

Protein and gene expression analyses in bone marrow stem cells mediated restoration of myocardium after ischemic insult

Lee, Kate L

The copyright of this thesis rests with the author and no quotation from it or information derived from it may be published without the prior written consent of the author

For additional information about this publication click this link.

<https://qmro.qmul.ac.uk/jspui/handle/123456789/559>

Information about this research object was correct at the time of download; we occasionally make corrections to records, please therefore check the published record when citing. For more information contact scholarlycommunications@qmul.ac.uk

**PROTEIN AND GENE EXPRESSION ANALYSES IN
BONE MARROW STEM CELL MEDIATED
RESTORATION OF MYOCARDIUM AFTER
ISCHEMIC INSULT**

Kate L Lee

Clinical Pharmacology
William Harvey Research Institute
Bart's and the London, Queen Mary University of London
John Vane Science Building
Charterhouse Square
EC1M 6BQ

Thesis submitted for the degree of PhD at the University of London in
January 2010

ABSTRACT

Myocardial Infarction (MI) is caused by occlusion of the coronary artery following atheromatous plaque rupture, the subsequent ischemia in the myocardium leads to myocyte necrosis unless treated quickly. Bone marrow derived stem cell treatment is a promising therapy for improving the outcome of patients with MI. The aim of this thesis was to study myocardial protein and gene expression changes in a rat ischemia/reperfusion (I/R) model in order to look for potential repair mechanisms of the myocardium triggered by endogenous bone marrow mononuclear cells (BMMNCs).

Rat myocardial samples were obtained from three experimental groups: one group had a sham operation, the other two groups had undergone myocardial I/R injury induced by left anterior descending (LAD) coronary artery ligation followed by treatment with either a BMMNC preparation or PBS. Comparative proteomic analyses were carried out using 2D electrophoresis; differentially expressed proteins were identified using LC-MS/MS. Western blotting was used to confirm the most significant findings including expression of 14-3-3 epsilon protein. Global comparative gene expression profiling was performed using Illumina RatRef12 BeadChips and QPCR was used to validate the top results. Bioinformatic tools were used to assess the biology of the differentially expressed genes and proteins.

Thirty-seven proteins were found to be differentially expressed in I/R injury compared to sham. These were primarily sarcomeric, energy production or stress response proteins and most were down-regulated. Expression levels were 'corrected' by BMMNC treatment for many of these proteins. Over 1500 genes were affected by I/R injury, 20 were affected by BMMNC treatment, and many of these were related to inflammation and apoptosis signalling and responses. The 14-3-3 epsilon protein was chosen for follow-up work as it presented as a good candidate for mechanistic involvement. This protein has many roles including interactions with the pro-apoptotic BCL2-associated agonist of cell death (Bad) protein. Western blotting was used to look at Bad expression and found it to be significantly increased in the

treatment group, although I could not reliably measure the expression of phosphorylated (serine 136) form of Bad. A preliminary pull-down assay was performed to look for binding partners of 14-3-3 epsilon. Two ATP synthase subunits, one of which is known to bind 14-3-3 epsilon, a protein involved in fatty acid β -oxidation and a protein of unknown function were found to bind. Further work will be required to follow up these findings and ascertain the exact role of 14-3-3 epsilon in cardioprotection. In summary, my data supports the power of profiling methods to derive new candidates for a role in repair mechanisms in this therapeutic model.

DECLARATION

The work presented in this thesis was performed on samples obtained from an animal model of ischemia/reperfusion injury with and without bone marrow cell treatment. The bone marrow cell preparation, animal model experiments, collection of phenotypic information from the model and measurements of Akt, p38 MAPK and GSK-3 β phosphorylation, and NF- κ B translocation by Western blotting were carried out by our collaborators in the William Harvey Research Institute and University College London. The harvesting and preservation of the myocardial samples used for my analyses was also carried out by collaborators.

For the gene expression studies I performed the cDNA preparation; hybridisation and reading of the chips was performed by Genome Centre Staff at Bart's and The London School of Medicine and Dentistry. Analysis of the gene expression data was carried out by me with some assistance from Dr Richard Dobson (Genome Centre staff).

I declare all the work pertaining to the 2DE analysis, mass spectrometry, Western blotting (14-3-3 epsilon, Sdha, Pebp1, Atp5b and Bad), QPCR, the pull-down assay, data analysis and the bioinformatics analyses presented in this thesis is my own work.

PUBLICATIONS & PRESENTATIONS

Publications

I have five publications arising from my participation in the Wellcome Trust Case Control Consortium:

- Wellcome Trust Case Control Consortium. Genome-wide association study of 14,000 cases of seven common diseases and 3,000 shared controls. *Nature*. 2007; 447; 661-78.
- Wellcome Trust Case Control Consortium. Association scan of 14,500 nonsynonymous SNPs in four diseases identifies autoimmunity variants. *Nat Genet*. 2007 Nov;39(11):1329-37.
- Wallace et al. Genome-wide Association Study Identifies Genes for Biomarkers of Cardiovascular Disease: Serum Urate and Dyslipidemia. *Am J Hum Genet* 2008 Jan;82: 139-149.
- Newton-Cheh et al. Genome-wide association study identifies eight loci associated with blood pressure. *Nat Genet*. 2009
- Wellcome Trust Case Control Consortium. Genome-wide association study of CNVs in 16,000 cases of eight common diseases and 3,000 shared controls. *Nature* 2010; 464; 713-722.

Other publications:

- Newhouse et al. Polymorphisms in the WNK1 Gene Are Associated with Blood Pressure Variation and Urinary Potassium Excretion. *PLoS One* 2009 April; 4: e5003.

Submitted:

- Lovell et al. Bone Marrow Mononuclear Cells Reduce Myocardial Reperfusion Injury by Activating the Pi3k/Akt Survival Pathway. *Atherosclerosis* 2010.

Oral Presentations

- Lee et al. Protein expression analyses in bone marrow stem cell mediated restoration of myocardium after ischemic insult. Presented at the William Harvey Review, William Harvey Research institute, Bart's and the London Queen Mary University, London, November 2008.

Poster Presentations

- Lee et al. Protein expression analyses in bone marrow stem cell mediated restoration of myocardium after ischemic insult. Poster presented at the 8th Sienna Meeting From Genome to Proteome: Integration and Proteome Completion Aug-Sep 2008.
- Lee et al. Protein expression analyses in bone marrow stem cell mediated restoration of myocardium after ischemic insult. Poster presented at the EuPA and DGP European Summer School "Proteomic Basics" July 2008.
(Attendance for this course was sponsored by a BSPR Fellowship)

ACKNOWLEDGEMENTS

I would like to thank the Medical Research Council for funding this study, and the British Heart Foundation for funding the work of our collaborators.

I would like to acknowledge the contributions of my supervisors Professor Munroe, Professor Mathur and Dr Leung for their support and mentorship; especially Professor Munroe for her patient and tireless guidance in writing this thesis.

I would also like to thank colleagues; Chaz and Rich, Mose and Mimi as well as those who have trodden this path before me and supplied advice and encouragement, especially Frankie. Finally I would like to thank my patient husband Casey for his support and proof reading skills.

CONTENTS	PAGE
1. Introduction	19
1.1 Myocardial infarction	19
1.1.1 Aetiology	
1.1.2 Prognosis	
1.1.3 Current therapy	
1.2 The promise of autologous progenitor cells	23
1.2.1 Autologous stem cells	
1.2.2 The evidence	
1.2.2.1 Animal models of bone marrow cell therapy for MI	
1.2.2.2 Human trials of bone marrow cell therapy for MI	
1.2.3 Mechanism	
1.2.3.1 IPC and cardioprotection	
1.2.3.2 Paracrine mechanism of BMMNCs	
1.3 Global protein and gene expression profiling	40
1.3.1 Proteomics	
1.3.1.1 Proteomics and CVD	
1.3.2 Transcriptomics	
1.3.2.1 Transcriptomics and CVD	
1.3.3 Integration of proteomic and genomic data	
1.3.4 Proteomics and gene expression studies of cardiac repair	
1.4 Rat model of I/R injury and restoration of myocardium associated with BMMNCs	53
2. Hypothesis and aims	57
2.1 Hypothesis	57
2.2 Aims	57
3. Materials and Methods	58
3.1 Model and bone marrow mononuclear cell preparation	58
3.1.1 Rat ischemia/reperfusion model	
3.1.2 Preparation and characterisation of bone marrow cells	
3.1.3 Collection of myocardial samples for proteomic and gene analysis	
3.2 Proteomic analyses	62
3.2.1 Sample preparation and quantification	

3.2.1.1	Protein lysate preparation from rat myocardial samples	
3.2.1.2	Protein quantification	
3.2.2	Two dimensional gel electrophoresis (2DE)	
3.2.2.1	Isoelectric focussing (IEF)	
3.2.2.2	SDS – polyacrylamide gel electrophoresis (PAGE)	
3.2.3	Image analysis	
3.2.4	Statistical analysis	
3.2.5	Protein identification by LC-MS/MS	
3.2.5.1	Excision and trypsin digestion of spots	
3.2.5.2	LC-MS/MS	
3.3	Validation of proteomic data by Western blotting	75
3.3.1	1D SDS-PAGE and blotting	
3.3.2	Antibody incubations and chemiluminescence	
3.3.3	Densitometry	
3.3.4	Statistical analysis	
3.4	Gene expression analyses	81
3.4.1	RNA preparation	
3.4.1.1	RNA extraction from tissue samples	
3.4.1.2	RNA quantification and quality assessment	
3.4.2	cDNA synthesis, purification and ‘in-vivo’ cRNA transcription	
3.4.3	Gene expression data pre-processing	
3.4.3.1	Quality assessment of gene expression data using BeadStudio	
3.4.3.2	Data preparation and normalisation	
3.4.4	Differential gene expression analysis using LIMMA	
3.5	Validation of differentially expressed genes	94
3.5.1	TaqMan gene expression assays	
3.5.2	RNA preparation	
3.5.3	QPCR using TaqMan gene expression assays	
3.5.4	Reference gene selection	
3.5.5	$\Delta\Delta C_t$ calculations and statistical analysis	
3.6	Bioinformatic analysis of protein and gene expression data	103
3.6.1	Protein ANalysis THrough Evolutionary Relationships (PANTHER)	
3.6.2	Database for Annotation, Visualization and Integrated Discovery (DAVID)	
3.6.3	Ingenuity Pathway Analysis (IPA)	

3.7 Studies of 14-3-3 epsilon	107
3.7.1 Validation of experiments using samples 10-18	
3.7.2 Expression and activation of BCL2-associated agonist of cell death (Bad)	
3.7.3 14-3-3 epsilon pull-down assay	
3.7.3.1 Bait protein immobilisation	
3.7.3.2 Prey protein preparation and capture	
3.7.3.3 Bait-Prey elution	
3.7.3.4 SDS-PAGE and protein detection	
3.7.3.5 LC-MS/MS protein identification	
4. Proteomic results	111
4.1 Wide-range protein profiling	111
4.1.1 Protein quantification	
4.1.2 2DE	
4.1.3 Differentially expressed proteins	
4.2 Narrow-range protein profiling	128
4.2.1 2DE	
4.2.1.1 pH 4.5-5.5 narrow-range 2DE analysis	
4.2.1.2 pH 5.5-6.7 narrow-range 2DE analysis	
4.2.2 Differentially expressed proteins	
4.3 Validation of proteomic data	139
5. Gene expression results	144
5.1 Gene expression profiles of samples 1-9 using Illumina RatRef12	144
5.1.1 Quality control and quantification of RNA and cRNA	
5.1.2 Quality control of the RatRef12 gene expression chip data	
5.2 Repeat of global expression profiles of samples 1-9 using Illumina RatRef12	152
5.2.1 Quality control and quantification of RNA and cRNA	
5.2.2 Quality control and pre-processing of the repeat of the RatRef12 gene expression chip data	
5.2.2.1 Quality control for the repeat chip data	
5.2.2.2 Pre-processing of the repeat chip data	
5.2.3 Differentially expressed genes discovered using LIMMA	
5.3 Validation of gene expression data	175
5.3.1 Reference gene selection	
5.3.2 QPCR using Taqman gene expression assays	
5.3.2.1 GeNorm	
5.3.2.2 $\Delta\Delta C_t$ calculations and statistical analysis	

5.3.2.3	QPCR analysis of Oas1k in samples 10-18	
6.	Bioinformatic results	183
6.1	Bioinformatic analysis of proteins found to be altered in 2DE analyses	183
6.1.1	Protein Analysis Through Evolutionary Relationships (PANTHER)	
6.1.1.1	Sham vs. MI	
6.1.1.2	MI vs. BMMNC	
6.1.2	Database for Annotation, Visualisation and Integrated Discovery (DAVID)	
6.1.2.1	Sham vs. MI	
6.1.2.2	MI vs. BMMNC	
6.1.3	Ingenuity Pathway Analysis (IPA)	
6.1.3.1	Sham vs. MI	
6.1.3.2	MI vs. BMMNC	
6.1.4	Summary	
6.2	Bioinformatic analysis of genes found to be differentially regulated in the Illumina RatRef12 analysis	220
6.2.1	Protein Analysis Through Evolutionary Relationships (PANTHER)	
6.2.1.1	Sham vs. MI	
6.2.1.2	MI vs. BMMNC	
6.2.2	Database for Annotation, Visualisation and Integrated Discovery (DAVID)	
6.2.2.1	Sham vs. MI	
6.2.2.2	MI vs. BMMNC	
6.2.3	Ingenuity Pathway Analysis (IPA)	
6.2.3.1	Sham vs. MI	
6.2.3.2	MI vs. BMMNC	
6.2.4	Summary	
7.	Studies of 14-3-3 epsilon and Bad proteins	252
7.1	Validation experiments using samples 10-18	252
7.2	Western blot analysis of Bad proteins	255
7.2.1	Bad	
7.2.2	Bad (phospho s136)	
7.3	Preliminary pull-down assay of his-tagged 14-3-3 epsilon	258
7.3.1	Pull-down assay and SDS-PAGE	
7.3.2	Protein identification by LC-MS/MS	

8. Discussion and Future Work	263
8.1 Proteomic changes in I/R model and treatment with BMMNCs	264
8.1.1 Mitochondrial/oxidative phosphorylation proteins	
8.1.2 Antioxidant proteins	
8.1.3 Energy metabolism proteins	
8.1.4 Heat shock proteins	
8.2 Candidate proteins for involvement in BMMNC afforded cardioprotection	272
8.3 Limitations of 2DE proteome analysis	277
8.4 Gene expression changes in I/R and after treatment with BMMNCs	282
8.5 Bioinformatic analysis of proteomic and gene expression datasets	288
8.6 Conclusions	289
8.7 Future work	291
10. References	295
11. Appendices	308
APPENDIX 1: Genome Centre protocol for Illumina direct hybridisation	308
APPENDIX 2: MASCOT search results from the wide-range 2DE analysis	313
APPENDIX 3: MASCOT search results from the pH 4.5-5.5 2DE analysis	323
APPENDIX 4: MASCOT search results from the pH 5.5-6.7 2DE analysis	327
APPENDIX 5: Abbreviations and identification codes for all proteins identified in the 2DE analyses	330
APPENDIX 6: Additional information on protein identifications which were based on a single peptide hit.	331
APPENDIX 7: LIMMA differential gene expression results	341
APPENDIX 8: Probe level data for the top 433 probes	348
APPENDIX 9: MASCOT search results from the 14-3-3 epsilon pull-down analysis	362
APPENDIX 10: Manuscript submitted to Atherosclerosis	368

LIST OF FIGURES	PAGE
Figure 1.1 Apical myocardial infarction	20
Figure 1.2 Progenitor cell classifications	24
Figure 1.3 Pathways thought to be involved in ischemic preconditioning	37
Figure 1.4 Tracking of BMMNCs 6 hours post-reperfusion	56
Figure 3.1 BSA standard curve macro in Excel	65
Figure 3.2 Assembly of XCell Blot Module [Invitrogen, UK]	76
Figure 3.3 An example of band volume normalisation using Gapdh as a loading control	80
Figure 3.4 RNeasy fibrous tissue kit procedure as shown in the handbook [Qiagen, UK]	83
Figure 3.5 R script used to perform the LIMMA analysis	93
Figure 3.6 Flowchart depicting the use of GeNorm to determine the most stable reference gene for a set of samples	99
Figure 3.7 Graphical out put of the example GeNorm analysis shown in figure 3.6	100
Figure 4.1 Venn diagram showing the distribution of 187 significantly differently expressed spots with >1.5 fold changes in the wide-range 2DE analysis	112
Figure 4.2 Venn diagram showing the distribution of 130 significantly differently expressed spots with >2.5 fold changes in the wide-range 2DE analysis	112
Figure 4.3 Graphs of p-values plotted against fold changes for 105 spots with significantly altered intensities in the pH 4-7 2DE analysis	114
Figure 4.4 Example of a wide range 2DE gel protduced for this analysis	119
Figure 4.5 The relative positions of peptides 1-16 along the length of ATP synthase subunit β	127
Figure 4.6 The relative positions of protein sequence covered by the 60kDa heat shock protein peptides identified in three spots from the narrow-range analyses	133
Figure 4.7 Example of the narrow range 2DE gel protduced for this analysis	134
Figure 4.8 Western blots of 14-3-3 epsilon (14-3-3 ϵ), succinate dehydrogenase (Sdha), and phosphatidylethanolamine-binding protein 1 (Pebp1) in samples 1-9	141
Figure 4.9 The average normalised spot volumes from the 2DE ananalysis (left) and normalised band volumes from Western blot (WB) analysis (right) for 14-3-3 epsilon (14-3-3 ϵ), succinate dehydrogenase (Sdha), and phosphatidylethanolamine-binding protein 1 (Pebp1) in samples 1-9	142
Figure 4.10 Bands detected using an antibody to ATP synthase subunit β	143
Figure 5.1 Summary from the Agilent Eukaryote Total RNA Nano Series II chip results for RNA extracted from samples 1-9	145
Figure 5.2 BeadStudio Plots of internal quality control features	148
Figure 5.3 Scatter plots of average signal data from two samples	149
Figure 5.4 Dendrogram produced by BeadStudio showing clustering of non-normalised probe data	151

Figure 5.5 Summary of the Agilent Eukaryote Total RNA Nano Series II chip results for RNA extracted from samples 1-9 for the repeat RatRef12 analysis	154
Figure 5.6 Summary of the Agilent Eukaryote Total RNA Nano Series II chip for results of repeat RNA extracts RNA 1r, RNA 2r and RNA 5r for the repeat RatRef12 analysis	155
Figure 5.7 Beadstudio Plots of internal quality control features	157
Figure 5.8 Scatter plots of average signal data from two samples	158
Figure 5.9 Dendrogram produced by BeadStudio showing clustering of non-normalised probe data	160
Figure 5.10 Venn diagram of distribution of differently expressed probes in the gene expression analysed using LIMMA	161
Figure 5.11 Graphs of FDR adjusted p-values plotted against log fold change (for probes with significant differential expression)	163
Figure 5.12 Graphical output of the GeNorm analysis	178
Figure 5.13 Graphs showing fold change (FC) results from the QPCR analysis (A-C) and LIMMA statistics from the Illumina RatRef12 chip analysis (D) for Iqgap1, Oas1k, and Sema4a	181
Figure 5.14 Graphs showing fold change (FC) results from the QPCR analysis for Oas1k in samples 10-18	182
Figure 6.1 PANTHER Pathways represented by the proteins differentially regulated in Sham vs. MI	184
Figure 6.2 PANTHER Biological processes represented by the proteins differentially regulated in Sham vs. MI	185
Figure 6.3 PANTHER Pathways represented by the proteins differentially regulated in MI vs. BMMNC	187
Figure 6.4 PANTHER Biological processes represented by the proteins differentially regulated in MI vs. BMMNC	188
Figure 6.5 KEGG Pathway - Oxidative Phosphorylation	198
Figure 6.6 Two of three networks associated with the proteins altered in Sham vs. MI	205
Figure 6.7 Three networks associated with the proteins altered in MI vs. BMMNC	215
Figure 6.8 PANTHER Pathways represented by the genes up-regulated in Sham vs. MI	222
Figure 6.9 PANTHER Pathways represented by the genes down-regulated in Sham vs. MI	223
Figure 6.10 PANTHER Biological processes represented by the genes up-regulated in Sham vs. MI	225
Figure 6.11 PANTHER Biological processes represented by the genes down-regulated in Sham vs. MI	226
Figure 6.12 PANTHER Biological processes represented by the genes differentially-regulated in MI vs. BMMNC	228
Figure 6.13 Networks associated with the genes altered in Sham vs. MI	240
Figure 6.14 Top network associated with the 15 genes altered in MI vs. BMMNC	249

Figure 6.15 Sphingosine-1-phosphate signalling	250
Figure 7.1 Western blots of 14-3-3 epsilon (14-3-3 ϵ), succinate dehydrogenase (Shda), and phosphatidylethanolamine-binding protein 1 (Pebp1) in samples 10-18	253
Figure 7.2 The normalised band volumes from Western blot analysis of samples 1-9 (left) and normalised band volumes from Western blot analysis of samples 10-18 (right) for 14-3-3 epsilon (14-3-3 ϵ), succinate dehydrogenase (Sdha), and phosphatidylethanolamine-binding protein 1 (Pebp1)	254
Figure 7.3 Western blots of Bad in samples 10-18	256
Figure 7.4 SDS-PAGE of the preliminary 14-3-3 epsilon pull-down assay	259
Figure 7.5 Band IDs from bait flow-through and eluate from the preliminary 14-3-3 epsilon pull-down assay	260
Figure 8.1 Mitochondrial oxidative phosphorylation chain	267
Figure 8.2 Signalling pathway potentially triggered by BMMNC treatment: Evidence from our model.	274
Figure 8.3 Example of wide- and narrow-range gel images	281

LIST OF TABLES	PAGE
Table 1.1 Summary of proteins found to be altered in expression or modified in 2DE comparative profiling experiments on animal models of I/R injury	43
Table 3.1 Myocardial samples collected for studies	61
Table 3.2 Lysis buffer preparation	63
Table 3.3 Concentrations of BSA standards used to obtain a calibration curve	64
Table 3.4 BSA standard curve preparation for performing the Bio-Rad protein assay on the NanoDrop 1000	66
Table 3.5 Rehydration buffer preparation	67
Table 3.6 12% SDS acrylamide gel solution preparation	68
Table 3.7 Displacing solution preparation	68
Table 3.8 Equilibration buffer preparation	69
Table 3.9 10 x SDS running buffer preparation	70
Table 3.10 10 x Tris buffered Saline (TBS) buffer	77
Table 3.11 1 x TBS-TWEEN buffer	77
Table 3.12 Reagents supplied in the RNeasy fibrous tissue kit [Qiagen, UK]	82
Table 3.13 Ambion TotalPrep reverse transcription master mix	87
Table 3.14 Ambion TotalPrep second strand master mix	87
Table 3.15 Ambion TotalPrep in-vivo transcription (IVT) master mix	88
Table 3.16 Promega reverse transcription master mix	95
Table 3.17 TaqMan QPCR master mix	96
Table 4.1 109 spots selected for protein identification by LC-MS/MS from the pH 4-7 2DE analysis	115
Table 4.2 Spots with significant fold changes for which a single protein ID was found from the wide-range analysis	121
Table 4.3 Proteins found to have significant fold changes in either the Sham vs. MI or the MI vs. BMMNC comparisons from the wide-range analysis	123
Table 4.4 Details of the ATP synthase subunit β peptides identified in 17 different spots in the wide-range analysis	126
Table 4.5 Seventeen spots selected for protein identification from the pH 4.4-5.5 narrow-range Progenesis 2DE analysis	129
Table 4.6 Fourteen spots selected for protein identification from the pH 5.5-6.7 narrow-range Progenesis 2DE analysis	131
Table 4.7 Details of the ATP synthase subunit β peptides identified in 2 different spots in the pH 4.5-5.5 narrow range analysis	132
Table 4.8 Spots with significant fold changes for which a single protein ID was found from the narrow range analyses	136
Table 4.9 Proteins found to have significant fold changes in either the Sham vs. MI or the MI vs. BMMNC comparisons from the narrow range analyses	138
Table 5.1 Preparation, quantification and QC of RNA samples	144

Table 5.2 Technical replicates of three RNA samples were processed into cRNA	146
Table 5.3 Nanodrop quantification of cRNA prepared using Ambion TotalPrep	146
Table 5.4 Quantification and QC of mRNA samples for repeated Illumina RatRef12 chip analysis	153
Table 5.5 Nanodrop quantification of cRNA prepared using the Ambion TotalPrep kit	156
Table 5.6 Top 30 probes found to be significantly altered in Sham vs. MI	166
Table 5.7 Top 10 probes found to be significantly down-regulated in Sham vs. MI	168
Table 5.8 Twenty probes found to be significantly altered in MI vs. BMMNC	169
Table 5.9 Top 15 qualitatively altered spots found to be ‘ON’ in MI compared to Sham	172
Table 5.10 Top 5 qualitatively altered spots found to be ‘ON’ in MI compared to Sham and ‘OFF’ in BMMNC compared to MI	173
Table 5.11 Three qualitatively altered spots found to be ‘OFF’ in MI compared to Sham	173
Table 5.12 Three qualitatively altered spots found to be ‘OFF’ in BMMNC compared to MI	174
Table 5.13 Suitability of 5 potential reference genes	176
Table 5.14 Normalised Ct values (Δ Ct) for each gene of interest (GOI), group averages and standard deviations	179
Table 5.15 P-values from the Student’s <i>t</i> -test performed on Δ Ct values from QPCR analysis in for <i>Iqgap1</i> , <i>Oas1k</i> , and <i>Sema4a</i>	180
Table 6.1 Four different lists of Refseq protein accession codes were entered into PANTHER	183
Table 6.2 Cluster 1-7 of 9 clusters of biological process GO terms associated with protein up-regulated in Sham vs. MI	190
Table 6.3 Cluster 1-12 of 19 clusters of biological process GO terms associated with protein down-regulated in Sham vs. MI	192
Table 6.4 Cluster 1 -9 of 14 clusters of biological process GO terms associated with protein up-regulated in MI vs. BMMNC	196
Table 6.5 One cluster of biological process GO terms associated with protein down-regulated in MI vs. BMMNC	197
Table 6.6 Proteins and endogenous chemicals included in the IPA analysis of Sham vs. MI proteomics data	201
Table 6.7 Top 10 canonical pathways associated with the 36 proteins altered in Sham vs. MI	207
Table 6.8 Table showing proteins and endogenous chemicals included in the IPA analysis of MI vs. BMMNC proteomics data	209
Table 6.9 Top 10 canonical pathways associated with the 27 proteins altered in MI vs. BMMNC	218
Table 6.10 Three different lists of Refseq gene accession codes were entered into PANTHER	220

Table 6.11 Group 1 -25 of 65 groups of biological process GO terms associated with genes up-regulated in Sham vs. MI	230
Table 6.12 Group 1 of 11 groups of biological process GO terms associated with genes down-regulated in Sham vs. MI	233
Table 6.13 Top 25 networks associated with the genes altered in Sham vs. MI	236
Table 6.14 Top 20 canonical pathways associated with the genes altered in Sham vs. MI	243
Table 6.15 Proteins and endogenous chemicals included in the IPA analysis of MI vs. BMMNC gene expression data	246
Table 6.16 Canonical Pathways associated with the genes altered in MI vs. BMMNC	250
Table 7.1 Proteins identified by LC-MS/MS from the bands illustrated in Figure 7.5	262

1. Introduction

Bone marrow derived progenitor cell therapy has been suggested as a novel therapeutic approach to cardiac repair following ischemia/reperfusion injury. Using a rat model of I/R injury in collaboration with Professors Mathur and Thiemermann we demonstrated that early injection of autologous bone marrow derived cells leads to a marked reduction in infarct size compared to controls. This research included measuring the mechanical and cellular improvements to myocardial function afforded by progenitor cell therapy and assessing the activation of some key survival signalling pathways.

The analyses I performed to study alterations in gene and protein expression in relation to the reduction in infarct size in the I/R model treated with progenitor cells forms the basis of this thesis. My aim was to use this data to look for clues to the cellular mechanisms by which the preservation of cardiac function was mediated.

1.1 Myocardial infarction

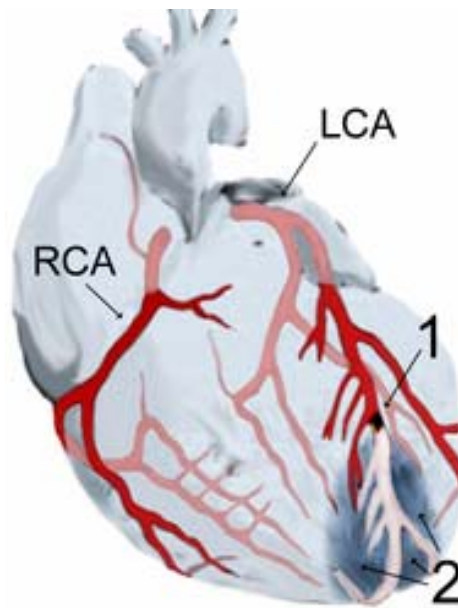
Myocardial infarction (MI) commonly known as a heart attack, is the descriptive term for death of myocardial tissue and resulting loss of overall cardiac function caused by a period of cardiac ischemia (interruption of blood flow). Taken together with stroke (infarction within the brain) these are the leading causes of mortality and morbidity worldwide [1].

1.1.1 Aetiology

Cardiac ischemia can occur when an atheromatous plaque in a coronary artery ruptures leading to acute thrombosis and either complete or intermittent occlusion of the coronary artery, see Figure 1.1. Atheromatous plaques are a lipid rich deposit in the intima of arteries which act as focal points for the accumulation of inflammatory and immune cells and debris, they are usually covered with a fibrous cap [2]. Partial

occlusion of the coronary artery can cause angina which is often characterised by exertional chest pain. Sustained chest pain is usually an indication of MI or unstable angina in which near-complete occlusion of the coronary artery occurs.

Figure 1.1 Apical myocardial infarction This figure illustrates the heart and the left coronary artery (LCA) and right coronary artery (RCA). 2 = area of infarction, shaded in dark grey. 1 = the position of the occlusion in the LCA. [3]



Ischemia is not simply hypoxia (lack of oxygen) but also involves a drop in the supply of metabolic substrates and a build up of metabolites [4]. Twenty minutes of ischemia will initiate necrosis of the cardiomyocytes and cause an inflammatory response leading to further tissue damage. Reperfusion reduces cell loss by initiating apoptosis (programmed cell death) which encourages rapid phagocytosis and a limited inflammatory response [5]. The final extent of myocardial damage is not only due to the ischemic insult, but is also due to cellular responses to reperfusion itself, termed ischemia/reperfusion (I/R) injury [6].

1.1.2 Prognosis

Cardiovascular disease (CVD) accounted for approximately a third of all annual deaths in the UK in 2007; coronary heart disease (CHD) is responsible for approximately half and stroke for a quarter of these CVD related deaths [7]. Nearly all the deaths from CHD were due to a heart attack [8]. Survival rates in patients who have suffered MI are highly dependant on the extent of the infarcted region which is determined by the duration of ischemia and size of the territory supplied by the occluded artery. Approximately 1/3 of patients with acute myocardial infarction die before reaching hospital and in total MI is fatal in around 40% of cases even with modern therapy. Infarcted myocardium eventually converts to scar tissue which is fibrotic and has reduced contractility. The loss of contractile function may lead to a compensating hypertrophy of the remaining myocardium. The increased demand of the hypertrophied myocardium can lead to LV failure and ventricular arrhythmia which are the leading causes of post hospital mortality and morbidity [9].

1.1.3 Current therapy

Therapeutic approaches that aim to reperfuse the area of infarct in the first few hours are crucial to limiting the infarct size. Thrombolytic therapy (such as streptokinase) and antiplatelet therapy (aspirin) are administered as soon as MI is diagnosed [10]. Primary angioplasty (direct balloon ‘unblocking’ of the coronary artery) for acute myocardial infarction is now becoming the first line treatment, it has been demonstrated to halve short-term mortality in some randomised clinical trials, although primary angioplasty must be performed within hours to have the most benefit [11, 12]. In the long term, patients are prescribed beta-blockers to inhibit beta-adrenergic stimulation which slows heart rate, lowers systemic blood pressure and reduces myocardial contractility thereby reducing the risk of ventricular arrhythmias [13, 14]. Angiotensin converting enzyme (ACE) inhibitors are also prescribed to inhibit fibrosis of the infarcted myocardium; part of the remodeling processes that can harm the contractile properties of the repaired myocardium and

reduce the haemodynamic changes due to ACE up-regulation [14-16]. Antiplatelet therapy (aspirin or clopidogrel) as well as lipid lowering statins can also be included in long term pharmacological interventions to reduce the potential for recurring MI [14]. Despite modern medical advances there is still a need to further reduce the mortality associated with MI. Efforts are being made to reduce the time from the onset of ischemia to the point of reperfusion, but a therapeutic strategy which limits I/R injury and which could be given at the onset of reperfusion may have a significant impact in improving prognosis.

1.2 The promise of autologous progenitor cells

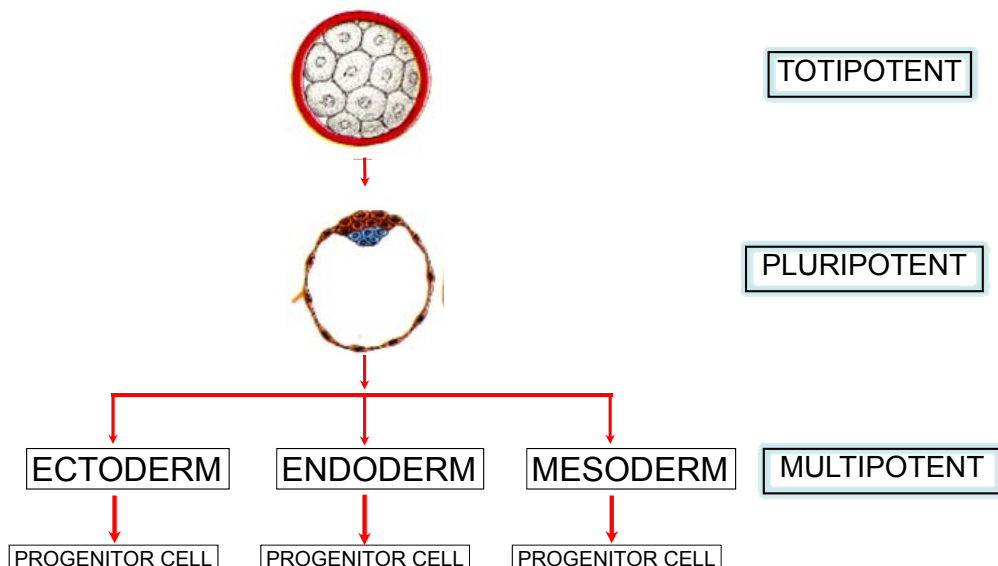
Recovery from MI depends on both the extent of the tissue area affected and the duration of ischemia. The ability of the myocardium to regenerate itself after damage is limited and after loss of cells due to infarct or other damage, remaining cardiomyocyte cells undergo hypertrophy to compensate [17]. It is now understood that the myocardium does have some ability for myocyte proliferation that may increase after cardiac damage [18]. This proliferation may be due to a limited resident progenitor cell population [19]. It has been suggested that these cardiac stem cells (CSC) reside in small niches and may differentiate into cardiomyocytes, smooth muscle cells and endothelial cells, making the heart a self renewing organ [20]. A recent study aimed to quantify cardiomyocyte renewal and their findings suggest that a 1% annual turnover at 25 years of age slows to 0.45% at age 75. This was calculated to equate to ~45% of cardiomyocytes that would have been replaced over an entire lifespan [21]. However this regenerative capacity appears to be hindered by injury as all myocardial cell types die in the area of infarct including the CSCs [20]. MI occurs more commonly in older people, for whom cardiac regeneration rates may have slowed, possibly in part due to lower CSC reserves, which would further reduce the hearts ability to renew large areas of damage without intervention [21].

The natural mechanisms of myocyte hypertrophy accompanied by increased fibrosis and scar formation are often not sufficient to maintain functional capacity of the myocardium after damage and may even be detrimental in the long term; the prognosis associated with damage to the heart from MI and hypertrophy is poor. Therapeutic methods that either protect myocytes from I/R induced cell death or encourage the homing and proliferation of resident progenitor cells or other circulating stem cells that could re-populate the myocardium would be an ideal solution for cardiac repair.

1.2.1 Adult derived stem cells

There are several classifications of stem cells which have the ability to self renew and go on to form several different types of fully differentiated cells, see figure 1.2. Stem cells can be derived from embryonic and adult sources and are defined by the range of cells they can differentiate into. Totipotent cells can form all the cell types of the body and the placenta, whereas pluripotent cells can form all cell types of the body but not the placenta. Both of these stem cell classifications are of embryonic sources [22]. Embryonic stem cells generate the greatest range of potential cell types and there are several studies showing these cells improve myocardial repair and function in mouse and rat models of MI [23-25]. The risks of immunorejection and ethical concerns however, lean towards autologous adult stem cells as a preferable option. Multipotent cells are obtained from a variety of adult tissues and are capable of differentiating into a limited range of cell types and their location appears to be an important factor in determining which cell types they can differentiate into [26].

Figure 1.2 Stem cell classifications Figure courtesy of Professor Mathur



One main source of autologous adult stem cells is the bone marrow. Bone marrow cells include a range of different cell types including mesenchymal stem cells (MSCs) and haematopoietic stem cells (HSCs). HSCs were originally thought to only give rise to red and white blood cells and platelets, whereas MSCs were progenitor cells for muscle, connective tissue and other mesenchymal derived cell types. However some experimental data has been interpreted as indicating that both of these cell types may have a much wider potential and may be coerced into forming cardiomyocytes, fibroblasts and indeed endothelial cells [27].

1.2.2 The evidence

1.2.2.1 Animal models of bone marrow cell therapy for MI

A frequently used ‘in-vivo’ model for studying MI is a rat model that has undergone left anterior descending (LAD) coronary artery ligation to induce cardiac ischemia. Similar models using mice are also popular due to the ability to perform experiments on transgenic animals that enable the functions of certain genes in relation to I/R to be assessed [28]. Other ‘in-vivo’ models such as canine and porcine infarct models are also useful, especially in certain aspects of stem cell research such as studying cell delivery methods that can be more directly applied to humans [29-31].

The first published evidence that bone marrow derived cells could invoke improved cardiac repair and function post-MI was performed in a rat model of myocardial injury. Bone marrow cells (BMCs) were isolated using a percoll gradient and either used fresh or after culturing for 7 days. Some cultures were treated with either transforming growth factor β (TGF- β) or 5-azacytidine (5-aza) added on the third day for 24 hours. The fresh and cultured cells were also phenotypically characterised by immunohistochemical staining for cardiac specific troponin I and myosin heavy chain (MHC). Following on from this, myocardial scarring was introduced by cryo-injury in adult Sprague-Dawley rats and after three weeks either freshly prepared BMSCs, cultured BMSCs, BMSCs cultured with 5-aza or cell culture medium were injected directly onto the scar. During culture of the BMCs it was noted that the cells

expressed cardiac specific proteins such as troponin I and MHC, and formed myotubules and this only occurred when the cells were treated with 5-aza. It was also noted that hematopoietic cells were eliminated during culturing process. Five weeks after transplantation, the scar area was smaller for the 5-aza group and these animals had thickened left ventricles, which translated into improved ventricular function as measured by peak systolic pressure. All scars transplanted with cells had increased angiogenesis as measured by capillary density. To identify the BMSCs within the scar, a further set of experiments were performed in which transplanted cells had been labelled with bromodeoxyuridine [BrdU]. Histological examination of samples collected after 5 weeks revealed BrdU positive cells within the scar tissue and indeed within some newly formed capillary walls [32]. This set of early experiments suggested that both the freshly prepared BMSCs and cultured BMSCs have the ability to either induce or form new vasculature in scarred myocardium. It was suggested that only cells that have been induced to differentiate into a cardiac-like phenotype by 5-aza could cause an increase in muscle mass sufficient to regain function.

Data from a study by Orlic *et al* (2001) was also interpreted to show that the BMCs transplanted 3-5 hours post-surgery were able to home and transdifferentiate in the infarct zone to replace dead myocytes [33]. They reported that BMCs, characterised as not expressing any differentiation markers (*lin-*) but expressing the receptor for stem cell factor (*c-kit*), when transplanted into the edge of the infarcted region of a mouse infarct model, generate new myocardial cells to replace the dead cells. Confirmation that the new myocardium was derived from the cell therapy came from an experiment where BMCs derived from male transgenic mice expressing enhanced green fluorescent protein (EGFP) were introduced into infarcted myocardium of female mice; subsequent immuno-staining for the Y chromosome histocompatibility antigen as well as expression of EGFP showed the donor cells had integrated into the female myocardium. The new cells were also found to express cardiac proteins common to fully competent myocardial cells such as myocyte enhancing factor 2 (MEF2) and the transcription factor GATA-4. There was however only a 40% success rate in the survival of the mice in this study which was thought to be due to

damage to the myocardium incurred during the procedure of injecting the BMCs into beating myocardium; also it was proposed that the female mice may have rejected the BMCs from male mice [33].

To get a more quantitative assessment for the migration and homing abilities of BMSCs, Sheik et al (2007) extracted bone marrow mononuclear cells (BMMNCs) from male transgenic mice expressing both firefly luciferase and EGFP and injected these (three hours post-surgery) into the tail vein of either sham operated or ischemia/reperfusion female mice. Cell migration and survival was recorded using bioluminescence imaging for 4 weeks. The BMMNCs were found in lung, spleen and femurs in both groups and the I/R group had much stronger fluorescent signals in the heart within the first 10 days [34]. Echocardiography showed a trend towards improved left ventricular fractional shortening (LVEF) which however was not statistically significant. This work did show that the cells were capable of homing even when introduced into the tail vein rather than directly transplanted to the heart.

The higher energetic demands of the damaged and hypertrophied myocardium can outstrip the ability of repaired vasculature in the damaged section of myocardium which leads to further cell loss and fibrosis. In 2001 Kocher *et al* studied the ability of different populations of BMCs to produce new vasculature as well as new myocardial cells. Human derived BMCs were separated into MSC (CD34⁻) and HSC (CD34⁺) fractions. The CD34⁺ fraction was then assessed for co-expression of CD117 (stem cell factor receptor), and vascular endothelial growth factor receptor-2 (VEGFR-2). A population of cells with co-expression of these factors was noted to have phenotypic characteristics of mature vascular endothelial cells and a further population of cells had characteristics of endothelial progenitor cells. CD34⁺ cells were then introduced intravenously to mice post-MI. These mice were found to have much improved neoangiogenesis in the infarct zone and in its periphery compared to control animals and compared to those treated with CD34⁻ cells [35].

Toma and colleagues (2002) studied human bone marrow derived mesenchymal stem cells (hMSCs), and labelled them using a β -galactosidase reporter gene (LacZ) expressing non-replicating virus. These cells (500,000-1 million) were then transplanted directly into the left ventricle of immunodeficient CB17 SCID/*beige* male mice and animals were sacrificed for histological analysis at 30 minutes, 4, 14, 21, 30 and 60 days after transplantation. Interestingly after 4 days the majority of β -gal⁺ cells were found in the spleen, liver and lungs. Up to 4 days, an estimated ~2200 β -gal⁺ cells remained in the heart, although the number seen decreased from this point. The fact these cells had dispersed indicated a strong capability for migration. Desmin was not expressed in β -gal⁺ cells after 4 days but was present in all the cells after 60 days, as was cardiac-specific troponin T, β -MHC, α -actinin and phospholamban. The cells were also found to have the structural characteristics of cardiomyocytes [36]. In a later study in which bone marrow derived MSCs from transgenic female mice expressing GFP were co-cultured with rat embryonic cardiomyocytes derived from male embryos. The MSCs did indeed express cardiac specific genes, and these were detected with mouse specific primers, but they also expressed collagen type IV (stromal cell marker absent in embryonic cardiomyocytes). Fusion was also investigated, by looking for cells with XXY chromosomes, and only a very low rate of this phenomenon was measured. The electrophysiological properties of the 'differentiated' MSCs were measured to look at the functional profile of these cell and these studies showed that the MSCs did not display spontaneous rhythmic activity and they were unable to produce action potentials [37]. A further study co-culturing HSCs and MSC with neonatal cardiomyocytes and differentiating factors were unable to produce evidence of transdifferentiation [38].

The studies described so far have indicated that bone marrow derived cells may home in on injured myocardium and some may in fact survive within the host myocardium. The introduction of these cells is also associated with an increased number of surviving, functioning myocytes and a corresponding improvement in cardiac function. However, to date there has been no definitive evidence that the introduced

cells in fact transdifferentiate and replace damaged myocardial cells. Studies measuring the expression of cardiac specific proteins in transplanted or co-cultured BMCs may in fact be measuring proteins taken-up by these cells rather than expressed by these cells. In the case of cells observed to have some physiological features in common with cardiomyocytes, they may still be unable to integrate and undergo spontaneous rhythmic contraction in unison with the surrounding myocardium [36, 37]. Indeed the number of BMCs homing and surviving within the damaged myocardium appear few. Studies in animal models trying to elucidate the best methods for introducing cells, the best type of cell and indeed the mechanism by which the cells might work are ongoing.

1.2.2.2 Human trials of bone marrow cell therapy for MI

Animal models are a useful research tool but relating the results from ‘in-vivo’ studies to a clinical setting involves caution as there are inter species differences in structural proteins and ion exchange proteins essential for contraction [39, 40]. In addition, animal models have a much reduced level of genetic variation, as they often involve inbred strains, and although this reduces confounding factors in an experiment, it does not necessarily reflect the human population. Experimental variation is also tightly controlled to levels not always possible in the clinical situation, for example, the time from onset of infarct to the application of therapy. The data from animal models suggests BMSCs may be an important therapeutic approach for MI. Finally in all of the various animal models of MI the background of inflammatory atherosclerotic disease inherent in most human subjects is lacking. Therefore several studies have been initiated to address whether the application of autologous bone marrow cell therapy in humans would incur the same beneficial outcome that had been observed in animal models.

Stamm et al (2003) performed one of the earliest exploratory experiments in humans. Six patients who had acute MI between 10 days and 3 months before admission for a coronary artery bypass graft (CABG) procedure were recruited into a small clinical trial. BMC transplantation took place during the CABG procedure, with AC133+

cells being injected into the infarct border. Improved LVEF and diastolic function were observed in four of the six recruited patients 2 weeks post-surgery and improvements in perfusion of the infarct were seen in five patients. Four patients had further complications following surgery, including supraventricular arrhythmia, and two patients had pericardial effusion (fluid around the heart) but a connection between these events and the cell therapy was difficult to ascertain [41]. These results are promising but without a control group, it is difficult to draw conclusions from this very small study.

Another early clinical trial in humans was performed by Strauer et al (2002), it included 20 patients with MI. All patients received standard treatment with 10 also receiving ficoll-separated BMCs using a balloon catheter 5 to 9 days after onset of MI. Follow-up consisted of left ventriculography and coronary angiography after 3 months. The percentage infarct region was found to be reduced significantly in the cell therapy group compared to control, and improvements in wall movement were also recorded. LVEF improved slightly but non-significantly in both groups. Other measurements of cardiac function e.g. stroke volume were also found to be improved in the cell treatment group [42].

These early studies indicated this therapeutic approach could yield positive outcomes in humans but further investigation into the behaviour (homing and survival) of the BMCs within patients was needed. Penicka et al (2007) tracked myocardially transplanted BMCs for 24 hours using radioisotope cell labelling in two groups of patients, 5 with acute MI (AMI) and 5 with chronic MI. Myocardial radioactivity was observed in all acute patients and in all but one of the chronic patients after 2 hours. At 20 hours radioactivity was only detected in three of the acute patients. Similar to the animal studies, strong signals were also detected in the spleen, liver and lungs at 2 and 20 hours [43]. The data shows the homing abilities of BMCs and this may be enhanced in acute MI.

There have been many larger clinical trials in the last few years looking at the benefits of cell based therapy for cardiac ischemia. Several gold-standard randomised controlled trials (RCT) have been carried out looking at BMC therapy in AMI with large enough cohorts to gain a more clear idea of the benefits of the therapy. One such trial was the BOne marrOw transfer to enhance ST-elevation infarct regeneration (BOOST) Trial [44]. In this trial 60 AMI patients were randomised to receive either best care or unselected bone marrow cell transplant ~5 days post percutaneous intervention (PCI). All patients had baseline MRI and further scans at 6 and 18 months after discharge. The primary endpoint was LVEF change after 6 and 18 months follow up compared to baseline. The LVEF at six months was significantly more improved in the treatment group than control, but at 18 months there was no significant difference between the improvements made in both groups [44].

Lunde et al (2006) randomised 100 patients to receive either ficoll-separated BMCs 6 days post-PCI or control. The control arm did not have the bone marrow aspiration procedure or sham injection. Single-photon-emission computed tomography (SPECT) and echocardiography were performed at baseline and at six months follow up. MRI was also performed. No statistically significant differences were found in LVEF, end-diastolic volume or infarct size at six months [45].

In a larger multi-centre trial, 204 AMI patients were randomised to receive either placebo medium or cell transplant with ficoll-separated BMCs ~4 days post PCI.. All patients had bone marrow cells aspirated. Angiograms were performed immediately before the procedure and at 4 month follow-up. The primary end-point in this study was the absolute change in LVEF at 4 months compared to baseline. In total 94 controls and 92 treatment angiograms were used for quantitative analysis. LVEF was found to be significantly higher (6%) in the treatment arm compared to control even after adjustments. Adverse clinical outcomes were also recorded at 4 months and at 1 year (for 168 patients). This data revealed no significant difference between the groups in any of the events independently (death, recurring MI, re-hospitalisation for

heart failure), but the incidence of the combined events was significantly lower in the treatment group [46].

A further study published alongside the two previously mentioned aimed to look at intracoronary infusion of enriched mononuclear cell preparations from either bone marrow or circulating blood in 75 patients. The patients had myocardial infarction at least three months prior to entry in the trial. The primary end points were LVEF and function of the LV in the area of infarct, both measured by angiography. After three months follow up, both primary end points were significantly improved in only the bone marrow cell preparations (3% in LVEF). In a cross over study, some of the patients were assigned to receive a different treatment at the time of the 3 month follow-up and again BMC treatment caused significant improvements in LVEF in patients who previously received either control or circulating blood cell preparation. Only 35 of the patients underwent MRI to assess infarct size, and reductions were not seen in any of the study groups [47]. The composition of the cell preparations were not fully characterised, therefore differences in functional improvement between the two cell preparations may be due to differences in cell composition.

Janssens et al (2006) randomised 67 AMI patients to receive either placebo medium or cell transplant with ficoll-separated BMCs within 24 hours of PCI. Again, all patients had bone marrow cells aspirated. MRI was performed at baseline and at 4 months follow-up. Cell therapy was not found to significantly improve LVEF in this study, however a reduction in infarct volume was recorded. Microvascular obstruction was also assessed in this study and the authors suggest that both LVEF and infarct size may be more improved in patients without microvascular obstruction, although the study was not powered to perform these calculations [48].

A recent review of published trial data found approximately 60 on-going trials, many of these were not RCT design, used cultured cells, or were not using patients with acute MI and therefore only 13 trials were assessed [49]. They found that none of the studies were large enough to demonstrate whether BMC treatment had an effect on

morbidity and mortality, indeed no significant differences were detected between treatment and control arms. Trends appeared to show the treatment was not associated with an increase in adverse events and there may be a short term benefit to LVEF [49]. A large amount of heterogeneity between study design and outcome measures make this ‘meta’-style analysis difficult to interpret. In general the results from human studies have been much less striking than what was observed in the animal models, but a generally positive trend has been attributed to bone marrow cell based therapy in two separate meta-analyses [49, 50].

The limitations within the clinical studies performed so far include differences in preparation of the cells to be injected (many studies using unselected heterogenous cell populations rather than purified HSCs); differences in the timing of cell transplantation (hours to months post PCI); and limited long-term outcome data to link any small improvements in LVEF with clinical benefit [51, 52]. The effect of cell infusion may be different in early treatment time points (hours or a few days) which may limit infarct size and lead to subsequent improvement in functional recovery compared to later time points (weeks to months) which don’t reduce infarct size but may improve function through a different mechanism. Recommendations for cell type, method of introduction and timing of introducing the cells as well as the mechanism of benefit are yet to be determined and further data from animal studies may enable better design of future clinical trials yielding more definitive results.

1.2.3 Mechanism

Initially transplanted autologous bone marrow derived cells were thought to differentiate and replace dead cells within the infarct, replacing myocytes (cardiogenesis) and vasculature (angiogenesis), however, data from animal models have shown that only a limited amount of transdifferentiation of BMCs occurs, if at all. Evidence suggests not enough of the transplanted cells survive within the infarct [53]. However, many progenitor cells secrete growth factors promoting vascular generation (e.g. vascular endothelial growth factor, VEGF) [54]. One of the strongest

mechanistic theories is that the BMCs are acting through a paracrine mechanism, whereby signals are secreted by the BMCs after they have homed-in on the site of injury, thereby inducing cell survival and angiogenesis.

What is this paracrine signal, from which constituent of the bone marrow cell preparation does this signal originate, and what is the target pathway or pathways of this signal? Clues about the details of the mechanism by which the BMCs work may be taken from looking at what we already know about other triggers of cardioprotection. Ischemic preconditioning (IPC) results in a striking level of cardioprotection from I/R injury and there have been decades of research into the triggers, mediating signalling pathways and potential end effectors of this phenomenon.

1.2.3.1 IPC and cardioprotection

IPC is a phenomenon in which one or more brief periods of non-lethal ischemia preceding a major infarct provides a significant level of protection to the myocardium downstream of the infarct. Aside from prompt reperfusion, IPC is the most effective intervention at reducing resultant infarct size, although without eventual reperfusion, the protection from IPC will be lost [55]. This protection appears to have two phases (windows) of protection, the first window is up to ~2 hours after preconditioning and the second window is days after preconditioning [56]. Some level of cardioprotection can also be initiated by causing brief periods of ischemia in a distal part of the body, termed remote preconditioning [57]. The discovery of IPC in 1986 [58] has provoked a huge amount of research and animal models have been used extensively to look at what mechanisms may be involved.

In terms of mechanism, the cardioprotective state is from 10 minutes after IPC and therefore suggests modification of pre-existing proteins may be involved [56]. The trigger is thought to be mediated through Gi-coupled receptors, with adenosine, bradykinin, norepinephrine and opioids all released by the heart during the

preconditioning stimulus and binding to these receptors with an additive effect [59], see Figure 1.3 overleaf.

The pathways that are downstream from the receptors which carry the cardioprotection message (mediators) are known to include protein kinase C (PKC). The evidence for PKC involvement is strong, blockade of PKC abolished cardioprotection triggered by adenosine, bradykinin and opioids [60-62]. Adenosine appears to directly activate PKC, whereas bradykinin and opioids activate phosphatidylinositol 3-OH kinase (Pi3k)/Akt pathway and then diverge on PKC further downstream [63]. Studies using wortmannin, a Pi3k inhibitor, have revealed the role of the Pi3k/Akt pathway in IPC and have shown that it acts upstream of PKC activation [64]. Rabbit cardiomyocytes either treated with Akt inhibitor, or rendered dominant negative for Akt show no reactive oxygen species (ROS) production in response to acetylcholine or bradykinin treatment, revealing an important mediatory role for Akt [65]. The same group also confirmed the involvement of nitric oxide (NO) and its place downstream of Akt in the signalling cascade. Guanylyl cyclase and protein kinase G (PKG) are also now thought to be downstream from NO [63], see Figure 1.3.

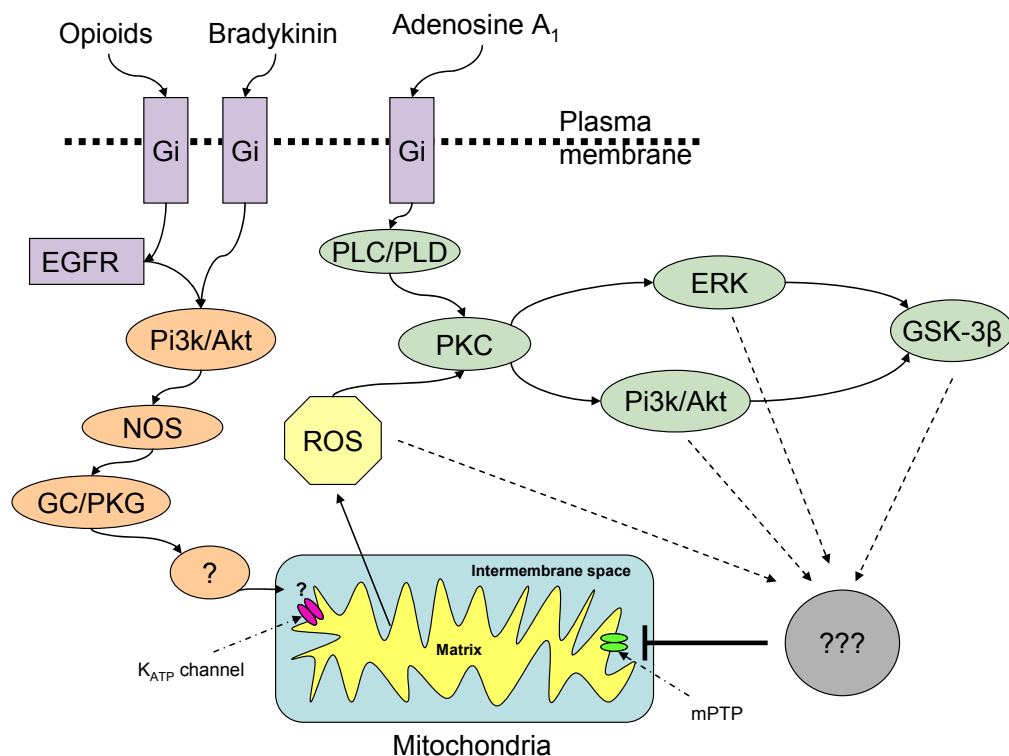
Free radicals are also thought to be involved in the cardioprotective response, possibly by directly activating protective protein kinases. Diazoxide mediated protection can be blocked by a free radical scavengers N-acetylcysteine and N-2-(mercaptopropionyl)glycine (MPG) [66]. It has also been shown that there is increased radical production from mitochondria triggered by ischemia [67].

Mitochondrial ATP sensitive potassium channels (mito- K_{ATP} channels) are thought to play an important role in IPC mediated cardioprotection, but how they are involved is only recently becoming clear. A theory put forward by Pain et al (2000) is that receptor occupancy leads to mito- K_{ATP} channel opening, causing ROS production and these free radicals activate downstream kinases [68]. In fact ROS is now known to activate PKC. Protein kinase G (PKG) has been shown to be capable of eliciting the

opening of mito- K_{ATP} channel channels, but is unlikely to be the final step in this signalling cascade, the intermediates between PKG and mito- K_{ATP} channel opening are as yet unknown [69].

Although some of the survival signals have been elucidated, final mechanisms for cardioprotection are still unknown. One further proposition is that the inhibition of the mitochondrial permeability transition pore (mPTP) opening plays an important role in IPC mediated myocardial protection, see Figure 1.3 [70, 71]. The opening of mPTP is thought to induce mitochondrial swelling and rupture, releasing apoptotic agents into the cytoplasm.

Figure 1.3 Pathways thought to be involved in ischemic preconditioning Protein kinase B (Akt), epidermal growth factor receptor (EGFR), extracellular signal-regulated kinase (ERK), guanylyl cyclase (GC), Gi protein coupled receptor (Gi), glycogen synthase kinase 3 beta (GSK-3 β), mitochondrial permeability transition pore (mPTP), nitric oxide synthase (NOS), protein kinase C (PKC), protein kinase G (PKG), phospholipase C (PLC), phospholipase D (PLD), phosphatidylinositol 3-OH kinase (Pi3k), reactive oxygen species (ROS). Adapted from Downey et al 2007 [63].



Glycogen synthase kinase 3 β (GSK-3 β) has been shown to inhibit mPTP opening [72]. GSK-3 β , unusually, exists in its active conformation, and phosphorylation causes it to be inactivated. PKC can directly phosphorylate GSK-3 β , or can initiate phosphorylation through ERK and Pi3k [63]. Many other potential candidates have been suggested (ROS, Pi3k/Akt, PKC, ERK, mito K_{ATP}), work is ongoing to elucidate the exact mechanism of mPTP opening [73]. Whether mPTP opening is the end effector of the ‘intrinsic’ mitochondrial apoptosis pathway, which involves the B-cell lymphoma protein 2 (BCL-2) protein family is controversial [74].

The mechanistic pathways behind the late phase of cardioprotection afforded by preconditioning appear to be similar to those involved in early phase. Studies using various inhibitors have also implicated important roles for COX-2, both endothelial and inducible nitric oxide (NO), and manganese superoxide dismutase (MnSOD) [56].

Elucidating cardioprotective mechanisms may enable high risk patients to be treated with pharmacological agents which trigger activation of these pathways possibly through binding to the Gi-coupled receptors. A carefully planned drug regimen would need to be used to maintain a cardioprotective response ready for a potential MI, the exact timing of which will be impossible to predict, but also to prevent over-agonising and dampening receptor response [56]. Such an approach would only be suitable for very high risk patients. The best strategy at present for MI patients in general is rapid reperfusion. But there is potential for an additional intervention whereby autologous cells or a pharmacological mimic thereof may be administered in conjunction with reperfusion to enhance recovery.

1.2.3.2 Paracrine mechanism of BMMNCs

Nakanishi et al (2008) hypothesised that growth factors and cytokines secreted by bone marrow derived MSCs may be responsible for activating resident stem cell populations in a paracrine manner. They found that not only did MSC conditioned medium promote the proliferation of isolated cardiac stem cells (CSCs) ‘in-vitro’, but also protected them from serum starvation-induced apoptosis. They also demonstrated that conditioned medium also led to increased Akt phosphorylation in the CSCs [75]. This study provided evidence that secreted factors may be involved, and also suggests Akt may be involved in bone marrow cell mediated protection.

Kubal et al (2006) performed a detailed ‘ex-vivo’ study using right atrial muscle slices from patients undergoing elective surgery. The tissue slices were subjected to 90 minutes simulated ischemia followed by 120 minutes reoxygenation. The tissue slices were either co-incubated with BMMNCs (obtained from the same patients),

BMMNCs plus a PKC inhibitor, PKC inhibitor alone or neither. The same set of experiments were carried out using a p38 MAPK inhibitor. Tissue injury as measured by creatine kinase release into the media was markedly reduced in the BMMNC treatment group, but the effects were countered by the PKC inhibitor. Cell necrosis and apoptosis were also much reduced in the BMMNC group and again these effects were ameliorated by the presence of the PKC inhibitor. The second set of experiments using the p38 MAPK inhibitor showed the same results [76]. This indicated that the BMMNCs might be working through PKC, p38 MAPK kinase signalling pathways, potentially indicating an overlap in the protective signal mediators involved in IPC.

Candidates, including interleukin-8 (IL-8), transforming growth factor β (TGF- β) and hepatocyte growth factor (HGF) among many others have evidence for involvement in mobilisation, homing, proliferation and survival, however, the mechanisms by which these processes occur in BMMNC mediated restoration of ischemic myocardium are not yet fully understood and therefore the design of therapeutic approaches cannot be refined [77].

1.3 Global protein and gene expression profiling

Proteomics and transcriptomics are terms and indeed fields with fairly recent origins. The suffix ‘omic’ refers to the totality of the subject. Proteomic techniques aim to study the entire proteome of an organism, tissue, or cell at a particular point in time under particular conditions i.e. measure the presence of all of the proteins and their modifications [78]. Transcriptomics aims to look at all of the gene expression activity present in an organism, tissue, or cell at a particular point in time under particular conditions. In reality, the whole picture is currently beyond the abilities of current analysis techniques, particularly for the proteome [79]. Although gene chip technology is enabling us to get a much more complete picture of gene expression in a sample, currently we are only able to visualise at best ~1000 different proteins in a 2DE analysis, perhaps twice that using a shotgun MS based proteomic method [80]. As ~12,000 different gene products are estimated to be expressed in a mammalian cell, only 8-16% of the proteome can be visualised at best [81]. The most common use of proteomic and transcriptomics is to perform an exercise in ‘spot-the-difference’ aimed at looking for differences between samples that reveal system-wide patterns or individual candidates that can act as biomarkers for diagnostic purposes or can indicate mechanism and thereby leading to potential new therapeutic targets. The results of such experiments will inform more targeted follow-up studies.

1.3.1 Proteomics

One of the most commonly applied proteomic methods is two-dimensional electrophoresis (2DE), which separates the proteins in a sample to enable visualisation. Proteins are separated according to charge (isoelectric point, pI) in the first dimension, then by mass (relative molecular mass, Mr) in the second. This method for visualisation allows differences between groups of samples to be detected by observing differences in the distribution and intensity of protein spots on the 2D gel after staining [82]. Identification of the proteins can be obtained using high performance liquid chromatography coupled to tandem mass spectrometry (MS/MS)

(LC-MS/MS) [83]. Information on post-translational modifications (PTMs) can be both observed in the 2DE patterns and further characterised using LC-MS/MS [84].

1.3.1.1 Proteomics and CVD

2DE has been used extensively for studying cardiovascular pathology, especially diseases of cardiac muscle which often result in cardiac failure. The technique is amenable to looking at changes at the protein level which accompany the structural changes at a cellular level. Such studies into cardiomyopathy and left ventricular hypertrophy (LVH) have been successful at finding alterations in cytoskeletal/contractile proteins and proteins involved in mitochondrial energy production which correlate with contractile dysfunction, and alterations in myocardial energetics which accompanies this form of cardiac remodelling [85]. The majority of 2DE studies to date have been global scale ‘fishing expeditions’ looking for differences that may lead to clues relating to the mechanisms of disease onset and progression. 2DE has been used for a global comparative proteomic comparison of disease vs. non-disease in an animal model of dilated cardiomyopathy (DCM) [86]. The findings of this comparison led to a more targeted study of the ubiquitin proteasome system in human DCM myocardial samples. This revealed a large increase in ubiquitination of many proteins within the DCM hearts compared to ischemic heart disease and healthy (unused) donor tissue controls [87].

The proteome of any particular tissue type or even a homogenous cell population is a complex group of proteins which are constantly being processed, modified and degraded. As a full picture of the entire proteome is currently unobtainable, many studies look at ‘sub-proteomes’ which may be based on cellular compartmentalisation (cytosolic, mitochondrial, membrane or nuclear extracts) or indeed on some other categorisation. The previously mentioned study separated ubiquitinated proteins for comparison by 2DE, another study looking at PKC kinase cascade signalling in IPC created sub-proteomes by co-immunoprecipitating PKC ϵ complexes using PKC ϵ monoclonal antibodies. This sub-proteome could then be further studied using 1D and 2DE as well as western blotting. These functional proteomic techniques led to the

discovery that PKC ϵ binds and phosphorylates a large number of proteins involved in a diverse array of functions from stress response to regulation of transcription and translation [88].

The 2DE approach has also been employed to look at ischemic vs. non ischemic myocardium in animal models and the approach has successfully found patterns of protein alterations in sarcomeric proteins, proteins involved in cellular energy metabolism and proteins of the mitochondrial respiration chain. Some of these studies have also compared the proteome after cardioprotective interventions such as IPC and the use of free-radical scavengers. See Table 1.1 for a list of proteins found to be altered in these studies.

2DE has been used to compare protein profiles from an I/R model using isolated rabbit hearts. Myocardial samples were obtained from two I/R injured groups, stunned (15 minutes of ischemia followed by 60 minutes reperfusion) and infarcted (60 minutes ischemia followed by 60 minutes of reperfusion) and a control group [89]. They identified many affected proteins which were categorised into cytoskeletal/sarcomeric proteins, energy metabolism proteins, redox regulation proteins (NADH oxidoreductase, cytochrome c oxidase, peroxidase and superoxide dismutase), stress response and others such as voltage-dependant anion channel 1 (VDAC1), fatty acid binding protein 3 and calcium independent phospholipase A2. Many of the proteins identified in this study were seen to be modified by ischemia, rather than being simply up-or down-regulated. Examples were VDAC1 in which a spot that appeared to be the native form decreased in both the stunned and infarcted myocardial samples and another spot (also VDAC1) which was of a lower molecular mass increased in both models of ischemia. There was also a significant decrease in the abundance of a spot identified as native Troponin T (pI 5.5) in both stunned and infarcted myocardium and an increase in the abundance of a seemingly basic (pI 7) form of Troponin T in the infarcted samples. The increased abundance of spots identified as myosin light chain 2 in the I/R injured samples also indicated cleavage of the native protein as both were smaller masses than the native

protein [89]. A follow up study looked at the proteome in the stunned I/R rabbit model with and without treatment with an oxygen free-radical scavenger, and discovered that therapy rectified some of the modifications in sarcomeric proteins caused by I/R injury, suggesting free radicals were responsible for sarcomeric damage and contractile dysfunction in stunned myocardium [90].

Table 1.1 Summary of proteins found to be altered in expression or modified in 2DE comparative profiling experiments on animal models of I/R injury. a = references in which this protein was found to alter in association with I/R injury compared to control; b = references in which this protein was found to alter in association with a cardioprotective intervention compared to no intervention; c = references in which this protein was found to alter in association with ischemia only (no reperfusion). References: 1 =[89]; 2 =[90]; 3 =[91]; 4 =[92]; 5 =[93].

Protein name	Reference(s)		
	a	b	c
2-oxoglutarate dehydrogenase	3	3	
3-Hydroxybutyrate dehydrogenase	3	3	
3-Mercaptopyruvate sulfurtransferase	5		
Actin alpha	1, 3	3	
Actinin alpha 2	1, 2	2	
Aldehyde dehydrogenase	5		
alpha B crystallin	1, 2	2	
ATP Synthase alpha	1, 2	2	5
ATP Synthase D	1, 2	2	
ATP Synthase delta	1, 2, 5	2	
ATP synthase F0 complex	3	3	
beta enolase	1, 2	2	
Calcium independent phospholipase A2	1		
Creatine kinase B	1, 2	2	
Creatine kinase M	1, 2, 4	2, 4	
Creatine kinase, Sarcomeric	1		
Cytochrome c oxidase	1, 2	2	
Dehydrogenase /Reductase SDR Family	2	2	
Delta(3,5)-delta(2,4)-dienoyl-CoA isomerase			5
Dihydrolipoamide dehydrogenase 1	1		
DJ-1 protein	5		5
Enolase 1 alpha	5		5
Enoyl-CoA hydratase-like protein	3	3	
Fatty acid binding protein 3	1		
Glutathione S-Transferase Mu	2	2	
Glyceraldehyde 3-phosphate-dehydrogenase			5

Table 1.1 continued

Protein name	Reference(s)		
	a	b	c
Heat shock protein 20kDa			5
Heat shock protein 27kDa	1, 2	2	
Heat shock protein 27kDa (phosphorylated)	2	2	
Heat shock protein 70kDa	1, 2	2	
Isocitrate dehydrogenase B			5
Isovaleryl coA dehydrogenase	5		
Lactate dehydrogenase	1	2	5
Lactate dehydrogenase, M subnit	2	2	
Long chain acyl-CoA dehydrogenase	3	3	
Malate dehydrogenase	3	3	
Microfilin	3	3	
Mitochondrial protein P1 precursor (chaperonin)	4	4	
Myoglobin	1		
Myosin H			5
Myosin light chain 1	5		
Myosin light chain 2	1, 2	2	
Myosin light chain 3	3	3	
NADH dehydrogenase	3	3	
NADH oxidoreductase	1, 2, 3	2, 3	
Peroxiredoxin 2	1, 2	2	
Peroxiredoxin 3	1, 2		
Peroxiredoxin 6	1, 2, 5	2	5
Phosphoglycerate mutase	1		
Prohibitin	3	3	
Pyruvate dehydrogenase	1, 3	3	
Rieske ion sulphur protein		3	
Skeletal LIM domain protein 2	1, 2	2	
Superoxide dismutase	1, 2, 4	2, 4	
Translation elongation factor	1, 3	3	
Translationally controlled tumour protein 1	1, 2	2	
Triose phosphate Isomerase	1, 2	2	
Tropomyosin	3	3	
Troponin C	1, 2	2	
Troponin T	1, 4	4	
Trypsinogen 11	2	2	
Ubiquinol cytochrome c reductase 1	2	2	5
Voltage-dependant anion channel 1	1, 2	2	
Voltage-dependant anion channel 2	3	3	

Another 2DE profiling study also using isolated rabbit hearts, they compared myocardial samples from control, I/R and IPC. In this study the mitochondrial protein fraction was isolated for 2DE analysis. Many proteins were found to be up- and down-regulated in I/R compared to control including; a reduction in TCA-cycle related proteins, an increase in the E1-beta subunit of pyruvate dehydrogenase, an

increase in NADH dehydrogenase (mitochondrial respiration chain, complex I), but a decrease in the rieske iron sulfur protein (mitochondrial respiration chain, complex III), a significant decrease in the expression of VDAC and a large increase in the expression of long chain acyl-CoA dehydrogenase. Almost all of these proteins were returned to levels similar to control in the IPC group [91]. These results give a snapshot of mitochondrial behaviour in response to I/R injury and IPC-induced protection.

An I/R model has also been created using isolated perfused rat hearts which were subjected to either: I/R, ischemia with no reperfusion, or control. Several different times of ischemia (15, 25 and 30 minutes) were looked at in both I/R and ischemia only. Protein was prepared from myocardial samples and from coronary effluents for 2DE analysis. The 2DE analysis revealed the majority of altered protein spots to be up-regulated in the ischemia group compared to control hearts after 25 minutes of ischemia; this effect was more pronounced for 30 minutes of ischemia. In the I/R samples compared to control the majority of proteins were down-regulated. There was also an increase in total protein concentration in effluent from I/R hearts compared to control. Enolase and myosin light chain 1 were both down-regulated in I/R and both appeared alongside ATP synthase in increased concentrations in the effluent. This study highlighted some of the individual proteins which are affected by I/R injury and also separated those which may specifically be up-regulated in ischemia from those alterations only seen once reperfusion ensues. This data also suggests that firstly protein expression may be up-regulated during ischemia and that there may be a 'flushing out' of proteins from ischemic tissue occurring during reperfusion [93]. This possibly adds an extra layer of complexity when interpreting the post I/R proteome.

Other proteomic analyses of I/R in animal models have aimed to look at protein differences that may elucidate the mechanisms behind IPC. An investigation on PKC ϵ 's mechanistic involvement in cardioprotection has been carried out using an array of proteomic techniques in concert with metabolomic analysis (profiling the

metabolome). Using transgenic mice with cardiac specific expression of either active (AE) or dominant negative (DN) PKC ϵ . The AE mice exhibited innate PKC ϵ dependant resistance to ischemic injury compared to wild type. Difference in-gel electrophoresis (DIGE), a 2DE method in which *Cye* (cyanine) dyes are used to label two different samples to be electrophoresed on the same 2D gel, was used to look at the myocardial proteome of wild type, AE and DN mice. This analysis revealed previously unknown PKC ϵ -influenced alterations in cytosolic glucose and energy metabolism proteins and also a strong negative influence of PKC ϵ inhibition on the pyruvate dehydrogenase complex [94]. The metabolic profiles obtained using nuclear magnetic resonance (NMR) showed discriminate differences between control AE and DN samples. This group also looked at metabolic profiles in the transgenic mice vs. control within an I/R model (LAD coronary artery ligation) and found further evidence of an improved metabolic recovery in AE hearts [94]. This study provides further clues of the mechanisms relating to PKC ϵ cardioprotection. It was not shown whether the moderate restoration of myocardial energetics measured is secondary to some other preceding cardioprotective action of PCK ϵ .

1.3.2 Transcriptomics

Transcriptomics is the study of gene expression, or the global analysis of mRNA within a sample. In cardiovascular disease, there have been many studies in cardiomyopathy and heart failure but there are only a limited number in MI [95]. There are two main approaches for studying gene expression, one being the comparison of the global gene expression in treated vs. non-treated (or disease vs. non-disease), the other is to look at the effect of genetic manipulation on gene expression to explore the functionality of specific candidate genes.

1.3.2.1 Transcriptomics and CVD

Early experiments looking at gene expression in I/R injury were limited by technology and only measured a small number of pre-specified genes [96, 97]. Expression of TNF- α , IL-1 β and IL-6 within the infarct area and in surrounding non-

infarct myocardium was measured 1, 8 and 20 weeks post surgery in a rat I/R model using quantitative polymerase chain reaction (QPCR). Expression levels of all three genes increased in the infarct area and decreased thereafter to levels lower than seen in surrounding non-infarct myocardium [97]. A further study looking at early (3 days) and late (21 days) gene expression changes, also in a rat I/R model, were measured using an RNase protection assay. The proto-oncogene *c-fos* was found to have a large (10 fold) increase at 3 days and remained 3 fold up-regulated even at 21 days. Previously noted up-regulation in the fetal form of MHC (β -MHC) was seen at 3 days but returned to normal levels at 21 days. Adult isoforms of Na-K ATPase decreased 5 fold at 3 days and again were returned to normal after 21 days [96]. These studies were very limited, and only a handful of genes for which there was prior evidence for involvement were measured.

Early cDNA microarrays enabled more global analysis of I/R influenced genes, but even these were limited to a few thousand. This approach however led to the discovery of genes not previously known to be affected by MI {e.g. cardiac ankyrin repeat protein (CARP) transforming growth factor β – stimulated clone (TSC)-22}, and indeed produced large enough datasets to cluster the affected genes into functional groups (e.g. protein expression, metabolism, cell signalling and cell structure) giving a better overall picture of the biological processes underlying MI and LV remodelling [98].

From the late 1990's GeneChips were available from Affymetrix containing much larger numbers of transcripts, these have been used in several studies looking at I/R in rat models [99-101]. Simkhovich et al (2003) looked at gene expression changes in young (4 months) and old (25 months) rats after three brief 3 minute periods of ischemia with 5 minutes reperfusion in between. The hearts were excised 24 hours after surgery and comparative gene expression analysis using Affymetrix U34A GeneChips was performed. In the ischemic tissue of younger rats compared to non-ischemic tissue, the majority of genes appeared to be down-regulated whereas many more up-regulated genes were found in the older rats [99]. Another study by the

same team looked at gene expression changes initiated by brief ischemic episodes, to look for potentially protective gene expression profiles again using Affymetrix U34A GeneChips. The samples included heart tissue from control, sham operated and ischemic as well as non-ischemic tissue from ischemia animals subjected to 20 mins ischemic followed by 4 hours reperfusion in 8-9 months old rats. These investigations found several genes (many inflammation-associated) to be up-regulated in non-ischemic tissue and sham operated tissue compared to control, possibly indicating some induction of gene expression related to operative stress. When comparing ischemic vs. non-ischemic tissue they found most of the altered genes were up-regulated including; heat shock proteins, activating transcription factor 3 (Atf3), early growth response 1 (Egr1), vascular endothelial growth factor (Vegf), b-cell translocation gene 2 (Btg2) and growth arrest and DNA damage inducible 45 α (Gadd45 α). Atrial myosin light chain 1 and sulfontransferase hydroxysteroid gene 2 (Sth2) were both found to be down-regulated [100]. The up-regulation of heat shock proteins, growth factors and other genes previously associated with inhibition of apoptosis, i.e Atf3, and were interpreted to indicate innate cardioprotective response. An increase in inflammation-associated genes, over and above those induced by surgery alone, was also noted.

Affymetrix U34A GeneChips have also been used to study gene expression changes induced by IPC and preconditioning triggered through the use of volatile anesthetics (APC). LV tissue was taken from animals after 110 minutes of isoflurane infusion (APC group), three 3 minute episodes of ischemia with 5 minutes reperfusion in between and 85 minutes reperfusion afterwards (IPC group), 110 minutes of no-flow ischemia (ischemia group) and a sham operated control group. In the APC group ~400 transcripts were altered by >2 fold, and these included an approximately equal number of up- and down-regulated genes compared to control, whereas ~290 transcripts were altered in IPC and the vast majority were up-regulated compared to control. Ischemia alone altered 78 transcripts including both up and down-regulated genes. The overlap between these lists of altered transcripts were relatively small

consistent with the idea that they represent different cardioprotective mechanisms [101].

All of the above studies show that comparative global gene-expression profiling can reveal clues regarding mechanisms of cardiac injury and protection in animal models. The same techniques have also been used to study the mechanism of BMSC-induced protection in I/R. As c-kit positive bone marrow derived cells have been used in many of the animal models of bone marrow cell transplantation in MI, Ayach et al (2006) wanted to look at the importance of c-kit. This group used the Affymetrix GeneChips to look at the gene expression changes in an I/R model using c-kit deficient (Wv) and wild-type (WT) mice with and without bone marrow derived HSC transplantation [102]. WT/WT and WT/Wv transplantations were also looked at in this study. Evidence for involvement of c-kit was clear as Wv mice suffered worse heart function than WT mice after MI. Transplantation of Wv mice with WT bone marrow cells rescued the defective cardiac repair that was seen in the Wv mice. The gene expression results revealed a strong up-regulation in genes which regulate natural-killer cells and natural-killer cell markers in bone marrow transplanted Wv animals compared to infarcted Wv animals. The anti-apoptotic genes; protein kinase B (Akt), bcl-2-associated X protein (BAX) and tyrosine kinase with immunoglobulin-like and EGF-like domains 1 (TIE1) as well as the angiogenic vascular endothelial growth factor (Vegf) were also up-regulated [102].

Ip et al (2007) used microarray chips to look at ischemic myocardium compared to non-ischemic myocardium following LAD induced ischemia in mice. They concentrated on a subset of genes on the Affymetrix chips, specifically chemokines, cytokines and cell adhesion genes [103]. They also studied the corresponding ligands and receptors in bone marrow derived MSCs. They found nine different receptors in the MSCs corresponding to eight cytokines to be up-regulated in ischemic myocardium. Selectively blocking some of these receptors and measuring MSC homing to the ischemic myocardium revealed a potential role for integrin β 1 but not integrin α 4 or CXCR4. As CXCR4 has previously been shown to be

important in HSC, they postulated different pathways for migration might exist in these two cell types [104].

1.3.3 Integration of proteomic and genomic data

The measurement of mRNA abundance in a sample or the qualitative comparisons between two samples that diverge by one biological variable enables some insight into gene regulation. Gene regulation is however poorly correlated with protein abundance and regulation which is more indicative of biological processes, as it is proteins and not mRNA which are functional units. The reason for this poor correlation is that although gene expression is inherently linked to protein production, subsequent processes of translation, post-transcriptional modification of proteins mean that every mRNA does not correlate to a molecule of protein; and the ever fluid nature of protein production and degradation also means that a quick glimpse of the transcriptome will not fully correlate to the proteome that exists in a biological sample at the same moment. The half lives of protein and mRNA range from 0.1-10 hours and 0.5-500 hours respectively [79]. It is important therefore to look at both thereby obtaining a view of the variation in genetic regulation and the variation in the biological system. How to integrate the two sets of data in a way in which they become more informative is a key issue.

Sampling processes also differentially affect the transcriptome and the proteome. During the processes of extracting and preserving samples the nucleic acid content is relatively stable as long as the operator is careful to limit RNA degradation by RNase enzymatic action. Proteins are however affected by various proteolytic enzymes, temperatures, pH etc. Even mRNAs present in low numbers can be measured by modern chip experiments, and the coverage of the transcriptome is ever improving. Low abundance proteins and hydrophobic membrane proteins are notoriously difficult to visualise and proteomic methods are limited in the ability to have a full view of proteins across the *pI* and molecular size scales. The proteome as seen by 2DE is limited to the *pI* range specified by the chosen IPG strip, even 2D gels made

using strips with a full pH 3-10 range rarely have high quality focussing of proteins at the extreme ends of the pH range, especially in very alkaline proteins [105]. Other proteomic approaches, such as shotgun proteomics, which is a 'bottom-up' approach where a complex protein sample is digested into peptides then analysed using LC-MS/MS, remove some of the limitations of gels-based methods. Low abundance and hydrophobic proteins are more easily identified, however, the ability to see all of the sample is still limited by the separation abilities of the LC (i.e. peptides run off the LC column and into the MS faster than they can be identified) [81]. Quantification issues also arise with the shotgun approach. Relative quantity between experimental groups can be calculated from the intensity of spots which are known to contain a particular protein in a 2DE analysis. Labelling with stable isotope tags is one method employed to quantify changes in protein expression with bottom-up methods, although label-free methods, such as peak area intensities and spectral counting, are becoming more popular [81]. In summary, in addition to the inherent differences between proteome and transcriptome, many proteomic techniques only visualise a portion of the global proteome and the portion viewed between different experiments may differ. This should be taken into account when integrating these two types of datasets.

1.3.4 Proteomic and gene expression studies of cardiac repair

Proteomic and gene expression studies have already been used to some extent to look for the biological responses of ischemic tissue to preconditioning as described. Recently, Fert-Bober et al (2008) produced a dataset which showed the merits of measuring both gene and protein expression to get a more complete picture of cellular responses. Protein expression alone after I/R showed a strong down-regulation in many proteins, whereas the gene expression data revealed this down-regulation was hiding an increase in transcriptional activity [93].

These approaches have not yet been used to compare gene and protein expression profiles of I/R injured myocardium and bone marrow cell 'restored' myocardium, and

to try to relate these findings directly to histological and functional measurements in the same model. It is possible results from such a study may reveal mechanistic information and may provide evidence for overlap of mechanism with that already well characterised in IPC. This information is especially important as human trials using bone marrow cells are ongoing and our knowledge of how these cells work is poor. There is a possibility that these cells may be secreting paracrine factors which could be pharmacologically mimicked therefore removing the need for cell harvesting. Even if the cells themselves were the best therapeutic approach there may also be a possibility to engineer them in some way to enhance whatever cardioprotective signals they are producing.

1.4 Rat model of I/R injury and restoration of myocardium associated with BMMNCs

In 2006 a set of experiments were initiated to study BMMNC treatment in a rat I/R model (LAD coronary artery ligation) in collaboration with Professors Mathur and Thiemermann and teams from the William Harvey Research Institute and University College London. Several parallel experiments were performed due to the mutually exclusive nature of the various assays to be performed. The main aims of these experiments were to study the effects of early introduction of bone marrow cells and to look for evidence of a paracrine mechanism of action.

The first experiment aimed to look at the early application of BMMNCs in a rat I/R model, and to measure changes in infarct size in comparison to IPC. Four groups were studied, these included sham surgery treated with PBS vehicle, I/R treated with PBS vehicle, I/R treated with BMMNCs and a preconditioned group with I/R and treated with PBS vehicle. Cells or PBS were delivered immediately upon reperfusion intravenously. The ischemic episode was 25 minutes, and 2 hours post reperfusion the area at risk (AAR) was measured by perfusing the heart with Evan's blue and the infarct was demarcated using nitro blue tetrazolium as previously described [106]. There was a 42% reduction in infarct size afforded by the BMMNC treatment, and this was comparable to the reduction afforded by IPC.

The second parallel experiment aimed to measure cell death by assessing apoptosis and necrosis, as well as caspase activation in this early intervention model. Three experimental groups were studied and included: sham surgery treated with PBS vehicle, I/R with PBS vehicle and I/R with BMMNCs. As before, the ischemic episode was 25 minutes, cardiomyocytes were isolated 2 hours post reperfusion. Apoptosis and necrosis were assessed immediately using flow cytometry (Annexin 5-FITC/propidium iodide dual staining), caspase-9 activity was assessed using Fluorescent-Labeled Inhibitor of CASpases (FLICA). Apoptosis, necrosis and

caspase activation were all found to be reduced in the BMMNC group compared to MI.

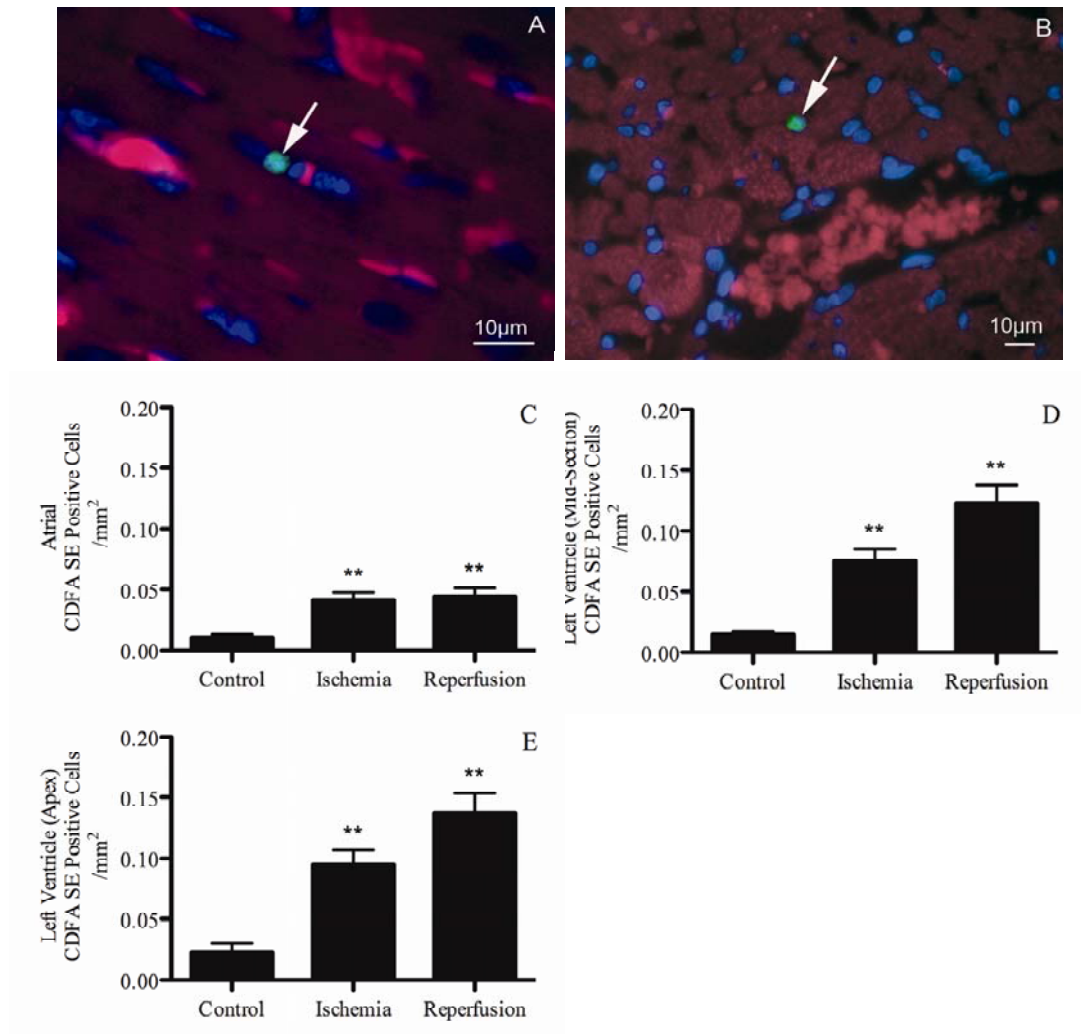
The third parallel experiment looked at cardiac function and the extent of myocardial fibrosis in the model. Three experimental groups were studied including sham surgery treated with PBS vehicle, I/R with PBS vehicle and I/R with BMMNCs. Baseline echocardiography was performed before surgery. The ischemic episode was 25 minutes for this experiment and 7 days after onset of reperfusion, echocardiography was repeated. Hearts were excised and sections stained with picrosirius red for histological assessment of fibrosis. Fibrosis was found to be reduced in the BMMNC group compared to MI, and this was accompanied by improvements in systolic and diastolic function as measured by left ventricular ejection fraction (LVEF), fractional area change (FAC) and Contractility index.

The final parallel experiment involved studying kinase signalling pathways known to be involved in IPC mediated cardioprotection, this was performed using five experimental groups including: sham surgery treated with PBS vehicle, I/R with PBS vehicle, I/R with BMMNCs, I/R with PBS vehicle and pi3k inhibitor (LY294002) and I/R with BMMNCs and LY294002. The ischemic episode was 25 minutes and assays were performed on protein lysates from cardiac samples taken 2 hours post reperfusion; Western blotting was used to measure protein expression. BMMNC were found to be associated with a Pi3k dependant phosphorylation of serine-473Akt (activation of Akt), serine-9GSK-3 β (inhibition of GSK-3 β), as well as phosphorylation of p38-MAPK and nuclear translocation of NF- κ B.

Separate studies were also carried out by Matthew Lovell (William Harvey Research Institute) looking at the presence of BMMNC cells stained with cell tracker dye carboxyfluorescein diacetate succinimidyl ester (CFDA SE) [Molecular probes, UK] in the hearts (whole, atria, ventricle and apex) 6 hours post reperfusion. Studies were performed in sham operated animals treated with cells, animals treated with cells upon initiation of ischemia and those treated with cells upon initiation of reperfusion.

The results of these studies showed that cells injected into the right internal jugular vein were present in heart tissue 6 hours post reperfusion (Figure 1.4 A and B). The cells were homing in on the the injured heart and there were more cells in the region downstream of the occlusion within the left ventricle (Figure 1.4 C, D and E). More cells successfully homed in if they were injected at the point at which reperfusion ensued (Figure 1.4 D and E). This study illustrates that the introduced cells do indeed home in on the site of injury in our model and it is estimated that 1% of cells are present after 6 hours. It also shows that injecting cells at the point of reperfusion improves the number of cells homing in on the injured myocardium, the viability of the cells was undetermined.

Figure 1.4 Tracking of BMMNCs 6 hours post-reperfusion. **A and B)** Histological sections of heart tissue stained with hematoxylin-eosin, with fluorescent CFDA SE stained BMMNC cells green. **C)** Stained BMMNC cells per mm² found in atrial sections. **D)** Stained BMMNC cells per mm² found in left ventricle sections. **E)** Stained BMMNC cells per mm² found in the apical section. *Experiments, data analysis and preparation of figures (Lovell).*



2. Hypothesis and aims

2.1 Hypothesis

The protein profile and gene expression pattern of rat myocardium with and without BMMNC treatment after experimentally induced infarct will differ, and these differences may guide us to 1) the pathways involved in myocardial regeneration, 2) the method of cellular repair and 3) may reveal similarities in the mechanism of BMMNC myocardial repair and IPC.

2.2 Aims

- 1.** To perform comparative proteomic analysis using 2DE to identify proteins which have been altered (expression or modification) by I/R injury and proteins subsequently altered by treatment with BMMNCs.
- 2.** To perform comparative gene expression profiling using the RatRef12 BeadChip (Illumina, UK) to determine if genes are differentially expressed in I/R injury and are activated by treatment with BMMNCs.
- 3.** To utilise bioinformatic tools in a search for patterns which may indicate specific signalling pathways involved in the cellular repair induced by BMMNC.

3. Materials and Methods

3.1 Model and bone marrow mononuclear cell preparation

All experiments were carried out in accordance with the Guide for Care and Use of Laboratory Animals published by the US National Institute of Health (NIH Publication No 85-23, revised 1996). The animals were purchased from Harlan, UK or Charles River UK, Ltd and were cared for in accordance with both the UK Home Office Guidance in the Operation of the Animals (Scientific Procedures) Act 1986, published by Her Majesty's Stationery Office, London, UK and the Guide for the Care and Use of Laboratory Animals, published by the American Physiological Society. All animal model work was carried out by our collaborators.

3.1.1 Rat ischemia/reperfusion model

The I/R model was created using male Wistar rats weighing 250-300g [Charles River UK, Ltd]. Two groups of animals underwent alternative procedures. The first group of animals were sham operated (Sham n = 3) and the second group had ischemia induced (n = 6) before being treated with either PBS vehicle (MI n = 3) or a bone marrow mononuclear cell (BMMNC) preparation (BMMNC n = 3) infused intravenously at the point of reperfusion.

All animals were anesthetised and ventilated; body temperature and mean arterial pressure (MAP) were monitored throughout the procedures. A thoractomy was performed and the pericardium was dissected to reveal the left anterior descending (LAD) coronary artery and a snare occluder was placed around the LAD. This was used to induce ischemia for 25 minutes before allowing reperfusion to ensue for 6 hours. For the sham animals, the thoractomy was undertaken but the LAD was not occluded.

3.1.2 Preparation and characterisation of bone marrow cells

The preparation and characterisation of bone marrow mononuclear cells was carried out by Matthew Lovell (Bart's and the London, UK). Cells were harvested from donor male Wistar rats which were killed using a schedule 1 listed technique of concussion. The fibias and tibias were excised and cleaned of all tissue before the bones were broken open and bone marrow cells were flushed out with Dulbecco's Modified Eagle's Medium (DMEM) and 10% fetal calves serum (FCS) [Sigma-Aldridge, UK]. The mononuclear cell fraction was then separated using Percoll [GE Healthcare Lifesciences, UK] density gradient centrifugation according to the manufacturer's protocol.

The cells were counted using a haemocytometer [Improved Neubauer, VWR International, UK] and viewed using a microscope [Keyence BZ8000, UK]. The viability of the cells was then tested by mixing an aliquot of the cell suspension with an equal volume of trypan blue [Invitrogen, UK]. After 5 minutes incubation at 37°C, the dead cells stain blue whereas viable cells are unstained.

Data on the presence of various cluster of differentiation (CD) antigens measured using fluorescence activated flow cytometry (FACS) [FACScan, Becton Dickinson, UK] were compared between the bone marrow cell preparation and whole bone marrow. These included CD45 which a leukocyte marker, CD45RA which is a marker of naïve T-cells, CD3 which is a T lymphocyte marker and CD90 which is thought to be a marker of several different cell types including MSCs and HSCs. The bone marrow cell preparation was enriched ~2-fold for CD45 and CD3 and 3 fold for CD90. The preparation was also characterised as being 7% c-Kit⁺ which is a HSC marker, specifically a stem cell factor receptor; 7% CD34⁺ which is also a HSC marker and 15% CD133⁺ which is a marker of HSCs and endothelial progenitor cells. CD45⁺ cells made up 54% of the population.

The cells to be used in the rat I/R model were washed immediately after being taken from the interface of the percoll gradient preparation and then re-suspended in PBS ready for injection into the right internal jugular vein at the start of reperfusion. Control I/R animals received a PBS injection instead of cells which will control for any effect of the saline in which the cells are suspended may have on the animals. This allows any differences between MI and BMMNC groups to be reasonably attributable to one or more components of the cellular content of the BMMNC preparation.

3.1.3 Collection of myocardial samples for proteomic and gene analysis

Tissue samples for proteomic and transcriptomic analyses were obtained from the excised hearts of sham, MI and BMMNC animals. All animals were sacrificed at 6 hours post reperfusion. Excised hearts were dyed with Evan's Blue dye to stain the perfused area and distinguish the unstained 'area at risk' (AAR) which is the area downstream from arterial ligand within which the actual area of infarct would lie. The AAR was dissected, rinsed with cold PBS and then wrapped in foil and snap frozen in liquid nitrogen before being stored at -80°C. A section of tissue at approximately the same size and position (LV apex) was excised from sham hearts. Myocardial samples from two experiments, performed at different time-points were obtained. Samples 1-9 were obtained from an experiment performed in 2007 and samples 10-18 came from an experiment using the same conditions, performed in the same laboratory by the same personnel in 2009 (Table 3.1). Samples 1-9 were used for proteomic and transcriptomic (gene expression) profiling. Samples 10-18 were used for studies of 14-3-3 epsilon as detailed in sections 3.7 and 7.0.

Table 3.1 Myocardial samples collected for studies

Experimental Group	SAMPLE_ID	Experimental Group	SAMPLE_ID
Sham -1	1	Sham -1	10
Sham-2	2	Sham-2	11
Sham-3	3	Sham-3	12
MI-1	4	MI-1	13
MI-2	5	MI-2	14
MI-3	6	MI-3	15
BMMNC-1	7	BMMNC-1	16
BMMNC-2	8	BMMNC-2	17
BMMNC-3	9	BMMNC-3	18

3.2 Proteomic analyses

Two dimensional gel electrophoresis (2DE) was used for profiling the proteomes of the myocardial samples from the rat I/R model. In the first instance, a wide pH range was analysed (pH 4-7), followed by two narrow-range analyses looking at pH 4.5-5.5 and pH 5.5-6.7. The same experimental procedures were used for all of these analyses. All methods used for 2DE proteome profiling experiments are described below.

3.2.1 Sample preparation and quantification

3.2.1.1 Protein lysate preparation from rat myocardial samples

Frozen tissue samples (~600mg per sample) were taken from the -80°C freezer and transported to the laboratory on dry ice. The samples were then crushed into fragments using a pre-chilled agate mortar and pestle. Approximately 80-140mg was taken and added to 1ml of lysis buffer (see Table 3.2). Complete protease inhibitor cocktail was supplied by Roche, UK. CHAPS and DTT were supplied by VWR International, UK. All other reagents were supplied by Sigma-Aldridge, UK.

The samples were then homogenised, using an Ultra-Turrax T8 with a small dispersing tool [IKA-Werke Staufen, Germany]. The remainder of the frozen samples were replaced in the -80°C freezer. The homogenates were vortexed before being placed in a sonication bath containing ice (to ensure the samples do not overheat) for 10 minutes. The homogenates were spun in a Sigma 1-15K microcentrifuge [Phillip Harris, UK] at 1500rpm (revolutions per minute) for 10 minutes at 17°C and the resulting supernatant was then split into aliquots of 500µl and stored at -20°C.

Table 3.2 Lysis buffer preparation

Reagent	Final conc. required	Volume to add
Urea *	9.5M	30g
3-[(3-Cholamidopropyl)dimethylammonio]-1-propane sulphonate (CHAPS)	4%	2g
(D,L)-1,4-Dithiothreitol (DTT)	1%	0.5g
Complete protease inhibitor	1x	1 tablet
Phosphatase inhibitor cocktail	1x	0.5µl
Milli-Q water		to 50ml

**Urea was made up to 45ml with Milli-Q water and stirred with Amberlite MB-1 and then filtered before the other reagents were added. Once prepared, lysis buffer was split into 50 x 1ml aliquots and stored at -80°C.*

3.2.1.2 Protein quantification

The concentration of the protein samples were assessed using the Bio-Rad protein assay [Bio-Rad, UK], a modified version of the Bradford Assay [107]. The assay is based on the colour change of Coomassie Brilliant Blue G-250 dye when combined with different concentrations of protein. The assay was originally performed in 3.6ml volumes and read by a UV-160 spectrophotometer [Shimadzu, UK]. The protocol was later modified for smaller volumes, specifically adapted to be read on the NanoDrop 1000 Spectrophotometer [Thermo Scientific, UK]. Samples that had been quantified with the original protocol were re-quantified using the NanoDrop protocol to ensure the consistency of results.

- Protein quantification by spectrophotometer

First 0.1N HCl:water (1:8) was prepared by adding 4.3ml of HCl to 495.7ml water (0.1N HCl), 62.5ml was then added to 437.5ml water. A working concentration of Bio-Rad dye reagent was prepared by adding 25ml of 4 x Bio-Rad solution to 75ml water and mixing gently. Standard curves were prepared using bovine serum albumin [Sigma-Aldridge UK] as detailed in Table 3.3, these were measured in the spectrophotometer at 595nm and the results checked to ensure that the curve had a

correlation of >0.98 before being aliquotted and stored at -20°C. Figure 3.1 shows how the standard curve was computed using Excel [Microsoft, US].

To perform the assay, 10µl of the pre-prepared standard curve solutions were added to 90µl of 0.1N HCl:water (1:8) and then dispensed into a cuvette [VWR, UK]. For the samples, 2µl was added to 8µl of lysis buffer and 90µl of 0.1N HCl:water (1:8) and this was dispensed into a cuvette. To each cuvette, 3.5ml of the working concentration dye reagent was added before being vortexed gently and left to settle for 2-3 minutes. The absorbance of the samples and standards were then measured on the spectrophotometer at 595nm; all readings were done in triplicate. The standard curve was computed in Excel [Microsoft, US] from which slope and intercept values were taken and used to calculate the concentration of the samples:

$$\text{total } \mu\text{g in the assay} = \frac{(\text{average absorbance at 595nm} - \text{intercept})}{\text{slope}}$$

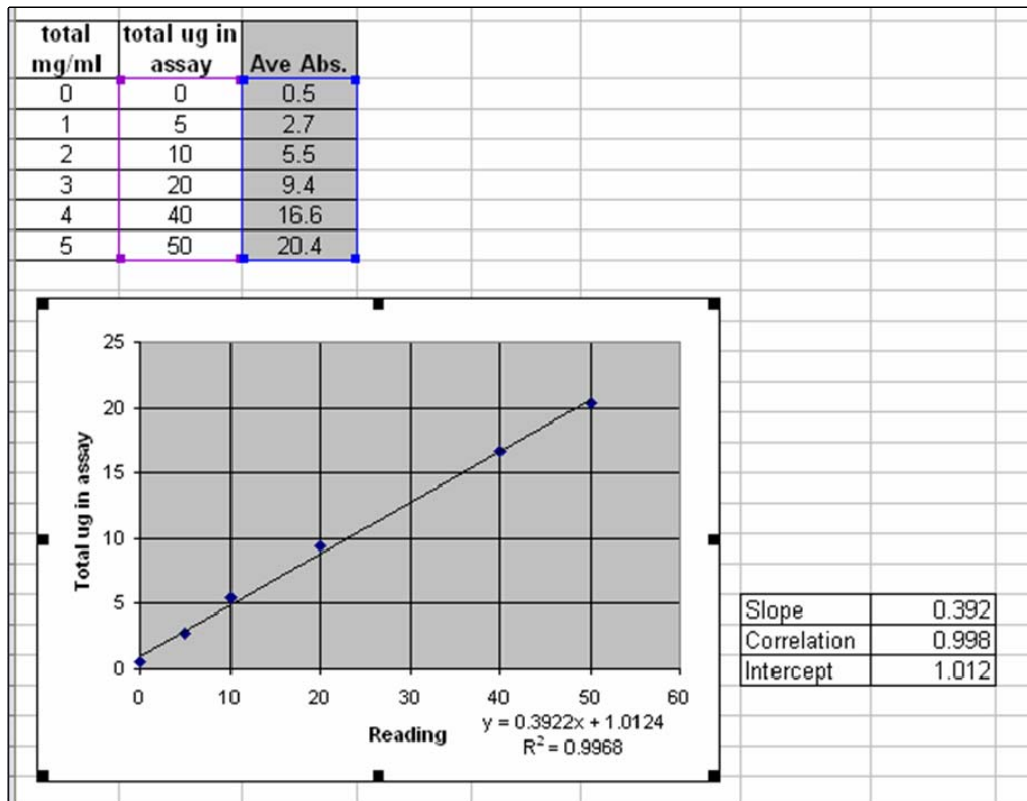
$$\text{concentration } (\mu\text{g}/\mu\text{l}) = \frac{\text{total } \mu\text{g in the assay}}{2}$$

Table 3.3 Concentrations of BSA standards used to obtain a calibration curve

Standards	Standards (mg/ml)	Vol of BSA stock (ul)	Vol of lysis buffer (ul)
0	0	0	500
1	0.5	50	450
2	1	100	400
3	2	200	300
4	4	400	100
5	5	500	0

BSA stocks at 5mg/ml BSA in lysis buffer were used.

Figure 3.1 BSA standard curve macro in Excel Curve is created from the ‘total μg in the assay’ (i.e. total μg in $10\mu\text{l}$ used in the assay) and the average absorbance at 595nm .



- Protein quantification by NanoDrop 1000

The ‘regular assay’ procedure was used as detailed in the NanoDrop 1000 manual [Thermo Scientific, UK]. A working concentration of Bio-Rad dye reagent was prepared by adding 12.5ml of $4 \times$ Bio-Rad solution to 37.5ml water and mixing gently. The BSA standard curve for this protocol was prepared as detailed in Table 3.4.

Table 3.4 BSA standard curve preparation for performing the Bio-Rad protein assay on the NanoDrop 1000

Standards	Standards (mg/ml)	Vol of BSA stock (ul)	Vol of lysis buffer (ul)
0	0	0	500
1	0.2	50	450
2	0.4	100	400
3	0.6	150	350
4	0.8	200	300
5	1	250	250

The BSA stocks were 2mg/ml BSA in lysis buffer.

The standards were prepared in triplicate by adding 10µl of standard to 490µl of the working concentration dye reagent. The samples were prepared by diluting 5µl in 45µl of lysis buffer, then adding 10µl of this dilution to 490µl of working concentration dye reagent. The samples were mixed thoroughly and left for 2-3 minutes before being read on the NanoDrop. The NanoDrop software has a Bradford assay setting which allows the user to record the blank (Standard 0) first, followed by the standard curve (up to five repetitions per standard), then the samples. All absorbance readings were exported to Excel [Microsoft, US] and protein concentrations were calculated as before.

3.2.2 Two dimensional gel electrophoresis (2DE)

3.2.2.1 Isoelectric Focussing (IEF)

Immobilised pH gradient (IPG) strips were rehydrated overnight in a total volume of 400µl (200µl lysis buffer containing 200µg total protein, 191µl rehydration buffer (Table 3.5) and 9µl Pharmalyte 3-10 [GE-healthcare Lifesciences, UK]) in a re-swelling tray [GE-healthcare Lifesciences, UK] and covered with silicone oil to prevent evaporation. For the rehydration buffer, Urea was supplied by Sigma-Aldridge, UK and all other reagents were from VWR International, UK.

The following day, the fully rehydrated IPG strips were placed onto the ceramic manifold of an Ettan IPGphor system for isoelectric focussing (IEF) [GE-Healthcare

Lifesciences, UK]. Dampened paper wicks were placed at either end to improve electrode contact and the manifold was again covered in silicon oil to prevent evaporation. IEF was carried out overnight at 20°C with 50µA per strip using a gradient of 0 to 100V for 1Vhour, 100V to 3400V for 7kVhours, followed by ‘Step n hold’ at 3500V for a total of ~65kVhours.

Table 3.5 Rehydration buffer preparation

Reagent	Final conc. required	Volume to add
Urea *	8M	25g
3-[(3-Cholamidopropyl)dimethylammonio]-1-propane sulphonate (CHAPS)	0.50%	0.25g
(D,L)-1,4-Dithiothreitol (DTT)	0.20%	0.1g
Bromophenol Blue	Trace of	Trace of
Milli-Q water		to 50ml

**Urea was made up to 45ml with Milli-Q water and stirred with Amberlite MB-1 and then filtered before the other reagents were added. Once prepared, rehydration buffer was split into 50 x 1ml aliquots and stored at -20°C.*

3.2.2.2 SDS – polyacrylamide gel electrophoresis (PAGE)

Large format, homogenous, 12% SDS PAGE gels were cast using the Ettan Dalt *twelve* system [GE-Healthcare Lifesciences, UK]. Glass plates (276mm x 216mm x 3mm) and plastic spacers (15mm x 216mm x 1.5mm) were assembled into gel casting cassettes and secured with gel-sealing tape. The reagents for the 12% SDS acrylamide gel solution are described in Table 3.6. All reagents were supplied by Sigma-Aldridge, UK. Bis-Acrylamide stock was deionised by stirring with amberlite MB-1 [Sigma-Aldridge Co] for 1 hour at room temperature, then the amberlite was removed by filtration before the Acrylamide gel solution was prepared.

Table 3.6 12% SDS acrylamide gel solution preparation

Reagent	Final conc. required	Volume to add
* Bis-Acrylamide 40% 37.5:1	12.50%	510ml
* 1.5M tris(hydroxymethyl)aminomethane (Tris) (pH8.8)	0.375M	425.1ml
10% Sodium dodecyl sulphate (SDS)	0.10%	17ml
10% Ammonium Persulphate (APS)	0.05%	8.5ml
N,N,N',N'-Tetramethylethylenediamine (TEMED)	0.02%	255µl
* Milli-Q water		739.14ml

** Combine water, acrylamide and 1.5M Tris, then de-gas for 1-2 hours before adding the other reagents.*

The casting equipment was assembled according to manufacturers' instructions and the acrylamide gel mix was poured into the system, followed by displacing solution (Table 3.7). Then 1-2ml of overlay solution (isobutanol and water 10:1) was pipetted onto the top edge of each gel. For the displacing solution, Bromophenol Blue was supplied by VWR International. All other reagents were supplied by Sigma-Aldridge, UK.

Table 3.7 Displacing solution preparation

Reagent	Final conc. required	Volume to add
1.5M Tris (pH8.8)	25%	25ml
Glycerol	50%	50ml
Milli-Q water	25%	25ml
Bromophenol Blue	Trace	Trace

Once the gels were set, the casting equipment was dismantled and cleaned. Gels were wrapped in damp tissue and cling-wrap to prevent drying out and were stored at 4°C until use.

Once IEF had been completed the IPG strips were equilibrated, first in equilibration buffer (Table 3.8) containing 2% DTT for 15 minutes then equilibration buffer containing 4.8% iodoacetamide for a further 15 minutes. Glycerol and Tris were supplied by Sigma-Aldridge, UK. Second dimension was performed using an Ettan Dalt *twelve* system [GE-Healthcare Lifesciences, UK]. The equilibrated IPG strips were placed in a horizontal alignment along the top edge of the SDS-PAGE gels. The strips were placed with the plastic backing in contact with the glass plate and the contact between the IPG strips and the SDS-PAGE gel was continual with no gaps. Molecular weight marker [GE Healthcare, UK] (3 μ l) was added to a 17 μ l of 1% agarose stained with bromophenol blue, and once solidified this was placed at one end of the gel. A 0.5% agarose solution (made with 1 x SDS running buffer, see below) was applied over the IPG strip to hold the strip in place.

1 x SDS running buffer was freshly prepared (10 x buffer stock detailed in Table 3.9). All reagents were supplied by Sigma-Aldridge, UK. The SDS buffer was poured into the Ettan Dalt *Twelve* tank [GE Healthcare, UK] to equilibrate to 10°C. A re-circulating cooling unit ensured the buffer remained at 10°C through out the run. The assembled gels were placed in the tank. The conditions for overnight running were 0.5W/gel for 1 hour, 0.75W/gel for 1 hour, 2W/gel for 22 hours.

Table 3.8 Equilibration buffer preparation

Reagent	Final conc. required	Volume to add
Urea	6M	18g
Sodium dodecyl sulphate (<i>SDS</i>)	2%	1g
Glycerol	30%	15g
tris(hydroxymethyl)aminomethane (Tris)	50mM	1.65ml of
Bromophenol Blue	Trace of	Trace of
Milli-Q water		to 50ml

Table 3.9 10 x SDS running buffer preparation

Reagent	Final conc. required	Volume to add
Tris base	250mM	60.5g
Glycine	192mM	288.2g
Sodium dodecyl sulphate (<i>SDS</i>)	1%	20g
Milli-Q water		to 2L

The gels were removed from the tank and cassettes when the dye-front was ~1cm from the bottom of the glass-plates. They were placed in fixing solution (30% methanol, 10% acetic acid) overnight and stained the following day using the Plus One silver staining kit [GE-Healthcare Lifesciences, UK] following manufacturers instructions. Stained images were scanned at medium-high resolution using a GS-800 scanner [Bio-Rad, UK].

3.2.3 Image analysis

Gels from each sample were produced in duplicate for both the wide-and narrow-range analyses. Two different software packages were used to analyse the gel images; PDQuest Advanced [Bio-Rad,UK] was used to analyse the wide-range gel images and Progenesis SameSpots [Nonlinear Dynamics, UK] was employed for analysing both sets of narrow-range gel images.

- PDQuest Advanced 2D gel image analysis.

Analysis using PDQuest Advanced software [BioRad, UK] was performed using the following workflow. The scanned images were all cropped using the same settings in the ‘advanced crop’ feature before being saved in a reduced file size format of 48 KB using Quantity One software [BioRad, UK]. Filters were used for 6 of the 18 gel images that had pepper type artifactual features (black speckles) that would reduce the impact of this ‘noise’ in the image during spot detection. Gels were then loaded into an experiment and spot detection parameters were set. Manual editing was then carried out for all gels. Artefacts and wrongly indicated spots were removed. The gel

with the most spots was chosen as the master (image to which the other images are matched) and automatic spot matching was initiated after marking several landmark spots. A second session of manual editing followed this. Spot intensity values were then 'normalised' using 'total density in gel' method. All spots indicated as differing by more than 1.5 fold were checked to make sure they were correctly detected and matched. Once any false spots were removed from the analysis all the normalised spot intensity values for all gels were exported to Excel [Microsoft, US].

- Progenesis SameSpots 2D gel image analysis

The workflow for Progenesis SameSpots analysis is as follows. Un-cropped gel images were loaded into SameSpots and automatic alignment was carried out on all of the gel images. The results from this were then checked manually gel by gel and if areas of the gel had not aligned sufficiently extra landmarks were added before auto alignment was repeated. This was repeated for all gels until they were aligned sufficiently. Progenesis analysis was then carried out. The top scoring spots were checked to ensure they were actual spots, were correctly outlined and aligned in each gel. Any spots which were artifactual or mismatched were excluded. After this, the normalised spot volumes for all of the spots were exported to Excel [Microsoft, US].

3.2.4 Statistical analysis

Excel [Microsoft, US] was used to calculate average, standard deviation, standard error and 95% upper and lower confidence intervals for each spot in each group using the normalised spot volumes for each gel. Fold changes and Student's *t*-test p-values were calculated for two intergroup comparisons; 'SHAM vs. MI' and 'MI vs. BMMNC'. All spots with significant differences (>1.5 fold) in either comparison were checked again in either PDQuest or Progenesis. All spots found to significantly differ by more than 2.5 fold (wide-range) or 1.5 fold (narrow-range) were excised for protein identification.

3.2.5 Protein identification by LC-MS/MS

3.2.5.1 Excision and trypsin digestion of spots

The spots were excised from the gel using a disposable pipette tip which had the end sliced off to increase the size of the aperture at the tip. The aperture was made to correspond roughly with the size of the spot to be excised. The excised piece of gel was then further cut with a razor blade to pieces no larger than 2mm cubed and placed in 1ml eppendorfs. The gel pieces were washed with 100mM ammonium bicarbonate (Ambic) for 15 minutes before the solution was decanted to waste and replaced with acetonitrile (ACN) for 5 minutes. The ACN was then decanted to waste and the dehydrated gel pieces were further dehydrated in a speedvac concentrator [Savant, UK] connected to a compressor vacuum pump [Compton, UK] for 10 minutes. The gel pieces were rehydrated in 10mM DTT dissolved in 100mM Ambic and heated to 56°C for 30 minutes. The DTT solution was decanted to waste and replaced with ACN for 5 minutes before decanting again and dehydrating the gel pieces in the speedvac for 10 minutes.

Gel pieces were rehydrated in 55mM Iodoacetamide dissolved in 100mM Ambic and placed in the dark for 20 minutes. The solution was again decanted to waste before the gel pieces were dehydrated in ACN for 5 minutes and then placed in the speedvac for 10 minutes. Finally the gel pieces were rehydrated in 50mM Ambic containing 13ng/μl bovine trypsin or methylated porcine trypsin [Sigma-Aldridge, Co]. The samples were placed at 4°C for 45-60 minutes to allow complete rehydration before being placed at 37°C for 1 hour. The samples were then left at room temperature overnight.

The following morning any remaining supernatant was decanted into a fresh labelled microcentrifuge tube and the gel pieces were washed in a small volume of 50mM Ambic for 15 minutes at 37°C. The supernatant was decanted to the fresh microcentrifuge tube and a further small volume of ACN was added before another 15 minute incubation at 37°C. The supernatant was added to the fresh

microcentrifuge tube before and then 50mM Ambic and the ACN steps were repeated. The fresh eppendorfs containing the supernatant laden with digested peptides were dried down to completion in the speedvac and stored at -20°C.

3.2.5.2 LC-MS/MS

For protein identification, the lyophilised peptide samples were re-suspended in 6µl of 50mM Ambic and were vortexed for 1 minute before incubation at 37°C for 5 minutes. They were briefly vortexed again and then centrifuged at maximum speed for 1 minute. The supernatant was transferred to a sample vial for injection. Samples were analysed using LC-MS/MS [CapLC and QTof-*micro*, Waters, UK].

Peptides were separated on a 75µm x 150mm Nanoease 3µm Atlantis dC18 column [Waters, UK]. A 30 minute solvent gradient of 1% to 95% B (A is 100ml H₂O and 50µl Formic acid, B is 20ml H₂O, 80ml ACN and 50µl Formic acid) was used at a flow rate of 200nl/min. Separated peptides were introduced into the mass analyser using a nanospray ESI source.

The QTof is a hybrid mass analyser combining quadrupole and time of flight (Tof) analysers. Peptide ions enter the QTof under vacuum, and are guided through the first quadrupole. These then pass through to the second quadrupole where collision induced dissociation (CID) occurs. The MS/MS fragment ions resulting from CID are then further resolved as they pass along the third quadrupole to the detector. Data was obtained using Data Dependant Acquisition (DDA) using two MS/MS channels.

The instrument was calibrated using glu-fibrinogen [Sigma-Aldridge, UK] prior to running samples to ensure mass accuracy. The raw peptide and fragment mass data was processed using ProteinLynx software [Waters, UK] and the processed peak list data (PKL file) was then used to search the SwissProt database using the MASCOT search engine [Matrix Science, UK]. For the MASCOT search, trypsin was set as the enzyme used, allowing up to one missed cleavage. Variable modifications were set for oxidation of methionine residues and carbamidomethylation of cysteine residues.

Peptide tolerance was set at +/- 2.0 Daltons and MS/MS tolerance of +/- 0.8 Daltons. MASCOT protein scores and percentage sequence coverage were calculated from only the peptides scoring over 35. For proteins only identified by a single peptide, the mass spectra were checked these are shown in Appendix 6. Expectation values are also included in the MASCOT data for these proteins. Proteins identified as specific isoforms were confirmed by BLASTing the peptide sequences which had scores over 35 [108].

3.3 Validation of proteomic data by Western blotting

Western blotting was used as a semi-quantitative method to validate observations made in the 2DE analysis. Specifically, antibodies for 14-3-3 epsilon (14-3-3ε), succinate dehydrogenase (Sdha), phosphatidylethanolamine-binding protein 1 (Pebp1) and ATP synthase subunit beta (Atp5b) were used to measure expression of these proteins in the samples from our experiment. Antibodies for Glyceraldehyde-3-phosphate dehydrogenase (Gapdh) were used to normalise protein loading. All antibodies were supplied by Abcam, UK. The methodology for Western blotting is detailed here.

Each assay required optimisation before a final blot was produced for densitometry and analysis. The Gapdh antibodies worked well with either 10µg or 20µg total protein loading which were the two concentrations at which all of our analytical assays were optimised to. The approximate antibody dilution suitable for western blotting was suggested by the manufacturer and this was always used as the starting point for optimisation.

3.3.1 1D SDS-PAGE and blotting

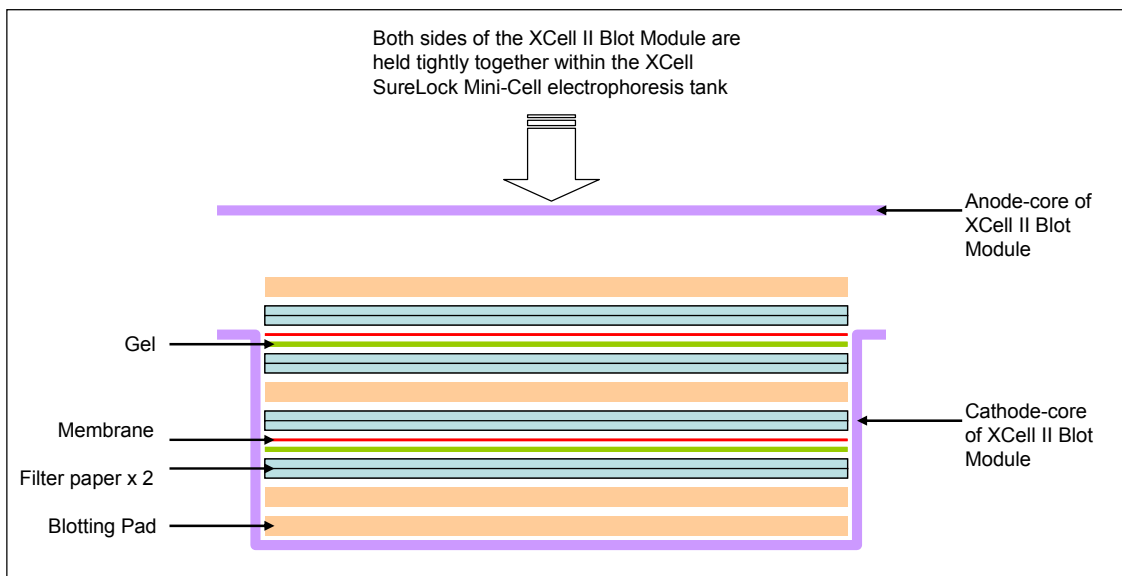
Protein lysates were electrophoretically separated on NuPAGE[®] Novex 10% Bis-Tris Gels in an XCell SureLock[™] Mini-Cell electrophoresis tank [both from Invitrogen, UK]. Unless otherwise stated, all reagents were supplied by Invitrogen.

Protein lysates were prepared by mixing with 'LDS' sample buffer at an appropriate concentration (determined by optimisation) in enough volume to load onto two gels (30µl). They were then heated to 70°C for 10 minutes to denature the proteins. Meanwhile, two pre-cast gels were placed in the tank and the combs were removed. Antioxidant (500µl) was added to 200ml of running buffer (1x) and this was poured into the central well of the tank and a pipette was used to wash out the wells. Once the samples had been incubated at 70°C, they were spun briefly in a microcentrifuge

and then 15µl of each sample preparation was loaded onto each gel, making two identical gels. See-Blue protein molecular weight marker [Invitrogen, UK] and CruzMarker TM molecular weight marker [Santa Cruz,UK] were also loaded onto the gels. The former is a pre-stained marker and the latter is designed to react with the secondary antibodies and therefore will be detected by chemiluminescence (see section 3.3.2.2). Running buffer (1x) was added to the outer chamber and electrophoresis was run at 200V for 50 minutes and then the gel cassettes were cracked open and the gels were prepared for transfer onto nitrocellulose membrane.

Blotting pads, nitrocellulose membranes (Hybond ECL from GE Healthcare), and blotting paper [Whatman, UK] were pre-soaked in transfer buffer [Invitrogen, UK]. The surfaces of the gels were rinsed in transfer buffer and the membrane was placed over it. Two ‘cut-to-size’ sheets of blotting paper were placed onto each side of the gel/membrane to make a sandwich. A falcon tube was then rolled over the sandwich to exclude any air bubbles. All gels were prepared in this way. An XCell II Blot Module [Invitrogen, UK] was then assembled with sponge blotting pads and the gel/membrane/filter paper sandwiches as shown in Figure 3.2.

Figure 3.2 Assembly of XCell Blot Module [Invitrogen, UK]



The module was closed and placed in the XCell SureLock™ Mini-Cell tank before being topped up with transfer buffer. The outer chamber was filled with deionised water and electrophoresis was run at 30V for 1hour. After one hour the tank was disassembled and the membranes which now held the separated protein samples were placed in 10ml of 3% skimmed milk made with tris buffered saline (TBS) containing 0.5% Tween (TBS-TWEEN) buffer (see Tables 3.10 and 3.11) and left overnight at 4°C.

Table 3.10 10 x Tris buffered Saline (TBS) buffer

Reagent	Final conc. required	Volume to add
NaCl	20mM	31.6g
Tris-HCl	137mM	79.46g
Milli-Q H2O		to 1L

Once solution was prepared, pH was adjusted to pH 7.6.

Table 3.11 1 x TBS-TWEEN buffer

Reagent	Final conc. required	Volume to add
10 x TBS buffer	1 x	100ml
Polysorbate 20 (TWEEN-20)	0.05%	0.5ml
Milli-Q H2O		to 1L

Once solution was prepared, pH was adjusted to pH 7.6.

3.3.2 Antibody incubations and chemiluminescence

After the membranes had been ‘blocked’ overnight in the milk solution, they were incubated for 90 minutes in 7ml of 3% milk made with TBS-TWEEN containing the relevant primary antibody at the appropriate concentration on a shaking platform. Following this the antibody solution was replaced by TBS-TWEEN and the membranes were incubated for 10 minutes on a shaking platform. This wash step was repeated twice before the secondary antibody incubation. The membranes were covered in 7ml of 3% milk made with TBS-TWEEN and the secondary, HRP

conjugated Goat anti-rabbit [Santa Cruz, UK] antibody at a concentration of 1 in 5000 and incubated on a shaking platform for one hour. A further three wash steps followed the secondary antibody incubation.

ECL Plus detection reagents [GE Healthcare, UK] were used to detect the HRP conjugated secondary antibodies on the membranes. The secondary antibodies are linked to horseradish peroxidase (HRP) which then reacts with the Acridan substrate (in the ECL Plus detection reagents) to generate acridinium ester, this is further oxidised by the peroxidase and produces a strong chemiluminescent signal detectable on autoradiographic film. Following the final wash step, the membranes were drained of TBS-TWEEN buffer and placed on a level clean surface. ECL detection reagents (Solution A and B in ratio 40:1) were mixed and gently poured over the membrane (0.1ml used per cm² membrane) and left to incubate for 5 minutes. The membranes were again drained and placed onto a pre-cut piece of cling wrap which was folded over to cover the membrane. The cling wrap covered membranes were then placed in an x-ray film cassette [GE Healthcare, UK] and taken to a dark-room.

A cut-to size piece of x-ray film (Hyperfilm ECL also from GE Healthcare) was placed over the membrane and the cassette was closed over it for 30 seconds. The film was then placed into 1 x Kodak GBX developing solution [Sigma-Aldridge, UK] till the bands appeared. The film was then rinsed briefly in water before being placed in 1 x Kodak GBX fixer solution. This first film was used to judge the optimal exposure time, and the exposure was repeated with some fresh film to ensure a clear image of the bands without overexposure which could lead to low dynamic range when quantifying the bands.

3.3.3 Densitometry

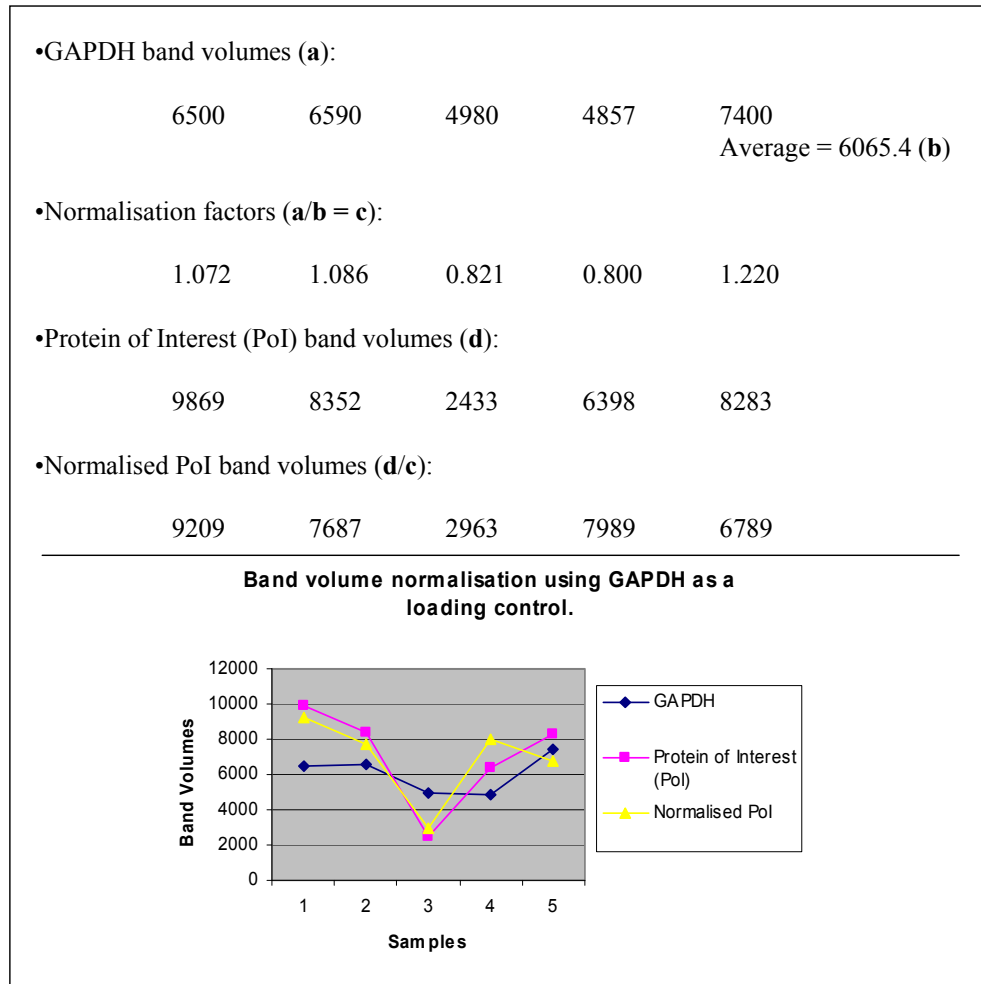
The developed Hyperfilms were scanned in using a Photosmart C3180 [Hewlett Packard, UK] at a resolution of 1200dpi in greyscale and saved as .tif images. These images were then analysed using TotalLab v1.10 software [Phoretix] which calculates

band volume by plotting band intensity $\times 10^3$ against band area. The volumes of the bands for the protein of interest and those of the GAPDH bands were then exported to Excel [Microsoft, US].

3.3.4 Statistical analysis

The band volumes for the protein of interest were normalised using the band volumes of Gapdh. This was done for each band by first dividing the value of each Gapdh band by the average of all the Gapdh bands to obtain a 'normalisation factor'. Each band volume of the protein of interest were then divided by this normalisation factor. Figure 3.3 below illustrates an example of this simple normalisation method.

Figure 3.3 An example of band volume normalisation using Gapdh as a loading control.



To investigate whether differences in expression measured using western blotting are statistically significant the normalised volumes of the protein of interest are analysed in GraphPad Prism 5 [GraphPad, UK]. A one-way ANOVA was used to see if there was a statistically significant difference between the three groups and this was followed by Bonferroni's post-hoc test for multiple comparisons to look at the statistical difference between pairs of groups. P-values of <0.05 were considered statistically significant.

3.4 Gene expression analyses

A whole genome scale comparative gene expression profiling experiment was carried out using Illumina's Rat Ref-12 BeadChip.

3.4.1 RNA preparation

3.4.1.1 RNA extraction from tissue samples

The RNeasy Fibrous Tissue Mini Kit [Qiagen, UK] was used to extract total RNA from the myocardial tissue samples 1-9. A fraction (20-30mg) of the crushed frozen tissue was taken and added to Precellys CK14 tubes containing ceramic beads and 300µl of RLT Buffer. The samples were then homogenised in a Precellys 24 bench top homogeniser [Bertin technologies]. The RNA extraction was then performed on these lysates following the protocol outlined in the RNeasy Fibrous Tissue Mini Kit handbook. Figure 3.4 shows a flow chart of the procedure and Table 3.12 lists the reagents supplied in the kit.

All steps were carried out at room temperature unless specified otherwise. The lysates were transferred into new eppendorfs along with 590µl of RNase-free water and 10µl of proteinase K and then incubated at 55°C for 10 minutes in a water bath. Following this incubation, the samples were spun for 3 minutes at 10,000 x g and the supernatant transferred to a new microcentrifuge tube.

The nucleic acid content was then precipitated from the solution by adding 0.5 volume of ethanol and mixing thoroughly with a pipette. This solution was immediately added to an RNeasy spin column which was placed in a collection tube and spun at room temperature for 15 seconds at 8,000 x g. The flow through was discarded and any remaining solution was added to the same column and the centrifugation step was repeated.

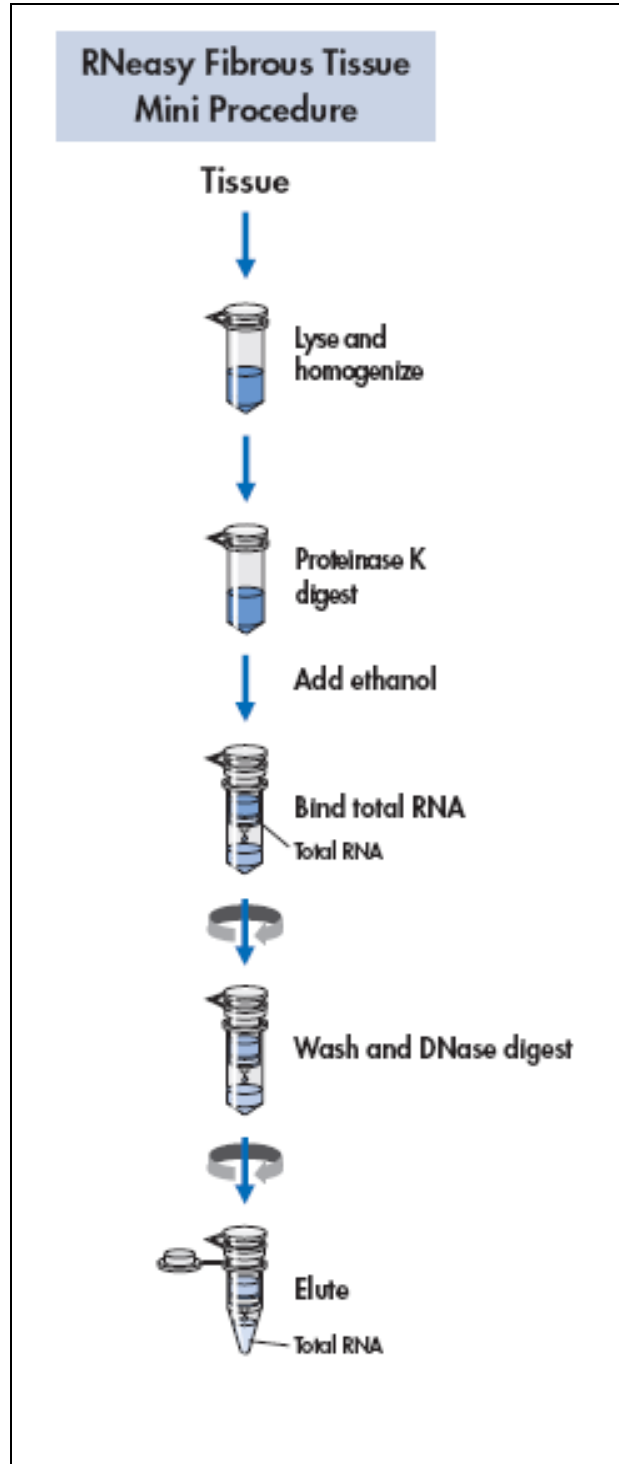
Table 3.12 Reagents supplied in the RNeasy fibrous tissue kit [Qiagen, UK]
 Buffer RPE requires the addition of 4 volumes of ethanol before use. β -Mercaptoethanol (β -ME) must be added to Buffer RLT before use.

RNeasy Kit Reagents
Proteinase K
Buffer RLT
Buffer RW1
Buffer RPE (concentrate)
Rnase-free Water
RNase-Free DNase Set:
RNase-Free DNase I (lyophilised)
Buffer RDD
RNase-Free Water

Once the nucleic acids had been captured on the spin column, a wash step was performed by adding 350 μ l of RW1 buffer to the column which was then spun at room temperature for 15 seconds at 8,000 x g and the flow-through was again discarded. DNase (10 μ l) was added to the column in 70 μ l of RDD buffer and was left on the bench top (room temperature) for 15 minutes to allow time for the enzyme to work. Another wash step was then performed by adding 350 μ l of RW1 buffer to the column which was then spun at room temperature for 15 seconds at 8,000 x g and the flow-through was again discarded.

500 μ l of RPE buffer containing a high concentration of ethanol was then added to the column to precipitate the RNA and the column was spun at room temperature for 15 seconds at 8,000 x g and flow through was discarded. The RPE precipitation step was repeated but with a longer centrifugation (2 minutes) to ensure all the ethanol was removed before RNA elution. The dried spin column was then placed in a fresh collection tube and 30 μ l of RNase free water was added to the column to elute the RNA. The column was spun at room temperature for 1 minute at 8,000 x g. A second volume of 20 μ l was added to the column and the centrifugation step was repeated. This ensured all of the total RNA was eluted in a final volume of 50 μ l.

Figure 3.4 RNeasy fibrous tissue kit procedure as shown in the handbook [Qiagen, UK]



3.4.1.2 RNA quantification and quality assessment

- NanoDrop 1000

To check the efficiency of the RNA extraction, the RNA samples were quantified using the NanoDrop 1000 Spectrophotometer. Using the RNA-40 setting, only 1µl of sample was required to measure absorbance at 260nm, 280nm and 230nm. The following ratios were then calculated; 260/280 ratio, which should be ~2.0 for pure RNA samples, and the 260/230 ratio which should be higher than the 260/280 ratio. The NanoDrop 1000 software also calculated the concentration of the sample according to Beer's Law. The modified version of the Beer-Lambert equation used for this calculation was:

$$c = (A \times e)/b$$

- **c** is the concentration of the nucleic acid sample.
- **A** is the absorbance units at 260nm.
- **e** is the wavelength dependant extinction coefficient (50ng-cm/µl for dsDNA, 33ng-cm/ul for ssDNA or 40ng-cm/µl for RNA).
- **b** is the path length in cm. (The absorbance was actually measured at a 1mm path length, but the reading is converted as if it were measured in a conventional 10mm path length by the NanoDrop 1000 software.

[Nanodrop user's manual, Thermo Scientific, UK.

<http://www.nanodrop.com/Library/nd-1000-v3.7-users-manual-8.5x11.pdf>].

- Agilent 2100 Bioanalyser

The Agilent 2100 bioanalyser can assess the quality and quantity of nucleic acid and protein samples using microfluidic 'chips' in which picogram quantities of sample can be electrophoretically separated and analysed. The RNA 6000 Nano Assay kit [Agilent] is specifically used to separate total RNA for size and quantity measurements. The associated software computes both quantity in ng/µl and an RNA

Integrity Number (RIN) which indicates the quality of the RNA in a sample independent of quantity.

The RNA 6000 Nano assay kit comes with chip, gel matrix, dye and a size marker. The samples were prepared and run on the chip according to manufacturer's instructions as follows. Reagents were allowed to come to room temperature whilst the electrodes of the bioanalyser were decontaminated with RNaseZAP. The gel matrix was prepared by adding 1ml to a spin filter and centrifuging for 10 minutes at 1,500 x g. 1µl of Nano dye concentrate was then added to 65µl of the filtered gel matrix and the solution was mixed thoroughly on a vortex.

A chip was then placed on the Agilent chip priming station and 9µl of the pre-prepared gel matrix/dye solution was pipetted into position (G) and the plunger was used to pressurize the gel into the system. A further 9µl was pipetted into the two positions marked G. The Nano marker was then added to the chip; 6µl pipetted into each sample well plus 5µl pipetted into the ladder well. The RNA samples, 1.5µl of each sample, were pre-heated to 70°C for 2 minutes on a thermocycler along with 1.5µl of the ladder before analysis in 0.2ml microtubes. Then 1µl of the denatured ladder was placed in the ladder well and 1µl of each sample was placed in the sample wells. The chip was then vortexed on the specially adapted vortex [Agilent] before being placed in the bioanalyser.

The correct assay programme was selected in the 2100 expert software and the run was initiated. Once the run was complete an electrophoresis file run summary was obtained. A RIN number of less than 8 may indicate RNA degradation has occurred and this may affect analysis results. A yield of 250ng of total RNA was required for the next stages of processing at a concentration of at least 25ng/µl.

3.4.2 cDNA synthesis, purification and ‘in-vivo’ cRNA transcription

The Ambion Illumina TotalPrep kit [Applied Biosystems, UK] was used to process total RNA samples prior to analysis on the Illumina Rat Ref12 BeadChip. The RNA was initially transcribed into cDNA which involves a polymerase chain reaction (PCR) which utilises reverse transcriptase as the reaction enzyme instead of DNA polymerase which is used in a standard PCR. Reverse transcriptase in this case is ‘Array Script’ which is a modified enzyme that has enhanced performance at synthesising full length cDNAs. The T7 oligo dT primer ensures all the generated cDNA contain a T7 promoter sequence which ensures all of the cDNAs are transcribed in the in-vivo transcription (IVT) stage.

In the next step the complementary strands for the newly generated cDNAs are synthesised using DNA polymerase, at the same time RNase H degrades the RNA present in the reaction. The double stranded cDNA is cleaned up and the degraded RNA is eliminated. The IVT step then generates biotin labelled RNA from all the cDNAs present using T7 enzyme. This reaction contains an excess of biotinylated dNTPs to allow transcription to continue uninhibited until the reaction stops, thereby allowing amplification of copies relative to the number of copies in the original sample. The cRNA is then cleaned up ready for hybridisation. The methods for cDNA and subsequent cRNA preparation are as per manufacturer’s protocols.

First 250ng of total RNA was made up to a volume of 11µl with RNase free water and placed in a 96 well skirted PCR plate [Thermo Scientific, UK]. This was placed on ice whilst the reverse transcription master mix was made up at room temperature in a nuclease free microcentrifuge tube, vortex mixed and spun briefly (see Table 3.13) then 9µl of the master mix was added to each sample to make a total volume of 20µl. The 96well plate was then sealed before being vortexed and briefly spun. The samples were then incubated at 42°C for 2 hours on a PTC-225 thermal cycler [MJ Research, UK].

Table 3.13 Ambion TotalPrep reverse transcription master mix Components are shown per reaction and also per 12 reactions (13.2 to account for pipetting error).

Reagent	1 reaction	13.2 reactions
T7 Oligo (dT) primer	1	13.2
10 x First strand buffer	2	26.4
dNTP mix	4	52.8
RNase Inhibitor	1	13.2
Array script	1	13.2

Once complete the plate is again spun briefly in a microcentrifuge before being placed on ice for the next step. The second strand master mix was prepared on ice (see Table 3.14) and again vortexed briefly to ensure components were well mixed. 80µl of this mix was pipetted into each sample to make 100µl total reaction volume and the plate was covered with a fresh seal. The plate is again vortexed and spun briefly, before being incubated at 16°C for 2 hours on a thermal cycler. Following this incubation the plate was placed on ice (or was placed at -20°C overnight).

Table 3.14 Ambion TotalPrep second strand master mix Components are shown per reaction and also per 12 reactions (13.2 to account for pipetting error).

Reagent	1 reaction	13.2 reactions
Nuclease-free water	63	831.6
10 x Second strand buffer	10	132
dNTP mix	4	52.8
DNA polymerase	2	26.4
Rnase H	1	13.2

For cDNA purification, nuclease-free water was pre-heated to 55°C and cDNA binding buffer was warmed to room temp. 1.5ml centrifuge tubes and cDNA filters were labelled before 250µl of cDNA binding buffer was added to the labelled 1.5ml eppendorfs. The samples were transferred one at a time from the 96 well plate and added to 250µl of buffer and mixed with a 1ml pipette before being put immediately

onto the filter cartridges. The cartridges were then spun for 1 minute at 10,000rcf (relative centrifugal force). The flow-through was discarded and 500µl of ethanol containing wash buffer was then added to the cartridge and they were spun again for 1 minute at 10,000rcf. The flow through was discarded and the filter was spun again to dry it out before it was transferred to a fresh labelled microcentrifuge tube for cDNA elution.

A small volume (10µl) of nuclease-free water was added to the filter and left to stand for 2 minutes at room temperature, before the filters were again spun for 1 minute at 10,000rcf. A further 9µl was added to the filter and the centrifugation was repeated to make a final elution volume of 17-18µl.

The Illumina oven was pre-heated to 37°C before beginning the cRNA in-vivo transcription (IVT) stage. The eluted cDNAs were made up to 17.5µl if they were less than 16µl, and the IVT master mix was made up at room temperature (see Table 3.15). The master mix was vortexed before 7.5µl was added to each cDNA sample, the tubes were then placed in the oven overnight. The exact length of time for this incubation was noted as this needed to be identical for all samples which are to be compared in the gene expression analysis. The following morning the reaction was stopped by adding 75µl of nuclease-free water.

Table 3.15 Ambion TotalPrep in-vivo transcription (IVT) master mix
Components are shown per reaction and also per 12 reactions (13.2 to account for pipetting error).

Reagent	1 reaction	13.2 reactions
T7 10 x reaction buffer	2.5	33
T7 enzyme mix	2.5	33
Biotin-NTP mix	2.5	33

Before starting cRNA purification the nuclease-free water was again pre-heated to 55°C and cRNA filters and microcentrifuge tubes were labelled. To each sample

350µl of cRNA binding buffer was added followed by 250µl of ethanol before being mixed thoroughly with a 1ml pipette. The mixed samples were then transferred immediately onto the cRNA filter cartridges and were spun for 1 minute at 10,000rcf. The flow-through was discarded and 650µl of wash buffer was added before a further centrifugation. The flow-through was discarded and the filter was spun again to dry it out. The filter was then placed in a new labelled microcentrifuge tube and 100µl of pre-heated nuclease-free water was added to the filter and left to stand at room temperature for 2 minutes before the cartridges were spun at 10,000rcf for 1.5 minutes.

The size distribution of the labelled cRNA was assessed on the Agilent 2100 Bioanalyser before the samples were hybridised onto an Illumina RatRef12 Beadchip by Genome Centre staff (the Genome Centre protocol for hybridisation is shown in Appendix 1) before being washed, stained and scanned on the Genome Analyser. The cRNA samples extracted from tissue samples 1-9 were hybridised onto the chip along with three technical replicates.

3.4.3 Gene expression data pre-processing

Once the chip had been scanned, the data was examined using the gene expression analysis module of Illumina's proprietary software package 'BeadStudio' which is designed for reading and viewing data generated by the Genome Analyser hardware. The gene expression module contains tools for looking at internal QC features on the chips, normalising data, performing background subtraction as well as statistical tools for performing a simple differential expression analysis.

3.4.3.1 Quality assessment of gene expression data using BeadStudio

A new 'Direct Hyb' gene expression project was created and named, and all the image data files from the chip were loaded. Once the project was created, the internal QC features were checked by looking at the control summary plots. These included several histograms, one summarising the results of each control feature. The first

three plots show data independent of samples and illustrate signals originating from the oligonucleotides that were spiked into the hybridisation solution.

- Plot 1 = 'Hybridisation controls' – This shows a histogram of high, medium and low relative quantity oligos. These should have high, medium and low intensity signals.
- Plot 2 = 'Low stringency' – This shows the signals of perfect match (PM and mismatch (MM2) oligos. This histogram should show the PM signal to be much higher than the MM2 signal.
- Plot 3 = 'Biotin and high stringency' - Both of these signals should be high especially the high stringency signal.
- Plot 4 = 'Negative controls' - This should indicate the background and noise to have low signals.
- Plot 5 = 'Gene intensity' – This shows the signal of the housekeeping genes against the signal from all the other genes together. This histogram should show a much higher signal coming from the housekeeping genes

Another tool used to check the data were the scatter plots. This tool was used to look at the average signals from probes in one sample against another. These checks will give some indication of how well matched any technical and biological replicates were and the relationship between samples of different experimental groups. Any strong skew or asymmetry in these plots would indicate poor sample quality or saturation at the higher intensities.

Clustering dendrograms were used to look at probe level data without normalisation to see if technical replicates clustered together and if the study groups clustered separately. Finally, the RIN numbers were also checked to see if they explained the cluster pattern of the samples.

3.4.3.2 Data preparation and normalisation

Following pre-processing, a new project was created with only the image data files of the samples to be analysed (i.e. excluding the technical replicates) were loaded and the study groups were defined. The data was then normalised using the quantile normalisation method. The normalised probe level data, with no background subtraction, was exported including the all fields as a .txt file. For the individual probes there are probe ID, gene symbol, search key (GI), chromosome, definition, synonyms, GI, accession, probe type and probe sequence. For every sample there are the average signal (normalised), detection p-value, bead standard error and average number of beads.

3.4.4 Differential gene expression analysis using LIMMA

Linear Models for Microarray Data (LIMMA) is an R software package especially designed to determine genes which are differentially expressed in large datasets produced by microarray analyses [109, 110]. LIMMA has also been shown to perform well in analysis of microarray experiments with a small n-number [111, 112]. The data files were prepared for LIMMA analysis in Excel. Firstly the non-detected probes were removed, the criteria for identifying non-detected probes are detection p-values >0.05 for 8 or 9 of the 9 samples. For the remaining probes, the following data was assembled in a format suitable for LIMMA analysis; average signal, array standard deviation, bead standard error, average number of beads and detection p-value. The file was saved as a comma separated values (CSV) format file. A second CSV file was created with the headings 'sample', 'disease' and 'time', the sample IDs were placed under 'sample' in the same order in which they appeared in the main data file. Sham, MI or BMMNC were placed under the disease file depending on which group the sample was from, and as the second variable (time) wasn't being used; the value '1' was entered for all samples. This file is named 'targets' and will be used to define the experimental design.

Once an 'R' workspace was opened the code detailed in Figure 3.5 below was entered to perform LIMMA analysis. The blue text contains details on what function each set of commands was performing. The .txt files containing the normalised gene expression data and the targets file are highlighted in bold text. The `write.table` function enables the statistical details to be written to a text file which can then be handled in Excel. The figures returned by the command `summary(results)` informed the number of results to get R to write to the text files.

The Illumina codes contained in the text files returned by LIMMA were then used to define which genes were determined as being significantly up or down-regulated in either Sham vs. MI, MI vs. MNC or Sham vs. MNC.

Figure 3.5 R script used to perform the LIMMA analysis Text in black is the code. Text in blue describes the functions of the various parts of the script.

```
> library(limma)
> library(beadarray)
Opens the libraries of command codes for LIMMA and Beadarray.

BSData=readBeadSummaryData("DATA_TABLE.csv",sep=" ",ProbeID="PROBE_ID",skip=0)
> BSData
Opens the .csv files containing the normalised data prepared earlier.

> targets<-readTargets("targets.csv",sep=" ")
> targets
Opens the .csv targets file containing the experimental design.

> f<-paste(targets$disease,sep=" ")
> f<-factor(f)
> design<-model.matrix(~0+f)
> colnames(design)<-levels(f)
> design
Determines the experimental design using the targets.csv file.

> fit<-lmFit(log2(exprs(BSData)),design)
> cont.matrix<-makeContrasts(Sham_MI="MI-Sham",MI_MNC="MNC-MI",Sham_MNC="MNC-Sham",levels=design)
> fit2<-contrasts.fit(fit, cont.matrix)
> fit2<-eBayes(fit2)
> colnames(fit2)
Instructions to perform the linear modelling using Bayes statistics on the log2 of the expression values in the data file 'BSData'. Then use the previously defined contrast matrix to perform three different two group comparisons, Sham vs. MI, MI vs. MNC and Sham vs. MNC.

> topTable(fit2, coef=1, number=10, adjust="fdr")
Returns a table detailing the top 10 results of the first contrast (Sham vs. MI) with p-values adjusted for fdr (false discovery rate).

> results<-decideTests(fit2)
> summary(results)
Returns a summary of the analyses done so far in terms of the number of probes with statistically significant positive or negative fold changes in the three comparisons performed.

> write.table(topTable(fit2, coef=1, number=1550, adjust="fdr"),file="shamvsMI1550.txt",sep=" ")
Writes a .txt file summarising the top 1550 results from the first contrast (Sham vs.MI).
```

3.5 Validation of differentially expressed genes

Validation of gene expression results was performed using quantitative real-time PCR (QPCR). The mRNA samples are converted into cDNA using in vitro reverse transcription and the cDNA population is then used as a template for a modified polymerase chain reaction (PCR) reaction termed QPCR. QPCR utilises the in-vitro transcription technique PCR to amplify specific transcripts in a prepared mRNA sample. The transcripts of interest should amplify at an equal rate and therefore their relative abundance at a certain time point during the exponential phase of amplification should be related to their proportion in the original mRNA sample. The abundance of transcripts is measured through the use of fluorescent probes or labels which can be detected on a fluorescence microplate reader.

Firstly several genes were tested to ascertain the most suitable genes to use for normalisation in our expression analysis, then comparative gene expression was determined by using the $\Delta\Delta C_T$ method to normalise gene expression and to calculate relative gene expression in the MI and BMMNC groups against the Sham group

3.5.1 TaqMan gene expression assays

TaqMan Gene Expression assays utilise 5' nuclease activity of the Taq polymerase enzyme. A short oligo (probe) which has a minor groove binder (MGB) and a non-fluorescent quencher at the 3' end and a fluorescent reporter dye at the 5' end. These probes are termed hydrolysis probes. The MGB binder increases binding of the probe and therefore shorter probes can be used and higher melting temperatures (T_m).

At the annealing/extension stage (60°C) of the PCR reaction a forward and reverse primer anneal to either end of the sequence of interest in the cDNA template, at the same time the TaqMan hydrolysis probe binds to a complementary sequence within the sequence of interest. The Taq polymerase then catalyses the polymerisation of a complementary strand extending for the primers in a 5' to 3' direction. When it

reaches the hydrolysis probe it will dislodge first the reporter dye from the probe, separating it from the influence of the quencher and creating a fluorescent signal. As Taq polymerase will only cleave probes that are complementarily bound to the sequence of interest whilst that sequence is being replicated then the amount of fluorescing reporter dye in the reaction is proportional to the number of copies of the sequence of interest.

3.5.2 RNA preparation

The RNeasy Fibrous Tissue Mini Kit [Qiagen] was used to extract RNA from the rat myocardial tissue samples as before and these were quantified and quality was assessed using the NanoDrop 1000 Spectrophotometer as before.

To prepare cDNA for QPCR a Reverse Transcription System kit [Promega, UK] was used. Firstly a master mix was prepared containing all the reaction components except the RNA template (See Table 3.16). Then 1 μ g of the RNA was then diluted to a final volume of 9.8 μ l in nuclease-free water. These samples were heated to 70°C for 1 minute in a thermal cycler and then 10.2 μ l of the master mix was added to the microtubes to make up 20 μ l reaction volumes. The tubes were incubated at room temperature for 10 minutes and then at 42°C for 15 minutes on a thermal cycler. The temperature was then taken up to 95°C for 5 minutes and down to 4°C for a further 5 minutes to denature and inactivate the reverse transcriptase enzyme. The cDNA samples could then be stored at -20°C until needed for the QPCR reaction.

Table 3.16 Promega reverse transcription master mix

Reagent	1 reaction	15 reactions
MgCl ₂ (25mM)	4	60
10 x Reverse Transcription Buffer	2	30
dNTP mix (10mM)	2	30
Recombinant RNasin Ribonuclease Inhibitor	0.5	7.5
AMV Reverse Transcriptase (15 units)	0.7	10.5
Random Primers	1	15
Nuclease free water	0.6	9

3.5.3 QPCR using TaqMan gene expression assays

Absolute QPCR ROX Mix [Thermo Scientific, UK] was used for the QPCR reaction. This pre-prepared reaction cocktail contains Thermo-Start™ DNA Polymerase, ROX Dye which is used as a passive internal reference for normalising the signal from the reporter dye, dNTPs and buffers for optimal reaction conditions.

cDNA samples were diluted 1:100 in nuclease-free water and 5µl of this dilution was pipetted into the wells of a 384 well optical reaction plate [Applied Biosystems, UK] in triplicate. The master mixes (see Table 3.17) were prepared on ice, one for each different gene (assay) to be used, in sufficient volume to do all the reactions plus a no-template control. The master mixes were then added to the diluted cDNA samples, 16µl of master mix for each 20µl reaction. Once the 384 well optical plate was prepared, it was sealed with an optical plate seal [Thermo Scientific, UK] and was briefly spun down in a Sigma 4K15C centrifuge [Phillip Harris, UK].

Table 3.17 TaqMan QPCR master mix

Reagent	1 reaction	30 reactions
Absolute QPCR ROX Mix	10	300
TaqMan assay	1	30
Nuclease-free water	4	120

A new ‘absolute quantification’ TaqMan 2900HT run was set up using the SDS v2.3 software, and the barcode of the optical reaction plate was scanned. A marker for each assay is selected in the detection manager, with a FAM fluorescent label and a non-fluorescent marker. The wells used for the reactions are highlighted and the marker is linked to them. The samples were then named in the left hand grid panel. The thermal profile was left as default i.e. 50°C for 2 minutes, 95°C for 10 minutes followed by 40 cycles of 95°C for 15 minutes and 60°C for 1 minute. The file was saved before the run was commenced. Once complete, the data was analysed using

the SDS v2.3 software and the data was exported to Excel [Microsoft, US]. Triplicate Ct values for each sample were averaged after removing any outliers as suggested by high CV values (CV>2).

3.5.4 Reference gene selection

As TaqMan gene expression assays are already optimised to be 100% efficient there is no real requirement to put a standard curve on every plate. Comparative gene expression can be determined by using the $\Delta\Delta$ Ct method to normalise gene expression and to calculate relative gene expression in one group against a reference group. Selecting a suitable reference gene is important to get accurate results as is the use of more than one reference gene [113].

Five reference genes for rat were available in-house these were ATP synthase subunit beta (ATP5B), beta-2 microglobulin (B2m), eukaryotic translation initiation factor 4A2 (Eif4a2), glyceraldehydes-3-phosphate dehydrogenase (Gapdh) and ubiquitin C (Ubc). Initially the performance of these as endogenous controls were looked at in the pre-existing Illumina chip data to see they are expressed at a reasonable level and to see how stable expression was across samples and also to see if there is any evidence that these genes are differentially expressed in our experiment, i.e affected by our experimental conditions. Statistics were performed to measure variation of signal across the samples (standard deviation and CV of the Average signal over all samples), one way ANOVA was also performed using GraphPad Prism 5 [GraphPad, UK] to look for differences between experimental groups. QPCR was then performed on each of the suitable best candidates in all of the cDNA samples (in triplicate).

The geNorm VBA Excel macro was downloaded from the geNorm website (<http://medgen.ugent.be/~jvdesomp/genorm/>). The QPCR data for all of the reference genes that were tested were put into an Excel data table with sample names

in the left column and gene names along the top. The values needed for this table were quantities (Q_{REF}) calculated using the ΔCt method:

$$\Delta Ct = Ct \text{ target} - Ct \text{ reference}$$

The reference was the sample with the smallest Ct (highest expression) which was then set to 1:

$$Q_{REF} = E^{\Delta Ct}$$

Q_{REF} = Quantity of reference converted from Ct values.

E = amplification efficiency (2 = 100%).

The geNorm macro was opened and the newly created table was uploaded and the macro was set to calculate. The macro calculated a measure of gene expression stability 'M' for each reference gene from the average pairwise variation 'V' for that gene against all the other tested reference genes. The 'M' value for the least stable gene was highlighted in red and this column was deleted and the calculations were repeated. This is repeated until you have the two best reference genes (see Figure 3.6 for an example). To check no additional genes would add value to the accuracy of the normalisation, the 'bar chart' symbol was selected and this will produce two types of chart both indicating the pairwise variation between two sequential normalisation factors. If this value was over 0.15 then the inclusion of data from the next best gene in the normalisation factor calculation would be desirable (see Figure 3.7 for an example). The cut-off value was suggested by Vandesompele et al 2002 [114].

Figure 3.6 Flowchart depicting the use of GeNorm to determine the most stable reference gene for a set of samples. 1) First the dataset is uploaded and the macro is told to make the calculations. 2) The column with the highest scoring gene ('M' value in red) is deleted and the analysis is repeated. 3) The highest scoring gene is again deleted and the analysis is repeated. 4) This is repeated till there are only the two best genes remaining.

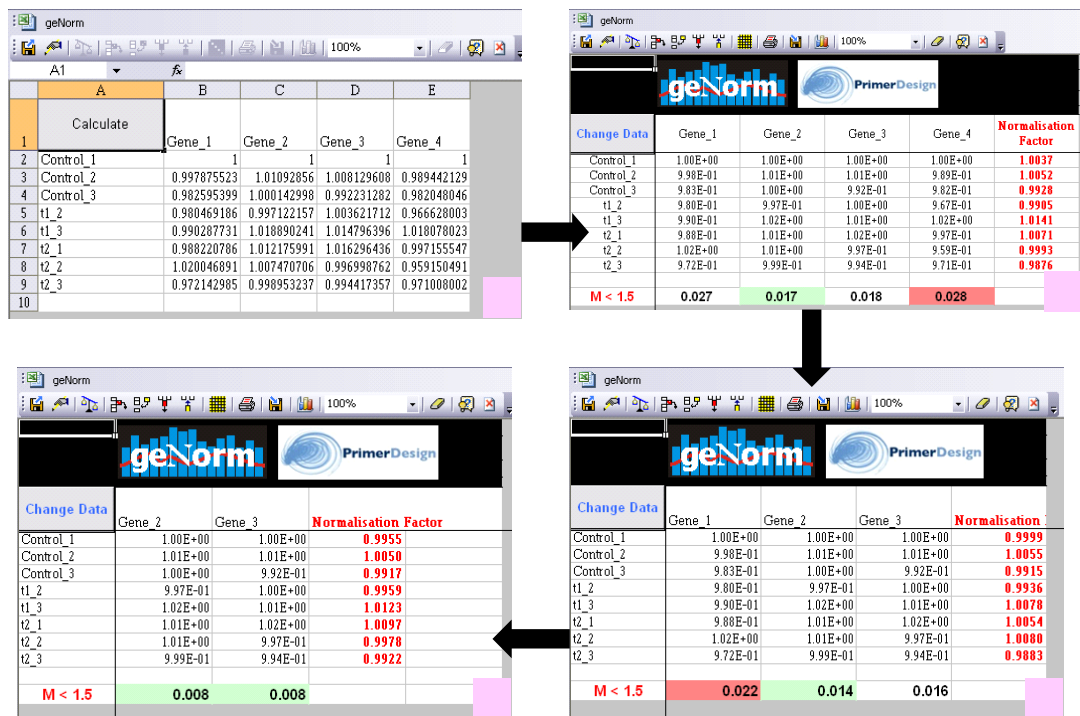
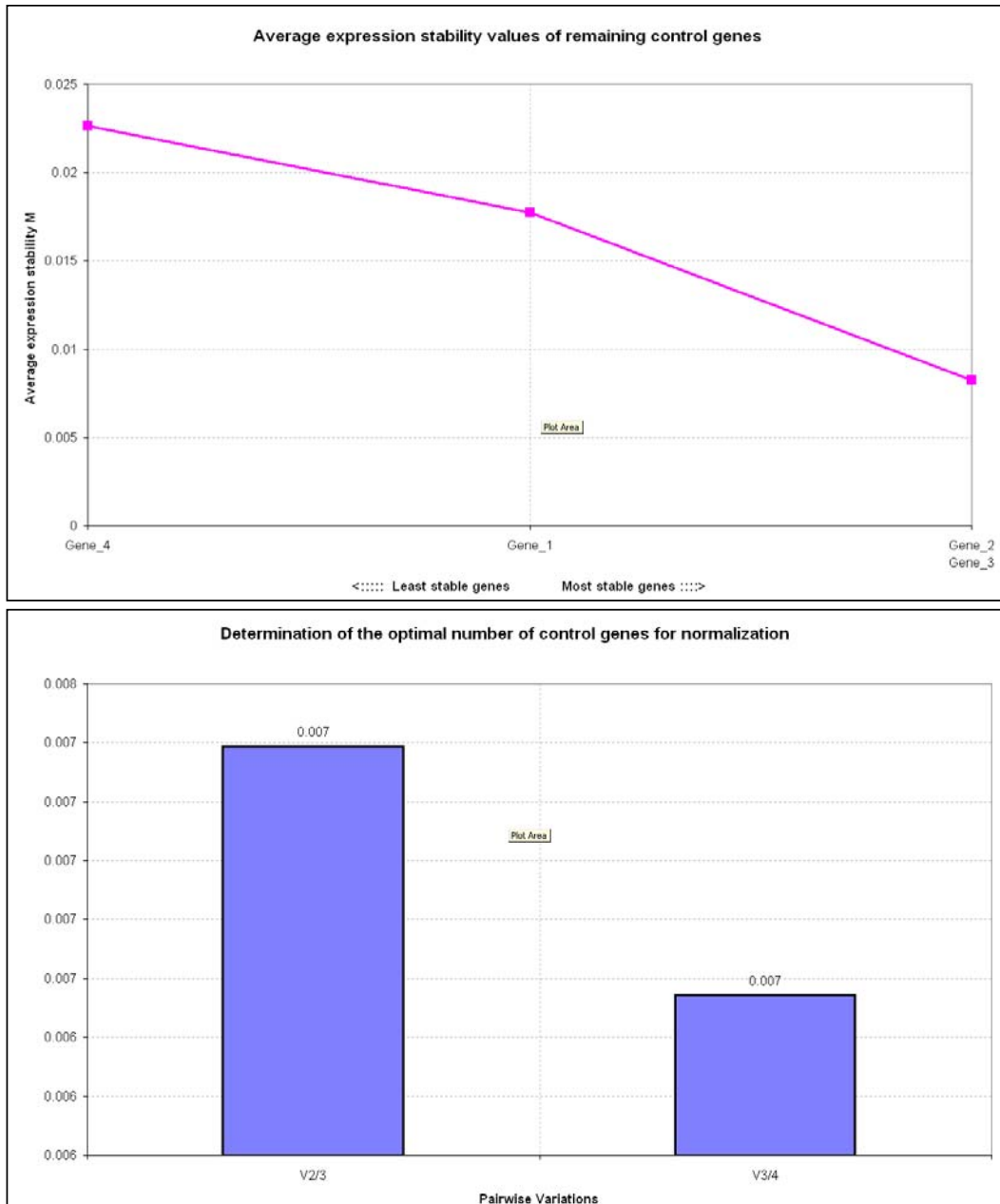


Figure 3.7 Graphical output of the example GeNorm analysis shown in Figure 3.6 The top chart plots the ‘M’ values for each gene, the two most stably expressed genes with the lowest ‘M’ value on the left. The bottom chart shows the pairwise variations for V2/3 (i.e between the normalisation factor calculated for the best 2 genes and the normalisation factor calculated from the best three genes), and V3/4 (i.e best three genes and the best four genes). Both values are <0.15 and so the additive effect of the third and fourth genes is negligible.



3.5.5 $\Delta\Delta\text{Ct}$ calculations and statistical analysis

The average Ct values for each of the reference genes suggested by GeNorm in each sample were calculated to give an average reference Ct (Ct_{REF}) value for each sample.

The ΔCt for each gene of interest ($\Delta\text{Ct}_{\text{GOI}}$) was calculated using the ΔCt method to calculate the difference between the Ct of the GOI and the Ct_{REF} :

$$\Delta\text{Ct}_{\text{GOI}} = \text{Ct}_{\text{GOI}} - \text{Ct}_{\text{REF}}$$

Then the average (AVE) and standard deviation (StDEV) of the $\Delta\text{Ct}_{\text{GOI}}$ was calculated for each of the experimental groups (Sham, MI and BMMNC).

The $\Delta\Delta\text{Ct}$ values were then calculated using the Sham group as reference:

$$\Delta\Delta\text{Ct}_{\text{Sham}} = \text{Ave } \Delta\text{Ct}_{\text{Sham}} - \text{Ave } \Delta\text{Ct}_{\text{Sham}} (= 0)$$

$$\Delta\Delta\text{Ct}_{\text{MI}} = \text{Ave } \Delta\text{Ct}_{\text{MI}} - \text{Ave } \Delta\text{Ct}_{\text{Sham}}$$

$$\Delta\Delta\text{Ct}_{\text{BMMNC}} = \text{Ave } \Delta\text{Ct}_{\text{BMMNC}} - \text{Ave } \Delta\text{Ct}_{\text{Sham}}$$

The $\Delta\Delta\text{Ct}$ values are then used to calculate fold changes (FC) between groups (relative expression) as shown below. In this case the FC of the MI group compared to Sham (FC1) and the FC of the BMMNC group compared to Sham (FC2). The Sham group value is also converted to 1 using the same calculation:

$$\text{FC1} = 2^{-\Delta\Delta\text{Ct}_{\text{MI}}}$$

$$\text{FC2} = 2^{-\Delta\Delta\text{Ct}_{\text{BMMNC}}}$$

$$\text{Sham} = 2^{-\Delta\Delta\text{Ct}_{\text{Sham}}} (= 1)$$

The StDEV of the group average Ct values were used to calculate 95% upper and lower confidence intervals (CI) which were shown on the histogram with the FC values. A Student's *t*-test was performed on the ΔCt_{GOI} values to look for significant differences between the Sham vs. MI and MI vs. BMMNC groups.

3.6 Bioinformatic analysis of protein and gene expression data

Several bioinformatics tools were employed to draw biologically relevant information from the lists of genes and proteins created in the comparative 2DGE and gene expression chip analyses. These tools were also used to look firstly at what information could be drawn from the proteomic analyses and from our gene expression analysis and then to combine the datasets and see if they yielded any extra information over and above that gained in looking at the datasets separately.

3.6.1 Protein ANalysis THrough Evolutionary Relationships (PANTHER)

PANTHER is an online database originally designed to look at the evolutionary relationship of sequence and protein function [115, 116]. An online tool interface has now been developed to utilise the database for expression data analysis among other things. Specifically the tool provides functional classification information when supplied with a list of genes or proteins.

When lists of gene or protein Refseq codes were entered into the ‘batch search’ function of PANTHER, the tool looked for genes in the database which matched those in the list. The resulting table shows the entered Refseq codes and gene names for these alongside the ‘best hit’ found in PANTHER and a score for this. A PANTHER score of 1 indicated a match couldn’t be found, a score of 0 was a perfect match and other scores in between were graded ‘closely related’, ‘related’ and ‘distantly related’. All of the PANTHER hits were returned along with PANTHER annotations for pathways, molecular functions and biological processes. PANTHER contains ~ 30 annotated biological process, ~30 molecular function categories as well as ~150 annotated pathways. These tables were exported. Before functional classification analysis was performed the threshold cut-off for the Panther score was set to exclude all genes with no hit, ‘distantly related’ hits and ‘related’ hits. This ensured only exact matches and closely related hits were included.

The 'pie-chart' function was then used to look at the pathways represented by the genes in the lists. Then the pie-chart showing the molecular functions and one showing the biological processes represented by our lists were studied and again data for these charts was exported as text files that could be looked at again in Excel [Microsoft, US].

Separate lists were entered into PANTHER for genes and proteins up- and down-regulated in the two comparisons to look for distinct pathways, functions or processes that were being up- or down-regulated

3.6.2 Database for Annotation, Visualization and Integrated Discovery (DAVID)

DAVID is a publicly available online tool for performing enrichment analysis on large gene lists produced from gene expression data [117, 118]. In a similar fashion to PANTHER, DAVID first matched a list of identifiers to genes in the database, and their annotations. DAVID includes many annotations from gene ontology (GO) terms and KEGG pathways, to annotations on protein domains and tissue expression. As before the separate gene lists for probes or proteins up- or down-regulated in either Sham vs. MI or MI vs. BMMNC were uploaded. For the gene expression data Illumina-ID codes were uploaded and 'RatRef12 Illumina chip dataset' was used as background upon which any enrichment was assessed. For the protein lists, the Uniprot accession codes were uploaded and *Rattus Norvegicus* was used as background. Functional annotation clustering was performed on each separate list of genes or proteins.

First the biological process (BP) GO terms were clustered. High stringency was chosen which gives smaller more specific clusters of terms rather than broader ones. The GO terms within each cluster, count (number of genes from list with this annotation), fold enrichment (the fold enrichment of this annotation in the uploaded gene list versus the proportion of this annotation in the background dataset), % (percentage of the inputted genes found with this annotation), p-value (modified

Fisher's exact test (EASE score) and benjamini adjusted p-values (corrected to control family-wide false discovery rate). In the analysis of proteomic data, GO terms with p-values of <0.05 were taken to be significantly associated. In the larger gene-expression dataset benjamini adjusted p-values of <0.05 were taken to be significantly associated.

Secondly we clustered the KEGG pathways represented in our gene lists. This time using a medium stringency setting and again we recorded the same output measures.

3.6.3 Ingenuity Pathway Analysis (IPA)

IPA is a literature mining tool and database resource (Ingenuity Systems®, www.ingenuity.com). Lists of proteins or genes with fold changes and p-values were entered into the online tool and a core-analysis was performed. IPA returned information on how the proteins/genes in the list are linked, which cellular functions, signalling pathways or disease states they were linked to and which other proteins they were linked to within these networks and pathways. From the large amount of information resulting from the core analysis, the most highly scoring networks were recorded, as were the top functions, and canonical pathways.

The lists were not split into up-and down-regulated members as the output of IPA shows direction of influence. A core analysis was performed on all of the proteomic data; Refseq codes, fold changes and p-values for Sham vs. MI (Observation 1) and MI vs. BMMNC (Observation 2). A second core analysis was performed on all of the significant LIMMA data; Refseq codes, log fold changes and adjusted p-values for Sham vs. MI (Observation 1) and the same data for MI vs. BMMNC (Observation 2).

In each core analysis, the functional/canonical pathway analysis used the Ingenuity Knowledge Base (genes only) as a reference set and both direct and indirect relationships were selected for the network analysis, including endogenous chemicals

e.g. hydrogen peroxide and Ca^{2+} . The most significantly associated functions and canonical pathways were looked at and the networks generated in each of these core analyses were saved. In the case of very large numbers of networks generated by the larger datasets, only the top five were looked at in detail. P-values for the association of a functional annotation or canonical pathway with the datasets are based on a right-tailed Fisher's Exact Test. Canonical pathways are returned with a \log_{10} p-value (negative values) from the Fisher's Exact Test and ratios which are calculated from the number of entered molecules found in the pathway divided by the total number of molecules in the pathway. Network scores are based on the number of genes/proteins they contain that are from the input dataset (focus molecules). The higher the score, the lower the probability of finding the observed number of focus molecules in a given network by random chance

3.7 Studies of 14-3-3 epsilon

3.7.1 Validation of experiments using samples 10-18

Western blotting was used to measure protein expression of 14-3-3ε, Sdha and Pebp1 in samples 10-18 (See Table 3.1). If expression changes between the groups reflected the results from samples 1-9 we would take this as validation for the use of freshly prepared samples for experiments which would further investigate findings of interest from our proteomic and gene expression analyses which were obtained using sample 1-9. The methodology for performing these western blots in samples 10-18 were identical to those described in section 3.3.

3.7.2 Expression and activation of BCL2-associated agonist of cell death (Bad)

Western blotting was used to measure BCL2-associated agonist of cell death (Bad) as well as the phosphorylated form, phosphorylated at serine 136, in protein lysates from samples 10-18. Antibodies for both Bad and phosphorylated Bad were supplied by Abcam, and an alternative antibody for phosphorylated Bad was purchased from Cell Signalling Technology [supplied by New England Biolabs, UK]. The methodology for these assays was the same as that described previously in section 3.3, except that the blocking step was reduced to 2-3 hours at room temperature on a shaker instead of overnight at 4°C, and the primary antibody incubations were left overnight at 4°C, then 2 hours at room temperature on a shaker.

3.7.3 14-3-3 epsilon pull-down assay

A pull-down assay was performed using the ProFound™ Pull-Down PolyHis Protein:Protein Interaction Kit [Pierce, US]. His-tagged 14-3-3 epsilon protein [Abcam, UK] was used as bait protein and freshly prepared protein lysates from samples 10-18 were used as prey. An initial experiment was performed to test the

methodology using 60µg of His-tagged 14-3-3 epsilon protein and a protein lysate prepared from a mix of three tissue samples, one from each experimental group.

3.7.3.1 Bait protein immobilisation

BupH™ Tris buffered saline (TBS) was made up to 500ml with Milli-Q water and filter sterilised using a 0.2µm filter and a 50ml syringe. The buffer was then stored at 4°C until required. Enough Handee™ spin columns for the experiment, one for each prey sample plus a no-bait control were labelled. Wash solution was made up by mixing TBS and Profound lysis buffer (1:1) and adding 4M imidazole stock to get a final concentration of 40mM. Only enough wash solution was prepared for immediate use. The immobilised cobalt chelate resin was thoroughly resuspended using a vortex mixer, and 25µl was pipetted into each column using a wide-bore pipette tip. 200µl of wash solution was added to each spin column, caps were placed over both ends and the column inverted several times. Both caps were removed and the column placed in a collection tube before being spun at 1,250 x g for 30 seconds. The flow-through was discarded and the bottom cap replaced. This wash step was repeated four times. After the fifth wash, 60µg of the bait protein was added to the column in 300µl total volume of wash solution and the top cap was replaced. The columns were then incubated at 4°C for 30 minutes on a rocking platform. Prey protein preparation was carried out during this incubation step.

Both caps were then removed and the columns were placed in a collection tube before being spun at 1,250 x g for 30sec. The flow-through was labelled as ‘bait-flow through’ and stored on ice. The resin was then washed five times using the same procedure as before.

3.7.3.2 Prey protein preparation and capture

Approximately 100mg of ground tissue from samples 12, 13 and 16 was added to 250µl of ice cold TBS containing protease inhibitor cocktail in a Precellys CK14 tubes, and this pooled sample was homogenised in a Precellys 24 bench top homogeniser [Bertin technologies]. An equal volume of Profound lysis buffer was

added and the sample was mixed gently then placed on ice for 30 minutes and inverted occasionally. The lysate was then decanted to a microcentrifuge tube and spun at 12,000 x g for 5 minutes. The supernatant was decanted and stored on ice. 4M imidazole was added to a final concentration of 40mM and the tube was immediately inverted to mix thoroughly and labelled 'prey lysate'.

The columns were removed from 4°C storage, and the top cap was removed. The full volume of prey protein lysate was added to the column except 10-15µl kept for quantification and SDS-PAGE. The top cap was replaced and the columns incubated at 4°C for at least 1 hour with gentle rocking. Both caps were then removed and the column was placed in a fresh collection tube and spun for 1,250 x g for 30 seconds. The flow through was labelled 'prey flow through' and placed on ice. The resin was then washed five times using the same procedure as before.

3.7.3.3 Bait-Prey elution

1ml of 290mM imidazole elution buffer was prepared by adding 63µl of 4M imidazole stock to 937µl wash solution already containing 40mM imidazole and mixing with a pipette. The bottom caps were applied to the columns and the top caps removed. 30µl of elution buffer was added to the spin columns and the top cap was replaced then the columns were incubated at room temperature for 5 minutes. Both caps were then removed from the columns and they were placed in a collection tube and spun for 1,250 x g for 1 minute. The flow-through was labelled Elution 1 and placed on ice.

3.7.3.4 SDS-PAGE and protein detection

Prey protein lysate, bait-flow through and eluate preparations were separated on SDS PAGE gels as described in section 3.3.1.1. Reducing agent was added to the samples (1.5µl to 15µl sample) along with 5µl of LDS buffer. Once run, the gel was silver stained using the plus one silver staining kit [GE Healthcare] according to manufacturer's instructions.

3.7.3.5 LC-MS/MS protein identification

Bands were cut from the gel using a scalpel, cut into pieces no bigger than 2mm² and placed in microcentrifuge tubes. Trypsin digestion was carried out using the same methodology already described in section 3.2.5. Lyophilised peptide samples were then reconstituted for LC/MS-MS and identification using the MASCOT database as described in section 3.2.6.

4. Proteomic results

4.1 Wide-range protein profiling

4.1.1 Protein quantification

Samples of 80-140mg were taken from myocardial samples 1-9 for protein lysate preparation. These protein lysates were quantified as being between 2-6 μ g/ul (total protein yields of between 1.6-7mg per sample, average 5mg). The average yield was 0.5mg of protein per 10 mg of starting material.

4.1.2 2DE

Two gels for each sample (18 gels in total) were analysed with PDQuest Advanced software [BioRad, UK]. An example of the gels produced for this analysis is shown in Figure 4.4. Normalised spot intensities for 1081 spots were analysed in Excel [Microsoft, US] to look for significant fold changes >1.5 . A total of 187 spots had fold changes >1.5 in either the Sham vs. MI, MI vs. BMMNC or both comparisons (Figure 4.1). This list was narrowed down to those with the most significant fold changes (FC >2.5). This left 130 spots (Figure 4.2). All 130 spots were then checked in the gel images to confirm these changes by visual inspection and to check if there was sufficient sample to yield identification.

105/130 spots were chosen to take forward for identification by LC-MS/MS. There were also 4 spots with qualitative differences; 2 spots which were not present in the MI gels but were present in both the Sham and BMMNC gels, and 2 other spots which were not present in the Sham gels but were present in the MI and BMMNC gels. These spots were also included and taken forward for LC-MS/MS (total n=109).

Figure 4.1 Venn diagram showing the distribution of 187 significantly differently expressed spots with >1.5 fold changes in the wide-range 2DE analysis Sham = sham operated group, MI = MI group treated with PBS, BMMNC = MI group treated with bone marrow mononuclear cells. Arrowheads indicate direction of expression change in the Sham vs. MI or the MI vs. BMMNC comparisons or Both comparisons.

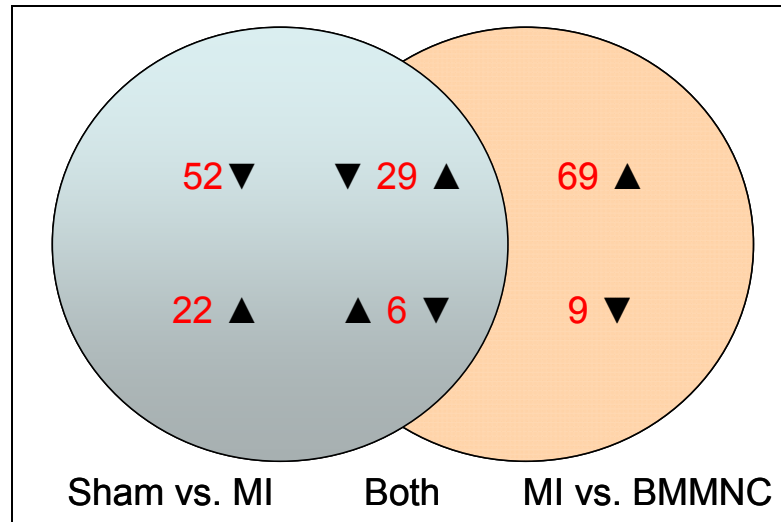
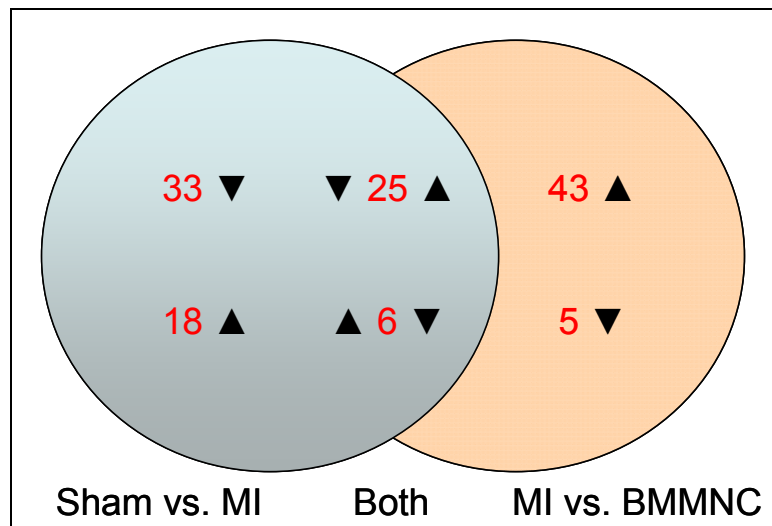


Figure 4.2 Venn diagram showing the distribution of 130 significantly differently expressed spots with >2.5 fold changes in the wide-range 2DE analysis Sham = sham operated group, MI = MI group treated with PBS, BMMNC = MI group treated with bone marrow mononuclear cells. Arrowheads indicate direction of expression change in the Sham vs. MI or the MI vs. BMMNC comparisons or Both comparisons.



The median and standard error of spot intensities as well as differences between groups, 95% confidence interval (CI) of the differences, and Student's *t*-test statistics for Sham vs. MI and MI vs. BMMNC comparisons for the 109 spots taken into protein identification are detailed in the Table 4.1. The distribution of fold changes and p-values of these spots (not including the 4 qualitatively altered spots) in both comparisons is shown in Figure 4.3. The larger proportion of spots were down-regulated in Sham vs. MI with up to 5 fold change and up-regulated in MI vs. BMMNC again up to 5 fold change.

Figure 4.3 Graphs of p-values plotted against fold changes for 105 spots with significantly altered intensities in the pH 4-7 2DE analysis Sham = sham operated group, MI = MI group treated with PBS, BMMNC = MI group treated with bone marrow mononuclear cells. **A** data for spots significantly altered in Sham vs. MI analysis. The points highlighted in blue show data for the spots which were also significantly different in MI vs. BMMNC. **B** data for spots significantly altered in MI vs. BMMNC analysis. The points highlighted in blue show data for the spots which were also significantly different in Sham vs. MI.

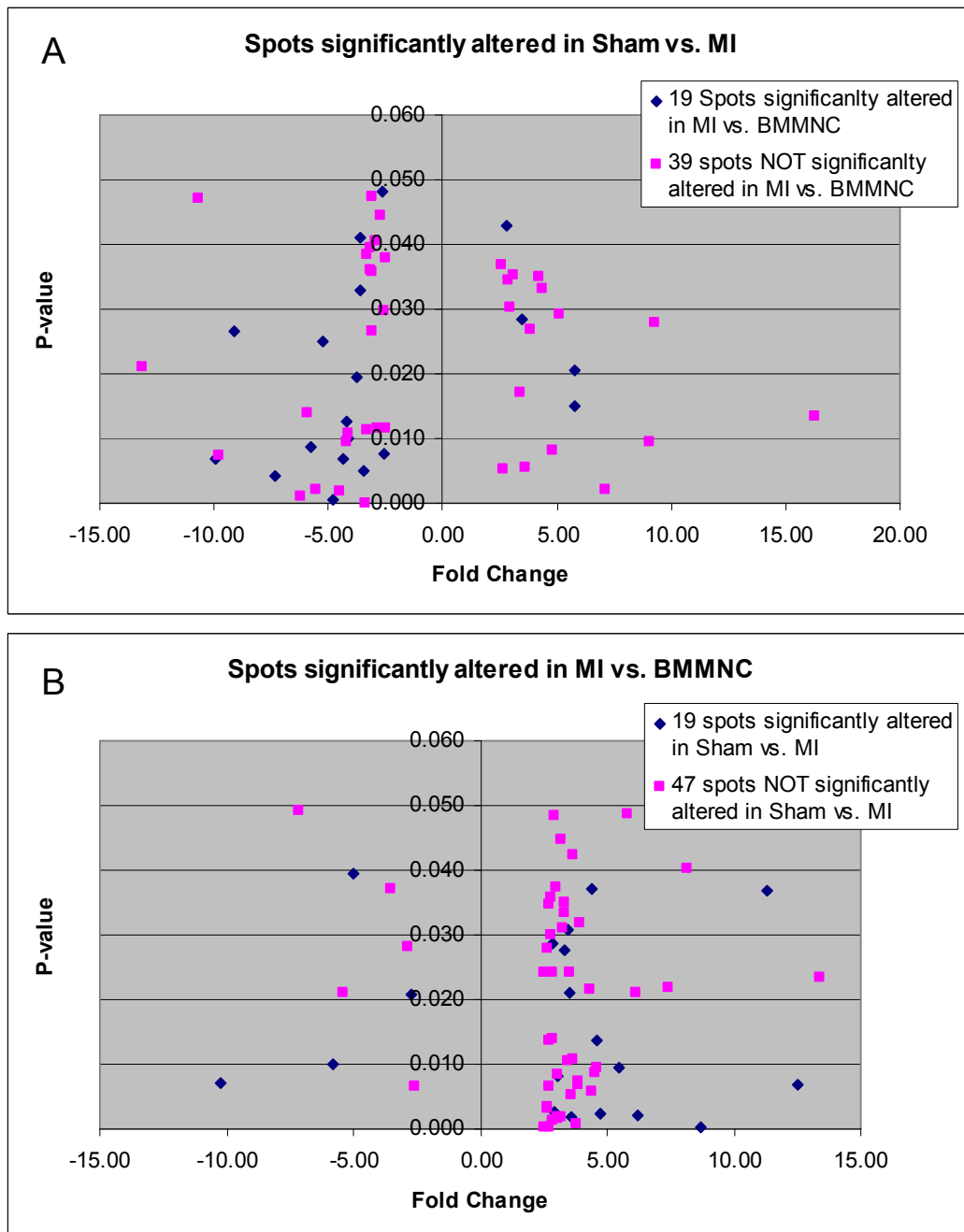


Table 4.1 109 spots selected for protein identification by LC-MS/MS from the pH 4-7 2DE analysis Sham = sham operated group, MI = MI group treated with PBS, BMMNC = MI group treated with bone marrow mononuclear cells. Median spot intensities and standard errors for each group are shown alongside the difference, 95% confidence interval and Student's t-test p-value for both Sham vs. MI and MI vs. BMMNC comparisons.

SSP	SHAM		MI		MNC		Change in intensity (MI/SHAM)			Change in intensity (BMMNC/MI)		
	Med.	SE	Med.	SE	Med.	SE	Difference	95% CI	p-value	Difference	95% CI	p-value
1206			487.8	96.56	229.0	148.12		On in MI		0.6		ns
1207	42.6	260.00	1530.6	330.15	1523.0	347.47	3.8	(2.15 - 5.52)	0.027	0.9		ns
1213	136.0	63.03	1056.0	157.18	693.0	197.05	7.1	(5.02 - 9.20)	0.002	0.6		ns
1223	73.9	56.30	10.8	12.32	137.8	56.06	0.2		ns	7.4	(2.89 - 11.98)	0.022
1224	493.69	147.22	87.61	124.58	893.49	142.04	0.4		ns	3.9	(2.53 - 5.30)	0.032
1225	312.0	61.87	11.6	13.78	233.9	94.57	0.1	(-0.02 - 0.17)	0.021	12.7		ns
1226	120.48	37.30	52.89	25.10	188.10	32.78	0.4		ns	3.0	(1.83 - 4.14)	0.037
1248	49.1	93.34			53.7	99.59		Off in MI				On in BMMNC
1301	739.1	221.10	146.0	156.50	684.0	55.51	0.3	(0.01 - 0.64)	0.036	2.1		ns
1304	672.9	239.84	114.8	68.51	556.1	172.21	0.2	(0.03 - 0.36)	0.025	4.6	(2.39 - 6.75)	0.014
1307	211.1	80.22	88.0	69.00	466.8	32.92	0.6		ns	3.2	(2.76 - 3.65)	0.002
1320	182.5	27.95	17.3	5.61	179.7	47.29	0.1	(0.04 - 0.16)	0.007	11.3	(5.95 - 16.66)	0.037
1424	331.0	121.77	342.8	67.56	803.2	92.83	0.7		ns	2.8	(2.18 - 3.52)	0.001
1429	1485.96	278.53	168.43	300.06	1714.20	309.05	0.4		ns	2.8	(1.79 - 3.82)	0.036
1430	258.6	68.41	23.8	6.82	271.9	73.49	0.1	(0.05 - 0.17)	0.027	12.5	(6.69 - 18.32)	0.007
1705	558.6	129.30	74.3	60.24	406.6	182.62	0.2	(0.03 - 0.45)	0.013	4.4	(1.77 - 7.07)	0.037
2119	210.0	166.12	1898.8	544.35	146.7	52.53	5.8	(2.53 - 8.99)	0.015	0.1	(0.04 - 0.15)	0.007
2226	420.9	115.81	139.9	41.72	324.0	78.51	0.3	(0.09 - 0.44)	0.020	2.9	(1.60 - 4.11)	0.029
2443	822.3	203.40	77.4	109.59	639.7	69.66	0.3		ns	3.6	(2.84 - 4.38)	0.005
2546	94.4	18.13	22.2	6.06	146.3	23.56	0.2	(0.11 - 0.38)	0.010	6.2	(4.08 - 8.34)	0.002
2607	18.5	33.03	258.6	32.73	213.1	59.97	4.8	(3.56 - 6.12)	0.008	0.9		ns
2609	777.2	121.29	301.0	68.67	783.6	55.55	0.5		ns	2.5	(2.16 - 2.86)	0.0003
2616	70.1	52.24	79.2	24.41	266.7	68.21	0.9		ns	3.3	(1.73 - 4.94)	0.035
2624	221.1	35.26	27.9	17.63	149.8	34.87	0.2	(0.05 - 0.41)	0.007	3.4	(1.87 - 4.99)	0.031
2626	95.1	30.14	68.6	23.54	301.7	91.19	1.0		ns	3.7	(1.71 - 5.65)	0.042
2701	39.5	78.78	366.4	83.13	441.1	323.49	2.9	(1.78 - 3.94)	0.034	1.7		ns
2712	631.5	180.42	184.6	102.51	715.4	244.00	0.4		ns	3.3	(1.63 - 4.90)	0.031
2722	36.3	17.57	21.9	7.86	134.4	32.10	0.5		ns	6.1	(3.36 - 8.92)	0.021
3208	216.1	68.85	123.4	57.84	469.2	48.71	0.5		ns	3.8	(3.11 - 4.54)	0.001
3209	258.8	91.71	30.9	50.70	470.1	103.23	0.4		ns	4.6	(2.63 - 6.60)	0.009
3228	140.9	89.60	1730.7	506.98	507.5	607.20	9.0	(4.19 - 13.90)	0.010	0.7		ns
3305	2089.7	390.71	502.1	203.38	1385.5	369.28	0.3	(0.09 - 0.56)	0.026	2.7		ns
3322	220.3	96.04			553.3	126.00		Off in MI				On in BMMNC
3433	811.3	136.32	461.2	102.82	1104.6	142.91	0.4	(0.17 - 0.60)	0.008	2.9	(2.16 - 3.73)	0.003

Table 4.1 continued.

SSP	SHAM		MI		MNC		Change in intensity (MI/SHAM)			Change in intensity (BMMNC/MI)		
	Med.	SE	Med.	SE	Med.	SE	Difference	95% CI	p-value	Difference	95% CI	p-value
3441	348.29	68.63	169.22	38.60	443.34	63.06	0.4		ns	3.0	(2.18 - 3.89)	0.008
3518	377.5	58.22	69.5	59.19	332.7	91.32	0.3	(-0.01 - 0.62)	0.011	2.9		ns
3523	551.1	129.94	256.8	55.88	637.8	48.63	0.5		ns	2.7	(2.36 - 3.14)	0.0002
3526	242.73	55.37	91.61	25.78	281.45	76.05	0.4		ns	3.2	(1.58 - 4.79)	0.045
3622	712.5	106.89	341.2	96.15	729.8	158.88	0.5		ns	2.5	(1.57 - 3.52)	0.024
3626	863.3	63.65	397.5	87.61	1075.1	161.82	0.5		ns	3.0	(2.23 - 3.87)	0.002
3627	326.7	118.43	221.5	20.72	531.0	74.46	0.4		ns	2.6	(1.93 - 3.35)	0.003
3629	285.7	66.51	111.4	38.11	462.1	81.22	0.4		ns	4.4	(3.03 - 5.76)	0.006
3632	113.8	33.21	55.4	24.43	209.8	41.26	0.6		ns	2.9	(1.81 - 3.93)	0.014
3636	270.6	49.01	32.2	26.40	384.8	46.73	0.2	(-0.012 - 0.37)	0.009	8.7	(6.76 - 10.64)	0.0004
3638	99.9	33.83	20.4	12.24	138.9	25.32	0.3	(0.06 - 0.50)	0.041	4.7	(3.11 - 6.34)	0.002
3706	409.7	65.23	164.3	47.79	738.6	136.53	0.5		ns	4.5	(2.95 - 6.06)	0.009
4207	524.5	164.16	802.8	238.61	435.2	110.88	2.0		ns	0.3	(0.14 - 0.56)	0.028
4217	903.56	209.86	161.41	117.70	197.14	101.48	0.3	(0.04 - 0.61)	0.047	1.0		ns
4235	50.0	26.86	23.0	7.03	188.1	41.90	0.3		ns	8.2	(4.36 - 11.95)	0.040
4244	238.0	51.56	22.9	10.24	173.3	41.23	0.1	(0.05 - 0.23)	0.004	5.5	(2.81 - 8.11)	0.009
4329	110.5	14.54	8.9	11.78	96.4	37.74	0.2	(-0.03 - 0.39)	0.002	5.4		ns
4406	721.4	140.81	188.0	125.34	922.2	144.33	0.4		ns	2.8	(1.81 - 3.86)	0.024
4418	75.6	65.92	76.5	30.65	392.7	75.29	0.6		ns	3.9	(2.31 - 5.44)	0.007
4511	400.3	89.46	50.0	61.54	505.2	88.15	0.4		ns	3.8	(2.50 - 5.20)	0.007
4513	95.23	6.54	38.34	19.65	156.51	30.81	0.5		ns	3.2	(1.80 - 4.50)	0.050
4521	426.8	306.05	44.7	141.22	752.4	71.75	0.4		ns	2.7	(2.12 - 3.24)	0.028
4522	295.8	67.87	130.8	42.86	421.3	41.77	0.6		ns	2.7	(2.06 - 3.25)	0.003
4523	691.1	89.08	73.8	86.61	403.7	130.40	0.2	(-0.02 - 0.46)	0.002	2.6		ns
4525	27.71	13.21	20.47	7.75	118.43	26.06	0.7		ns	4.3	(2.03 - 6.64)	0.022
4702	362.2	74.95	196.0	56.06	483.4	89.06	0.5		ns	2.7	(1.88 - 3.54)	0.006
4703	140.7	41.45	84.3	45.50	294.2	75.91	0.7		ns	2.7	(1.54 - 3.92)	0.035
4722	178.5	31.16	16.4	34.68	207.4	49.49	0.4	(-0.01 - 0.77)	0.048	3.3	(1.88 - 4.79)	0.028
4734	116.9	33.58	46.3	13.31	120.3	34.12	0.4	(0.21 - 0.56)	0.030	1.9		ns
4740	73.96	54.44	352.83	38.71	143.83	106.81	2.6	(2.00 - 3.15)	0.037	0.6		ns
4741	50.8	64.33	58.0	24.54	245.6	46.22	0.6		ns	3.4	(2.20 - 4.65)	0.011
5311	237.03	75.58	805.08	176.20	723.36	82.71	2.9	(1.55 - 4.31)	0.030	0.9		ns
5315	34.70	6.36	8.62	1.74	8.27	24.66	0.2	(0.13 - 0.35)	0.011	5.0		ns
5408	462.1	81.80	110.2	63.93	435.4	50.44	0.4	(0.09 - 0.70)	0.038	2.4		ns
5422	58.09	7.41	9.51	3.20	38.88	18.03	0.2	(0.06 - 0.28)	0.014	5.5		ns
5501	304.76	82.79	51.41	42.67	260.90	47.80	0.4		ns	2.8	(1.77 - 3.80)	0.030
5601	549.0	42.09	131.6	32.75	362.4	20.96	0.3	(0.18 - 0.42)	0.00005	2.2		ns
5618	214.0	60.27	82.5	26.17	168.3	48.73	0.3	(0.11 - 0.52)	0.039	2.3		ns

Table 4.1 continued.

SSP	SHAM		MI		MNC		Change in intensity (MI/SHAM)			Change in intensity (BMMNC/MI)		
	Med.	SE	Med.	SE	Med.	SE	Difference	95% CI	p-value	Difference	95% CI	p-value
5715	297.4	68.71	1034.7	422.40	485.8	126.94	4.2	(1.66 - 6.79)	0.035	0.4		ns
5805	68.1	58.86	436.3	98.64	465.0	184.05	3.1	(1.65 - 4.54)	0.035	1.2		ns
6123	414.9	106.53	33.9	13.72	88.4	76.84	0.1	(0.02 - 0.16)	0.047	3.9		ns
6413	217.9	119.81	1003.8	358.86	483.1	173.02	4.3	(1.83 - 6.87)	0.033	0.5		ns
6424	666.28	136.76	142.75	51.98	519.16	163.44	0.3	(0.11 - 0.49)	0.038	3.2		ns
6425	472.7	60.58	31.0	36.97	211.2	195.97	0.2	(-0.01 - 0.33)	0.001	5.6		ns
6533	119.8	50.88	539.4	84.12	795.0	58.49	3.6	(2.47 - 4.76)	0.006	1.5		ns
6538	179.5	61.92	97.4	23.11	237.1	31.58	0.3	(0.09 - 0.46)	0.033	3.6	(2.67 - 4.48)	0.002
6545	327.4	66.83	24.3	32.13	365.9	1416.03	0.2	(0.02 - 0.46)	0.016	25.7		ns
6603	89.93	16.82	393.30	75.99	160.83	49.96	3.4	(1.98 - 4.88)	0.017	0.5		ns
6616	69.7	56.65	216.5	51.88	21.1	28.47	3.5		ns	0.2	(-0.05 - 0.42)	0.021
6636	73.8	29.65	54.9	9.36	189.4	50.56	0.8		ns	2.9	(1.44 - 4.39)	0.048
6732	94.7	26.36	290.3	43.99	208.0	21.75	2.6	(1.93 - 3.35)	0.005	0.6		ns
6746	121.13	26.77	289.95	89.33	80.84	22.70	2.5		ns	0.3	(0.14 - 0.43)	0.037
6813	226.80	48.49	68.00	28.53	131.83	36.14	0.3	(0.07 - 0.56)	0.036	1.8		ns
7110			174.4	508.95	23.5	45.40		On in MI		0.1		ns
7111	775.4	210.42	209.4	78.54	491.4	156.98	0.2	(0.08 - 0.40)	0.009	2.6		ns
7112	122.4	41.78	18.5	4.08	69.5	45.67	0.1	(0.05 - 0.15)	0.007	7.1		ns
7228	17.6	63.73	1039.8	299.68	692.5	167.62	16.2	(8.75 - 23.74)	0.013	0.4		ns
7306	348.1	53.40	61.0	33.94	352.6	69.19	0.2	(0.04 - 0.38)	0.001	3.5	(1.90 - 5.14)	0.021
7323	690.6	163.55	1689.3	151.49	602.2	248.60	2.4		ns	0.4	(0.09 - 0.69)	0.007
7327	18.8	55.22	451.6	86.47	274.0	50.06	5.1	(2.79 - 7.48)	0.029	0.8		ns
7508	132.0	58.73	394.6	48.28	103.3	57.82	2.8	(2.08 - 3.51)	0.043	0.4	(0.06 - 0.68)	0.021
7515	175.0	21.33	85.3	15.95	205.6	27.55	0.4		ns	3.0	(2.29 - 3.78)	0.002
7608	52.2	19.59	489.2	130.60	338.9	126.82	9.3	(4.44 - 14.06)	0.028	0.7		ns
7612	44.8	26.50	174.3	39.00	31.9	8.07	3.4	(2.13 - 4.77)	0.029	0.2	(0.09 - 0.25)	0.010
7702	136.1	40.33	42.2	19.75	183.0	42.28	0.4		ns	3.7	(2.15 - 5.18)	0.011
7722	31.3	9.89	260.5	67.25	41.4	10.18	5.8	(2.41 - 9.17)	0.021	0.2	(0.11 - 0.29)	0.039
7723	314.1	82.71	99.4	26.05	275.5	58.44	0.4	(0.21 - 0.53)	0.045	2.4		ns
7730	101.6	20.08	46.3	8.07	76.6	30.21	0.4	(0.26 - 0.54)	0.012	2.5		ns
7737	170.2	41.43	53.4	18.41	117.7	36.79	0.3	(0.13 - 0.54)	0.040	2.5		ns
8128	511.6	99.61	194.5	79.76	380.8	134.24	0.4	(0.10 - 0.61)	0.012	1.9		ns
8520	136.2	17.54	22.6	21.09	136.6	14.96	0.3	(0.01 - 0.56)	0.005	3.0	(2.36 - 3.73)	0.008
8525	158.8	99.49	19.7	8.98	366.2	149.02	0.1		ns	13.4	(4.31 - 22.43)	0.023
8526	88.67	32.58	53.09	12.28	184.79	36.30	0.4		ns	3.5	(1.92 - 5.08)	0.024
8710	274.7	87.42	174.8	35.96	373.4	88.51	0.5		ns	2.7	(1.66 - 3.71)	0.014
8853	242.8	90.52	101.5	36.04	317.4	97.84	0.4		ns	3.4	(1.76 - 4.95)	0.033

4.1.3 Differentially expressed proteins

Of the 109 spots selected for protein identification 45 spots yielded no identification and 13 spots contained more than one protein. 51 spots yielded single protein identification including a total of 28 different proteins, 5 proteins were found in more than one spot. An example of the 2DE gels produced by this analysis is shown in Figure 4.4, the spots from which a single protein identification was obtained are highlighted. All of the MASCOT search results for the wide-range analysis are detailed in Appendix 2. A summary of the 51 spots with single protein identification is shown in Table 4.2 and the fold change and p-values for these proteins, organised into functional categories is shown in Table 4.3.

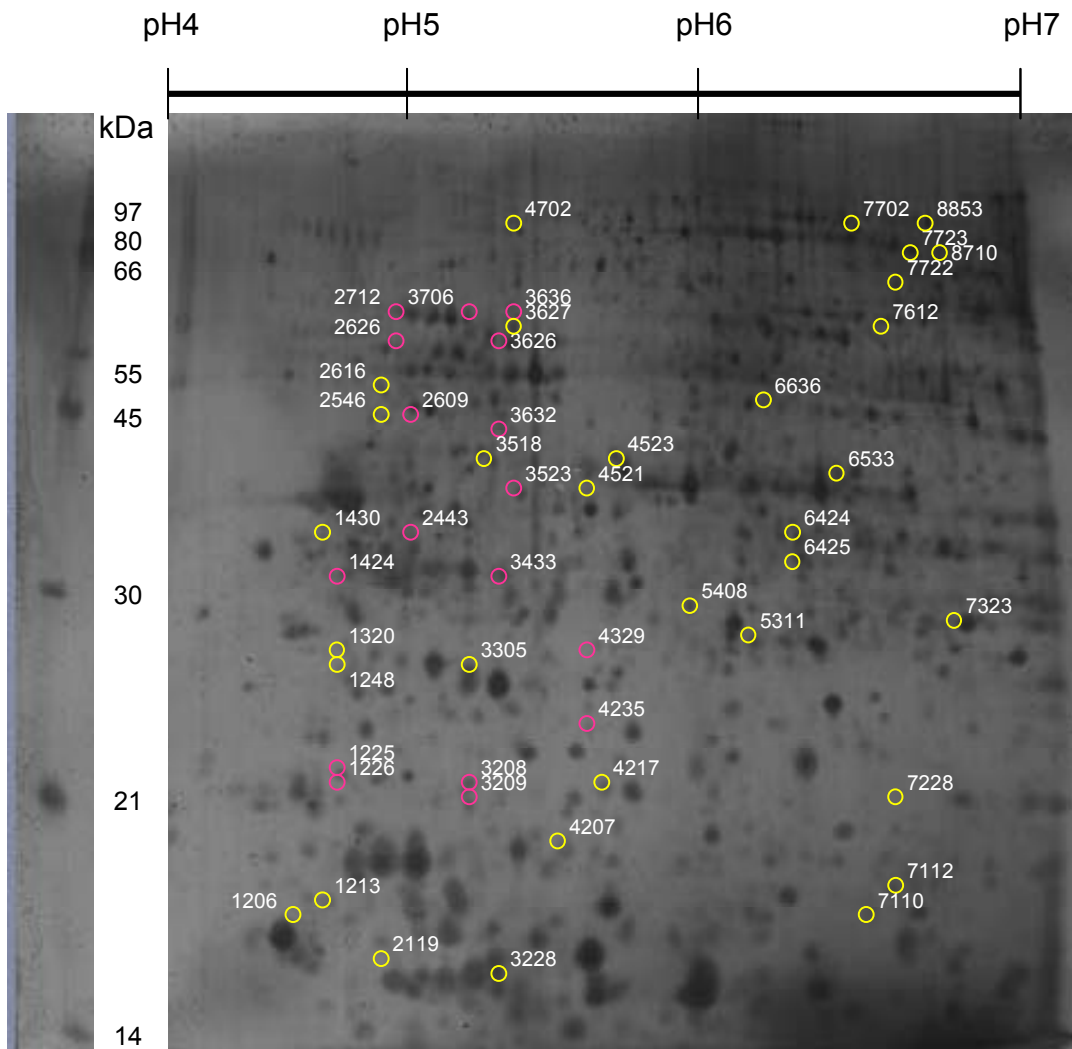
ATP synthase subunit β (Atp5b) was found in 17 different spots, L-lactate dehydrogenase B (Ldhb) chain was found in 3 different spots (although the peptide found in spot 4521 could not be distinguished from L-lactate dehydrogenase A chain), rat serum albumin (Alb) and myosin regulatory light chain-2 (Myl2) were also each found in 3 different spots and stress-70 protein (Hspa9) was found in 2 different spots.

All of the Atp5b spots were down-regulated in Sham vs. MI and up-regulated in MI vs. BMMNC, only spots 3626, 3636 and 3433 were significantly altered in both comparisons. The fold changes seen in these 17 spots ranged from 2 to 13 fold. All spots had an estimated mass of between 19 and 57kDa and a range of pI from 4.5 to 5.4. The theoretical mass of Atp5b is 56.3kDa and pI is 5.2. The details of all 17 spots and the Atp5b peptides identified in each are shown in Table 4.4 and Figure 4.5.

The most statistically significant alterations in Sham vs. MI were in the down-regulated Ldhb, tubulin α -4A chain (Tuba4a) and Atp5b and in the up-regulated enoyl-CoA hydratase (Echs1) and Myl2. Some of the highest fold change values in Sham vs. MI were seen in the down-regulated Atp5b, tropomyosin (Tpm1), NADH-ubiquinone oxidoreductase 75kDa subunit (Ndufs1) and 14-3-3 epsilon (Ywhae) and

the up-regulated Myl2 and Alb. Three spots with qualitative differences yielded protein identification results. These were galectin-5 (Lgals5) and Myl2 which were both absent in Sham and present in the MI gels, and troponin T (Tnnt2) which was present in Sham but absent in the MI gels.

Figure 4.4 Example of a wide-range 2DE gel produced for this analysis Image shows the positions of spots which differed significantly and from which protein identifications were obtained. Spots identified as ATP synthase subunit β shown in pink, all others in yellow. Numbers next to spots are SSP identifiers assigned by PDQuest.



Other proteins altered in Sham vs. MI were peroxiredoxin-6 (Prdx6) which was up-regulated and thioredoxin-dependent peroxide reductase (Prdx3) which was down-regulated. The heat shock protein stress-70 (Hspa9) was also down-regulated.

Some of the above proteins were also altered in MI vs. BMMNC. Many of the spots identified as Atp5b were up-regulated in MI vs. BMMNC, as was one of the spots identified as L-lactate dehydrogenase (B or A chain). Tpm1 and Ywhae were also strongly up-regulated in MI vs. BMMNC and Echs1 was significantly down-regulated. Hspa9 and Hspa8 were both up-regulated in MI vs. BMMNC.

Other proteins of interest shown to be altered in MI vs. BMMNC were Cytochrome b-c1 complex subunit 6 (Uqcrh) which was down-regulated by 10 fold (5 fold up-regulation in Sham vs. MI). Adenylyl cyclase-associated protein 1 (Cap1) and Desmin (Des) were significantly up-regulated in MI vs. BMMNC after being down-regulated in Sham vs. MI.

Table 4.2 Spots with significant fold changes for which a single protein ID was found from the wide-range analysis. SSP are spot identification numbers assigned by PDQuest software. Mascot details are as follows; mascot score (the sum of the peptide scores), the number of peptides found and the sequence coverage of these peptides (only including peptides with individual scores over 35). Theoretical *Mr* and *pI* values for the protein identified are shown as well as the observed *Mr* and *pI* of the spot as estimated from its position in the gel.

SSP	Observed in gel		Theoretical		Protein name	UniProtKB/Swiss-Prot Accession	Mascot		
	Mr	PI	Mr	PI			Score	pep's	% sc
1206	17500	4.40	18868	4.86	Myosin regularory light chain 2	P08733	57	1	8
1207	19000	4.40	113780	8.4	NAD(P) transhydrogenase	Q61941	58	1	2
1213	17500	4.40	18868	4.86	Myosin regularory light chain 2	P08733	108	2	16
1225	21000	4.50	56318	5.19	ATP synthase subunit beta	P10719	192	2	7
1226	19000	4.50	56318	5.19	ATP synthase subunit beta	P10719	105	2	6
1248	25000	4.50	35709	4.95	Troponin T, cardiac muscle	P50753	59	1	3
1320	29000	4.50	32661	4.69	Tropomyosin alpha-1 chain (or Tropomyosin beta chain)	P04692	58	1	4
1424	34000	4.60	56318	5.19	ATP synthase subunit beta	P10719	131	2	8
1430	34500	4.40	29155	4.63	14-3-3 protein epsilon	P62260	164	3	20
2119	14500	4.80	10417	4.90	Cytochrome b-c1 complex subunit 6	Q5M9I5	131	1	20
2443	35000	4.80	56318	3.00	ATP synthase subunit beta	P10719	91	1	3
2546	45000	4.80	51556	7.16	Adenylyl cyclase-associated protein 1	Q08163	55	1	4
2609	47500	4.80	56318	5.19	ATP synthase subunit beta	P10719	457	6	12
2616	47500	4.80	32803	4.80	40S ribosomal protein SA	P38983	50	1	4
2626	52500	4.90	56318	5.19	ATP synthase subunit beta	P10719	167	3	8
2712	57500	4.90	56318	5.19	ATP synthase subunit beta	P10719	707	8	26
3208	22000	5.00	56318	5.19	ATP synthase subunit beta	P10719	51	1	4
3209	20000	5.00	56318	5.19	ATP synthase subunit beta	P10719	144	2	5
3228	15000	5.20	18868	4.86	Myosin regularory light chain 2	P08733	135	3	20
3305	25000	5.00	22142	5.03	Myosin light chain 3	P16409	334	5	33
3433	34000	5.00	56318	5.19	ATP synthase subunit beta	P10719	436	6	18
3441	35000	5.00	68686	6.09	Serum albumin	P02770	46	1	2
3518	42500	5.10	73812	5.97	Stress-70 protein (aka HSPA9)	P48721	85	1	2
3523	40000	5.20	56318	5.19	ATP synthase subunit beta	P10719	280	4	14
3626	54500	5.20	56318	5.19	ATP synthase subunit beta	P10719	711	9	29

Table 4.2 continued.

SSP	Observed in gel		Theoretical		Protein name	UniProtKB/Swiss-Prot Accession	Mascot		
	Mr	PI	Mr	PI			Score	pep's	% sc
3627	57000	5.20	53424	5.21	Desmin	P48675	463	7	20
3632	47000	5.20	56318	5.19	ATP synthase subunit beta	P10719	314	5	16
3636	57000	5.10	56318	5.19	ATP synthase subunit beta	P10719	226	5	15
3706	57000	5.10	56318	5.19	ATP synthase subunit beta	P10719	215	3	9
4207	19000	5.40	223370	5.59	Myosin-6	P02563	279	4	3
4217	21500	5.50	42000	5.23	Actin , alpha cardiac muscle 1 (or ACTS, or ACTA)	P68035	218	3	10
4235	24000	5.40	56318	5.19	ATP synthase subunit beta	P10719	110	2	4
4329	29000	5.40	56318	5.19	ATP synthase subunit beta	P10719	69	1	2
4521	37000	5.40	36589	5.70	L-lactate dehydrogenase B chain (or LDHA)	P42123	72	1	3
4523	43000	5.60	49892	4.95	Tubulin alpha-4A chain	Q5XIF6	191	3	11
4702	60000	5.20	73812	5.97	Stress-70 protein (aka HSPA9)	P48721	739	10	21
5311	29000	6.00	28277	7.14	Thioredoxin-dependent peroxide reductase (Peroxiredoxin-3)	Q9Z0V6	89	2	0
5408	32000	5.80	24803	5.64	Peroxiredoxin-6	O35244	388	7	44
5715	70000	5.90	68686	6.09	Serum albumin	P02770	379	5	11
6424	38500	6.20	36589	5.70	L-lactate dehydrogenase B chain	P42123	85	1	4
6425	37000	6.20	36589	5.70	L-lactate dehydrogenase B chain	P42123	77	1	6
6636	50000	6.10	~70000	~5.45	Heat shock cognate 71Da (aka HSPA8)	P63018	46	1	2
7110	16000	6.30	16186	6.17	Galectin-5	P47967	157	3	21
7112	17000	6.50	79362	5.65	NADH-ubiquinone oxidoreductase 75 kDa subunit	Q66HF1	102	2	2
7323	31500	6.60	31496	8.39	Enoyl-CoA hydratase	P14604	71	1	3
7608	52500	6.50	68686	6.09	Serum albumin	P02770	177	3	6
7702	70000	6.40	58307	5.85	Hydroxysteroid dehydrogenase-like protein 2	Q4V8F9	75	2	4
7722	62000	6.60	67123	8.76	Dihydrolipoyllysine-residue acetyltransferase component of pyruvate dehydrogenase complex	P08461	228	4	9
7723	67500	6.60	71570	6.75	Succinate dehydrogenase [ubiquinone] flavoprotein subunit	Q920L2	73	1	2
8710	67000	6.60	66140	6.15	WD repeat-containing protein 1	Q5RKI0	157	4	11
8853	67500	6.70	79293	7.70	Methylcrotonoyl-CoA carboxylase subunit alpha (mouse)	Q5I0C3	166	3	6

Table 4.3 Proteins found to have significant fold changes in either the Sham vs. MI or the MI vs. BMMNC comparisons from the wide-range analysis. SSP are spot identification numbers assigned by PDQuest software. Sham = sham operated group, MI = MI group treated with PBS, BMMNC = MI group treated with bone marrow mononuclear cells. Fold changes are shown alongside the p-values (Student's *t*-test). 'On' and 'Off' in the FC column indicate presence or absence of the spots, e.g. in spot 1206 'On' indicates the spot was absent in Sham but present in MI.

SSP	Protein name	SHAM vs. MI		MI vs. BMMNC	
		FC	p-value	FC	p-value
Mitochondrial/Oxidative Phosphorylation					
1225	ATP synthase subunit beta	-13.1	0.021	12.7	ns
1226	ATP synthase subunit beta	-2.4	ns	3.0	0.037
1424	ATP synthase subunit beta	-1.5	ns	2.8	0.001
2443	ATP synthase subunit beta	-3.7	ns	3.6	0.005
2609	ATP synthase subunit beta	-2.0	ns	2.5	0.000
2626	ATP synthase subunit beta	-1.0	ns	3.7	0.042
2712	ATP synthase subunit beta	-2.4	ns	3.3	0.031
3208	ATP synthase subunit beta	-1.9	ns	3.8	0.001
3209	ATP synthase subunit beta	-2.6	ns	4.6	0.009
3433	ATP synthase subunit beta	-2.6	0.008	2.9	0.003
3523	ATP synthase subunit beta	-1.9	ns	2.7	0.000
3626	ATP synthase subunit beta	-2.2	0.002	3.0	0.002
3632	ATP synthase subunit beta	-1.7	ns	2.9	0.014
3636	ATP synthase subunit beta	-5.7	0.009	8.7	0.0004
3706	ATP synthase subunit beta	-2.1	ns	4.5	0.009
4235	ATP synthase subunit beta	-3.3	ns	8.2	0.040
4329	ATP synthase subunit beta	-5.6	0.002	5.4	ns
2119	Cytochrome b-c1 complex subunit 6	5.8	0.015	-10.2	0.007
7112	NADH-ubiquinone oxidoreductase 75 kDa subunit	-9.8	0.007	7.1	ns
1207	NAD(P) transhydrogenase	3.83	0.027	-1.11	ns
7723	Succinate dehydrogenase [ubiquinone] flavoprotein subunit	-2.7	0.045	2.4	0.026

Table 4.3 continued.

SSP	Protein name	SHAM vs. MI		MI vs. BMMNC	
		FC	p-value	FC	p-value
Energy Metabolism					
7722	Dihydrolipoyllysine-residue acetyltransferase component of pyruvate dehydrogenase complex	5.8	0.021	-5.0	0.039
7323	Enoyl-CoA hydratase	2.4	0.002	-2.6	0.007
6425	L-lactate dehydrogenase B chain	-6.2	0.001	5.6	ns
6424	L-lactate dehydrogenase B chain	-3.3	0.038	3.2	ns
4521	L-lactate dehydrogenase B chain (or LDHA)	-2.8	ns	2.7	0.028
8853	Methylcrotonoyl-CoA carboxylase subunit alpha (mouse)	-2.7	ns	3.4	0.033
Antioxidants					
5408	Peroxiredoxin-6	-2.5	0.038	2.4	0.018
5311	Thioredoxin-dependent peroxide reductase (PRDX3)	2.9	0.030	-1.1	ns
Heat Shock Proteins					
6636	Heat shock cognate 71Da (aka HSPA8)	-1.3	ns	2.9	0.048
3518	Stress-70 protein (aka HSPA9)	-3.3	0.011	2.9	ns
4702	Stress-70 protein (aka HSPA9)	-1.9	ns	2.7	0.006

Table 4.3 continued.

SSP	Protein name	SHAM vs. MI		MI vs. BMMNC	
		FC	p-value	FC	p-value
Cytoskeletal/Sarcomeric					
4217	Actin , alpha cardiac muscle 1 (or ACTS, or ACTA)	-3.1	0.047	1.0	ns
3627	Desmin	-2.4	0.045	2.6	0.003
3305	Myosin light chain 3	-3.1	0.026	2.7	ns
1206	Myosin regulatory light chain 2	On	-	-1.6	ns
1213	Myosin regulatory light chain 2	7.1	0.002	-1.7	ns
3228	Myosin regulatory light chain 2	9.1	0.010	-1.5	ns
4207	Myosin-6	2.0	ns	-2.9	0.028
1320	Tropomyosin alpha-1 chain (or Tropomyosin beta chain)	-9.95	0.007	11.30	0.037
1248	Troponin T, cardiac muscle	Off	-	On	-
4523	Tubulin alpha-4A chain	-4.5	0.002	2.6	ns
Others					
1430	14-3-3 protein epsilon	-9.1	0.027	12.5	0.007
2616	40S ribosomal protein SA	-1.2	ns	3.3	0.035
2546	Adenylyl cyclase-associated protein 1	-4.1	0.010	6.2	0.002
7110	Galectin-5	On	-	-9.9	ns
7702	Hydroxysteroid dehydrogenase-like protein 2	-2.7	ns	3.7	0.011
8710	WD repeat-containing protein 1	-2.1	ns	2.7	0.014
5715	Serum albumin	4.23	0.035	-2.61	ns
7608	Serum albumin	9.25	0.028	-1.45	ns
3441	Serum albumin	-2.36	ns	3.04	0.008

Table 4.4 Details of the ATP synthase subunit β peptides identified in 17 different spots in the wide-range analysis. A SSP are spot identification numbers assigned by PDQuest software. Significant fold changes are shown for both the Sham vs. MI and the MI vs. BMMNC comparisons. Then the ‘Observed’ *Mr* and *pI* as determined from the position of the spot in the gel are shown. Mascot details are as follows; mascot score (the sum of the peptide scores), the number of peptides found and the sequence coverage of these peptides (only including peptides with individual scores over 35), and the peptides identified for this spot are shown in the right hand column (* see Table B). **B** The amino acids included in peptides 1-16 (M) is oxidation of methionine.

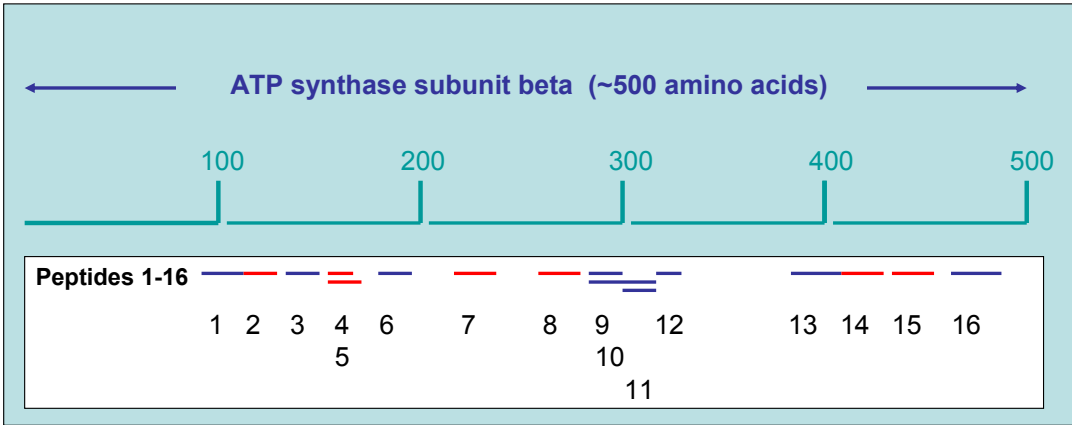
A

SSP	Sham vs. MI	MI vs. BMMNC	Obs. Mr	Obs. pI	Mascot			Peptides identified *
					Score	pep's	% sc	
1226		3.0	19.0	4.5	105	2	6	13, 14
3209		4.6	20.0	5.0	144	2	5	2, 4
1225	-13.1		21.0	4.5	192	2	7	13, 14
3208		3.8	22.0	5.0	51	1	4	3
4235		8.2	24.0	5.4	110	2	4	2, 14
4329	-5.6		29.0	5.4	69	1	2	2
1424		2.8	34.0	4.6	131	2	8	13, 15
3433	-2.6	2.9	34.0	5.0	436	6	18	1, 2, 4, 5, 7, 10
2443		3.6	35.0	4.8	91	1	3	13
3523		2.7	40.0	5.2	280	4	14	8, 10, 13, 14
3632		2.9	47.0	5.2	314	5	16	4, 8, 13, 14, 15
2609		2.5	47.5	4.8	457	6	12	2, 4, 7, 9, 10, 11
2626		3.7	52.5	4.9	167	3	8	2, 4, 13
3626	-2.2	3.0	54.5	5.2	711	9	29	2, 3, 4, 7, 9, 10, 12, 13, 15
3636	-5.7	8.7	57.0	5.1	226	5	15	3, 4, 12, 14, 16
3706		4.5	57.0	5.1	215	3	9	2, 8, 13
2712		3.3	57.5	4.9	707	8	26	2, 4, 7, 9, 10, 11, 13, 15

B

1	95-109	9	282-294
2	110-121 (M)	10	282-310
3	125-143	11	295-310
4	144-155 (M)	12	311-324
5	144-159 (M)	13	388-406
6	189-198	14	407-422 (M)
7	213-225 (M)	15	433-456 (M)
8	265-279 (M)	16	463-480

Figure 4.5 The relative positions of peptides 1-16 along the length of ATP synthase subunit β . Peptides indicated in red include an oxidated methionine.



4.2 Narrow-range protein profiling

4.2.1 2DE

4.2.1.1 pH 4.5-5.5 narrow-range 2DE analysis

17 gel images were selected to be analysed by Progenesis, two images for each sample except for one of the Sham samples for which an image had to be dropped due to low quality. Once gels were aligned and the analysis was run the first 150 spots were checked to remove artefacts wrongly identified as spots. Data for all the spots (~2500) were then exported to Excel [Microsoft, US] and statistics were calculated in the same manner as for the wide-range analysis including Student's *t*-test p-values and fold changes calculated for Sham vs. MI and MI vs. BMMNC.

96 spots were identified as having significant (*t*-test) fold changes >1.5 in either Sham vs. MI or MI vs. BMMNC. After reviewing these 96 spots in Progenesis and excluding spots with poor alignment and definition, 17 were selected to be taken forward for protein identification by LC-MS/MS (see Table 4.5).

Table 4.5 Seventeen spots selected for protein identification from the pH 4.4-5.5 narrow-range Progenesis 2DE analysis Sham = sham operated group, MI = MI group treated with PBS, BMMNC = MI group treated with bone marrow mononuclear cells. Median spot intensities and standard errors for each group are shown alongside the difference, 95% confidence interval and Student's t-test p-value for both Sham vs. MI and MI vs. BMMNC comparisons.

Spot	SHAM		MI		BMMNC		Change in intensity MI/Sham			Change in intensity BMMNC/MI		
	Med.	SE	Med.	SE	Med.	SE	Difference	95% CI	p-value	Difference	95% CI	p-value
17	16456.3	4431.3	5640.1	1772.5	8480.4	1374.9	0.4	(0.15 - 0.59)	0.020	1.5		ns
21	8890.0	1877.1	3321.8	381.8	3923.2	548.8	0.4	(0.34 - 0.50)	0.010	1.0		ns
32	25970.6	4797.7	10230.7	2151.3	10346.0	1971.2	0.4	(0.28 - 0.60)	0.007	1.2		ns
35	11583.3	2135.0	6222.6	290.6	7095.7	1593.0	0.5	(0.42 - 0.50)	0.017	1.2		ns
40	9421.0	4032.9	26788.2	889.6	17615.3	3641.5	2.2	(2.04 - 2.34)	0.017	0.7	(0.37 - 0.93)	0.046
48	19787.0	1447.0	9636.8	3353.0	12276.5	4568.0	0.5	(0.17 - 0.81)	0.010	1.6		ns
54	2798.3	508.9	1384.3	245.1	2081.2	696.7	0.5	(0.32 - 0.64)	0.012	1.7		ns
60	22653.6	4681.6	11979.1	1371.5	16697.1	1627.3	0.5	(0.40 - 0.61)	0.023	1.3		ns
63	4282.4	371.7	6774.7	857.7	8899.7	758.3	1.6	(1.25 - 1.99)	0.018	1.1		ns
66	25427.2	3840.9	13570.1	2168.5	12566.8	418.5	0.6	(0.40 - 0.78)	0.017	1.0		ns
73	3522.3	486.8	2327.3	76.2	2637.9	391.5	0.6	(0.57 - 0.65)	0.026	1.2		ns
75	27861.0	1725.5	17381.1	1804.0	18996.7	2817.7	0.6	(0.47 - 0.71)	0.000	1.2		ns
77	2093.8	204.8	3818.1	354.3	3779.6	324.6	1.5	(1.24 - 1.86)	0.028	1.1		ns
1182	30814.0	6956.4	15009.9	887.0	17102.4	5783.5	0.5	(0.45 - 0.56)	0.024	1.2		ns
1281	34504.8	1132.9	19194.1	2708.5	12648.8	3342.6	0.6	(0.39 - 0.72)	0.010	1.0		ns
1364	5998.1	563.0	3530.0	657.7	5045.9	1661.7	0.6	(0.38 - 0.82)	0.027	1.7		ns
1663	38987.4	4766.1	23396.9	4432.4	40817.8	6880.9	0.7	(0.44 - 0.87)	0.042	1.5	(1.01 - 2.03)	0.049

4.2.1.2 pH 5.5-6.7 narrow-range 2DE analysis

The analysis was initially attempted with all 18 gel images, but the images from one batch of gels were aligning poorly with the others. To achieve good alignment in the experiment and therefore to be able to analyse as many spots as possible, only nine gel images were used for this analysis, one from each sample. Once gels were aligned and the analysis was run the first 150 spots were checked to remove artefacts wrongly identified as spots. Data for all the spots (~2600) was then exported to Excel [Microsoft, US] and statistics were calculated in the same manner as for the wide-range analysis including Student's *t*-test p-values and fold changes calculated for Sham vs. MI and MI vs. BMMNC.

94 spots were identified as having significant (*t*-test) fold changes >1.5 in either Sham vs. MI or MI vs. BMMNC. After checking these 94 spots in Progenesis and excluding spots with poor alignment and definition, 14 were selected to be taken forward for protein identification by LC-MS/MS (see Table 4.6).

Table 4.6 Fourteen spots selected for protein identification from the pH 5.5-6.7 narrow-range Progenesis 2DE analysis Sham = sham operated group, MI = MI group treated with PBS, BMMNC = MI group treated with bone marrow mononuclear cells. Median spot intensities and standard errors for each group are shown alongside the difference, 95% confidence interval and Student's t-test p-value for both Sham vs. MI and MI vs. BMMNC comparisons.

Spot	SHAM		MI		BMMNC		Change in intensity MI/Sham			Change in intensity BMMNC/MI		
	Med.	SE	Med.	SE	Med.	SE	Difference	95% CI	p-value	Difference	95% CI	p-value
29	8735.992	617.74	5558.378	908.20	12429.01	1143.667	0.65	(0.46 - 0.84)	0.041	1.94	(1.56 - 2.31)	0.018
34	18169.01	1289.21	11292.49	853.45	21551.9	2266.008	0.68	(0.58 - 0.78)	0.025	1.81	(1.43 - 2.20)	0.018
35	8308.627	948.29	4885.619	867.98	10435.32	1214.333	0.62		ns	1.78	(1.33 - 2.22)	0.049
36	2404.492	262.51	1463.403	142.25	1876.293	41.88562	0.56	(0.46 - 0.67)	0.018	1.25		ns
39	901.7728	41.37	580.4419	62.77	526.7505	70.22686	0.69	(0.55 - 0.83)	0.023	0.85	(0.62 - 1.08)	0.390
40	4820.258	252.30	7663.654	653.48	4678.896	642.1923	1.48	(1.23 - 1.74)	0.026	0.58	(0.41 - 0.75)	0.028
47	15318.98	566.70	8966.973	619.22	13567.18	1070.384	0.61	(0.53 - 0.69)	0.002	1.38	(1.15 - 1.60)	0.048
49	18272.07	2154.48	14653.65	863.18	23616.89	1006.345	0.78		ns	1.56	(1.43 - 1.69)	0.003
55	15529.82	1089.72	9726.604	981.33	14224.74	374.0915	0.67	(0.54 - 0.80)	0.030	1.46	(1.38 - 1.53)	0.013
1090	5961.77	1141.30	10343.13	522.75	6971.644	1756.699	1.83	(1.65 - 2.01)	0.020	0.62		ns
1112	10372.36	1216.51	6442.62	1464.36	14588.66	1344.001	0.70		ns	1.81	(1.45 - 2.16)	0.039
1189	6443.015	640.87	10478.82	1216.55	10479.68	2394.395	1.76	(1.39 - 2.12)	0.023	0.75		ns
1303	18950.07	1647.97	9461.704	2063.09	13524.28	1919.984	0.59	(0.37 - 0.81)	0.048	1.40		ns
1331	8171.816	905.59	4696.44	245.64	6083.712	945.8495	0.60	(0.54 - 0.66)	0.033	1.34		ns

4.2.2 Differentially expressed proteins

Of the 35 spots in total that were selected for protein identification from the two narrow-range analyses, more than one protein was identified in three spots, and no identity was obtained in six spots. In total 22 spots yielded a single protein identity (12 from pH4.5-5.5 and 10 from the pH5.5-6.7 analysis) and 16 different proteins were identified. Examples of 2DE gels from both the narrow-range experiments are shown in Figure 4.7. All of the MASCOT search results are detailed in Appendices 3 and 4. A summary table of the 22 spots with single protein identification from each narrow-range analysis are shown in Table 4.8A and B and the fold change and p-values for these 24 spots, organised into functional categories is shown in Table 4.9.

The 12 spots with single protein identifications from the pH 4.5-5.5 narrow range analysis identified seven different proteins. Atp5b subunit was found in two spots, both with a ~2 fold decrease in Sham vs. MI but no significant difference in MI vs. BMMNC. Both of these spots had a lower observed mass than the predicted mass of the full length protein (Table 4.7). Two spots were identified as Tpm1, both of which had increased in Sham vs. MI by ~1.5 fold but no significant difference in MI vs. BMMNC; again one of the spots had a mass much smaller than that predicted for this protein.

Table 4.7 Details of the ATP synthase subunit β peptides identified in 2 different spots in the pH 4.5-5.5 narrow range analysis. SSP are spot identification numbers assigned by Progenesis software. Significant fold changes are shown for both the Sham vs. MI and the MI vs. BMMNC comparisons. The ‘Observed’ *Mr* and *pI* as determined from the position of the spot in the gel are shown. Mascot details are as follows; mascot score (the sum of the peptide scores), the number of peptides found and the sequence coverage of these peptides (only including peptides with individual scores over 35), and the peptides identified for this spot are shown in the right hand column (* see Table 4.3 B).

SSP	Sham vs. MI	MI vs. BMMNC	Obs. Mr	Obs. pI	Mascot			Peptides identified *
					Score	pep's	% sc	
21	-2.39		45	5.00	166	3	7	1, 4, 6
1281	-1.80		15	4.95	209	2	6	13, 14

The 60 kDa heat shock protein (Hspd1) was found in 2 spots in the pH 4.5-5.5 analysis (spots 75 and 1364), both with a 1.7 fold down-regulation in Sham vs. MI and no significant difference in MI vs. BMMNC. These two spots have much lower mass than predicted for the full length protein (35 and 40 compared to 61kDa). This protein was also found in the pH 5.5-6.7 analysis (spot 1090) but had a 1.8 fold up-regulation in Sham vs. MI. This spot is again much smaller than the predicted mass of the full size protein but larger (49kDa) than both of the spots found in the pH 4.5-5.5 analysis. In the two spots from the pH 4.5-5.5 analysis, Hspd1 peptides identified covered 26% of the amino acid sequence between 293 and 493 for spot 75 and 12% of the amino acid sequence between 251 and 493 for spot 1364. In spot 1090 from the pH 5.5-6.7 analysis, Hspd1 peptides identified covered 42% of the amino acid sequence between 61 and 446. This is illustrated in Figure 4.6.

Figure 4.6 The relative positions of protein sequence covered by the 60kDa heat shock protein peptides identified in three spots from the narrow-range analyses.

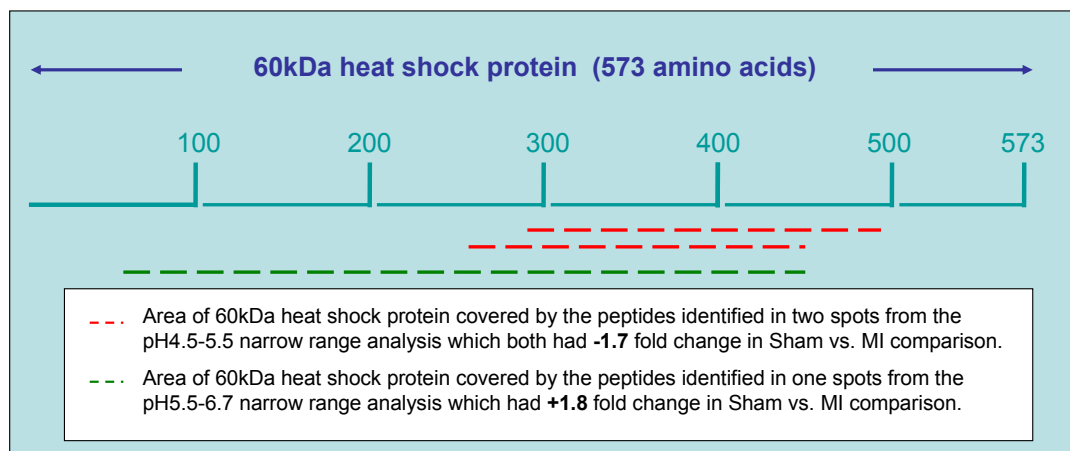
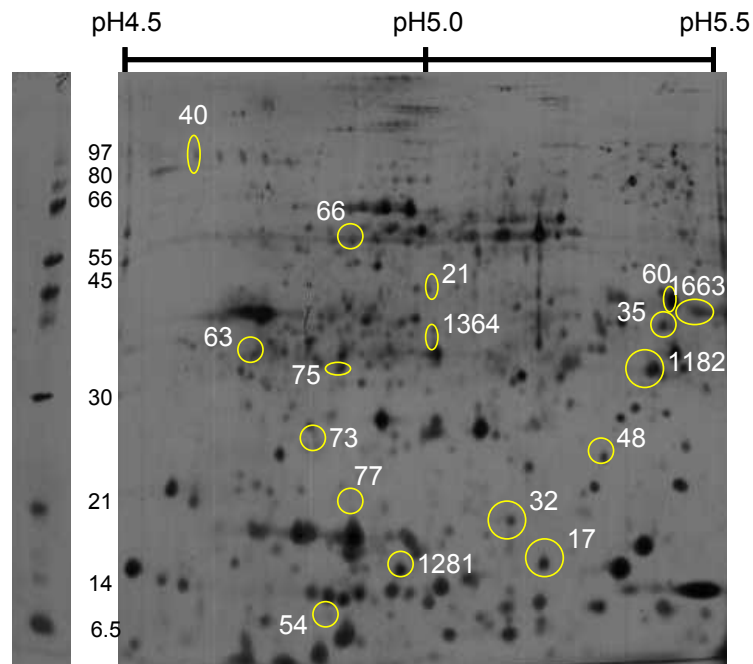
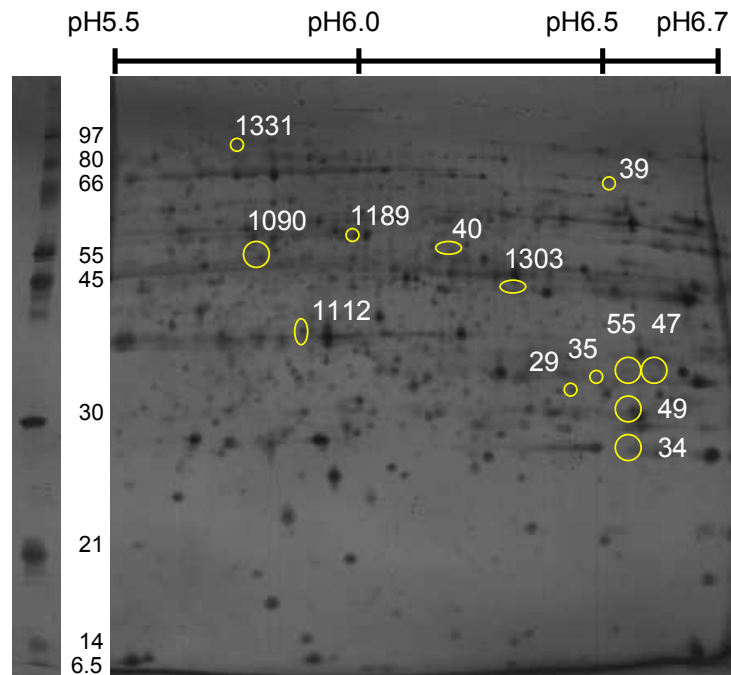


Figure 4.7 Examples of the narrow range 2DE gels produced in this analysis **A)** Example of a pH4.5-5.5 2DE gel. **B)** Example of a pH5.5-6.7 2DE gel. Images shows the positions of spots which differed significantly and from which protein identifications were obtained. Numbers next to spots are SSP identifiers assigned by Progenesis.

A



B



A fragment of Myosin-6 (Myh6) was identified from spot 1663 shown to be down-regulated in Sham vs. MI. This was the only protein identified from the pH 4.5-5.5 analysis which had a significant difference in the MI vs. BMMNC analysis. Two other proteins were identified as being down-regulated in Sham vs. MI but unaltered in MI vs. BMMNC, namely phosphatidylethanolamine-binding protein 1 (Pebp1) and heat shock protein beta-8 (Hspb8). In the pH 4.5-5.5 analysis, four proteins were found in more than one spot. Actin (Actc1) was found in three spots all of which had ~2 fold decrease in Sham vs. MI but no significant difference in MI vs. BMMNC.

In the pH 5.5-6.7 analysis, 10 different proteins were identified, including Hspd1 already mentioned. Two different forms of creatine kinase were identified (Ckm and Ckmt2) in two spots which both had significant down-regulation in Sham vs. MI and were both up-regulated in MI vs. BMMNC. Subunit 10 of NADH dehydrogenase 1 alpha (Ndufa10) was identified as being significantly down-regulated in Sham vs. MI and up-regulated in MI vs. BMMNC. Several energy metabolism proteins were identified, which were down-regulated in Sham vs. MI, namely short chain acyl-CoA dehydrogenase (Acads), phosphoglycerate mutase 1 (Pgam1) and electron transfer flavoprotein subunit alpha (Etf). Pgam1 and Etf were also significantly up-regulated in MI vs. BMMNC. Another energy metabolism protein lipoamide acyltransferase component of branched-chain alpha keto acid dehydrogenase (Dbt) was up-regulated in Sham vs. MI but was not significantly altered in MI vs. BMMNC.

A table detailing all of the proteins identified in the 2DE analyses along with full protein names, accession codes, and the abbreviations used throughout this thesis can be found in Appendix 5.

Table 4.8 Spots with significant fold changes for which a single protein ID was found from the narrow range analyses.

A) Spots from the pH 4.5-5.5 range analysis. **B)** Spots from the pH 5.5-6.7 range analysis. SSP are spot identification numbers assigned by Progenesis software. Mascot details are as follows; mascot score (the sum of the peptide scores), the number of peptides found and the sequence coverage of these peptides (only including peptides with individual scores over 35). Theoretical *Mr* and *pI* values for the protein identified are shown as well as the observed *Mr* and *pI* of the spot as estimated from its position in the gel.

A

SSP	Observed in gel		Theoretical		Protein name	UniProtKB/ Swiss-Prot Accession	Mascot		
	Mr	PI	Mr	PI			Score	pep's	% sc
21	45000	5.00	56318	5.19	ATP synthase subunit beta	ATPB_RAT	166	3	7%
35	42000	5.40	41992	5.23	Actin, alpha cardiac muscle 1	ACTC_RAT	229	3	13%
48	25000	5.30	20788	5.48	Phosphatidylethanolamine-binding protein 1	PEBP1_RAT	388	5	41%
60	43000	5.40	41992	5.23	Actin, alpha cardiac muscle 1	ACTC_RAT	1220	19	48%
63	37000	4.70	32661	4.69	Tropomyosin alpha-1 chain	TPM1_RAT	70	1	5%
73	27500	4.80	21579	4.92	Heat shock protein beta-8 (HSPB8)	HSPB8_RAT	73	2	10%
75	35000	4.85	60917	5.91	60 kDa heat shock protein	CH60_RAT	895	11	26%
77	20000	4.90	32661	4.69	Tropomyosin alpha-1 chain	TPM1_RAT	132	3	9%
1182	35000	5.35	41992	5.23	Actin, alpha cardiac muscle 1	ACTC_RAT	909	10	27%
1281	15000	4.95	56318	5.19	ATP synthase subunit beta	ATPB_RAT	209	2	6%
1364	40000	5.00	60917	5.91	60 kDa heat shock protein	CH60_RAT	316	5	12%
1663	42000	5.45	223370	5.59	Myosin-6	MYH6_RAT	155	3	2%

Table 4.8 B

SSP	Observed in gel		Theoretical		Protein name	UniProtKB/ Swiss-Prot Accession	Mascot		
	Mr	PI	Mr	PI			Score	pep's	% sc
29	35000	6.4	47443	8.64	Creatine kinase, sarcomeric	KCRS_MOUSE	183	3	6%
35	37500	6.45	43018	6.58	Creatine kinase M-type	KCRM_RAT	82	2	4%
47	37000	6.6	34929	8.62	Electron transfer flavoprotein subunit alpha	ETFA_RAT	232	4	18%
49	37000	6.55	28814	6.67	Phosphoglycerate mutase 1	PGAM1_RAT	333	4	24%
55	37000	6.55	73812	5.97	Stress-70 protein (HSPA9)	GRP75_RAT	241	4	7%
1090	49000	5.8	60917	5.91	60 kDa heat shock protein	CH60_RAT	1453	21	42%
1112	41000	5.9	40468	7.64	NADH dehydrogenase [ubiquinone] 1 alpha subcomplex subunit 10	NDUAA_RAT	679	9	38%
1189	52000	6	53127	8.88	Lipoamide acyltransferase component of branched-chain alpha-keto acid dehydrogenase complex	ODB2_MOUSE	758	13	19%
1303	48000	6.3	44737	8.47	Short-chain specific acyl-CoA dehydrogenase	ACADS_RAT	286	5	12%
1331	85000	5.75	83717	6.95	Elongation factor G 1	EFG1_RAT	120	3	4%

Table 4.9 Proteins found to have significant fold changes in either the Sham vs. MI or the MI vs. BMMNC comparisons from the narrow range analyses SSP are spot identification numbers assigned by PDQuest software. Fold changes are shown alongside the p-values (*t*-test).

SSP	Protein name	SHAM vs. MI		MI vs. BMMNC	
		FC	p-value	FC	p-value
Mitochondrial/Oxidative Phosphorylation					
21	ATP synthase subunit beta	-2.4	0.010	1.0	ns
1281	ATP synthase subunit beta	-1.8	0.010	1.0	ns
1112	NADH dehydrogenase [ubiquinone] 1 alpha subcomplex subunit 10	-1.4	ns	1.8	0.039
Energy Metabolism					
1303	Short-chain specific acyl-CoA dehydrogenase	-1.7	0.048	1.4	ns
47	Electron transfer flavoprotein subunit alpha	-1.6	0.002	1.4	0.048
1189	Lipoamide acyltransferase component of branched-chain alpha-keto acid dehydrogenase complex	1.8	0.023	-1.3	ns
49	Phosphoglycerate mutase 1	-1.3	ns	1.6	0.003
Heat Shock Proteins					
55	Stress-70 protein (aka HSPA9)	-1.5	0.03	1.5	0.013
75	60 kDa heat shock protein	-1.7	0.000	1.2	ns
1364	60 kDa heat shock protein	-1.7	0.027	1.7	ns
73	Heat shock protein beta-8 (HSPB8)	-1.6	0.026	1.2	ns
1090	60 kDa heat shock protein	1.8	0.020	-1.6	ns
Cytoskeletal/Sarcomeric					
35	Actin, alpha cardiac muscle 1	-2.2	0.017	1.2	ns
60	Actin, alpha cardiac muscle 1	-2.0	0.023	1.3	ns
1182	Actin, alpha cardiac muscle 1	-2.0	0.024	1.2	ns
1663	Myosin-6	-1.5	0.042	1.5	0.049
63	Tropomyosin alpha-1 chain	1.6	0.018	1.1	ns
77	Tropomyosin alpha-1 chain	1.5	0.028	1.1	ns
Others					
48	Phosphatidylethanolamine-binding protein 1	-2.0	0.010	1.6	ns
1331	Elongation factor G 1	-1.7	0.033	1.3	ns
29	Creatine kinase, sarcomeric	-1.5	0.041	1.9	0.018
35	Creatine kinase M-type	-1.6	0.049	1.8	0.049

4.3 Validation of proteomic data

Four proteins were chosen for Western blotting to verify the results obtained from both the wide- and narrow-range 2DE experiments. 14-3-3 epsilon and the mitochondrial protein Sdha were chosen for validation as they were functionally interesting proteins which had significant changes in both Sham vs. MI and MI vs. BMMNC comparisons. Atp5b was found not only to differ significantly in our analysis but it was also identified as having several different fragments. Western blotting was used to visualise these. Pebp1 was significantly altered in Sham vs. MI in our narrow range analysis, it was chosen to verify this analysis.

- 14-3-3 epsilon (14-3-3ε)

An assay using a rabbit polyclonal to 14-3-3ε antibody was used to detect a band at approximately 29kDa using an antibody dilution of 1 in 1000 and 20µg total protein loading. The bands from 14-3-3ε and the GAPDH gel run simultaneously can be seen in Figure 4.6. The average normalised band volumes and associated statistics are in Figure 4.7. The average spot intensity data is also shown in Figure 4.7 for comparison. The western blotting revealed a significant 3 fold decrease in 14-3-3ε concentration in Sham vs. MI and a significant 3.2 fold increase in MI vs. BMMNC. The direction of regulation reflected the 2DE data but western blotting fold changes were much more modest than the 2DE data (-9 fold and +12.5 fold respectively).

- Succinate dehydrogenase (Sdha)

An assay using a rabbit polyclonal to Sdha antibody was used to detect a band at approximately 73kDa using an antibody dilution of 1 in 280 and 20ug total protein loading. The bands from Sdha and the GAPDH gel run simultaneously can be seen in Figure 4.6. The average normalised band volumes and associated statistics are in Figure 4.7. The average spot intensity data is also shown in Figure 4.7 for comparison. The western blotting revealed significant differences between the groups in concentration of Sdha. A 1.5 fold decrease in MI compared to Sham did not reach significance in post hoc testing, but a 1.7 fold increase in BMMNC

compared to Sham did reach significance. The fold changes seen in the western blot analysis were slightly smaller than those measured in 2DE analysis.

- Phosphatidylethanolamine-binding protein 1 (Pebp1)

An assay using a rabbit polyclonal to Pebp1 antibody was used to detect a band at approximately 21kDa using an antibody dilution of 1 in 5000 and 10ug total protein loading. The bands from Pebp1 and the GAPDH gel run simultaneously can be seen in Figure 4.6. The average normalised band volumes and associated statistics are in Figure 4.7. The average spot intensity data is also shown in Figure 4.7 for comparison. The direction of change in Pebp1 reflected the 2DE data but did not reach significance.

- ATP synthase subunit β (Atp5b)

An assay using a rabbit polyclonal to ATP synthase beta antibody was optimised at 20ug of total protein lysate, a 1 in 1000 antibody dilution and blocking in 3% milk overnight with 1.5 hour incubations for both primary and secondary antibodies. The antibodies picked up multiple bands between the sizes of 34 and 56kDa. The estimated mass of ATP synthase subunit beta is ~56kDa. Quantification was not performed on this assay however the multiple bands are shown in Figure 4.8. Although quantification was not performed, the sham bands were of a much stronger intensity than MI. BMMNC bands were also more intense than MI but slightly fainter than Sham, reflecting the 2DE results. The same distribution of bands can be seen in all three samples.

Figure 4.8 Western blots of 14-3-3 epsilon (14-3-3 ϵ), succinate dehydrogenase (Sdha), and phosphatidylethanolamine-binding protein 1 (Pebp1) in samples 1-9
 S = sham operated group, M = MI group treated with PBS, B = MI group treated with bone marrow mononuclear cells. Both Pebp1 and Sdha were only measured in 2 of the 3 MI samples. Glyceraldehyde 3-phosphate dehydrogenase (Gapdh) was used for normalisation.

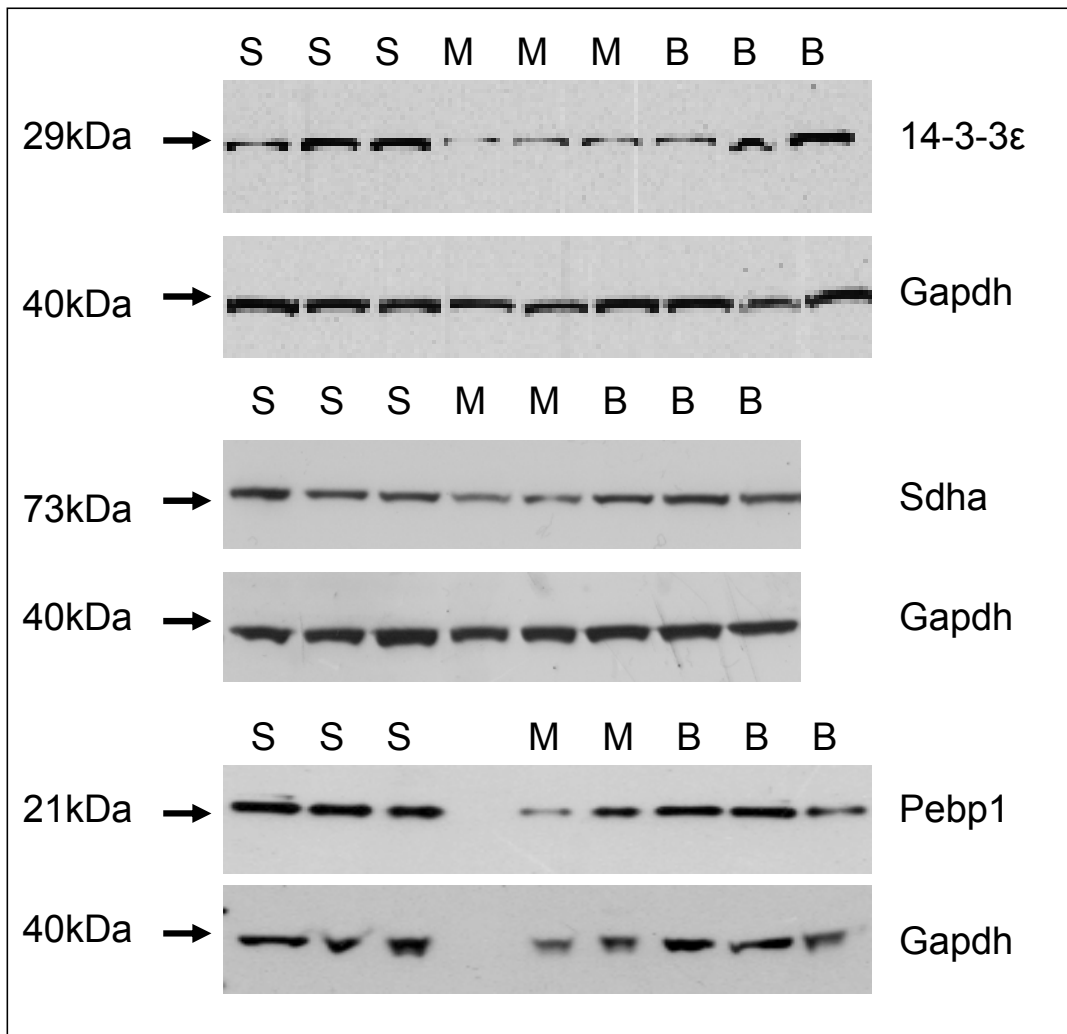


Figure 4.9 The average normalised spot volumes from the 2DE analysis (left) and normalised band volumes from Western blot (WB) analysis (right) for 14-3-3 epsilon (14-3-3ε), succinate dehydrogenase (Sdha), and phosphatidylethanolamine-binding protein 1 (Pebp1) in samples 1-9 Sham = sham operated group, MI = MI group treated with PBS, BMMNC = MI group treated with bone marrow mononuclear cells. Error bars indicate standard deviation. 2DE graphs; significance in Sham vs. MI and MI vs. BMMNC comparisons indicated by the bars, * = *t*-test p-value of 0.05-0.01, ** = *t*-test p-value <0.01, ns = not significant. WB graphs; significance in one way ANOVA indicated in top right hand corner of charts, significance in Sham vs. MI and MI vs. BMMNC comparisons indicated by the bars, * = post-hoc bonferroni p-value of 0.05-0.01, ** = post-hoc bonferroni p-value <0.01, ns = not significant.

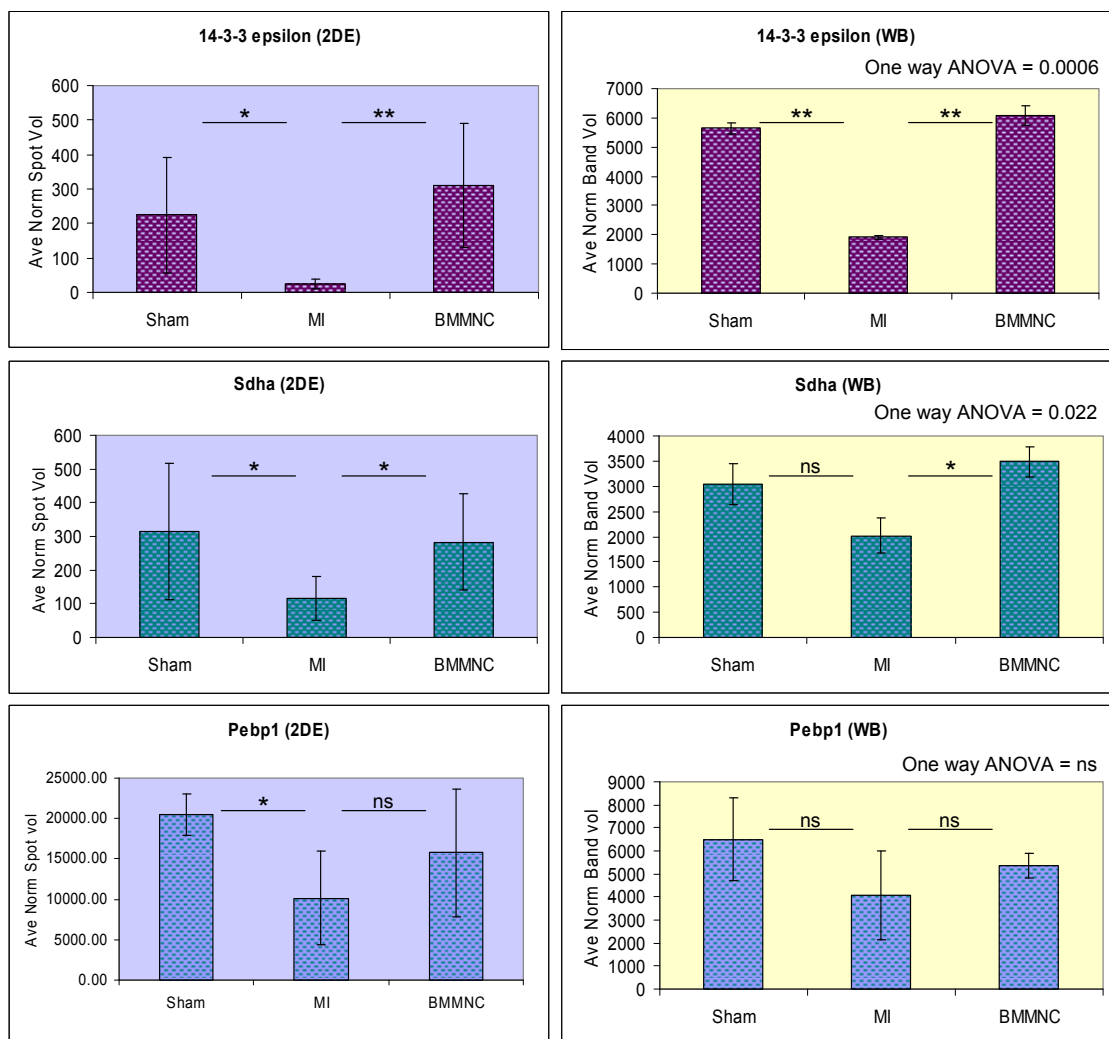
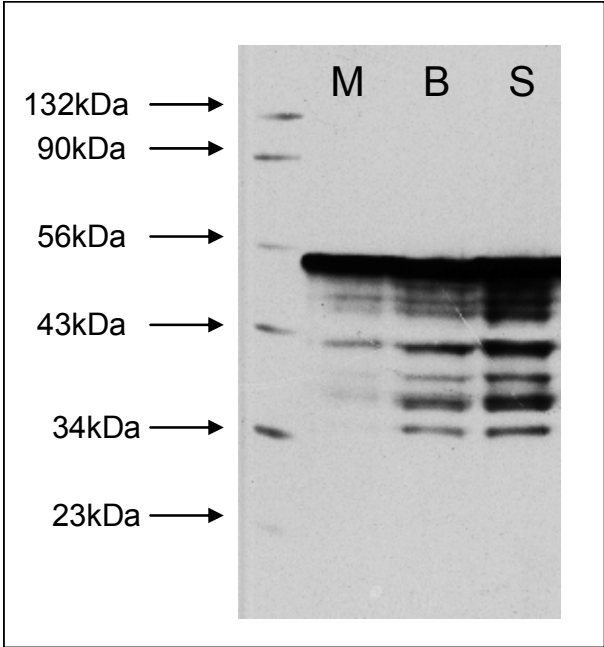


Figure 4.10 Bands detected using an antibody to ATP synthase subunit β S = sham operated group, M = MI group treated with PBS, B = MI group treated with bone marrow mononuclear cells. The Santa Cruz protein molecular weight ladder is on the left of the blot image and the masses of the ladder (in kDa) are labelled on the left of the figure.



5. Gene expression results

5.1 Global expression profiles of samples 1-9 using Illumina RatRef12

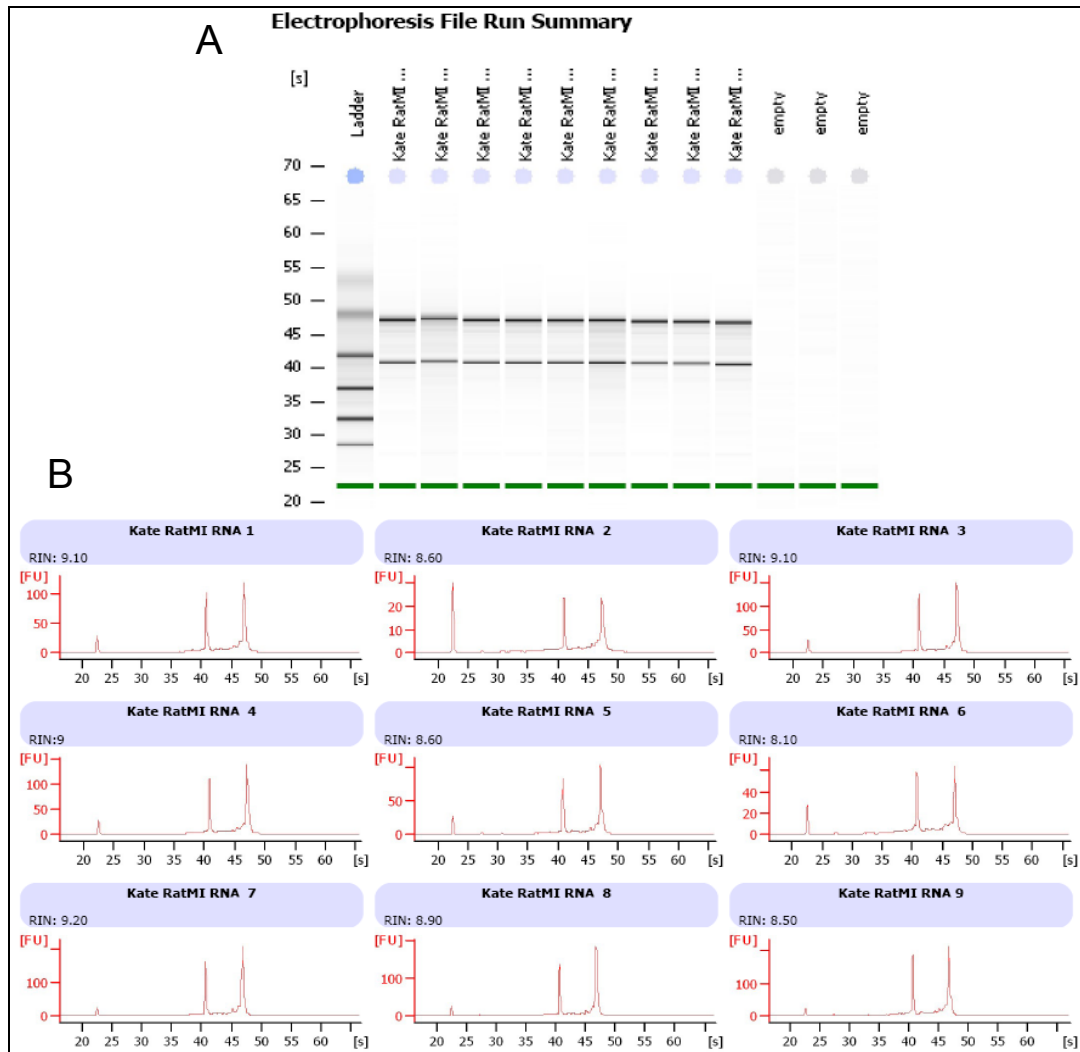
5.1.1 Quality control and quantification of RNA and cRNA

Total RNA was extracted from tissue samples 1-9 using the RNeasy Fibrous Tissue Mini Kit from Qiagen. Approximately 20-30mg of tissue was used from each sample. Yields of RNA ranged from 55-350ng/μl (2.5-17.5μg in total) as recorded by the Agilent bioanalyser 2100, see Table 5.1.

Table 5.1 Preparation, quantification and QC of RNA samples The mRNA samples were prepared from tissue samples 1-9. RNA concentration (ng/μl) and 260/280 ratios are shown for two repeated readings on the Nanodrop. RNA concentration (ng/μl) and RIN scores as read by the Agilent Bioanalyser are shown in the left hand columns.

RNA_ID	SAMPLE_ID (Tissue)	Nanodrop					Agilent results	
		Nano conc. ng/ul	260/280 Ratio	Nano conc. ng/ul	260/280 Ratio	Ave. nano conc. ng/ul	Agilent conc. ng/ul	RIN
Rat MI 1	7	160.3	2.04	153.2	2.07	156.75	185	9.1
Rat MI 2	6	45.7	1.93	45.3	2.09	45.5	55	8.6
Rat MI 3	3	146.6	2.09	158.9	2.02	152.75	210	9.1
Rat MI 4	1	134.3	2.07	129.9	2.06	132.1	200	9
Rat MI 5	4	114.6	2.06	115	2.08	114.8	158	8.6
Rat MI 6	9	91.6	2.09	91.6	2.05	91.6	130	8.1
Rat MI 7	2	151.9	2.07	146	2.08	148.95	261	9.2
Rat MI 8	8	154.8	2.09	145.1	2.07	149.95	245	8.9
Rat MI 9	5	192.6	2.08	201.9	2.07	197.25	335	8.5

Figure 5.1 Summary from the Agilent Eukaryote Total RNA Nano Series II chip results for RNA extracted from samples 1-9 A) electrophoresis results. B) electropherograms including the RIN score for each sample.



All of the RNA samples had a RIN score of over 8, their purity is illustrated in the Agilent Bioanalyser summary in Figure 5.1. In a total RNA extraction, mRNA will only make up 1-3% of the total RNA, >80% is ribosomal RNA, specifically 18S and 28S units. Non-degraded samples should therefore show clear well defined peaks representing these two components, these peaks will appear as broader humps in degraded samples. The first small peak visible in the electropherograms represents the marker.

Approximately, 250ng from each sample (1-9) was selected for cDNA synthesis, purification, cRNA ‘in-vivo’ transcription and labelling using the Ambion Illumina TotalPrep Amplification kit. For this purpose, 100ng/ul stocks were made up for all except Rat MI 2 for which the mRNA concentration was too low; for this sample a 55ng/ul stock was made. One RNA sample from each group was processed in duplicate to assess experimental reproducibility; these were labelled Rat MI 7a, Rat MI 8a and Rat MI 9a and were replicates of Rat MI 7, Rat MI 8 and Rat MI 9 respectively (see Table 5.2).

Table 5.2 Technical replicates of three RNA samples were processed into cRNA

Original RNA sample_ID	Technical replicate for cRNA prep.
Rat MI 7	Rat MI 7a
Rat MI 8	Rat MI 8a
Rat MI 9	Rat MI 9a

The resultant cRNA was quantified using the nanodrop and quality was again assessed using the Agilent Bioanalyser. The cRNA concentrations as determined by the nanodrop ranged from 200-500ng/ul (Table 5.3). The 12 samples were then hybridised to the chip by Genome Centre staff.

Table 5.3 Nanodrop quantification of cRNA prepared using Ambion TotalPrep

cRNA_ID	Nano Conc (ng/ul)
Rat MI 1	454.3
Rat MI 2	453.1
Rat MI 3	425.5
Rat MI 4	410.3
Rat MI 5	504.4
Rat MI 6	200.5
Rat MI 7	428.1
Rat MI 8	406.4
Rat MI 9	328
Rat MI 7a	326.3
Rat MI 9a	459.9
Rat MI 8a	358.8

5.1.2 Quality control of the RatRef12 gene expression chip data

The results from the internal quality control features on the RatRef12 chip were all above accepted ranges, this illustrated the chip run had been successful (Figure 5.2). The hybridization controls showed the high, medium and low values as expected. Both background and noise were well below the accepted levels of 30-60. The low stringency control showed $PM > MM^2$. The gene intensity showed that the housekeeping genes had a much higher average intensity than the average of all the genes. Finally the biotin and high stringency control plot also showed high values.

Scatter plots were used to check for any large differences in signal that may be due to poor data quality. Figure 5.3 shows three scatter plots which compare a technical replicate (scatter plot 1), biological replicates (scatter plot 2) and two samples from different groups (scatter plot 3). A good level of convergence was seen in plot 1, a greater level of divergence was seen in plot 2 and again in plot 3. Plot three shows several points clustering below the line of equal fit indicating several genes had higher expression in sample 8 (Sham) than in sample 7 (MI).

Figure 5.2 BeadStudio Plots of internal quality control features

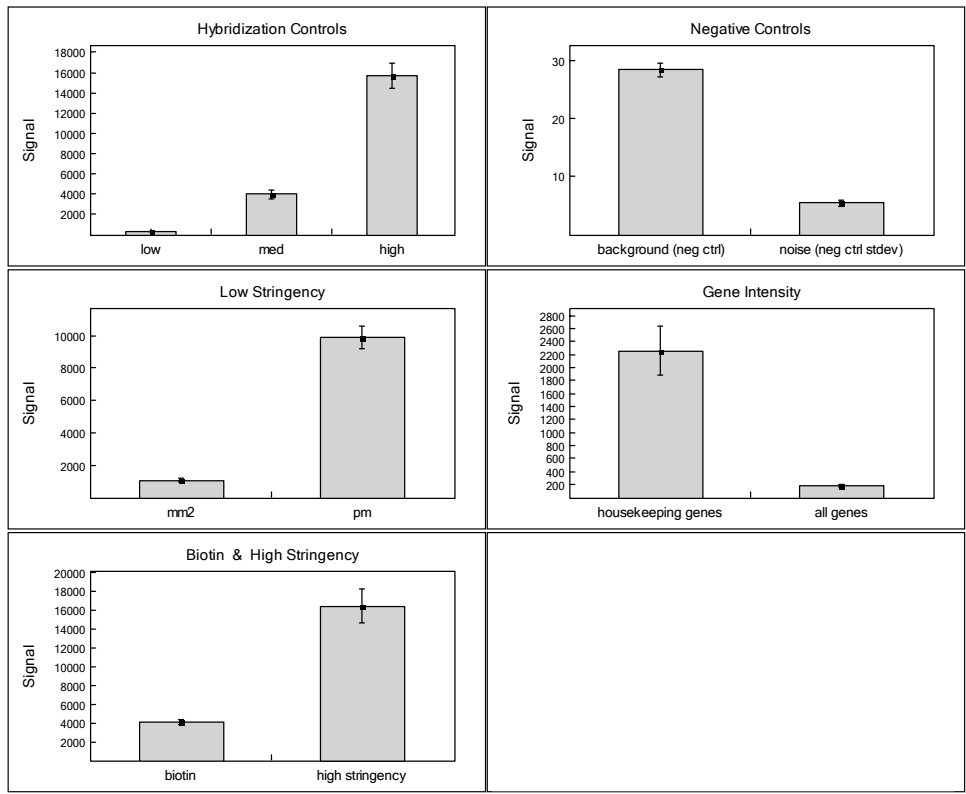
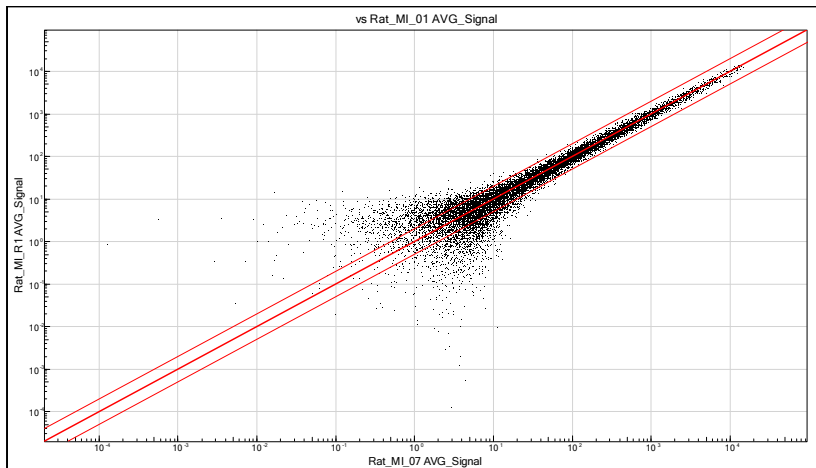
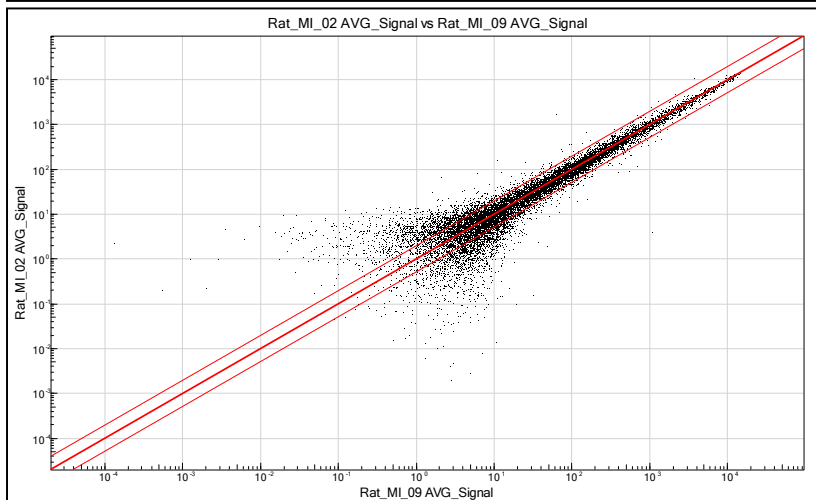


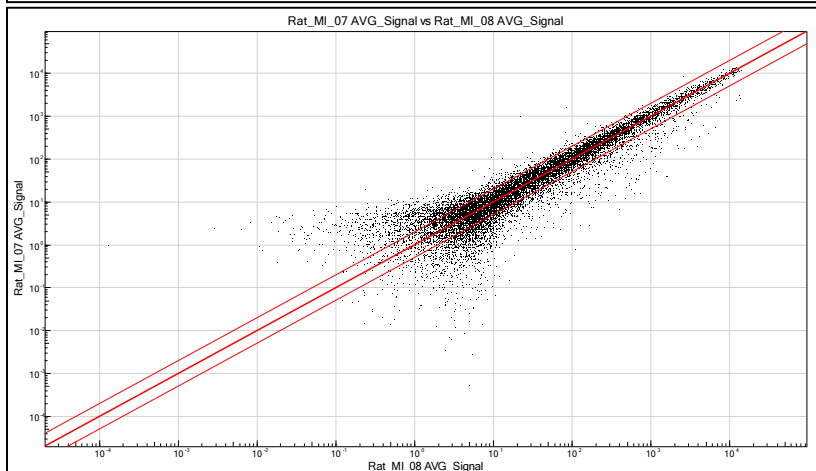
Figure 5.3 Scatter plots of average signal data from two samples Scatter plot 1 shows sample 7 and 7a (technical replicates). Scatter plot 2 shows sample 2 and 9 (closely related samples, both from MI). Scatter plot 3 shows sample 7 and 8 (distantly related MI and Sham)



Scatter plot 1



Scatter plot 2

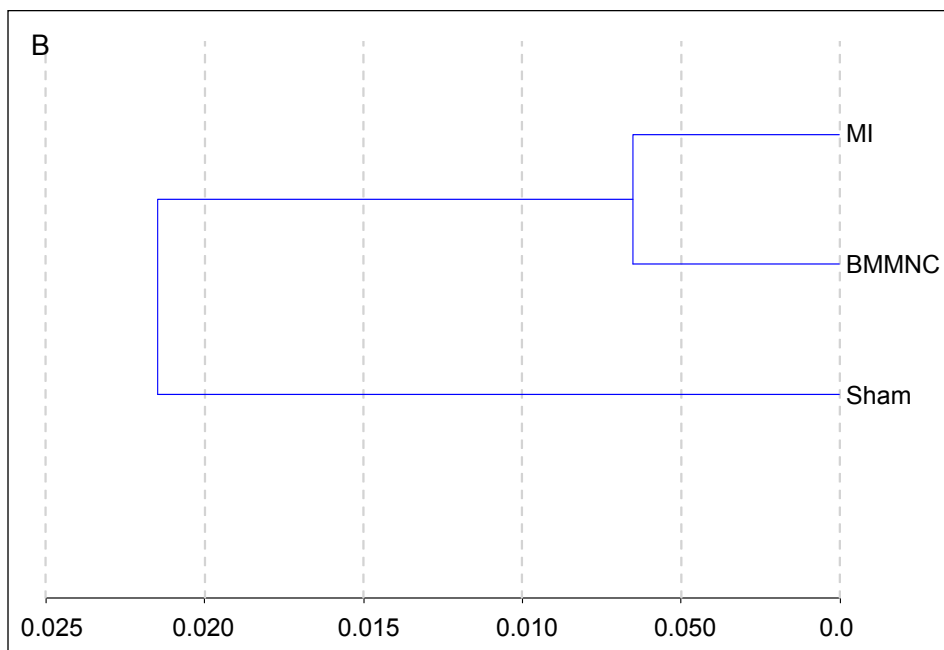
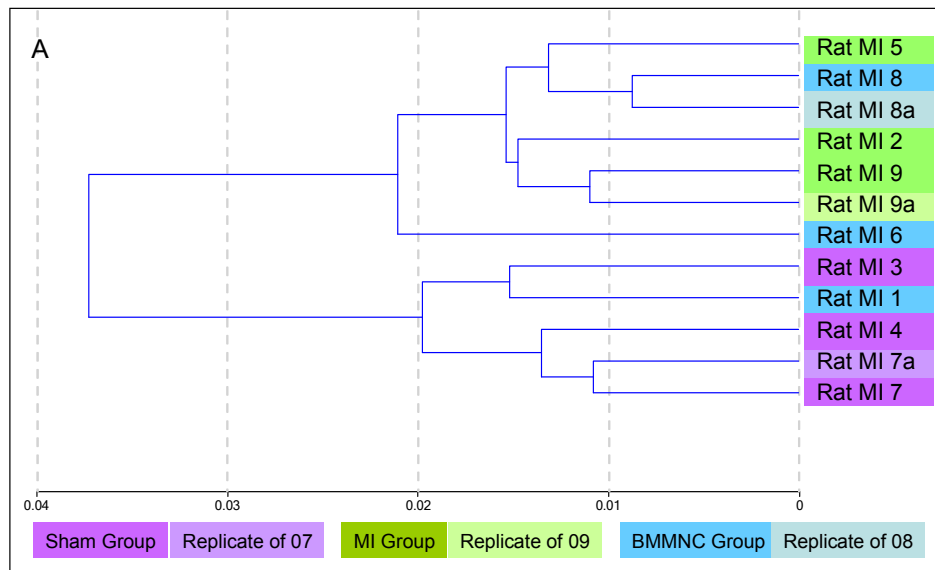


Scatter plot 3

Clustering of the non-processed probe expression data (Figure 5.4 A) reveals that all the samples on the chip were highly related with all samples clustering below ~ 0.037 . Clustering of the technical replicates shows they bear the closest relationships with each pair of technical replicates clustering < 0.012 . The clustering shows that there are two main clusters, the first contains all of the Sham samples and one sample from the BMMNC group. The second cluster contains all of the MI samples and two of the BMMNC samples.

Clustering of the groups according to differentially expressed probes (Figure 5.4 B) indicated the MI and BMMNC group were more highly related to each other than to the Sham group. This data indicates that there are few probes differentially expressed between MI and BMMNC. More probes were differentially expressed between Sham and MI as well as between Sham and BMMNC.

Figure 5.4 Dendrograms produced by BeadStudio showing clustering of non-normalised probe data Sham = sham operated group, MI = MI group treated with PBS, BMMNC = MI group treated with bone marrow mononuclear cells **A)** Shows a dendrogram illustrating clustering for non-normalised data of all samples and replicates. Pink indicates Sham samples and the paler pink indicates 7a which is a replicate of the Sham sample 7. Green indicates MI samples and the paler green indicates 9a which is a replicate of the MI sample 9. Blue indicates BMMNC samples and the paler blue indicates 8a which is a replicate of the BMMNC sample 8. **B)** Shows a dendrogram illustrating experimental groups clustered according to differentially expressed probes.



5.2 Repeat of global expression profiling for samples 1-9 using Illumina RatRef12

5.2.1 Quality control and quantification of RNA and cRNA

The same 9 tissue samples were used in the repeat experiment but this time the samples were heavily ground whilst still frozen before a portion was removed for RNA extraction. The exact quantity of tissue used for each extraction was not measured as the samples were now more prone to defrosting during processing. The amount of tissue was estimated to be 15-25mg. RNA yields were all between 55 to 374ng/ul according to the nanodrop, but the Agilent Bioanalyser estimated them to be approximately 10 times higher (see Table 5.4 A). Figure 5.5 shows the Agilent summary report for these samples, an error in the ladder (see Figure 5.5 A) would explain the high RNA quantification results, and therefore only the Nanodrop quantifications were used.

The RNA qualities were poor for two samples (RNA 1 and RNA 5) and yield was low for one sample (RNA 2) therefore RNA preparation was repeated for these three samples (RNA 1r, RNA 2r and RNA 5r). These three new RNA preparations yielded 43-313ng/ul according to the Nanodrop (see table 5.4 B). All repeated RNA samples were again assessed using the Agilent Bioanalyser. RNA quality was good for all of the samples except RNA 1 and RNA 1r. Agilent quantifications were again very high which was due to an error with the ladder, as seen in the first lane of the image in Figure 5.6 A.

Table 5.4 Quantification and QC of mRNA samples for repeated Illumina RatRef12 chip analysis The mRNA samples were prepared from c.15-25mg tissue samples 1-9. **A)** Quantification and QC results of first attempt at RNA preparations from tissue samples 1-9 for the repeated Illumina chip analysis. **B)** Quantification and QC results from the three repeated RNA preparations (RNA 1r, RNA 2r and RNA 5r). RNA 1, RNA 2 and RNA 5 were run alongside RNA 1r, RNA 2r and RNA 5r in the Agilent analysis.

A

RNA_ID	SAMPLE_ID (Tissue)	Nanodrop		Agilent	
		Nano conc. ng/ul	260/280 Ratio	Agilent conc. ng/ul	RIN
RNA 1	7	269.66	2.04	2,363	5
RNA 2	4	55.23	1.93	479	8.1
RNA 3	1	185.71	2.09	1895	8.6
RNA 4	8	170.12	2.07	1797	8.8
RNA 5	5	108.31	2.06	1149	N/A
RNA 6	2	186.27	2.09	2040	8.8
RNA 7	9	117.78	2.07	1294	8.3
RNA 8	6	114.04	2.09	1356	8.8
RNA 9	3	374.45	2.08	5026	8.7

B

RNA_ID	SAMPLE_ID (Tissue)	Nanodrop		Agilent results	
		Nano conc. ng/ul	260/280 Ratio	Agilent conc. ng/ul	RIN
RNA 1r	7	313.38	2.1	14111	4.3
RNA 2r	4	43.51	2.12	1636	8.2
RNA 5r	5	55.87	2.14	2003	8.2
RNA 1				12369	4.6
RNA 2				2158	8.6
RNA 5				4253	8.4

Figure 5.5 Summary of the Agilent Eukaryote Total RNA Nano Series II chip results for RNA extracted from samples 1-9 for the repeat RatRef12 analysis. A) electrophoresis results. Red markers indicate a failed ladder and a failed RIN score. B) electropherograms including the RIN score for each sample.

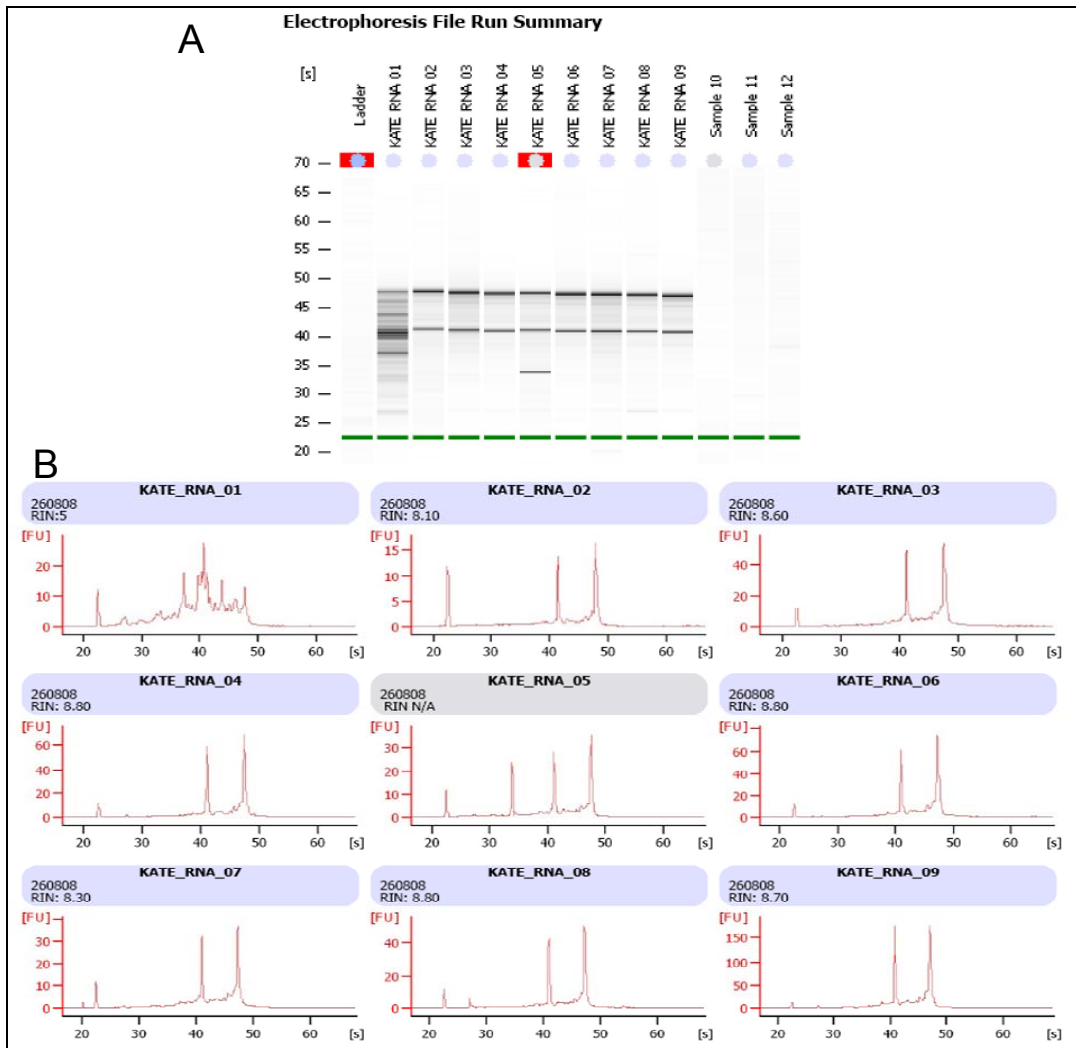
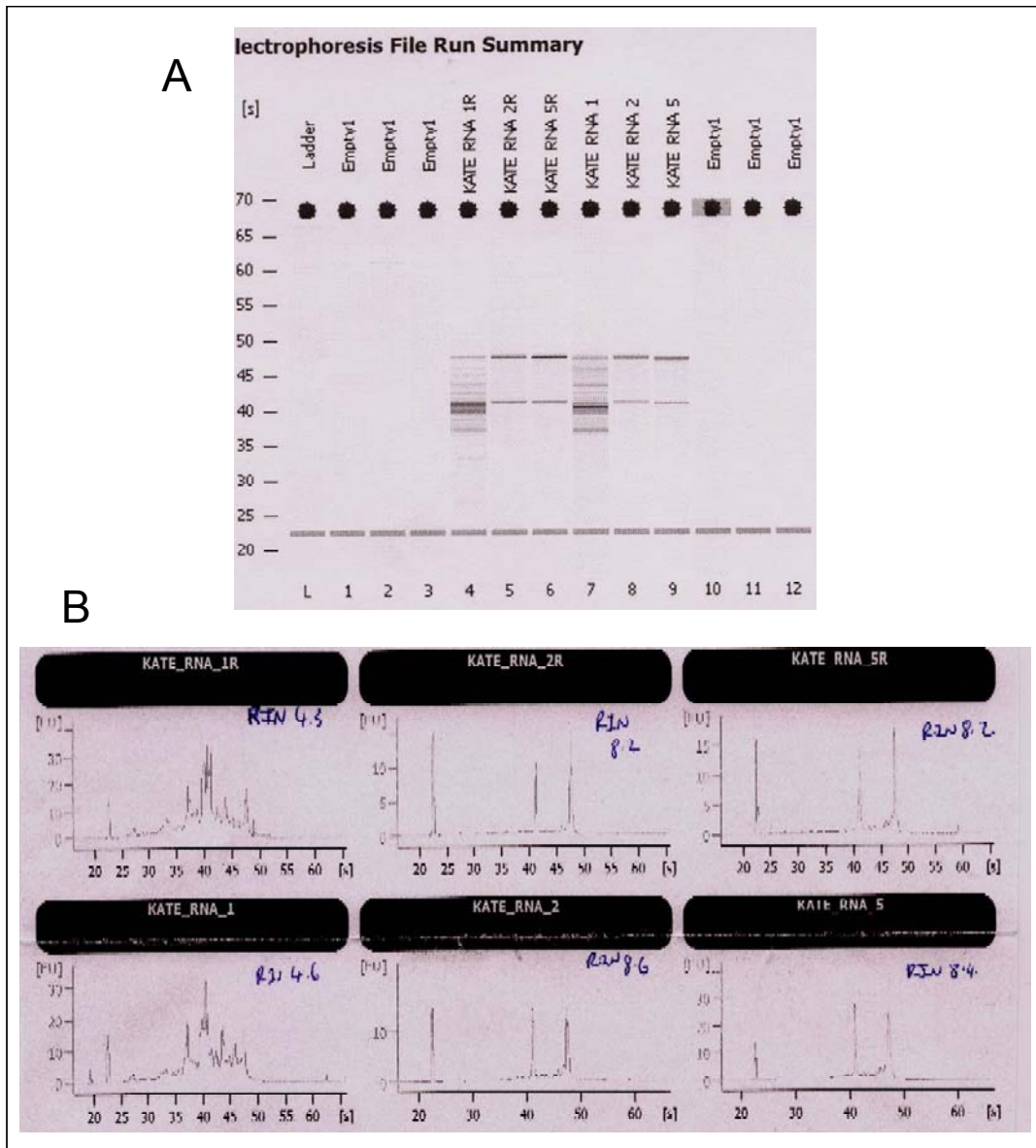


Figure 5.6 Summary of the Agilent Eukaryote Total RNA Nano Series II chip for results of repeat RNA extracts RNA 1r, RNA 2r and RNA 5r for the repeat RatRef12 analysis. RNA 1, RNA 2 and RNA 5 were also run. A) electrophoresis results. B) electroferograms including the RIN score for each sample.



After repeating three of the RNA extractions, eight of the nine samples had RNA with RIN scores > 8. RNA 1 and RNA 1r both had low RIN scores of below 5. The RNA samples RNA 1, 2, 3, 4, 5r, 6, 7, 8, 9 and 1r were all taken forward for cDNA synthesis, purification, cRNA in vivo transcription and labelling. As before, 100ng/ul stocks were made up for each except for RNA 2 and RNA 5r where 50ng/ul stocks were prepared.

The resultant cRNA at the end of processing was quantified using the nanodrop and quality was again checked using the Agilent Bioanalyser. The cRNA samples were determined to be between 95 and 495ng/ul (Table 5.5). The cRNA produced from RNA 1r was of a low concentration and so was not used for hybridisation.

Table 5.5 Nanodrop quantification of cRNA prepared using the Ambion TotalPrep kit

cRNA_ID	Nano Conc (ng/ul)
RNA 1	327.3
RNA 2	448.3
RNA 3	446.1
RNA 4	495.2
RNA 5r	360.5
RNA 6	450.9
RNA 7	428.3
RNA 8	465.7
RNA 9	430.5
RNA 1r	95.7

To look at reproducibility in the hybridisation stages three cRNA samples (RNA 1, RNA 2 and RNA 3), one from each group, were hybridised twice to the chip and referred to as (RNA 1a, RNA 2a and RNA 3a), 12 samples in total.

5.2.2 Quality control and pre-processing for the repeat of the RatRef12 gene expression chip data

5.2.2.1 Quality control for the repeat chip data

The results from the internal quality control features on the RatRef12 chip were again all within accepted ranges showing the chip run had again been successful as shown in Figure 5.7. The hybridization controls showed the high, medium and low values as expected. Both background and noise were well below the accepted levels of 30-60. The low stringency control showed PM>MM2. The gene intensity showed that the housekeeping genes had a much higher average intensity than the average of all the genes. Finally the biotin and high stringency control plot also showed high values. Scatter plots were again used to check for any large differences in signal that may indicate poor data quality. These are shown in Figure 5.8 below.

Figure 5.7 Beadstudio Plots of internal quality control features All QC tools were used except the 'Labelling and Background' feature. Mm2 = mismatch oligos pm = perfect match oligos.

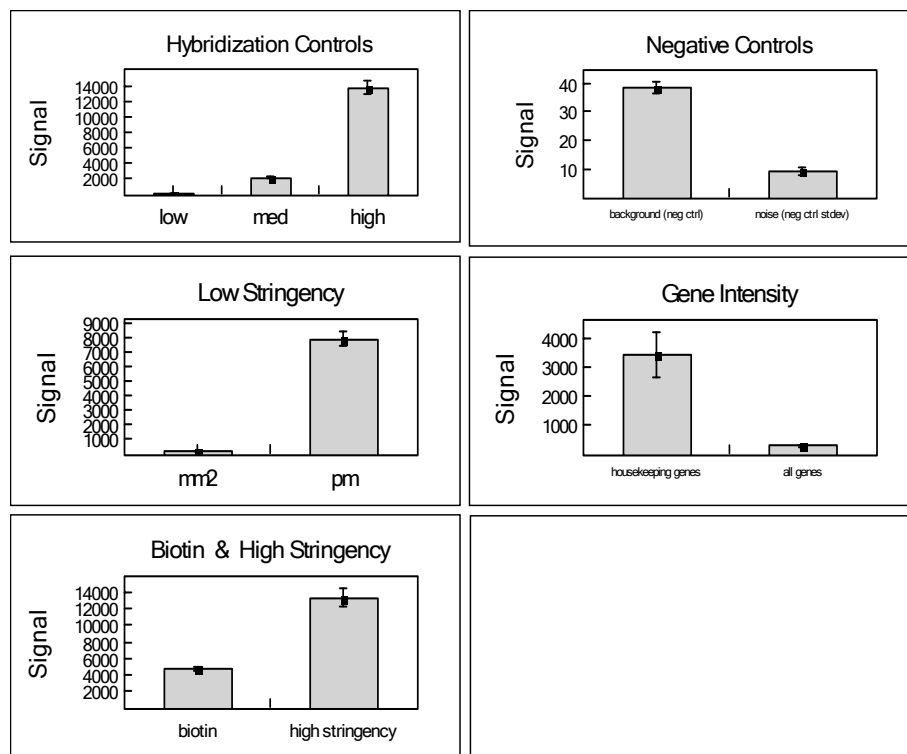
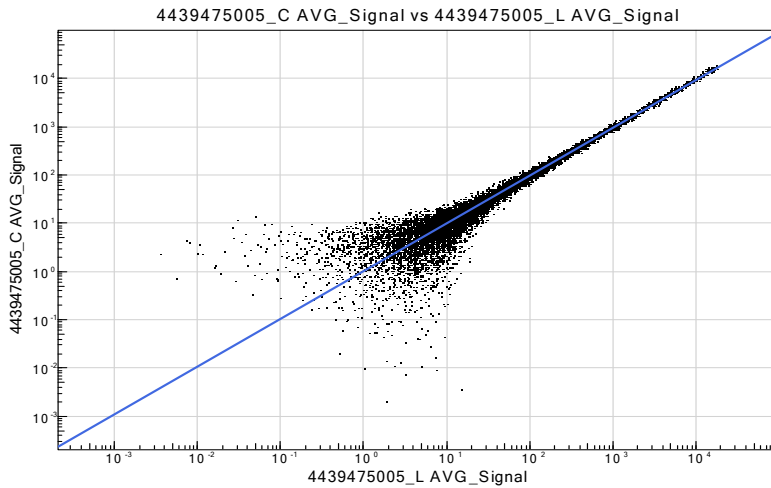
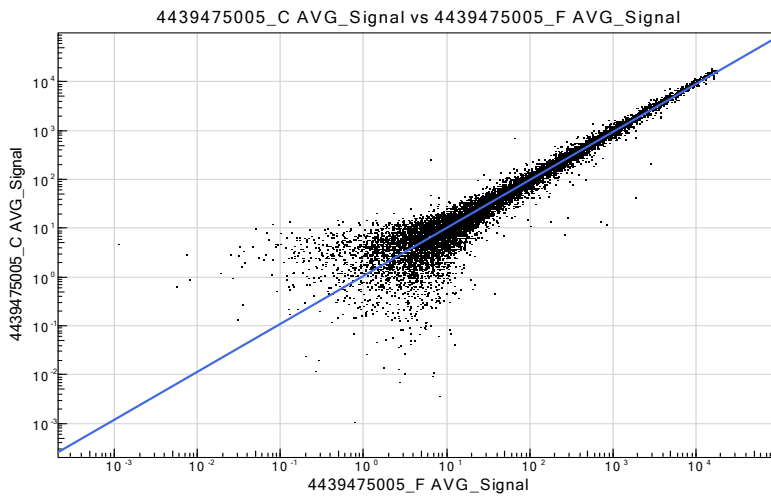


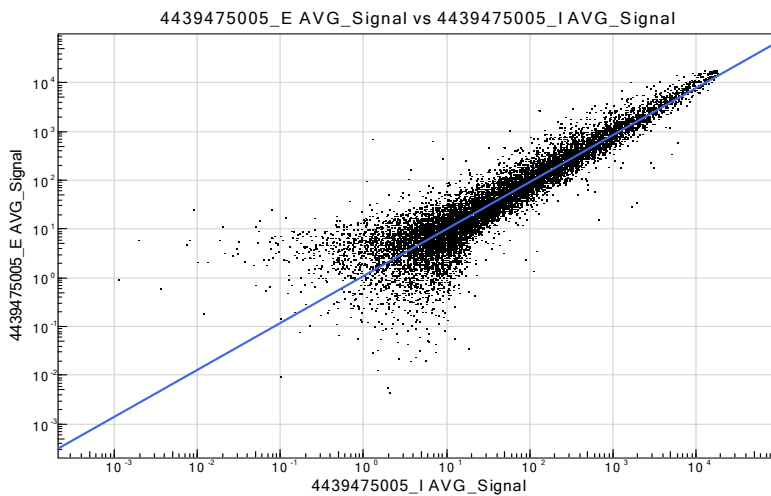
Figure 5.8 Scatter plots of average signal data from two samples Scatter plot 1 shows sample 3 and 3a (technical replicates). Scatter plot 2 shows sample 3 and 6 (closely related samples, both from Sham). Scatter plot 3 shows sample 5 and 9 (distantly related MI and Sham)



Scatter plot 1



Scatter plot 2



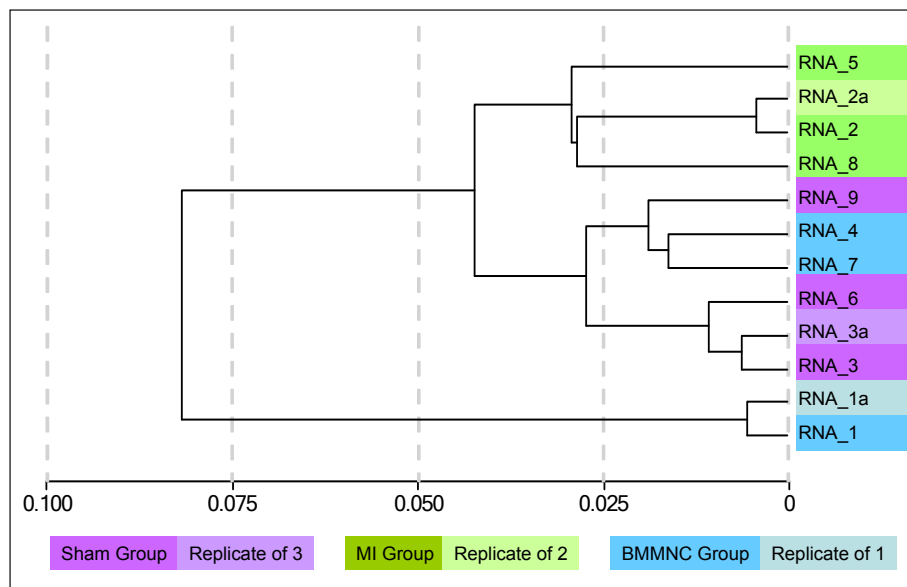
Scatter plot 3

Clustering of the samples according to non processed probe level data is shown in Figure 5.9 A. The samples were more divergent compared to the first chip experiment with all samples clustering below 0.045 apart from RNA 1 which was strongly divergent from the others. The technical replicates all clustered together well, with 3 and 3a just over 0.005, and the other two pairs (1 and 1a, 2 and 2a) just below 0.005.

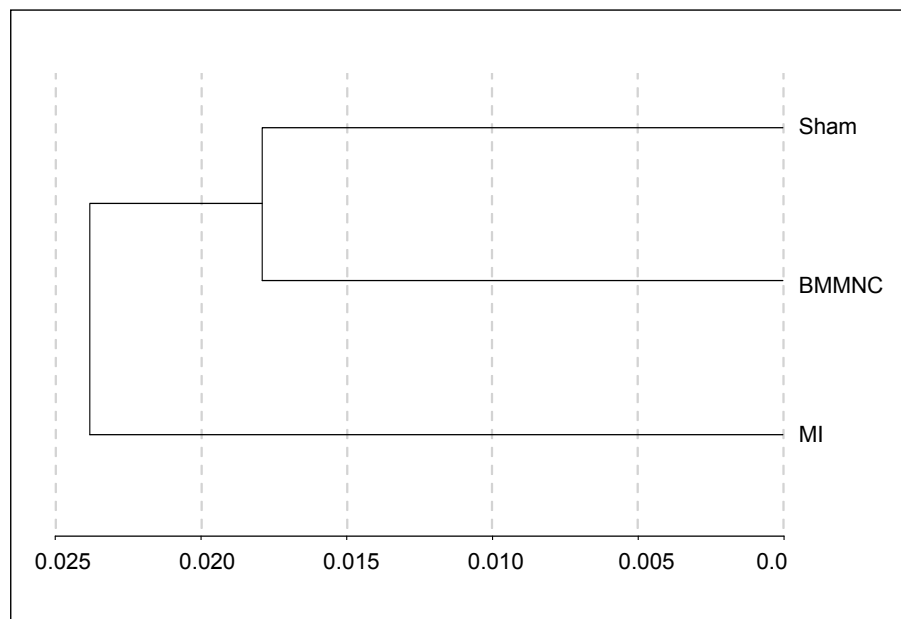
There are three main clusters. Sample RNA 1 and its technical replicate 1a are in one cluster, highly divergent from the other samples as already mentioned. This is the sample which had a very poor RIN score of <5 in comparison to all other samples which had scores >8. The second cluster contains all of the MI samples and the technical replicate of RNA 2 (RNA 2a). The third cluster contains the Sham samples RNA 3 and RNA 6 which are closely related. The other Sham sample, RNA 9 is also in this cluster closely associated with the two BMMNC samples RNA 4 and RNA 7. Clustering of the groups according to differently expressed probes is illustrated in Figure 5.9 B. This dendrogram shows that Sham and BMMNC are the most closely related groups and are divergent from the MI group. This data indicates there are few probes differentially expressed between the Sham and BMMNC groups.

Figure 5.9 Dendrograms produced by BeadStudio showing clustering of non-normalised probe data Sham = sham operated group, MI = MI group treated with PBS, BMMNC = MI group treated with bone marrow mononuclear cells. **A)** Shows a dendrogram illustrating clustering for non-normalised data of all samples and replicates. Pink highlighting indicates Sham samples and the paler pink shading indicates a replicate of the Sham sample 1. Green highlighting indicates MI samples and the paler green shading indicates a replicate of the MI sample 2. Blue highlighting indicates BMMNC samples and the paler blue shading indicates a replicate of the BMMNC sample 3. **B)** Shows a dendrogram illustrating experimental groups clustered according to differentially expressed probes.

A



B



5.2.2.2 Pre-processing of the repeat chip data

Sample 1 was excluded from all further analysis as the probe level data was most certainly affected by low quality of starting material. The probe level intensity data was normalised using Quantile method in BeadStudio and then all data was exported to Excel [Microsoft, US]. Non-detected probes were removed from the dataset (probes with detection p-values >0.05 in 8 or 9 of the 9 samples) leaving a total of 11,701 probes.

5.2.3 Differentially expressed genes discovered using LIMMA

Analysis using LIMMA of the Sham vs. MI comparison revealed 860 probes to be significantly up-regulated and 677 to be down-regulated (FDR adjusted p-value of ≤ 0.05), 13% of the probes had significant differences between the two groups (see Figure 5.10). In MI vs. BMMNC comparison there were 19 probes significantly down-regulated, 18 of which were in the list of probes significantly up-regulated in Sham vs. MI comparison. Only one probe was significantly up-regulated by BMMNC treatment, this probe was also found to be significantly altered in Sham vs. MI.

Figure 5.10 Venn diagram of distribution of differentially expressed probes in the gene expression analysed using LIMMA Sham = sham operated group, MI = MI group treated with PBS, BMMNC = MI group treated with bone marrow mononuclear cells.

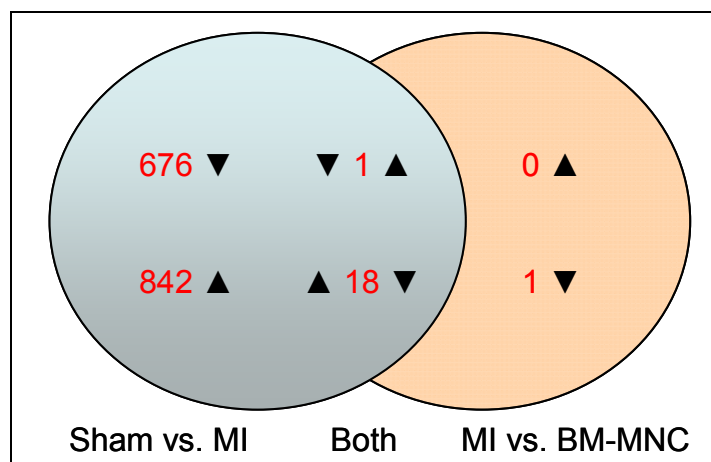
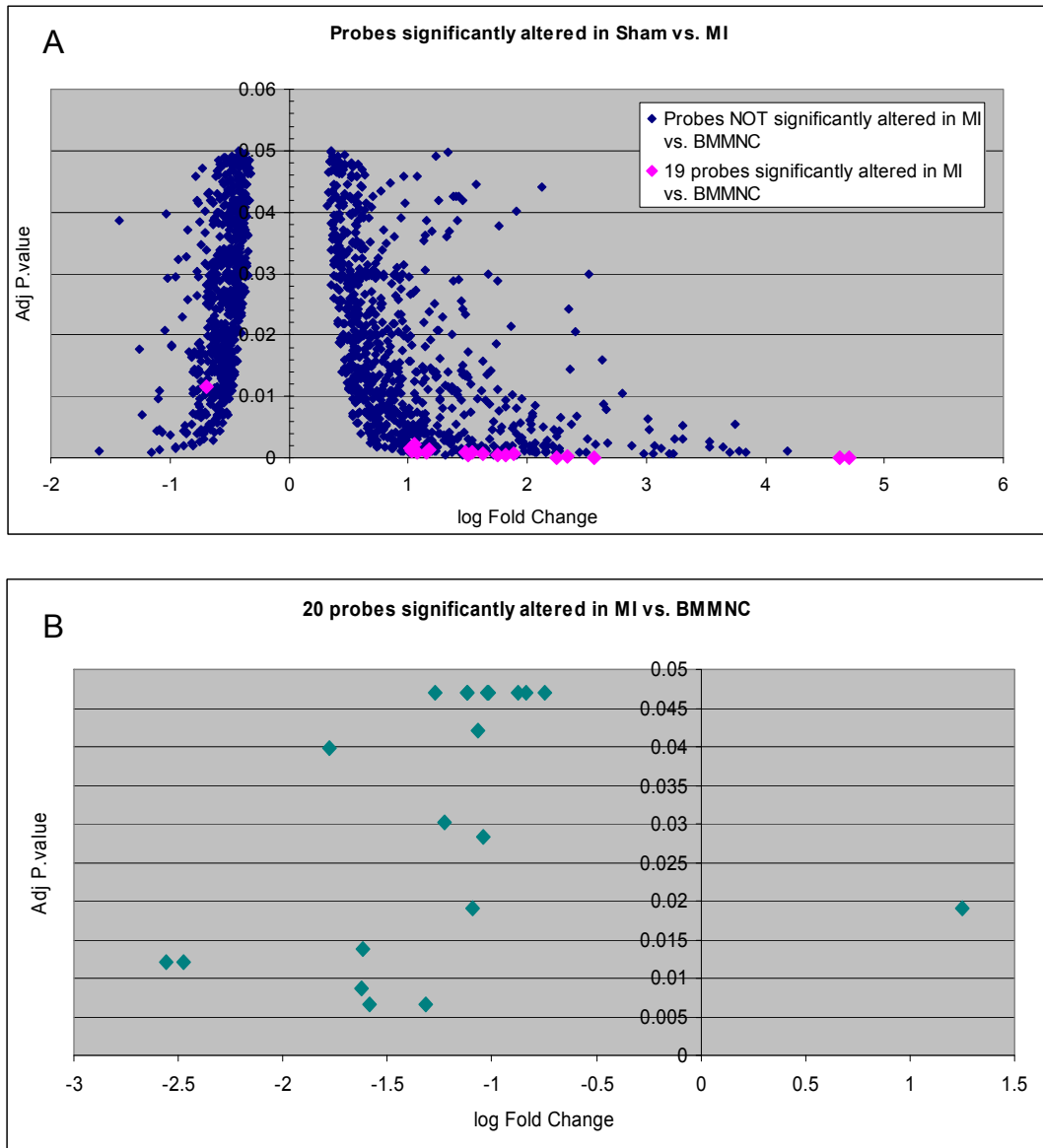


Figure 5.11 shows the distribution of the data for both the Sham vs. MI and the MI vs. BMMNC comparisons. The probes found to be significantly altered by treatment were all probes that also had highly significant differences in MI compared to Sham (highlighted pink in graph 5.11 A). Approximately 40% of the up-regulated probes had highly significant alterations ($p < 0.01$) in MI whereas only about 10% of the down-regulated probes had significance values $p < 0.01$.

Figure 5.11 Graphs of FDR adjusted p-values plotted against log fold change (for probes with significant differential expression) Sham = sham operated group, MI = MI group treated with PBS, BMMNC = MI group treated with bone marrow mononuclear cells. **A)** shows the data for probes significantly altered in Sham vs. MI analysis. The points highlighted in pink are the data for those probes which also had significant alterations in MI vs. BMMNC. **B)** shows data for probes significantly altered in MI vs. BMMNC analysis



A list of the top 433 probes {including all probes with significant difference in MI vs. BMMNC ($p < 0.05$) and all probes with significant alteration in Sham vs. MI

($p < 0.01$) identified in the LIMMA analysis are shown in Appendix 6 and further details of these probes are shown in Appendix 7. Table 5.6 shows the top 30 probes altered in Sham vs. MI according to FDR adjusted p-values, these probes are all up-regulated. The top 10 probes that were found to be down-regulated in Sham vs. MI are listed in Table 5.7. Of the top 30 probes up-regulated in Sham vs. MI, 13 were also found to be significantly down-regulated in MI vs. BMMNC. All 20 probes found to be significantly altered in MI vs. BMMNC are in Table 5.8.

The five most significantly up-regulated probes in Sham vs. MI were also found to be the most significantly down-regulated in MI vs. BMMNC. These probes were from transcripts encoding the sema domain immunoglobulin domain transmembrane domain and short cytoplasmic domain 4A (Sema4a), 2' -5' oligoadenylate synthetase 1K (Oas1k), a transcript predicted to be Stefin A2 (Stfa2), and a transcript similar to Stfa2. The first two (Sema4a and Oas1k) were up-regulated in Sham vs. MI by 5 and 6 fold respectively and were subsequently down-regulated in the BMMNC group. Both the Stfa2 probes were up-regulated by around 25 fold in Sham vs. MI, and expression significantly down-regulated by 3 fold in MI vs. BMMNC. The GLI pathogenesis-related 1 (glioma) (Glipr1), was also both significantly up-regulated in Sham vs. MI and down-regulated in MI vs. BMMNC.

The other eight probes significantly up-regulated in Sham vs. MI (Table 5.6) which are also significantly altered in MI vs. BMMNC are shown in Table 5.8 and are; antigen presenting cell lectin-like receptor A1 (Aplra1), coagulation factor 5 (mapped) (F5_mapped), endothelial differentiation G-protein-coupled receptor 6 (predicted) (Edg6_predicted) a.k.a. sphingosine-1-phosphate receptor 4 (S1PR4), coronin actin binding protein 1A (Coro1a), embigin (Emb), resistin like alpha (Retnla), serine/threonine kinase 17b (apoptosis-inducing) (Stk17b), as well as a hypothetical protein (LOC308990).

Of the top 30 most significantly up-regulated probes in Sham vs. MI, 17 were not significantly altered in MI vs. BMMNC. Six however were up-regulated by >5 fold;

liver glycogen phosphorylase (Pygl), lymphocyte selectin (Sell), matrix metalloproteinase 8 (Mmp8), napsin A aspartic peptidase (Napsa), a transcript similar to Clecsf12 protein (predicted) and a transcript similar to a hypothetical protein (LOC199675). The other nine were more modestly up-regulated and these included gamma cytoplasmic actin (Actg_predicted), lymphocyte cytosolic protein 1 (Lcp1), PDZ and LIM domain 7 (Pdlim7), Kruppel-like factor 5 (Klf5), nuclear factor erythroid derived 2 (Nfe2), and ERBB receptor feedback inhibitor 1 (Errfi1) an epidermal growth factor (EGF) receptor.

The 10 most significantly down-regulated probes in Sham vs. MI all had no significant alterations in MI vs. BMMNC. A probe from a transcript predicted to be leucine-rich repeat-containing 10 (Lrrc10_predicted) was down-regulated 3 fold, protein kinase C and casein kinase substrate in neurons 2 (Pacsin2) and a transcript similar to RIKEN cDNA D430028G21 (MGC93707) were both down-regulated by >2 fold. The other 7 probes were down-regulated by <2 fold and include; G7c protein (G7c), ATP-binding cassette sub-family C (CFTR/MRP) member 8 (Abcc8), molybdenum cofactor synthesis 2 transcript variant 1 (Mocs2), coenzyme Q3 homolog methyltransferase (yeast) (Coq3) and a transcript predicted to be mitochondrial ribosomal protein L50 (Mrpl50_predicted).

Of the 20 probes found to be significantly altered in MI vs. BMMNC, all were down-regulated except calsequestrin 2 (Casq2) which was up-regulated by ~2.5 fold. Only one, the ring finger protein 149 (Rnf149) probe was not significantly altered in Sham vs. MI. Other than the 13 probes already mentioned which were in the top 30 most significantly up-regulated in Sham vs. MI; carbohydrate (keratan sulfate Gal-6) sulfotransferase 1 (Chst1), a transcript predicted to be docking protein 3 (Dok3_predicted) and a transcript predicted to be sortilin-related receptor L (DLR class) A repeats-containing (Sorl1_predicted) were among the other probes significantly down-regulated in MI vs. BMMNC.

Table 5.6 Top 30 probes found to be significantly altered in Sham vs. MI Illumina probe ID, gene symbol, definition and accession code are detailed alongside the log fold change and FDR adjusted p-value for the Sham vs. MI analysis.

PROBE DATA				LIMMA RESULTS	
Probe ID	Symbol	Accession	Definition	logFC	P.Val
ILMN_1376428	Sema4a	NM_001012078.1	sema domain, immunoglobulin domain (Ig), transmembrane domain (TM) and short cytoplasmic domain, (semaphorin) 4A (Sema4a), mRNA.	2.25	2.81E-05
ILMN_1358567	Oas1k	NM_001009489.1	2' -5' oligoadenylate synthetase 1K (Oas1k), mRNA.	2.57	2.81E-05
ILMN_1364315	RGD1560676_predicted	XM_573293.1	similar to stefin A2 (predicted) (RGD1560676_predicted), mRNA.	4.70	2.81E-05
ILMN_1352951	Stfa2_predicted	XM_001070786.1	stefin A2 (predicted) (Stfa2_predicted), mRNA.	4.63	2.81E-05
ILMN_1376740	Glipr1	NM_001011987.1	GLI pathogenesis-related 1 (glioma) (Glipr1), mRNA.	2.34	0.000263
ILMN_1651187	LOC497712	XM_579055.1	hypothetical gene supported by NM_001001511 (LOC497712), mRNA.	1.72	0.000327
ILMN_1362269	Actg_predicted	XM_213540.3	actin, gamma, cytoplasmic (predicted) (Actg_predicted), mRNA.	1.77	0.000327
ILMN_1349760	Pygl	NM_022268.1	liver glycogen phosphorylase (Pygl), mRNA.	2.34	0.00039
ILMN_1650752	Aplra1	NM_001005896.1	antigen presenting cell lectin-like receptor A1 (Aplra1), mRNA.	1.82	0.000418
ILMN_1350326	LOC308990	NM_001025001.1	hypothetical protein LOC308990 (LOC308990), mRNA.	1.51	0.000425
ILMN_1376765	Lcp1	NM_001012044.1	lymphocyte cytosolic protein 1 (Lcp1), mRNA.	1.91	0.000425
ILMN_1371753	F5_mapped	XM_222831.4	coagulation factor 5 (mapped) (F5_mapped), mRNA.	1.75	0.000498
ILMN_1369190	Pdlim7	NM_173125.1	PDZ and LIM domain 7 (Pdlim7), mRNA.	1.46	0.000498
ILMN_1361302	Klf5	NM_053394.2	Kruppel-like factor 5 (Klf5), mRNA.	1.31	0.000498
ILMN_1351274	RGD1565374_predicted	XM_573339.2	similar to hypothetical protein LOC199675 (predicted) (RGD1565374_predicted), mRNA.	3.23	0.000572
ILMN_1371493	Edg6_predicted	XM_234930.2	endothelial differentiation, G-protein-coupled receptor 6 (predicted) (Edg6_predicted), mRNA.	1.63	0.00067
ILMN_1364468	Coro1a	NM_130411.2	coronin, actin binding protein 1A (Coro1a), mRNA.	1.89	0.000703
ILMN_1349113	Sell	NM_019177.1	selectin, lymphocyte (Sell), mRNA.	3.06	0.000705

Table 5.6 continued

PROBE DATA				LIMMA RESULTS	
Probe ID	Symbol	Accession	Definition	logFC	P.Val
ILMN_1376772	Stom	NM_001011965.1	stomatin (Stom), mRNA.	1.45	0.000754
ILMN_1371081	Mmp8	NM_022221.1	matrix metalloproteinase 8 (Mmp8), mRNA.	3.20	0.000754
ILMN_1374896	Napsa	NM_031670.1	napsin A aspartic peptidase (Napsa), mRNA.	2.98	0.000754
ILMN_1359464	Emb	NM_053719.1	embigin (Emb), mRNA.	1.08	0.000766
ILMN_1362534	Retnla	NM_053333.1	resistin like alpha (Retnla), mRNA.	1.54	0.000766
ILMN_1370817	Stk17b	NM_133392.1	serine/threonine kinase 17b (apoptosis-inducing) (Stk17b), mRNA.	1.48	0.000766
ILMN_1350897	Pfc_mapped	XM_001056015.1	properdin factor, complement (mapped) (Pfc_mapped), mRNA.	1.37	0.000766
ILMN_1376557	Nfe2	NM_001012224.1	nuclear factor, erythroid derived 2 (Nfe2), mRNA.	2.06	0.000766
ILMN_1349895	RGD1565140_predicted	XM_001067977.1	similar to Clecsf12 protein (predicted) (RGD1565140_predicted), mRNA.	2.49	0.000766
ILMN_1374845	MGC105649	NM_001008518.1	hypothetical LOC302884 (MGC105649), mRNA.	2.16	0.000766
ILMN_1366212	Errfi1	NM_001014071.1	ERBB receptor feedback inhibitor 1 (Errfi1), mRNA.	2.44	0.000819
ILMN_1368490	LOC24906	NM_031537.1	RoBo-1 (LOC24906), mRNA.	1.53	0.000842

Table 5.7 Top 10 probes found to be significantly down-regulated in Sham vs. MI Illumina probe ID, gene symbol, definition and accession code are detailed alongside the log fold change and FDR adjusted p-value for the Sham vs. MI analysis.

PROBE DATA				LIMMA RESULTS	
Probe ID	Symbol	Accession	Definition	logFC	P.Val
ILMN_1368846	Pacsin2	NM_130740.2	protein kinase C and casein kinase substrate in neurons 2 (Pacsin2), mRNA.	-1.15914	0.0009676
ILMN_1348962	Lrrc10_predicted	XM_001080952.1	leucine-rich repeat-containing 10 (predicted) (Lrrc10_predicted), mRNA.	-1.59641	0.0011253
ILMN_1348979	MGC93707	NM_001005556.1	similar to RIKEN cDNA D430028G21 (MGC93707), mRNA.	-1.08306	0.0013971
ILMN_1353208	G7c	NM_212499.1	G7c protein (G7c), mRNA.	-0.94906	0.0014257
ILMN_1374611	RGD1306595	NM_001025626.1	similar to hypothetical protein (RGD1306595), mRNA.	-0.95577	0.001684
ILMN_1366054	Abcc8	NM_013039.1	ATP-binding cassette, sub-family C (CFTR/MRP), member 8 (Abcc8), mRNA.	-0.88671	0.0020688
ILMN_1367596	Mocs2	XM_001067999.1	molybdenum cofactor synthesis 2, transcript variant 1 (Mocs2), mRNA.	-0.8026	0.0020688
ILMN_1359089	Coq3	NM_019187.1	coenzyme Q3 homolog, methyltransferase (yeast) (Coq3), mRNA.	-0.81278	0.0025027
ILMN_1359659	Mrpl50_predicted	XM_342835.2	mitochondrial ribosomal protein L50 (predicted) (Mrpl50_predicted), mRNA.	-0.75424	0.0026191
ILMN_1359578	RGD1305574_predicted	XM_341388.2	similar to polymerase (RNA) III (DNA directed) (155kD) (predicted) (RGD1305574_predicted), mRNA.	-0.63994	0.0027451

Table 5.8 Twenty probes found to be significantly altered in MI vs. BMMNC Illumina probe ID, gene symbol and definition and accession code are detailed alongside the log fold change and FDR adjusted p-value for the MI vs. BMMNC analysis.

PROBE DATA				LIMMA RESULTS	
Probe ID	Symbol	Accession	Definition	logFC	P.Val
ILMN_1376428	Sema4a	NM_001012078.1	sema domain, immunoglobulin domain (Ig), transmembrane domain (TM) and short cytoplasmic domain, (semaphorin) 4A (Sema4a), mRNA.	-1.32	0.006666
ILMN_1358567	Oas1k	NM_001009489.1	2' -5' oligoadenylate synthetase 1K (Oas1k), mRNA.	-1.59	0.006666
ILMN_1650752	Aplra1	NM_001005896.1	antigen presenting cell lectin-like receptor A1 (Aplra1), mRNA.	-1.63	0.008608
ILMN_1364315	RGD1560676_predicted	XM_573293.1	similar to stefin A2 (predicted) (RGD1560676_predicted), mRNA.	-2.56	0.012004
ILMN_1352951	Stfa2_predicted	XM_001070786.1	stefin A2 (predicted) (Stfa2_predicted), mRNA.	-2.48	0.012004
ILMN_1376740	Glipr1	NM_001011987.1	GLI pathogenesis-related 1 (glioma) (Glipr1), mRNA.	-1.62	0.013690
ILMN_1376641	Chst1	NM_001011955.1	carbohydrate (keratan sulfate Gal-6) sulfotransferase 1 (Chst1), mRNA.	-1.10	0.018974
ILMN_1357616	Casq2	NM_017131.1	calsequestrin 2 (Casq2), mRNA.	1.25	0.018974
ILMN_1350326	LOC308990	NM_001025001.1	hypothetical protein LOC308990 (LOC308990), mRNA.	-1.04	0.028309
ILMN_1371493	Edg6_predicted	XM_234930.2	endothelial differentiation, G-protein-coupled receptor 6 (predicted) (Edg6_predicted), mRNA.	-1.22	0.030115
ILMN_1372230	Rnf149	XM_343561.3	ring finger protein 149 (Rnf149), mRNA.	-1.78	0.039782
ILMN_1370914	Dok3_predicted	XM_001069255.1	docking protein 3 (predicted) (Dok3_predicted), mRNA.	-1.07	0.042063
ILMN_1371753	F5_mapped	XM_222831.4	coagulation factor 5 (mapped) (F5_mapped), mRNA.	-1.12	0.046911
ILMN_1364468	Coro1a	NM_130411.2	coronin, actin binding protein 1A (Coro1a), mRNA.	-1.27	0.046911
ILMN_1359464	Emb	NM_053719.1	embigin (Emb), mRNA.	-0.75	0.046911
ILMN_1362534	Retnla	NM_053333.1	resistin like alpha (Retnla), mRNA.	-1.12	0.046911
ILMN_1370817	Stk17b	NM_133392.1	serine/threonine kinase 17b (apoptosis-inducing) (Stk17b), mRNA.	-1.02	0.046911

Table 5.8 continued.

PROBE DATA				LIMMA RESULTS	
Probe ID	Symbol	Accession	Definition	logFC	P.Val
ILMN_1370198	LOC363060	NM_001014209.1	similar to RIKEN cDNA 1600029D21 (LOC363060), mRNA.	-0.87	0.046911
ILMN_1366128	RGD1562311_predicted	XR_008266.1	similar to PIRA5 (predicted) (RGD1562311_predicted), mRNA.	-0.83	0.046911
ILMN_1363716	Sorl1_predicted	XM_001065506.1	sortilin-related receptor, L(DLR class) A repeats-containing (predicted) (Sorl1_predicted), mRNA.	-1.02	0.046911

Several of the probes (75) within the 1538 which had a significant change in either the Sham vs. MI or MI vs. BMMNC comparisons had qualitative differences. There were 69 probes which were not significantly detected in any of the Sham samples (detection p-values >0.05) but were detected in all of the MI samples. These were termed to be 'ON' in MI. Seventy one were found to be significantly up-regulated in the LIMMA analysis. Forty three of the 71 were not altered in MI vs. BMMNC, but three were significantly down-regulated in MI vs. BMMNC according to LIMMA and 23 were not significantly detected in BMMNC ('OFF' in BMMNC). Only one of these was identified as significantly altered in the LIMMA analysis, this was the probe with the highest average probe intensity in the MI group. The top 15 probes which were 'ON' in MI compared to Sham and which were also detected in the BMMNC group are in Table 5.9. The top 5 probes found to be 'ON' in MI compared to Sham and 'OFF' in BMMNC compared to MI are in Table 5.10.

Three probes were not significantly detected in any of the Sham samples but were detected in all of the MI samples ('ON' in MI). All three were determined to be significantly altered by LIMMA analysis, see Table 5.11. Two of these probes were significantly detected in the both of the BMMNC samples ('ON' in BMMNC) including cytoplasmic linker associated protein 1 (Clasp1); the third was detected in one of the BMMNC samples and not in the other. The intensity values in these probes, even when significantly detected is quite low.

Three probes were significantly detected in all of the MI samples but were not significantly detected in any of the BMMNC samples ('OFF' in BMMNC), see Table 5.12. None of them had a significantly altered expression in MI vs. BMMNC according to the LIMMA analysis results. All three were significantly detected in at least one of the Sham samples and so could not be classed as being 'ON' in MI compared to Sham. All were however shown to be significantly up-regulated in Sham vs. MI according to LIMMA. The intensity values, even in the MI group, did not go above 100.

Table 5.9 Top 15 qualitatively altered probes found to be ‘ON’ in MI compared to Sham Sham = sham operated group, MI = MI group treated with PBS, BMMNC = MI group treated with bone marrow mononuclear cells. Illumina probe ID, gene symbol and average probe intensities for Sham, MI and BMMNC are detailed alongside the significant LIMMA results; log fold change and FDR adjusted p-value for the Sham vs. MI analysis (logFC_1 and P.Val_1) and the log fold change and FDR adjusted p-value for the MI vs. BMMNC analysis (logFC_2 and P.Val_2). The direction of the qualitative differences are detailed in the right-hand columns. Average intensities shaded grey were from probes which were not significantly detected (all detection p-values >0.05). The average intensities shaded blue indicate that not all probes were significantly detected (some detection p-values >0.05).

PROBE DATA					LIMMA RESULTS				QUALITATIVE:	
Probe ID	Symbol	Ave Sham	Ave MI	Ave BMMNC	logFC_1	P.Val_1	logFC_2	P.Val_2	Sham → MI	MI → BMMNC
ILMN_1352340	Il8rb	38.1	188.4	84.7	2.21	0.00187	-	-	ON	-
ILMN_1351430	Serpib10	36.5	156.0	53.0	2.04	0.00114	-	-	ON	-
ILMN_1371753	F5_mapped	43.3	146.1	67.1	1.75	0.00050	-1.12	0.04691	ON	-
ILMN_1360221	Tacstd1	36.9	133.2	87.6	1.77	0.00773	-	-	ON	-
ILMN_1350326	LOC308990	43.1	123.6	59.7	1.51	0.00042	-1.04	0.02831	ON	-
ILMN_1370914	Dok3_predicted	45.5	103.7	49.4	1.18	0.00130	-1.07	0.04206	ON	-
ILMN_1362050	RGD1563994_predicted	37.6	96.9	49.4	1.33	0.00391	-	-	ON	-
ILMN_1362786	Cias1_predicted	42.6	95.9	59.4	1.16	0.00609	-	-	ON	-
ILMN_1376946	Clec4d	43.5	95.6	46.8	1.11	0.00584	-	-	ON	-
ILMN_1358847	Fcar	41.2	94.5	49.3	1.18	0.00285	-	-	ON	-
ILMN_1361075	RGD1560915_predicted	43.6	87.3	60.9	0.95	0.02231	-	-	ON	-
ILMN_1372294	LOC499078	40.5	86.7	48.4	1.08	0.00315	-	-	ON	-
ILMN_1353222	hshin7	36.9	86.2	66.5	1.13	0.02195	-	-	ON	-
ILMN_1650491	Arl5b	42.7	79.2	54.6	0.87	0.01237	-	-	ON	-
ILMN_1369853	Il22ra2	43.5	77.2	54.9	0.78	0.03376	-	-	ON	-

Table 5.10 Top 5 qualitatively altered probes found to be ‘ON’ in MI compared to Sham and ‘OFF’ in BMMNC compared to MI Sham = sham operated group, MI = MI group treated with PBS, BMMNC = MI group treated with bone marrow mononuclear cells. Illumina probe ID, gene symbol and average probe intensities for Sham, MI and BMMNC are detailed alongside the significant LIMMA results; log fold change and FDR adjusted p-value for the Sham vs. MI analysis (logFC_1 and P.Val_1) and the log fold change and FDR adjusted p-value for the MI vs. BMMNC analysis (logFC_2 and P.Val_2). The direction of the qualitative difference are detailed in the right-hand columns. Average intensities shaded grey were from probes which were not significantly detected (all detection p-values >0.05).

PROBE DATA					LIMMA RESULTS				QUALITATIVE:	
Probe ID	Symbol	Ave Sham	Ave MI	Ave BMMNC	logFC_1	P.Val_1	logFC_2	P.Val_2	Sham → MI	MI → BMMNC
ILMN_1650752	Aplra1	31.6	112.7	36.0	1.82	0.00042	-1.63	0.00861	ON	OFF
ILMN_1373925	Pirb	35.3	109.6	45.3	1.50	0.01304	-	-	ON	OFF
ILMN_1374520	RGD1563073_predicted	38.5	85.6	42.0	1.14	0.00201	-	-	ON	OFF
ILMN_1354457	LOC316207	34.1	78.9	41.9	1.19	0.00285	-	-	ON	OFF
ILMN_1350738	Gpr109a	33.3	76.0	43.2	1.18	0.00097	-	-	ON	OFF

Table 5.11 Three qualitatively altered probes found to be ‘OFF’ in MI compared to Sham Sham = sham operated group, MI = MI group treated with PBS, BMMNC = MI group treated with bone marrow mononuclear cells. Illumina probe ID, gene symbol and average probe intensities for Sham, MI and BMMNC are detailed alongside the significant LIMMA results; log fold change and FDR adjusted p-value for the Sham vs. MI analysis (logFC_1 and P.Val_1) and the log fold change and FDR adjusted p-value for the MI vs. BMMNC analysis (logFC_2 and P.Val_2). The direction of the qualitative differences are detailed in the right-hand columns. Average intensities shaded grey were from probes which were not significantly detected (all detection p-values >0.05). The average intensities shaded blue indicate that not all probes were significantly detected (some detection p-values >0.05).

PROBE DATA					LIMMA RESULTS				QUALITATIVE:	
Probe ID	Symbol	Ave Sham	Ave MI	Ave BMMNC	logFC_1	P.Val_1	logFC_2	P.Val_2	Sham → MI	MI → BMMNC
ILMN_1360605	Clasp1	56.5	43.0	54.1	-0.39	0.03613	-	-	OFF	ON
ILMN_1356665	RGD1310121_predicted	55.4	40.5	48.8	-0.45	0.02562	-	-	OFF	ON
ILMN_1362596	MGC114379	51.0	39.7	47.4	-0.36	0.03257	-	-	OFF	-

Table 5.12 Three qualitatively altered probes found to be ‘OFF’ in BMMNC compared to MI Sham = sham operated group, MI = MI group treated with PBS, BMMNC = MI group treated with bone marrow mononuclear cells. Illumina probe ID, gene symbol and average probe intensities for Sham, MI and BMMNC are detailed alongside the significant LIMMA results; log fold change and FDR adjusted p-value for the Sham vs. MI analysis (logFC_1 and P.Val_1) and the log fold change and FDR adjusted p-value for the MI vs. BMMNC analysis (logFC_2 and P.Val_2). The direction of the qualitative difference are detailed in the right-hand columns. Average intensities shaded grey were from probes which were not significantly detected (all detection p-values >0.05). The average intensities shaded blue indicate that not all probes were significantly detected (some detection p-values >0.05).

PROBE DATA					LIMMA RESULTS				QUALITATIVE:	
Probe ID	Symbol	Ave Sham	Ave MI	Ave BMMNC	logFC_1	P.Val_1	logFC_2	P.Val_2	Sham → MI	MI → BMMNC
ILMN_1375210	RGD1561730_predicted	48.7	71.0	44.6	0.53	0.04793	-	-	-	OFF
ILMN_1376826	Il13ra2	48.1	68.4	44.6	0.50	0.03140	-	-	-	OFF
ILMN_1366137	Actn1	47.8	67.9	47.0	0.51	0.01627	-	-	-	OFF

5.3 Validation of gene expression data

5.3.1 Reference gene selection

Five reference genes for rat were available 'in-house' for testing. These were ATP synthase subunit beta (Atp5b), beta-2 microglobulin (B2m), eukaryotic translation initiation factor 4A2 (Eif4a2), glyceraldehydes-3-phosphate dehydrogenase (Gapdh) and ubiquitin C (Ubc). Initially the performance of these genes as endogenous controls was checked in the Illumina chip data, to assess if; 1) they were expressed at reasonable levels, 2) expression was stable across samples, 3) there was any evidence that these genes were differentially expressed in our experiment, i.e affected by our experimental conditions. The resulting statistics are shown in Table 5.13, including the coefficient of variation (CV) which indicates overall stability of expression of each gene and one way ANOVA statistics looking for within group variation.

Two genes, Atp5b and Ubc had minimal coefficient of variance, 4 and 7% respectively. The other genes also had relatively good stability. Gapdh was the least stable with a CV of 11%. None of the genes had significant differential expression according to the LIMMA analysis, but a one-way ANOVA revealed that B2m is the gene most likely to have significant variation between our experimental groups. This indicates that 4 of the 5 genes were potentially suitable reference genes. These four were assessed further using QPCR in 8 of the 9 experimental samples 1-9 (one sample from the Sham group (tissue sample 3) had no tissue remaining).

Table 5.13 Suitability of 5 potential reference genes Sham = sham operated group, MI = MI group treated with PBS, BMMNC = MI group treated with bone marrow mononuclear cells. **A)** Illumina data from the 5 potential genes indicates average signal (AVE_Signal) and standard deviation (ARRAY_STDEV) **B)** Statistical analysis of variation across all samples; average (Ave), standard deviation (StDev) and coefficient of variance (CV) and variation between groups (One way ANOVA).

A

SYMBOL	PROBE_ID	Sham		MI		BMMNC	
		AVG_Signal	ARRAY_STDEV	AVG_Signal	ARRAY_STDEV	AVG_Signal	ARRAY_STDEV
Atp5b	ILMN_1350324	15547	1144	15883	1037	16797	1615
B2m	ILMN_1368656	15256	869	18016	837	15975	1030
Eif4a2	ILMN_1372755	2862	318	3108	375	3367	1090
Gapdh	ILMN_1649859	9064	1291	7634	310	9337	1121
Ubc	ILMN_1350494	14326	817	14027	1484	12478	1572

B

SYMBOL	PROBE_ID	STATS			
		Ave	StDev	CV	One_Way_ANOVA
Atp5b	ILMN_1350324	16076	647	4	ns
B2m	ILMN_1368656	16416	1432	9	0.0245
Eif4a2	ILMN_1372755	3113	252	8	ns
Gapdh	ILMN_1649859	8678	915	11	ns
Ubc	ILMN_1350494	13610	992	7	ns

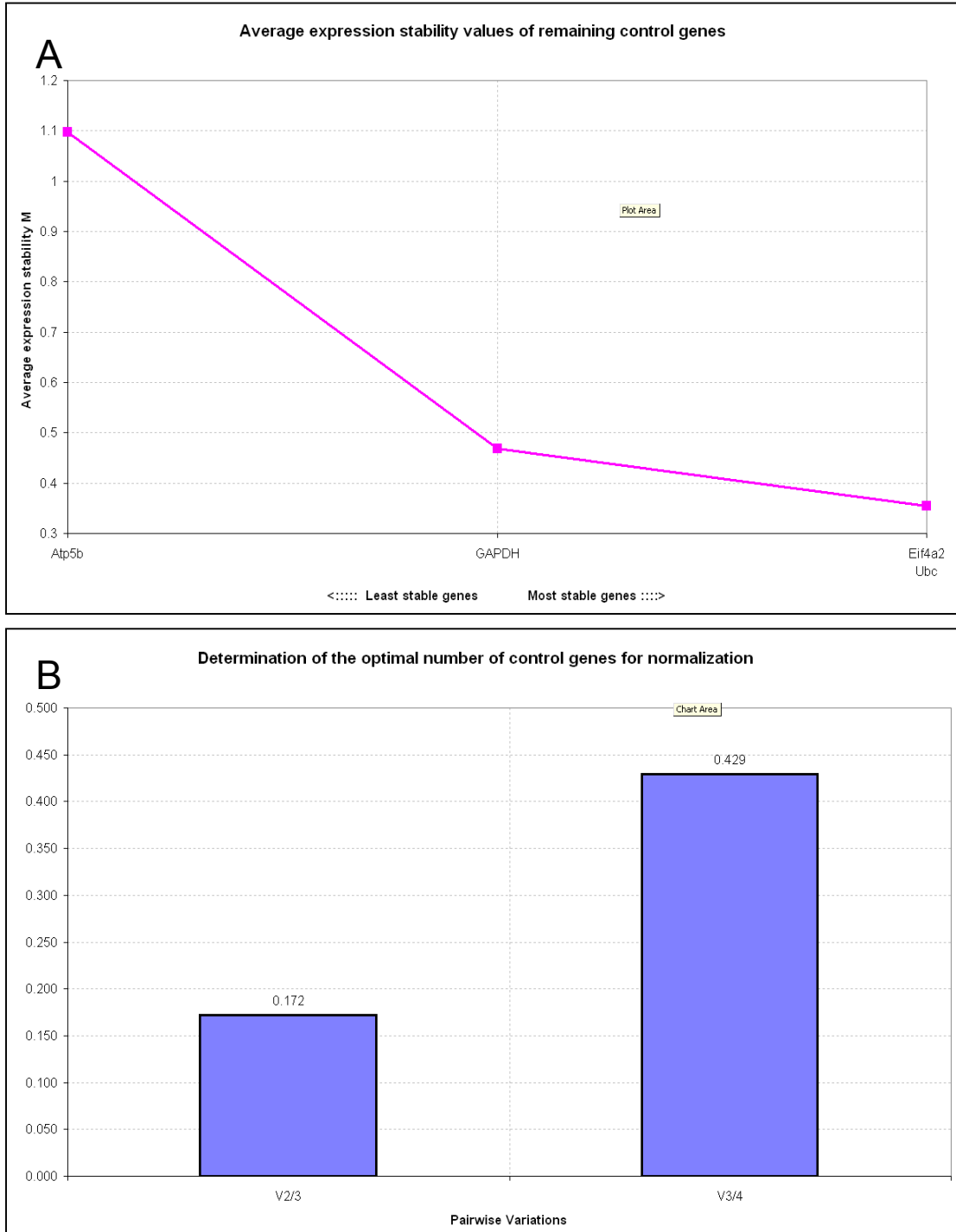
5.3.2 QPCR using TaqMan gene expression assays

Three genes were followed up using QPCR; Sema4a, Oas1k and Iqgap1. Both Sema4a and Oas1k had the highest and most significant alterations in expression in both the Sham vs. MI and the MI vs. BMMNC comparisons. The adjusted p-values in MI vs. BMMNC were several orders of magnitude higher than Sham vs. MI. Iqgap1 had much lower fold change difference and much higher adjusted p-values. QPCR results for these three gene would help to determine the reliability of the gene expression dataset from the most highly significant data to data with lesser significance. Reactions were performed in triplicate for each cDNA sample and for the reference genes. The amplification curves were checked in SDS2.3 [Applied Biosystems, U.K] and wells with errors were noted, the data was exported to Excel [Microsoft, US] for analysis. Triplicate Ct values for each sample were averaged after removing any outliers as suggested by high CV values (CV>2).

5.3.2.1 *GeNorm*

The Ct values for the reference genes were converted into ‘quantities’ (Q) and entered into the GeNorm macro. The macro found the gene with the highest M value (1.724) was Atp5b, this column was discarded and the analysis was rerun and showed that GAPDH was the next highest value with 0.526. This meant that Ubc and Eif4a2 were the best performing reference genes with an M value of 0.355. The charts were checked with data for all 4 genes uploaded to check the pairwise variation values (Figure 5.12). As seen in Figure 5.12 B the V2/3 value is 0.172, which is above the 0.15 threshold suggested by Vandesompele et al 2002 [114] therefore including the data for third best gene (GAPDH) in the normalisation factor calculation would be desirable. The V3/4 was 0.429 indicating this gene should also be included.

Figure 5.12 Graphical output of the GeNorm analysis **A)** plots the ‘M’ values for each gene, the two most stably expressed genes with the lowest ‘M’ value on the left. **B)** shows the pairwise variations for V2/3 (i.e between the normalisation factor calculated for the best 2 genes and the normalisation factor calculated from the best three genes), and V3/4 (i.e best three genes and the best four genes).



5.3.2.2 $\Delta\Delta Ct$ calculations and statistical analysis.

The average Ct values for all four reference genes in each sample were calculated to give an average reference Ct (Ct_{REF}) value. These values were used to calculate the ΔCt for each gene of interest (ΔCt_{GOI}) and then average and standard deviations in each experimental group were calculated Table 5.14.

Table 5.14 Normalised Ct values (ΔCt) for each gene of interest (GOI), group averages and standard deviations Sham = sham operated group, MI = MI group treated with PBS, BMMNC = MI group treated with bone marrow mononuclear cells. Only two of the three Sham samples were tested and one of the MI samples failed in two of the three GOI. **A)** Results from Sema4a. **B)** Results from Oas1k. **C)** Results from Iqgap1.

A

Sample	ΔCt	Group Ave ΔCt	Group StDev
Sham 2	5.18	5.68	0.71
Sham 3	6.18		
MI 1	4.26	4.43	0.25
MI 2	-		
MI 3	4.61		
BMMNC 1	4.18	5.05	0.77
BMMNC 2	5.33		
BMMNC 3	5.64		

B

Sample	ΔCt	Group Ave ΔCt	Group StDev
Sham 2	6.89	6.04	1.20
Sham 3	5.19		
MI 1	3.16	3.27	0.15
MI 2	-		
MI 3	3.37		
BMMNC 1	2.29	3.61	1.23
BMMNC 2	4.74		
BMMNC 3	3.80		

C

Sample	ΔCt	Group Ave ΔCt	Group StDev
Sham 2	4.48	4.59	0.15
Sham 3	4.70		
MI 1	4.35	4.10	0.29
MI 2	3.79		
MI 3	4.17		
BMMNC 1	3.90	4.04	0.42
BMMNC 2	4.52		
BMMNC 3	3.70		

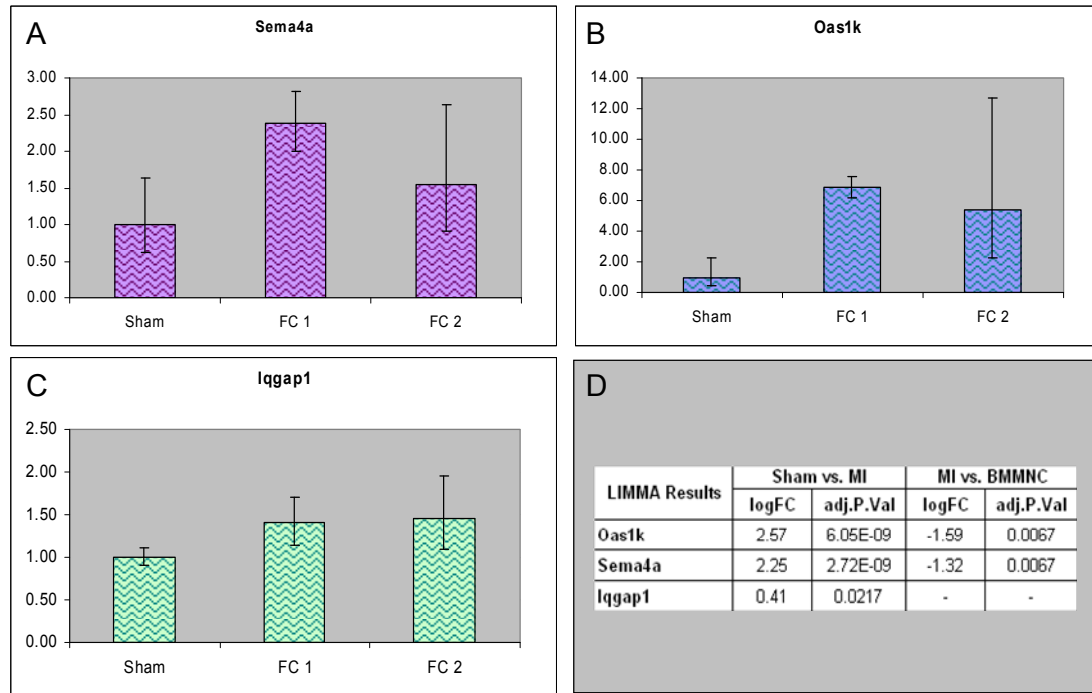
The ΔC_t were then used to calculate $\Delta\Delta C_t$ using Sham as the reference group and fold changes were calculated from this. These fold changes are shown in Figure 5.13 with error bars indicating 95% confidence interval on the fold change values. The pattern of gene expression over the three groups was similar to the LIMMA data in all three genes i.e. Sema4a and Oas1k had strong up-regulation in MI group compared to Sham and a lesser down-regulation in BMMNC compared to MI. Iqgap also showed an up-regulation in MI compared to Sham, but no difference between MI and BMMNC. Large error bars are present in the FC2 calculations from Sema4a and Oas1k.

To look for statistical differences the ΔC_t values were used to perform a Student's *t*-test. As mentioned previously, one of the three Sham samples was not analysed due to lack of tissue sample for RNA extraction and one of the three MI samples failed in both the Oas1k and the Sema4a. This meant an n of 2 in some of the *t*-tests. No significant differences were found (Table 5.15).

Table 5.15 P-values from the Student's *t*-test performed on ΔC_t values from QPCR analysis in for Iqgap1, Oas1k, and Sema4a

	Sham vs. MI	MI vs. BMMNC
Sema4a	0.150	0.422
Oas1k	0.084	0.734
Iqgap1	0.124	0.842

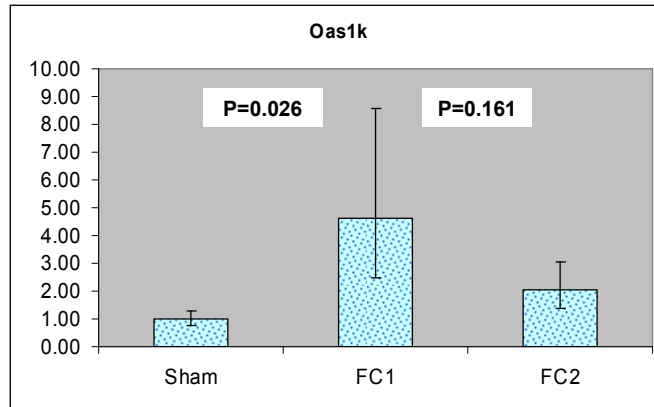
Figure 5.13 Graphs showing fold change (FC) results from the QPCR analysis (A-C) and LIMMA statistics from the Illumina RatRef12 chip analysis (D) for *Iqgap1*, *Oas1k*, and *Sema4a* A-C) The FC of the MI group compared to Sham (FC1) and the FC of the BMMNC group compared to Sham (FC2). Error bars indicate upper and lower 95% confidence interval (CI) of the FC. D) Log fold changes and FDR adjusted p-values for Sham vs. MI and MI vs. BMMNC as calculated by LIMMA from the Illumina RatRef12 chip analysis.



5.3.2.3 QPCR analysis of *Oas1k* in samples 10-18

QPCR analysis was also performed on cDNA prepared from tissue samples 10-18 for one of the genes (*Oas1k*). The four previously used endogenous controls and *Oas1k* were run in triplicate on one plate. GeNorm analysis of the endogenous controls data suggested the use of just *Ubc* and *Eif4a2* for normalisation in this sample set. $\Delta\Delta C_t$ calculations were performed as before and Figure 5.14 shows the results for *Oas1k* gene expression. Again, the error bar is especially large for the FC1 calculation. P-values for Sham vs. MI and MI vs. BMMNC are shown in the white boxes.

Figure 5.14 Graphs showing fold change (FC) results from the QPCR analysis for *Oas1k* in samples 10-18. The FC of the MI group compared to Sham (FC1) and the FC of the BMMNC group compared to Sham (FC2). Error bars indicate upper and lower 95% confidence interval (CI) of the FC. P values for Sham vs. MI and MI vs. BMMNC are shown in the white boxes.



6. Bioinformatic results

6.1 Bioinformatic analysis of proteins found to be altered in 2DE analyses

6.1.1 Protein ANalysis THrough Evolutionary Relationships (PANTHER)

Four different lists of proteins were entered into PANTHER the number of proteins in each list is shown in Table 6.1.

Table 6.1 Four different lists of Refseq protein accession codes were entered into PANTHER

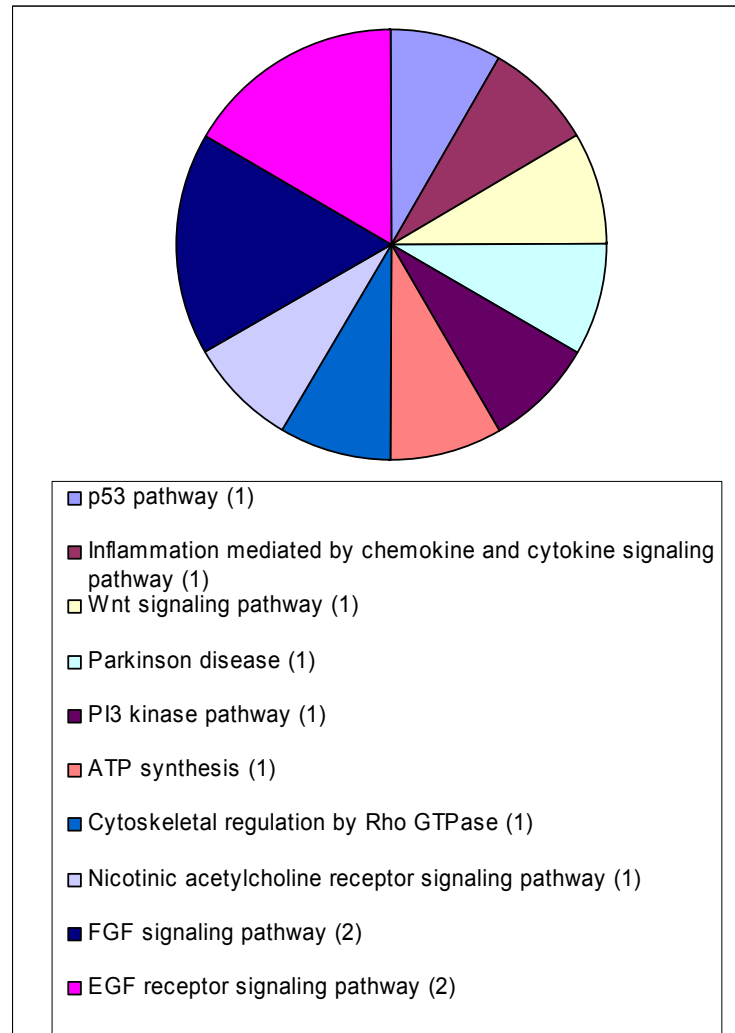
PANTHER Dataset	Number of Proteins
Sham vs. MI - Up	11
Sham vs. MI - Down	23
MI vs. BMMNC - Up	22
MI vs. BMMNC - Down	4

6.1.1.1 Sham vs. MI

From the proteins up-regulated in Sham vs. MI, all 11 were mapped by PANTHER, with exact hits. Of the 23 proteins down-regulated in Sham vs. MI, PANTHER hits were found for 22; stress-70 protein was un-mapped.

The 11 up-regulated proteins were not represented by any different PANTHER pathways. The 22 down-regulated proteins represented 10 different pathways, as shown in Figure 6.1. The epidermal growth factor (EGF) and fibroblast growth factor (FGF) pathways are represented by the presence of both Ywhae and Pebp1. The other eight pathways were only represented by a single protein from our dataset, either Myh6, Atp5b or Ywhae.

Figure 6.1 PANTHER Pathways represented by the proteins differentially regulated in Sham vs. MI Pathways represented by 22 proteins found to be Down-regulated in Sham vs. MI. Numbers in brackets indicate the number of proteins associated with the term.

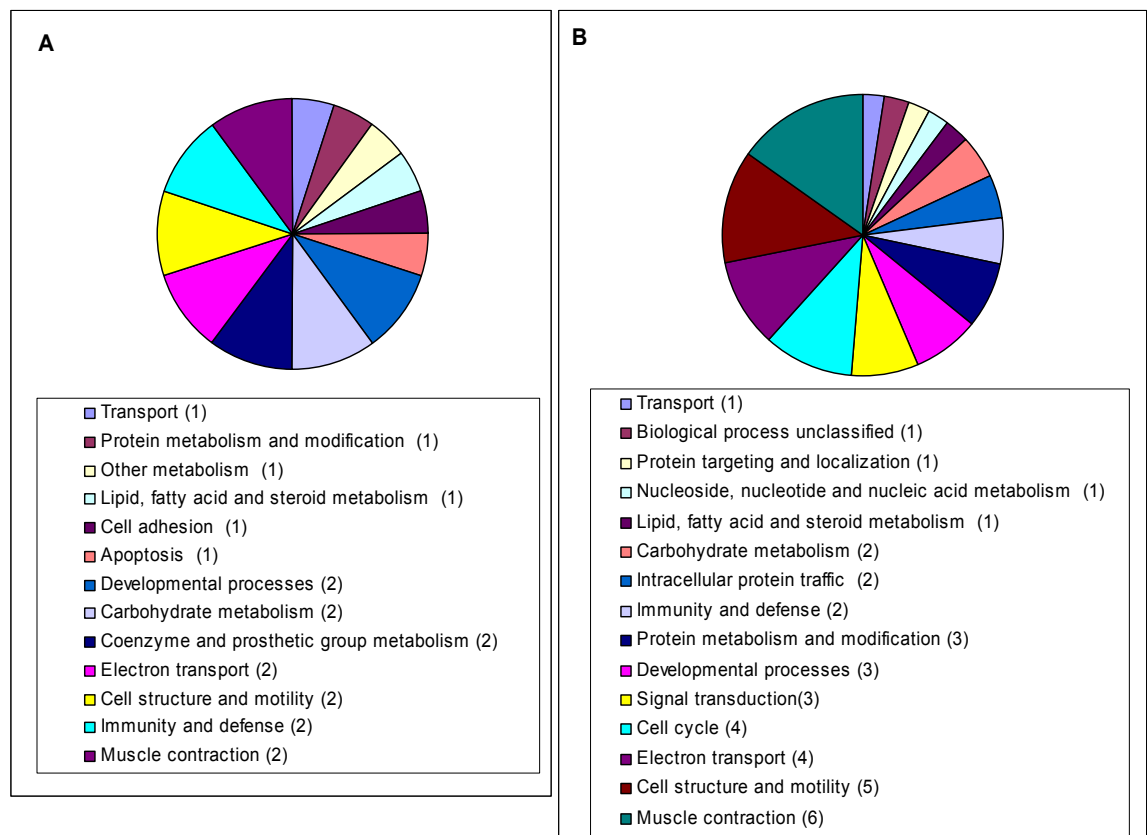


The most highly represented biological process represented in both the up- and down-regulated proteins in Sham vs. MI was ‘muscle contraction’, represented by Tpm1 and Myl 2 from the up-regulated proteins and Ckm, Ckmt2, Myh6, Tnnt2, Tpm1 and myosin light chain 3 (Myl3), see Figure 6.2.

Many other biological processes were included in both up-regulated and down-regulated lists including; carbohydrate metabolism, cell structure and motility, immunity and defence and electron transport. Carbohydrate metabolism was represented by dihydrolipoyllysine-residue acetyltransferase component of

pyruvate dehydrogenase complex a.k.a E2 component of pyruvate dehydrogenase (Dlat) and Echs1 from up-regulated protein list; succinate dehydrogenase (Sdha) and Ldhb from down-regulated protein list. Cell structure and motility was represented by Tpm1 and Myl2 from the up-regulated list; Cap1, Tuba4a, Actc1, Des and Tpm1 from the down-regulated list. Immunity and defence was represented by Prdx3 and Lgal5 from up-regulated list; Prdx6 and Hspb8 from the down-regulated list. Finally, electron transport was represented by NAD(P) transhydrogenase (Nnt) and Uqcrh from the up-regulated list; Acads, Ndufs1, Sdha and Atp5b from the down-regulated list.

Figure 6.2 PANTHER Biological processes represented by the proteins differentially regulated in Sham vs. MI **A)** Processes represented by 11 proteins found to be Up-regulated in Sham vs. MI. **B)** Processes represented by 22 proteins found to be Down-regulated in Sham vs. MI. Numbers in brackets indicate the number of proteins associated with the term.



Biological processes unique to the up-regulated protein list included coenzyme and prosthetic group metabolism (Dlat and Echs1). Biological processes only associated with the down-regulated proteins included; cell cycle (Myh6, Ywhae,

Tuba4a and Actc1) signal transduction (Cap1, Ywhae and Pebp1) and intracellular protein traffic (Tuba4a and Actc1).

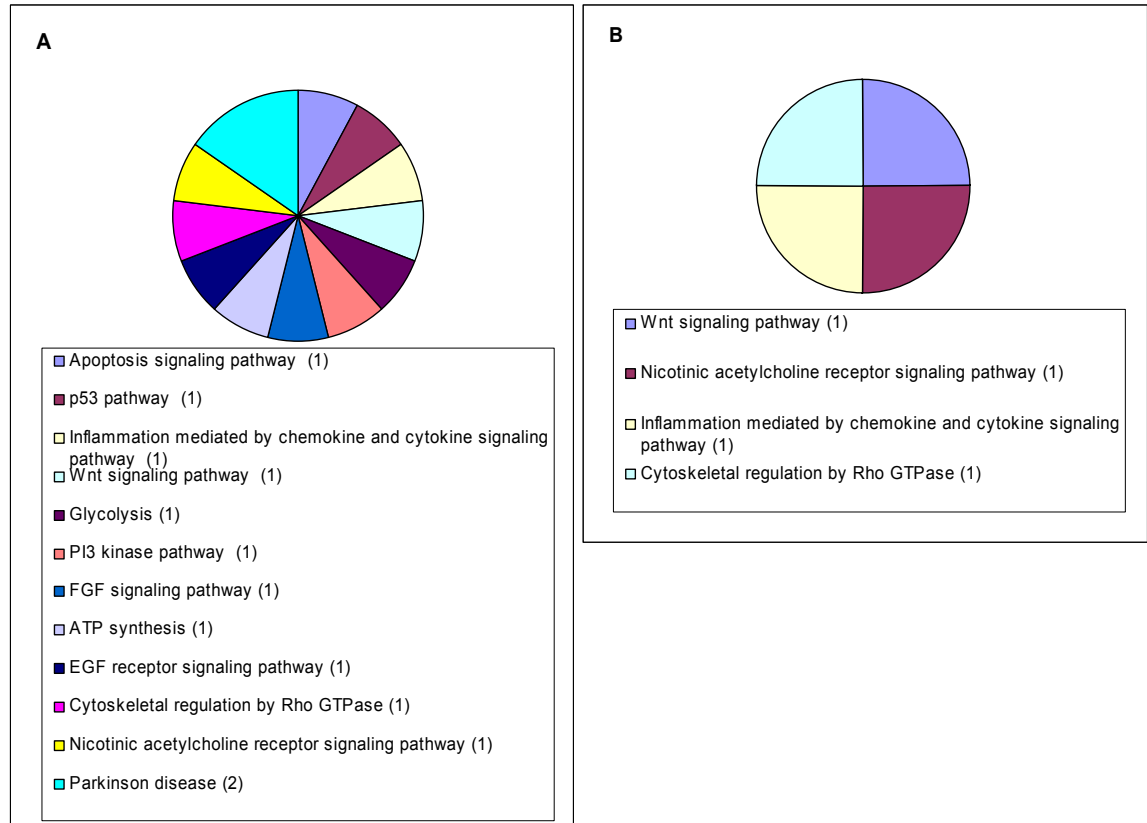
The molecular functions represented by these proteins reveal two functions to be highly represented by several proteins in both lists. From the list of proteins up-regulated 'Oxidoreductase' is represented by the presence of four different proteins, Nnt, Prdx3, Echs1 and Uqcrh. The same function was also represented by five of the proteins down-regulated; Acads, Prdx6, Ndufa10, Sdha and Ldhd. Two up-regulated proteins were cytoskeletal, namely Tpm1 and Myl2, however eight cytoskeletal proteins were down-regulated; Myh6, Tnnt2, Cap1, Tuba4a, Actc1, Des and Myl3.

6.1.1.2 MI vs. BMMNC

The two lists of Refseq protein accession codes for proteins up- and down-regulated in MI vs. BMMNC were successfully mapped by PANTHER except Hspa9 from the up-regulated proteins list. Myh6 was in both the up and down-regulated protein list.

The pathways represented by up-regulated proteins from the MI vs. BMMNC comparison (Figure 6.3 A) include Parkinson's disease represented by Ywhae and Hspb8, All other pathways are represented by a single protein from the list. The EGF, FGF Pi3 kinase and p53 signalling pathways are represented by Ywhae. Apoptosis is represented by hspb8; glycolysis by Pgam1 and ATP synthesis by Atp5b. Myh6 accounts for the other four pathways including Wnt signalling. All four pathways represented by the down-regulated proteins are represented by only one protein, namely Myh6 (Figure 6.3 B).

Figure 6.3 PANTHER Pathways represented by the proteins differentially regulated in MI vs. BMMNC **A)** Pathways represented by 21 proteins found to be Up-regulated in MI vs. BMMNC. **B)** Pathways represented by 4 proteins found to be Down-regulated in MI vs. BMMNC. Numbers in brackets indicate the number of proteins associated with the term.

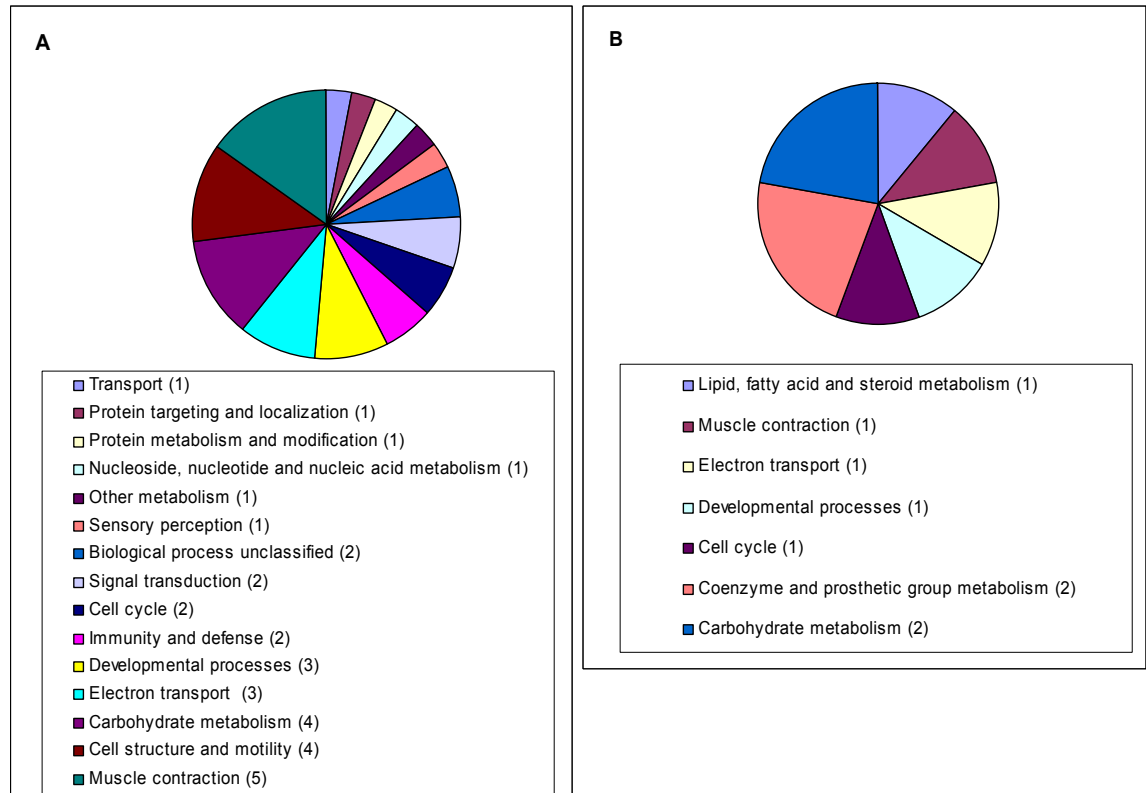


Many biological processes were represented by the proteins both up- and down-regulated in MI vs. BMMNC including carbohydrate metabolism, muscle contraction and electron transport. Carbohydrate metabolism was represented by Ldhb, methylcrotonoyl-CoA carboxylase alpha (Mccc1), Sdha and Pgam1 from the up-regulated list and both Dlat and Echs1 from the down-regulated list. Muscle contraction was represented by Ckm, Ckmt2, Myh6, Tnnt2, Tpm1 from the up-regulated list and Myh6 from the down-regulated list. Electron transport was represented by Atp5b, Ndufa10 and Sdha from the up-regulated list; Uqcrh from the down-regulated list.

Processes unique to the up-regulated proteins included cell structure and motility (Cap1, Ndufa10, Des and Tpm1), signal transduction (Cap1, Ywhae and Pebp1) and immunity and defence (Prdx6 and Hspb8). Whereas the processes unique to

the down-regulated proteins were; coenzyme and prosthetic group metabolism (Dlat and Echs1) and fatty acid steroid metabolism (Echs1).

Figure 6.4 PANTHER Biological processes represented by the proteins differentially regulated in MI vs. BMMNC **A)** Processes represented by 22 proteins found to be Up-regulated in MI vs. BMMNC. **B)** Processes represented by 4 proteins found to be Down-regulated in MI vs. BMMNC. Numbers in brackets indicate the number of proteins associated with the term.



The molecular functions represented by the two lists of proteins altered in MI vs. BMMNC reveal two functions to be highly represented in both lists. From the list of proteins up-regulated ‘Oxidoreductase’ is represented by the presence of five different proteins; Ldhb, Ndufa10, Sdha, Prdx6 and hydroxysteroid dehydrogenase-like protein 2 (Hsd12). The same function was also represented by two of the proteins down-regulated; Echs1 and Uqcrh. Six up-regulated proteins were cytoskeletal but only one cytoskeletal protein was down-regulated (Myh6).

6.1.2 Database for Annotation, Visualization and Integrated Discovery (DAVID)

The same four protein lists that were entered into PANTHER were also entered into DAVID (see Table 6.1).

6.1.2.1 Sham vs. MI

The cluster analysis of the biological process GO terms associated with the proteins up-regulated in Sham vs. MI returned 9 clusters. Only GO terms in the first seven groups had p-values <0.05. The first cluster of terms were all related to negative regulation of cellular processes, the second were related to positive regulation of hydralase and catalytic activity, the third relates to stress responces, circulation made up the fourth cluster, reaction to ROS was the fifth cluster. Groups 1 -7 are shown in Table 6.2.

The clustering of biological process GO terms associated with the proteins down-regulated in Sham vs. MI returned 19 clusters. There were significant p-values in clusters 1-13 (these are detailed in Table 6.3). These thirteen clusters contained terms associated with muscle contraction (cluster 1), muscle and organ development (cluster 2 and 5), transport and localisation (cluster 3 and 6), stress response (cluster 4) and apoptosis (cluster 7).

Table 6.2 Cluster 1 -7 of 9 clusters of biological process GO terms associated with proteins up-regulated in Sham vs. MI The GO terms within each cluster, count (number of proteins from list with this annotation), % (percentage of the input proteins found with this annotation), p-value (modified Fisher's exact test (EASE score) and fold enrichment (the fold enrichment of this annotation in the uploaded protein list versus the proportion of this annotation in the background dataset). Only significantly associated GO terms (p-value <0.05) are shown.

Cluster	GO Biological Process Term	Count	%	PValue	Fold Enrichment
1	GO:0043066~negative regulation of apoptosis	4	33	0.00097	17
	GO:0043069~negative regulation of programmed cell death	4	33	0.00101	16
	GO:0060548~negative regulation of cell death	4	33	0.00102	16
	GO:0051704~multi-organism process	4	33	0.00188	13
	GO:0051093~negative regulation of developmental process	4	33	0.00402	10
	GO:0042981~regulation of apoptosis	4	33	0.00738	8
	GO:0043067~regulation of programmed cell death	4	33	0.00764	8
	GO:0010941~regulation of cell death	4	33	0.00773	8
	GO:0050793~regulation of developmental process	4	33	0.01757	6
	GO:0010033~response to organic substance	4	33	0.01858	6
2	GO:0051345~positive regulation of hydrolase activity	3	25	0.00320	30
	GO:0051336~regulation of hydrolase activity	3	25	0.01172	16
	GO:0043085~positive regulation of catalytic activity	3	25	0.03073	9
3	GO:0042542~response to hydrogen peroxide	3	25	0.00129	48
	GO:0032496~response to lipopolysaccharide	3	25	0.00241	35
	GO:0002237~response to molecule of bacterial origin	3	25	0.00338	30
	GO:0009617~response to bacterium	3	25	0.00831	19
	GO:0002520~immune system development	3	25	0.01188	15
	GO:0051707~response to other organism	3	25	0.01196	15
	GO:0009607~response to biotic stimulus	3	25	0.01717	13
4	GO:0003013~circulatory system process	3	25	0.00430	26
	GO:0008015~blood circulation	3	25	0.00430	26
5	GO:0000302~response to reactive oxygen species	4	33	0.00003	52
	GO:0006979~response to oxidative stress	4	33	0.00020	28
	GO:0044093~positive regulation of molecular function	4	33	0.00323	11
	GO:0050790~regulation of catalytic activity	4	33	0.00767	8
	GO:0065009~regulation of molecular function	4	33	0.01186	7

Table 6.2 continued

Cluster	GO Biological Process Term	Count	%	PValue	Fold Enrichment
6	GO:0065008~regulation of biological quality	5	42	0.00585	5
	GO:0006950~response to stress	5	42	0.00735	5
	GO:0048523~negative regulation of cellular process	5	42	0.00760	5
	GO:0048519~negative regulation of biological process	5	42	0.01108	4
	GO:0048518~positive regulation of biological process	5	42	0.01920	4
7	GO:0048584~positive regulation of response to stimulus	3	25	0.01006	17
	GO:0048583~regulation of response to stimulus	3	25	0.03288	9

Table 6.3 Cluster 1-13 of 19 clusters of biological process GO terms associated with proteins down-regulated in Sham vs. MI The GO terms within each cluster, count (number of proteins from list with this annotation), % (percentage of the input proteins found with this annotation), p-value (modified Fisher's exact test (EASE score) and fold enrichment (the fold enrichment of this annotation in the uploaded protein list versus the proportion of this annotation in the background dataset). Only significantly associated GO terms (p-value <0.05) are shown.

Cluster	GO Biological Process Term	Count	%	PValue	Fold Enrichment
1	GO:0033275~actin-myosin filament sliding	3	13	0.00003	351
	GO:0030049~muscle filament sliding	3	13	0.00003	351
	GO:0070252~actin-mediated cell contraction	3	13	0.00005	251
	GO:0043462~regulation of ATPase activity	3	13	0.00017	146
	GO:0045214~sarcomere organization	3	13	0.00030	110
2	GO:0060415~muscle tissue morphogenesis	5	21	0.00000	91
	GO:0055008~cardiac muscle tissue morphogenesis	5	21	0.00000	91
	GO:0006941~striated muscle contraction	5	21	0.00000	71
	GO:0030048~actin filament-based movement	4	17	0.00000	180
	GO:0048738~cardiac muscle tissue development	5	21	0.00000	44
	GO:0060048~cardiac muscle contraction	4	17	0.00000	123
	GO:0008016~regulation of heart contraction	5	21	0.00000	42
	GO:0003015~heart process	4	17	0.00001	102
	GO:0060047~heart contraction	4	17	0.00001	102
	GO:0055010~ventricular cardiac muscle morphogenesis	4	17	0.00001	102
	GO:0003007~heart morphogenesis	5	21	0.00001	38
	GO:0030239~myofibril assembly	4	17	0.00001	97
	GO:0055002~striated muscle cell development	4	17	0.00001	94
	GO:0006936~muscle contraction	5	21	0.00001	31
	GO:0031032~actomyosin structure organization	4	17	0.00002	75
	GO:0055001~muscle cell development	4	17	0.00002	75
	GO:0030705~cytoskeleton-dependent intracellular transport	4	17	0.00002	69
	GO:0003012~muscle system process	5	21	0.00002	28
	GO:0010927~cellular component assembly involved in morphogenesis	4	17	0.00003	63
	GO:0051146~striated muscle cell differentiation	4	17	0.00007	47
	GO:0003013~circulatory system process	5	21	0.00013	18
	GO:0008015~blood circulation	5	21	0.00013	18

Table 6.3 continued.

Cluster	GO Biological Process Term	Count	%	PValue	Fold Enrichment
2 cont.	GO:0014706~striated muscle tissue development	5	21	0.00017	17
	GO:0060537~muscle tissue development	5	21	0.00020	16
	GO:0030036~actin cytoskeleton organization	5	21	0.00023	15
	GO:0030029~actin filament-based process	5	21	0.00027	15
	GO:0007517~muscle organ development	5	21	0.00040	13
	GO:0007507~heart development	5	21	0.00040	13
	GO:0042692~muscle cell differentiation	4	17	0.00052	24
	GO:0048729~tissue morphogenesis	5	21	0.00055	12
	GO:0048646~anatomical structure formation involved in morphogenesis	5	21	0.00161	9
	GO:0044057~regulation of system process	5	21	0.00174	9
	GO:0007010~cytoskeleton organization	5	21	0.00195	9
	GO:0032989~cellular component morphogenesis	5	21	0.00301	8
	GO:0009887~organ morphogenesis	6	25	0.00596	5
	GO:0009888~tissue development	5	21	0.02292	4
3	GO:0006810~transport	11	46	0.00114	3
	GO:0051234~establishment of localization	11	46	0.00123	3
	GO:0051179~localization	11	46	0.00500	2
4	GO:0009408~response to heat	4	17	0.00032	28
	GO:0009266~response to temperature stimulus	4	17	0.00084	20
	GO:0009628~response to abiotic stimulus	4	17	0.03046	6
5	GO:0048856~anatomical structure development	12	50	0.00031	3
	GO:0048731~system development	11	46	0.00112	3
	GO:0032502~developmental process	12	50	0.00147	3
	GO:0007275~multicellular organismal development	11	46	0.00295	3
6	GO:0046907~intracellular transport	6	25	0.00112	7
	GO:0051649~establishment of localization in cell	6	25	0.00419	5
	GO:0051641~cellular localization	6	25	0.00609	5

Table 6.3 continued.

Cluster	GO Biological Process Term	Count	%	PValue	Fold Enrichment
7	GO:0006915~apoptosis	5	21	0.00307	8
	GO:0012501~programmed cell death	5	21	0.00331	7
	GO:0008219~cell death	5	21	0.00466	7
	GO:0016265~death	5	21	0.00493	7
8	GO:0010926~anatomical structure formation	7	29	0.00395	4
	GO:0022607~cellular component assembly	6	25	0.00599	5
	GO:0044085~cellular component biogenesis	6	25	0.00927	4
9	GO:0051336~regulation of hydrolase activity	5	21	0.00092	11
	GO:0051345~positive regulation of hydrolase activity	4	17	0.00148	17
	GO:0050790~regulation of catalytic activity	5	21	0.02626	4
	GO:0043085~positive regulation of catalytic activity	4	17	0.03707	5
10	GO:0009117~nucleotide metabolic process	4	17	0.01303	8
	GO:0006753~nucleoside phosphate metabolic process	4	17	0.01303	8
	GO:0055086~nucleobase, nucleoside and nucleotide metabolic process	4	17	0.01752	7
11	GO:0046034~ATP metabolic process	3	13	0.01666	14
	GO:0009205~purine ribonucleoside triphosphate metabolic process	3	13	0.02073	13
	GO:0009199~ribonucleoside triphosphate metabolic process	3	13	0.02101	13
	GO:0009144~purine nucleoside triphosphate metabolic process	3	13	0.02216	12
	GO:0009141~nucleoside triphosphate metabolic process	3	13	0.02424	12
	GO:0009150~purine ribonucleotide metabolic process	3	13	0.02672	11
	GO:0009259~ribonucleotide metabolic process	3	13	0.02831	11
	GO:0006163~purine nucleotide metabolic process	3	13	0.04704	8
12	GO:0048468~cell development	6	25	0.01822	4
	GO:0048869~cellular developmental process	7	29	0.03722	3
13	GO:0048545~response to steroid hormone stimulus	4	17	0.01303	8

6.1.2.2 MI vs. BMMNC

Biological process GO terms associated with the proteins up-regulated in MI vs. BMMNC grouped into 14 clusters. Clusters 1-9 all contained terms with p-values <0.05. Clusters 1 to 9 contained terms related to the following; transport and localisation (cluster 1 and 2), muscle development and contraction (cluster 3 and 4) and circulation (cluster 5). Groups 1 to 9 are detailed in Table 6.4.

There were only 4 proteins down-regulated in MI vs. BMMNC, and the biological process GO terms formed one cluster, this group included two terms relating to cellular catabolic process and is shown in Table 6.5.

Clustering of associated KEGG pathway terms was not possible for the proteomic data. There was only a single pathway associated with the Sham vs. MI down-regulated and MI vs. BMMNC up-regulated gene lists, this was oxidative phosphorylation (Figure 6.5). The four proteins associated with this pathway were NADH-ubiquinone oxidoreductase 75kDa subunit (Ndufs1), succinate dehydrogenase (Sdha), cytochrome b-c1 complex subunit Rieske (Uqcrcfs1) and ATP synthase subunit β (Atp5b).

Table 6.4 Clusters 1 -9 of 14 clusters of biological process GO terms associated with proteins up-regulated in MI vs. BMMNC
 The GO terms within each cluster, count (number of genes from list with this annotation), % (percentage of the inputted genes found with this annotation), p-value (modified Fisher's exact test (EASE score) and fold enrichment (the fold enrichment of this annotation in the uploaded gene list versus the proportion of this annotation in the background dataset). Only significantly associated GO terms (p-value <0.05) are shown.

Cluster	GO Biological Process Term	Count	%	PValue	Fold Enrichment
1	GO:0006810~transport	12	55	0.00003	4
	GO:0051234~establishment of localization	12	55	0.00004	4
	GO:0051179~localization	12	55	0.00020	3
2	GO:0051641~cellular localization	7	32	0.00038	6
	GO:0046907~intracellular transport	6	27	0.00052	8
	GO:0051649~establishment of localization in cell	6	27	0.00201	6
3	GO:0030049~muscle filament sliding	3	14	0.00002	406
	GO:0033275~actin-myosin filament sliding	3	14	0.00002	406
	GO:0070252~actin-mediated cell contraction	3	14	0.00004	290
	GO:0043462~regulation of ATPase activity	3	14	0.00012	169
	GO:0030048~actin filament-based movement	3	14	0.00014	156
	GO:0045214~sarcomere organization	3	14	0.00022	127
	GO:0055010~ventricular cardiac muscle morphogenesis	3	14	0.00046	88
	GO:0030239~myofibril assembly	3	14	0.00050	85
	GO:0055002~striated muscle cell development	3	14	0.00054	81
	GO:0055001~muscle cell development	3	14	0.00084	66
	GO:0055008~cardiac muscle tissue morphogenesis	3	14	0.00090	63
	GO:0060415~muscle tissue morphogenesis	3	14	0.00090	63
	GO:0030705~cytoskeleton-dependent intracellular transport	3	14	0.00101	60
	GO:0006941~striated muscle contraction	3	14	0.00147	50
	GO:0051146~striated muscle cell differentiation	3	14	0.00218	41
	GO:0008016~regulation of heart contraction	3	14	0.00411	29
	GO:0003007~heart morphogenesis	3	14	0.00509	26
	GO:0006936~muscle contraction	3	14	0.00734	22
	GO:0042692~muscle cell differentiation	3	14	0.00812	21
	GO:0003012~muscle system process	3	14	0.00945	19
GO:0014706~striated muscle tissue development	3	14	0.02494	11	

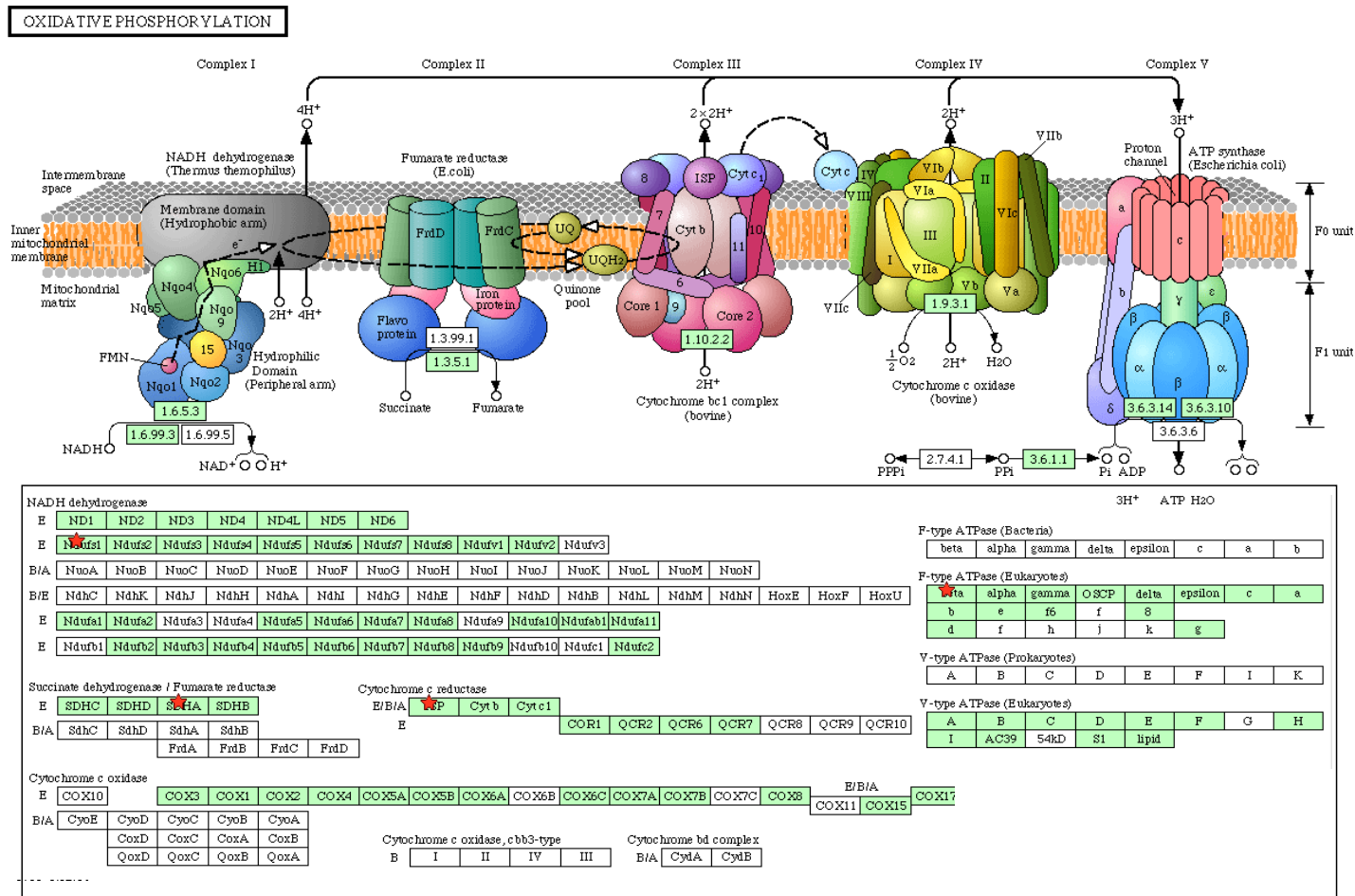
Table 6.4 continued.

Cluster	GO Biological Process Term	Count	%	PValue	Fold Enrichment
3 cont.	GO:0060537~muscle tissue development	3	14	0.02680	11
	GO:0007507~heart development	3	14	0.03754	9
	GO:0007517~muscle organ development	3	14	0.03754	9
	GO:0048729~tissue morphogenesis	3	14	0.04361	8
4	GO:0030036~actin cytoskeleton organization	4	18	0.00220	14
	GO:0030029~actin filament-based process	4	18	0.00247	14
	GO:0007010~cytoskeleton organization	4	18	0.01087	8
	GO:0032989~cellular component morphogenesis	4	18	0.01502	7
5	GO:0008015~blood circulation	4	18	0.00144	17
	GO:0003013~circulatory system process	4	18	0.00144	17
6	GO:0048646~anatomical structure formation involved in morphogenesis	4	18	0.00944	8
	GO:0010926~anatomical structure formation	5	23	0.04394	3
8	GO:0010926~anatomical structure formation	5	23	0.04394	3
9	GO:0048856~anatomical structure development	8	36	0.02768	2

Table 6.5 One cluster of biological process GO terms associated with proteins down-regulated in MI vs. BMMNC The GO terms within each cluster, count (number of genes from list with this annotation), % (percentage of the inputted genes found with this annotation), p-value (modified Fisher's exact test (EASE score) and fold enrichment (the fold enrichment of this annotation in the uploaded gene list versus the proportion of this annotation in the background dataset). Only significantly associated GO terms (p-value <0.05) are shown.

Cluster	GO Biological Process Term	Count	%	PValue	Fold Enrichment
1	GO:0044248~cellular catabolic process	3	75	0.01087	12
	GO:0009056~catabolic process	3	75	0.02956	7

Figure 6.5 KEGG Pathway - Oxidative Phosphorylation Proteins identified as being down-regulated in Sham vs. MI and up-regulated in MI vs. BMMNC are highlighted by red stars.



6.1.3 Ingenuity Pathway Analysis (IPA)

Data from 73 spots for which there was a single protein identity were uploaded in the form of RefSeq ID's with fold changes and p-values for both the Sham vs. MI and the MI vs. BMMNC comparisons.

6.1.3.1 *Sham vs. MI*

31 proteins differentially expressed in Sham vs. MI mapped in IPA (Table 6.6 A), and these were associated within three different networks along with a further 42 different proteins and endogenous chemicals (Table 6.6 B). Networks 1 and 2 had scores of 35 and 33 respectively; network 3 had a much lower score of 2. Networks 1 and 2 are shown in Figures 6.6 A and B.

Network 1 contains 16 proteins from our dataset and is mainly related to cardiovascular system development and function and has several major hubs including nuclear factor kappa-light-chain-enhancer of activated B cells (NFkB) complex, p38 mitogen activated protein kinase (p38 MAPK), protein kinase C (Pkc), Insulin and Myosin see Figure 6.6 A. NFkB is linked to one down regulated protein (Pebp1) and three up-regulated proteins (Dbt, Alb and Hspd1). There is evidence that Hspd1 and Albumin (both up-regulated) are involved in increased translocation and activation of NFkB [119-121]. Whereas, the down-regulated Pebp1 has been shown to antagonise activation of NFkB [122]. P38 MAPK, which increases activation of NFkB, is linked to two down-regulated proteins (Des and Hspb8) and to the up-regulated hspd1. Both heat shock proteins have been shown to increase activation of p38 MAPK as part of apoptosis signalling cascades [123, 124]. Insulin is linked to Alb, Actc1 and Ywhae. Insulin has been shown to increase the binding of Ywhae and Pkc α ; Ywhae overexpression has also been shown to increase downstream ERK1/2 and Akt activation [125]. Insulin has also been shown to regulate transcription of Albumin [126]. The Myosin hub consists of links between the myofibrillar/contractile proteins, including Actc1, Tnnt2, Myh6 and Myl2.

Network 2 contains 15 proteins from our dataset and is mainly related to lipid metabolism and small molecule biochemistry and contains several major hubs including tumour necrosis factor (Tnf), v-myc myelocytomatosis viral oncogene homolog (Myc), and the endogenous chemicals cholesterol, beta-estradiol and hydrogen peroxide see Figure 6.6 B. Myc is thought to cause reduced expression of Tpm1 and increase expression of Prdx6. Myc also interacts with Ywhae [127]. Myc also has known but undefined associations with Tuba4a and Ndufs1. Tnf has known associations with Tpm1 and Ldhd, and is also known to decrease expression of Acads [128].

Network 3 consists of the interaction of membrane metallo-endopeptidase (Mme) with NADP transhydrogenase a.k.a nicotinamide nucleotide transhydrogenase (Nnt).

Table 6.6 Proteins and endogenous chemicals included in the IPA analysis of Sham vs. MI proteomics data A) Proteomic results mapped into IPA for core analysis. B) Associated proteins and endogenous chemicals also included in the Sham vs. MI IPA core analysis. Protein symbol and Entrez gene names are shown alongside the network(s) the protein/chemical is found in, the sub-cellular localisation and molecule type.

A

Symbol	Entrez Gene Name	Networks	Location	Type(s)
TNNT2	troponin T type 2 (cardiac)	1	Cytoplasm	other
ATP5B	ATP synthase, H ⁺ transporting, mitochondrial F1 complex, beta polypeptide	1	Cytoplasm	transporter
YWHAE	tyrosine 3-monooxygenase/tryptophan 5-monooxygenase activation protein, epsilon polypeptide	1	Cytoplasm	other
CAP1	CAP, adenylate cyclase-associated protein 1 (yeast)	1	Plasma Membrane	other
ACTC1	actin, alpha, cardiac muscle 1	1	Cytoplasm	enzyme
MYL3	myosin, light chain 3, alkali; ventricular, skeletal, slow	1	Cytoplasm	other
DES	desmin	1	Cytoplasm	other
PEBP1	phosphatidylethanolamine binding protein 1	1	Cytoplasm	other
CKM	creatine kinase, muscle	1	Cytoplasm	kinase
HSPB8	heat shock 22kDa protein 8	1	Cytoplasm	kinase
MYH6	myosin, heavy chain 6, cardiac muscle, alpha	1	Cytoplasm	enzyme
DBT	dihydrolipoamide branched chain transacylase E2	1	Cytoplasm	enzyme
HSPD1	heat shock 60kDa protein 1 (chaperonin)	1	Cytoplasm	enzyme
ALB	albumin	1	Extracellular Space	transporter
MYL2	myosin, light chain 2, regulatory, cardiac, slow	1	Cytoplasm	other
TPM1	tropomyosin 1 (alpha)	1,2	Cytoplasm	other
NDUFS1	NADH dehydrogenase (ubiquinone) Fe-S protein 1, 75kDa (NADH-coenzyme Q reductase)	2	Cytoplasm	enzyme
LDHB	lactate dehydrogenase B	2	Cytoplasm	enzyme
TUBA4A	tubulin, alpha 4a	2	Cytoplasm	other
HSPA9	heat shock 70kDa protein 9 (mortalin)	2	Cytoplasm	other
SDHA	succinate dehydrogenase complex, subunit A, flavoprotein (Fp)	2	Cytoplasm	enzyme

Table 6.6 A continued.

Symbol	Entrez Gene Name	Networks	Location	Type(s)
PRDX6	peroxiredoxin 6	2	Cytoplasm	enzyme
ACADS	acyl-Coenzyme A dehydrogenase, C-2 to C-3 short chain	2	Cytoplasm	enzyme
GFM1	G elongation factor, mitochondrial 1	2	Cytoplasm	translation regulator
ETFA	electron-transfer-flavoprotein, alpha polypeptide	2	Cytoplasm	transporter
CKMT2	creatine kinase, mitochondrial 2 (sarcomeric)	2	Cytoplasm	kinase
ECHS1	enoyl Coenzyme A hydratase, short chain, 1, mitochondrial	2	Cytoplasm	enzyme
PRDX3	peroxiredoxin 3	2	Cytoplasm	enzyme
DLAT	dihydrolipoamide S-acetyltransferase	2	Cytoplasm	enzyme
HCG 25371 (Uqcrh)	ubiquinol-cytochrome c reductase hinge protein-like	2	Cytoplasm	enzyme
NNT	nicotinamide nucleotide transhydrogenase	3	Cytoplasm	enzyme

Table 6.6 B

Symbol	Entrez Gene Name	Networks	Location	Type(s)
Actin	--	1	unknown	group
Akt	--	1	unknown	group
ATPase	--	1	unknown	group
Insulin	--	1	unknown	group
Mlc	--	1	unknown	group
Mlcp	--	1	Cytoplasm	complex
MYL4	myosin, light chain 4, alkali; atrial, embryonic	1	Cytoplasm	other
Myosin	--	1	Cytoplasm	complex
Myosin Light Chain Kinase	--	1	unknown	group
NFkB (complex)	--	1	Nucleus	complex
P38 MAPK	--	1	unknown	group
Pkc(s)	--	1	unknown	group
RNA polymerase II	--	1	Nucleus	complex
SLC9A8	solute carrier family 9 (sodium/hydrogen exchanger), member 8	1	Cytoplasm	transporter

Table 6.6 B continued.

Symbol	Entrez Gene Name	Networks	Location	Type(s)
SPAST	spastin	1	Nucleus	enzyme
Tni	--	1	unknown	group
Tropomyosin	--	1	unknown	group
Troponin t	--	1	unknown	group
TNNC1	troponin C type 1 (slow)	1,2	Cytoplasm	other
ABCC9	ATP-binding cassette, sub-family C (CFTR/MRP), member 9	2	Plasma Membrane	ion channel
ACADVL	acyl-Coenzyme A dehydrogenase, very long chain	2	Cytoplasm	enzyme
AGT	angiotensinogen (serpin peptidase inhibitor, clade A, member 8)	2	Extracellular Space	other
ATP	--	2	unknown	chemical - endogenous mammalian
ATP5O	ATP synthase, H+ transporting, mitochondrial F1 complex, O subunit	2	Cytoplasm	transporter
beta-estradiol	--	2	unknown	chemical - endogenous mammalian
CFD	complement factor D (adipsin)	2	Extracellular Space	peptidase
cholesterol	--	2	unknown	chemical - endogenous mammalian
CNN1	calponin 1, basic, smooth muscle	2	Cytoplasm	other
CTNNB1	catenin (cadherin-associated protein), beta 1, 88kDa	2	Nucleus	transcription regulator
FCGRT	Fc fragment of IgG, receptor, transporter, alpha	2	Plasma Membrane	transmembrane receptor
hydrogen peroxide	--	2	unknown	chemical - endogenous mammalian

Table 6.6 B continued.

Symbol	Entrez Gene Name	Networks	Location	Type(s)
MYC	v-myc myelocytomatosis viral oncogene homolog (avian)	2	Nucleus	transcription regulator
PKD3	pyruvate dehydrogenase kinase, isozyme 3	2	Cytoplasm	kinase
PPARGC1B	peroxisome proliferator-activated receptor gamma, coactivator 1 beta	2	Nucleus	transcription regulator
PRDX2	peroxiredoxin 2	2	Cytoplasm	enzyme
SLC25A13	solute carrier family 25, member 13 (citrin)	2	Cytoplasm	transporter
TNF	tumor necrosis factor (TNF superfamily, member 2)	2	Extracellular Space	cytokine
TRAF6	TNF receptor-associated factor 6	2	Cytoplasm	enzyme
MME	membrane metallo-endopeptidase	3	Plasma Membrane	peptidase
NAD(P) transhydrogenase (AB-specific)	--	3	unknown	group
NAD(P) transhydrogenase (B-specific)	--	3	unknown	group
phosphate	--	3	unknown	chemical - endogenous mammalian

Figure 6.6 Two of three networks associated with the proteins altered in Sham vs. MI A) Network 1. B) Network 2. Proteins highlighted in red were found to be up-regulated, and those highlighted in green were down-regulated in Sham vs. MI. Full names of these proteins can be found in Table 6.5.

A

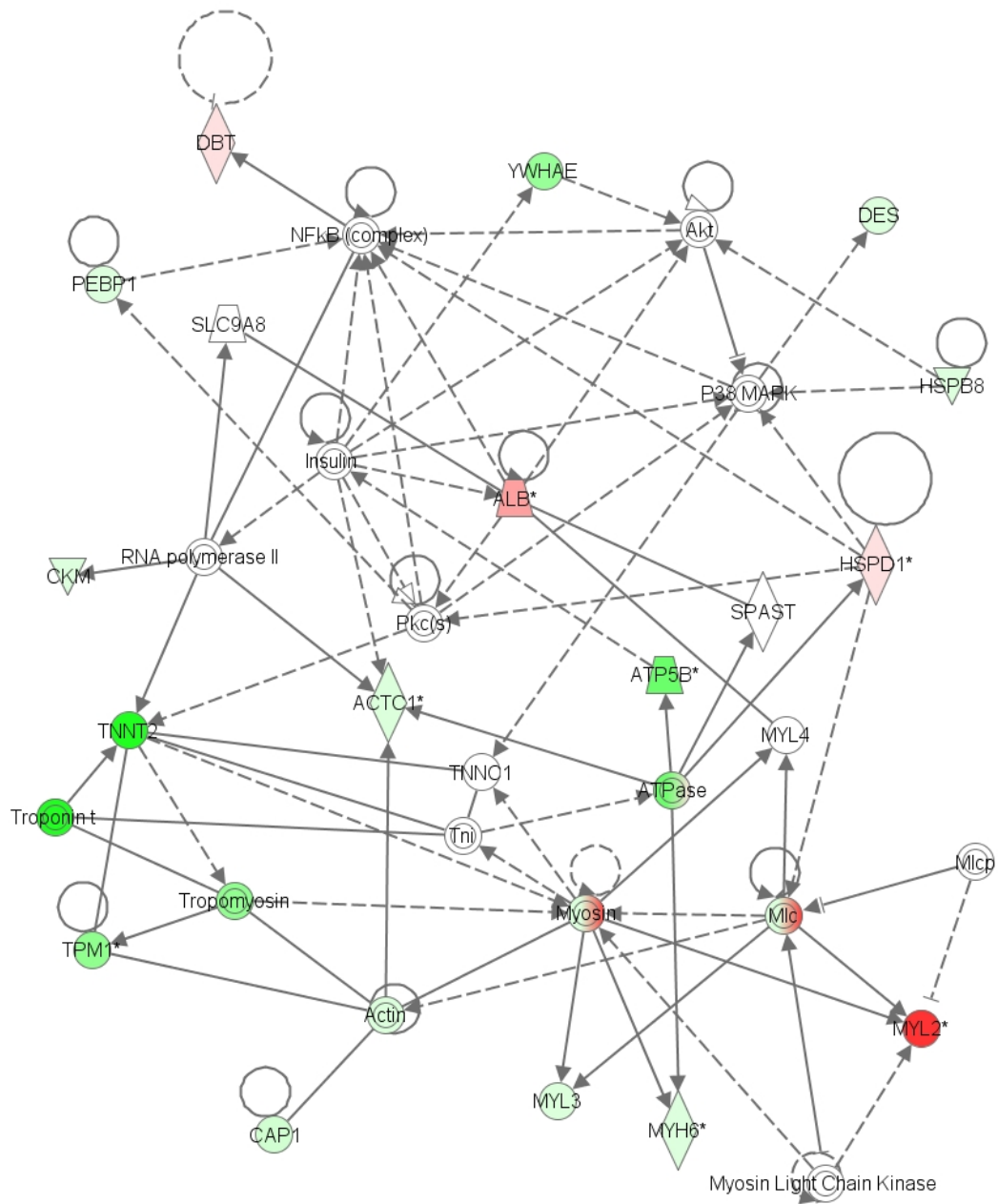
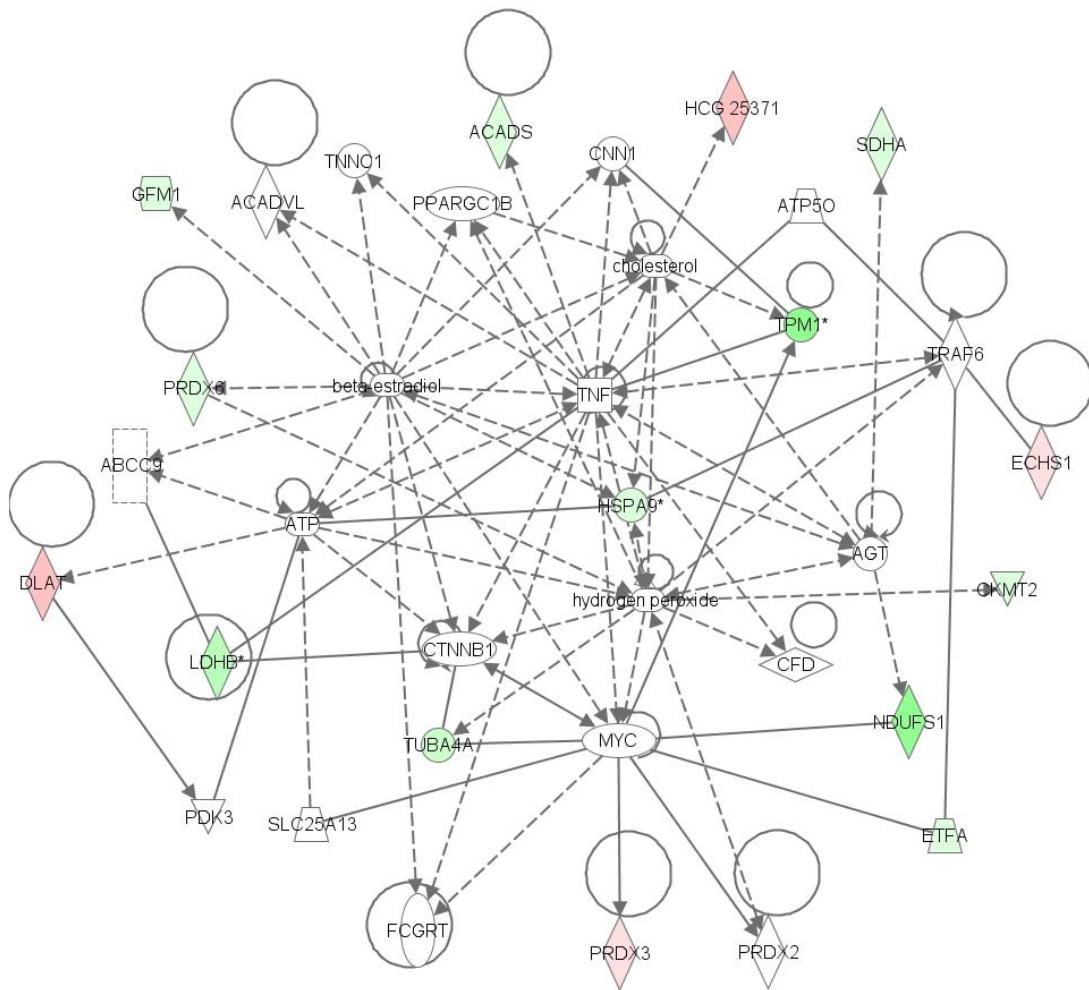


Figure 6.6 B



The top canonical pathways associated with the proteins altered in Sham vs. MI are shown in Table 6.7. Pathways relating to small molecule biochemistry make up the main part of these pathways. Calcium signalling is highlighted due to the presence of proteins involved in muscle cell contraction. There are several proteins involved in oxidative phosphorylation and the up-regulation of Prdx3 suggests mitochondrial dysfunction.

Table 6.7 Top 10 canonical pathways associated with the 36 proteins altered in Sham vs. MI

Ingenuity Canonical Pathways	-log(p-value)	Ratio	Molecules
Butanoate Metabolism	6.74E+00	3.79E-02	SDHA,ECHS1,DBT,PRDX6,ACADS
Calcium Signaling	5.85E+00	2.93E-02	TPM1,MYH6,MYL2,TNNT2,ACTC1,MYL3
Mitochondrial Dysfunction	3.81E+00	2.34E-02	SDHA,PRDX3,NDUFS1,ATP5B
Oxidative Phosphorylation	3.56E+00	2.41E-02	SDHA,NDUFS1,HCG 25371,ATP5B
Tight Junction Signaling	3.47E+00	2.40E-02	MYH6,MYL2,ACTC1,MYL3
Propanoate Metabolism	3.44E+00	2.31E-02	ECHS1,LDHB,ACADS
Valine, Leucine and Isoleucine Degradation	3.38E+00	2.70E-02	ECHS1,DBT,ACADS
ILK Signaling	3.28E+00	2.15E-02	MYH6,MYL2,ACTC1,MYL3
Regulation of Actin-based Motility by Rho	3.12E+00	3.26E-02	MYL2,ACTC1,MYL3
Actin Cytoskeleton Signaling	3.02E+00	1.72E-02	MYH6,MYL2,ACTC1,MYL3

6.1.3.2 MI vs. BMMNC

25 proteins that were differentially expressed in Sham vs. MI were mapped in IPA (Table 6.8 A). These were associated within three different networks along with a further 79 different proteins and endogenous chemicals (Table 6.8 B). These three networks are shown in Figures 6.7 A-C. Networks 1 and 2 had scores of 27 and 22 respectively, network 3 had a much lower score of 5.

Network 1 contains 12 proteins from our dataset and is mainly related to cell cycle and muscle system development and function. Hepatocyte nuclear factor 4 alpha (Hnf4a), Beta-estradiol (E2), transforming growth factor beta 1 (Tgf- β) and 14-3-3 zeta (Ywhaz) are all hubs within this network see Figure 6.7 A. Binding of Hnf4a and two of our proteins (Mccc1 and Hsd12) is known to occur in the liver [129]. E2 is a hormone with many different roles besides its main actions on reproductive function. It has been linked to cardioprotection during hypoxia/reoxygenation induced apoptosis through the inhibition of mitochondrial ROS formation (antioxidant properties) and p38 α MAPK activation, activation of Pi3k, and activation of p38 β MAPK [130]. E2 has also been shown to limit Angiotensin II (Ang II) induced hypertrophy [131]. These modes of functionality explain why it has been linked to expression of structural proteins Myh6 and Tnnt2 and expression of Ckm and modification of the antioxidant Prdx6. Tgf- β is involved in many functions, but mainly growth arrest and signals through Smad and p38 MAPK/JNK pathways [132]. Tgf β has known to increase the expression of both Tpm1 and Tnnt2 and inhibit expression of Ckm [133-135]. Ywhaz is a

molecular chaperone related to the epsilon isoform found in our dataset and has uncharacterised associations with Ndufa10, Pgam1 and Echs1.

Network 2 contains ten proteins from dataset and is mainly related to DNA replication, recombination and repair as well as energy production. The main hubs within this network are Ywhae, Ang II receptor type 1 (Agtr1), Insulin and Vascular endothelial growth factor (Vegf), see Figure 6.7 B. Ywhae is only linked to a single other protein (Hsp70) from our dataset and this is due to evidence of a binding interaction [136]. In a study of the effects of Agtr1 mediated effects of Ang II on beta arrestin complex formation; Ywhae, Atp5b and Sdha were all identified as proteins which dissociate from beta arrestin upon Agtr1 stimulation [137]. Insulin is linked to both Ywhae and Alb and these connections were detailed in section 6.1.3.1. Glycated Alb has been shown to increase expression of Vegf and Vegf has also been linked to increased expression of Etfa (up-regulated in MI vs. BMMNC) [138, 139].

Table 6.8 Table showing proteins and endogenous chemicals included in the IPA analysis of MI vs. BMMNC proteomics data A) Proteomic results mapped into IPA for core analysis. **B)** Associated proteins and endogenous chemicals also included in the Sham vs. MI IPA core analysis. Protein symbol and Entrez gene names are shown alongside the network(s) the protein/chemical is found in, the sub-cellular localisation and molecule type.

A

Symbol	Entrez Gene Name	Networks	Location	Type(s)
HCG 25371 (Uqcrh)	ubiquinol-cytochrome c reductase hinge protein-like	1	Cytoplasm	enzyme
MYH6	myosin, heavy chain 6, cardiac muscle, alpha	1	Cytoplasm	enzyme
ECHS1	enoyl Coenzyme A hydratase, short chain, 1, mitochondrial	1	Cytoplasm	enzyme
PGAM1	phosphoglycerate mutase 1 (brain)	1	Cytoplasm	phosphatase
CKM	creatine kinase, muscle	1	Cytoplasm	kinase
NDUFA10 (includes EG:4705)	NADH dehydrogenase (ubiquinone) 1 alpha subcomplex, 10, 42kDa	1	Cytoplasm	enzyme
CKMT2	creatine kinase, mitochondrial 2 (sarcomeric)	1	Cytoplasm	kinase
PRDX6	peroxiredoxin 6	1	Cytoplasm	enzyme
MCCC1	methylcrotonoyl-Coenzyme A carboxylase 1 (alpha)	1	Cytoplasm	enzyme
HSDL2	hydroxysteroid dehydrogenase like 2	1	Cytoplasm	transporter
TPM1	tropomyosin 1 (alpha)	1	Cytoplasm	other
TNNT2	troponin T type 2 (cardiac)	1	Cytoplasm	other
DLAT	dihydrolipoamide S-acetyltransferase	2	Cytoplasm	enzyme
ETF1A	electron-transfer-flavoprotein, alpha polypeptide	2	Cytoplasm	transporter
SDHA	succinate dehydrogenase complex, subunit A, flavoprotein (Fp)	2	Cytoplasm	enzyme
HSPA9	heat shock 70kDa protein 9 (mortalin)	2	Cytoplasm	other
LDHB	lactate dehydrogenase B	2	Cytoplasm	enzyme
HSPA8	heat shock 70kDa protein 8	2	Cytoplasm	enzyme
ALB	albumin	2	Extracellular Space	transporter
ENSMUSG00000047676 (RPSA)	ribosomal protein SA pseudogene	2	Plasma Membrane	transmembrane receptor
ATP5B	ATP synthase, H ⁺ transporting, mitochondrial F1 complex, beta polypeptide	2	Cytoplasm	transporter

Table 6.8 A continued.

Symbol	Entrez Gene Name	Networks	Location	Type(s)
YWHAE	tyrosine 3-monooxygenase/tryptophan 5-monooxygenase activation protein, epsilon polypeptide	2	Cytoplasm	other
DES	desmin	3	Cytoplasm	other
WDR1	WD repeat domain 1	3	Extracellular Space	other
CAP1	CAP, adenylate cyclase-associated protein 1 (yeast)	3	Plasma Membrane	other

Table 6.8 B

Symbol	Entrez Gene Name	Networks	Location	Type(s)
beta-estradiol	--	1	unknown	chemical - endogenous mammalian
CNN1	calponin 1, basic, smooth muscle	1	Cytoplasm	other
Cofilin	--	1	unknown	group
CYC1	cytochrome c-1	1	Cytoplasm	enzyme
dCTP	--	1	unknown	chemical - endogenous mammalian
DSTN	destrin (actin depolymerizing factor)	1	Cytoplasm	other
GH1	growth hormone 1	1	Extracellular Space	cytokine
HNF4A	hepatocyte nuclear factor 4, alpha	1	Nucleus	transcription regulator
hydrogen peroxide	--	1	unknown	chemical - endogenous mammalian
MAP3K5 (includes EG:293015)	mitogen-activated protein kinase kinase kinase 5	1	unknown	kinase
MAPK13	mitogen-activated protein kinase 13	1	Cytoplasm	kinase

Table 6.8 B continued.

Symbol	Entrez Gene Name	Networks	Location	Type(s)
MLL2	myeloid/lymphoid or mixed-lineage leukemia 2	1	Nucleus	transcription regulator
SIK1	salt-inducible kinase 1	1	Cytoplasm	kinase
TEAD3	TEA domain family member 3	1	Nucleus	transcription regulator
TGFB1	transforming growth factor, beta 1	1	Extracellular Space	growth factor
TMOD2	tropomodulin 2 (neuronal)	1	Cytoplasm	other
Tni	--	1	unknown	group
TNNC1	troponin C type 1 (slow)	1	Cytoplasm	other
TNNT1	troponin T type 1 (skeletal, slow)	1	unknown	other
Tropomyosin	--	1	unknown	group
Troponin t	--	1	unknown	group
WNT11	wingless-type MMTV integration site family, member 11	1	Extracellular Space	other
YWHAZ	tyrosine 3-monooxygenase/tryptophan 5-monooxygenase activation protein, zeta polypeptide	1	Cytoplasm	enzyme
AGTR1	angiotensin II receptor, type 1	2	Plasma Membrane	G-protein coupled receptor
ATP5	--	2	unknown	group
ATP5A1	ATP synthase, H ⁺ transporting, mitochondrial F1 complex, alpha subunit 1, cardiac muscle	2	Cytoplasm	transporter
ATP5E	ATP synthase, H ⁺ transporting, mitochondrial F1 complex, epsilon subunit	2	Cytoplasm	transporter
ATP5O	ATP synthase, H ⁺ transporting, mitochondrial F1 complex, O subunit	2	Cytoplasm	transporter
Caspase	--	2	unknown	group
CLIC4	chloride intracellular channel 4	2	Cytoplasm	ion channel
DNAJC13	DnaJ (Hsp40) homolog, subfamily C, member 13	2	unknown	other
FBXO45	F-box protein 45	2	unknown	other
GPR37	G protein-coupled receptor 37 (endothelin receptor type B-like)	2	Plasma Membrane	G-protein coupled receptor

Table 6.8 B continued.

Symbol	Entrez Gene Name	Networks	Location	Type(s)
Hsp70	--	2	unknown	group
HSPA2	heat shock 70kDa protein 2	2	Cytoplasm	other
Insulin	--	2	unknown	group
IRS4	insulin receptor substrate 4	2	Cytoplasm	other
MYOCD	myocardin	2	Nucleus	transcription regulator
PACRG	PARK2 co-regulated	2	Cytoplasm	other
PEG3	paternally expressed 3	2	Nucleus	kinase
RICTOR	RPTOR independent companion of MTOR, complex 2	2	Cytoplasm	other
SDH	--	2	unknown	group
SDHD	succinate dehydrogenase complex, subunit D, integral membrane protein	2	Cytoplasm	enzyme
SPAST	spastin	2	Nucleus	enzyme
SRPK2	SFRS protein kinase 2	2	Nucleus	kinase
TBK1	TANK-binding kinase 1	2	Cytoplasm	kinase
VEGFA	vascular endothelial growth factor A	2	Extracellular Space	growth factor
ACADM	acyl-Coenzyme A dehydrogenase, C-4 to C-12 straight chain	3	Cytoplasm	enzyme
ACTG1	actin, gamma 1	3	Cytoplasm	other
APOB	apolipoprotein B (including Ag(x) antigen)	3	Extracellular Space	transporter
CBL	Cas-Br-M (murine) ecotropic retroviral transforming sequence	3	Nucleus	transcription regulator
CFL1	cofilin 1 (non-muscle)	3	Nucleus	other
CRYAB	crystallin, alpha B	3	Nucleus	other
D-glucose	--	3	unknown	chemical - endogenous mammalian
F Actin	--	3	Cytoplasm	complex
fatty acid	--	3	unknown	chemical - endogenous mammalian

Table 6.8 B continued.

Symbol	Entrez Gene Name	Networks	Location	Type(s)
FOXA2	forkhead box A2	3	Nucleus	transcription regulator
HSPB1	heat shock 27kDa protein 1	3	Cytoplasm	other
INSR	insulin receptor	3	Plasma Membrane	kinase
IRS1	insulin receptor substrate 1	3	Cytoplasm	other
LDHA	lactate dehydrogenase A	3	Cytoplasm	enzyme
lipid	--	3	unknown	chemical - endogenous mammalian
MEF2	--	3	unknown	group
MEF2C	myocyte enhancer factor 2C	3	Nucleus	transcription regulator
melatonin	--	3	unknown	chemical - endogenous mammalian
norepinephrine	--	3	unknown	chemical - endogenous mammalian
PDPK1	3-phosphoinositide dependent protein kinase-1	3	Cytoplasm	kinase
PPARG	peroxisome proliferator-activated receptor gamma	3	Nucleus	ligand-dependent nuclear receptor
PRKCA	protein kinase C, alpha	3	Cytoplasm	kinase
PRKCB	protein kinase C, beta	3	Cytoplasm	kinase
PRKCE	protein kinase C, epsilon	3	Cytoplasm	kinase
SKIV2L	superkiller viralicidic activity 2-like (<i>S. cerevisiae</i>)	3	Cytoplasm	translation regulator
SLC2A4	solute carrier family 2 (facilitated glucose transporter), member 4	3	Plasma Membrane	transporter
TEAD4	TEA domain family member 4	3	Nucleus	transcription regulator
THRA	thyroid hormone receptor, alpha (erythroblastic leukemia viral (v-erb-a) oncogene homolog, avian)	3	Nucleus	ligand-dependent nuclear receptor

Table 6.8 B continued.

Symbol	Entrez Gene Name	Networks	Location	Type(s)
TUBB3	tubulin, beta 3	3	Cytoplasm	other
VAMP2	vesicle-associated membrane protein 2 (synaptobrevin 2)	3	Plasma Membrane	other
VIM	vimentin	3	Cytoplasm	other
HNRNPK	heterogeneous nuclear ribonucleoprotein K	2,3	Nucleus	other

Figure 6.7 Three networks associated with the proteins altered in MI vs. BMMNC **A) Network 1. B) Network 2. C) Network 3.** Proteins highlighted in red were found to be up-regulated, and those highlighted in green were down-regulated in MI vs. BMMNC. Full names of these proteins can be found in Table 6.7.

A

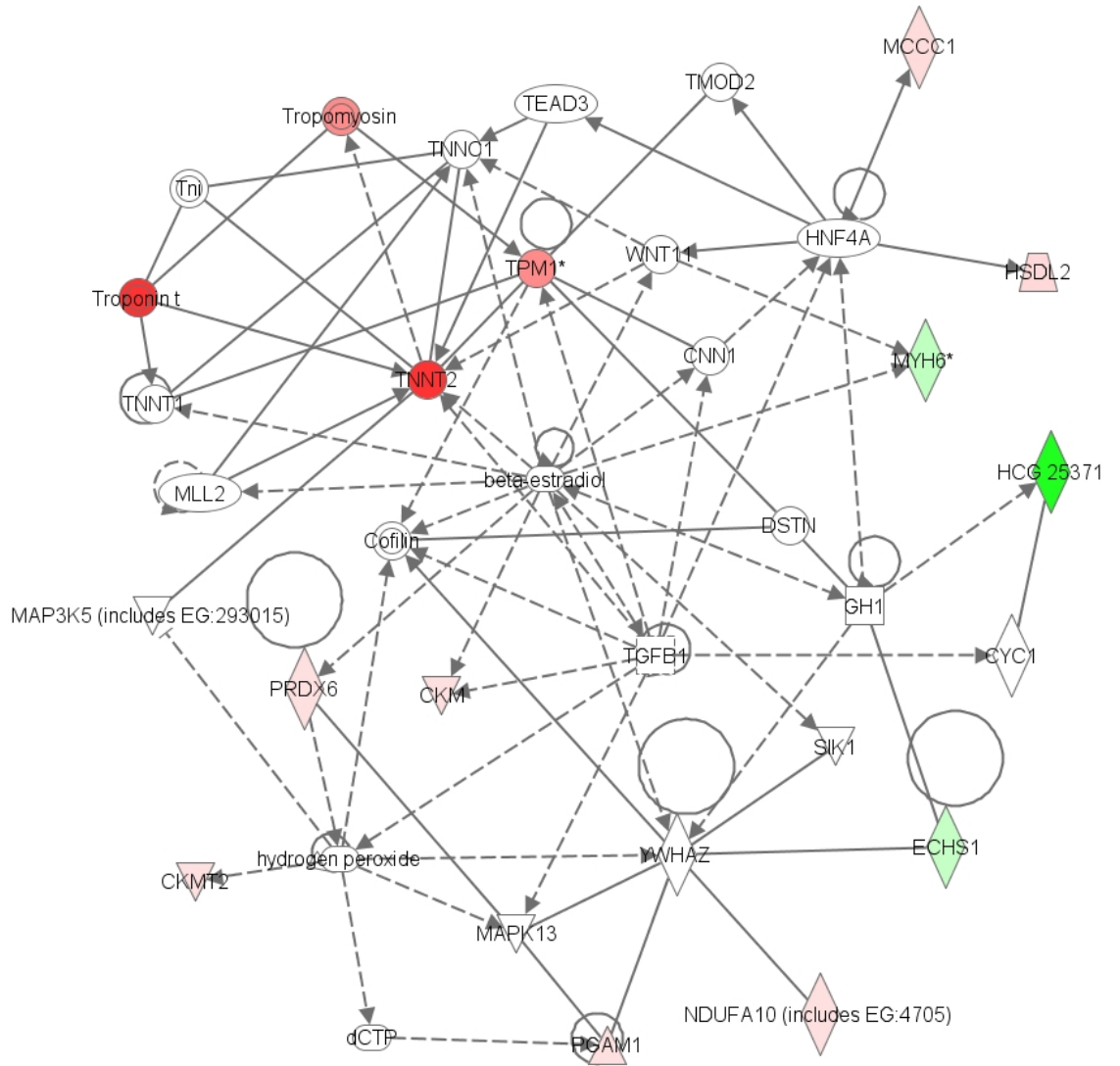


Figure 6.7 B

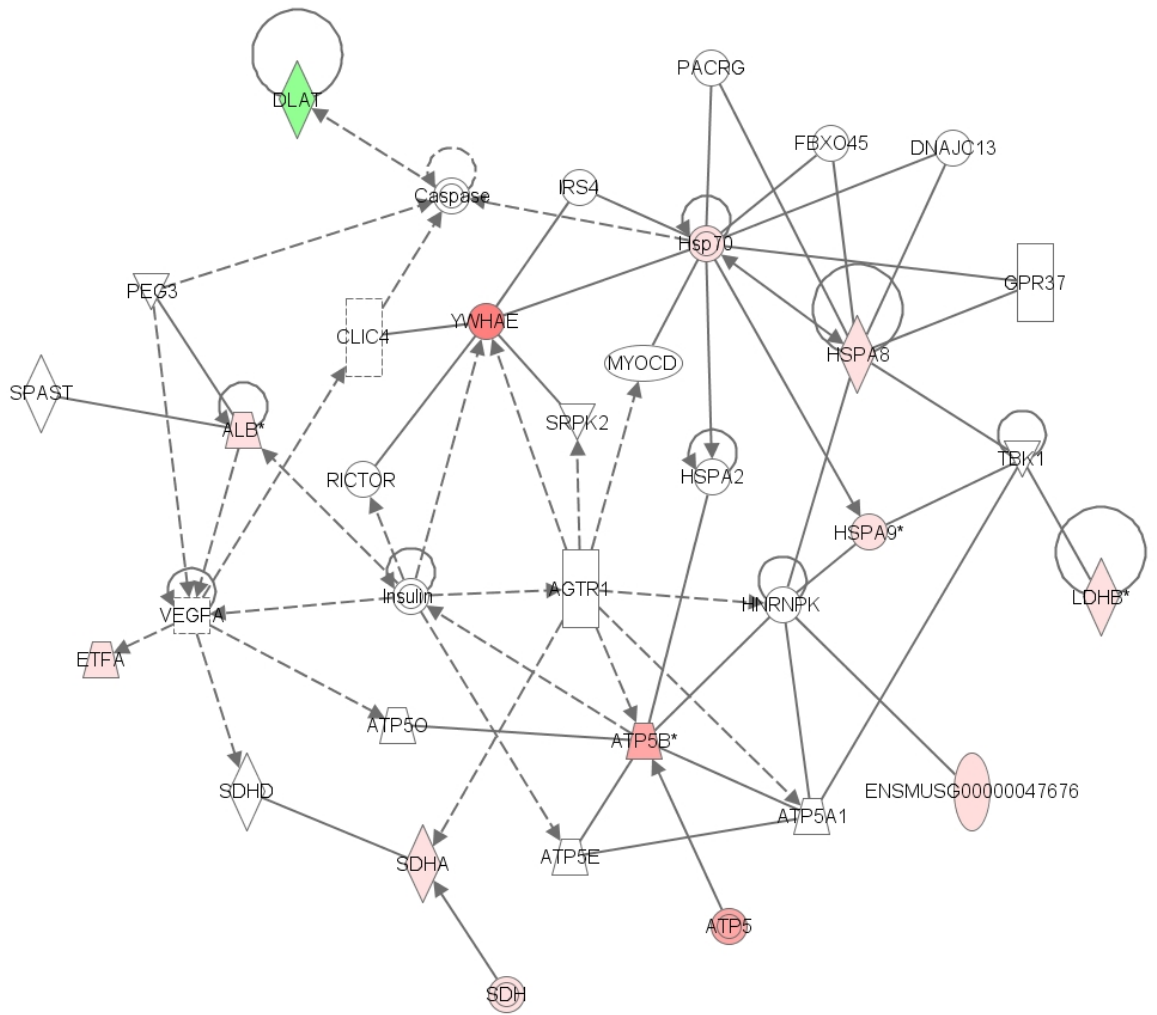
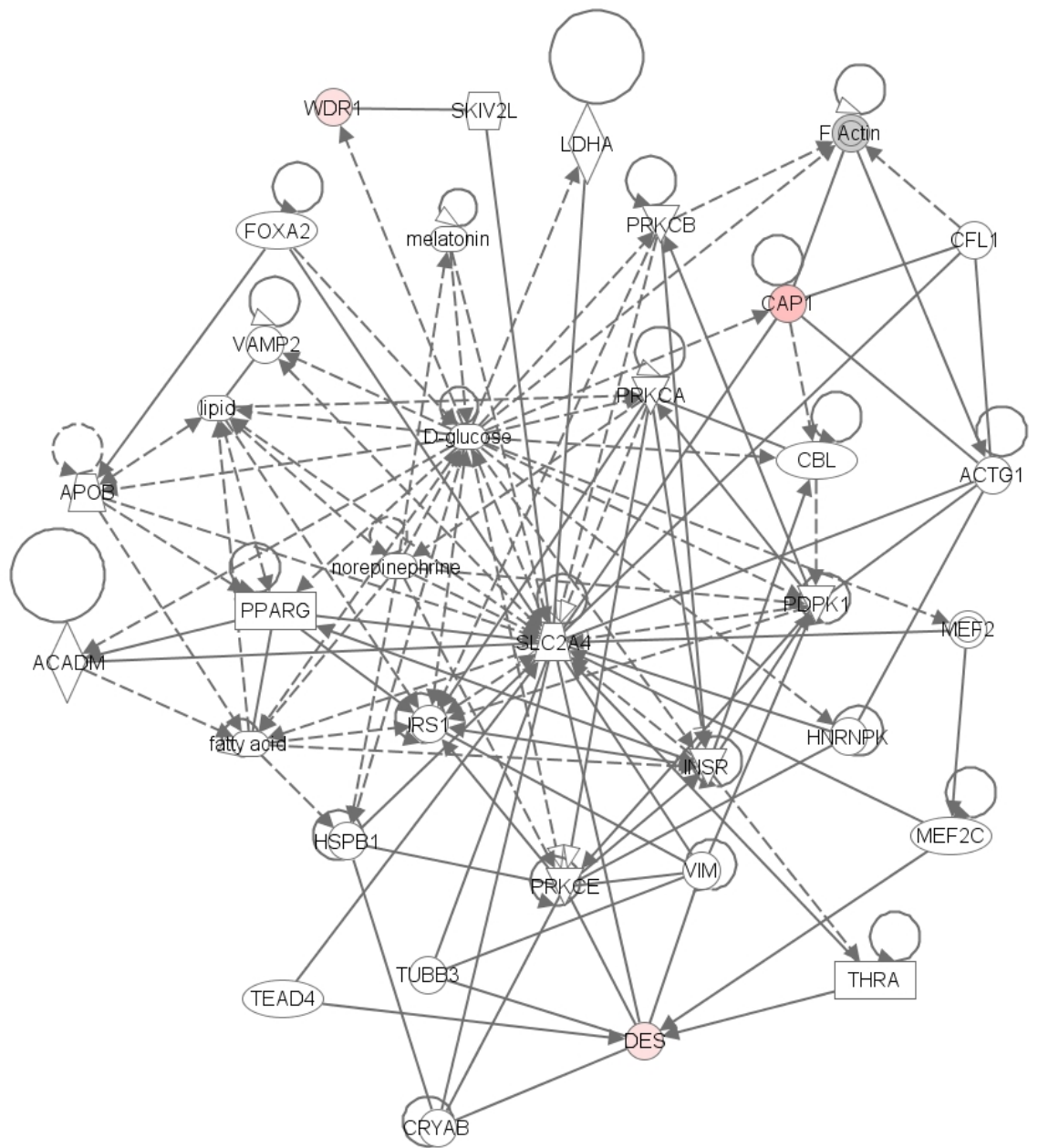


Figure 6.7 C



Network 3 contained only three proteins from our dataset and is linked to the functions of carbohydrate metabolism and molecular transport see Figure 6.7 C. There are several major hubs in this network, but the ones linked to the proteins from our dataset are solute carrier family 2 (facilitated glucose transporter) member 4 (Slc2a4) aka Glut-4, D-glucose and protein kinase C epsilon (Prkce). Glut-4 as a major hub and the interactions with many proteins from the MI vs. BMMNC dataset come from one study looking at insulin dependant interactions [140]. Glucose has a regulatory role in Wdr1 function, and an uncharacterised association with Des and Prkce is also highlighted.

The top ten canonical pathways associated with the proteins altered in MI vs. BMMNC are shown in Table 6.9. Oxidative phosphorylation and mitochondrial dysfunction are in the top as the expression changes in many of the proteins involved in these pathways were reversed in MI vs. BMMNC. Again many of the associated pathways relate to small molecule biochemistry.

Table 6.9 Top 10 canonical pathways associated with the 27 proteins altered in MI vs. BMMNC

Ingenuity Canonical Pathways	-log(p-value)	Ratio	Molecules
Oxidative Phosphorylation	4.00E+00	2.41E-02	SDHA,HCG 25371,NDUFA10 (includes EG:4705),ATP5B
Butanoate Metabolism	3.86E+00	2.27E-02	SDHA,ECHS1,PRDX6
Glycolysis/Gluconeogenesis	3.27E+00	2.11E-02	DLAT,PGAM1,LDHB
Mitochondrial Dysfunction	2.92E+00	1.75E-02	SDHA,NDUFA10 (includes EG:4705), ATP5B
Urea Cycle and Metabolism of Amino Groups	2.85E+00	2.50E-02	CKMT2,CKM
Calcium Signaling	2.57E+00	1.46E-02	TPM1,MYH6,TNNT2
Propanoate Metabolism	2.28E+00	1.54E-02	ECHS1,LDHB
Valine, Leucine and Isoleucine Degradation	2.25E+00	1.80E-02	ECHS1,MCCC1
Arginine and Proline Metabolism	2.13E+00	1.09E-02	CKMT2,CKM
Pyruvate Metabolism	2.12E+00	1.34E-02	DLAT,LDHB

6.1.4 Summary

- PANTHER analysis revealed muscle contraction, signal transduction and electron transport to be among the most highly represented processes in the down-regulated Sham vs. MI list, and in the up-regulated MI vs. BMMNC list. Individual pathways were poorly covered by our proteomics datasets .
- DAVID highlighted that annotations relating to muscle structure and function were over-represented in the down-regulated Sham vs. MI list (in the up-regulated MI vs. BMMNC list). Both apoptosis and functions related to oxidative stress were over-represented by proteins up-regulated in Sham vs. MI.
- The networks created by IPA for the proteomics data are dominated by interactions identified in a limited number of studies looking at undefined protein-protein interactions [129, 140, 141]. NFkB and p38 MAPK were highlighted as potentially important interactors in Sham vs. MI altered proteins. Tgfβ1 and Slc4a2 were highlighted in the MI vs. BMMNC networks. Beta-estradiol and Insulin were highlighted in both Sham vs. MI and MI vs. BMMNC networks.
- The terms oxidative phosphorylation, oxidoreductase and mitochondrial dysfunction were highly associated with the proteomics dataset in all the bioinformatics analyses.
- The proteomics dataset was relatively small (<100 different proteins) which resulted in several annotations being associated to only a small number of proteins from our dataset ..

6.2 Bioinformatic analysis of genes found to be differentially regulated in the Illumina RatRef12 analysis.

6.2.1 Protein ANalysis THrough Evolutionary Relationships (PANTHER)

Three different lists of genes were entered into PANTHER, the number of genes in each list is shown in Table 6.10. The MI vs. BMMNC included 19 down-regulated genes and the only up-regulated gene, cardiac calsequestrin (Casq2).

Table 6.10 Three different lists of Refseq gene accession codes were entered into PANTHER

PANTHER Dataset	Number of Genes
Sham vs. MI - Up	860
Sham vs. MI - Down	677
MI vs. BMMNC	20

6.2.1.1 Sham vs. MI

The pathways represented by the 715/860 mapped up-regulated genes in Sham vs. MI are shown in Figure 6.8. The pathways represented by the 544/677 genes down-regulated in Sham vs. MI are shown in Figure 6.9.

Several pathways were represented in both lists including; inflammation mediated by chemokine and cytokine signalling pathway which was represented by 42 up-regulated genes and five down-regulated genes, integrin signalling was represented by 23 up-regulated genes and 2 down-regulated genes and angiogenesis was represented by 20 up-regulated and 2 down-regulated genes. Platelet derived growth factor (Pdgf) signalling was represented by 16 up-regulated genes and 5 down-regulated genes and Wnt signalling was represented by 12 up-regulated and 6 down-regulated genes. Oxidative stress response, TGF- β signalling and several growth factor signalling pathways were also common to both lists.

Pathways that were unique to the up-regulated gene list were apoptosis signalling, B-cell activation, Pi3k pathway and T-cell activation. Pathways unique to the down-regulated list included glycolysis, ubiquitin proteasome pathway and heme biosynthesis.

Figure 6.8 PANTHER Pathways represented by the genes up-regulated in Sham vs. MI Numbers in brackets indicate the number of proteins associated with the term.

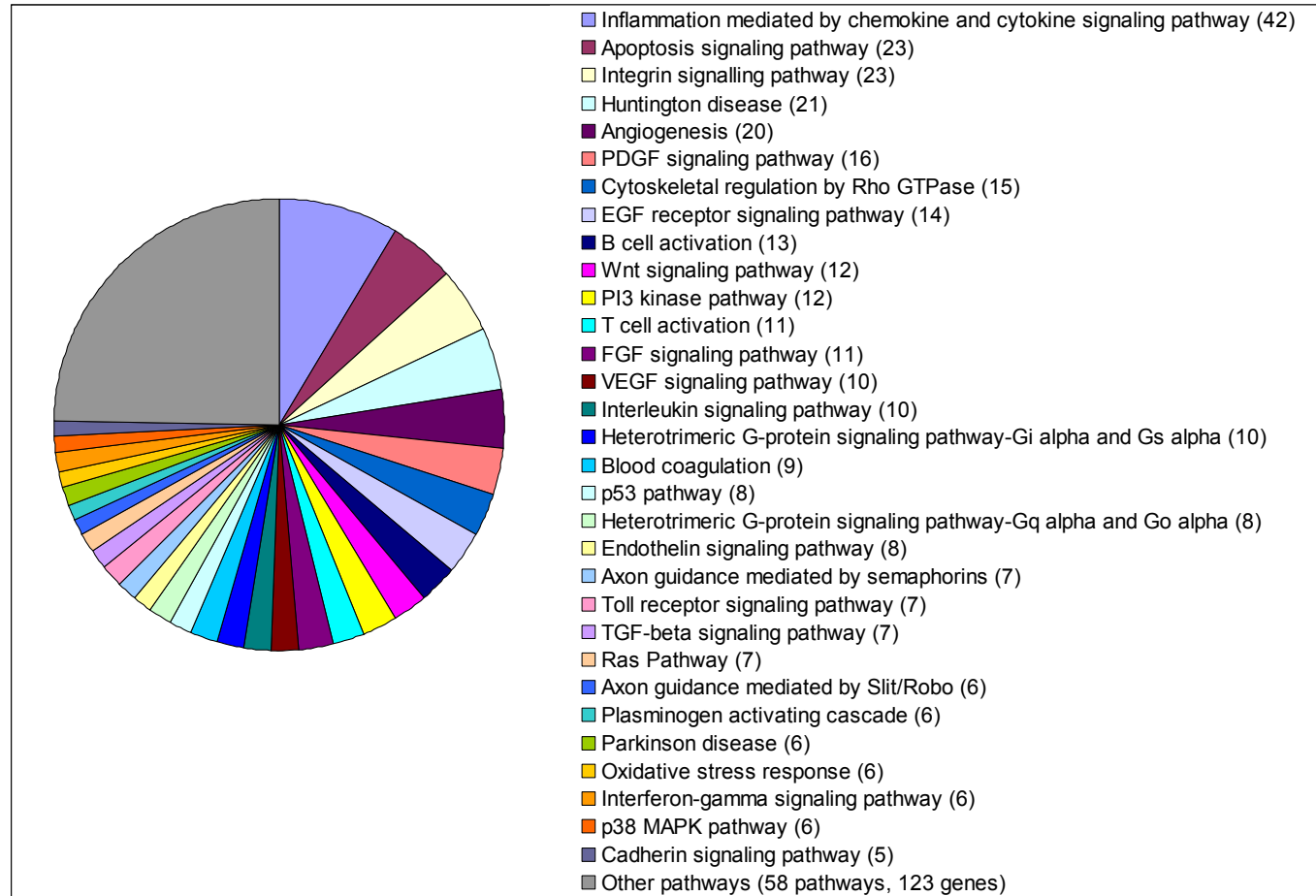
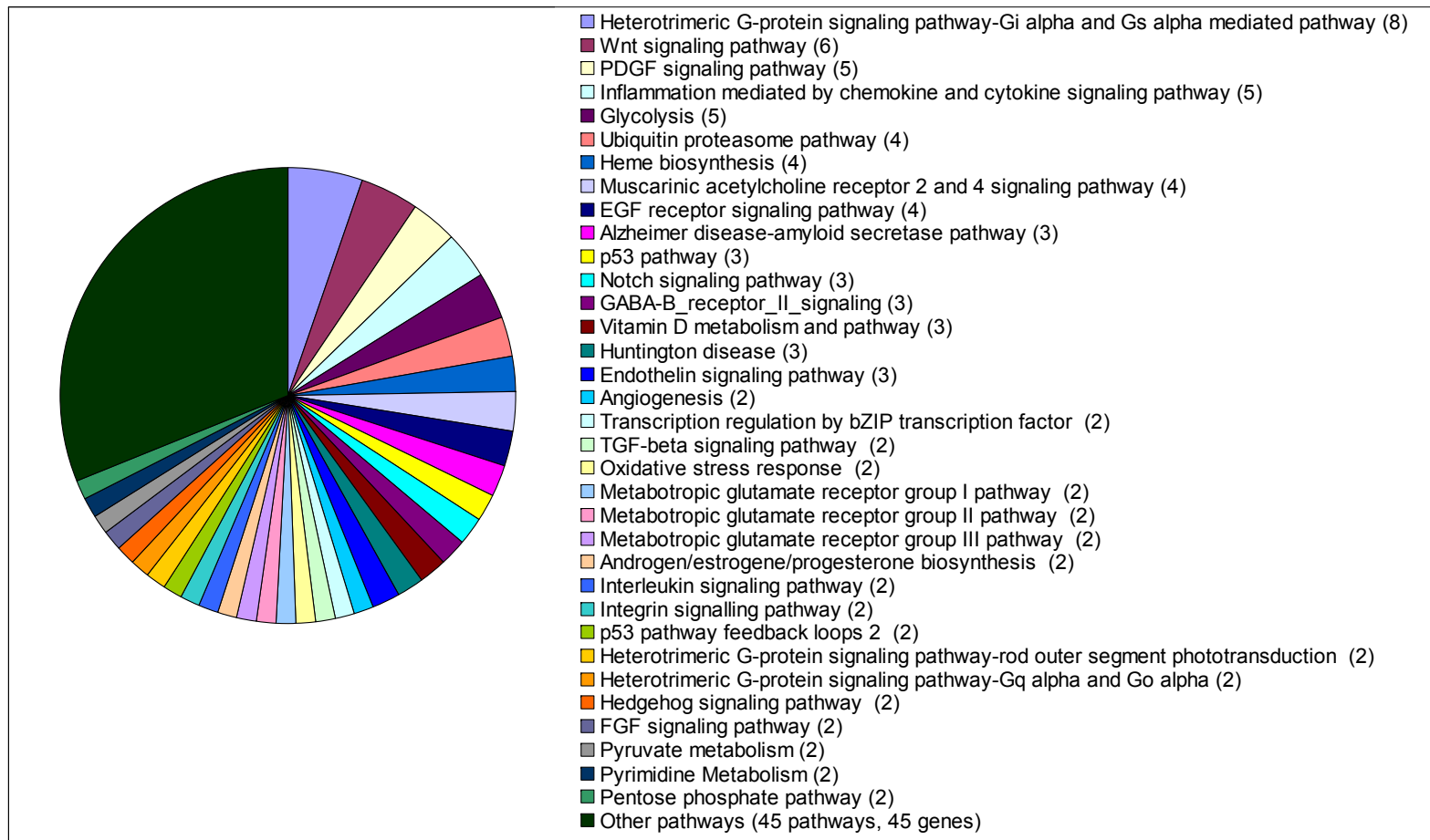


Figure 6.9 PANTHER Pathways represented by the genes down-regulated in Sham vs. MI Numbers in brackets indicate the number of proteins associated with the term.



Biological processes represented by the up- and down-regulated lists are shown in Figure 6.10 and 6.11. All of the processes were represented by members of both gene lists. Top in both lists were signal transduction (216 up-regulated and 56 down-regulated genes), protein metabolism and modification (132 up-regulated and 94 down-regulated genes), nucleic acid metabolism (121 up-regulated and 77 down-regulated genes) and immunity and defence (128 up-regulated and 29 down-regulated genes). There were 111 unclassified up-regulated genes and 138 unclassified down-regulated genes.

Many of the genes had no molecular function classification. The most highly represented molecular functions in both up- and down-regulated genes were nucleic acid binding, select regulatory molecules and transcription factors.

Figure 6.10 PANTHER Biological processes represented by the genes up-regulated in Sham vs. MI Numbers in brackets indicate the number of proteins associated with the term.

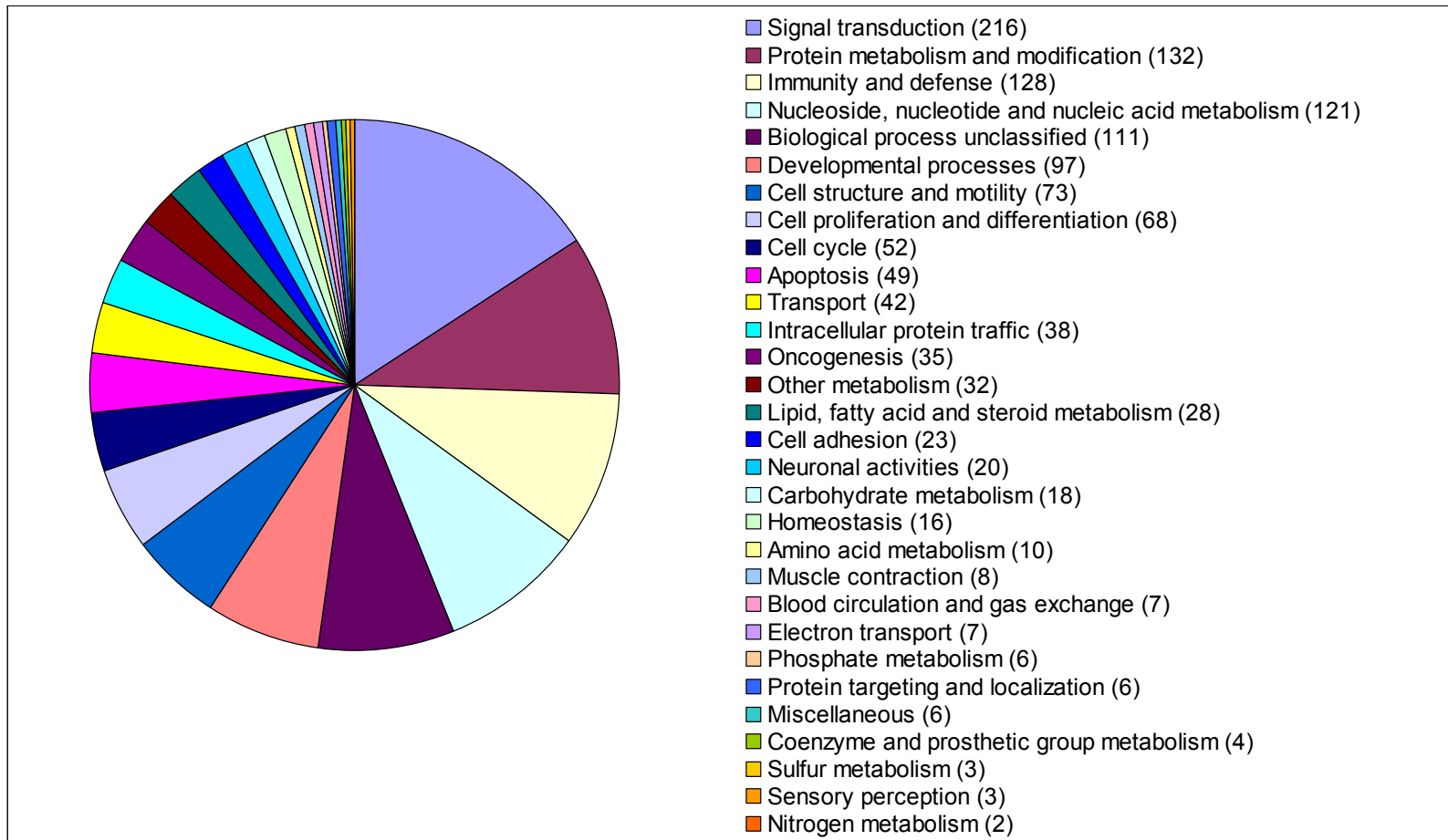
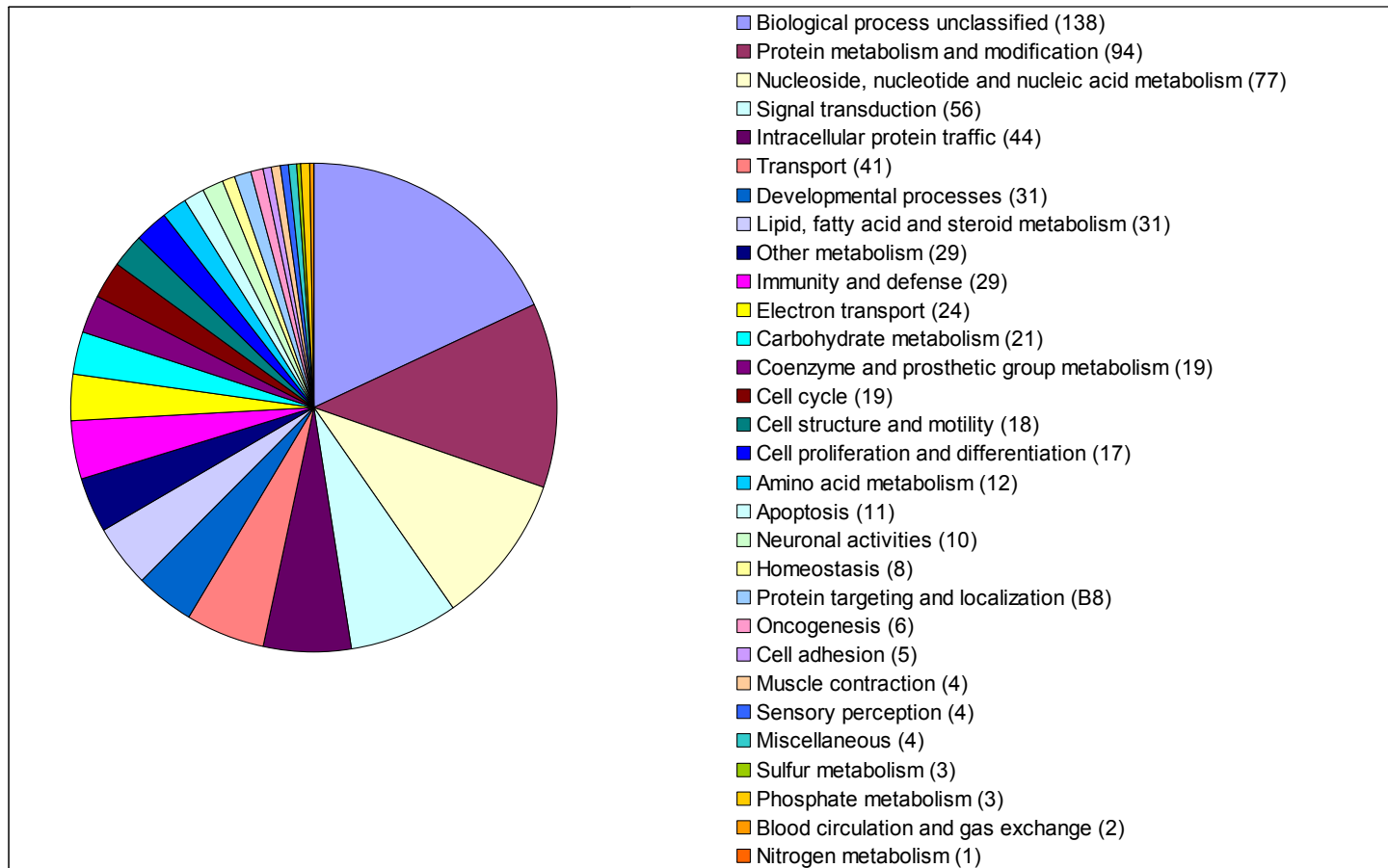


Figure 6.11 PANTHER Biological processes represented by the genes down-regulated in Sham vs. MI Numbers in brackets indicate the number of proteins associated with the term.



6.2.1.2 MI vs. BMMNC

Only a single pathway (angiogenesis) was associated with the 17 genes mapped by PANTHER, this was only linked to docking protein 3 (Dok3).

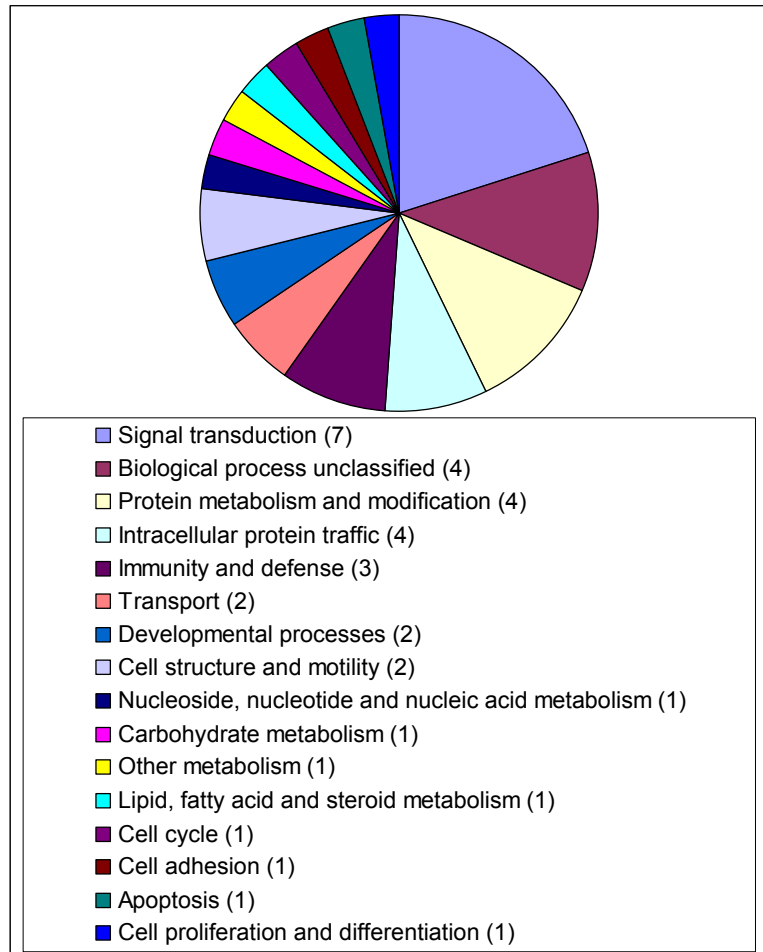
Of the biological processes altered in MI vs. BMMNC, the most highly represented were 'signal transduction', associated with embigin (Emb), coronin actin binding protein 1A (Coro1a), sema domain immunoglobulin domain (Ig) transmembrane domain (TM) and short cytoplasmic domain (semaphorin) 4A (Sema4a), endothelial differentiation G-protein-coupled receptor 6 (Edg6), docking protein 3 (Dok3), antigen presenting cell lectin-like receptor A1 (Alpra1) and the up-regulated Casq2.

'Protein metabolism and modification' was the next process represented by 4 genes; serine/threonine kinase 17b (apoptosis-inducing) (Stk17b), ring finger protein 149 (Rnf149), stefin A2 (Stfa2) and similar to stefin A2 (RDG1560676). These were followed by 'intracellular protein traffic' (Coro1a, sortilin-related receptor, L(DLR class) A repeats-containing (Sorl1) and Alpra1) and 'immunity and defence' (2' -5' oligoadenylate synthetase 1K (Oas1k), Sema4a, Alpra1).

Three other processes were represented by more than one member of the list 'transport' (Sorl1 and Coro1a) 'developmental processes' (Emb and Sema4a) and 'cell structure and motility' (Coro1a and Dok3). All of the processes linked to this list are shown in Figure 6.12.

There were several molecular functions associated with 13 of the 17 genes, the most common of these was 'receptor' associated with Sorl1, Edg6 and Alpra1. This was followed by 'transferase' associated with Oas1k and carbohydrate (keratan sulfate Gal-6) sulfotransferase 1 (Chst1) and 'select regulatory molecule' (Stfa2 and Stfa2). The process 'select calcium binding protein' was associated with the only up-regulated gene Casq2.

Figure 6.12 PANTHER Biological processes represented by the genes differentially-regulated in MI vs. BMMNC Numbers in brackets indicate the number of proteins associated with the term.



6.2.2 Database for Annotation, Visualization and Integrated Discovery (DAVID)

The same three lists that were entered into PANTHER analysis were also entered into DAVID (see Table 6.10).

6.2.2.1 Sham vs. MI

Of the probes up-regulated in Sham vs. MI, 823 mapped to DAVID ID's and when clustering analysis was performed on the biological process GO terminology, the terms grouped into 65 clusters. Terms with significant Benjamini corrected p-values (<0.05) were found in clusters 1-25 and these are detailed in Table 6.11. The general themes of the top 5 clusters were anatomical development, cell death, chemotaxis, vasculature development and immune system development. Other clusters were related to NF-kappa- β regulation and mononuclear cell proliferation.

665 probes down-regulated in Sham vs. MI mapped to DAVID ID's and clustering analysis on biological process GO terms produced 11 clusters. Only cluster 1 had significant Benjamini corrected p-values, (detailed in Table 6.12) contains terms relating to cellular metabolic processes and includes nearly 300 of the genes from our list. Other clusters were related to protein transport, ubiquinone metabolic processing, glycolysis, and ATP metabolism.

Table 6.11 1 -25 of 65 clusters of biological process GO terms associated with genes up-regulated in Sham vs. MI The GO terms within each cluster, count (number of genes from list with this annotation), % (percentage of the input genes found with this annotation), p-value (modified Fisher's exact test (EASE score) and fold enrichment (the fold enrichment of this annotation in the uploaded gene list versus the proportion of this annotation in the background dataset) and Benjamini adjusted p-values (corrected to control family-wide false discovery rate).

Group	GO Biological Process Term	Count	%	PValue	Fold Enrichment	Benjamini
1	GO:0007275~multicellular organismal development	175	21.26%	0.00000	1.84	0.00000
	GO:0048856~anatomical structure development	169	20.53%	0.00000	1.83	0.00000
	GO:0048731~system development	152	18.47%	0.00000	1.92	0.00000
2	GO:0008219~cell death	82	9.96%	0.00000	2.43	0.00000
	GO:0016265~death	82	9.96%	0.00000	2.43	0.00000
	GO:0012501~programmed cell death	78	9.48%	0.00000	2.38	0.00000
	GO:0006915~apoptosis	77	9.36%	0.00000	2.37	0.00000
3	GO:0006935~chemotaxis	25	3.04%	0.00000	5.11	0.00000
	GO:0042330~taxis	25	3.04%	0.00000	5.11	0.00000
	GO:0007626~locomotory behavior	29	3.52%	0.00000	3.65	0.00000
4	GO:0001944~vasculature development	34	4.13%	0.00000	3.87	0.00000
	GO:0001568~blood vessel development	33	4.01%	0.00000	3.83	0.00000
	GO:0048514~blood vessel morphogenesis	30	3.65%	0.00000	3.96	0.00000
	GO:0001525~angiogenesis	27	3.28%	0.00000	4.35	0.00000
	GO:0048646~anatomical structure formation	29	3.52%	0.00000	3.73	0.00000
5	GO:0002520~immune system development	33	4.01%	0.00000	3.37	0.00000
	GO:0048534~hemopoietic or lymphoid organ development	32	3.89%	0.00000	3.40	0.00000
	GO:0030097~hemopoiesis	30	3.65%	0.00000	3.42	0.00000
6	GO:0042035~regulation of cytokine biosynthetic process	14	1.70%	0.00000	5.55	0.00005
	GO:0042089~cytokine biosynthetic process	15	1.82%	0.00000	5.00	0.00007
	GO:0042107~cytokine metabolic process	15	1.82%	0.00000	4.92	0.00009
7	GO:0043066~negative regulation of apoptosis	29	3.52%	0.00000	2.68	0.00021
	GO:0043069~negative regulation of programmed cell death	29	3.52%	0.00000	2.66	0.00023
	GO:0006916~anti-apoptosis	23	2.79%	0.00001	3.04	0.00033

Table 6.11 continued.

Group	GO Biological Process Term	Count	%	PValue	Fold Enrichment	Benjamini
8	GO:0002460~adaptive immune response based on somatic	15	1.82%	0.00000	4.83	0.00010
	GO:0002250~adaptive immune response	15	1.82%	0.00000	4.83	0.00010
	GO:0002449~lymphocyte mediated immunity	14	1.70%	0.00000	4.84	0.00023
	GO:0019724~B cell mediated immunity	12	1.46%	0.00002	4.96	0.00099
	GO:0016064~immunoglobulin mediated immune response	11	1.34%	0.00009	4.65	0.00360
9	GO:0030036~actin cytoskeleton organization and biogenesis	27	3.28%	0.00000	3.21	0.00002
	GO:0030029~actin filament-based process	27	3.28%	0.00000	3.02	0.00006
	GO:0007010~cytoskeleton organization and biogenesis	36	4.37%	0.00235	1.70	0.05524
10	GO:0006417~regulation of translation	20	2.43%	0.00000	3.52	0.00019
	GO:0031326~regulation of cellular biosynthetic process	20	2.43%	0.00003	3.04	0.00124
	GO:0009889~regulation of biosynthetic process	22	2.67%	0.00003	2.83	0.00135
11	GO:0043549~regulation of kinase activity	26	3.16%	0.00003	2.56	0.00126
	GO:0051338~regulation of transferase activity	26	3.16%	0.00004	2.48	0.00193
	GO:0045859~regulation of protein kinase activity	25	3.04%	0.00005	2.53	0.00205
12	GO:0042108~positive regulation of cytokine biosynthetic	10	1.22%	0.00002	6.13	0.00105
	GO:0045727~positive regulation of translation	11	1.34%	0.00002	5.36	0.00118
	GO:0031328~positive regulation of cellular biosynthetic	11	1.34%	0.00007	4.75	0.00301
	GO:0009891~positive regulation of biosynthetic process	12	1.46%	0.00021	3.87	0.00803
13	GO:0043122~regulation of I-kappaB kinase/NF-kappaB	16	1.94%	0.00001	3.95	0.00049
	GO:0007249~I-kappaB kinase/NF-kappaB cascade	19	2.31%	0.00005	3.01	0.00218
	GO:0043123~positive regulation of I-kappaB kinase/NF-	14	1.70%	0.00008	3.70	0.00335
	GO:0009967~positive regulation of signal transduction	17	2.07%	0.00362	2.24	0.07849
14	GO:0032944~regulation of mononuclear cell proliferation	11	1.34%	0.00002	5.36	0.00118
	GO:0050670~regulation of lymphocyte proliferation	11	1.34%	0.00002	5.36	0.00118
	GO:0032943~mononuclear cell proliferation	13	1.58%	0.00003	4.41	0.00126
	GO:0046651~lymphocyte proliferation	13	1.58%	0.00003	4.41	0.00126
	GO:0042129~regulation of T cell proliferation	9	1.09%	0.00024	5.19	0.00876

Table 6.11 continued.

Group	GO Biological Process Term	Count	%	PValue	Fold Enrichment	Benjamini
14 cont.	GO:0051249~regulation of lymphocyte activation	12	1.46%	0.00029	3.74	0.01005
	GO:0050865~regulation of cell activation	12	1.46%	0.00039	3.62	0.01209
	GO:0050863~regulation of T cell activation	9	1.09%	0.00369	3.49	0.07921
15	GO:0043086~negative regulation of catalytic activity	14	1.70%	0.00017	3.46	0.00634
	GO:0033673~negative regulation of kinase activity	11	1.34%	0.00037	3.95	0.01173
	GO:0006469~negative regulation of protein kinase activity	11	1.34%	0.00037	3.95	0.01173
	GO:0051348~negative regulation of transferase activity	11	1.34%	0.00051	3.80	0.01529
16	GO:0033674~positive regulation of kinase activity	18	2.19%	0.00023	2.78	0.00848
	GO:0051347~positive regulation of transferase activity	18	2.19%	0.00034	2.69	0.01085
	GO:0045860~positive regulation of protein kinase activity	17	2.07%	0.00047	2.72	0.01451
17	GO:0030030~cell projection organization and biogenesis	26	3.16%	0.00034	2.19	0.01106
	GO:0048858~cell projection morphogenesis	26	3.16%	0.00034	2.19	0.01106
	GO:0032990~cell part morphogenesis	26	3.16%	0.00034	2.19	0.01106
18	GO:0008361~regulation of cell size	20	2.43%	0.00014	2.70	0.00555
	GO:0016049~cell growth	19	2.31%	0.00024	2.68	0.00873
	GO:0001558~regulation of cell growth	15	1.82%	0.00114	2.72	0.02973
19	GO:0006796~phosphate metabolic process	65	7.90%	0.00029	1.57	0.01015
	GO:0006793~phosphorus metabolic process	65	7.90%	0.00029	1.57	0.01015
	GO:0006468~protein amino acid phosphorylation	49	5.95%	0.00080	1.63	0.02224
	GO:0016310~phosphorylation	54	6.56%	0.00126	1.55	0.03249
20	GO:0030005~cellular di-, tri-valent inorganic cation	22	2.67%	0.00011	2.58	0.00451
	GO:0055066~di-, tri-valent inorganic cation homeostasis	22	2.67%	0.00011	2.58	0.00451
	GO:0030003~cellular cation homeostasis	23	2.79%	0.00032	2.34	0.01068
	GO:0055080~cation homeostasis	23	2.79%	0.00032	2.34	0.01068
	GO:0055082~cellular chemical homeostasis	25	3.04%	0.00054	2.16	0.01596
	GO:0006873~cellular ion homeostasis	25	3.04%	0.00054	2.16	0.01596
	GO:0019725~cellular homeostasis	29	3.52%	0.00099	1.94	0.02606

Table 6.11 continued.

Group	GO Biological Process Term	Count	%	PValue	Fold Enrichment	Benjamini
21	GO:0030182~neuron differentiation	28	3.40%	0.00083	1.99	0.02281
	GO:0022008~neurogenesis	33	4.01%	0.00098	1.85	0.02612
	GO:0048699~generation of neurons	30	3.65%	0.00150	1.86	0.03700
22	GO:0044238~primary metabolic process	330	40.10%	0.00029	1.14	0.01010
	GO:0044237~cellular metabolic process	325	39.49%	0.00073	1.13	0.02069
23	GO:0051726~regulation of cell cycle	28	3.40%	0.00028	2.14	0.00988
	GO:0000074~regulation of progression through cell cycle	27	3.28%	0.00053	2.09	0.01588
24	GO:0042533~tumor necrosis factor biosynthetic process	4	0.49%	0.00133	15.21	0.03347
	GO:0032640~tumor necrosis factor production	4	0.49%	0.00133	15.21	0.03347
	GO:0042534~regulation of tumor necrosis factor biosynthetic	4	0.49%	0.00133	15.21	0.03347
25	GO:0007599~hemostasis	12	1.46%	0.00156	3.08	0.03816

Table 6.12 1 of 11 clusters of biological process GO terms associated with genes down-regulated in Sham vs. MI The GO terms within each cluster, count (number of genes from list with this annotation), % (percentage of the input genes found with this annotation), p-value (modified Fisher's exact test (EASE score), fold enrichment (the fold enrichment of this annotation in the uploaded gene list versus the proportion of this annotation in the background dataset), and Benjamini adjusted p-values (corrected to control family-wide false discovery rate).

Group	GO Biological Process Term	Count	%	PValue	Fold Enrichment	Benjamini
1	GO:0008152~metabolic process	285	42.86%	0.00000	1.28	0.00000
	GO:0044237~cellular metabolic process	259	38.95%	0.00000	1.31	0.00000
	GO:0044238~primary metabolic process	243	36.54%	0.00001	1.22	0.00457

Clustering of KEGG terms associated with the 823 mapped genes which were up-regulated in Sham vs. MI produced three clusters but none contained significant corrected p-values. The first cluster contains several pathways relating to signalling, including B-cell receptor signalling (significant), natural killer cell cytotoxicity and VEGF signalling. The second and third clusters consist of pathways relating to cancer.

KEGG terms associated with the 665 genes down-regulated in Sham vs. MI also grouped into three clusters, although corrected p-values show only significance for the first pathway in the first cluster. This first pathway is valine, leucine and isoleucine degradation and is shown with fatty acid metabolism and butanoate metabolism in the first cluster. The second cluster is glycolysis related pathways and the third is phospholipid metabolism.

6.2.2.2 MI vs. BMMNC

All of the 20 genes altered in MI vs. BMMNC mapped to David IDs. Only a single cluster of biological process GO terms was found and this contained no significant terms. The three terms within the cluster were all relating to intracellular signalling. The KEGG pathways associated with these genes did not cluster.

6.2.3 Ingenuity Pathway Analysis (IPA)

Significant fold changes (not logged) and adjusted p-values were entered for all 1538 probes for which a difference was found in either Sham vs. MI or MI vs. BMMNC.

6.2.3.1 Sham vs. MI

1248 genes were differentially expressed in Sham vs. MI that mapped in IPA. 690 of these were associated within 25 networks (set as maximum number of networks to return) along with 177 other genes and endogenous chemicals. Details of the 25 networks are shown in Table 6.13. All networks scored from 47 to 21 and each contained between 35 and 23 genes from our dataset.

Network 1 has Glut-4 as a major hub linking ~30 genes from our dataset (Figure 6.13 A). Approximately two thirds of these genes are down-regulated in our dataset. All of the relationships are protein-protein associations that were found in the same study already mentioned [140]. Slc2a4 itself was found to be down-regulated in Sham vs. MI. Another hub gene in this network is ADP-ribosylation factor 6 (Arf6) which was up-regulated in our dataset and is linked to 5 other up-regulated genes.

Table 6.13 Top 25 networks associated with the genes altered in Sham vs. MI Network ID (1-25) is shown on the left and all the genes in that network are listed with either red arrows (up-regulated) or green arrows (down-regulated), focus molecules (ones from our dataset) are in bold. The network score is shown alongside the number of focus molecules in the network and the general functions represented by the network.

△ ID	Molecules in Network	Score	Focus	Top Functions
1	↓ACADS, ↑ARF6, ↑ARG1, ↓ASRGL1, ↓BCAT2, ↓BCKDHA, ↑BIN1, ↓BNIP1, ↓CASQ2, ↓CDIPT, ↑CLIC1, ↓DLST, ↑EIF4A1, ↑EPDR1, ↑FAM65B, ↓HADH, ↑HNRNP1, ↓HSD17B4, ↓JPH2, ↓MRPL49, ↑NDRG1, ↑PABPC1, ↓PARK7, ↓PECR, ↑PGD, ↓RAB14, ↓RINT1, ↓SC65, ↓SGCG, ↓SLC2A4, ↓SLC7A5, ↑STOM, ↑TARS, ↑TUBB6, ↑YARS	47	35	Amino Acid Metabolism, Small Molecule Biochemistry, Molecular Transport
2	↑ANGPT2, Arf, ↑ARF2, ↑ARF4, ↑BOP1, ↑CCL6, ↑CDR2, ↑CFLAR, ↑DDX18, ↑DDX52, ↑EMP1, ↑FBL, ↑FBXL5, ↑GCLC, ↑GNL2, ↓GPI, ↑H3F3C (includes EG:440093), ↑HAMP, ↑HIVEP2, ↑IPO13, ↑LIMS1, ↑MORF4L2, ↓MRPS34, ↑MYC, ↑NOP58, ↑P4HA1, ↑PELO, ↑PLS3, ↓PTGES2, ↑SLC11A1, ↓SLC25A12, ↓SLC25A13, ↓SLC25A19, ↓SSBP2, ↑TAF1C	44	34	RNA Post-Transcriptional Modification, Amino Acid Metabolism, Molecular Transport
3	↓ABCFC3, ↓C11ORF59, ↓C21ORF33, ↓CSPG4, ↓CSR2, ↑EEF1A1, ↑EEF1A2, ENaC, ↑ERAF, ↑G6PD, ↓HBXIP, Histone h3, ↑IL6R, Integrin alpha 3 beta 1, ↑LAPTM5, ↓LETM1, ↑LITAF, ↓MOCS2, ↓MRPS9, ↑NDFIP2, ↓NEDD4, ↑NOC2L, ↓OLA1, ↓ORMDL3, ↓PAICS, ↑PMEPA1, Protein-synthesizing GTPase, ↓RABIF*, ↑RELN, ↑SCNN1A, ↓SDHAF2, ↓SF3B2, ↓SGK1, ↑SPP1, ↓TUFM	37	31	Protein Synthesis, Molecular Transport, Cellular Movement
4	↓ACOT13, ↑ACTB*, ↑AKAP2, ↑ANXA2, ↓CHSY1, ↓COX17, ↓COX5B, ↓DDT, ↓DSTYK, eIF, Eif2, ↑EIF5, ↓EIF2B4, ↑EIF2S1, ↑EIF2S2, ↑EMD, ↑FAM129B, ↓FHL2, ↓IKBKE, ↓LAGE3, ↑LRRCS9, ↑MAT2A, ↓MAVS, MIR1, MIR124, ↑NARG1, ↓PLEKHB2, ↑PRKAR1A, ↑RAB11A, ↑RBM47, ↓SMARCC1, ↑TAGLN2, ↑TMBIM1, ↓UBE2M, ↓YLPM1	36	31	Protein Synthesis, Infection Mechanism, Embryonic Development
5	↑ABL1, ↑ACAP1, ↓ADAMTSL4, ↓APBA3, ATYPICAL PROTEIN KINASE C, ↑BCR, ↑BHLHE40, ↑CD200R1, ↓DDR1, ↓DNPEP, ↑DOK2, ↑DOK3, ↑ENAH, ↑EPHA2, ↑F2RL2, ↑GABPB1 (includes EG:2553), ↓GNS, ↑INPP5D, ↑MDM2, ↑PHLDA1, ↑PLAC8, ↑PLSCR1, ↓RAD52, ↑RASD1, ↑RGS2, ↑RYBP, Sapk, ↑SEMA6D, Shc, ↑SLPI, ↓SNX17, ↑TDRD7, ↑TIAM1, ↑TM4SF1, ↓WNK2	35	32	Hematological System Development and Function, Tissue Morphology, Cellular Growth and Proliferation
6	ADCY, ↑ADCY4, ↓ADCY6, ↑AFF4, ↓CCDC85B, ↑CDK9, ↓CYTSA, ↑EGR2, Filamin, ↑FLNA, G alpha, ↑GNA13, ↑GNA13, ↑GNAT2, ↑GNG10, ↓GPSM1, ↑HMGCR, ↓IRF2BP1, ↓MAPK8IP1, ↑NAT9, ↑NEDD9, ↑NUP54, ↓OSTM1, ↑PMP22, ↓PMS1, ↑RGS3, ↑RIPK1, ↑RIPK3, ↓RUNX1, ↑SMAD1, Tnf receptor, ↑UPP1, ↓VPS24, ↓VPS4A, ↓ZNF76	35	31	Genetic Disorder, Neurological Disease, Cell Signaling
7	↑APOLD1, ↑ASNS, ↑ATF3, ↑ATF4, ↑BATF, ↑BATF3, ↓BCL10, c-Src, ↓CARD9, ↑CASP8, Caspase, Cbp/p300, ↑CEBPG, ↑CREB3L1, ↑CREM*, ↓HABP4, ↓HMBS, ↓INHA, JUN/JUNB/JUND, ↑MAFF, ↑MAFK, ↑MALT1, ↑MIDN*, musculoaponeurotic fibrosarcoma oncogene, ↑NFE2, ↓NFE2L1, ↑NFE2L2, ↓NFI3, ↑NLRC4, ↑NLRP3, ↑PRKCQ, SRC, ↓STK39, ↑UGDH, ↓WWP1	33	29	Antigen Presentation, Antimicrobial Response, Humoral Immune Response
8	↑ACTG1, ↑ACTR3, Alpha actin, Arp2/3, ↑ARPC3, ↑ARPC5, ↑ARPC1B, ↑ASL, ↑CAP1, ↑CFL1, ↓CFL2, Cofilin, ↑CORO1A, ↑COTL1, ↑ELL, ↑EMB, ↑EPCAM, F Actin, ↑FOS, G-Actin, ↓ITSN2, ↓KBTBD10, ↓MAEA, ↓NAE1, ↓NIPSNAP1, ↓PARVB, ↓PCYT2, ↓PGAM2, Profilin, ↓SCHIP1, ↑SEC23B, ↓SNF8, ↓TIA1, ↑VASP, ↑WAS	32	29	Cellular Assembly and Organization, Cell Morphology, Cellular Function and Maintenance

Table 6.13 continued.

△ ID	Molecules in Network	Score	Focus	Top Functions
9	↓ABCD3, ↓ACP6, ↓ACTC1, ↑ANPEP, ↓ATP1A2, ↓ATP1B1, ATPase, ↑BAZ1A, ↓COPE, ↑CSDA, ↑DDX39, E2f, ↑HLA-C, ↑HSP90B1, ↑HSPA5, ↑KLRA1 (includes EG:10748), ↑LGALS3, MHC Class I (complex), MHC CLASSI (family), ↑NASP, ↑PCNA, ↑PDPN, ↑PGRMC1, ↓PICK1, Pkc(s), ↑PVR, ↑PVRL3, ↑SERP1, ↑SFXN1*, ↓SIRT3, ↑SMARCA5, TCR, ↓TMEM132A, ↑XBP1, ↓YIF1A	32	29	Endocrine System Disorders, Metabolic Disease, Cell-To-Cell Signaling and Interaction
10	↑ADAMTS4, ↑BMX, ↓CLPP, Dynamin, ↓EFNB3, ↓ELP2, ↑FGL2, ↑IFITM1, JAK, ↑JAK3, ↑LMCD1, ↓MRPL19, ↑OSMR, ↓PACSIN2, ↓PACSIN3, ↑PDK3, peptidase, ↑PHKA1, Phosphorylase, ↓PLIN3, ↑PTPN2, ↑PYGL, ↓PYGM, Rab5, ↓RAB4A, ↓RUFY1, ↑SDCBP, STAT, ↓STAT1, STAT1/3/5, ↓STX8, ↓TRIM63, ↓TYMP, ↓ULK1, ↓VPS45	31	28	Cellular Function and Maintenance, Carbohydrate Metabolism, Cell Morphology
11	Actin, ↑ACTN1, ↑ADORA2A, ↑ADRB2*, AKAP, ↑AKAP12, Alpha Actinin, ↑CDC42EP3, ↑CSNK2A2, ↑CTTNBP2NL, ↓CYTH2, ↑CYTIP, ↓DCTN3*, ↑ENCL, GADD45, ↑GADD45A, ↑GADD45B, ↑GADD45G, ↑HSF2, ↑KCNJ5, ↓KCNQ1, ↑KLHL2, Pak, ↑PAK1IP1, ↓PFDN6, ↑PIM1, Pka, PP2A, ↓PPP2CB, ↓PPP2R5B, ↑PRKAG1, ↑RHOQ, ↓SIK1, ↑STRN3, ↑TES	31	28	Post-Translational Modification, Cell Cycle, Cell Signaling
12	↑CSF3R, DNA-directed RNA polymerase, ↑FLNB, Glutathione transferase, GST, ↓GSTK1, ↓GSTM2, ↓GSTM5, ↓GSTO1, ↓GSTT2, IL-2R, ↑JAK2, Jnk, ↓LRPPRC, ↓NPHP1, PLC gamma, ↓POLR1A, ↓POLR3A, ↓POLRMT, ↑PRAM1, ↑PTAFR, ↑PTK2B, ↑PTPN6, ↑PTPRO, ↑RGS1, ↓RPRD1A, ↑SIGLEC7, ↑SKAP2, ↑SLC1A5, SOCS, ↑SOCS3, ↑SOCS4, ↑SOCS5, ↑UBASH3B, ↓VDAC3	31	28	Gene Expression, Hematological Disease, Organismal Injury and Abnormalities
13	↑ACSL4, Alpha tubulin, ↓AMHR2, ↓CKB, ↑CSRP1, ↑DENND4A, ↑ERRFIL, ↑FES, ↓GLG1, ↑GP9, ↑GP1BB, ↑HNRNP, HSP, ↑IQGAP1, ↓KLC4, ↓MAPT, ↑NAPSA, ↑PAFAH1B1, ↓PANK1, PFK, ↓PFKL, ↓PFKM, ↑PGLYRP1, Phosphofructokinase, ↑RAL14, ↑SIK1, ↓SPR, ↓ST5*, ↓TBCD, ↑TRA2B, ↑TUBB3, ↑TUBB2A, Tubulin, ↓UCP2, ↑YWHAZ	30	30	Genetic Disorder, Hematological Disease, Cell Morphology
14	↓CKS1B, ↓CLASP1, ↓CLASP2, ↓DAP3, ↑DNAJA1, ↑DNAJB1, ↑DNAJB4, DNAJC, ↓DNAJC14, ↓DNAJC15, ↓DNAJC18, ↑DUSP1, ↑DUSP6, ERK, ERK1/2, ↑HSBP1, Hsp90, Hsp22/Hsp40/Hsp90, ↑HSP90AA1, ↓IP6K2, ↑MAP3K8, Mapk, ↓MAPRE3, Mek, ↑NLRP12, P38 MAPK, ↓PEBP1, ↓PLXNB1, ↑PTPN1, ↑RND3, ↑SEMA4A, ↑SEMA4D, ↓SMYD2, ↑STP1, ↑TRIB1	29	27	Endocrine System Development and Function, Small Molecule Biochemistry, Drug Metabolism
15	↑ADSS, ↑E2F5, ↑EDN1, ↑EDN2, ↑EDNRB, Endothelin, Endothelin Receptor, Gata, ↓GATA4, ↓GATA6, ↑GEM, ↑GNL3, ↑ID3, Importin alpha, Importin beta, ↑IPOS, ↓KLF15, ↓MLX, NADH dehydrogenase, NADH2 dehydrogenase, NADH2 dehydrogenase (ubiquinone), ↓NDUFA8, ↓NDUFA13, ↓NDUFB4, ↓NDUFS7, ↓NDUFS8, ↑NES, ↓NKX2-5, ↓NPPA, ↑NUP153, ↑PDLIM7, ↑PPAN-P2RY11, ↓PRKD2, ↑RANBP1, ↑SRFBP1	28	27	Cardiovascular System Development and Function, Cell Morphology, Skeletal and Muscular System Development and Function
16	Beta Arrestin, C/ebp, ↑CCL3, ↑CCL7, ↑CCL13, ↑CCR1, ↑CCR5, CHEMOKINE, ↑CXCL3, ↑CXCR4, ↑ETF1, ↑FCAR, G alphaI, ↑GDF15, Gpcr, ↑GPSM3, ↑IER3, Iga, ↑IL8RB, ↑JAK1, ↑KLF4, ↑KLF6, ↑LTBP1, NFkB (complex), ↓NKIRAS1, ↑NKRF, ↑NOS2, ↑ODC1, PDGF BB, ↑PF4, ↑PLP2, ↑REL, ↑RETNLA, Tqf beta, ↑THBD	27	26	Cellular Movement, Hematological System Development and Function, Immune Cell Trafficking
17	↑ANXA1, ↑APBB1IP, ↓CALM3, Calmodulin, Cpla2, G, ↑KCNN4, ↑KRAS, ↑LTB4R, ↑MARCKS (includes EG:4082), ↓MIF, Myosin, ↑NRAS, PI3K p85, PLA2, ↓PLA2G5, ↓PLA2G6, ↓PLA2G12A, ↑RABGEF1, Ras, Ras homolog, ↑RASSF1, ↑RASSF5, ↑RNF111, ↑RRAD, ↑SELL, Sos, ↑TLR2, ↓TMOD1, ↑TPM3*, ↑TPM4, Tropomyosin, ↑TRPM2, ↑TRPV4, ↑VAV1	25	25	Carbohydrate Metabolism, Lipid Metabolism, Molecular Transport

Table 6.13 continued.

△ ID	Molecules in Network	Score	Focus	Top Functions
18	Akt, ↑ARHGDI3, ↑CASP3, ↓CAT, CD14-Myd88-Tlr2-Tlr6, ↑CNKSR3, ↑HNRNPAB, Hsp27, ↑HSPB1, IKK (complex), IL1, IL-1R, IL-1R/TLR, ↑IL1R1, ↑IL1R2, ↑IL1RN, IRAK, ↑LMNB1, ↑LOXL2, MAGI, ↑MYD88, ↑NCF4, PARP, ↓PARP4, ↑PTEN, ↑RAC2, ↑RHOH, ↑SIGIRR, ↑SNAIL, ↑TAX1BP1, ↓THAP11, ↑TIPARP, ↑TLR6, ↑TOLLIP, ↓UNC84A	25	25	Infectious Disease, Inflammatory Disease, Respiratory Disease
19	14-3-3, ↑AKAP13, ↓ALAD, Alcohol group acceptor phosphotransferase, ↑CD24, ↑CD37, ↑CD53, ↑CLEC4C, Fc gamma receptor, ↑FCER1G, Fcgr2, ↑FCGR1A, FCGR1A/2A/3A, ↑FCGR2A, ↑FCGR2B, ↑FGR, ↑HCK, ↑HMG20B, IgG, ↓KIF1C, ↑LOC498276, ↑MAP3K6, MHC Class II, ↑PAK2, PI3K, ↑PRKCH, Rac, ↑RAC1, ↓RIT1, ↓SH3KBP1, STAT5a/b, ↑SWAP70, ↓TACC2, ↑TNFRSF12A, ↑YWHAQ (includes EG:22630)	24	25	Cell-To-Cell Signaling and Interaction, Cellular Function and Maintenance, Hematological System Development and Function
20	3',5'-cyclic-nucleotide phosphodiesterase, ↑ADAM17, ↑AHR, ↓ALDOA, ↑ANGPTL4, ↓BCL2A1, ↓BTRC, ↓CCS, Ck2, ↓CXORF40A, ↑HIF1A, ↑MCL1, ↑MED7 (includes EG:9443), Mlc, ↓MYL7, ↑NAP1L1, ↑NR4A3*, ↑PDE10A, ↑PDE4B, ↓PDE6D, ↑PLXNA2, ↓PMM1, ↓PSMD4, Rb, ↑ROCK2, ↑SAT1, ↓SAT2, Smad, ↑SPHK1, ↑STK17B, ↑TNFRSF1A, ↓UBACL1, ↓UBE2R2 (includes EG:54926), Ubiquitin, ↑WEE1	24	29	Cardiovascular System Development and Function, Organismal Development, Cell Death
21	↓AIFM1, ↑BAG3, BCR, ↑CBLB, ↑DAPP1, ↑FAM189A2, Fcer1, Gcn5l, ↓GLS, ↑HBEGF, Hsp70, ↑HSPA14, IFN ALPHA RECEPTOR, ↓KCNAS, ↓KCNJ12, ↑MAP4K1, Mre11, NCK, ↑NFAM1, ↓NIT1, Nos, ↑OLR1, ↑PLCG2, ↑PPP1R15A (includes EG:23645), Ptk, ↑PTPRC, ↑SLA, ↓SNTA1, ↑SYK, SYK/ZAP, ↑TAFSL, ↑TNF2, ↑TWF1, VAV, ↓XRCC6	23	24	Cellular Growth and Proliferation, Hematological System Development and Function, Cell Signaling
22	↓AVEN, ↑BAMBI, BCL2, ↓BCL2A1, BIK, CD3, CEBPA, ↑CTGF, ↑DGAT2, ↑ESM1, ↓EXTL2, ↑GADD45A, ↓GIMAP5, ↑GLRX, ↑HRC, IFI27, ↑IFIT1, ↑IL10, ITGAL, ITGAX, ↑KANK1, KATNA1, ↑LGALS3, ↑LITAF, ↑LST1, MIR124-1, ↑PTPRC, ↑RASSF5, ↑SERPINE1*, ↑SLC30A7, SMARCA4, SWI-SNF, tyrosine kinase, ↑YOD1, ↓ZBTB48	22	23	Renal and Urological Disease, Inflammatory Disease, Renal Nephritis
23	Ahr-aryl hydrocarbon-Arnt, ↓CPT1B, Ctbp, ↑DDX5, Esr1-Esr1-estrogen-estrogen, Estrogen Receptor, ↑FUS, ↓GTF2I, Insulin, ↑MAFB, ↑MED21, ↓MKKS, N-cor, ↓NR0B2, ↑NR1P1, Nuclear factor 1, ↑PGF, ↑PLIN2, ↓POLR2B, ↑PTBP1, ↑PTGS2, Rar, ↓RARB, ↑RBBP8, RNA polymerase II, Rxr, ↓RXRB, ↑SDAD1, ↑SFPO, ↑SLC20A1, ↑SNRPA, ↓SPAG7, ↑TGIF1, Thyroid hormone receptor, Vegf	21	23	Dermatological Diseases and Conditions, Inflammatory Disease, Gene Expression
24	↑ABCB1B, Adaptor protein 2, ↓AKR1C14, Ap1, ↑BDNF, ↓BLVRB, ↑CBR3, Clathrin, Creb, ↑CXORF21, ↓CYP27A1, ↓CYP4F6, ↑CYP4F16*, ↑DAB2, ↑EGR1, ↓ETFDH, ETS, ↑ETS1, ↑ETS2, ↑FTL*, ↑HAS1, ↑HMOX1, ↑ITGB7, ↑LTB, Neurotrophin, Nfat (family), ↑NGF, Oxidoreductase, ↓OXNAD1, ↑PTHLH, ↑SRGN, ↑TIMP1, ↑TLR13, ↑TNFSF14, Trk Receptor	21	26	Organ Morphology, Cellular Development, Cell Morphology
25	↑A2M, ↑ADAMTS1, ↑CD44, Collagen type I, Collagen(s), Complement component 1, ↑CTGF, ↑CYR61, ↑ELANE, Elastase, ↑FCN1, Fibrin, Fibrinogen, ↑FN1, Igfbp, ↑IGFBP3, Integrin, ↑ITGAM, Laminin, ↑LRG1, LRP, Mmp, ↑MMP3, ↑MMP8, ↑MMP9, Plasminogen Activator, ↑PLAT, ↑PLAU, ↑RNASE1, ↑SERPINB1, ↑SERPINE1*, ↑SOAT1, ↑TFPI2, ↓UROD, ↑VCAN	21	23	Cell-To-Cell Signaling and Interaction, Cardiac Damage, Cardiovascular Disease

Network 2 has over 30 genes from our list associated with Myc, which was found to be up-regulated (Figure 6.13 B). Many of the associations are known non-specific protein-protein interactions. Myc is thought to be involved in regulating the expression of several genes including Afr4 and 6, angiopoietin 2 (Angpt2), block of proliferation 1 (Bop1), Nop58 ribonucleoprotein homolog (Nop58) and fibrillarin (Fbl), which are all up-regulated in our dataset. Myc is also supposed to increase expression of glucose phosphate isomerase (Gpi) which was down-regulated in our dataset. Myc is also known to down-regulate the expression of several other genes which are up-regulated in our analysis including LIM and senescent cell antigen-like domains 1 (Lims1), Casp8 and FADD-like apoptosis regulator (Cflar) and H3 histone family 3C (H3f3c). Single stranded DNA binding protein 2 (Ssbp2) was down-regulated in our analysis and is known to inhibit expression of Myc.

Network 3 has several interlinked small hubs; histone h3, eukaryotic translation elongation factor 1 alpha 1 (Eef1a1), serum/glucocorticoid regulated kinase 1 (Sgk1) and neural precursor cell expressed developmentally down-regulated 4 (Nedd4) (see Figure 6.13 C). Nedd4 is down-regulated in our analysis and is associated with several up-regulated proteins including eNaC which it inhibits. SGK1 is up-regulated in our dataset and is linked in this network to 5 down-regulated proteins, and also binds eNaC (and possibly increases phosphorylation of eNaC, reducing the inhibition by Nedd4). Sgk1 is also thought to inhibit NEDD4. Eef1a1 is up-regulated in our analysis and is shown to be associated with several genes from our dataset which were down-regulated. Histone H3 (up-regulated) is associated with several up- and down-regulated genes in Network 3.

Figure 6.13 Networks associated with the genes altered in Sham vs. MI A) Network 1. B) Network 2. C) Network 3. Genes highlighted in red were found to be up-regulated, and those highlighted in green were down-regulated in Sham vs. MI.

A

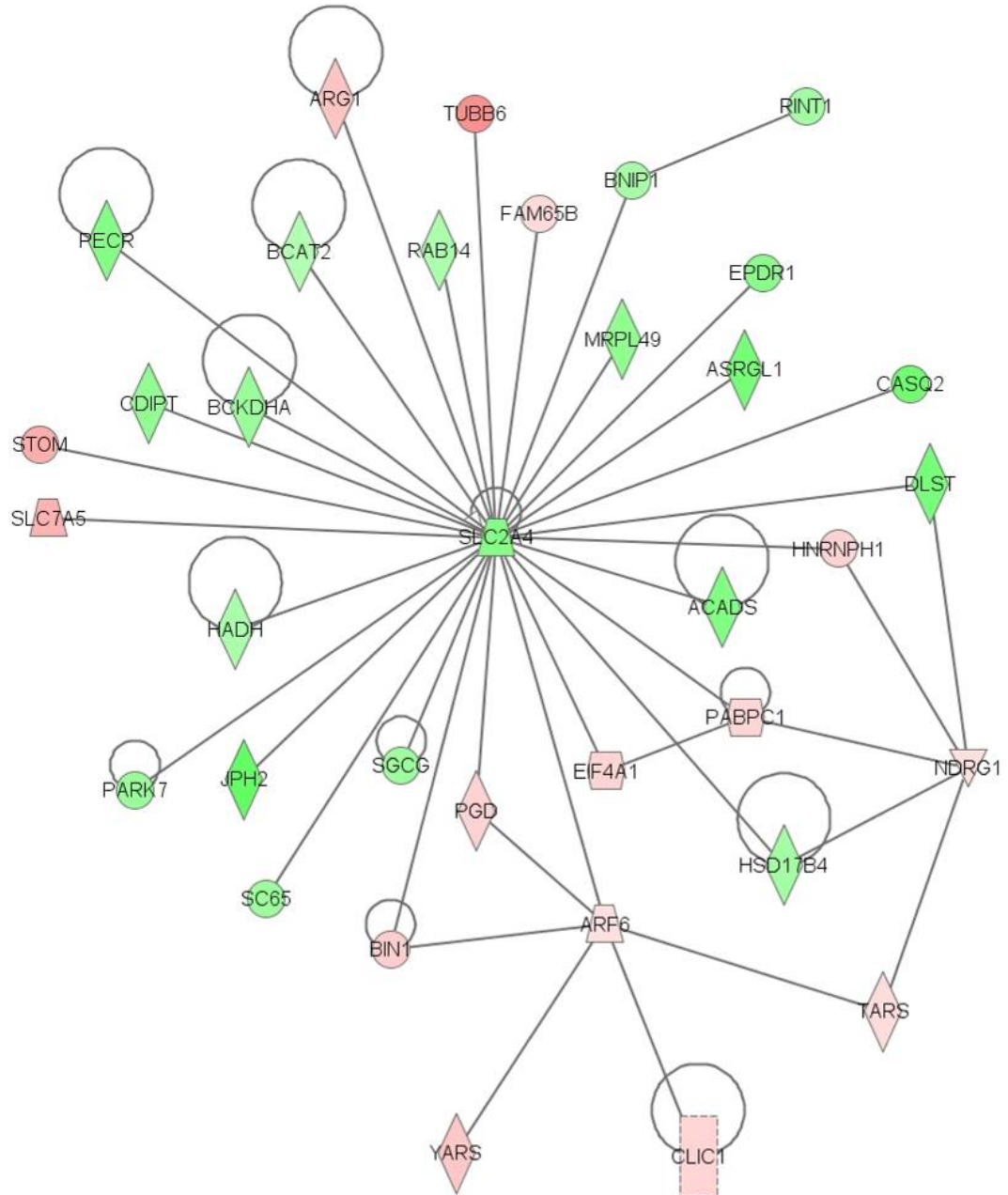


Figure 6.13 B

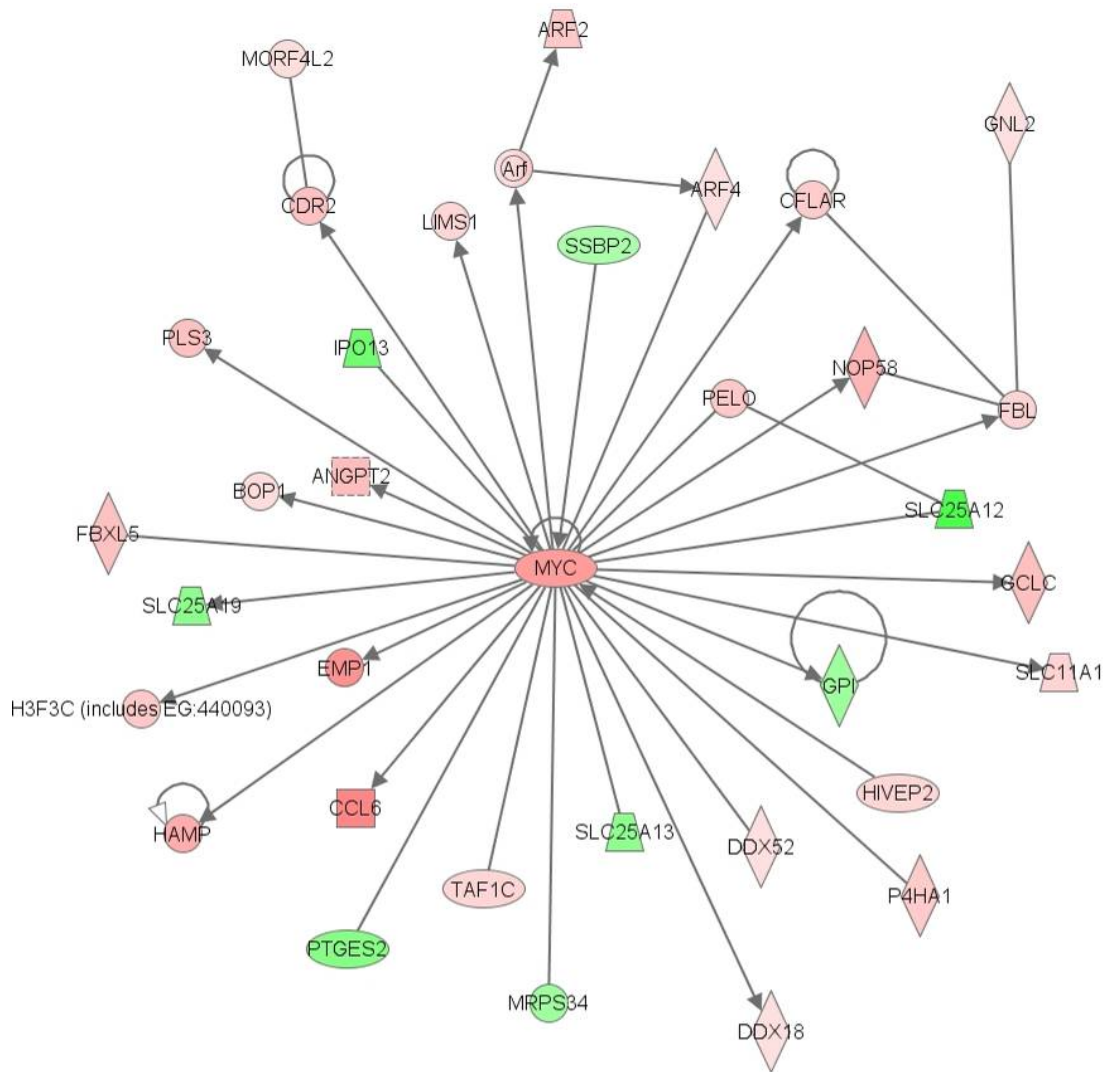
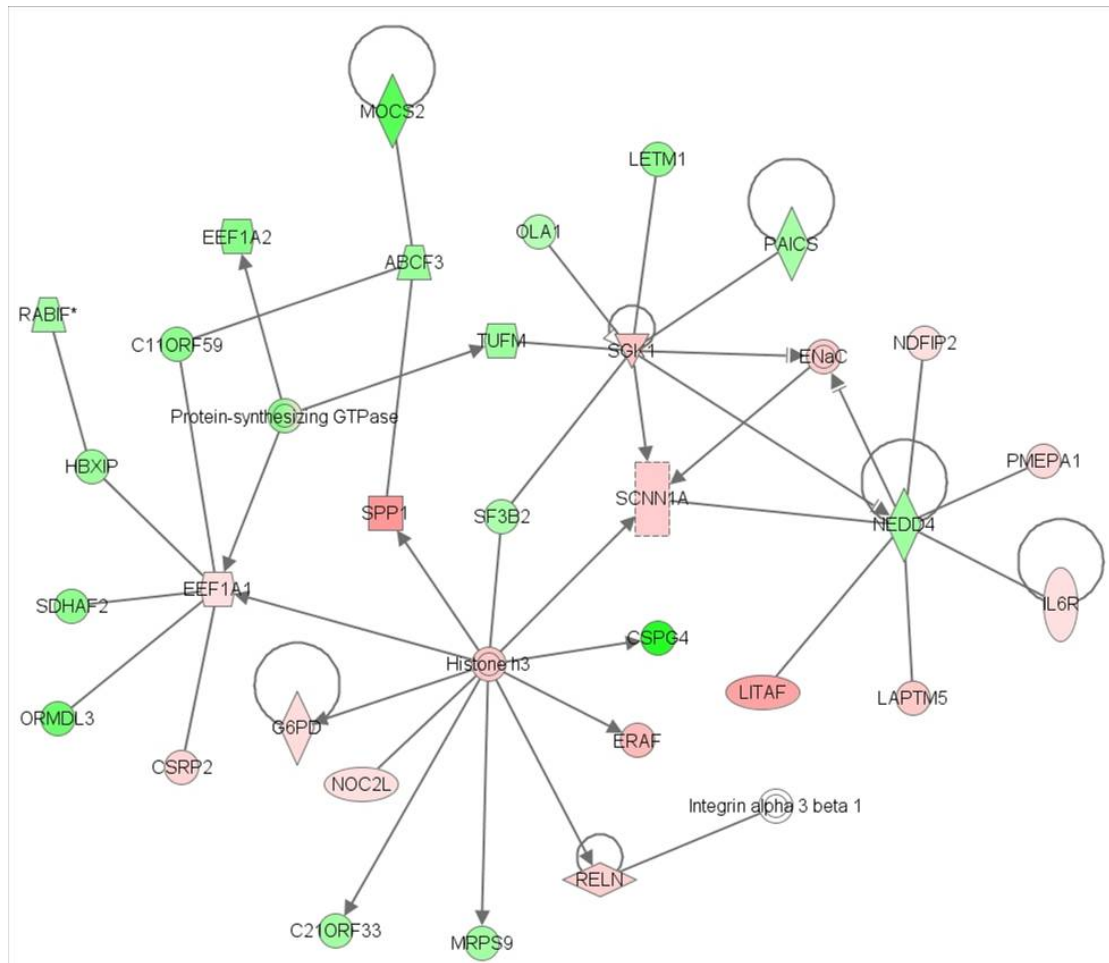


Figure 6.13 C



The main canonical pathways highlighted by the transcriptomic data are signalling pathways, some involved in inflammatory response (IL-10, IL-8, Fcγ-receptor, and acute phase response signalling) some involved in oxidative stress response (Nrf2). The top 20 of these are detailed in Table 6.14.

Table 6.14 Top 20 canonical pathways associated with the genes altered in Sham vs. MI

Ingenuity Canonical Pathways	-log(p-value)	Ratio	Molecules
Fc gamma Receptor-mediated Phagocytosis in Macrophages and Monocytes	8.27E+00	2.57E-01	RAC2,PTK2B,ARPC1B,ARPC5,FCGR1A,PTEN,HMOX1,ARF6,ACTR3,HCK,ARPC3,ACTC1,VASP,FGR,PRKCQ,FCGR2A,ACTB,RAC1,ACTG1,INPP5D,PLA2G6,WAS,SYK,RAB11A,VAV1,PRKCH
ILK Signaling	6.22E+00	1.82E-01	RAC2,FLNB,FN1,PPP2R5B,HIF1A,RHOH,ITGB7,PGF,PTEN,MYC,PARVB,RHOG,FLNA,PPAP2B,ATF4,ILKAP,NOS2,ACTC1,ACTN1,CFL1,TNFRSF1A,ACTB,SNAI1,RAC1,RHOJ,ACTG1,MYL7,PPP2CB,FOS,RHOQ,RND3,CFL2,PTGS2,MMP9
Integrin Signaling	4.94E+00	1.65E-01	RAC2,ARPC1B,ARPC5,ABL1,KRAS,LIMS1,RHOH,ITGB7,PTEN,TSPAN3,PARVB,ARF6,ACTR3,RHOG,ARF4,ARPC3,ILKAP,ACTC1,VASP,ACTN1,PAK2,NRAS,ACTB,RAC1,RHOJ,ARF2,ACTG1,MYL7,ITGAM,RHOQ,RND3,WAS,PLCG2
IL-10 Signaling	4.91E+00	2.29E-01	CCR1,SOCS3,CCR5,JAK1,IL10,FCGR2A,BLVRB,IKBKE,IL1R1,FCGR2B,IL1R2,HMOX1,FOS,IL1RN,IL1B,LBP
B Cell Receptor Signaling	4.81E+00	1.75E-01	RAC2,ABL1,KRAS,FCGR2B,PTEN,PTPRC,ATF4,ETS1,PTPN6,NRAS,CALM3,PRKCQ,MAP3K6,FCGR2A,EGR1,RAC1,IKBKE,MALT1,INPP5D,DAPP1,BCL10,SYK,PLCG2,MAP3K8,VAV1,PIK3AP1,BCL2A1
NRF2-mediated Oxidative Stress Response	4.50E+00	1.64E-01	FTL,GSTM5,DNAJB4,GCLC,KRAS,DNAJC15,DNAJA1,CLPP,HMOX1,GSTM2,ATF4,GSTTT2,DNAJB1,ACTC1,NFE2L2,GSTK1,PRKCQ,NRAS,ACTB,MAFK,MAFF,ACTG1,GSTO1,TXNRD1,FOS,STIP1,CAT,DNAJC18,DNAJC14,PRKCH
Leukocyte Extravasation Signaling	4.02E+00	1.55E-01	RAC2,MMP3,PTK2B,ABL1,RHOH,ROCK2,TIMP1,MMP8,ARHGAP12,RASSF5,ACTC1,ACTN1,VASP,ITK,PRKCQ,CXCR4,ACTB,RAC1,BMX,NCF4,ACTG1,GNAI3,ITGAM,ARHGAP9,WAS,PLCG2,CD44,VAV1,PRKCH,MMP9
TREM1 Signaling	3.94E+00	2.03E-01	RAC2,TREM1,IL10,TYROBP,RAC1,JAK2,FCGR2B,CCL3,TLR2,CCL7,PLCG2,TLR6,TLR13,IL1B
Colorectal Cancer Metastasis Signaling	3.93E+00	1.41E-01	RAC2,JAK1,MMP3,ADCY4,KRAS,JAK2,RHOH,PRKAG1,PGF,MYC,RHOG,MMP8,WNT4,NOS2,STAT1,NRAS,CASP3,TNFRSF1A,IL6R,RAC1,ADCY6,RHOJ,GNG10,TLR2,FOS,RHOQ,RND3,TLR6,PRKACA,TLR13,PTGER2,PTGS2,JAK3,MMP9,PRKAR1A
Acute Phase Response Signaling	3.88E+00	1.57E-01	SOCS3,RAC2,HAMP,FTL,FN1,KRAS,JAK2,HMOX1,LBP,SERPINE1,C3,NRAS,MYD88,TNFRSF1A,C1S,IL6R,RAC1,IKBKE,SOCS4,IL1R1,FOS,HP,RIPK1,TF,IL1RN,IL1B,A2M,SOCS5
NF-kappaB Signaling	3.83E+00	1.64E-01	RAC2,BMP4,BMP2,KRAS,NGF,IL1R2,PRKCQ,NRAS,TNFRSF1A,MYD88,RAC1,IL1R1,MALT1,TLR2,CSNK2A2,RIPK1,IL1RN,BCL10,PLCG2,TLR6,FCER1G,PRKACA,IL1B,BTRC,MAP3K8
Production of Nitric Oxide and Reactive Oxygen Species in Macrophages	3.79E+00	1.41E-01	RAC2,JAK1,PPP2R5B,JAK2,RHOH,RHOG,NOS2,STAT1,PTPN6,PRKCQ,MAP3K6,TNFRSF1A,RAC1,IKBKE,RHOJ,NCF4,TLR2,PPP2CB,FOS,RHOQ,RND3,PLCG2,CAT,PRKCH,MAP3K8,JAK3

Table 6.14 continued.

Ingenuity Canonical Pathways	-log(p-value)	Ratio	Molecules
Semaphorin Signaling in Neurons	3.79E+00	2.50E-01	PAK2,FES,CFL1,RAC1,RHOJ,RHOH,ROCK2,SEMA4D,RHOG,RHOQ,RND3,CFL2,PLXNB1
Oncostatin M Signaling	3.66E+00	2.86E-01	JAK1,NRAS,MMP3,OSM,OSMR,KRAS,PLAU,JAK2,STAT1,JAK3
IL-8 Signaling	3.59E+00	1.45E-01	RAC2,ANGPT2,PTK2B,KRAS,RHOH,PGF,ROCK2,HMOX1,RHOG,IL8RB,GNA13,PRKCQ,PAK2,NRAS,RAC1,HBEGF,IKBKE,RHOJ,GNG10,MYL7,GNAI3,ITGAM,RHOQ,RND3,PRKCH,PTGS2,MMP9
Endothelin-1 Signaling	3.59E+00	1.45E-01	ADCY4,KRAS,MYC,PLCD3,HMOX1,EDN1,GNAT2,PLA2G5,GNA13,NOS2,CASP8,NRAS,PRKCQ,CASP3,PLA2G12A,EDNRB,YWHAZ,ADCY6,GNAI3,PLA2G6,FOS,RNF111,PLCG2,PRKCH,SPR,PTGS2,PTGER2
Role of Macrophages, Fibroblasts and Endothelial Cells in Rheumatoid Arthritis	3.52E+00	1.26E-01	SOCS3,RAC2,FN1,MMP3,PDGFA,LTB,KRAS,JAK2,IL17RA,FCGR1A,CEBPG,PGF,MYC,ROCK2,IL1R2,PLCD3,OSM,ATF4,WNT4,NOS2,ADAMTS4,MIF,CALM3,PRKCQ,NRAS,MYD88,IL10,TNFRSF1A,C1S,IL6R,RAC1,IKBKE,IL1R1,TLR2,FOS,HP,RIPK1,IL1RN,PLCG2,TLR6,TLR13,IL1B,PRKCH
Regulation of Actin-based Motility by Rho	3.48E+00	1.83E-01	RAC2,PAK2,CFL1,ARPC1B,ACTB,ARPC5,RAC1,RHOJ,RHOH,MYL7,RHOQ,ACTR3,RHOH,RND3,WAS,ARPC3,ACTC1
Sphingosine-1-phosphate Signaling	3.46E+00	1.70E-01	RAC2,PTK2B,CASP3,PDGFA,ADCY4,ADCY6,RAC1,RHOJ,RHOH,S1PR4,PLCD3,GNAI3,RHOG,RHOQ,RND3,PLCG2,SPHK1,GNA13,CASP8
Ephrin Receptor Signaling	3.42E+00	1.38E-01	RAC2,RGS3,ARPC1B,PDGFA,ARPC5,ABL1,KRAS,JAK2,PGF,ROCK2,ACTR3,GNAT2,ARPC3,ATF4,EFNB3,GNA13,PAK2,NRAS,CFL1,CXCR4,RAC1,GNG10,GNAI3,SDCBP,WAS,CFL2,EPHA2

6.2.3.2 *MI vs. BMMNC*

15 genes were differentially expressed in MI vs. BMMNC that mapped in IPA (Table 6.15 A). These were associated with 63 other genes (other genes associated with network 1 shown in Table 6.15 B) within 10 different networks. Network 1 scored 11 and has 5 molecules from our dataset. The other networks all contained only one gene from our dataset and all scored only 3 or 2. Network 1 is illustrated in Figure 6.14.

A major hub in network 1 was FBJ murine osteosarcoma viral oncogene homolog (Fos) a gene found to be significantly up-regulated in Sham vs. MI, it is also a central hub of network 8 in the Sham vs. MI IPA core analysis (Table 6.13). Fos was not significantly differentially regulated in the MI vs. BMMNC dataset. Within this network Fos is known to decrease the expression of embigin (Emb) which is down-regulated in MI vs. BMMNC.

Micro RNA 214 (Mir214) is known to target Sorl1 and Chst1 from our dataset as well as several other genes only found to differ in Sham vs. MI (Fos, Egr1 and Prkaca). Signal transducer and activator of transcription 6, interleukin-4 induced (Stat6) also links Fos and several proteins not in this dataset with down-regulated resistin like alpha (Retnla).

Table 6.15 Proteins and endogenous chemicals included in the IPA analysis of MI vs. BMMNC gene expression data A Gene expression results mapped into IPA for core analysis. B The associated genes and endogenous chemicals also included in the Sham vs. MI IPA core analysis which were found in network 1. Protein symbol and Entrez gene names are shown alongside the network(s) the protein/chemical is found in, the sub-cellular localisation and molecule type.

A

Symbol	Entrez Gene Name	Networks	Location	Type(s)
CHST1	carbohydrate (keratan sulfate Gal-6) sulfotransferase 1	1	Cytoplasm	enzyme
EMB	embigin homolog (mouse)	1	Plasma Membrane	other
F5	coagulation factor V (proaccelerin, labile factor)	1	Plasma Membrane	other
RETNLA	resistin like alpha	1	Extracellular Space	other
SORL1	sortilin-related receptor, L(DLR class) A repeats-containing	1	Plasma Membrane	transporter
RNF149	ring finger protein 149	2	Unknown	other
CASQ2	calsequestrin 2 (cardiac muscle)	3	Cytoplasm	other
CLEC4C	C-type lectin domain family 4, member C	4	Plasma Membrane	other
S1PR4	sphingosine-1-phosphate receptor 4	5	Plasma Membrane	G-protein coupled receptor
DOK3	docking protein 3	6	Cytoplasm	other
CORO1A	coronin, actin binding protein, 1A	7	Cytoplasm	other
GLIPR1	GLI pathogenesis-related 1	8	Extracellular Space	other
SEMA4A	sema domain, immunoglobulin domain (Ig), transmembrane domain (TM) and short cytoplasmic domain, (semaphorin) 4A	9	Plasma Membrane	other
STK17B	serine/threonine kinase 17b	10	Nucleus	kinase
1600029D21RIK	RIKEN cDNA 1600029D21 gene		Unknown	other

Table 6.15 B

Symbol	Entrez Gene Name	Networks	Location	Type(s)
A2M	alpha-2-macroglobulin	1	Extracellular Space	transporter
APP	amyloid beta (A4) precursor protein	1	Plasma Membrane	other
COL1A1	collagen, type I, alpha 1	1	Extracellular Space	other
EGR1	early growth response 1	1	Nucleus	transcription regulator
ELAVL1	ELAV (embryonic lethal, abnormal vision, Drosophila)-like 1 (Hu antigen R)	1	Cytoplasm	other
ETS1	v-ets erythroblastosis virus E26 oncogene homolog 1 (avian)	1	Nucleus	transcription regulator
F3	coagulation factor III (thromboplastin, tissue factor)	1	Plasma Membrane	transmembrane receptor
FABP4	fatty acid binding protein 4, adipocyte	1	Cytoplasm	transporter
FCER2	Fc fragment of IgE, low affinity II, receptor for (CD23)	1	Plasma Membrane	other
FOS	FBJ murine osteosarcoma viral oncogene homolog	1	Nucleus	transcription regulator
FURIN	furin (paired basic amino acid cleaving enzyme)	1	Cytoplasm	peptidase
IFNG	interferon, gamma	1	Extracellular Space	cytokine
Ige	--	1	Extracellular Space	complex
IGHE	immunoglobulin heavy constant epsilon	1	Extracellular Space	other
IL13	interleukin 13	1	Extracellular Space	cytokine
LGALS3	lectin, galactoside-binding, soluble, 3	1	Extracellular Space	other
MAF	v-maf musculoaponeurotic fibrosarcoma oncogene homolog (avian)	1	Nucleus	transcription regulator
MIR125A (includes EG:406910)	microRNA 125a	1	Unknown	microRNA
MIR214 (includes EG:406996)	microRNA 214	1	Unknown	microRNA
NCOA3	nuclear receptor coactivator 3	1	Nucleus	transcription regulator
NMI	N-myc (and STAT) interactor	1	Cytoplasm	transcription regulator
NPPA	natriuretic peptide precursor A	1	Extracellular Space	other
PACS1	phosphofurin acidic cluster sorting protein 1	1	Cytoplasm	other

Table 6.15 B continued.

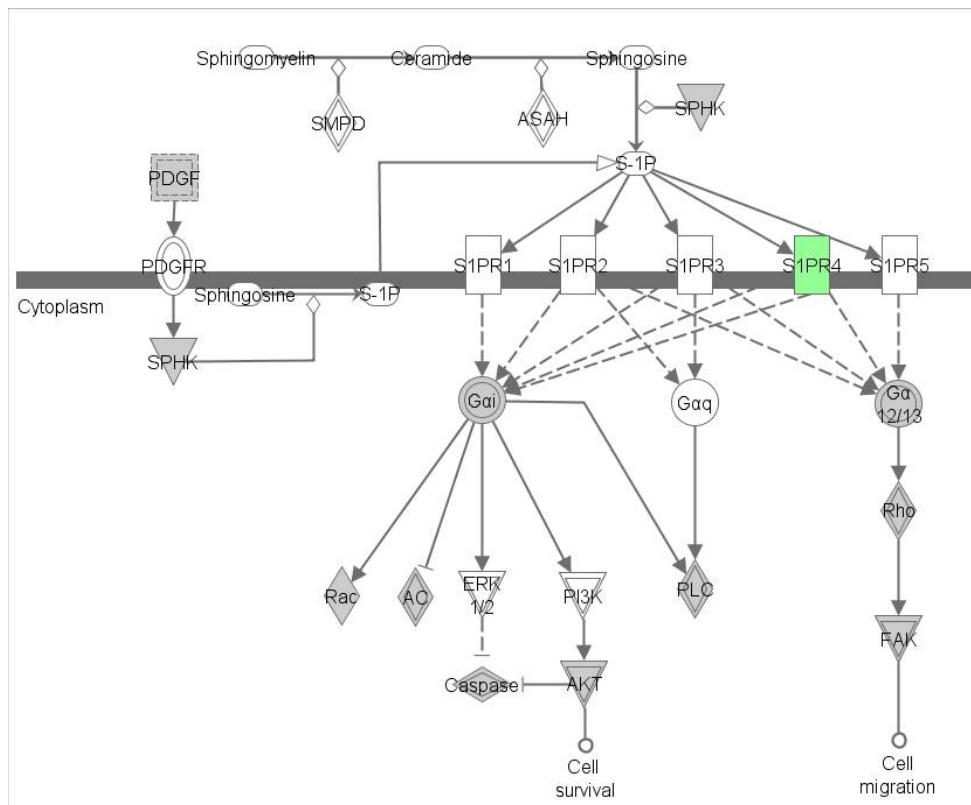
Symbol	Entrez Gene Name	Networks	Location	Type(s)
PRKACA	protein kinase, cAMP-dependent, catalytic, alpha	1	Cytoplasm	kinase
PRKD1	protein kinase D1	1	Cytoplasm	kinase
STAT	--	1	Unknown	group
STAT5A	signal transducer and activator of transcription 5A	1	Nucleus	transcription regulator
STAT5B	signal transducer and activator of transcription 5B	1	Nucleus	transcription regulator
STAT6	signal transducer and activator of transcription 6, interleukin-4 induced	1	Nucleus	transcription regulator

Table 6.16 Canonical Pathways associated with the genes altered in MI vs. BMMNC

Ingenuity Canonical Pathways	-log(p-value)	Ratio	Molecules
Coagulation System	1.45E+00	2.70E-02	F5
Ceramide Signaling	1.11E+00	1.15E-02	S1PR4
Sphingosine-1-phosphate Signaling	1.00E+00	8.93E-03	S1PR4
Human Embryonic Stem Cell Pluripotency	9.30E-01	6.76E-03	S1PR4
Calcium Signaling	7.87E-01	4.85E-03	CASQ2
Axonal Guidance Signaling	5.01E-01	2.48E-03	SEMA4A

S1pr4 (a.k.a Egd6) is present in three different pathways. Its role in those pathways is essentially the same and is best illustrated in ‘sphingosine-1-phosphate signalling’ which is illustrated in Figure 6.15. S1pr4 (Edg6) S1pr5 (Edg8) are both known to activate Gai complexes which are known to activate ERK1/2 and Pi3k activating cell survival pathways [143, 144].

Figure 6.15 Sphingosine-1-phosphate signalling The gene highlighted in green was found to be down-regulated in MI vs. BMMNC. Those in grey were found to be differentially expressed in Sham vs. MI, but not in MI vs. BMMNC.



6.2.4 Summary

- PANTHER pathway analysis revealed apoptosis and inflammation (including b-cell and t-cell activation) to be over-represented by genes up-regulated in Sham vs. MI. DAVID also highlighted apoptosis and immune system activation. General cellular metabolism were overrepresented in the down-regulated genes in Sham vs. MI.
- A very large amount of information was provided by IPA network analysis for the Sham vs. MI gene list. An interesting finding was that the transport protein Glut-4 and the transcription factor Myc were connected to many of the genes altered in Sham vs. MI.
- Canonical pathway analysis on Sham vs. MI genes revealed inflammation (reflecting results from DAVID and PANTHER) and oxidative stress which was also highlighted in the proteomic dataset bioinformatics analyses.
- The small number of genes differentially regulated in MI vs. BMMNC led to very little information from any of the bioinformatic analyses. However one network highlighted two transcription factors as being interesting in relation to the MI vs. BMMNC affected genes (Fos and Stat6), however they were each only linked to a single gene from our dataset.
- Sphingosine-1-phosphate receptor 4 (S1pr4) was highlighted in several pathways focusing on ceramide signalling and the activation of downstream survival kinases, including Akt/Pi3k which are known to be involved in cardioprotection signals initiated through IPC.

7. Studies of 14-3-3 epsilon and Bad proteins

7.1 Validation experiments using samples 10-18

Western blotting of 14-3-3 ϵ , Sdha and Pepb1 were performed on samples 10-18 and results were compared to the Western blot analyses for samples 1-9. The experimental conditions were as described in section 4.3. Images of the Western blots for each protein are shown in Figure 7.1. The Gapdh loading controls for the 14-3-3 ϵ and Pepb1 western blots did not show uniformity across samples, suggesting perhaps that protein loading was not uniform. The calculations were however corrected to the Gapdh band intensities as before. The average normalised band volumes for samples 10-18 are shown alongside samples 1-9 (Figure 7.2).

Results for 14-3-3 ϵ showed a significant difference between experimental groups for samples 10-18. The change in Sham vs. MI was non significant (3 fold significant decrease in samples 1-9) however there was a significant 14 fold increase in MI vs. BMMNC (3.2 fold in samples 1-9). The MI associated decrease in 14-3-3 epsilon observed in samples 1-9 was not seen in samples 10-18, but there was a strong up-regulation of 14-3-3 ϵ in both sample sets.

For Sdha significant differences between the experimental groups was observed. Although both sample sets did not have significant differences in Sham vs. MI, there was a significant 2 fold up-regulation in MI vs. BMMNC (1.75 fold in samples 1-9). The magnitude of the expression change is very similar.

Pepb1 showed a similar pattern of regulation in samples 10-18 to that observed in samples 1-9. None of the differences between the groups reached significance in either sample set.

The similarity of the differential regulation between experimental groups for these three proteins in separately prepared sets of myocardial samples suggested they were suitable to use for further studies of one of our proteins of interest (14-3-3ε).

Figure 7.1 Western blots of 14-3-3 epsilon (14-3-3ε), succinate dehydrogenase (Sdha), and phosphatidylethanolamine-binding protein 1 (Pebp1) in samples 10-18 S = Sham operated group, M = MI group treated with PBS, B = MI group treated with bone marrow mononuclear cells. Glyceraldehyde 3-phosphate dehydrogenase (Gapdh) was used for normalisation. (See Figure 4.6 for western blots of these three proteins in samples 1-9)

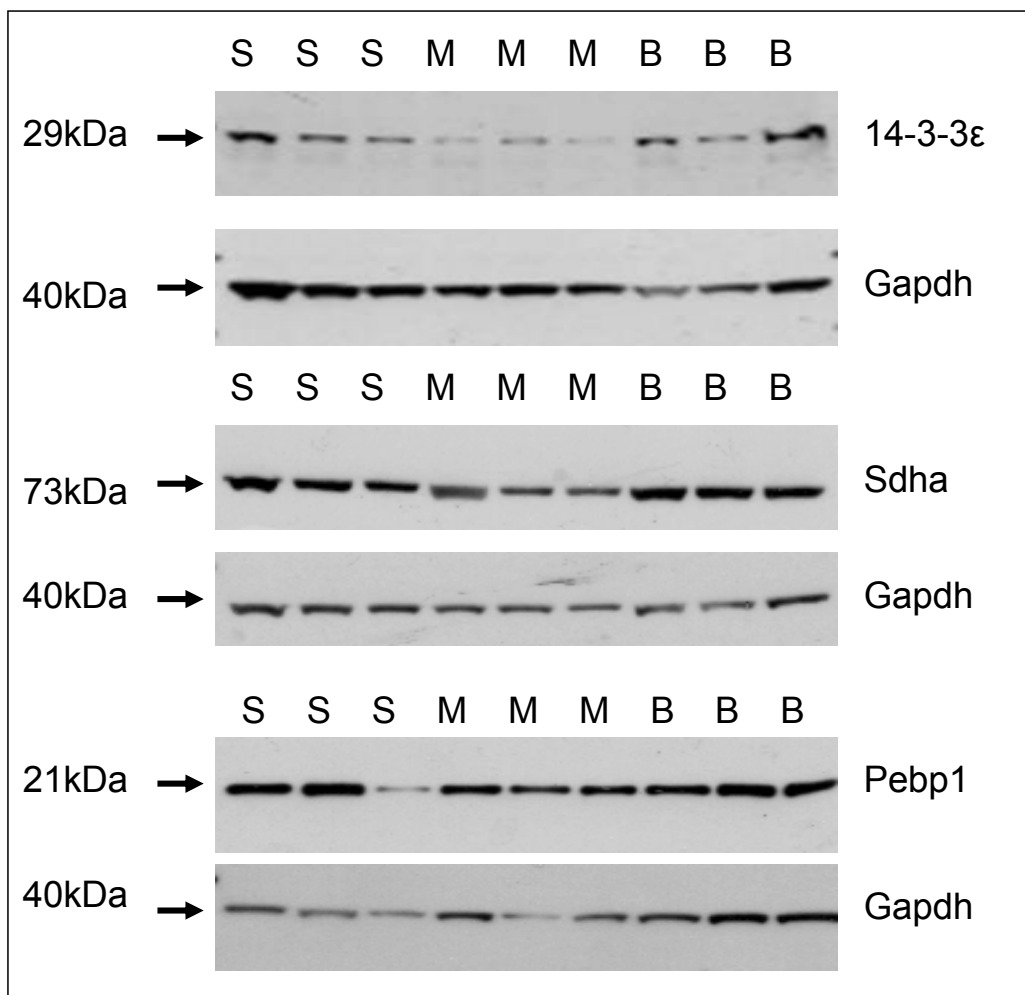
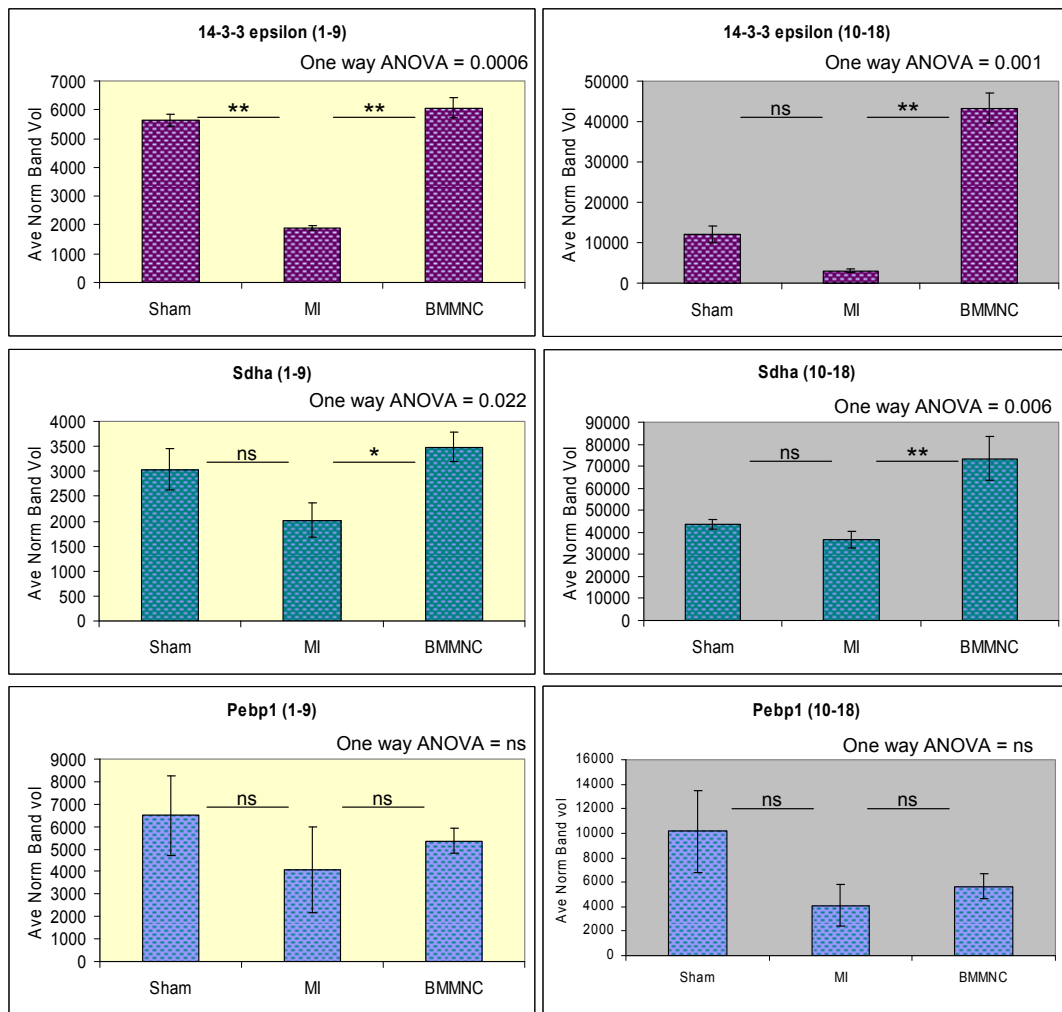


Figure 7.2 The normalised band volumes from Western blot analysis of samples 1-9 (left) and normalised band volumes from Western blot analysis of samples 10-18 (right) for 14-3-3 epsilon (14-3-3 ϵ), succinate dehydrogenase (Sdha), and phosphatidylethanolamine-binding protein 1 (Pebp1) Sham = sham operated group, MI = MI group treated with PBS, BMMNC = MI group treated with bone marrow mononuclear cells. Error bars indicate standard deviation. Significance in one way ANOVA indicated in top right hand corner of charts, significance in Sham vs. MI and MI vs. BMMNC comparisons indicated by the bars, * = post-hoc bonferroni p-value of 0.05-0.01, ** = post-hoc bonferroni p-value <0.01, ns = not significant.



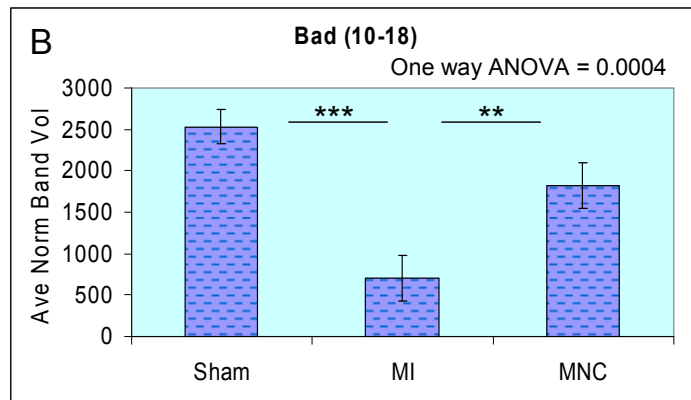
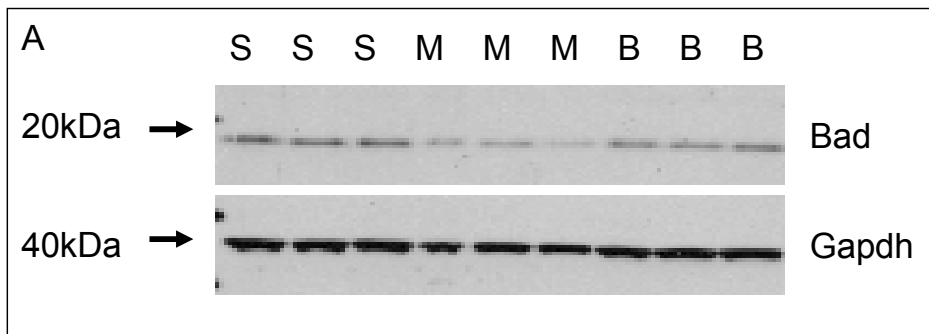
7.2 Western blot analysis of Bad proteins

Western blotting was also performed on samples 10-18 using antibodies for the pro-apoptotic protein Bad which is known to interact with 14-3-3 ϵ in its phosphorylated form. We first measured non-phosphorylated Bad to ascertain whether it was present in our protein lysates, then we attempted to measure Bad phosphorylated at serine 136, which is part of the phosphorylated binding motif for 14-3-3 ϵ .

7.2.1 Bad

An assay using a rabbit monoclonal to Bad antibody was used to detect a band at approximately 20kDa using an antibody dilution of 1 in 2000 and 30ug total protein loading. The bands from Bad and the Gapdh gel run simultaneously can be seen in Figure 7.3 A. The average normalised band volumes and associated statistics are in Figure 7.3 B. Bad protein was down-regulated 3 fold in Sham vs. MI and was up-regulated 2.3 fold in MI vs. BMMNC, both differences were highly significant.

Figure 7.3 Western blots of Bad in samples 10-18 A) S = Sham operated group, M = MI group treated with PBS, B = MI group treated with bone marrow mononuclear cells. Glyceraldehyde 3-phosphate dehydrogenase (Gapdh) was used for normalisation. B) Normalised band volumes Sham = sham operated group, MI = MI group treated with PBS, BMMNC = MI group treated with bone marrow mononuclear cells. Error bars indicate standard deviation. Significance in one way ANOVA indicated in top right hand corner of charts, significance in Sham vs. MI and MI vs. BMMNC comparisons indicated by the bars, ** = post-hoc bonferroni p-value <0.01, *** = post-hoc bonferroni p-value <0.001.



7.2.2 Bad (phospho s136)

An assay using two different rabbit polyclonal to Bad (phospho s136) antibodies was not optimised after attempting several different variations in conditions including, primary antibody dilutions of 1 in 300, 1 in 1000 and 1 in 7000 (Abcam's recommended dilution) for the Abcam antibody and 1 in 350, 1 in 500 and 1 in 1000 for the New England Biolab supplied antibody. Protein lysate concentrations utilised were from 10-40ug total loading. Overnight primary antibody incubations were tried as well as 1.5 hour incubations. BSA (fraction V) as a blocking agent as well as 5% non-fat milk, in concentrations of Tween-20 from 0.05% to 0.15% were also tested. Both antibodies produced multiple bands from 90-20kDa, but none of the tested conditions produced clear bands in the expected 22kDa range.

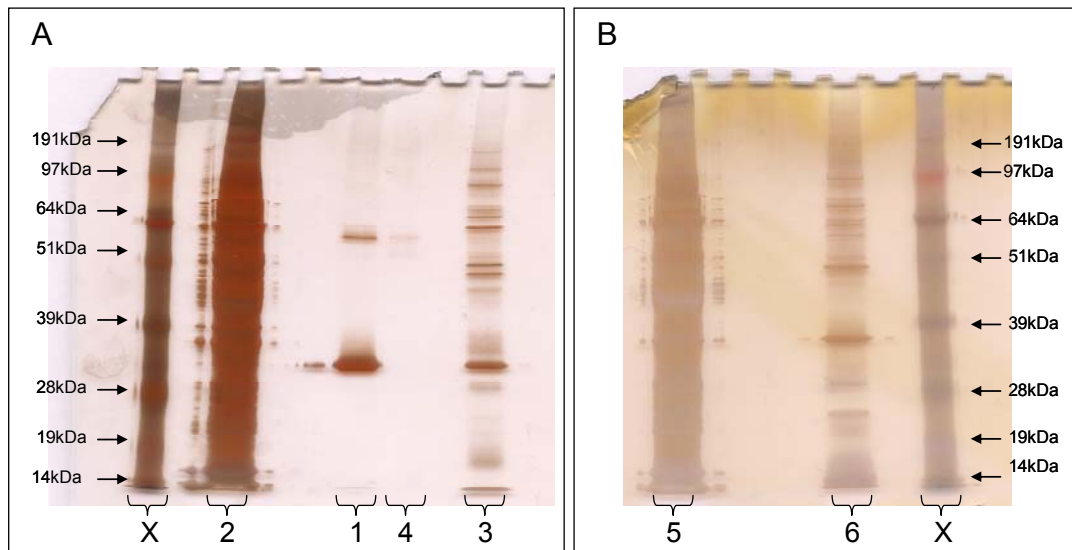
7.3 Preliminary pull-down assay of his-tagged 14-3-3 epsilon

7.3.1 Pull-down assay and SDS-PAGE

The pull-down methodology was tested using 60ug of his-tagged 14-3-3ε and the ProFound™ Pull-Down PolyHis Protein:Protein Interaction Kit [Pierce, US]. The protein lysate was prepared from a mix of three tissue samples, one from each experimental group from samples 10-18.

During the procedure, the no-bait control column collapsed before the prey could be added, however the procedure was continued and the bait flow-through, prey flow-through and the eluate from the 60ug bait column were separated on an SDS-PAGE gel along with the bait-flow through for the no-bait control column (Figure 7.4 A). The no-bait control was repeated the next day using the same prey protein preparation which had been frozen overnight and the prey-flow through and eluate from this was run on a second SDS-PAGE gel (Figure 7.4 B).

Figure 7.4 SDS-PAGE of the preliminary 14-3-3 epsilon pull-down assay A) & B)
 Two SDS-PAGE gels were run with the products from the pull-down assay. 1, 2 & 3 are from the column loaded with 60µg his-tagged 14-3-3ε bait; 1 = Bait flow-through, 2 = Prey flow-through, 3 = Eluate. 4, 5 & 6 are from the column loaded with buffer only (no-bait control); 4 = Bait flow-through, 5 = Prey flow-through, 6 = Eluate. X = Mw marker.

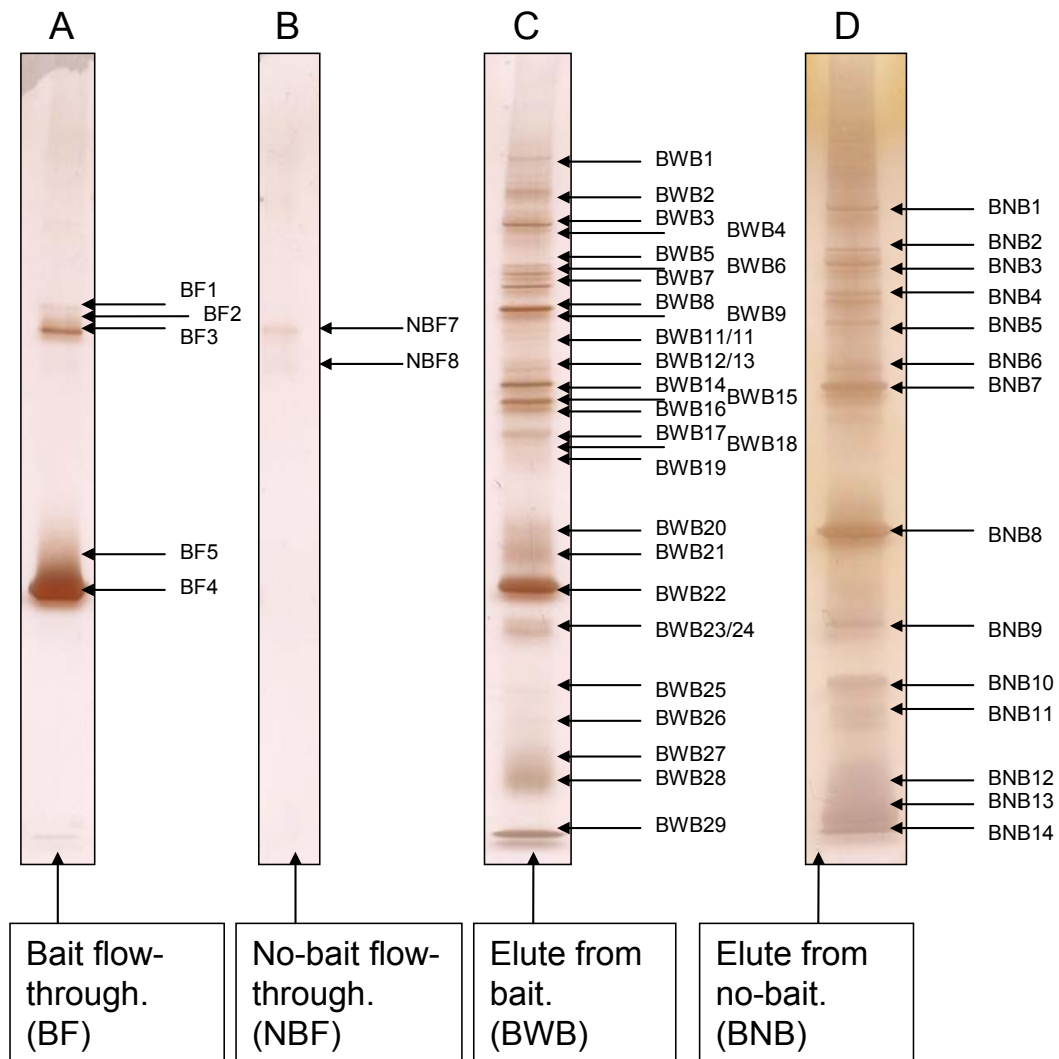


Several bands were visible that were in both the bait and no bait control eluate. There were also differences in the patterns of the bands from the two eluates. The bands from the bait flow through and from the eluates were given unique IDs as illustrated in Figure 7.5. Bands were then excised and processed for protein identification using LC-MS/MS.

7.3.2 Protein identification by LC-MS/MS

Detailed results from the MASCOT searches are shown in Appendix 8. A summary of the proteins identified are shown in Table 7.1. Bovine milk proteins and the rat serum albumin were among the identified proteins but were excluded from the summarised results table (Table 7.1). The only protein identified from the bait flow through was 14-3-3 epsilon. The fainter, higher mass bands did not yield an identification.

Figure 7.5 Band IDs from bait flow-through and eluate from the preliminary 14-3-3 epsilon pull-down assay **A)** Bait flow through from the 60ug his-tagged 14-3-3ε column. **B)** Bait flow through from the no-bait control column. **C)** Eluate from the 60ug his-tagged 14-3-3ε column. **D)** Eluate from the no-bait control column.



Several proteins were found in both the bait and no-bait control eluate suggesting their presence in the bait eluate was due to non-specific binding. These were haemoglobin, cytochrome b-c1 complex subunit 6 and cytochrome c1, heme protein. Proteins identified only in the no-bait control were NADH ubiquinone oxidoreductase, elongation factor 1-alpha, succinyl-CoA ligase [GDP-forming] subunit alpha, NADH dehydrogenase [ubiquinone] flavoprotein 2, NADH

dehydrogenase [ubiquinone] iron-sulfur protein 6 and cytochrome c oxidase subunit 6B1. Proteins identified only in the bait eluate were oxoglutarate dehydrogenase E1 component, ATP synthase subunit beta, trifunctional enzyme subunit beta, sarcomeric creatine kinase, up-regulated during skeletal muscle growth protein 5 (Usmg5) and ATP synthase subunit e. Two of these six proteins, oxoglutarate dehydrogenase and creatine kinase, had peptide scores too low to be confident in the identification.

Table 7.1 Proteins identified by LC-MS/MS from the bands illustrated in Figure 7.5 Estimated relative molecular mass (*Mr*) of the bands is shown on the left. Proteins identified from the bait flow through (BF) are shown in pink. Proteins identified from the no-bait control eluate (BNB) and in orange and from the 60ug 14-3-3ε bait eluate (BWB) are shown in green. Protein names are shown alongside the band IDs shown in Figure 7.5. Protein names highlighted in grey had scores below threshold.

Estimated <i>Mr</i> of Band	Bait Flow-through (BF)		Bands No Bait (BNB)		Bands With Bait (BWB)	
	Band ID	Protein Name	Band ID	Protein Name	Band ID	Protein Name
190kDa					BWB3	oxoglutarate dehydrogenase E1 component, mitochondrial
120kDa			BNB3	NADH-ubiquinone oxidoreductase 75 kDa subunit, mitochondrial		
62kDa					BWB14	ATP synthase subunit beta, mitochondrial
60kDa			BNB7	Elongation factor 1-alpha	BWB15	Trifunctional enzyme subunit beta, mitochondrial
55kDa					BWB17	Creatine kinase, sarcomeric mitochondrial (mouse)
52kDa			BNB8	Succinyl-CoA ligase [GDP-forming] subunit alpha, mitochondrial		
50 kDa					BWB20	14-3-3 protein epsilon
50 kDa	BF4	14-3-3 epsilon			BWB21	14-3-3 protein epsilon
50 kDa	BF5	14-3-3 epsilon			BWB22	14-3-3 protein epsilon
47kDa					BWB24	Cytochrome c1, heme protein, mitochondrial (mouse)
45kDa			BNB9	Cytochrome c1, heme protein, mitochondrial (Bovine)		
40kDa			BNB10	NADH dehydrogenase [ubiquinone] flavoprotein 2, mitochondrial		
35kDa					BWB26	Hemoglobin subunit alpha-1/2
31kDa			BNB11	Hemoglobin subunit beta-2		
30kDa					BWB27	Hemoglobin subunit alpha-1/2
22kDa			BNB12	Hemoglobin subunit beta-2	BWB28	Hemoglobin subunit alpha-1/2
20kDa			BNB13	Hemoglobin subunit alpha-1/2		
18kDa			BNB14	Cytochrome b-c1 complex subunit 6, mitochondrial	BWB29	Cytochrome b-c1 complex subunit 6, mitochondrial
				NADH dehydrogenase [ubiquinone] iron-sulfur protein 6, mitochondrial		Up-regulated during skeletal muscle growth protein 5
				Cytochrome c oxidase subunit 6B1 (mouse)		ATP synthase subunit e, mitochondrial
				Hemoglobin subunit alpha-1/2		

8. Discussion and Future Work

This thesis describes the results from protein and gene expression profiling studies in a rat model of I/R injury and BMMNC therapy. I found numerous alterations in mitochondrial, energy metabolism and stress related proteins, many of these changes are consistent with what has been reported in previous models of I/R injury. BMMNC treatment was shown to ‘correct’ many of the protein alterations induced by I/R injury, and increased expression of some proteins to above sham levels (heat shock proteins, myosin regulatory light chain 2, and some subunits of the mitochondrial oxidative phosphorylation chain). There are no prior reports in the literature comparing I/R induced changes in the proteome with those following treatment with BMMNCs.

Validation was performed for a handful of differentially expressed proteins. Western blotting confirmed the changes in 14-3-3 epsilon (Ywhae/14-3-3 ϵ) expression, this is a protein known to have pro-survival functions including an ability to bind and inhibit the Bcl-2 related protein Bad (phosphorylated form) [145]. Bad phosphorylation is thought to be one of the many downstream actions of the Pi3k/Akt pathway, a system activated in our model [146, 147]. Pilot experiments on 14-3-3 ϵ did not provide data supporting an interaction with Bad, but a pull-down assay found an interaction with two subunits of ATP synthase, one of which has previously been shown to interact with 14-3-3 ϵ .

Gene expression was also found to be affected by I/R injury, with hundreds of genes showing increased or decreased expression. Many of these genes are involved in inflammatory/immunological responses and apoptosis/cell death signalling, both are aspects of cellular behaviour recognised as being associated with I/R injury. A few BMMNC induced changes in gene expression were observed, however these could not be validated by QPCR.

8.1 Proteomic changes in I/R and after treatment with BMMNCs

Numerous proteins were identified as being affected by I/R injury and BMMNC treatment in both the wide-range and narrow-range 2DE analyses. Many of these protein changes are likely to be modifications to existing proteins rather than increases or decreases in actual expression. The timepoint at which samples were collected for proteomic analysis (namely 6hr post reperfusion and treatment) is possibly too soon to see results of changes in rates of protein expression. Many proteins were observed in decreased amounts in MI group compared to Sham and these changes are likely to be degradation of proteins by proteases during the processes of cellular damage and death. Proteins which seem to increase in I/R are likely to be modified forms with the native version being undetected in our analysis, giving the appearance of a protein having much increased expression from near zero levels. The proteins we identified as being affected mostly fall within the functional categories of mitochondrial/oxidative phosphorylation, antioxidants, energy metabolism and heat shock/stress as well as cytoskeletal/sarcomeric proteins. Protein changes in the first four categories will be discussed below.

8.1.1 Mitochondrial/oxidative phosphorylation proteins

Subunits of complex I, II, III and V of the oxidative phosphorylation chain were all found to be altered by I/R injury in our model, see Figure 8.1. Many of these changes were seen to be ‘corrected’ in the treatment group however expression in some of the subunits increased after treatment compared to sham levels (Ndufa10). I/R induced changes in some of these proteins have been observed before in 2DE studies, and the ‘correction’ of these changes have been seen in both IPC and free radical scavenger treatment, both known to improve outcome after MI, in isolated perfused rabbit hearts [90, 91].

Complex I (NADH dehydrogenase) is made of 45 different subunits, seven of which are encoded by the mitochondrial genome [148]. Two different subunits of complex

I, NADH-ubiquinone oxidoreductase 75kDa subunit (Ndufs1) and NADH dehydrogenase [ubiquinone] 1 alpha subcomplex 10 (Ndufa10) were identified in our study as being differentially expressed. A fragment of the native Ndufs1 was found to be significantly down-regulated in Sham vs. MI, and up-regulated in MI vs. BMMNC but not significantly. Ndufa10 was not significantly altered in Sham vs. MI but did show a significant up-regulation in MI vs. BMMNC. Two different subunits of Complex I (Ndufa10, and Ndufv2) have been found to be up-regulated in I/R in an isolated perfused rabbit heart model, these were both subsequently found to be down-regulated in IPC which is the opposite direction of regulation to what we observed [91]. Another study using a perfused rabbit heart model identified three further subunits of Complex I (Ndufs3, Ndufv1 and Ndufab1) from four spots of interest. One of the spots identified as Ndufs3 was up-regulated in I/R and subsequently down-regulated after treatment with oxygen free radical scavenger (MPG), the other, a slightly higher *Mr* variant, was down-regulated in I/R but unchanged by treatment. The Ndufv1 spot was up-regulated in I/R and down-regulated in treatment, whereas the opposite was true of the Ndufab1 spot [90].

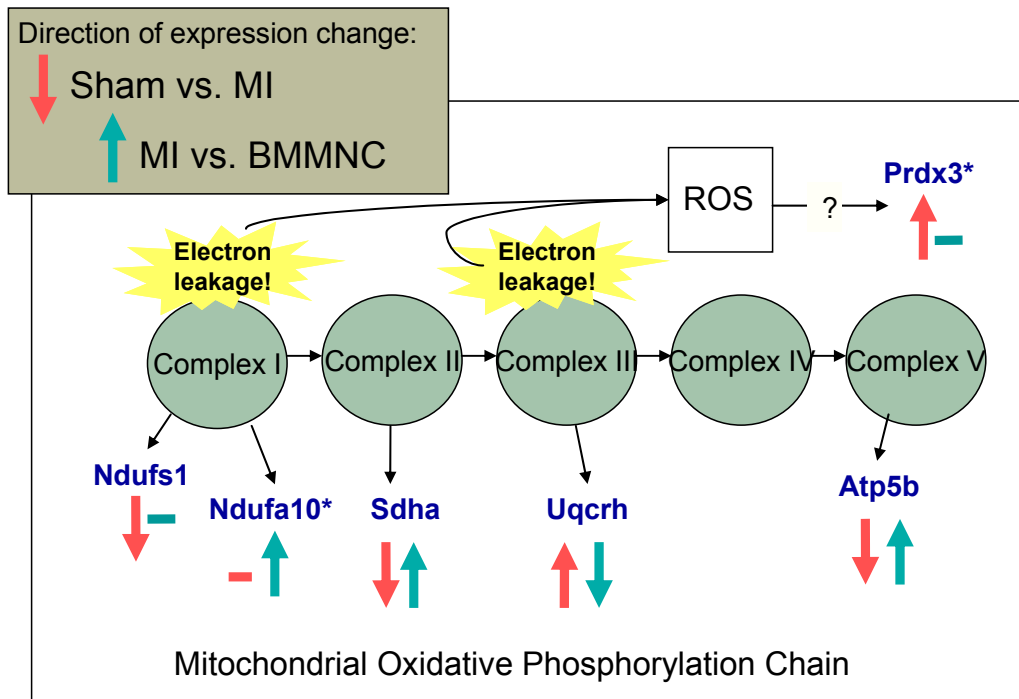
NADH dehydrogenase is a very large protein complex and the functions of all 45 different subunits are still not fully understood. It is clear from our results and others that I/R affects this complex but there may be a variation in the reaction of different subunits to I/R. The difference between the changes we observed for Ndufa10 and those observed by Kim et al (2006) may be related to differences in the model or we may have measured different variants, there is no information on observed *Mr* and *pI* in their dataset to check this.

The flavoprotein subunit of succinate dehydrogenase (Sdha) which is complex II of the oxidative phosphorylation chain was found to be down-regulated in Sham vs. MI and was subsequently up-regulated in MI vs. BMMNC in our study. This complex has only four subunits and has not been identified in any of the proteomic analyses of I/R.

Complex III (ubiquinone-cytochrome b-c1 oxidoreductase) has 11 different subunits [149]. One of these were identified in our study as being differentially regulated; cytochrome b-c1 complex, subunit 6 (Uqcrh). Uqcrh was found to be up-regulated in Sham vs. MI and down-regulated in MI vs. BMMNC . Uqcrfs1 (rieske subunit of cytochrome b-c1 complex) was identified in an isolated rabbit heart model of I/R, in this study it was found to be down-regulated in I/R but unchanged in IPC [91]. Cytochrome b-c1 complex, core protein 1 (Uqcrc1) has previously been shown to be up-regulated in I/R and down-regulated in after treatment with MPG [90]. Our data and that of others suggests the Complex III subunits may react to I/R in different ways, as was seen with Complex I subunits.

ATP synthase is often referred to as complex V of the oxidative phosphorylation chain. The β subunit (Atp5b) was identified in our study in 17 different spots, these showed Atp5b to be down-regulated in Sham vs. MI and up-regulated in MI vs. BMMNC. The Atp5 β Western blot shown in figure 4.10 suggests that fragments of Atp5 β are present in all of the test groups. The fainter bands in the MI may indicate that there is less Atp5 β in the I/R injured tissue possibly due to further degradation. The higher mass band representing the full length protein (~56kDa) was too overexposed to see differences between the groups. Atp5b was identified in a previous proteomic analysis of a hepatic I/R injury mouse model as being down-regulated by I/R and subsequently up-regulated by IPC [150].

Figure 8.1 Mitochondrial oxidative phosphorylation chain Proteins found to differ in our studies are indicated in blue, significant changes are indicated by salmon and teal arrows Sham vs. MI. * indicated that the native protein was identified. NADH-ubiquinone oxidoreductase 75 kDa subunit (Ndufs1), NADH dehydrogenase [ubiquinone] 1 alpha subcomplex subunit 10 (Ndufa10), succinate dehydrogenase [ubiquinone] flavoprotein subunit (Sdha), cytochrome b-c1 complex subunit 6 (Uqcrh), ATP synthase subunit β (Atp5b), thioredoxin-dependent peroxide reductase (Prdx3).



In general, there appears to be some overlap in the proteomic alterations that occur in I/R injury across species and across models whether it is in-vivo, ex-vivo or even in different organs (liver). Alterations in the expression of these proteins, especially the different regulation seen in different subunits of the larger complexes, suggest disarray of oxidative phosphorylation enzymes which would lead to mitochondrial dysfunction. Mitochondrial dysfunction is a well characterised aspect of I/R injury, the mitochondria are known to play an important role in the intrinsic mechanism of apoptosis. Our data reveals a recovery or even an increase in expression levels of mitochondrial oxidative phosphorylation proteins after BMMNC treatment suggests the mitochondria have been protected from I/R damage and have been able to recover

function. As mitochondrial damage is closely linked to apoptosis, there is evidence that protection of mitochondria inhibits the progression of apoptosis [151].

8.1.2 Antioxidant proteins

The cytoplasmic antioxidant, peroxiredoxin-6 (Prdx6) was found to be down-regulated in I/R and up-regulated in treatment in our model. A lower *pI* version of thioredoxin-dependant peroxide reductase (Prdx3), which is a mitochondrion specific antioxidant, was found to be up-regulated after I/R injury and remained unchanged from this in the treatment group. Prdx3 is illustrated in Figure 8.1, these data may be further evidence that changes to proteins in the mitochondrial oxidative phosphorylation chain result in increased production of reactive oxygen species (ROS). ROS would cause further damage to mitochondrial function by inactivating NADH dehydrogenase, NADH oxidase, succinate dehydrogenase and ATP synthase [152]. Nonn et al (2003) found that Prdx3-transfected cells showed resistance to hypoxia-induced ROS formation and resistance to apoptosis [153]. Prdx3 may be part of an innate cellular mechanism to protect mitochondria from ROS-induced damage during ischemia.

Prdx3 and Prdx6 have both been identified in other 2DE studies looking at I/R injury. Prdx6 was found to be up-regulated after ischemia but down-regulated after I/R in an isolated rat heart model [93]. Prdx6 was up-regulated in both stunned and injured myocardium after reperfusion in an isolated rabbit heart model, but down-regulated after treatment with oxygen free radical scavenger MPG [89, 90]. In the same model, Prdx3 was observed to be down-regulated in both stunned and injured myocardium and up-regulated after treatment with MPG [89, 90]. These conflicting results may be explained by the presence of different *pI* variants of these proteins (i.e a shift from one *pI* to another) as observed by Cullingford et al (2006). Peroxiredoxins and heat shock proteins were found to be altered in response to oxidative stress in neonatal rat cardiomyocytes. Both acidic and basic forms of Prdx3 and Prdx6 were identified as well as several other forms. The acidic forms of both of

these proteins were up-regulated by oxidative stress whereas the basic forms were down-regulated and this shift to a more acidic form is suggested to be super-oxidation of cysteine-residues [154]. The *pI* of Prdx6 identified in our proteomic analysis suggests this is a basic isoform and Prdx3 is more acidic than theoretical, which may explain why the two antioxidants are seen to be regulated differently.

8.1.3 Energy metabolism proteins

Various energy metabolism proteins were also affected by I/R in our model. Cellular energy metabolism is known to be seriously affected during ischemia and reperfusion. Cardiac substrate preference under normal conditions is a mixture of glycolysis, glucose oxidation and free fatty acids. This is altered during ischemia, in part due to a reduction in phosphocreatine and ATP, which results in an increase in fatty acid metabolism and a reduction in glucose oxidation. The outcome of this is an increase in lactic acid and faster consumption of oxygen, and eventually loss of cellular function [151].

Energy substrate metabolism enzymes have been identified in several previous 2DE analyses of I/R injury. Dihydrolipoyllysine-residue acetyltransferase component of pyruvate dehydrogenase complex (Dlat) was found to be up-regulated in Sham vs. MI, and down-regulated in MI vs. BMMNC in our study. Pyruvate dehydrogenase was also found to be up-regulated after I/R in two different studies using isolated rabbit hearts [89, 91] this change was reversed in IPC [91]. However, other studies have seen changes in energy metabolism enzymes which differ from our results. In our study lactate dehydrogenase was found to be down-regulated in two different spots in Sham vs. MI. Lactate dehydrogenase was however up-regulated in I/R (1 hour ischemia and 1 hour reperfusion) in isolated rabbit hearts, but was unchanged after 15 minutes ischemia and 1 hour reperfusion [89].

In our study, Enoyl-CoA hydratase was up-regulated in Sham vs. MI and down-regulated in MI vs. BMMNC. This protein however has been found to be down-

regulated after 30 minutes ischemia and 2h reperfusion in isolated rabbit hearts and the expression change was corrected after IPC [91].

The differences in protein expression results between our study and others for these proteins may be due to the differences in study designs. For example, differences in the species used, differences in the type of model used (i.e. regional ischemia initiated by coronary artery ligation in our model vs. global ischemia simulated by anoxia, achieved by substitution of nitrogen for oxygen in the perfusate in Kim et al (2006) [91], and the timings used for ischemia and reperfusion (i.e. 25 minutes ischemia followed by 6 hours reperfusion in our model, whereas reperfusion was only 1-2 hours in the other studies). Cardiac substrate preference is quite dynamic over the course of ischemia and reperfusion so differences in the timings of the experiments would lead to different results in terms of the regulation of energy metabolism proteins that would be recorded. There are also important differences between anoxia and ischemia models. In ischemia (especially in-vivo) a lack of circulation would lead to poor supply and clearance of metabolites in the infarct, whereas isolated perfused hearts in which oxygen removal is the only variable, metabolites can still be cleared. Perfusate is also different from blood in what it brings to the myocardium in terms of energy substrates.

Metabolic pathways for different substrates overlap and are also further complicated by the alternative use of amino acids and ketone bodies as metabolites [155]. The few proteins we have observed as changing in our model do not give a definitive picture of what alterations are occurring in the system, only evidence that the systems are being perturbed.

8.1.4 Heat shock proteins

Various heat shock proteins (Hsp) were also found to be differentially expressed in our study. Both Hspa9 and Hspb8 were down-regulated. Previous studies have also identified various heat shock proteins to be differentially expressed. White et al

(2005) found several spots containing Hsps in an isolated rabbit heart model of I/R. They had two different I/R timings, as described before (15 minutes ischemia / 60 minutes reperfusion [stunned] and 60 minutes ischemia / 60 minutes reperfusion [infarct]), they also sub-fractionated the protein sample and ran separate 2DE analyses on whole tissue extracts, a myofilament enriched fraction and a cytosolic enriched fraction. Hsp27kDa (Hspb1) was identified in one spot in both whole and cytosolic fractions and was up-regulated in both fractions in both models. Hsp 70kDa (Hspa9) was identified in two spots in the whole tissue extract and although one Hspa9 spot was up-regulated in both models, the other was down-regulated in both models [89]. Although Hspa9 was found to be up-regulated back to sham levels in MI vs. BMMNC in our study, Hspb8 expression were unaffected, suggesting the mechanism of cardioprotection in BMMNC's may not involve heat shock proteins. However, in light of the varying results seen in the paper by White and colleagues, there should be a more detailed study of the behaviour of these proteins before their actions could be ruled out.

8.2 Candidate proteins for involvement in BMMNC afforded cardioprotection

One protein, 14-3-3 epsilon is a very good candidate for being directly involved in the cardioprotection afforded by treatment with BMMNCs. Expression changes in this protein were confirmed by Western blotting. 14-3-3 proteins are highly conserved molecular chaperones with more than 200 different client species [156]. They bind to phosphorylated serine or threonine motifs and thereby mediate many different signal transduction pathways [156]. There are seven mammalian isoforms in the 14-3-3 protein family including β , γ , ϵ , η , σ , τ and ζ plus α and δ which are phosphorylated forms of β and ζ [157]. Much of the research to date in the literature on 14-3-3 proteins does not specify the isoform under investigation and although 14-3-3 epsilon is suggested to have early evolutionary divergence from the other members of the family, an analysis of substrate specificities indicates a high level of overlap between the binding motifs recognised by the different isoforms [157, 158]. This suggests that many functions will be common to several isoforms.

One of the well documented functions of 14-3-3 proteins is the promotion of cell survival through the inhibition of several apoptotic pathways [145]. 14-3-3 proteins are specifically known to be involved in cell survival signalling via their interaction with the B-cell lymphoma (BCL-2) protein Bad. In fact all of the mammalian isoforms bind and inhibit Bad [159]. The BCL-2 family of proteins comprises a core of ~12 proteins split into three classes, namely class I, class II and BH3-only. All are highly involved in the control of the mitochondrial apoptosis pathway, otherwise referred to as the intrinsic apoptotic pathway. Class I includes Bcl-xL and Bcl-2 and these inhibit apoptosis. Class II members promote apoptosis and include Bax and Bak among others. The BH3-only group contain a BH3 domain and includes Bad. The BH3-only members can bind the anti-apoptotic Class I members thereby promoting apoptosis [160].

Phosphorylation of serine 136 and serine 112 in the Bad protein creates a binding motif for 14-3-3 and subsequent binding leads to improved accessibility of serine 155

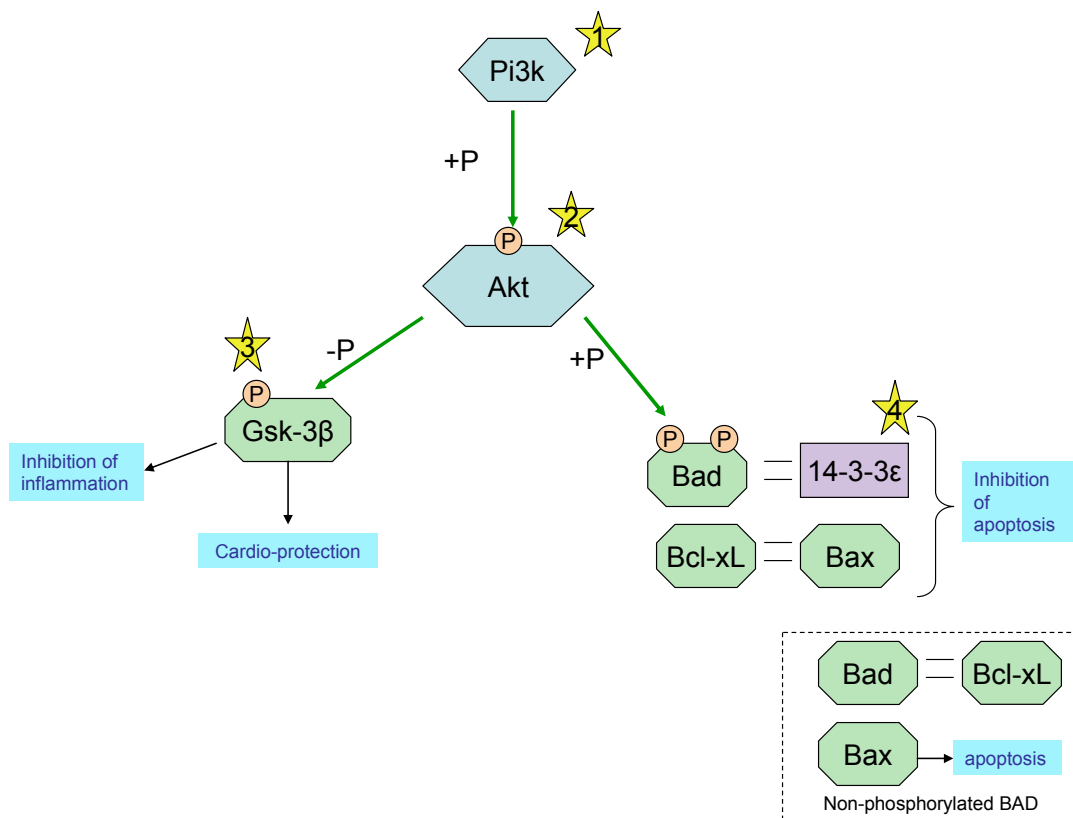
(in the BH3 domain of Bad). Serine 155 is then phosphorylated by protein kinase A (PKA). Phosphorylation of serine 155 by PKA disrupts the interaction of Bad and Bcl-xL causing Bcl-xL to be released to bind preferentially to the BH3 domain of Bax inhibiting the pro-apoptotic function of this member of the BCL-2 family [161-163]. Therefore the phosphorylation state of Bad appears to be important in regulating mitochondrial apoptosis in conjunction with its interaction with 14-3-3.

Akt is thought to be the agent responsible for phosphorylation of Bad at serine 136 and therefore, the Pi3k/Akt pathway is thought to be involved in initiating the suppression of this otherwise pro-apoptotic pathway [146, 147]. The serine/threonine kinases Rsk-1 causes phosphorylation of Bad at serine 112 in response to protein kinase C activation [164]. Calcineurin has been shown to dephosphorylate Bad causing it to dissociate with 14-3-3 and thereby induce apoptosis [165]. Several studies have also shown that Jnk1/2 works in opposition to Akt in apoptosis signaling by interfering with Bad/14-3-3 binding. Jnk1/2 phosphorylates serine 128 in Bad causing dissociation from 14-3-3, part of the pro-survival actions of Akt may be suppression of Jnk1/2 as well as its own direct actions on the phosphorylation state of Bad [166]. Interestingly Caspase-3, which is activated by the pro-apoptotic Class I BCL-2 proteins through cytochrome c release from leaking mitochondria, has been shown to cleave 14-3-3 ϵ and prevent its interaction with Bad thereby further promoting apoptosis [167]. Many of these kinase pathways are known to be involved in cardioprotection.

The candidacy of 14-3-3 ϵ in cardioprotection is also supported by additional studies in the rat model developed as part of this programme of studies. Western blot analysis of Akt (which is thought to be involved in IPC induced cardioprotection) showed that BMMNC treatment led to phosphorylation of serine 473 of Akt, and this activation was abolished by treatment with the Pi3k inhibitor LY294002 (see section 1.4). The anti-apoptotic effect of 14-3-3 would be dependant on Akt being activated and phosphorylating Bad. Phosphorylated Bad would then be bound to 14-3-3 leaving Bcl-xL to bind and sequester pro-apoptotic Bax (see Figure 8.2).

Further Western blotting showed inhibition of Gsk-3 β was initiated through the phosphorylation of serine 9 in the BMMNC group (also shown in Figure 8.2). Gsk-3 β inhibition through phosphorylation of serine 9 is thought to be pro-survival and there are several kinases which may initiate this phosphorylation including Akt [168].

Figure 8.2 Signalling pathway potentially triggered by BMMNC treatment: Evidence from our model Stars indicate evidence from Western blotting and proteomics data produced in our programme of studies. Akt has been shown to be phosphorylated (activated) by BMMNC and appears to be Pi3k dependant (star 1 and 2). Gsk-3 β has also been shown to be phosphorylated (inactivated) by treatment (star 3). 14-3-3 ϵ was shown to be one of the up-regulated proteins in the treatment group (star 4). +P = activated through phosphorylation, -P = inactivated through phosphorylation.



Western blotting experiments to compare the two different batches of rat myocardial samples (samples 1-9 and 10-18) showed similar patterns of expression, however a striking difference was the 3-fold reduction in 14-3-3 ϵ observed in Sham vs. MI in samples 1-9 that was not observed in samples 10-18. However, up-regulation of 14-3-3 ϵ was observed in MI vs. BMMNC in both sample sets. This may indicate a level of experimental variation between batches, which may be expected as they were produced at different time points. However, there is certainly similarity in the expression patterns, especially in MI vs. BMMNC. This comparison is where we might expect to find changes which may indicate mechanistic action of BMMNC treatment.

In our preliminary investigations of 14-3-3 ϵ and Bad we were able to show that overall protein expression of Bad was reduced in I/R injury and significantly increased \sim 3 fold after BMMNC treatment. However, we were unable to measure phosphorylation of serine 136 in Bad which would have indicated whether it was in a configuration conducive to 14-3-3 binding.

To look at which proteins were interacting with 14-3-3 ϵ in our samples, a pull-down assay was performed using his-tagged 14-3-3 ϵ as bait and protein lysate (treated with phosphatase inhibitors to preserve phosphorylated motifs) as prey. A preliminary pull-down experiment revealed two different subunits of ATP synthase to bind. ATP synthase subunit β (Atp5b) has a known 14-3-3 binding motif and has previously been shown to bind with 14-3-3 in an affinity chromatography assay using protein extracts from HeLa cells [169]. Several other studies also note an interaction of 14-3-3 proteins and ATP synthase in plants [170, 171]. A phosphorylation dependant interaction between ATP synthase and 14-3-3 may also be anti-apoptotic [172]. Atp5b was identified as a differentially regulated protein in our study, being significantly down-regulated in Sham vs. MI and significantly up-regulated in MI vs. BMMNC. ATP synthase subunit e (Atp5i) is part of the membrane bound F₀ complex of ATP synthase. Very little is known about the functional capacity of this subunit. It is known to be important for maintaining dimerisation and oligomerisation

of mitochondrial F_1F_0 , which may be important in maintaining mitochondrial cristae structure [173]. Subunit e may have been pulled-down in a complex with the β subunit, rather than due to a direct interaction with 14-3-3 ϵ .

8.3 Limitations of 2DE proteome analysis

Due to variation in biological systems, a reasonable number of replicates are usually required to obtain statistically significant results; an 'n' of three is the absolute minimum from which any meaningful data can be obtained but larger 'n' is required as variation increases and the size of the difference you want to detect decreases. The pattern of expression change of four proteins (14-3-3ε, Sdha, Pepb1 and Atp5b) observed in the 2DE analysis was confirmed by Western blotting. However, the exact fold change values observed by profiling were not always validated, illustrating that 2DE results must be confirmed before any firm conclusions can be made. The low number of replicates in our study makes verification of results even more pressing.

A common method for highlighting spots with a significant difference between groups is to use a simple statistical test. We took a spot-by-spot approach, meaning we looked at data from each spot separately, not taking into account the entire dataset when considering whether a spot was significantly different between groups [174]. This approach negated the need to perform correction for multiple testing, which aims to lower the false discovery rate which is increased in proportion to the number of tests performed. Most methods of correction would lower the p-value threshold for significant data by a large margin, especially as many 2DE analyses include 1-2000 spots. This in all likelihood would result in very little significant data and overcorrection will increase the false negative rate. There has been no consensus on the best way to analyse a 2DE datasets. With so few samples, it is impossible to check for 'normal' distribution so the decision to use parametric or non-parametric test is not a simple one. A t-test will compare the means of each of the two groups that are to be compared and will look for statistical differences based upon the ratio of the difference and the standard error of the difference [175]. As our comparisons were between two groups of independent samples the student's t-test is an appropriate tool. However, it could be argued that a non-parametric test such as the Mann Whitney U test which also compares two independent groups but which does not

assume the data is normally distributed should be used in this analysis. The Mann Whitney test looks at the scale of the difference between groups and does not take standard error into account [175]. However with a low number of replicates, the power of the Mann Whitney U test may be reduced [174, 176]. Both Student's t-test and Mann Whitney U tests were performed on the spot intensity data and the two tests were found to produce a very similar list of significantly altered spots. The Student's t-test was chosen to present in this thesis and a p-value of <0.05 was taken as being significant. We also used a fold-change cut-off as 1.5 as differences below this value are often thought of as being the limit of changes detectable by 2DE. However it must be noted that using a fold change cut-off will lead to some significant findings being overlooked. In the case of the wide-range analysis, a large number of spots passed the criteria of having a p-value <0.05 and being >1.5 fold change difference between groups. For this analysis we chose a cut-off value of 2.5 fold change to highlight the most interesting spots to prioritise for protein identification. Both of the narrow-range analyses produced much smaller numbers of spots with p-value <0.05 and >1.5 fold change difference, therefore all of these spots were taken forward for analysis. There is as yet no gold-standard statistical analysis for 2DE data, which is another reason why it is important to validate findings with a different technique such as Western blotting.

Comparative 2DE gels give a window onto the proteome but this window is limited to the range of proteins which are solubilised in the buffers used for protein sample preparation, and are sufficiently resolved within the 2DE gels (across the pH range of the IPG strip and across the length of the second dimension gel). In this study we only had the potential to observe proteins in the range of pH4-7 and then only those which were solubilised and well focussed in the 2DE gels. This would have also excluded any proteins with very low abundance and particularly hydrophobic proteins which are also difficult to visualise using 2DE and would be under-represented. Another limitation to the amount of the proteome observed in 2DE experiments comes as a consequence of variability between gels. For example, spots can be missing from one gel but well resolved in another for technical reasons rather than

biological ones, and regions of the gels may migrate differently (warping) which leads to difficulties in matching spots across the gels. If there is any doubt as to the appropriate matching of spots, then these spots should be excluded from analysis.

There are several ways to maximise the amount of proteome visualised using 2DE. These include sub-fractionating the protein sample, based on solubility or on subcellular compartmentalisation. Running separate 2DE analyses on the different fractions will allow a larger portion of the proteome to be visualised. The use of fractionation on the basis of subcellular compartmentalisation may also reveal translocation of various proteins in response to the experimental conditions.

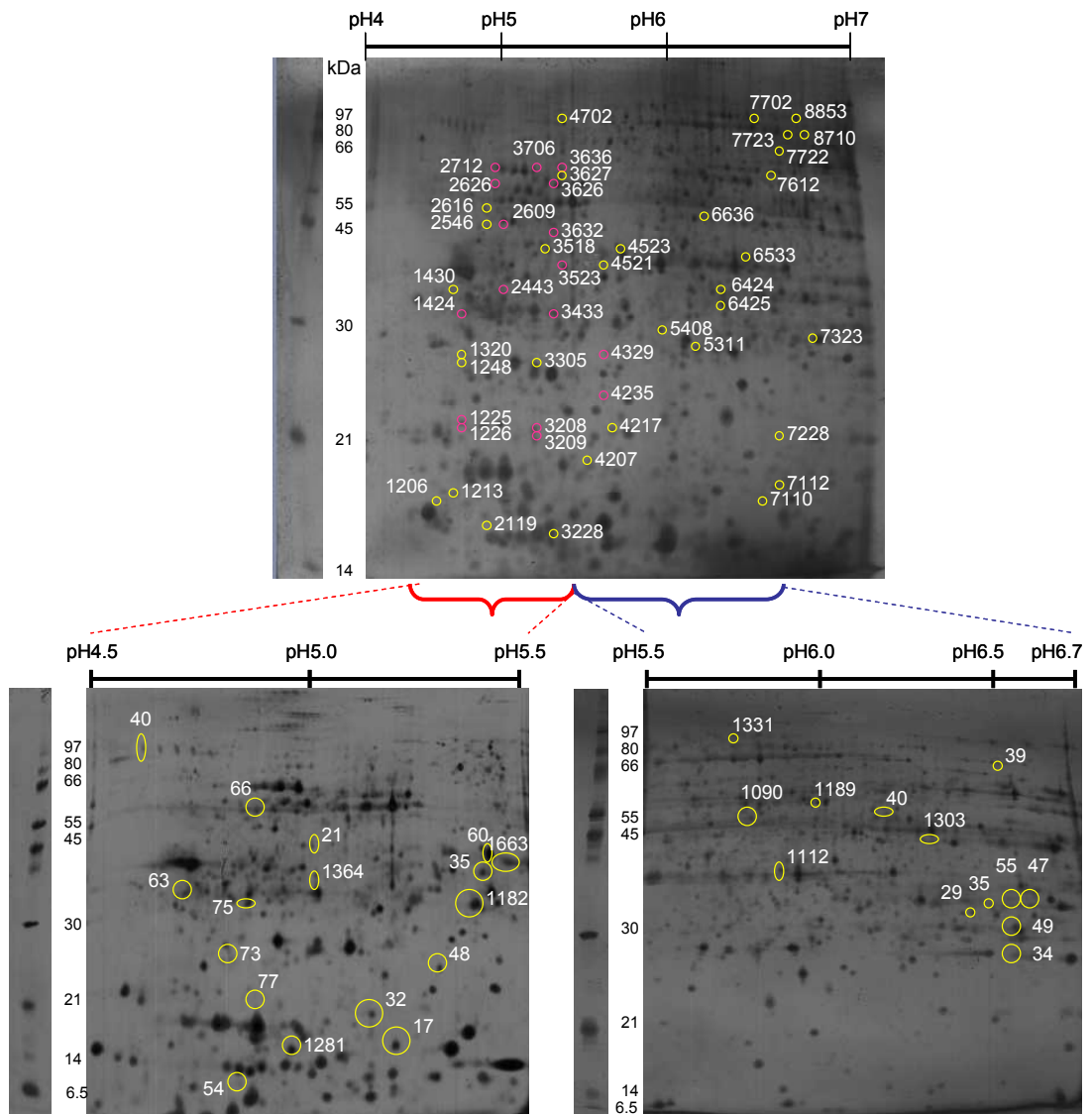
To increase the proportion of the proteome we could analyse in this study, two narrow-range analyses were performed. These two pH ranges in the wide-range gels were dense with spots and in some cases spots were too dense to be matched and analysed with confidence. High density of separated spots also causes many spots to yield more than one protein identification, in these cases, no conclusions can be drawn from the spot intensity data. By stretching both of these pH ranges over a larger area it was hoped that better separation could be achieved and some new proteins would be identified that had not been identified in the wide-range analysis.

Five proteins were identified in the narrow-range analyses that were already picked up by the wide-range analysis; these were ATP synthase subunit beta, stress 70 protein, actin, myosin-6 and tropomyosin. A further 14 different proteins were identified in the narrow-range analyses. The effect of improved resolution in these pH ranges is illustrated in Figure 8.3, which shows examples of our 2DE gels from the wide-range analysis and both of the narrow-range analyses.

Another 2DE method which addresses the issues of gel to gel variability, especially in regards to variations in the running pattern of spots, is difference gel electrophoresis (DIGE). DIGE employs the use of fluorescent dyes to differentially label two samples which can then be separated on the same gel [177]. A sample from each

group is stained with a different fluorescent dye, pooled and then run together, proteins co-migrate enabling improved matching [178]. Additionally there is an option to use an internal control, which is made up from an equal portion of all samples stained with a third fluorescent dye and also run on the same gel. The internal control should contain all of the protein species present in the different samples and further improve matching [179].

Figure 8.3 Example wide- and narrow-range gel images The top image is an example of a pH 4-7 gel image with the positions of identified proteins marked. Pink circles indicate spots identified as ATP synthase beta, all other proteins labelled in yellow. The two lower images show examples of the narrow-range gel images. A pH 4.5-5.5 gel image is on the left and a pH 5.5-6.7 gel image is on the right. Positions of identified proteins marked with circles. The pH range is indicated on the top of the gel images and the M_r is labelled on the left in kDa.



8.4 Gene expression changes in I/R and after treatment with BMMNCs

There were numerous genes altered in Sham vs. MI (>1500), 44% of which were down-regulated and 56% were up-regulated. Very few genes were altered in MI vs. BMMNC (20). Many of the genes which were observed to be altered in regulation in Sham vs. MI, have a function related to inflammatory response, integrin signalling and cytokine chemokine signalling. Platelet derived growth factor (PDGF) signalling and transforming growth factor β (TGF- β) signalling were also strongly represented. As with the proteomic data, the 6 hour timescale must be considered as quite an early timepoint to observe changes in gene expression regulation within the existing cell population of the myocardial tissue.

In the I/R damaged myocardial sample we expect the actual area of infarct to be made up of dead and dying cardiomyocytes and damaged extracellular matrix (ECM) as opposed to healthy myocardium made up of healthy cardiomyocytes and intact ECM. The dead and dying cardiomyocytes will trigger an inflammatory response. There is also likely to be an activation of cardiac fibroblasts (which make up ~90% of the remaining myocardial cell population) which are responsible for regulation of the ECM [180]. Although many fibroblasts are likely to be damaged and subjected to I/R induced cell death along with the cardiomyocytes, they are probably a little more hardy to I/R induced damage as they have much lower energy requirements. Although, there was no histological evidence of tissue composition of the samples used for these proteomic and gene expression analysis.

In the early stages of response to I/R injury activated cardiac fibroblasts induce the degradation of ECM through increased expression of matrix metalloproteinases (MMPs) [181]. The MMPs 8, 9 and 3 were found to be elevated in expression as well as tissue inhibitor of metalloproteinase (TIMP1) in Sham vs. MI. Interleukin 1 beta (IL-1 β), IL-1 receptor type I and II and IL-1 receptor agonists as well as tumour necrosis factor (TNF) receptors were also found to be increased in expression in I/R injury. IL-1 β can stimulate increased expression of MMP9 and 3 and this is

augmented by TNF α via p38 MAPK signalling [182]. Induction of MMP9 expression by IL-1 β may also be through impaired iNOS function and via NF- κ B activation [183]. These genes reflect the known initial stages of fibroblast response to injury.

Of the genes found to be altered in Sham vs. MI, many were associated with inflammation and with apoptosis signalling, both cellular responses which make biological sense in relation to the phenotype, indicating that the analysis was reasonably successful at identifying genes changing in Sham vs. MI. A large number of the genes and gene families we identified as differing in Sham vs. MI have also been found to differ in other gene expression analyses of I/R injured tissue.

Gabrielson et al (2007) compared gene expression profiles after an acute ischemic episode in healthy myocardial biopsies and chronic ischemic biopsies taken from patients undergoing bypass surgery using Affymetrix HG_U133 A Genechip[®] arrays. They found several genes to be up-regulated by acute ischemia in the chronic ischemia samples compared to normal, many of these genes were also identified as being up-regulated in this analysis. These included; a disintegrin-like and metallopeptidase (reprolysin type) with thrombospondin type 1 motif 1 (Adamts1), activating transcription factor 3 (Atf3), chemokine (C-C motif) ligand 2 (Ccl2), Ccl3, dual specificity phosphatase 1 (Dusp1), Dusp5, early growth response 1 (Egr1), Egr2, FBJ murine osteosarcoma viral oncogene homolog (Fos), growth arrest and DNA-damage-inducible 45 beta (Gadd45b), Gadd45g, matrix metalloproteinase 9 (Mmp9), myelocytomatosis viral oncogene homolog (Myc), nuclear receptor subfamily 4, group A, member 3 (Nr4a3), and S100 calcium binding protein A8 (calgranulin A) (S100a8) [184]. Gabrielsen and colleagues also found various subunits of NADH dehydrogenase (ubiquinone) to be down-regulated in the acute ischemic episode in their study [184]. Several NADH dehydrogenase subunits were also identified as being down-regulated in our dataset. Some of the cytokines, chemokines and adhesion molecules identified by Ip et al (2007) as being differentially regulated by ischemia in a mouse model were also identified in our analysis. These included;

Adamts1, Ccl2, Ccl6, Ccl7, Ccr1, chemokine (C-X-C motif) ligand 2 (Cxcl2), interleukin 1 receptor type II (Il1r2), interleukin 1 receptor antagonist transcript variant 1 (Il1rn), Mmp8, plasminogen activator, tissue (Plat), plasminogen activator, urokinase (Plau), and tissue inhibitor of metalloproteinase 1 (Timp1) [103].

The 20 genes found to be altered in MI vs BMMNC were nearly all down regulated (with the exception of calsequestrin 2). No particular pathway was highlighted by this list of genes as shown by the bioinformatic analyses, but there are several functionally interesting genes in the list. Apoptosis inducing serine/threonine kinase 17 beta (Stk17b) or DRAK2, was found to be down-regulated and is thought to be a positive regulator of apoptosis [185]. One candidate responsible for negative regulation of this gene may be Cyclooxygenase-2 (COX-2) [186]. Expression of COX-2 is known to be upregulated in the preconditioned heart and this may be initiated through Janus tyrosine kinase/signal transducers and activators of transcription (Jak/Stat) signalling, however the activity of COX-2 appears to be linked to inducible nitric oxide synthase (iNOS) production of NO [187, 188]. 2' 5' oligoadenylate synthetases are a family of interferon inducible enzymes which block protein synthesis (by causing mRNA degradation) as a response to infection. Oas1k is homologous to human OAS3 (100kDa) isoform which is known to form dimers of 2'-5' linked oligomers of adenosine and these are not thought to be capable of activating RNase L and therefore OAS3 is unlikely to have the same functionality as OAS1 and OAS2 [189]. Analogues of dimeric 2'-5' adenosine however have been shown to regulate gene expression and DNA replication through inhibition of DNA topoisomerase I [190]. Rebouillat et al (2006) found expression of OAS3 caused human cells to be sensitive to apoptosis initiated by caspase-9 activation, and downstream cleavage of caspase-3 and Poly (ADP-ribose) polymerase (PARP) [191]. Down-regulation of this gene could also give some resistance to apoptosis.

Expression of Edg6, a sphingosine-1-phosphate receptor specifically expressed in lymphoid tissue and thought to be involved in lymphocyte trafficking, has been shown to be indirectly controlled by Pi3k through the transcription factor FOXO1 in

T-cells and hence the down-regulation of Edg6 in the treated group may be a consequence of parallel Pi3k signalling [192, 193]. Sema4a is a class 4 semaphorin and also appears to have a role in inflammatory responses. It is expressed on both B-cells and dendritic cells, and is involved in T-cell activation [194]. Sema4a has previously been shown to be involved in autoimmune myocarditis and autoimmune encephalomyelitis through regulation of T-cell differentiation [195, 196]. An anti-angiogenic action of Sema4a in endothelial cells has been shown to be mediated through negative regulation of vascular endothelial growth factor (VEGF) signalling [197]. Down-regulation of Sema4a would therefore allow enhanced endothelial cell migration and vascular genesis. Dok-3 which is expressed on B-cells and macrophages is thought to be involved in negative regulation of B-cell activation [198, 199].

These genes, although not apparently in the same signalling network as far as current evidence shows, all appear to be expressed and involved in the regulation of lymphocytes and may suggest a modulation of the adaptive immune response in treated myocardium which may be linked to apoptosis resistance. These results provide many different interactions of interest to be explored in future work.

Three genes were followed up for QPCR validation; sema domain immunoglobulin domain (Ig) transmembrane domain (TM) and short cytoplasmic domain (semaphorin) 4A (Sema4a), 2' -5' oligoadenylate synthetase 1K (Oas1k) and IQ motif containing GTPase activating protein 1 (Iqgap1). Sema4a was found to be the most highly significantly altered gene in both the Sham vs. MI and the MI vs. BMMNC comparisons. There was a 2.25 log fold-change in Sham vs. MI (adjusted p-value of 2.72e-9) and a -1.3 log fold change in MI vs. BMMNC (adjusted p-value of 0.007). The QPCR results for this gene also showed up-regulation after I/R and a subsequent down-regulation in BMMNC, although these changes were not found to be statistically significant. Oas1k was the second most highly significantly altered gene in both the Sham vs. MI and the MI vs. BMMNC comparisons. There was a 2.57 log fold-change in Sham vs. MI (adjusted p-value of 6.05e-9) and a -1.6 log fold

change in MI vs. BMMNC (adjusted p-value of 0.007). The QPCR data for this gene showed an up-regulation in I/R, which did not reach statistical significance and no change was seen after BMMNC. This gene was also measured by QPCR in samples 10-18, these results showed an up-regulation in I/R, which reached statistical significance ($p = 0.026$) and a down-regulation in BMMNC, which did not reach significance. *Iqgap1* had a modest but statistically significant up-regulation in Sham vs. MI (log fold change of 0.41 and an adjusted p-value of 0.022) and was included in the QPCR analysis to see if we could validate less significant differences. The QPCR results for this gene showed a modest non-statistically significant up-regulation in I/R and no change in BMMNC.

The QPCR results for all three genes, in general, reflected the results observed in the RatRef12 chip analysis. Statistical significance however, was only reached in the Sham vs. MI comparison for *Oas1k* in tissue samples 10-18. There were amplification failures for some samples in these analyses and it is clear that RNA quality can be compromised during the process of finely grinding the sample to allow improved sampling. Combined with low numbers of replicates, these factors are most likely to be responsible for the large error bars seen in the QPCR results which may account for the lack of statistically significant changes between groups.

There was some overlap in the gene expression dataset and the proteomics data; subunits d and h of ATP synthase were found in the gene expression dataset (beta subunit in the proteomics dataset), Actin, Acads, Creatine kinase, Galectin 5, *Pepb1* and *Cap1* as well as different subunits of succinate dehydrogenase and lactate dehydrogenase were all identified in both datasets. In many instances, the same direction of change was seen in both datasets. *Cap1* was identified as being down regulated in the proteomics data (Sham vs. MI) but gene expression was up-regulated. The simplistic view of down-regulation in the proteomics dataset may be misleading as the *Cap1* protein may have been modified rather than down-regulated in expression. Due to such modifications and the dynamic relations between an mRNA being expressed, a protein being translated, processed and modified, as well as the

technical limitations inherent in comparative proteomics as mentioned previously, there will not always be a direct relationship between mRNA content and proteins observed in a 2DE analysis. Different nomenclature can also make the task of comparing two datasets difficult.

There were very few gene expression changes in MI vs. BMMNC, and both the p-values and fold changes for these few results were more modest than those seen in the Sham vs. MI data. The QPCR validation as mentioned above was also weak for the MI vs. BMMNC differences. The lack of differentially expressed genes observed in the BMMNC group in our study indicates that myocardial restoration may be achieved through mechanisms not relying on gene expression, which would favour the theory of a paracrine mechanism being important or it may be a consequence of the 6 hour timepoint used in this study. It would be preferable to confirm these findings using a larger number of experimental replicates also using a different platform for the gene expression chip analysis (for example Affymetrix, US). Measuring gene expression at a later timepoint or possibly a performing a time-series investigation would be of interest.

8.5 Bioinformatic analysis of proteomic and gene expression datasets

Global proteomic and gene expression analyses similar to the ones presented here result in large lists of proteins and genes which are potentially involved in producing the phenotype under scrutiny. To obtain biological meaning from these lists, a literature search on each protein could be performed to ascertain individual functions, this process however is very time consuming. Most proteins or genes act in concert, and indeed can have different actions depending on cellular location and interactors. There are now several bioinformatic tools which will look for over-representation of functions, or pathways within a list of proteins. The information gathered using these tools can be used to prioritise any further investigation. In the case of our gene and protein datasets, some general functional groupings were revealed to be affected in our study, such as oxidative phosphorylation, apoptosis and inflammation.

Overall, there was little in the way of key findings which implicated a mechanism for the actions of BMMNCs in our bioinformatic analyses. This may be due to a relatively small size of the proteomic dataset (which is in part due to the restricted view of the proteome we are able to access using 2DE), and the even smaller list of genes affected in MI vs. BMMNC. As the effects of BMMNCs appear to be mediated not through transcriptional activation, but through activation and mobilisation of the existing protein populations, bioinformatics results from the proteomic data may be more likely to contain clues to the mechanism.

8.6 Conclusions

BMMNC therapy in our model was shown to considerably reduce infarct size (through reduced apoptosis and necrosis) to an extent comparable to that achieved through IPC and this correlated with improved cardiac function. Survival kinase signalling pathways (Pi3k/Akt and Gsk-3 β) known to be affected in IPC were also shown to be affected by BMMNC in our study. The proteomic and gene expression data presented here have revealed many I/R induced changes which are in agreement with what is currently understood about I/R injury, and this indicates the validity of our data. The proteomic data also shows that many I/R induced protein alterations are corrected by BMMNC therapy, this also reflects the results from other 2DE analysis looking at IPC and pharmacological preconditioning in rodent models. Myocardial restoration by BMMNC was not associated with many alterations in gene expression, which may be evidence of a mechanism which relies on modification and mobilisation of the existing protein population, possibly in response to a paracrine signal. However, differential regulation in a few genes with potentially interesting functional parallels in B-cell and T-cell regulation as well as apoptosis resistance is worthy of further investigation.

Knowledge of the signalling cascades which are activated by the paracrine signal may narrow down the possible identity of the signal itself. However, when considering the possible source for this paracrine signal we must remember the nature of the bone marrow cell preparation used for treatment. Mononuclear cells were enriched through percoll density gradient centrifugation but the cell preparation may be expected to include a mixture of several different cell types. Several CD markers were measured in the BMMNC preparation used in this analysis but this only gives a limited picture of the range of cells in the preparation. Evidence from studies conducted by Prokopi et al (2009) indicated that platelets, platelet derived microparticles and indeed megakaryocytes maybe contaminating the BMMNC prep and through mechanical perturbations inherent in the preparation procedures, the platelets within the preparation may be in an activated state [200]. Platelets are

anuclear cells originating from megakaryocytes and contain secretory granules which carry a wide variety of proteins with many different functions including contain growth factors such as VEGF and chemokines; they also carry membrane bound integrins and receptors on their surface [201]. This adds an extra dimension to the interpretation of data as immune modulation and angiogenesis are among the many varied functions of platelets and platelet α -granules and must therefore be considered as potentially responsible for the cardioprotective effects of the BMMNC preparation.

In summary, there are now several pieces of evidence that suggest BMMNC cells work in a paracrine manner. Data from our study indicates that whatever this paracrine signal is, it may invoke similar pathways to what has been observed in IPC, post-conditioning and pharmacological conditioning. There is a need to further characterise the signalling pathways initiated by BMMNC treatment, in the same way there has been lots of research characterising pathways involved in other cardioprotective mechanisms. Improved definition of the mechanisms may uncover a downstream drug target for a drug which can be administered at the point of reperfusion. No one has previously performed a proteomic and gene expression profile of myocardial tissue after treatment with BMMNCs, my experiments have revealed 14-3-3 ϵ as one of the candidates to be considered for further study.

8.7 Future work

There are many further experiments which can be done based on the findings from our global profiling studies. The investigation of proteins interacting with 14-3-3 ϵ within our model remains incomplete and one of the first experiments that could be done is a more comprehensive pull-down assay. Such an experiment would look at interactors within our samples and indeed differences in 14-3-3 ϵ interactions between groups. These results may indicate if 14-3-3 ϵ interacts with Bad, or indeed it may show that other interactions form the basis for its functions within our model and several novel interactors may yet be forthcoming. Identifying these interacting proteins would indicate if there is a role for 14-3-3 ϵ in our model and help to elucidate whether it is involved directly in cardioprotection or not. Obtaining data on the phosphorylation state of Bad in our model would also be an important piece of evidence of the involvement of 14-3-3 and Bad and should be a priority. If these experiments revealed evidence for the involvement of Bad and 14-3-3 ϵ in BMMNC afforded cardioprotection, the dependence of this upon Pi3k/Akt activation could then be assessed using Pi3k inhibitors. Measuring the presence of Bad in mitochondrial preparations and cytosolic fractions from our myocardial samples in Sham, I/R, BMMNC and BMMNC with a Pi3k inhibitor may also indicate whether Bad is translocating to the mitochondria in I/R, whether this is attenuated by BMMNC treatment and if this translocation is Pi3k dependant. Bad is thought to interact with receptors on the mitochondrial membrane and initiate the opening of the permeability transition pore, therefore initiating apoptosis, there are currently several research groups trying to define the exact mechanisms involved [160]. In terms of BMMNC mechanism, the paracrine message is likely to be upstream of Pi3k/Akt signalling, therefore once the pathways that lead from Pi3k/Akt activation to apoptosis are confirmed, focus should be concentrated on what lies up-stream from Pi3k/Atk activation.

As well as looking at known elements of apoptotic/protective signalling pathways to assess their regulation after BMMNC treatment and trying to assess the nature of the

paracrine trigger of this response; we must also consider the source of the trigger. Any of the components of the BMMNC preparation may be responsible for delivering the trigger and so a more detailed characterisation of the cell preparation should be a high priority. Measuring CD markers is the most common way to get a 'phenotype' of a mixture of cells, but this method lacks specificity and only gives an idea of composition. One key aspect of the bone marrow cell preparation used in this study may be the presence of contaminating platelets or megakaryocytes and these should be quantified in any further work. Further purifying the bone marrow cell preparation would allow a set of parallel experiments to look at the ability of different cell types (and supernatant from these isolated cell populations) to see if they can elicit any affect on cardiomyocytes post I/R. Initially these could be performed on cell cultures (cultured adult rat cardiomyocytes (with the limitation that experiments would have to be completed within 48 hours), neonatal rat cardiomyocytes which can be cultured for 5-10 days or possibly stem cell-derived or induced pluripotent cardiomyocyte-like cells which are being developed by Harding and colleagues at Imperial College London; with successful cell types being tested further in our I/R rat model. The use of these novel in-vitro myocyte models would have to be validated against the conventional adult cells to assess response to I/R in relevant systems.

We have shown 2DE methods yield some success in looking for mechanisms of BMMNC cardioprotection; to obtain further data more in-depth proteomic based methods could be employed. A large amount of data was produced in these 2DE analyses, but only a fraction of the proteome was screened for alterations. Further experiments could be performed to enhance our view of the proteome. For example, sub-fractionating myocardial samples according to subcellular location before performing 2DE analysis would enhance the number of proteins we can see, and will enrich our dataset with more insoluble proteins. Phosphoprotein specific stains could also be used to look at phosphorylation modifications, as these have been shown to be common in the signalling pathways which we know about so far. A shotgun approach, such as multidimensional protein identification technology (MudPIT), could also be used as this may cover areas of the proteome not seen using 2DE [202].

As so many proteins were down-regulated in the I/R group and up-regulated with treatment, it would be of interest to perform a time-course experiment to ascertain how early after reperfusion protein expression is up-regulated in the treatment group, or to see if protein expression in this group remains at levels comparable to sham throughout reperfusion. The expression of some of the proteins and genes identified in this work and the activation of some key signalling kinases could be measured in these time-course experiments.

Additionally, once more of the details of signalling pathways involved in BMMNC myocardial repair are understood, targeted experiments could be performed using cell-based models of hypoxia/ischemia (which have already shown value in the study of IPC) with and without BMMNC co-culture [203]. Targeting of the potentially involved signalling proteins with inhibitors in such a model may enable more details of signalling pathways to be elucidated. Cell based models are often further from the human condition than are animal models, but are often cheaper and faster experiments to perform and findings from these models can then be taken on and used to perform more informed experiments in animal models and indeed humans. Another commonly used approach is the use of transgenic mice. Mice in which a certain gene of interest is under or over-expressed (in a cardiac specific manner) can be used to assess the physiological and molecular reactions to I/R injury (and BMMNC therapy) [204]. This can also enable the role of proteins of interest to be elucidated.

For the time being there remain many basic questions about BMMNC therapy for I/R injury to be answered. We have shown proteomics to be a helpful tool for answering these questions. Once some of the key cardioprotective pathways involved in BMMNC have been identified, the aspect of BMMNC treatment (whether paracrine signal or otherwise) which triggers these pathways may become clear. Once the exact mechanism of BMMNC treatment is understood, this information may enable a pharmacological target to be identified which could be inhibited or activated in

conjunction with fast reperfusion to limit reperfusion injury and thereby rescue more of the myocardium. These types of studies may translate into improvements in morbidity and mortality rates resulting from MI in the future.

REFERENCES

1. Murray, C.J. and A.D. Lopez, *Mortality by cause for eight regions of the world: Global Burden of Disease Study*. Lancet, 1997. **349**(9061): p. 1269-76.
2. Hansson, G.K., *Inflammation, atherosclerosis, and coronary artery disease*. N Engl J Med, 2005. **352**(16): p. 1685-95.
3. Wikipedia. *Myocardial Infarction*. Wikipedia [cited 2009 2nd December 09]; Available from: http://en.wikipedia.org/wiki/Myocardial_infarction.
4. Ostadal, B., Kolar, F, *Cardiac Ischemia: From Injury to Protection*. 1999: Kluwer Academic Publishers.
5. Clarke, M., M. Bennett, and T. Littlewood, *Cell death in the cardiovascular system*. Heart, 2007. **93**(6): p. 659-64.
6. Yellon, D.M. and D.J. Hausenloy, *Myocardial reperfusion injury*. N Engl J Med, 2007. **357**(11): p. 1121-35.
7. BHF. *G30 UK CHD statistics factsheet 2009-10*. BHF Publications 2009 [cited 2009 2nd November]; Available from: <http://www.bhf.org.uk/publications.aspx>.
8. BHF. *Coronary heart disease statistics factsheet 2008/2009*. BHF Publications 2006 [cited 2009 2nd November]; Available from: <http://www.bhf.org.uk/publications.aspx>.
9. Tiyyagura, S.R. and S.P. Pinney, *Left ventricular remodeling after myocardial infarction: past, present, and future*. Mt Sinai J Med, 2006. **73**(6): p. 840-51.
10. Antman, E.M., et al., *ACC/AHA guidelines for the management of patients with ST-elevation myocardial infarction--executive summary. A report of the American College of Cardiology/American Heart Association Task Force on Practice Guidelines (Writing Committee to revise the 1999 guidelines for the management of patients with acute myocardial infarction)*. J Am Coll Cardiol, 2004. **44**(3): p. 671-719.
11. Keeley, E.C., J.A. Boura, and C.L. Grines, *Primary angioplasty versus intravenous thrombolytic therapy for acute myocardial infarction: a quantitative review of 23 randomised trials*. Lancet, 2003. **361**(9351): p. 13-20.
12. Pinto, D.S., et al., *Door-to-balloon delays with percutaneous coronary intervention in ST-elevation myocardial infarction*. Am Heart J, 2006. **151**(6 Suppl): p. S24-9.
13. Chen, J., et al., *Are beta-blockers effective in elderly patients who undergo coronary revascularization after acute myocardial infarction?* Arch Intern Med, 2000. **160**(7): p. 947-52.
14. Antman, E.M., et al., *ACC/AHA guidelines for the management of patients with ST-elevation myocardial infarction; A report of the American College of Cardiology/American Heart Association Task Force on Practice Guidelines (Committee to Revise the 1999 Guidelines for the Management of patients with acute myocardial infarction)*. J Am Coll Cardiol, 2004. **44**(3): p. E1-E211.

15. Sun, Y. and K.T. Weber, *Angiotensin converting enzyme and myofibroblasts during tissue repair in the rat heart*. J Mol Cell Cardiol, 1996. **28**(5): p. 851-8.
16. Porter, K.E. and N.A. Turner, *Cardiac fibroblasts: at the heart of myocardial remodeling*. Pharmacol Ther, 2009. **123**(2): p. 255-78.
17. Dengler, T.J. and H.A. Katus, *Stem cell therapy for the infarcted heart ("cellular cardiomyoplasty")*. Herz, 2002. **27**(7): p. 598-610.
18. Beltrami, A.P., et al., *Adult cardiac stem cells are multipotent and support myocardial regeneration*. Cell, 2003. **114**(6): p. 763-76.
19. Ahuja, P., P. Sdek, and W.R. MacLellan, *Cardiac myocyte cell cycle control in development, disease, and regeneration*. Physiol Rev, 2007. **87**(2): p. 521-44.
20. Anversa, P., et al., *Life and death of cardiac stem cells: a paradigm shift in cardiac biology*. Circulation, 2006. **113**(11): p. 1451-63.
21. Bergmann, O., et al., *Evidence for cardiomyocyte renewal in humans*. Science, 2009. **324**(5923): p. 98-102.
22. Lovell, M.J. and A. Mathur, *The role of stem cells for treatment of cardiovascular disease*. Cell Prolif, 2004. **37**(1): p. 67-87.
23. Min, J.Y., et al., *Transplantation of embryonic stem cells improves cardiac function in postinfarcted rats*. J Appl Physiol, 2002. **92**(1): p. 288-96.
24. Hodgson, D.M., et al., *Stable benefit of embryonic stem cell therapy in myocardial infarction*. Am J Physiol Heart Circ Physiol, 2004. **287**(2): p. H471-9.
25. Singla, D.K., et al., *Transplantation of embryonic stem cells into the infarcted mouse heart: formation of multiple cell types*. J Mol Cell Cardiol, 2006. **40**(1): p. 195-200.
26. Mathur, A. and J.F. Martin, *Stem cells and repair of the heart*. Lancet, 2004. **364**(9429): p. 183-92.
27. Semsarian, C., *Stem cells in cardiovascular disease: from cell biology to clinical therapy*. Intern Med J, 2002. **32**(5-6): p. 259-65.
28. Smits, A.M. and J.F.M. Smits, *Ischemic heart disease: models of myocardial hypertrophy and infarction*. Drug Discovery Today: Disease Models, 2004. **1**(3): p. 273-278.
29. Vulliamy, P.R., et al., *Intra-coronary arterial injection of mesenchymal stromal cells and microinfarction in dogs*. Lancet, 2004. **363**(9411): p. 783-4.
30. Silva, G.V., et al., *Mesenchymal stem cells differentiate into an endothelial phenotype, enhance vascular density, and improve heart function in a canine chronic ischemia model*. Circulation, 2005. **111**(2): p. 150-6.
31. Amado, L.C., et al., *Multimodality noninvasive imaging demonstrates in vivo cardiac regeneration after mesenchymal stem cell therapy*. J Am Coll Cardiol, 2006. **48**(10): p. 2116-24.
32. Tomita, S., et al., *Autologous transplantation of bone marrow cells improves damaged heart function*. Circulation, 1999. **100**(19 Suppl): p. II247-56.
33. Orlic, D., et al., *Bone marrow cells regenerate infarcted myocardium*. Nature, 2001. **410**(6829): p. 701-5.

34. Sheikh, A.Y., et al., *Molecular imaging of bone marrow mononuclear cell homing and engraftment in ischemic myocardium*. *Stem Cells*, 2007. **25**(10): p. 2677-84.
35. Kocher, A.A., et al., *Neovascularization of ischemic myocardium by human bone-marrow-derived angioblasts prevents cardiomyocyte apoptosis, reduces remodeling and improves cardiac function*. *Nat Med*, 2001. **7**(4): p. 430-6.
36. Toma, C., et al., *Human mesenchymal stem cells differentiate to a cardiomyocyte phenotype in the adult murine heart*. *Circulation*, 2002. **105**(1): p. 93-8.
37. Rose, R.A., et al., *Bone marrow-derived mesenchymal stromal cells express cardiac-specific markers, retain the stromal phenotype, and do not become functional cardiomyocytes in vitro*. *Stem Cells*, 2008. **26**(11): p. 2884-92.
38. Koninckx, R., et al., *Human bone marrow stem cells co-cultured with neonatal rat cardiomyocytes display limited cardiomyogenic plasticity*. *Cytotherapy*, 2009. **11**(6): p. 778-92.
39. Sham, J.S., S.N. Hatem, and M. Morad, *Species differences in the activity of the Na(+)-Ca²⁺ exchanger in mammalian cardiac myocytes*. *J Physiol*, 1995. **488 (Pt 3)**: p. 623-31.
40. Hasenfuss, G., *Animal models of human cardiovascular disease, heart failure and hypertrophy*. *Cardiovasc Res*, 1998. **39**(1): p. 60-76.
41. Stamm, C., et al., *Autologous bone-marrow stem-cell transplantation for myocardial regeneration*. *Lancet*, 2003. **361**(9351): p. 45-6.
42. Strauer, B.E., et al., *Repair of infarcted myocardium by autologous intracoronary mononuclear bone marrow cell transplantation in humans*. *Circulation*, 2002. **106**(15): p. 1913-8.
43. Penicka, M., et al., *One-day kinetics of myocardial engraftment after intracoronary injection of bone marrow mononuclear cells in patients with acute and chronic myocardial infarction*. *Heart*, 2007. **93**(7): p. 837-41.
44. Meyer, G.P., et al., *Intracoronary bone marrow cell transfer after myocardial infarction: eighteen months' follow-up data from the randomized, controlled BOOST (BOne marrOw transfer to enhance ST-elevation infarct regeneration) trial*. *Circulation*, 2006. **113**(10): p. 1287-94.
45. Lunde, K., et al., *Intracoronary injection of mononuclear bone marrow cells in acute myocardial infarction*. *N Engl J Med*, 2006. **355**(12): p. 1199-209.
46. Schachinger, V., et al., *Intracoronary bone marrow-derived progenitor cells in acute myocardial infarction*. *N Engl J Med*, 2006. **355**(12): p. 1210-21.
47. Assmus, B., et al., *Transcoronary transplantation of progenitor cells after myocardial infarction*. *N Engl J Med*, 2006. **355**(12): p. 1222-32.
48. Janssens, S., et al., *Autologous bone marrow-derived stem-cell transfer in patients with ST-segment elevation myocardial infarction: double-blind, randomised controlled trial*. *Lancet*, 2006. **367**(9505): p. 113-21.
49. Martin-Rendon, E., et al., *Stem cell treatment for acute myocardial infarction*. *Cochrane Database Syst Rev*, 2008(4): p. CD006536.
50. Abdel-Latif, A., et al., *Adult bone marrow-derived cells for cardiac repair: a systematic review and meta-analysis*. *Arch Intern Med*, 2007. **167**(10): p. 989-97.

51. Schwartz, R.S., *The politics and promise of stem-cell research*. N Engl J Med, 2006. **355**(12): p. 1189-91.
52. Rosenzweig, A., *Cardiac cell therapy--mixed results from mixed cells*. N Engl J Med, 2006. **355**(12): p. 1274-7.
53. Hofmann, M., et al., *Monitoring of bone marrow cell homing into the infarcted human myocardium*. Circulation, 2005. **111**(17): p. 2198-202.
54. Dimmeler, S., A.M. Zeiher, and M.D. Schneider, *Unchain my heart: the scientific foundations of cardiac repair*. J Clin Invest, 2005. **115**(3): p. 572-83.
55. Kloner, R.A., et al., *Medical and cellular implications of stunning, hibernation, and preconditioning: an NHLBI workshop*. Circulation, 1998. **97**(18): p. 1848-67.
56. Yellon, D.M. and J.M. Downey, *Preconditioning the myocardium: from cellular physiology to clinical cardiology*. Physiol Rev, 2003. **83**(4): p. 1113-51.
57. Hausenloy, D.J. and D.M. Yellon, *Remote ischaemic preconditioning: underlying mechanisms and clinical application*. Cardiovasc Res, 2008. **79**(3): p. 377-86.
58. Murry, C.E., R.B. Jennings, and K.A. Reimer, *Preconditioning with ischemia: a delay of lethal cell injury in ischemic myocardium*. Circulation, 1986. **74**(5): p. 1124-36.
59. Cohen, M.V., C.P. Baines, and J.M. Downey, *Ischemic preconditioning: from adenosine receptor to KATP channel*. Annu Rev Physiol, 2000. **62**: p. 79-109.
60. Goto, M., et al., *Role of bradykinin in protection of ischemic preconditioning in rabbit hearts*. Circ Res, 1995. **77**(3): p. 611-21.
61. Sakamoto, J., et al., *Limitation of myocardial infarct size by adenosine A1 receptor activation is abolished by protein kinase C inhibitors in the rabbit*. Cardiovasc Res, 1995. **29**(5): p. 682-8.
62. Miki, T., M.V. Cohen, and J.M. Downey, *Opioid receptor contributes to ischemic preconditioning through protein kinase C activation in rabbits*. Mol Cell Biochem, 1998. **186**(1-2): p. 3-12.
63. Downey, J.M., A.M. Davis, and M.V. Cohen, *Signaling pathways in ischemic preconditioning*. Heart Fail Rev, 2007. **12**(3-4): p. 181-8.
64. Tong, H., et al., *Ischemic preconditioning activates phosphatidylinositol-3-kinase upstream of protein kinase C*. Circ Res, 2000. **87**(4): p. 309-15.
65. Krieg, T., et al., *Acetylcholine and bradykinin trigger preconditioning in the heart through a pathway that includes Akt and NOS*. Am J Physiol Heart Circ Physiol, 2004. **287**(6): p. H2606-11.
66. Baines, C.P., M. Goto, and J.M. Downey, *Oxygen radicals released during ischemic preconditioning contribute to cardioprotection in the rabbit myocardium*. J Mol Cell Cardiol, 1997. **29**(1): p. 207-16.
67. Becker, L.B., et al., *Generation of superoxide in cardiomyocytes during ischemia before reperfusion*. Am J Physiol, 1999. **277**(6 Pt 2): p. H2240-6.
68. Pain, T., et al., *Opening of mitochondrial K(ATP) channels triggers the preconditioned state by generating free radicals*. Circ Res, 2000. **87**(6): p. 460-6.

69. Costa, A.D., et al., *Protein kinase G transmits the cardioprotective signal from cytosol to mitochondria*. *Circ Res*, 2005. **97**(4): p. 329-36.
70. Hausenloy, D.J., M.R. Duchon, and D.M. Yellon, *Inhibiting mitochondrial permeability transition pore opening at reperfusion protects against ischaemia-reperfusion injury*. *Cardiovasc Res*, 2003. **60**(3): p. 617-25.
71. Argaud, L., et al., *Specific inhibition of the mitochondrial permeability transition prevents lethal reperfusion injury*. *J Mol Cell Cardiol*, 2005. **38**(2): p. 367-74.
72. Juhaszova, M., et al., *Glycogen synthase kinase-3beta mediates convergence of protection signaling to inhibit the mitochondrial permeability transition pore*. *J Clin Invest*, 2004. **113**(11): p. 1535-49.
73. Hausenloy, D.J., S.B. Ong, and D.M. Yellon, *The mitochondrial permeability transition pore as a target for preconditioning and postconditioning*. *Basic Res Cardiol*, 2009. **104**(2): p. 189-202.
74. Baines, C.P., *The mitochondrial permeability transition pore and ischemia-reperfusion injury*. *Basic Res Cardiol*, 2009. **104**(2): p. 181-8.
75. Nakanishi, C., et al., *Activation of cardiac progenitor cells through paracrine effects of mesenchymal stem cells*. *Biochem Biophys Res Commun*, 2008. **374**(1): p. 11-6.
76. Kubal, C., et al., *Bone marrow cells have a potent anti-ischemic effect against myocardial cell death in humans*. *J Thorac Cardiovasc Surg*, 2006. **132**(5): p. 1112-8.
77. Vandervelde, S., et al., *Signaling factors in stem cell-mediated repair of infarcted myocardium*. *J Mol Cell Cardiol*, 2005. **39**(2): p. 363-76.
78. Wolff, S., et al., *Towards the entire proteome of the model bacterium *Bacillus subtilis* by gel-based and gel-free approaches*. *J Chromatogr B Analyt Technol Biomed Life Sci*, 2007. **849**(1-2): p. 129-40.
79. Waters, K.M., J.G. Pounds, and B.D. Thrall, *Data merging for integrated microarray and proteomic analysis*. *Brief Funct Genomic Proteomic*, 2006. **5**(4): p. 261-72.
80. Kubota, K., T. Kosaka, and K. Ichikawa, *Combination of two-dimensional electrophoresis and shotgun peptide sequencing in comparative proteomics*. *J Chromatogr B Analyt Technol Biomed Life Sci*, 2005. **815**(1-2): p. 3-9.
81. Ahn, N.G., et al., *Achieving in-depth proteomics profiling by mass spectrometry*. *ACS Chem Biol*, 2007. **2**(1): p. 39-52.
82. Gorg, A., W. Weiss, and M.J. Dunn, *Current two-dimensional electrophoresis technology for proteomics*. *Proteomics*, 2004. **4**(12): p. 3665-85.
83. Griffiths, W.J. and Y. Wang, *Mass spectrometry: from proteomics to metabolomics and lipidomics*. *Chem Soc Rev*, 2009. **38**(7): p. 1882-96.
84. Chen, G. and B.N. Pramanik, *Application of LC/MS to proteomics studies: current status and future prospects*. *Drug Discov Today*, 2009. **14**(9-10): p. 465-71.
85. McGregor, E. and M.J. Dunn, *Proteomics of heart disease*. *Hum Mol Genet*, 2003. **12 Spec No 2**: p. R135-44.

86. Weekes, J., et al., *Bovine dilated cardiomyopathy: proteomic analysis of an animal model of human dilated cardiomyopathy*. Electrophoresis, 1999. **20**(4-5): p. 898-906.
87. Weekes, J., et al., *Hyperubiquitination of proteins in dilated cardiomyopathy*. Proteomics, 2003. **3**(2): p. 208-16.
88. Ping, P., et al., *Functional proteomic analysis of protein kinase C epsilon signaling complexes in the normal heart and during cardioprotection*. Circ Res, 2001. **88**(1): p. 59-62.
89. White, M.Y., et al., *Proteomics of ischemia/reperfusion injury in rabbit myocardium reveals alterations to proteins of essential functional systems*. Proteomics, 2005. **5**(5): p. 1395-410.
90. White, M.Y., et al., *Proteomics of ischemia and reperfusion injuries in rabbit myocardium with and without intervention by an oxygen-free radical scavenger*. Proteomics, 2006. **6**(23): p. 6221-33.
91. Kim, N., et al., *Potential biomarkers for ischemic heart damage identified in mitochondrial proteins by comparative proteomics*. Proteomics, 2006. **6**(4): p. 1237-49.
92. Buerke, M., et al., *Proteome analysis of myocardial tissue following ischemia and reperfusion--effects of complement inhibition*. Biochim Biophys Acta, 2006. **1764**(10): p. 1536-45.
93. Fert-Bober, J., et al., *Effect of duration of ischemia on myocardial proteome in ischemia/reperfusion injury*. Proteomics, 2008. **8**(12): p. 2543-55.
94. Mayr, M., et al., *Proteomic and metabolomic analysis of cardioprotection: Interplay between protein kinase C epsilon and delta in regulating glucose metabolism of murine hearts*. J Mol Cell Cardiol, 2009. **46**(2): p. 268-77.
95. Ginsburg, G.S., D. Seo, and C. Frazier, *Microarrays coming of age in cardiovascular medicine: standards, predictions, and biology*. J Am Coll Cardiol, 2006. **48**(8): p. 1618-20.
96. Gidh-Jain, M., et al., *Alterations in cardiac gene expression during ventricular remodeling following experimental myocardial infarction*. J Mol Cell Cardiol, 1998. **30**(3): p. 627-37.
97. Ono, K., et al., *Cytokine gene expression after myocardial infarction in rat hearts: possible implication in left ventricular remodeling*. Circulation, 1998. **98**(2): p. 149-56.
98. Stanton, L.W., et al., *Altered patterns of gene expression in response to myocardial infarction*. Circ Res, 2000. **86**(9): p. 939-45.
99. Simkhovich, B.Z., et al., *Age-related changes of cardiac gene expression following myocardial ischemia/reperfusion*. Arch Biochem Biophys, 2003. **420**(2): p. 268-78.
100. Simkhovich, B.Z., et al., *Brief episode of ischemia activates protective genetic program in rat heart: a gene chip study*. Cardiovasc Res, 2003. **59**(2): p. 450-9.
101. Sergeev, P., et al., *Trigger-dependent gene expression profiles in cardiac preconditioning: evidence for distinct genetic programs in ischemic and anesthetic preconditioning*. Anesthesiology, 2004. **100**(3): p. 474-88.

102. Ayach, B.B., et al., *Stem cell factor receptor induces progenitor and natural killer cell-mediated cardiac survival and repair after myocardial infarction*. Proc Natl Acad Sci U S A, 2006. **103**(7): p. 2304-9.
103. Ip, J.E., et al., *Mesenchymal stem cells use integrin beta1 not CXC chemokine receptor 4 for myocardial migration and engraftment*. Mol Biol Cell, 2007. **18**(8): p. 2873-82.
104. Wright, D.E., et al., *Hematopoietic stem cells are uniquely selective in their migratory response to chemokines*. J Exp Med, 2002. **195**(9): p. 1145-54.
105. Gorg, A., et al., *2-DE with IPGs*. Electrophoresis, 2009. **30** **Suppl 1**: p. S122-32.
106. Thiemermann, C., et al., *Inhibition of the activity of poly(ADP ribose) synthetase reduces ischemia-reperfusion injury in the heart and skeletal muscle*. Proc Natl Acad Sci U S A, 1997. **94**(2): p. 679-83.
107. Bradford, M.M., *A rapid and sensitive method for the quantitation of microgram quantities of protein utilizing the principle of protein-dye binding*. Anal Biochem, 1976. **72**: p. 248-54.
108. Altschul, S.F., et al., *Basic local alignment search tool*. J Mol Biol, 1990. **215**(3): p. 403-10.
109. Smyth, G.K., *Linear models and empirical bayes methods for assessing differential expression in microarray experiments*. Stat Appl Genet Mol Biol, 2004. **3**: p. Article3.
110. Smyth, G.K., *Limma: linear models for microarray data.*, in *Bioinformatics and Computational Biology Solutions using R and Bioconductor*, R.C. Gentleman, V. Dudoit, S. Irizarry, R. Huber, W., Editor. 2005, Springer: New York. p. 397-420.
111. Kooperberg, C., et al., *Significance testing for small microarray experiments*. Stat Med, 2005. **24**(15): p. 2281-98.
112. Jeffery, I.B., D.G. Higgins, and A.C. Culhane, *Comparison and evaluation of methods for generating differentially expressed gene lists from microarray data*. BMC Bioinformatics, 2006. **7**: p. 359.
113. Bustin, S.A., et al., *The MIQE guidelines: minimum information for publication of quantitative real-time PCR experiments*. Clin Chem, 2009. **55**(4): p. 611-22.
114. Vandesompele, J., et al., *Accurate normalization of real-time quantitative RT-PCR data by geometric averaging of multiple internal control genes*. Genome Biol, 2002. **3**(7): p. RESEARCH0034.
115. Thomas, P.D., et al., *Applications for protein sequence-function evolution data: mRNA/protein expression analysis and coding SNP scoring tools*. Nucleic Acids Res, 2006. **34**(Web Server issue): p. W645-50.
116. Mi, H., et al., *PANTHER version 6: protein sequence and function evolution data with expanded representation of biological pathways*. Nucleic Acids Res, 2007. **35**(Database issue): p. D247-52.
117. Dennis, G., Jr., et al., *DAVID: Database for Annotation, Visualization, and Integrated Discovery*. Genome Biol, 2003. **4**(5): p. P3.

118. Huang, D.W., B.T. Sherman, and R.A. Lempicki, *Systematic and integrative analysis of large gene lists using DAVID bioinformatics resources*. Nat. Protocols, 2008. **4**(1): p. 44-57.
119. Kol, A., et al., *Chlamydial and human heat shock protein 60s activate human vascular endothelium, smooth muscle cells, and macrophages*. The Journal of Clinical Investigation, 1999. **103**(4): p. 571-577.
120. Lander, H.M., et al., *Activation of the Receptor for Advanced Glycation End Products Triggers a p21ras-dependent Mitogen-activated Protein Kinase Pathway Regulated by Oxidant Stress*. Journal of Biological Chemistry, 1997. **272**(28): p. 17810-17814.
121. Tang, S., et al., *Albumin stimulates interleukin-8 expression in proximal tubular epithelial cells in vitro and in vivo*. The Journal of Clinical Investigation, 2003. **111**(4): p. 515-527.
122. Yeung, K.C., et al., *Raf Kinase Inhibitor Protein Interacts with NF- κ B-Inducing Kinase and TAK1 and Inhibits NF- κ B Activation*. Mol. Cell. Biol., 2001. **21**(21): p. 7207-7217.
123. Kol, A., et al., *Cutting Edge: Heat Shock Protein (HSP) 60 Activates the Innate Immune Response: CD14 Is an Essential Receptor for HSP60 Activation of Mononuclear Cells*. J Immunol, 2000. **164**(1): p. 13-17.
124. Gober, M.D., et al., *Forced Expression of the H11 Heat Shock Protein Can Be Regulated by DNA Methylation and Trigger Apoptosis in Human Cells*. Journal of Biological Chemistry, 2003. **278**(39): p. 37600-37609.
125. Oriente, F., et al., *Protein Kinase C- α Regulates Insulin Action and Degradation by Interacting with Insulin Receptor Substrate-1 and 14-3-3 ϵ* . Journal of Biological Chemistry, 2005. **280**(49): p. 40642-40649.
126. Messina, J.L. and R.S. Weinstock, *Evidence for diverse roles of protein kinase-C in the inhibition of gene expression by insulin: the tyrosine aminotransferase, albumin, and phosphoenolpyruvate carboxykinase genes [published erratum appears in Endocrinology 1995 May; 136(5):2039]*. Endocrinology, 1994. **135**(6): p. 2327-2334.
127. Koch, H.B., et al., *Large-scale identification of c-MYC-associated proteins using a combined TAP/MudPIT approach*. Cell Cycle, 2007. **6**(2): p. 205-17.
128. Ruan, H., H.J. Pownall, and H.F. Lodish, *Troglitazone Antagonizes Tumor Necrosis Factor- α -induced Reprogramming of Adipocyte Gene Expression by Inhibiting the Transcriptional Regulatory Functions of NF- κ B*. Journal of Biological Chemistry, 2003. **278**(30): p. 28181-28192.
129. Odom, D.T., et al., *Control of pancreas and liver gene expression by HNF transcription factors*. Science, 2004. **303**(5662): p. 1378-81.
130. Kim, J.K., et al., *Estrogen Prevents Cardiomyocyte Apoptosis through Inhibition of Reactive Oxygen Species and Differential Regulation of p38 Kinase Isoforms*. Journal of Biological Chemistry, 2006. **281**(10): p. 6760-6767.
131. Pedram, A., et al., *Estrogen Inhibits Cardiac Hypertrophy: Role of Estrogen Receptor- β to Inhibit Calcineurin*. Endocrinology, 2008. **149**(7): p. 3361-3369.

132. Heldin, C.-H., M. Landström, and A. Moustakas, *Mechanism of TGF- β signaling to growth arrest, apoptosis, and epithelial-mesenchymal transition*. Current Opinion in Cell Biology, 2009. **21**(2): p. 166-176.
133. Chambers, R.C., et al., *Global expression profiling of fibroblast responses to transforming growth factor- β 1 reveals the induction of inhibitor of differentiation-1 and provides evidence of smooth muscle cell phenotypic switching*. Am J Pathol, 2003. **162**(2): p. 533-46.
134. Shi-wen, X., et al., *CCN2 is necessary for adhesive responses to transforming growth factor- β 1 in embryonic fibroblasts*. J Biol Chem, 2006. **281**(16): p. 10715-26.
135. Murakami, M., M. Ohkuma, and M. Nakamura, *Molecular mechanism of transforming growth factor- β -mediated inhibition of growth arrest and differentiation in a myoblast cell line*. Dev Growth Differ, 2008. **50**(2): p. 121-30.
136. Wang, X., et al., *Interactions between Extracellular Signal-regulated Protein Kinase 1, 14-3-3 ϵ , and Heat Shock Factor 1 during Stress*. Journal of Biological Chemistry, 2004. **279**(47): p. 49460-49469.
137. Xiao, K., et al., *Functional specialization of β -arrestin interactions revealed by proteomic analysis*. Proceedings of the National Academy of Sciences, 2007. **104**(29): p. 12011-12016.
138. Treins, C., et al., *Regulation of vascular endothelial growth factor expression by advanced glycation end products*. J Biol Chem, 2001. **276**(47): p. 43836-41.
139. Wright, G.L., et al., *VEGF stimulation of mitochondrial biogenesis: requirement of AKT3 kinase*. FASEB J., 2008. **22**(9): p. 3264-3275.
140. Foster, L.J., et al., *Insulin-dependent interactions of proteins with GLUT4 revealed through stable isotope labeling by amino acids in cell culture (SILAC)*. J Proteome Res, 2006. **5**(1): p. 64-75.
141. Ewing, R.M., et al., *Large-scale mapping of human protein-protein interactions by mass spectrometry*. Mol Syst Biol, 2007. **3**: p. 89.
142. Beard, N.A., D.R. Laver, and A.F. Dulhunty, *Calsequestrin and the calcium release channel of skeletal and cardiac muscle*. Prog Biophys Mol Biol, 2004. **85**(1): p. 33-69.
143. Kihara, A., et al., *Metabolism and biological functions of two phosphorylated sphingolipids, sphingosine 1-phosphate and ceramide 1-phosphate*. Prog Lipid Res, 2007. **46**(2): p. 126-44.
144. Brinkmann, V., *Sphingosine 1-phosphate receptors in health and disease: mechanistic insights from gene deletion studies and reverse pharmacology*. Pharmacol Ther, 2007. **115**(1): p. 84-105.
145. Masters, S.C., et al., *Survival-promoting functions of 14-3-3 proteins*. Biochem Soc Trans, 2002. **30**(4): p. 360-5.
146. Datta, S.R., et al., *Akt phosphorylation of BAD couples survival signals to the cell-intrinsic death machinery*. Cell, 1997. **91**(2): p. 231-41.
147. del Peso, L., et al., *Interleukin-3-induced phosphorylation of BAD through the protein kinase Akt*. Science, 1997. **278**(5338): p. 687-9.


148. Carroll, J., et al., *Bovine complex I is a complex of 45 different subunits*. J Biol Chem, 2006. **281**(43): p. 32724-7.
149. Iwata, S., et al., *Complete structure of the 11-subunit bovine mitochondrial cytochrome bc1 complex*. Science, 1998. **281**(5373): p. 64-71.
150. Xu, C., et al., *Proteomic analysis of hepatic ischemia/reperfusion injury and ischemic preconditioning in mice revealed the protective role of ATP5beta*. Proteomics, 2009. **9**(2): p. 409-19.
151. Gerstenblith, G., *Derangements in Cardiac Metabolism in the Ischemic State and Consequences of Reperfusion*. Advanced Studies in Medicine, 2004. **4**(6B): p. S464-S471.
152. Zhang, Y., et al., *The oxidative inactivation of mitochondrial electron transport chain components and ATPase*. J Biol Chem, 1990. **265**(27): p. 16330-6.
153. Nonn, L., M. Berggren, and G. Powis, *Increased expression of mitochondrial peroxiredoxin-3 (thioredoxin peroxidase-2) protects cancer cells against hypoxia and drug-induced hydrogen peroxide-dependent apoptosis*. Mol Cancer Res, 2003. **1**(9): p. 682-9.
154. Cullingford, T.E., et al., *Effects of oxidative stress on the cardiac myocyte proteome: modifications to peroxiredoxins and small heat shock proteins*. J Mol Cell Cardiol, 2006. **40**(1): p. 157-72.
155. Sambandam, N. and G.D. Lopaschuk, *AMP-activated protein kinase (AMPK) control of fatty acid and glucose metabolism in the ischemic heart*. Prog Lipid Res, 2003. **42**(3): p. 238-56.
156. Porter, G.W., F.R. Khuri, and H. Fu, *Dynamic 14-3-3/client protein interactions integrate survival and apoptotic pathways*. Semin Cancer Biol, 2006. **16**(3): p. 193-202.
157. Yaffe, M.B., et al., *The structural basis for 14-3-3:phosphopeptide binding specificity*. Cell, 1997. **91**(7): p. 961-71.
158. Wang, W. and D.C. Shakes, *Molecular evolution of the 14-3-3 protein family*. J Mol Evol, 1996. **43**(4): p. 384-98.
159. Subramanian, R.R., et al., *Functional conservation of 14-3-3 isoforms in inhibiting bad-induced apoptosis*. Exp Cell Res, 2001. **271**(1): p. 142-51.
160. Youle, R.J. and A. Strasser, *The BCL-2 protein family: opposing activities that mediate cell death*. Nat Rev Mol Cell Biol, 2008. **9**(1): p. 47-59.
161. Masters, S.C., et al., *14-3-3 inhibits Bad-induced cell death through interaction with serine-136*. Mol Pharmacol, 2001. **60**(6): p. 1325-31.
162. Tan, Y., et al., *BAD Ser-155 phosphorylation regulates BAD/Bcl-XL interaction and cell survival*. J Biol Chem, 2000. **275**(33): p. 25865-9.
163. Datta, S.R., et al., *14-3-3 proteins and survival kinases cooperate to inactivate BAD by BH3 domain phosphorylation*. Mol Cell, 2000. **6**(1): p. 41-51.
164. Tan, Y., et al., *p90(RSK) blocks bad-mediated cell death via a protein kinase C-dependent pathway*. J Biol Chem, 1999. **274**(49): p. 34859-67.
165. Wang, H.G., et al., *Ca²⁺-induced apoptosis through calcineurin dephosphorylation of BAD*. Science, 1999. **284**(5412): p. 339-43.

166. Wang, X.T., et al., *Opposing effects of Bad phosphorylation at two distinct sites by Akt1 and JNK1/2 on ischemic brain injury*. Cell Signal, 2007. **19**(9): p. 1844-56.
167. Won, J., et al., *Cleavage of 14-3-3 protein by caspase-3 facilitates bad interaction with Bcl-x(L) during apoptosis*. J Biol Chem, 2003. **278**(21): p. 19347-51.
168. Tong, H., et al., *Phosphorylation of glycogen synthase kinase-3beta during preconditioning through a phosphatidylinositol-3-kinase--dependent pathway is cardioprotective*. Circ Res, 2002. **90**(4): p. 377-9.
169. Pozuelo Rubio, M., et al., *14-3-3-affinity purification of over 200 human phosphoproteins reveals new links to regulation of cellular metabolism, proliferation and trafficking*. Biochem J, 2004. **379**(Pt 2): p. 395-408.
170. Bunney, T.D., H.S. van Walraven, and A.H. de Boer, *14-3-3 protein is a regulator of the mitochondrial and chloroplast ATP synthase*. Proc Natl Acad Sci U S A, 2001. **98**(7): p. 4249-54.
171. Reiland, S., et al., *Large-scale Arabidopsis phosphoproteome profiling reveals novel chloroplast kinase substrates and phosphorylation networks*. Plant Physiol, 2009. **150**(2): p. 889-903.
172. Peluso, J.J., X. Liu, and J. Romak, *Progesterone maintains basal intracellular adenosine triphosphate levels and viability of spontaneously immortalized granulosa cells by promoting an interaction between 14-3-3sigma and ATP synthase beta/precursor through a protein kinase G-dependent mechanism*. Endocrinology, 2007. **148**(5): p. 2037-44.
173. Bisetto, E., et al., *Functional and stoichiometric analysis of subunit e in bovine heart mitochondrial F(0)F(1)ATP synthase*. J Bioenerg Biomembr, 2008. **40**(4): p. 257-67.
174. Chich, J.-F., et al., *Statistics for proteomics: Experimental design and 2-DE differential analysis*. Journal of Chromatography B, 2007. **849**(1-2): p. 261-272.
175. Norman, G.R., Streiner, D.L., *Biostatistics: The Bare Essentials*. Second Edition ed. 2000, Hamilton, London: B. C. Decker Inc.
176. Thomas, J.G., et al., *An efficient and robust statistical modeling approach to discover differentially expressed genes using genomic expression profiles*. Genome Res, 2001. **11**(7): p. 1227-36.
177. Unlu, M., M.E. Morgan, and J.S. Minden, *Difference gel electrophoresis: a single gel method for detecting changes in protein extracts*. Electrophoresis, 1997. **18**(11): p. 2071-7.
178. Minden, J.S., et al., *Difference gel electrophoresis*. Electrophoresis, 2009. **30 Suppl 1**: p. S156-61.
179. Timms, J.F. and R. Cramer, *Difference gel electrophoresis*. Proteomics, 2008. **8**(23-24): p. 4886-97.
180. Agocha, A.E. and M. Eghbali-Webb, *A simple method for preparation of cultured cardiac fibroblasts from adult human ventricular tissue*. Molecular and Cellular Biochemistry, 1997. **172**(1): p. 195-198.
181. Brown, R.D., et al., *The cardiac fibroblast: therapeutic target in myocardial remodeling and failure*. Annu Rev Pharmacol Toxicol, 2005. **45**: p. 657-87.

182. Brown, R.D., et al., *Cytokines regulate matrix metalloproteinases and migration in cardiac fibroblasts*. Biochemical and Biophysical Research Communications, 2007. **362**(1): p. 200-205.
183. Knipp, B.S., et al., *Increased MMP-9 expression and activity by aortic smooth muscle cells after nitric oxide synthase inhibition is associated with increased nuclear factor- κ B and activator protein-1 activity*. Journal of Surgical Research, 2004. **116**(1): p. 70-80.
184. Gabrielsen, A., et al., *Gene expression signals involved in ischemic injury, extracellular matrix composition and fibrosis defined by global mRNA profiling of the human left ventricular myocardium*. J Mol Cell Cardiol, 2007. **42**(4): p. 870-83.
185. Sanjo, H., T. Kawai, and S. Akira, *DRAKs, Novel Serine/Threonine Kinases Related to Death-associated Protein Kinase That Trigger Apoptosis*. Journal of Biological Chemistry, 1998. **273**(44): p. 29066-29071.
186. Doherty, G.A., et al., *Regulation of the apoptosis-inducing kinase DRAK2 by cyclooxygenase-2 in colorectal cancer*. Br J Cancer, 2009. **101**(3): p. 483-91.
187. Shinmura, K., et al., *Inducible Nitric Oxide Synthase Modulates Cyclooxygenase-2 Activity in the Heart of Conscious Rabbits During the Late Phase of Ischemic Preconditioning*. Circ Res, 2002. **90**(5): p. 602-608.
188. Xuan, Y.-T., et al., *Mechanism of cyclooxygenase-2 upregulation in late preconditioning*. Journal of Molecular and Cellular Cardiology, 2003. **35**(5): p. 525-537.
189. Sarkar, S.N. and G.C. Sen, *Novel functions of proteins encoded by viral stress-inducible genes*. Pharmacol Ther, 2004. **103**(3): p. 245-59.
190. Hovanessian, A.G. and J. Justesen, *The human 2'-5' oligoadenylate synthetase family: unique interferon-inducible enzymes catalyzing 2'-5' instead of 3'-5' phosphodiester bond formation*. Biochimie, 2007. **89**(6-7): p. 779-88.
191. Rebouillat, D., et al., *Characterization of the gene encoding the 100-kDa form of human 2',5' oligoadenylate synthetase*. Genomics, 2000. **70**(2): p. 232-40.
192. Takuwa, Y., et al., *Subtype-specific, differential activities of the EDG family receptors for sphingosine-1-phosphate, a novel lysophospholipid mediator*. Molecular and Cellular Endocrinology, 2001. **177**(1-2): p. 3-11.
193. Fabre, S., et al., *FOXO1 Regulates L-Selectin and a Network of Human T Cell Homing Molecules Downstream of Phosphatidylinositol 3-Kinase*. J Immunol, 2008. **181**(5): p. 2980-2989.
194. Kumanogoh, A. and H. Kikutani, *Immune semaphorins: a new area of semaphorin research*. J Cell Sci, 2003. **116**(Pt 17): p. 3463-70.
195. Kumanogoh, A., et al., *Class IV semaphorin Sema4A enhances T-cell activation and interacts with Tim-2*. Nature, 2002. **419**(6907): p. 629-33.
196. Makino, N., et al., *Involvement of Sema4A in the progression of experimental autoimmune myocarditis*. FEBS Lett, 2008. **582**(28): p. 3935-40.
197. Toyofuku, T., et al., *Semaphorin-4A, an activator for T-cell-mediated immunity, suppresses angiogenesis via Plexin-D1*. EMBO J, 2007. **26**(5): p. 1373-1384.

198. Robson, J.D., D. Davidson, and A. Veillette, *Inhibition of the Jun N-Terminal Protein Kinase Pathway by SHIP-1, a Lipid Phosphatase That Interacts with the Adaptor Molecule Dok-3*. Mol. Cell. Biol., 2004. **24**(6): p. 2332-2343.
199. Ng, C.-H., S. Xu, and K.-P. Lam, *Dok-3 plays a nonredundant role in negative regulation of B-cell activation*. Blood, 2007. **110**(1): p. 259-266.
200. Prokopi, M., et al., *Proteomic analysis reveals presence of platelet microparticles in endothelial progenitor cell cultures*. Blood, 2009. **114**(3): p. 723-32.
201. Blair, P. and R. Flaumenhaft, *Platelet alpha-granules: basic biology and clinical correlates*. Blood Rev, 2009. **23**(4): p. 177-89.
202. Wolters, D.A., M.P. Washburn, and J.R. Yates, 3rd, *An automated multidimensional protein identification technology for shotgun proteomics*. Anal Chem, 2001. **73**(23): p. 5683-90.
203. Diaz, R.J. and G.J. Wilson, *Studying ischemic preconditioning in isolated cardiomyocyte models*. Cardiovasc Res, 2006. **70**(2): p. 286-96.
204. Ramachandran, A., S. Jha, and D.J. Lefer, *REVIEW paper: pathophysiology of myocardial reperfusion injury: the role of genetically engineered mouse models*. Vet Pathol, 2008. **45**(5): p. 698-706.

APPENDIX 1: Genome Centre protocol for Illumina direct hybridisation



Whole-Genome Gene Expression with IntelliHyb™ Seal Experienced User Card

Hyb BC

Hands-on time: ~ 20 minutes

Incubation time: ~ 16–24 hours

Dispense the resuspended cRNA samples onto BeadChips. Incubate the BeadChips in the Illumina Hybridization Oven to hybridize the samples onto the BeadChips.

New Materials	Quantity
HYB	20 µl (6-Sample) 10 µl (8 or 12-Sample)
HCB	200 µl
RNase-free water	10 µl (6-Sample) 5 µl (8 or 12-Sample)

Preparation

- Preheat the oven (with rocking platform) to 58°C.
- Prepare cRNA samples dried down, if necessary to achieve required concentration.
- Add RNase-free water to RNA and mix:
 - For the **6-Sample** chip, add 10 µl RNase-free water to 1.5 µg RNA and mix.
 - For the **8-Sample** or **12-Sample** chip, add 5 µl RNase-free water to 750 ng RNA and mix.
- Leave at room temperature (~22°C) for 10 minutes to resuspend cRNA.
- Place the HYB and HCB tubes in the 58°C oven for 10 minutes to dissolve any salts that may have precipitated in storage. Inspect the solution; if any salts remain undissolved, incubate at 58°C for another 10 minutes. After cooling to room temperature, mix thoroughly before using.
- Add HYB to each cRNA sample:
 - For the **6-Sample** chip, add 20 µl HYB to each cRNA sample.
 - For the **8-Sample** or **12-Sample** chip, add 10 µl HYB to each cRNA sample.

Steps

- 1. Place the Illumina Hyb Chamber gaskets into the BeadChip Hyb Chamber.
- 2. Dispense 200 µl HCB into the humidifying buffer reservoirs. Only add buffer to reservoirs next to loaded BeadChips.

APPENDIX 1: continued




Whole-Genome Gene Expression with IntelliHyb™ Seal Experienced User Card

- 3. Seal the Hyb Chamber with lid and keep on bench at room temperature until ready to load BeadChips into the Hyb Chamber.
- 4. Remove all BeadChips from their packages.
- 5. Holding the BeadChip by the coverseal tab with tweezers or with powder-free gloved hands, slide the BeadChip into the Hyb Chamber insert so that the barcode lines up with barcode symbol on the insert.
- 6. Preheat the assay sample at 65°C for 5 minutes.
- 7. Briefly vortex, then briefly centrifuge to collect the liquid in the bottom of the tube. Allow sample to cool to room temperature before using. Pipette sample immediately after cooling to room temp.
- 8. Load the Hyb Chamber inserts containing BeadChips into the Hyb Chamber.
- 9. Dispense assay sample onto the large sample port of each array:
 - For the 6-Sample chip, add 30 µl.
 - For the 8-Sample or 12-Sample chip, add 15 µl.
- 10. Seal lid onto the Hyb Chamber carefully to avoid dislodging the Hyb Chamber insert(s).
- 11. Incubate for 16-20 hours at 58°C with rocker speed at 5.

Next step

Proceed to **Wash and Stain BeadChip**.



Whole-Genome Gene Expression with IntelliHyb™ Seal

Experienced User Card

Wash and Stain BeadChip

Estimated processing time: ~ 65 minutes

Prepare for wash steps. Remove BeadChips from the overnight hybridization. Remove BeadChip coverseals. Wash, block, and stain BeadChips.

New Materials	Quantity
High-Temp Wash Buffer	500 ml
Wash E1BC	2.5 L
Block E1 Buffer	6 ml/chip
Streptavidin-Cy3	2 µl of 1 mg/ml stock per chip
100% Ethanol	250 ml
Pyrex No. 3140 Beaker	1

Preparation

Prepare for High-Temp Wash & Overnight Incubation

- 1. Prepare 1X High-Temp Wash buffer (add 50 ml 10X stock to 450 ml RNase-free water).
- 2. Place waterbath insert into heat block, and add 500 ml prepared 1X High-Temp Wash buffer.
- 3. Set heat block temp to 55°C and pre-warm High-Temp Wash buffer to that temperature.
- 4. Close heat block lid and leave overnight.

Next Day

- Make the Wash E1BC solution (add 7.5 ml E1BC buffer to 2.5 L RNase-free water).
- Pre-warm Block E1 buffer (4 ml/chip) to room temperature.
- Prepare Block E1 buffer (2 ml/chip) with streptavidin-Cy3 (2 µl of 1 mg/ml stock per chip). Use a single conical tube for all BeadChips. Store in dark until detection step.
- Place 1.5 L of diluted Wash E1BC buffer in a Pyrex No. 3140 beaker.

Steps

Seal Removal

APPENDIX 1: continued



Whole-Genome Gene Expression with IntelliHyb™ Seal

Experienced User Card

- 1. Remove the Hyb Chamber from the oven and disassemble.



If you are processing multiple chambers, remove them from the oven and process the BeadChips one at a time. Process all BeadChips in the first chamber as described in steps 2–5 below, then remove second chamber from the oven, process all of its BeadChips, and so on until all chambers are processed.

- 2. Using powder-free gloved hands, remove all BeadChips from the Hyb Chamber and submerge them face up at the bottom of the beaker.
- 3. Using powder-free gloved hands, remove the coverseal from the first BeadChip. Ensure that the entire BeadChip remains submerged during removal.
- 4. Using tweezers or powder-free gloved hands, transfer the peeled BeadChip into the slide rack submerged in the staining dish containing 250 ml Wash E1BC solution.
- 5. Repeat steps 3 and 4 for all BeadChips from the same Hyb Chamber.
- 6. Use the slide rack handle to transfer the rack into the Hybex Waterbath insert containing High-Temp Wash buffer.

High-Temp Wash

- Incubate static for 10 minutes with the Hybex lid closed.

1st Room-Temp Wash

- 1. During the 10-minute High-Temp Wash buffer incubation, add fresh 250 ml Wash E1BC solution to a clean staining dish.
- 2. After the 10-minute High-Temp Wash buffer incubation is complete, immediately transfer the slide rack into the staining dish containing E1BC.
- 3. Briefly agitate using rack, then shake on orbital shaker for 5 minutes at the highest speed possible without allowing solution to splash out of dish.


Ethanol Wash

- 1. Transfer rack to a clean staining dish containing 250 ml 100% Ethanol (use fresh from Ethanol source bottle).
- 2. Briefly agitate using rack handle, then shake on orbital shaker for 10 minutes.

2nd Room-Temp Wash

- 1. Transfer rack to a clean staining dish containing fresh 250 ml Wash E1BC solution.

APPENDIX 1: continued

	<p>Whole-Genome Gene Expression with IntelliHyb™ Seal Experienced User Card</p>
	<p><input type="checkbox"/> 2. Briefly agitate using rack handle, then shake on orbital shaker for 2 minutes.</p>
	<p>Block</p>
	<p><input type="checkbox"/> 1. Pipette 4 ml Block E1 buffer into the wash tray(s). <input type="checkbox"/> 2. Transfer the BeadChip, face up, into BeadChip wash tray(s) on rocker. <input type="checkbox"/> 3. Rock at medium speed for 10 minutes.</p>
	<p>Detect</p>
	<p><input type="checkbox"/> 1. Pipette 2 ml Block E1 buffer + streptavidin-Cy3 into fresh wash tray(s). <input type="checkbox"/> 2. Transfer the BeadChip, face up, into wash tray(s) on rocker. <input type="checkbox"/> 3. Place cover on tray and rock at medium speed for 10 minutes.</p>
	<p>3rd Room-Temp Wash</p>
	<p><input type="checkbox"/> 1. Add 250 ml of Wash E1BC solution to a clean staining dish. <input type="checkbox"/> 2. Transfer the BeadChip to the slide rack submerged in the staining dish. <input type="checkbox"/> 3. Briefly agitate using rack, and then shake at room temperature on orbital shaker for 5 minutes.</p>
	<p>Dry</p>
	<p><input type="checkbox"/> 1. Prepare centrifuge with plateholders, paper towels, and balance rack. Set speed to 275 relative centrifugal force. <input type="checkbox"/> 2. Centrifuge the rack of BeadChips at room temperature for 4 minutes. If processing only one slide rack, redistribute the BeadChips between two racks, or counterbalance it with another rack loaded with an equal number of used BeadChips to maintain centrifuge balance. <input type="checkbox"/> 3. Store dry chips in slide box until scanned.</p>

APPENDIX 2: MASCOT search results from wide-range 2DE analysis SSP are spot identification numbers assigned by PDQuest. Next to the protein name are total scores assigned by mascot, the number of peptides matched in MASCOT, the species, the theoretical mass (*Mr*) and *pI* of the full length protein, the % coverage of the peptides matched. Only peptides with ion scores over 35 are shown in the matched peptides column, and the corresponding ion score for these are also shown. The shaded rows indicate the final MASCOT score, number of matched peptides and the coverage as calculated from the peptides with scores over 35.

SSP		Protein Name	MASCOT Score	Queries matched	Species	Theoretical		coverage	Matched peptides	MASCOT ion Score
						Mr	pI			
1206	MLRV_RAT	Myosin regulatory light chain 2, ventricular/cardiac muscle isoform	142	8	Rat	18868	4.86	45%	K.GADPEETILNAFK.V	57
1206	MLRV_RAT	Myosin regulatory light chain 2	57	1	Rat	18868	4.86	8%		
1207	NNTM_MOUSE	NAD(P) transhydrogenase, mitochondrial precursor	58	1	Mouse	113780	8.4	2%	R.SLGVGYAAVDNPIFYKPNTAMLLGDAK.K (M)	58
1207	NNTM_MOUSE	NAD(P) transhydrogenase	58	1	Mouse	113780	8.4	2%		
1213	MLRV_RAT	Myosin regulatory light chain 2, ventricular/cardiac muscle isoform	211	7	Rat	18868	4.86	43%	K.GADPEETILNAFK.V	70
									K.NLVHIITHGEEKD.-	38
1213	MLRV_RAT	Myosin regulatory light chain 2,	108	2	Rat	18868	4.86	16%		
1223		Cationic trypsin precursor peptides only								
1223		NO RESULT								
1224		Cationic trypsin precursor peptides only								
1224		NO RESULT								
1225	ATPB_RAT	ATP synthase subunit beta, mt precursor	203	6	Rat	56318	5.19	10%	R.AIAELGIYPVAVDPLDTSR.I	87
									R.IMDPNIVGSEHYDVAR.G (M)	108
1225	ATPB_RAT	ATP synthase subunit beta	192	2	Rat	56318	5.19	7%		
1226	ATPB_RAT	ATP synthase subunit beta, mt precursor	50	1	Rat	56318	5.19	3%	R.AIAELGIYPVAVDPLDTSR.I	50
	CCS_RAT	Copper chaperone for superoxide dismutase	33	1	Rat	28871	5.79	4%	R.QAVLKGMGSSQLK.N (M)	33
1226	ATPB_RAT	ATP synthase subunit beta, mt precursor	55	1	Rat	56318	5.19	3%	R.IMDPNIVGSEHYDVAR.G	55
1226	ATPB_RAT	ATP synthase subunit beta	105	2	Rat	56318	5.19	6%		
1248	TNNT2_RAT	Troponin T, cardiac muscle	64	2	Rat	35709	4.95	8%	R.LFMPNLVPPK.I (M)	59
1248	TNNT2_RAT	Troponin T, cardiac muscle	59	1	Rat	35709	4.95	3%		
1301	CASA1_BOVIN	Alpha-S1-casein precursor	149	7	Bovine	24513	4.98	15%	R.FFVAPFPEVFGK.E	38
									R.YLGYLEQLLR.L	78
1301	CASA1_BOVIN	Alpha-S1-casein	116	2	Bovine					
1304	TPM1_RAT	Tropomyosin alpha-1 chain	159	5	Rat	32661	4.69	13%	K.ATDAEADVASLNR.R	74
									K.HIAEDADR.K	44
	TBB2C_RAT	Tubulin beta-2C chain	110	3	Rat	49769	4.79	6%	R.INVYYNEATGGK.Y	59
									R.AVLVDLEPGTMDSVR.S (M)	51
1304	TPM1_RAT	Tropomyosin alpha-1 chain	118	2	Rat	32661	4.69	7%		
1304	TBB2C_RAT	Tubulin beta-2C chain	110	2	Rat	49769	4.79	6%		
1307	ATPB_RAT	ATP synthase subunit beta, mt precursor	233	1	Rat	56318	5.19	5%	R.VALTGLTVAEYFRDQEGQDVLLFIDNIFR.F	233
	TNNT2_RAT	Troponin T, cardiac muscle	80	2	Rat	35709	4.95	8%	R.DAEDGPVEDSKPKPSR.L	54
1307	ATPB_RAT	ATP synthase subunit beta	233	1	Rat	56318	5.19	5%		
1307	TNNT2_RAT	Troponin T, cardiac muscle	54	1	Rat	35709	4.95	5%		
1320	TPM1_RAT	Tropomyosin alpha-1 chain	58	1	Rat	32661	4.69	4%	K.ATDAEADVASLNR.R	58
	TPM2_RAT	Tropomyosin beta chain	58	1	Rat	32817	4.66	4%	K.ATDAEADVASLNR.R	58
	TBB2C_RAT	Tubulin beta-2C chain	33	1	Rat	49769	4.79	2%	R.INVYYNEATGGK.Y	33
1320		Tropomyosin (general)	58	1	Rat	32661	4.69	4%		

APPENDIX 2: continued

SSP		Protein Name	MASCOT Score	Queries matched	Species	Theoretical		coverage	Matched peptides	MASCOT ion Score
						Mr	PI			
1424	ATPB_RAT	ATP synthase subunit beta, mitochondrial precursor	131	2	Rat	56318	5.19	8%	R.AIAELGIYPAVDPLDSTR.I K.SLQDIIAALGMDLSEEDKLTVSR.A (M)	79 52
1424	ATPB_RAT	ATP synthase subunit beta	131	2	Rat	56318	5.19	8%		
1429		Cationic trypsin precursor peptides only								
1429		NO RESULT								
1430	1433E_RAT	14-3-3 protein epsilon	75	2	Rat	29155	4.63	8%	K.VAGMDVELTVEER.N (M)	67
1430	1433E_RAT	14-3-3 protein epsilon	123	5	Rat	29155	4.63	22%	R.QMVEVELK.L (M) K.AAFDDAIAELDTLSEESYKSTLIMQLLR.D (M)	44 53
1430	1433E_RAT	14-3-3 protein epsilon	164	3	Rat	29155	4.63	20%		
1705		Cationic trypsin precursor peptides only								
1705		NO RESULT								
2119	QCR6_RAT	Cytochrome b-c1 complex subunit 6, mitochondrial precursor	146	3	Rat	10417	4.9	28%	R.SQTEEDCTEELDFLHAR.D (C)	131
2119	QCR6_RAT	Cytochrome b-c1 complex subunit 6	131	1	Rat	10417	4.9	20%		
2226	1433T_RAT	14-3-3 protein theta	47	1	Rat	27761	4.69	9%	R.SICTTVLELLDKYLIANATNPESK.V (C)	47
	HSP7C_RAT	Heat shock cognate 71 kDa protein	60	2	Rat	70827	5.37	2%	R.LSKEDIER.M	38
2226	1433T_RAT	14-3-3 protein theta	47	1	Rat	27761	4.69	9%		
2226	HSP7C_RAT	Heat shock cognate 71 kDa protein	60	1	Rat	70827	5.37	1%		
2443	ATPB_RAT	ATP synthase subunit beta, mitochondrial precursor	121	2	Rat	56318	5.19	6%	R.AIAELGIYPAVDPLDSTR.I	91
2443	ATPB_RAT	ATP synthase subunit beta	91	1	Rat	56318	5.19	3%		
2546	CAP1_RAT	Adenylyl cyclase-associated protein 1	88	2	Rat	51556	7.16	8%	K.LSDLLAPISEQIQEVITFR.E	55
2546	CAP1_RAT	Adenylyl cyclase-associated protein 1	55	1	Rat	51556	7.16	4%		
2607		Cationic trypsin precursor peptides only								
2607		NO RESULT								
2609	ATPB_RAT	ATP synthase subunit beta, mitochondrial precursor	456	9	Rat	56318	5.19	12%	R.TIAMDGTEGLVR.G (M) R.IMNVIGEPIDER.G (M) K.TVLIMELINNVAK.A (M) R.VALTGLTVAEYFR.D R.VALTGLTVAEYFRDQEGQDVLFFIDNIFR.F R.DQEGQDVLFFIDNIFR.F	65 54 56 60 136 86
2609	ATPB_RAT	ATP synthase subunit beta	457	6	Rat	56318	5.19	12%		
2616	RSSA_RAT	40S ribosomal protein SA	50	1	Rat	32803	4.8	4%	K.FAAATGATPIAGR.F	50
2616	RSSA_RAT	40S ribosomal protein SA	50	1	Rat	32803	4.8	4%		
2624		Cationic trypsin precursor peptides only								
2624		NO RESULT								
2626	ATPB_RAT	ATP synthase subunit beta, mitochondrial precursor	197	4	Rat	56318	5.19	13%	R.TIAMDGTEGLVR.G (M) R.IMNVIGEPIDER.G (M) R.AIAELGIYPAVDPLDSTR.I	45 50 72
2626	ATPB_RAT	ATP synthase subunit beta	167	3	Rat	56318	5.19	8%		
2701	SPA3K_RAT	Serine protease inhibitor A3K precursor	573	9	Rat	46532	5.31	25%	K.IAELFSELDER.T R.TSMVLVNYLLFK.G (M) K.FSISTDYNLEEVLPGLGIR.K R.KIFSQQADLSR.I K.IFSQQADLSR.I K.AVLVDVDETEGEGAAATAVTAALK.S K.IAELFSDLER.T R.TSMVLVNYLLFK.G (M) R.LGGEVSVACK.L (C)	47 60 135 45 59 168 54 60 54
	SPA3L_RAT	Serine protease inhibitor A3L precursor	134	4	Rat	46248	5.48	15%		
	FETUA_RAT	Alpha-2-HS-glycoprotein precursor	54	1	Rat	37958	6.05	3%		
2701	SPA3K_RAT	Serine protease inhibitor A3K	514	6	Rat	46532	5.31	18%		
2701	FETUA_RAT	Alpha-2-HS-glycoprotein	54	1	Rat	37958	6.05	3%		

APPENDIX 2: continued

SSP		Protein Name	MASCOT Score	Queries matched	Species	Theoretical		coverage	Matched peptides	MASCOT ion Score
						Mr	PI			
2712	ATPB_RAT	ATP synthase subunit beta, mitochondrial precursor	733	14	Rat	56318	5.19	30%	R.TIAMDGTEGLVR.G (M) R.IMNVIGEPIDER.G (M) K.TVLIMELINNAK.A (M) R.VALTGLTVAEYFR.D R.VALTGLTVAEYFRDQEGQDVLLFIDNIFR.F R.DQEGQDVLLFIDNIFR.F R.AIAELGIYPAVDPLDSTR.I K.SLQDIIAALGMDLSEEDKLTVSR.A (M)	55 59 68 100 158 102 75 90
2712	ATPB_RAT	ATP synthase subunit beta	707	8	Rat	56318	5.19	26%		
2722		Cationic trypsin precursor peptides only								
2722		NO RESULT								
3208	ATPB_RAT	ATP synthase subunit beta, mitochondrial precursor	55	2	Rat	56318	5.19	5%	K.VLDSGAPIKIPVGPETLGR.I	51
3208	ATPB_RAT	ATP synthase subunit beta	51	1	Rat	56318	5.19	4%		
3209	ATPB_RAT	ATP synthase subunit beta, mitochondrial precursor	176	5	Rat	56318	5.19	13%	R.TIAMDGTEGLVR.G (M) R.IMNVIGEPIDER.G (M)	77 67
3209	ATPB_RAT	ATP synthase subunit beta	144	2	Rat	56318	5.19	5%		
3228	MLRV_RAT	Myosin regulatory light chain 2, ventricular/cardiac muscle isoform	163	4	Rat	18868	4.86	32%	K.EAFTIMDQNR.D (M) R.DGFIDKNDLR.D R.VNVKNEEIDEMIK.E (M)	34 65 36
3228	MLRV_RAT	Myosin regulatory light chain 2	135	3	Rat	18868	4.86	20%		
3305	MYL3_RAT	Myosin light chain 3	334	7	Rat	22142	5.03	33%	R.ALGQNPTQAEVLR.V K.MMDFETFLPMLQHISK.N 3 (M) K.DTGTYEDEFVEGLR.V R.VFDKEGNGTVMGAELR.H (M) R.HVLATLGER.L	88 72 57 42 75
3305	MYL3_RAT	Myosin light chain 3	334	5	Rat	22142	5.03	33%		
3322		Cationic trypsin precursor peptides only								
3322		NO RESULT								
3433	ATPB_RAT	ATP synthase subunit beta, mitochondrial precursor	478	9	Rat	56318	5.19	28%	R.LVLEVAQHLGESTVR.T R.TIAMDGTEGLVR.G (M) R.IMNVIGEPIDER.G (M) R.IMNVIGEPIDERGPIK.T (M) K.TVLIMELINNAK.A (M) R.VALTGLTVAEYFRDQEGQDVLLFIDNIFR.F	72 79 63 46 50 126
3433	ATPB_RAT	ATP synthase subunit beta	436	6	Rat	56318	5.19	18%		
3441	ALBU_RAT	Serum albumin precursor	46	1	Rat	68686	6.09	2%	K.DVFLGTFLYEYSR.R	46
3441	ALBU_RAT	Serum albumin	46	1	Rat	68686	6.09	2%		
3518	GRP75_RAT	Stress-70 protein, mitochondrial precursor	149	7	Rat	73812	5.97	8%	R.QAASSLQOASLK.L	85
3518	GRP75_RAT	Stress-70 protein	85	1	Rat	73812	5.97	2%		
3523	ATPB_RAT	ATP synthase subunit beta, mitochondrial precursor	281	4	Rat	56318	5.19	14%	K.VALVYQGMNEPPGAR.A (M) R.VALTGLTVAEYFRDQEGQDVLLFIDNIFR.F R.AIAELGIYPAVDPLDSTR.I R.IMDPNIVGSEHYDVAR.G (M)	82 36 56 107
3523	ATPB_RAT	ATP synthase subunit beta	280	4	Rat	56318	5.19	14%		

APPENDIX 2: continued

SSP		Protein Name	MASCOT Score	Queries matched	Species	Theoretical		coverage	Matched peptides	MASCOT ion Score
						Mr	PI			
3526	K2C5_RAT	Keratin, type II cytoskeletal 5	127	5	Rat	61788	7.6	5%	R.SLDLDSIIAEVK.A	76
	HSP7C_RAT	Heat shock cognate 71 kDa protein	114	3	Rat	70827	5.37	5%	R.TLSSSTQASIEIDSLYEGIDFYTSITR.A	85
	H4_RAT	Histone H4 [Contains: Osteogenic growth peptide	59	1	Rat	11360	11.36	9%	R.ISGLIYEETR.G	59
3526	HSP7C_RAT	Heat shock cognate 71 kDa protein	85	1	Rat	70827	5.37	2%		
3526	K2C5_RAT	Keratin, type II cytoskeletal 5	76	1	Rat	61788	7.6	4%		
3526	H4_RAT	Histone H4 [Contains: Osteogenic growth peptide	59	1	Rat	11360	11.36	9%		
3622	ATPB_RAT	ATP synthase subunit beta, mitochondrial precursor	824	16	Rat	56318	5.19	37%	R.TIAMDGTEGLVR.G (M)	57
									R.IMNVIGEPIDER.G (M)	67
									K.QFAPIHAEAPEFIEMSVQEILVTGIK.V (M)	79
									K.TVLIMELINNVAKA (M)	73
									R.VALTGLTVAEYFR.D	115
									R.VALTGLTVAEYFRDQEGQDVLFDNIFR.F	156
									R.DQEGQDVLFDNIFR.F	101
									R.FTQAGSEVSALLGR.I	87
									R.AIAELGIYPAVDPLDSTSR.I	79
									K.SLQDIIAILGMDELSEEDKLTVSR.A (M)	122
									R.FLSQPPQVAEVEFTGHMGK.L	82
	DESM_RAT	Desmin	43	2	Rat	53424	5.21	4%	R.TSGGAGGLGSLR.A	43
3622	ATPB_RAT	ATP synthase subunit beta	1018	11	Rat	56318	5.19	35%		
3622	DESM_RAT	Desmin	43	1	Rat	53424	5.21	3%		
3626	ATPB_RAT	ATP synthase subunit beta, mitochondrial precursor	723	15	Rat	56318	5.19	30%	R.TIAMDGTEGLVR.G (M)	69
									K.VLDSGAPIKIPVGPETLGR.I	97
									R.IMNVIGEPIDER.G (M)	70
									K.TVLIMELINNVAKA (M)	73
									R.VALTGLTVAEYFR.D	52
									R.VALTGLTVAEYFRDQEGQDVLFDNIFR.F	97
									R.FTQAGSEVSALLGR.I	84
									R.AIAELGIYPAVDPLDSTSR.I	80
									K.SLQDIIAILGMDELSEEDKLTVSR.A (M)	89
3626	ATPB_RAT	ATP synthase subunit beta	711	9	Rat	56318	5.19	29%		
3627	DESM_RAT	Desmin	486	10	Rat	53424	5.21	23%	R.TSGGAGGLGSLR.A	63
									R.APSYGAGELLDLFLADAVNQEFLATR.T	80
									R.FLEQQNAALAAEVNR.L	118
									R.VAELYEEEMR.E (M)	49
									R.QVEVLTNQR.A	50
									R.ADVDAATLAR.I	54
									R.INLPIQTFALSALNFR.E	49
3627	DESM_RAT	Desmin	463	7	Rat	53424	5.21	20%		
3629	ATPB_RAT	ATP synthase subunit beta	193	7	Rat	56318	5.19	15%	K.VALVYQGMNEPPGAR.A	62
									R.IMDPNIVGSEHYDVAR.G	71
	ACTA_RAT	Actin, aortic smooth muscle	82	3	Rat	41982	5.23	10%	K.AGFAGDDAPR.A	47
3629	ATPB_RAT	ATP synthase subunit beta	125	4	Rat	56318	5.19	10%	K.VVDLLAPYAK.G	44
									R.AIAELGIYPAVDPLDSTSR.I	60
3629	ATPB_RAT	ATP synthase subunit beta	237	4	Rat	56318	5.19	11%		
3629	ACTA_RAT	Actin, aortic smooth muscle	47	1	Rat	41982	5.23	3%		

APPENDIX 2: continued

SSP		Protein Name	MASCOT Score	Queries matched	Species	Theoretical		coverage	Matched peptides	MASCOT ion Score
						Mr	PI			
3632	ATPB_RAT	ATP synthase subunit beta, mitochondrial precursor	239	4 (4)	Rat	56318	5.19	11%	R.IMNVIGEPIDER.G (M)	42
									K.VALVYGGMNEPPGAR.A (M)	36
									R.AIAELGIYPAVDPLDSTSR.I	60
									R.IMDPNIVGSEHYDVAR.G (M)	101
									K.SLQDIIAALGMDELSEEDKLTVSR.A (M)	75
	ATPB_RAT	ATP synthase subunit beta, mitochondrial precursor	114	4 (1)	Rat	56318	5.19	13%		
3632	ATPB_RAT	ATP synthase subunit beta	314	5	Rat	56318	5.19	16%		
3636	ATPB_RAT	ATP synthase subunit beta, mitochondrial precursor	202	11	Rat	56318	5.19	27%	R.IMNVIGEPIDER.G	39
									R.IMDPNIVGSEHYDVAR.G	56
									R.FLSQPFQVAEVFTGHMGK.L	39
3636	ATPB_RAT	ATP synthase subunit beta, mitochondrial precursor	196	8	Rat	56318	5.19	17%	K.VLDSGAPIKIPVGPETLGR.I	37
									R.FTQAGSEVSALLGR.I	55
3636	ATPB_RAT	ATP synthase subunit beta	226	5	Rat	56318	5.19	15%		
3638		Cationic trypsin precursor peptides only								
3638		NO RESULT								
3706	ATPB_RAT	ATP synthase subunit beta, mitochondrial precursor	246	4	Rat	56318	5.19	10%	R.TIAMDGTEGLVR.G (M)	71
									K.VALVYGGMNEPPGAR.A (M)	76
									R.AIAELGIYPAVDPLDSTSR.I	68
3706	ATPB_RAT	ATP synthase subunit beta	215	3	Rat	56318	5.19	9%		
4207	MYH6_RAT	Myosin-6	278	9	Rat	223488	5.54	3%	R.VVDSLQTSLEAETR.S	73
									R.SRNEALR.V	35
									R.NTLLQAELEELR.A	54
									R.NTLLQAELEELRAVVEQTER.S	117
	MYH3_RAT	Myosin-3	35	2	Rat	223720	5.64	0%	R.SRNEAIR.L	35
4207	MYH6_RAT	Myosin-6	279	4	Rat	223370	5.59	3%		
4217	ACTC_RAT	Actin, alpha cardiac muscle 1	219	3	Rat	41992	5.23	10%	K.SYELPDGQVITIGNER.F	114
									K.EITALAPSTMK.I (M)	36
									K.QEYDEAGPSIVHR.K	68
		Actin, alpha skeletal muscle	219	3	Rat	42024	5.23	10%	K.SYELPDGQVITIGNER.F	114
									K.EITALAPSTMK.I (M)	36
									K.QEYDEAGPSIVHR.K	68
		Actin, aortic smooth muscle	217	3	Rat	41982	5.23	10%	K.SYELPDGQVITIGNER.F	114
									K.EITALAPSTMK.I (M)	36
									K.QEYDEAGPSIVHR.K	68
4217	ACTC_RAT	Actin, alpha cardiac muscle 1 (or Actin, alpha skeletal muscle)	218	3	Rat	~42000	5.23	10%		
4235	ATPB_RAT	ATP synthase subunit beta, mitochondrial precursor	111	3	Rat	56318	5.19	4%	R.TIAMDGTEGLVR.G (M)	69
									R.IMNVIGEPIDER.G (M)	41
4235	ATPB_RAT	ATP synthase subunit beta	110	2	Rat	56318	5.19	4%		
4244	ATPB_RAT	ATP synthase subunit beta, mitochondrial precursor	86	1	Rat	56318	5.19	3%	R.AIAELGIYPAVDPLDSTSR.I	86
	MYL3_RAT	Myosin light chain 3	35	1	Rat	22142	5.03	6%	R.ALGQNPTQAEVLR.V	35
4244	ATPB_RAT	ATP synthase subunit beta	86	1	Rat	56318	5.19	3%		
4244	MYL3_RAT	Myosin light chain 3	35	1	Rat	22142	5.03	6%		
4329	ATPB_RAT	ATP synthase subunit beta, mitochondrial precursor	69	1	Rat	56318	5.19	2%	R.TIAMDGTEGLVR.G (M)	69
4329	ATPB_RAT	ATP synthase subunit beta	69	1	Rat	56318	5.19	2%		

APPENDIX 2: continued

SSP		Protein Name	MASCOT Score	Queries matched	Species	Theoretical		coverage	Matched peptides	MASCOT ion Score
						Mr	PI			
4406	ATPB_RAT	ATP synthase subunit beta, mitochondrial precursor	348	8	Rat	56318	5.19	16%	R.VALTGLTVAEYFRDQEGQDVLLFIDNIFR.F R.AIAELGIYPAVDPLDSTSR.I K.SLQDIILGMDLSEEDKLTVSR.A (M) K.SYELPDGQVITIGNER.F	173 69 44 107
	ACTC_RAT	Actin, alpha cardiac muscle 1 (or ACTA, ACTB, ACTG, ACTH and ACTS)	120	1	Rat	41992	5.23	7%		
4406		ATP synthase subunit beta	286	3	Rat	56318	5.19	15%		
4406		Actin, alpha cardiac muscle 1	107	1	Rat	41992	5.23	4%		
4418		Cationic trypsin precursor peptides only								
4418		NO RESULT								
4511		Cationic trypsin precursor peptides only								
4511		NO RESULT								
4513		Cationic trypsin precursor peptides only								
4513		NO RESULT								
4521	LDHA_RAT	L-lactate dehydrogenase A chain	72	1	Rat	36427	8.45	3%	R.VIGSGCNLDSAR.F (C)	72
	LDHB_RAT	L-lactate dehydrogenase B chain	72	1	Rat	36589	5.7	3%	R.VIGSGCNLDSAR.F (C)	72
4521	LDHA_RAT	L-lactate dehydrogenase (or LDHB)	72	1	Rat	36427	8.45	3%		
4522		Cationic trypsin precursor peptides only								
4522		NO RESULT								
4523	TBA4A_RAT	Tubulin alpha-4A chain	225	4	Rat	49892	4.95	14%	R.AVFVDLEPTVIDEIR.N R.NLDIERPTYTNLNR.L R.FDGALNVDLTEFQTNLVPYPR.I	83 51 57
4523	TBA4A_RAT	Tubulin alpha-4A chain	191	3	Rat	49892	4.95	11%		
4525		Cationic trypsin precursor peptides only								
4525		NO RESULT								
4702	GRP75_RAT	Stress-70 protein, mitochondrial	440	23	Rat	73812	5.97	27%	K.NAVITVPAYFNDSQR.Q K.DAGQISGLNVLR.V R.VINEPTAAALAYGLDK.S K.SQVFSTAADGQTOVEIK.V K.LLGOFTLIGIPPAPR.G R.VEAVNMAEGIIHDTETK.M	69 79 78 58 52 110
4702	GRP75_RAT	Stress-70 protein, mitochondrial	383	14	Rat	73812	5.97	19%	R.AQFEGIVTDLIKR.T K.SDIGEVILVGGMTR.M K.VQQTVDLDFGR.A R.QAASSLQQASLK.L	77 73 60 83
4702	GRP75_RAT	Stress-70 protein	739	10	Rat	73812	5.97	21%		
4703		Cationic trypsin precursor peptides only								
4703		NO RESULT								
4722		Cationic trypsin precursor peptides only								
4722		NO RESULT								
4734		Cationic trypsin precursor peptides only								
4734		NO RESULT								
4740		Cationic trypsin precursor peptides only								
4740		NO RESULT								

APPENDIX 2: continued

SSP		Protein Name	MASCOT Score	Queries matched	Species	Theoretical		coverage	Matched peptides	MASCOT ion Score
						Mr	PI			
4741	DESM_RAT	Desmin	252	8	Rat	53424	5.21	25%	R.TSGGAGGLGSLR.A	54
									R.QVEVLTNQR.A	50
	ALBU_RAT	Serum albumin precursor	205	4	Rat	68686	6.09	8%	K.DVFLGTFLYEYSR.R	57
									R.LPCVEDYLSAILNR.L (C)	102
4741	DESM_RAT	Desmin	281	9	Rat	53424	5.21	24%	R.APSYGAGELLDVSLADAVNQEFATR.T	93
									R.FLEQQNAALAAEVNR.L	107
									R.DGEVVSEATQQHEVL.-	35
4741	DESM_RAT	Desmin	339	5	Rat	53424	5.21	17%		
4741	ALBU_RAT	Serum albumin	159	2	Rat	68686	6.09	4%		
5311	PRDX3_RAT	Thioredoxin-dependent peroxide reductase, mitochondrial precursor	89	2	Rat	28277	7.14	16%	R.GLFIIDPNGVIK.H	37
									K.AFQFVETHGEVCPANWTPESPTIKPSPTASK.E (C)	52
5311	PRDX3_RAT	Thioredoxin-dependent peroxide reductase	89	2	Rat	28277	7.14	16%		
5315		Cationic trypsin precursor peptides only								
5315		NO RESULT								
5408	PRDX6_RAT	Peroxioredoxin-6	430	11	Rat	24803	5.64	51%	M.PGGLLLGDEAPNFEANTTIGHIR.F	64
									R.DFTPVCTTELGR.A (C)	40
									K.LIALSIDSVEDHFAWSK.D	73
									R.VVFIFGPDK.K	36
									K.LSILYPATTGR.N	52
									R.VVDSLQLTASNVPVATPVDWK.K	86
5408	PRDX6_RAT	Peroxioredoxin-6	202	10	Rat	24803	5.64	34%	R.NFDEILR.V	37
5408	PRDX6_RAT	Peroxioredoxin-6	388	7	Rat	24803	5.64	44%		
5422		Cationic trypsin precursor peptides only								
5422		NO RESULT								
5501		Cationic trypsin precursor peptides only								
5501		NO RESULT								
5601		Cationic trypsin precursor peptides only								
5601		NO RESULT								
5618		Cationic trypsin precursor peptides only								
5618		NO RESULT								
5715	ALBU_RAT	Serum Albumin precursor	472	7	Rat	68648	5.75	14%	K.GLVLIAFSQYLQK.C	76
									K.LVQEVTDFAKT	56
									K.DVFLGTFLYEYSR.R	80
									K.APQVSTPTLVEAAR.N	70
									R.LPCVEDYLSAILNR.L (C)	97
5715	ALBU_RAT	Serum Albumin	379	5	Rat	68686	6.09	11%		
5805		Cationic trypsin precursor peptides only								
5805		NO RESULT								
6123	UBE2N_RAT	Ubiquitin-conjugating enzyme E2 N	216	6 (3)	Rat	17113	6.13	19%	R.LLAEPVPGIK.A	47
									R.LLAEPVPGIKAEPDESNA.R.Y	105
									K.SNEAQAIETAR.A	64
	KAP0_RAT	cAMP-dependent protein kinase type I-alpha regulatory subunit	44	1	Rat	43068	5.27	4%	R.LGPSDYFGEIALLMNRPR.A (M)	44
6123	UBE2N_RAT	Ubiquitin-conjugating enzyme E2 N	216	3	Rat	17113	6.13	19%		
6123	KAP0_RAT	cAMP-dependent protein kinase type I-alpha regulatory subunit	44	1	Rat	43068	5.27	4%		

APPENDIX 2: continued

SSP	Protein Name	MASCOT Score	Queries matched	Species	Theoretical		coverage	Matched peptides	MASCOT ion Score
					Mr	PI			
6413	Cationic trypsin precursor peptides only								
6413	NO RESULT								
6424	LDHB_RAT L-lactate dehydrogenase B chain	127	4	Rat	36589	5.7	9%	R.VIGSGCNLDSAR.F (C)	85
6424	LDHB_RAT L-lactate dehydrogenase B chain	85	1	Rat	36589	5.7	4%		
6425	LDHB_RAT L-lactate dehydrogenase B chain	105	4	Rat	36589	5.7	10%	R.VIGSGCNLDSAR.F (C)	77
6425	LDHB_RAT L-lactate dehydrogenase B chain	77	1	Rat	36589	5.7	6%		
6533	MYOZ2_MOUSE Myozenin-2	44	1		29743	8.53	4%	R.FLAFANPLSGR.R	44
6533	NO RESULT								
6538	Cationic trypsin precursor peptides only								
6538	NO RESULT								
6545	Cationic trypsin precursor peptides only								
6545	NO RESULT								
6603	ALBU_RAT Serum albumin precursor	134	3	Rat	68686	6.09	6%	K.APQVSTPTLVEAAR.N	43
								R.LPCVEDYLSAILNR.L (C)	61
	HBB1_RAT Hemoglobin subunit beta-1	108	3	Rat	15969	7.88	15%	K.VNPDDVGGGEALGR.L	55
								R.LLVVYPWTQR.Y	52
	MYG_RAT Myoglobin	63	2	Rat	17146	7.83	9%	K.HGCTVLTALGTILKK.K (C)	49
6603	ALBU_RAT Serum albumin	104	2	Rat	68686	6.09	5%		
6603	HBB1_RAT Hemoglobin subunit beta-1	107	2	Rat	15969	7.88	15%		
6603	MYG_RAT Myoglobin	49	1	Rat	17146	7.83	9%		
6616	Cationic trypsin precursor peptides only								
6616	NO RESULT								
6636	HSP7C_RAT Heat shock cognate 71 kDa protein	46	1	Rat	70827	5.37	2%	K.STAGDTHLGGEDFDNR.M	46
	HSP72_RAT Heat shock-related 70 kDa protein 2	46	1	Rat	69599	5.51	2%	K.STAGDTHLGGEDFDNR.M	46
6636	HSP7C_RAT Heat shock cognate 71Da OR HSP72	46	1	Rat	70827	5.37	2%		
6732	Cationic trypsin precursor peptides only								
6732	NO RESULT								
6746	Cationic trypsin precursor peptides only								
6746	NO RESULT								
6813	EZRI_RAT Ezrin	152	8	Rat	69348	5.83	11%	K.APDFVFYAPR.L	44
								K.ALQLEEEER.R	40
	ENOA_RAT Alpha-enolase	35	1	Rat	47098	6.16	4%	R.AAVPSGASTGIYEALR.D	35
6813	EZRI_RAT Ezrin	84	2	Rat	69348	5.83	3%		
6813	ENOA_RAT Alpha-enolase	35	1	Rat	47098	6.16	4%		
7110	LEG5_RAT Galectin-5	158	6	Rat	16186	6.17	21%	R.FDENAVVR.N	52
								R.NTQINNSWGPEER.S	47
								R.SLPGSMFISR.G (M)	58
7110	LEG5_RAT Galectin-5	157	3	Rat	16186	6.17	21%		
7111	Cationic trypsin precursor peptides only								
7111	NO RESULT								
7112	NDUS1_RAT NADH-ubiquinone oxidoreductase 75 kDa subunit, mt precursor	124	3	Rat	79362	5.65	3%	K.VGMQIPR.F (M)	54
								K.VVAACAMPVMK.G (C); 2 (M)	48
7112	NDUS1_RAT NADH-ubiquinone oxidoreductase 75 kDa subunit	102	2	Rat	79362	5.65	2%		
7228	CRYAB_RAT Alpha-crystallin B chain	129	7	Rat	20076	6.76	61%	R.QDEHGFSR.E	43
7228	NO RESULT								

APPENDIX 2: continued

SSP		Protein Name	MASCOT Score	Queries matched	Species	Theoretical		coverage	Matched peptides	MASCOT ion Score
						Mr	PI			
7306	ATPA_RAT	ATP synthase subunit alpha, mitochondrial precursor	96	2	Rat	59717	9.22	6%	K.QVAGTMKLELAQYR.E (M)	35
									R.EVAFAQFGSDLDAATQQLLSR.G	60
	NSA2_RAT	Ribosome biogenesis protein NSA2 homolog	36	1	Rat	30019	10.25	2%	R.KPPKYEK.F	36
	ATPA_RAT	ATP synthase subunit alpha, mitochondrial precursor	116	3	Rat	59717	9.22	6%	R.EVAFAQFGSDLDAATQQLLSR.G	94
									K.LKEIVTNFLAGFEP.-	72
	K2C5_RAT	Keratin, type II cytoskeletal (various)	62	1	Rat	61788	7.6	2%	R.SLDLDSIAEVK.A	62
7306	ATPA_RAT	ATP synthase subunit alpha	201	3	Rat	59717	9.22	9%		
7306	K2C5_RAT	Keratin, type II cytoskeletal (various)	62	1	Rat	61788	7.6	2%		
7306	NSA2_RAT	Ribosome biogenesis protein NSA2 homolog	36	1	Rat	30019	10.25	2%		
7323	ECHM_RAT	Enoyl-CoA hydratase, mitochondrial precursor	71	1	Rat	31496	8.39	3%	R.EGMSAFVEKR.K (M)	73
7323	ECHM_RAT	Enoyl-CoA hydratase	71	1	Rat	31496	8.39	3%		
7327		Cationic trypsin precursor peptides only								
7327		NO RESULT								
7508		Cationic trypsin precursor peptides only								
7508		NO RESULT								
7515		Cationic trypsin precursor peptides only								
7515		NO RESULT								
7608	ALBU_RAT	Serum albumin	256	8	Rat	68686	6.09	14%	K.DVFLGTFLYEYSR.R	59
									R.RHPDYSVSLLLR.L	45
									K.TNCELYEK.L (C)	39
									K.QTALAELVK.H	50
7608	ALBU_RAT	Serum albumin	99	4	Rat	68686	6.09	8%	K.APQVSTPTLVEAAR.N	60
7608	ALBU_RAT	Serum albumin	349	5	Rat	68686	6.09	21%		
7612	ALDH2_RAT	Aldehyde dehydrogenase, mitochondrial precursor	96	6	Rat	56453	6.63	12%	R.VVGNPFDSR.T	44
7612		NO RESULT								
7702	HSDL2_RAT	Hydroxysteroid dehydrogenase-like protein 2	73	2	Rat	58307	5.85	4%	R.VDLMMSVNTR.G 2 (M)	40
									R.IVKDLSLDEVVRA	35
7702	HSDL2_RAT	Hydroxysteroid dehydrogenase-like protein 2	75	2	Rat	58307	5.85	4%		
7722	ODP2_RAT	Dihydropolyllysine-residue acetyltransferase component of pyruvate dehydrogenase complex, mitochondrial precursor	239	7	Rat	67123	8.76	9%	K.ILVPEGTR.D	41
									K.AAPAAAAAPPGR.V	47
									R.VAFTPAGVFIDIPISNIR.R	89
									K.GLETIASDVVSLASK.A	51
7722	ODP2_RAT	Dihydropolyllysine-residue acetyltransferase component of pyruvate dehydrogenase complex	228	4	Rat	67123	8.76	9%		
7723	DHSA_RAT	Succinate dehydrogenase [ubiquinone] flavoprotein subunit, mitochondrial	73	1	Rat	71570	6.75	2%	R.LGANSLLDLVWFGR.A	73
7723	DHSA_RAT	Succinate dehydrogenase [ubiquinone] flavoprotein subunit	73	1	Rat	71570	6.75	2%		
7730		Cationic trypsin precursor peptides only								
7730		NO RESULT								
7737		Cationic trypsin precursor peptides only								
7737		NO RESULT								
8128		Cationic trypsin precursor peptides only								
8128		NO RESULT								
8520		Cationic trypsin precursor peptides only								
8520		NO RESULT								
8525		Cationic trypsin precursor peptides only								
8525		NO RESULT								

APPENDIX 2: continued

SSP		Protein Name	MASCOT Score	Queries matched	Species	Theoretical		coverage	Matched peptides	MASCOT ion Score
						Mr	PI			
8526		Cationic trypsin precursor peptides only								
8526		NO RESULT								
8710	WDR1_RAT	WD repeat-containing protein 1	199	13	Rat	66140	6.15	24%	R.NIDNPAVADIYTEHAHQVVAK.Y	41
									R.IAVVGEGR.E	36
									R.LATGSDDNCAAFFEGPPFK.F (C)	35
8710	WDR1_RAT	WD repeat-containing protein 1	130	9	Rat	66140	6.15	19%	K.YAPSGFYASGDISGK.L	45
8710	WDR1_RAT	WD repeat-containing protein 1	157	4	Rat	66140	6.15	11%		
8853	MCCA_RAT	Methylcrotonoyl-CoA carboxylase subunit alpha, mitochondrial	215	6	Rat	79279	6.66	10%	K.QEGIFIGPPSTAIR.D	47
									K.IPLSQEEIPLQGHAFEAR.I	81
									R.TNVDLLR.L	38
8853	MCCA_RAT	Methylcrotonoyl-CoA carboxylase subunit alpha	166	3	Rat	79279	6.66	6%		

APPENDIX 3: MASCOT search results from pH 4.5-5.5 2DE analysis Spot numbers were assigned by Progenesis. Next to the protein name are total scores assigned by mascot, the number of peptides matched in MASCOT, the species, the theoretical mass (*Mr*) and *pI* of the full length protein, the % coverage of the peptides matched. Only peptides with ion scores over 35 are shown in the matched peptides column, and the corresponding ion score for these are also shown. The shaded rows indicate the final MASCOT score, number of matched peptides and the coverage as calculated from the peptides with scores over 35.

	Protein Name	MASCOT Score	Queries matched	Species	Theoretical		coverage	Matched peptides	MASCOT ion Score
					Mr	PI			
	Human keratin and porcine trypsin peptides only								
	NO RESULT								
ATPB_RAT	ATP synthase subunit beta, mitochondrial	197	10	Rat	56318	5.19	14%	R.LVLEVAQHLGESTVR.T R.IMNVIGEPIDER.G K.VVDLLAPYAK.G	71 52 43
ATPB_RAT	ATP synthase subunit beta	166	3	Rat	56318	5.19	7%		
ATPB_RAT	ATP synthase subunit beta, mitochondrial	422	9	Rat	56318	5.19	15%	R.LVLEVAQHLGESTVR.T R.TIAMDGTEGLVR.G K.VLDSGAPIKIPVGPETLGR.I R.IMNVIGEPIDER.G R.IMNVIGEPIDER.G (M) R.IMNVIGEPIDERGPIK.T K.VVDLLAPYAK.G	87 60 78 65 62 44 46
DESM_RAT	Desmin	199	3	Rat	53424	5.21	9%	K.LQEEIQLREEAENLAAFR.A	116
DESM_RAT	Desmin	215	4	Rat	53424	5.21	10%	R.FLEQQNAALAAEVNR.L R.VDVERDNLIDDLQR.L	84 73
ATPB_RAT	ATP synthase subunit beta, mitochondrial	187	9	Rat	56318	5.19	9%	K.IPVGPETLGR.I	35
ATPB_RAT	ATP synthase subunit beta	477	8	Rat	56318	5.19	14%		
DESM_RAT	Desmin	273	3	Rat	53424	5.21	10%		
ACTC_RAT	Actin, alpha cardiac muscle 1	402	21	Rat	41992	5.23	48%	R.VAPEEHPTLLTEAPLNPK.A K.SYELPDGQVITIGNER.F K.QEYDEAGPSIVHR.K	69 100 60
ACTC_RAT	Actin, alpha cardiac muscle 1	229	3	Rat	41992	5.23	13%		
	Human keratin and porcine trypsin peptides only								
	NO RESULT								
PEBP1_RAT	Phosphatidylethanolamine-binding protein 1	441	19	Rat	20788	5.48	57%	R.VDYGGVTVDELGK.V K.LYTLVLTDPDAPSR.K K.GNDISSGTVLYSEYVGGPPK.D K.YHLGAPVAGTCFQAEWDDSVPK.L (C) K.LHDQLAGK.-	78 66 115 77 52
PEBP1_RAT	Phosphatidylethanolamine-binding protein 1	388	5	Rat	20788	5.48	41%		
	Human keratin and porcine trypsin peptides only								
	NO RESULT								

APPENDIX 3: continued

	Protein Name	MASCOT Score	Queries matched	Species	Theoretical		coverage	Matched peptides	MASCOT ion Score
					Mr	PI			
ACTC_RAT	Actin, alpha cardiac muscle 1	978	44	Rat	41992	5.23	57%	K.DSYVVGDEAQS.K.R	58
								K.DSYVVGDEAQS.K.R.G	61
								K.IWHHTFYNEL.R.V	42
								R.VAPEEHPTLLTEAPLNPK.A	102
								R.TTGIVLDSGDGVTHNVPIYEGYALPHAIMR.L	53
								R.TTGIVLDSGDGVTHNVPIYEGYALPHAIMR.L	94
								R.DLTDYLMK.I	42
								R.DLTDYLMK.I (M)	40
								R.GYSFVTTAER.E	49
								K.LCYVALDFENEMATAASSSSLEK.S (C)	57
								K.SYELPDGQVITIGNER.F	94
								R.KDLYANNVLSGGTTMYPGIADR.M	46
								R.KDLYANNVLSGGTTMYPGIADR.M (M)	40
								K.DLYANNVLSGGTTMYPGIADR.M	103
								K.DLYANNVLSGGTTMYPGIADR.M (M)	115
								K.EITALAPSTMK.I	52
								K.EITALAPSTMK.I (M)	52
								K.IIAPPERK.Y	36
								K.QEYDEAGPSIVHR.K	84
ACTC_RAT	Actin, alpha cardiac muscle 1	1220	19	Rat	41992	5.23	48%		
TPM1_RAT	Tropomyosin alpha-1 chain	98	2	Rat	32661	4.69	9%	R.IQLVEEELDRAQER.L	70
TPM2_RAT	Tropomyosin beta chain	98	2	Rat	32817	4.66	9%	R.IQLVEEELDRAQER.L	70
TPM3_RAT	Tropomyosin alpha-3 chain	98	2	Rat	28989	4.75	10%	R.IQLVEEELDRAQER.L	70
TPM4_RAT	Tropomyosin alpha-4 chain	98	2	Rat	28492	4.66	10%	R.IQLVEEELDRAQER.L	70
TPM1_RAT	Tropomyosin alpha-1 chain (OR TPM2, 3 or 4)	70	1	Rat	32661	4.69	5%		
DESM_RAT	Desmin	828	22	Rat	53424	5.21	49%	R.QVEVLNQR.A	51
								R.VDVERDNLIDDLQR.L	79
								K.LQEEIQLREEAENLAAFR.A	131
								R.ADVDAATLAR.I	70
								R.AQYETIAAK.N	39
								R.FASEASGYQDNARLEEEIR.H	45
								K.LLEGEESR.I	56
								R.DGEVSEATQQQHEVL.-	57
ATPB_RAT	ATP synthase subunit beta, mitochondrial	70	1	Rat	56318	5.19	3%	R.AIAELGIYPAVDPLDSTSR.I	70
DESM_RAT	Desmin	554	13	Rat	53424	5.21	31%	R.APSYGAGELLDLDFSLADAVNQEFLATR.T	112
								R.FLEQQNAALAAEVNR.L	104
								R.INLPIQTFSSALNFR.E	63
								R.INLPIQTFSSALNFRFETSPEQR.G	35
DESM_RAT	Desmin	842	12	Rat	53424	5.21	36%		
ATPB_RAT	ATP synthase subunit beta	70	1	Rat	56318	5.19	3%		

APPENDIX 3: continued

	Protein Name	MASCOT Score	Queries matched	Species	Theoretical		coverage	Matched peptides	MASCOT ion Score
					Mr	PI			
HSPB8_RAT	Heat shock protein beta-8	136	4	Rat	21579	4.92	19%	R.LSSAWPGLR.S K.QEGGIVSK.N	35 38
HSPB8_RAT	Heat shock protein beta-8	73	2	Rat	21579	4.92	10%		
CH60_RAT	60 kDa heat shock protein, mitochondrial	787	19	Rat	60917	5.91	34%	K.APGFGDNR.K K.VGEVIVTKDDAMLLK.G K.VGEVIVTKDDAMLLK.G (M) R.IQEITEQLDITTSYEYKEK.L R.VTDALNATR.A R.CIPALDSLKPANEDQK.I (C) K.NAGVEGSLIVEK.I	49 105 80 113 61 84 81
CH60_RAT	60 kDa heat shock protein, mitochondrial	571	16	Rat	60917	5.91	24%	K.VGLQVVAVK.A K.NQLKDMAIATGGAVFGEEGLNLEDVQAHD LGK.V (M) K.VGEVIVTK.D K.LSDGVAVLK.V R.AAVEEGIVLGGGCALLR.C (C)	64 52 47 65 94
CH60_RAT	60 kDa heat shock protein	895	11	Rat	60917	5.91	26%		
TPM1_RAT	Tropomyosin alpha-1 chain	166	9	Rat	32661	4.69	12%	K.QLEDELVSLQK.K R.IQLVEEELDR.A R.IQLVEEELDRAQER.L	39 53 40
TPM1_RAT	Tropomyosin alpha-1 chain	132	3	Rat	32661	4.69	9%		
ACTC_RAT	Actin, alpha cardiac muscle 1	670	17	Rat	41992	5.23	45%	R.TTGIVLDSGDGVTHNVPIYEGYALPHAIMR.L R.TTGIVLDSGDGVTHNVPIYEGYALPHAIMR.L R.GYSFVTTAER.E K.SYELPDGQVITIGNER.F R.KDLYANNVLSGGTTMYPGIADR.M K.DLYANNVLSGGTTMYPGIADR.M (M) K.EITALAPSTMK.I K.QEYDEAGPSIVHR.K	125 149 41 87 68 130 43 73
ACTA_RAT	Actin, aortic smooth muscle	668	17	Rat	41982	5.23	45%	R.TTGIVLDSGDGVTHNVPIYEGYALPHAIMR.L R.TTGIVLDSGDGVTHNVPIYEGYALPHAIMR.L R.GYSFVTTAER.E K.SYELPDGQVITIGNER.F R.KDLYANNVLSGGTTMYPGIADR.M K.DLYANNVLSGGTTMYPGIADR.M (M) K.EITALAPSTMK.I K.QEYDEAGPSIVHR.K	125 149 41 87 68 130 43 73
ACTC_RAT	Actin, alpha cardiac muscle 1	510	19	Rat	41992	5.23	34%	R.KDLYANNVLSGGTTMYPGIADR.M (M) K.DLYANNVLSGGTTMYPGIADR.M R.KDLYANNVLSGGTTMYPGIADR.M (M) K.DLYANNVLSGGTTMYPGIADR.M K.DLYANNVLSGGTTMYPGIADR.M (M)	70 123 70 123 70
ACTA_RAT	Actin, aortic smooth muscle	510	19	Rat	41982	5.23	34%	R.KDLYANNVLSGGTTMYPGIADR.M (M) K.DLYANNVLSGGTTMYPGIADR.M K.DLYANNVLSGGTTMYPGIADR.M (M)	70 123 70
ACTH_RAT	Actin, gamma-enteric smooth muscle	510	19	Rat	41850	5.31	34%	R.KDLYANNVLSGGTTMYPGIADR.M (M) K.DLYANNVLSGGTTMYPGIADR.M	70 123
ACTC_RAT	Actin, alpha cardiac muscle 1	909	10	Rat	41992	5.23	27%		

APPENDIX 3: continued

	Protein Name	MASCOT Score	Queries matched	Species	Theoretical		coverage	Matched peptides	MASCOT ion Score
					Mr	PI			
ATPB_RAT	ATP synthase subunit beta, mitochondrial	209	5	Rat	56318	5.19	6%	R.AIAELGIYPAVDPLDSTSR.I R.IMDPNIVGSEHYDVAR.G (M)	96 113
ATPB_RAT	ATP synthase subunit beta	209	2	Rat	56318	5.19	6%		
CH60_RAT	60 kDa heat shock protein, mitochondrial	324	9	Rat	60917	5.91	25%	K.ISSVQSIVPALEIANHR.K K.VGEVIVTKDDAMLLK.G R.VTDALNATR.A R.AAVEEGIVLGGGCALLR.C (C)	127 41 37 73
CH60_RAT	60 kDa heat shock protein, mitochondrial	180	10	Rat	60917	5.91	20%	K.LSDGVAVLK.V	38
CH60_RAT	60 kDa heat shock protein	316	5	Rat	60917	5.91	12%		
MYH6_RAT	Myosin-6	153	7	Rat	223370	5.59	2%	R.NTLLQAELEELRAVVEQTER.S K.LAEQELIETSER.V R.QAEEAEEQANTNLSK.F	63 42 50
MYH6_RAT	Myosin-6	155	3	Rat	223370	5.59	2%		

APPENDIX 4: MASCOT search results from pH 5.5-6.7 2DE analysis Spot numbers were assigned by Progenesis. Next to the protein name are total scores assigned by mascot, the number of peptides matched in MASCOT, the species, the theoretical mass (*Mr*) and *pI* of the full length protein, the % coverage of the peptides matched. Only peptides with ion scores over 35 are shown in the matched peptides column, and the corresponding ion score for these are also shown. The shaded rows indicate the final MASCOT score, number of matched peptides and the coverage as calculated from the peptides with scores over 35.

	Protein Name	MASCOT Score	Queries matched	Species	Theoretical		coverage	Matched peptides	MASCOT ion Score
					Mr	PI			
KCRS_MOUSE	Creatine kinase, sarcomeric mitochondrial	189	6	Mouse	47443	8.64	17%	R.EVENVAITALEGLK.G	56
								K.LSEMTEQDQQR.L (M)	63
KCRS_MOUSE	Creatine kinase, sarcomeric mitochondrial	146	5	Mouse	47443	8.64	15%	R.EVENVAITALEGLK.G	43
								K.LSEMTEQDQQR.L	64
KCRS_MOUSE	Creatine kinase, sarcomeric	183	3	Mouse	47443	8.64	6%		
UCRI_RAT	Cytochrome P-450 complex subunit Rieske, mitochondrial	97	5	Rat	29427	9.04	13%	R.AEVLDTK.S	37
	NO RESULT								
KCRM_RAT	Creatine kinase M-type	120	6	Rat	43018	6.58	10%	K.VLTPDLYNK.L	45
								K.GGDDLDPNYVLSSR.V	37
KCRM_RAT	Creatine kinase M-type	82	2	Rat	43018	6.58	4%		
	Human Keratin and Porcine Trypsin peptides only								
	NO RESULT								
ACON_RAT	Aconitate hydratase, mitochondrial	130	7	Rat	85380	7.87	11%	R.VDVSPTSQR.L	41
	NO RESULT								
ENOB_RAT	Beta-enolase	130	3	Rat	46984	7.08	12%	R.AAVPSGASTGIYEALR.D	119
ALBU_RAT	Serum albumin	1	47	Rat	68686	6.09	1%	R.FPNAEFAEITK.L	47
ENOB_RAT	Beta-enolase	149	4	Rat	46984	7.08	14%	K.TLGPALLEK.K	38
								R.IEEALGDK.A	43
ENOB_RAT	Beta-enolase	200	3	Rat	46984	7.08	8%		
ALBU_RAT	Serum Albumin	47	1	Rat	68686	6.09	1%		
ETFA_RAT	Electron transfer flavoprotein subunit alpha, mitochondrial	201	4	Rat	34929	8.62	18%	R.LGGEVSCLVAGTK.C (C)	70
								K.LNVAPVSDIIEIK.S	50
								K.LLYDLADQLHAAVGASR.A	73
ETFA_RAT	Electron transfer flavoprotein subunit alpha, mitochondrial	149	6	Rat	34929	8.62	22%	R.AAVDAGFVPNDMQVGQTGK.I	39
ETFA_RAT	Electron transfer flavoprotein subunit alpha	232	4	Rat	34929	8.62	18%		
PGAM1_RAT	Phosphoglycerate mutase 1	408	14	Rat	28814	6.67	43%	R.DAGYEFDICFTSVQKR.A (C)	72
								R.YADLTEDQLPSCESLKDITR.A (C)	145
								R.ALPFWNEEIVPQIK.E	73
								K.AMEAVAAQGK.V (M)	43
PGAM1_RAT	Phosphoglycerate mutase 1	333	4	Rat	28814	6.67	24%		
GRP75_RAT	Stress-70 protein, mitochondrial	245	5	Rat	73812	5.97	9%	K.VLENAEGAR.T	55
								R.TTPSVVAFTPDGER.L	58
GRP75_RAT	Stress-70 protein, mitochondrial	238	4	Rat	73812	5.97	7%	K.NAVITVPAYFNDSQR.Q	51
								K.DAGQISGLNVL.R.V	77
GRP75_RAT	Stress-70 protein	241	4	Rat	73812	5.97	7%		

APPENDIX 4: continued

	Protein Name	MASCOT Score	Queries matched	Species	Theoretical		coverage	Matched peptides	MASCOT ion Score
					Mr	PI			
CH60_RAT	60 kDa heat shock protein, mitochondrial	1340	31	Rat	60917	5.91	48%	R.TVIIEQSWGSPK.V	52
								R.GVMLAVDAVIAELKK.Q (M)	57
								K.DIGNIISDAMK.K	60
								K.TLNDELEIIEGMK.F	72
								R.GYISPYFINTSK.G	58
								K.CEFQDAYVLLSEK.K [c]	83
								K.ISSVQSIVPALEIANHR.K	107
								R.KPLVIAEDVDGEALSTLVLR.L	68
								K.VGLQWVAVK.A	68
								K.APGFGDNR.K	55
								K.VGEVIVTK.D	44
								K.VGEVIVTKDDAMLLK.G	102
								K.VGEVIVTKDDAMLLK.G (M)	72
								R.IQEITEQLDITTSEYEKEK.L	101
								K.LSDGVAVLK.V	63
								K.VGGTSDVEVNEK.K	70
								R.VTDALNATR.A	58
								R.AAVEEGIVLGGGCALLR.C ©	90
CH60_RAT	60 kDa heat shock protein, mitochondrial	795	25	Rat	60917	5.91	30%	K.LVQDVANNTNEEAGDGTATVLR.S	99
								K.TLNDELEIIEGMKFDR.G	39
								K.CEFQDAYVLLSEK.I (C)	35
CH60_RAT	60 kDa heat shock protein	1453	21	Rat	60917	5.91	42%		
NDUAA_RAT	NADH dehydrogenase [ubiquinone] 1 alpha subcomplex subunit 10, mitochondrial	726	19	Rat	40468	7.64	45%	R.LLQYSDALEHLLSTGQGVVLR.S	147
								R.SIYSDVFLEAMYNQGFIR.K (M)	36
								K.VTSAYLQDIEDAYK.K	65
								K.VTSAYLQDIEDAYK.K.T	123
								K.VVEDIEYLNYNK.G	72
								R.EVLNYYTVVYLPVPEITIGAHQGSR.I	77
NDUAA_RAT	NADH dehydrogenase [ubiquinone] 1 alpha subcomplex subunit 10, mitochondrial	348	10	Rat	40468	7.64	31%	R.DIAEQLGMK.H	37
								R.LQSWLYASR.L	58
								R.LTLPEYLPVPEITIGAHQGSR.I	64
NDUAA_RAT	NADH dehydrogenase [ubiquinone] 1 alpha subcomplex subunit 10	679	9	Rat	40468	7.64	38%		

APPENDIX 4: continued

	Protein Name	MASCOT Score	Queries matched	Species	Theoretical		coverage	Matched peptides	MASCOT ion Score
					Mr	PI			
ODB2_MOUSE	Lipoamide acyltransferase component of branched-chain alpha-keto acid dehydrogenase complex, mitochondrial	468	12	Mouse	53127	8.88	20%	R.YDGVIKR.L	39
								R.LAMENNIK.L	46
								R.LAMENNIK.L (M)	46
								K.LSEVVGSGK.D	55
								K.QTGAILPPSPK.S	60
								K.AQIMNVWSADHR.V	82
								R.VIDGATMSR.F	65
								R.VIDGATMSR.F (M)	51
								K.SYLENPAFMLLDLK.-	79
ODB2_MOUSE	Lipoamide acyltransferase component of branched-chain alpha-keto acid dehydrogenase complex, mitochondrial	445	15	Mouse	53127	8.88	19%	K.TLATPAVR.R	51
								K.LSEVVGSGKDGR.I	64
								K.LREELKPVALAR.G	41
								K.SYLENPAFMLLDLK.- (M)	79
ODB2_MOUSE	Lipoamide acyltransferase component of branched-chain alpha-keto acid dehydrogenase complex	758	13	Mouse	53127	8.88	19%		
ACADS_RAT	Short-chain specific acyl-CoA dehydrogenase, mitochondrial	260	9	Rat	44737	8.47	16%	R.ASSTANLIFEDCR.I (C)	53
								K.IAMQTLDMGR.I	54
								K.LADMALALESAR.L	75
								K.LADMALALESAR.L (M)	56
								R.ITEIYEGTSEIQR.L	48
ACADS_RAT	Short-chain specific acyl-CoA dehydrogenase	286	5	Rat	44737	8.47	12%		
EFG1_RAT	Elongation factor G 1, mitochondrial	130	5	Rat	83717	6.95	7%	K.GIIDLIEER.A	45
								R.AIYFDGDFGQIVR.Y	41
								R.YDEIPADLR.A	34
EFG1_RAT	Elongation factor G 1	120	3	Rat	83717	6.95	4%		

APPENDIX 5: Abbreviations and identification codes for all proteins identified in the 2DE analyses

Protein Name	Abbrev.	RefSeq ACCESSION	UniProtKB/Swiss-Prot Accession	UniProtKB/Swiss-Prot
Short-chain specific acyl-CoA dehydrogenase, mitochondrial	Acads	NP_071957.1	P15651	ACADS_RAT
Actin , alpha cardiac muscle 1	Actc1	NP_062056.1	P68035	ACTC_RAT
Serum albumin precursor	Alb	NP_599153.2	P02770	ALBU_RAT
ATP synthase subunit beta, mitochondrial	Atp5b	NP_599191.1	P10719	ATPB_RAT
Adenylyl cyclase-associated protein 1	Cap1	NP_071778.2	Q08163	CAP1_RAT
Creatine kinase M-type	Ckm	NP_036662.1	P00564	KCRM_RAT
Creatine kinase, sarcomeric mitochondrial	Ckmt2	NP_940807.1	Q6P8J7	KCRS_MOUSE
Lipoamide acyltransferase component of branched-chain alpha-keto acid dehydrogenase complex, mitochondrial	Dbt	NP_034152.1	P53395	ODB2_MOUSE
Desmin	Des	NP_071976.1	P48675	DESM_RAT
Dihydrolipoyllysine-residue acetyltransferase component of pyruvate dehydrogenase complex	Dlat	NP_112287.1	P08461	ODP2_RAT
Enoyl-CoA hydratase	Echs1	NP_511178.1	P14604	ECHM_RAT
Electron transfer flavoprotein subunit alpha, mitochondrial	EtfA	NP_001009668.1	P13803	ETFARAT
Elongation factor G 1, mitochondrial	Gfm1	NP_446077.1	Q07803	EFG1_RAT
Hydroxysteroid dehydrogenase-like protein 2	Hsdl2	NP_001020868.1	Q4V8F9	HSDL2_RAT
Heat shock cognate 71Da	Hspa8	NP_077327.1	P63018	HSP7C_RAT
Stress-70 protein	Hspa9	NP_001094128.1	P48721	GRP75_RAT
Heat shock protein beta-8	Hspb8	NP_446064.1	Q9EPX0	HSPB8_RAT
60 kDa heat shock protein, mitochondrial	Hspd1	NP_071565.2	P63039	CH60_RAT
L-lactate dehydrogenase B chain	Ldhb	NP_036727.1	P42123	LDHB_RAT
Galectin-5	Lgals5	NP_037108.1	P47967	LEG5_RAT
Methylcrotonoyl-CoA carboxylase subunit alpha, mitochondrial (mouse)	Mccc1	NP_001009653.1	Q510C3	MCCA_RAT
Myosin-6	Myh6	NP_058935.1	P02563	MYH6_RAT
Myosin regularory light chain 2, ventricular/cardiac muscle isoform	Myl2	NP_001030329.1	P08733	MLRV_RAT
Myosin light chain 3	Myl3	NP_036738.1	P16409	MYL3_RAT
NADH dehydrogenase [ubiquinone] 1 alpha subcomplex subunit 10, mitochondrial	Ndufa10	NP_872612.1	Q561S0	NDUAA_RAT
NADH-ubiquinone oxidoreductase 75 kDa subunit	Ndufs1	NP_001005550.1	Q66HF1	NDUS1_RAT
NAD(P) transhydrogenase, mitochondrial precursor	Nnt	NP_032736.2	Q61941	NNTM_MOUSE
Phosphatidylethanolamine-binding protein 1	Pebp1	NP_058932.1	P31044	PEBP1_RAT
Phosphoglycerate mutase 1	Pgam1	NP_445742.1	P25113	PGAM1_RAT
Thioredoxin-dependent peroxide reductase	Prdx3	NP_071985.1	Q9Z0V6	PRDX3_RAT
Peroxiredoxin-6	Prdx6	NP_446028.1	Q35244	PRDX6_RAT
40S ribosomal protein SA	Rpsa	NP_058834.1	P38983	RSSA_RAT
Succinate dehydrogenase [ubiquinone] flavoprotein subunit, mitochondrial	Sdha	NP_569112.1	Q920L2	DHSA_RAT
Troponin T, cardiac muscle	Tnnt2	NP_036808.1	P50753	TNNT2_RAT
Tropomyosin alpha-1 chain	Tpm1	NP_001029241.1	P04692	TPM1_RAT
Tubulin alpha-4A chain	Tuba4a	NP_001007005.1	Q5XIF6	TBA4A_RAT
Cytochrome b-c1 complex subunit 6	Ugcrh	NP_001009480.1	Q5M9I5	QCR6_RAT
WD repeat-containing protein 1	Wdr1	NP_001014157.1	Q5RKI0	WDR1_RAT
14-3-3 protein epsilon	Ywhae	NP_113791.1	P62260	1433E_RAT

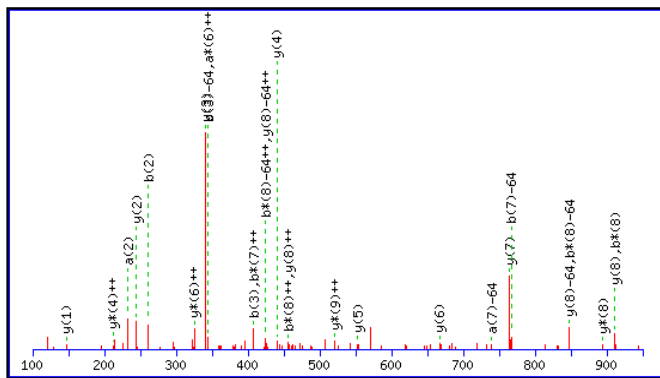
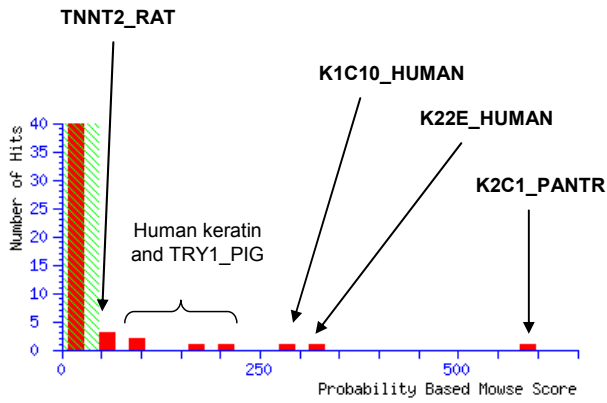
APPENDIX 6: Additional information on protein identifications which were based on a single peptide hit. A) Table of proteins which were identified by a single peptide hit. Spot numbers were assigned by PDQuest (Progenesis for 63). Next to the protein name are the species, the theoretical mass (*Mr*) and *pI* of the full length protein, the % coverage of the peptides matched. The peptide sequence, ion scores and Expect value are also shown. Further detail of MASCOT fragment assignments for single ion scores below 65 are in Appendix 6 B. **B)** Fragment assignments (MASCOT results) for 7 proteins with identifications based on single peptides with ion scores below 65 (See table in Appendix 6 A).

APPENDIX 6 A:

SSP		Protein Name	Species	Theoretical		coverage	Matched peptides	MASCOT ion Score	Expect
				Mr	PI				
2119	QCR6_RAT	Cytochrome b-c1 complex subunit 6	Rat	10417	4.9	20%	R.SQTEEDCTEELFDLHAR.D (C)	131	8.30E-11
2443	ATPB_RAT	ATP synthase subunit beta	Rat	56318	5.19	3%	R.AIAELGIYPAVDPLDSTR.I	91	7.80E-07
3518	GRP75_RAT	Stress-70 protein	Rat	73812	5.97	2%	R.QAASSLQQASLK.L	85	6.40E-06
6424	LDHB_RAT	L-lactate dehydrogenase B chain	Rat	36589	5.7	4%	R.VIGSGCNLDSAR.F (C)	85	7.00E-06
6425	LDHB_RAT	L-lactate dehydrogenase B chain	Rat	36589	5.7	6%	R.VIGSGCNLDSAR.F (C)	77	4.60E-05
7723	DHSA_RAT	Succinate dehydrogenase [ubiquinone] flavoprotein subunit	Rat	71570	6.75	2%	R.LGANSLLDLVVFGR.A	73	9.90E-05
4521	LDHA_RAT	L-lactate dehydrogenase (or LDHB)	Rat	36427	8.45	3%	R.VIGSGCNLDSAR.F (C)	72	1.40E-04
7323	ECHM_RAT	Enoyl-CoA hydratase	Rat	31496	8.39	3%	R.EGMSAFVEKR.K (M)	73	1.10E-04
63	TPM1_RAT	Tropomyosin alpha-1 chain (OR TPM2, 3 or 4)	Rat	32661	4.69	5%	R.IQLVEEELDRAQER.L	70	1.60E-04
4329	ATPB_RAT	ATP synthase subunit beta	Rat	56318	5.19	2%	R.TIAMDGTEGLVR.G (M)	69	2.40E-04
1248	TNNT2_RAT	Troponin T, cardiac muscle	Rat	35709	4.95	3%	R.LFMPNLVPPK.I (M)	59	0.007
1207	NNTM_MOUSE	NAD(P) transhydrogenase	Rat	113780	8.4	2%	R.SLGVGYAAVDNPIFYKPNTAMLL	58	0.002
1320	TPM1_RAT	Tropomyosin alpha-1 chain (or Tropomyosin beta chain)	Rat	32661	4.69	4%	K.ATDAEADVASLNR.R	58	0.003
1206	MLRV_RAT	Myosin regulatory light chain 2	Rat	18868	4.86	8%	K.GADPEETILNAFK.V	57	0.005
2546	CAP1_RAT	Adenylyl cyclase-associated protein 1	Rat	51556	7.16	4%	K.LSDLLAPISEIQIEVITFR.E	55	0.003
3208	ATPB_RAT	ATP synthase subunit beta	Rat	56318	5.19	4%	K.VLDSGAPIKIPVGPETLGR.I	51	0.006
2616	RSSA_RAT	40S ribosomal protein SA	Rat	32803	4.8	4%	K.FAAATGATPIAGR.F	50	0.024
3441	ALBU_RAT	Serum albumin	Rat	68686	6.09	2%	K.DVFLGTFLYEYSR.R	46	0.037
6636	HSP7C_RAT	Heat shock cognate 71Da OR HSP72	Rat	70827	5.37	2%	K.STAGDTHLGGEDFDNR.M	46	0.043

APPENDIX 6 B:

1248_Troponin T, cardiac muscle



Monoisotopic mass of neutral peptide $M_r(\text{calc})$: 1170.6471

Variable modifications:

M3 : Oxidation (M), with neutral losses 0.0000 (shown in table), 63.9983

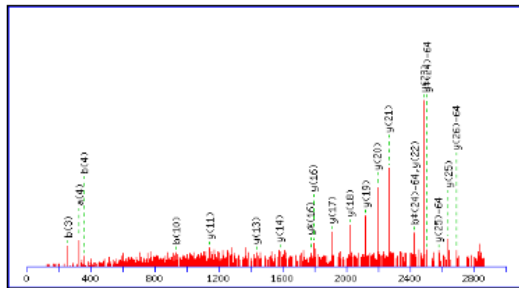
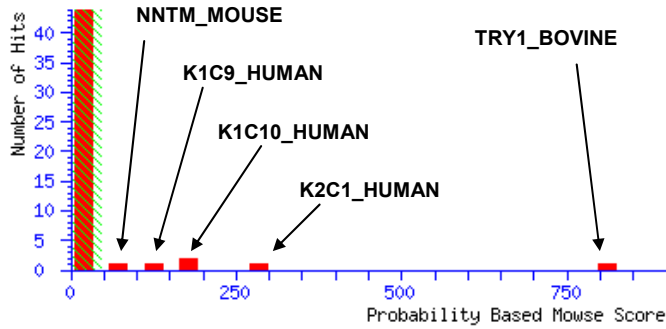
Ions Score: 56 **Expect:** 0.0068

Matches (Bold Red): 27/148 fragment ions using 34 most intense peaks

#	a	a ⁺⁺	a [*]	a ^{*++}	b	b ⁺⁺	b [*]	b ^{*++}	Seq.	y	y ⁺⁺	y [*]	y ^{*++}	#
1	86.0964	43.5519			114.0913	57.5493			L					10
2	233.1648	117.0861			261.1598	131.0835			F	1058.5703	529.7888	1041.5438	521.2755	9
3	380.2002	190.6038			408.1952	204.6012			M	911.5019	456.2546	894.4754	447.7413	8
4	477.2530	239.1301			505.2479	253.1276			P	764.4665	382.7369	747.4400	374.2236	7
5	591.2959	296.1516	574.2694	287.6383	619.2908	310.1491	602.2643	301.6358	N	667.4137	334.2105	650.3872	325.6972	6
6	704.3800	352.6936	687.3534	344.1804	732.3749	366.6911	715.3484	358.1778	L	553.3708	277.1890	536.3443	268.6758	5
7	803.4484	402.2278	786.4219	393.7146	831.4433	416.2253	814.4168	407.7120	V	440.2867	220.6470	423.2602	212.1337	4
8	900.5012	450.7542	883.4746	442.2410	928.4961	464.7517	911.4695	456.2384	P	341.2183	171.1128	324.1918	162.5995	3
9	997.5539	499.2806	980.5274	490.7673	1025.5489	513.2781	1008.5223	504.7648	P	244.1656	122.5864	227.1390	114.0731	2
10									K	147.1128	74.0600	130.0863	65.5468	1

APPENDIX 6 B: continued.

1207_NAD(P) transhydrogenase

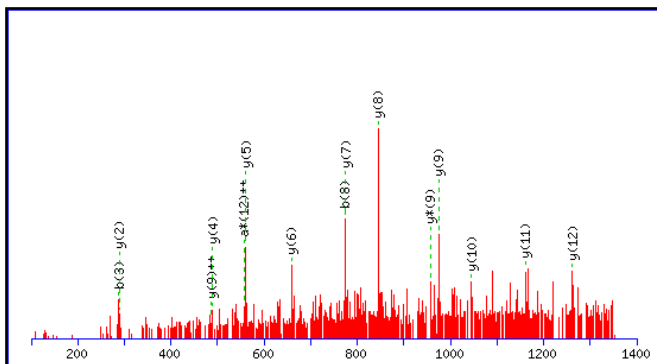
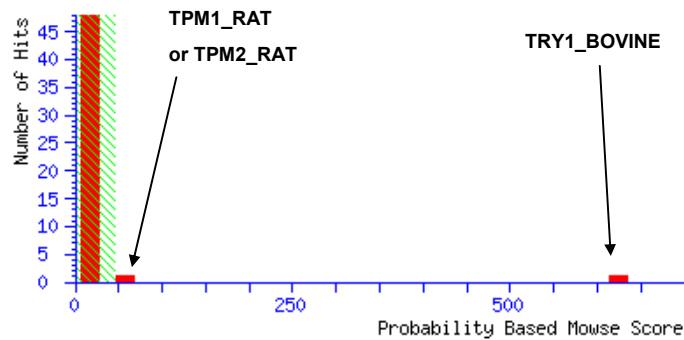


Monoisotopic mass of neutral peptide H₀(calc): 2840.4418
 Variable modifications:
 M2L : Oxidation (M), with neutral losses 0.0000 (shown in table), 62.9983
 Ions Score: 5% Expect: 0.0017
 Matches (Bold Red): 21/400 fragment ions using 45 most intense peaks

#	a	a ⁺⁺	a ⁺	a ⁺⁺⁺	b	b ⁺⁺	b ⁺	b ⁺⁺⁺	Seq.	y	y ⁺⁺	y ⁺	y ⁺⁺⁺	#
1	60.0444	30.5258			88.0393	44.5233			S					27
2	173.1285	87.0679			201.1234	101.0653			L	2754.4171	1377.7122	2737.3906	1369.1989	26
3	230.1499	115.5786			258.1448	129.5761			G	2641.3331	1321.1702	2624.3065	1312.6569	25
4	329.2183	165.1128			357.2132	179.1103			V	2584.3116	1292.6594	2567.2850	1284.1462	24
5	386.2398	193.6235			414.2347	207.6210			G	2485.2432	1243.1252	2468.2166	1234.6120	23
6	549.3031	275.1552			577.2980	289.1527			Y	2428.2217	1214.6145	2411.1952	1206.1012	22
7	620.3402	310.6738			648.3352	324.6712			A	2265.1584	1133.0828	2248.1318	1124.5696	21
8	691.3774	346.1923			719.3723	360.1898			A	2194.1213	1097.5643	2177.0947	1089.0510	20
9	790.4458	395.7265			818.4407	409.7240			V	2123.0842	1062.0457	2106.0576	1053.5324	19
10	905.4727	453.2400			933.4676	467.2374			D	2024.0157	1012.5115	2006.9892	1003.9982	18
11	1019.5156	510.2615	1002.4891	501.7482	1047.5106	524.2589	1030.4840	515.7456	N	1908.9888	954.9980	1891.9623	946.4848	17
12	1116.5684	558.7878	1099.5419	550.2746	1144.5633	572.7853	1127.5368	564.2720	P	1794.9459	897.9766	1777.9193	889.4633	16
13	1229.6525	615.3299	1212.6259	606.8166	1257.6474	629.3273	1240.6208	620.8141	I	1697.8931	849.4502	1680.8666	840.9389	15
14	1376.7209	688.8641	1359.6943	680.3508	1404.7158	702.8615	1387.6892	694.3483	F	1584.8090	792.9082	1567.7825	784.3949	14
15	1539.7842	770.3957	1522.7577	761.8825	1567.7791	784.3932	1550.7526	775.8799	Y	1437.7406	719.3740	1420.7141	710.8607	13
16	1667.8792	834.4432	1650.8526	825.9299	1695.8741	848.4407	1678.8475	839.9274	K	1274.6773	637.8423	1257.6508	629.3290	12
17	1764.9319	882.9696	1747.9054	874.4563	1792.9268	896.9671	1775.9003	888.4538	P	1146.5823	573.7948	1129.5558	565.2815	11
18	1878.9749	939.9911	1861.9483	931.4778	1906.9698	953.9885	1889.9432	945.4753	N	1049.5296	525.2684	1032.5030	516.7552	10
19	1980.0225	990.5149	1962.9960	982.0016	2008.0175	1004.5124	1990.9909	995.9991	T	935.4867	468.2470	918.4601	459.7337	9
20	2051.0597	1026.0335	2034.0331	1017.5202	2079.0546	1040.0309	2062.0280	1031.5176	A	834.4390	417.7231	817.4124	409.2098	8
21	2198.0951	1099.5512	2181.0685	1091.0379	2226.0900	1113.5486	2209.0634	1105.0353	M	763.4019	382.2046	746.3753	373.6913	7
22	2311.1791	1156.0932	2294.1526	1147.5799	2339.1740	1170.0907	2322.1475	1161.5774	L	616.3665	308.6869	599.3399	300.1736	6
23	2424.2632	1212.6352	2407.2366	1204.1220	2452.2581	1226.6327	2435.2316	1218.1194	L	503.2824	252.1448	486.2558	243.6316	5
24	2481.2847	1241.1460	2464.2581	1232.6327	2509.2796	1255.1434	2492.2530	1246.6301	G	390.1983	195.6028	373.1718	187.0895	4
25	2596.3116	1298.6594	2579.2850	1290.1462	2624.3065	1312.6569	2607.2800	1304.1436	D	333.1769	167.0921	316.1503	158.5788	3
26	2667.3487	1334.1780	2650.3222	1325.6647	2695.3436	1348.1754	2678.3171	1339.6622	A	218.1499	109.5786	201.1234	101.0653	2
27									K	147.1128	74.0600	130.0863	65.5468	1

APPENDIX 6 B: continued.

1320_Tropomyosin alpha-1 chain (or Tropomyosin beta chain)

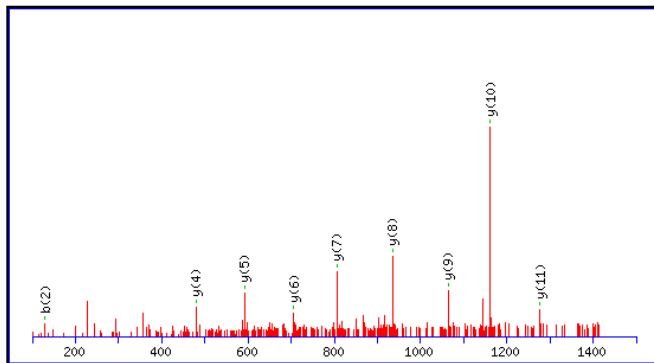
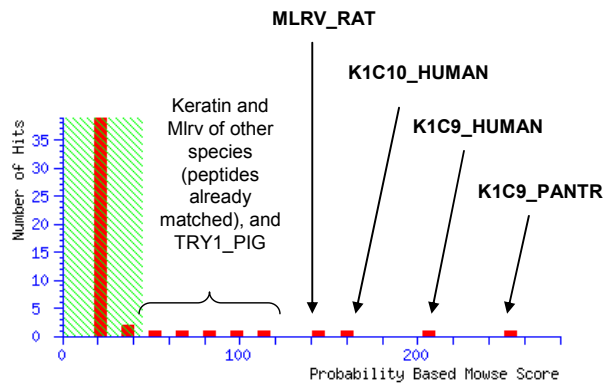


Monoisotopic mass of neutral peptide $M_r(\text{calc})$: 1331.6317
 Ions Score: 58 Expect: 0.0031
 Matches (**Red**): 15/100 fragment ions using 44 most intense peaks

#	a	a ⁺⁺	a ⁺	a ⁺⁺⁺	b	b ⁺⁺	b ⁺	b ⁺⁺⁺	Seq.	y	y ⁺⁺	y ⁺	y ⁺⁺⁺	#
1	44.0495	22.5284			72.0444	36.5258			A					13
2	145.0972	73.0522			173.0921	87.0497			T	1261.6019	631.3046	1244.5753	622.7913	12
3	260.1241	130.5657			288.1190	144.5631			D	1160.5542	580.7807	1143.5277	572.2675	11
4	331.1612	166.0842			359.1561	180.0817			A	1045.5273	523.2673	1028.5007	514.7540	10
5	460.2038	230.6055			488.1987	244.6030			E	974.4901	487.7487	957.4636	479.2354	9
6	531.2409	266.1241			559.2358	280.1216			A	845.4476	423.2274	828.4210	414.7141	8
7	646.2679	323.6376			674.2628	337.6350			D	774.4104	387.7089	757.3839	379.1956	7
8	745.3363	373.1718			773.3312	387.1692			V	659.3835	330.1954	642.3569	321.6821	6
9	816.3734	408.6903			844.3683	422.6878			A	560.3151	280.6612	543.2885	272.1479	5
10	903.4054	452.2063			931.4003	466.2038			S	489.2780	245.1426	472.2514	236.6293	4
11	1016.4895	508.7484			1044.4844	522.7458			L	402.2459	201.6266	385.2194	193.1133	3
12	1130.5324	565.7698	1113.5059	557.2566	1158.5273	579.7673	1141.5008	571.2540	N	289.1619	145.0846	272.1353	136.5713	2
13									R	175.1190	88.0631	158.0924	79.5498	1

APPENDIX 6 B: continued.

1206_Myosin regulatory light chain 2



Monoisotopic mass of neutral peptide $M_r(\text{calc})$: 1403.6932

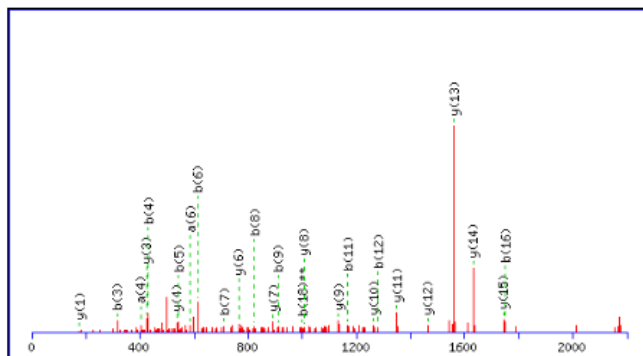
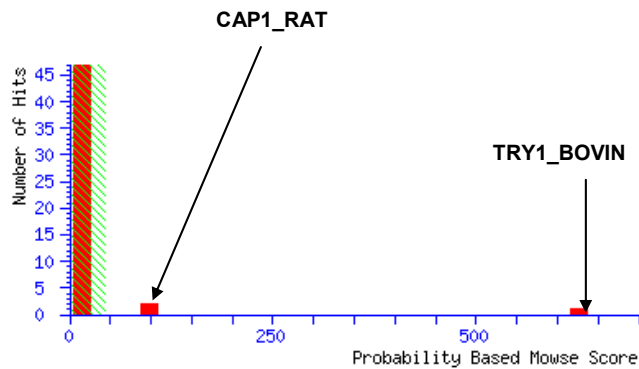
Ions Score: 57 Expect: 0.0046

Matches (**Bold Red**): 9/108 fragment ions using 19 most intense peaks

#	a	a ⁺⁺	a [*]	a ^{*++}	b	b ⁺⁺	b [*]	b ^{*++}	Seq.	y	y ⁺⁺	y [*]	y ^{*++}	#
1	30.0338	15.5206			58.0287	29.5180			G					13
2	101.0709	51.0391			129.0659	65.0366			A	1347.6791	674.3432	1330.6525	665.8299	12
3	216.0979	108.5526			244.0928	122.5500			D	1276.6420	638.8246	1259.6154	630.3113	11
4	313.1506	157.0790			341.1456	171.0764			P	1161.6150	581.3111	1144.5885	572.7979	10
5	442.1932	221.6003			470.1882	235.5977			E	1064.5623	532.7848	1047.5357	524.2715	9
6	571.2358	286.1216			599.2307	300.1190			E	935.5197	468.2635	918.4931	459.7502	8
7	672.2835	336.6454			700.2784	350.6429			T	806.4771	403.7422	789.4505	395.2289	7
8	785.3676	393.1874			813.3625	407.1849			I	705.4294	353.2183	688.4028	344.7051	6
9	898.4516	449.7295			926.4466	463.7269			L	592.3453	296.6763	575.3188	288.1630	5
10	1012.4946	506.7509	995.4680	498.2376	1040.4895	520.7484	1023.4629	512.2351	N	479.2613	240.1343	462.2347	231.6210	4
11	1083.5317	542.2695	1066.5051	533.7562	1111.5266	556.2669	1094.5000	547.7537	A	365.2183	183.1128	348.1918	174.5995	3
12	1230.6001	615.8037	1213.5735	607.2904	1258.5950	629.8011	1241.5685	621.2879	F	294.1812	147.5942	277.1547	139.0810	2
13									K	147.1128	74.0600	130.0863	65.5468	1

APPENDIX 6 B: continued.

2546_ Adenylyl cyclase-associated protein 1



Monoisotopic mass of neutral peptide $M_r(\text{calc})$: 2171.1838

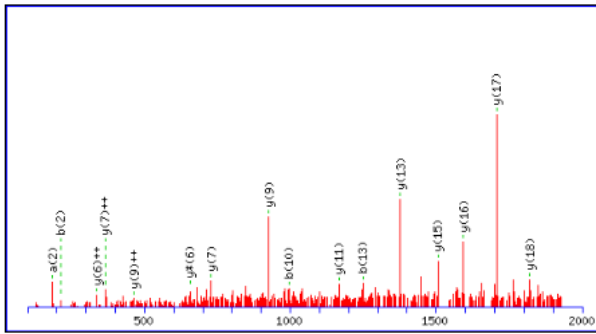
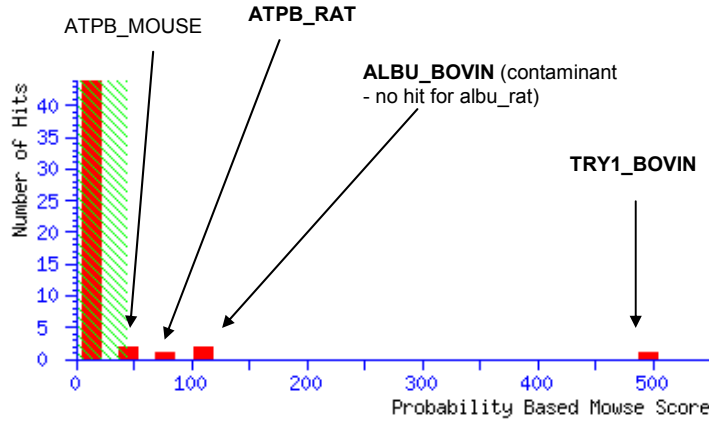
Ions Score: 55 Expect: 0.0026

Matches (Bold Red): 26/176 fragment ions using 74 most intense peaks

#	a	a ⁺⁺	a ⁺	a ⁺⁺⁺	b	b ⁺⁺	b ⁺	b ⁺⁺⁺	Seq.	y	y ⁺⁺	y ⁺	y ⁺⁺⁺	#
1	86.0964	43.5519			114.0913	57.5493			L					19
2	173.1285	87.0679			201.1234	101.0653			S	2059.1070	1030.0571	2042.0804	1021.5439	18
3	288.1554	144.5813			316.1503	158.5788			D	1972.0750	986.5411	1955.0484	978.0278	17
4	401.2395	201.1234			429.2344	215.1208			L	1857.0480	929.0277	1840.0215	920.5144	16
5	514.3235	257.6654			542.3184	271.6629			L	1743.9640	872.4856	1726.9374	863.9723	15
6	585.3606	293.1840			613.3556	307.1814			A	1630.8799	815.9436	1613.8534	807.4303	14
7	682.4134	341.7103			710.4083	355.7078			P	1559.8428	780.4250	1542.8162	771.9118	13
8	795.4975	398.2524			823.4924	412.2498			I	1462.7900	731.8986	1445.7635	723.3854	12
9	882.5295	441.7684			910.5244	455.7658			S	1349.7060	675.3566	1332.6794	666.8433	11
10	1011.5721	506.2897			1039.5670	520.2871			E	1262.6739	631.8406	1245.6474	623.3273	10
11	1139.6307	570.3190	1122.6041	561.8057	1167.6256	584.3164	1150.5990	575.8032	Q	1133.6313	567.3193	1116.6048	558.8060	9
12	1252.7147	626.8610	1235.6882	618.3477	1280.7096	640.8585	1263.6831	632.3452	I	1005.5728	503.2900	988.5462	494.7767	8
13	1380.7733	690.8903	1363.7468	682.3770	1408.7682	704.8877	1391.7417	696.3745	Q	892.4887	446.7480	875.4621	438.2347	7
14	1509.8159	755.4116	1492.7894	746.8983	1537.8108	769.4090	1520.7843	760.8958	E	764.4301	382.7187	747.4036	374.2054	6
15	1608.8843	804.9458	1591.8578	796.4325	1636.8792	818.9433	1619.8527	810.4300	Y	635.3875	318.1974	618.3610	309.6841	5
16	1721.9684	861.4878	1704.9418	852.9746	1749.9633	875.4853	1732.9367	866.9720	I	536.3191	268.6632	519.2926	260.1499	4
17	1823.0161	912.0117	1805.9895	903.4984	1851.0110	926.0091	1833.9844	917.4958	T	423.2350	212.1212	406.2085	203.6079	3
18	1970.0845	985.5459	1953.0579	977.0326	1998.0794	999.5433	1981.0528	991.0301	F	322.1874	161.5973	305.1608	153.0840	2
19									R	175.1190	88.0631	158.0924	79.5498	1

APPENDIX 6 B: continued.

3208_ATP synthase subunit beta

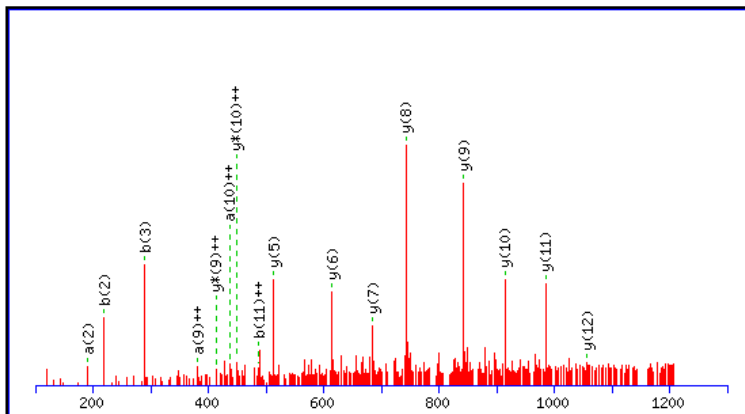
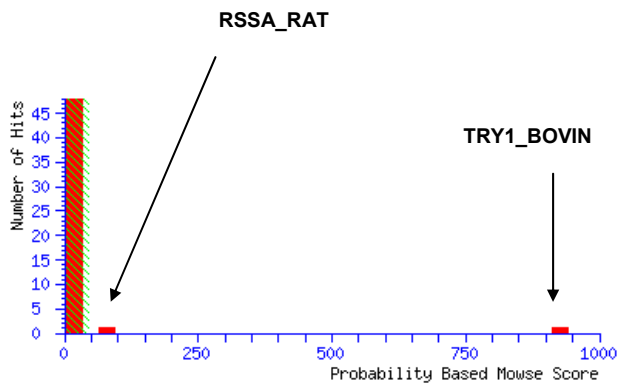


Monoisotopic mass of neutral peptide $M_r(\text{calc})$: 1918.0888
 Ions Score: 51 Expect: 0.0059
 Matches (Bold Red): 16/184 fragment ions using 26 most intense peaks

#	a	a ⁺⁺	a ⁺	a ⁺⁺⁺	b	b ⁺⁺	b ⁺	b ⁺⁺⁺	Seq.	y	y ⁺⁺	y ⁺	y ⁺⁺⁺	#
1	72.0808	36.5440			100.0757	50.5415			V					19
2	185.1648	93.0861			213.1598	107.0835			L	1820.0276	910.5175	1803.0011	902.0042	18
3	300.1918	150.5995			328.1867	164.5970			D	1706.9436	853.9754	1689.9170	845.4621	17
4	387.2238	194.1155			415.2187	208.1130			S	1591.9166	796.4619	1574.8901	787.9487	16
5	444.2453	222.6263			472.2402	236.6237			G	1504.8846	752.9459	1487.8580	744.4327	15
6	515.2824	258.1448			543.2773	272.1423			A	1447.8631	724.4352	1430.8366	715.9219	14
7	612.3352	306.6712			640.3301	320.6687			P	1376.8260	688.9166	1359.7995	680.4034	13
8	725.4192	363.2132			753.4141	377.2107			I	1279.7732	640.3903	1262.7467	631.8770	12
9	853.5142	427.2607	836.4876	418.7475	881.5091	441.2582	864.4825	432.7449	K	1166.6892	583.8482	1149.6626	575.3350	11
10	966.5982	483.8028	949.5717	475.2895	994.5932	497.8002	977.5666	489.2869	I	1038.5942	519.8007	1021.5677	511.2875	10
11	1063.6510	532.3291	1046.6245	523.8159	1091.6459	546.3266	1074.6194	537.8133	P	925.5102	463.2587	908.4836	454.7454	9
12	1162.7194	581.8633	1145.6929	573.3501	1190.7143	595.8608	1173.6878	587.3475	V	828.4574	414.7323	811.4308	406.2191	8
13	1219.7409	610.3741	1202.7143	601.8608	1247.7358	624.3715	1230.7093	615.8583	G	729.3890	365.1981	712.3624	356.6849	7
14	1316.7936	658.9005	1299.7671	650.3872	1344.7886	672.8979	1327.7620	664.3846	P	672.3675	336.6874	655.3410	328.1741	6
15	1445.8362	723.4218	1428.8097	714.9085	1473.8312	737.4192	1456.8046	728.9059	E	575.3148	288.1610	558.2882	279.6477	5
16	1546.8839	773.9456	1529.8574	765.4323	1574.8788	787.9431	1557.8523	779.4298	T	446.2722	223.6397	429.2456	215.1264	4
17	1659.9680	830.4876	1642.9414	821.9744	1687.9629	844.4851	1670.9364	835.9718	L	345.2245	173.1159	328.1979	164.6026	3
18	1716.9894	858.9984	1699.9629	850.4851	1744.9844	872.9958	1727.9578	864.4825	G	232.1404	116.5738	215.1139	108.0606	2
19									R	175.1190	88.0631	158.0924	79.5498	1

APPENDIX 6 B: continued.

2616_40S ribosomal protein SA



Monoisotopic mass of neutral peptide Mr(calc): 1202.6408

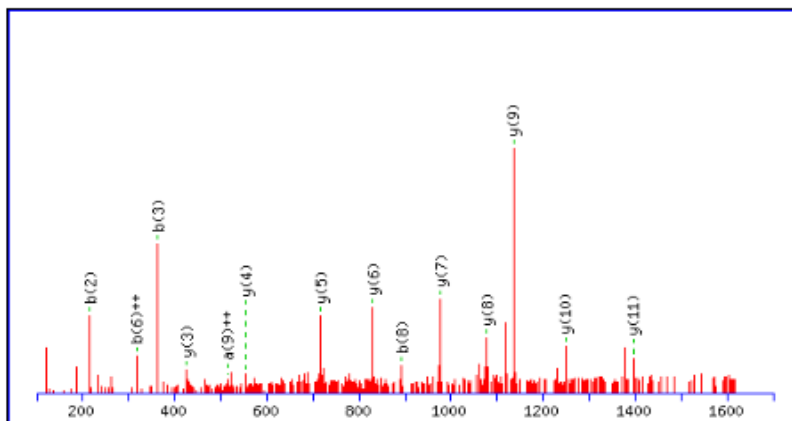
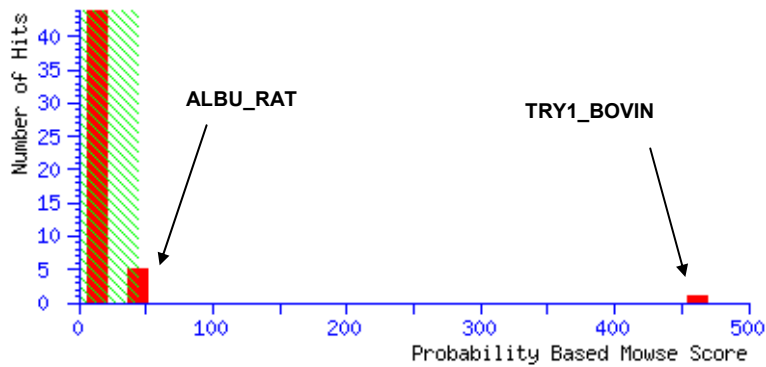
Ions Score: 50 **Expect:** 0.024

Matches (Bold Red): 16/96 fragment ions using 29 most intense peaks

#	a	a ⁺⁺	b	b ⁺⁺	Seq	y	y ⁺⁺	y [*]	y ⁺⁺⁺	#
1	120.0808	60.5440	148.0757	74.5415	F					13
2	191.1179	96.0626	219.1128	110.0600	A	1056.5796	528.7935	1039.5531	520.2802	12
3	262.1550	131.5811	290.1499	145.5786	A	985.5425	493.2749	968.5160	484.7616	11
4	333.1921	167.0997	361.1870	181.0972	A	914.5054	457.7563	897.4789	449.2431	10
5	434.2398	217.6235	462.2347	231.6210	T	843.4683	422.2378	826.4417	413.7245	9
6	491.2613	246.1343	519.2562	260.1317	G	742.4206	371.7139	725.3941	363.2007	8
7	562.2984	281.6528	590.2933	295.6503	A	685.3992	343.2032	668.3726	334.6899	7
8	663.3461	332.1767	691.3410	346.1741	T	614.3620	307.6847	597.3355	299.1714	6
9	760.3988	380.7030	788.3937	394.7005	P	513.3144	257.1608	496.2878	248.6475	5
10	873.4829	437.2451	901.4778	451.2425	I	416.2616	208.6344	399.2350	200.1212	4
11	944.5200	472.7636	972.5149	486.7611	A	303.1775	152.0924	286.1510	143.5791	3
12	1001.5415	501.2744	1029.5364	515.2718	G	232.1404	116.5738	215.1139	108.0606	2
13					R	175.1190	88.0631	158.0924	79.5498	1

APPENDIX 6 B: continued.

3441_Serum albumin



Monoisotopic mass of neutral peptide $M_r(\text{calc})$: 1608.7824

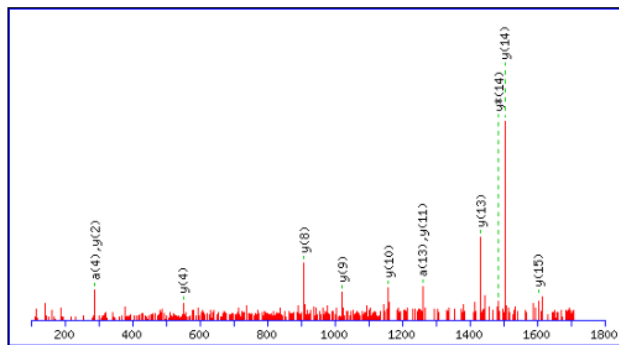
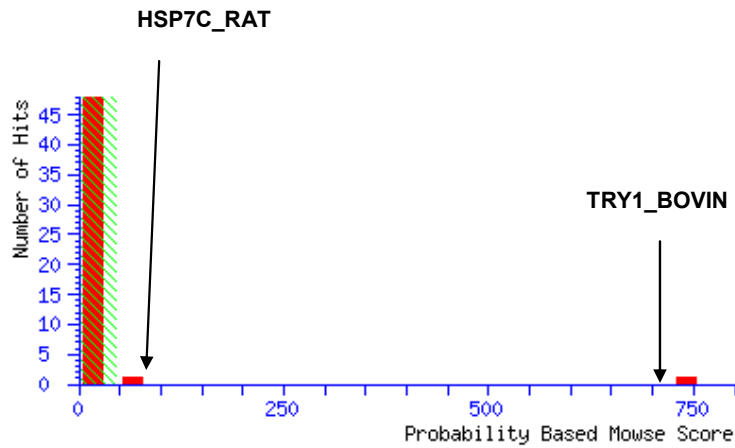
Ions Score: 46 Expect: 0.037

Matches : 14/96 fragment ions using 30 most intense peaks ([help](#))

#	a	a ⁺⁺	b	b ⁺⁺	Seq.	y	y ⁺⁺	y [*]	y ⁺⁺⁺	#
1	88.0393	44.5233	116.0342	58.5207	D					13
2	187.1077	94.0575	215.1026	108.0550	Y	1494.7627	747.8850	1477.7362	739.3717	12
3	334.1761	167.5917	362.1710	181.5892	F	1395.6943	698.3508	1378.6678	689.8375	11
4	447.2602	224.1337	475.2551	238.1312	L	1248.6259	624.8166	1231.5994	616.3033	10
5	504.2817	252.6445	532.2766	266.6419	G	1135.5419	568.2746	1118.5153	559.7613	9
6	605.3293	303.1683	633.3243	317.1658	T	1078.5204	539.7638	1061.4938	531.2506	8
7	752.3978	376.7025	780.3927	390.7000	F	977.4727	489.2400	960.4462	480.7267	7
8	865.4818	433.2445	893.4767	447.2420	L	830.4043	415.7058	813.3777	407.1925	6
9	1028.5451	514.7762	1056.5401	528.7737	Y	717.3202	359.1638	700.2937	350.6505	5
10	1157.5877	579.2975	1185.5827	593.2950	E	554.2569	277.6321	537.2304	269.1188	4
11	1320.6511	660.8292	1348.6460	674.8266	Y	425.2143	213.1108	408.1878	204.5975	3
12	1407.6831	704.3452	1435.6780	718.3426	S	262.1510	131.5791	245.1244	123.0659	2
13					R	175.1190	88.0631	158.0924	79.5498	1

APPENDIX 6 B: continued.

6636_Heat shock cognate 71Da OR HSP72



Monoisotopic mass of neutral peptide Mr(calc): 1690.7183
 Ions Score: 46 Expect: 0.043
 Matches (Bold Red): 12/124 fragment ions using 25 most intense peaks

#	a	a ⁺⁺	a ⁺	a ⁺ ++	b	b ⁺⁺	b ⁺	b ⁺ ++	Seq.	y	y ⁺⁺	y ⁺	y ⁺ ++	#
1	60.0444	30.5258			88.0393	44.5233			S					16
2	161.0921	81.0497			189.0870	95.0471			T	1604.6936	802.8504	1587.6670	794.3371	15
3	232.1292	116.5682			260.1241	130.5657			A	1503.6459	752.3266	1486.6193	743.8133	14
4	289.1506	145.0790			317.1456	159.0764			G	1432.6088	716.8080	1415.5822	708.2947	13
5	404.1776	202.5924			432.1725	216.5899			D	1375.5873	688.2973	1358.5607	679.7840	12
6	505.2253	253.1163			533.2202	267.1137			T	1260.5604	630.7838	1243.5338	622.2705	11
7	642.2842	321.6457			670.2791	335.6432			H	1159.5127	580.2600	1142.4861	571.7467	10
8	755.3682	378.1878			783.3632	392.1852			L	1022.4538	511.7305	1005.4272	503.2172	9
9	812.3897	406.6985			840.3846	420.6959			G	909.3697	455.1885	892.3432	446.6752	8
10	869.4112	435.2092			897.4061	449.2067			G	852.3482	426.6778	835.3217	418.1645	7
11	998.4538	499.7305			1026.4487	513.7280			E	795.3268	398.1670	778.3002	389.6537	6
12	1113.4807	557.2440			1141.4756	571.2414			D	666.2842	333.6457	649.2576	325.1325	5
13	1260.5491	630.7782			1288.5440	644.7757			F	551.2572	276.1323	534.2307	267.6190	4
14	1375.5761	688.2917			1403.5710	702.2891			D	404.1888	202.5980	387.1623	194.0848	3
15	1489.6190	745.3131	1472.5924	736.7999	1517.6139	759.3106	1500.5874	750.7973	N	289.1619	145.0846	272.1353	136.5713	2
16									R	175.1190	88.0631	158.0924	79.5498	1

APPENDIX 7: LIMMA differential gene expression results for the top 433 probes. Including all probes with significant difference in MI vs. BMMNC ($p < 0.05$) and all probes with significant alteration in Sham vs. MI ($p < 0.01$). Illumina probe IDs and gene symbols are shown alongside the log fold change (log FC), FDR adjusted p-value and B statistic for the Sham vs. MI, MI vs. BMMNC and Sham vs. BMMNC comparisons.

ID	SYMBOL	Sham vs. MI			MI vs. BMMNC			Sham vs. BMMNC		
		logFC	adj.P.Val	B	logFC	adj.P.Val	B	logFC	adj.P.Val	B
ILMN_1376428	Sema4a	2.252	0.00003	11.029	-1.319	0.00667	5.530	0.933	0.03663	2.992
ILMN_1358567	Oas1k	2.567	0.00003	10.480	-1.585	0.00667	5.316			
ILMN_1352951	Sifa2_predicted	4.630	0.00003	10.298	-2.477	0.01200	4.250	2.153	0.03663	2.980
ILMN_1364315	RGD1560676_predicted	4.700	0.00003	10.146	-2.559	0.01200	4.214	2.141	0.03795	2.720
ILMN_1376740	Glipr1	2.341	0.00026	8.189	-1.619	0.01369	3.970			
ILMN_1651187	LOC497712	1.715	0.00033	7.778				1.068	0.03795	2.609
ILMN_1362269	Actg_predicted	1.769	0.00033	7.710				1.089	0.03952	2.491
ILMN_1349760	Pygl	2.342	0.00039	7.438						
ILMN_1650752	Aplra1	1.819	0.00042	7.273	-1.627	0.00861	4.846			
ILMN_1350326	LOC308990	1.509	0.00042	7.151	-1.041	0.02831	3.052			
ILMN_1376765	Lcp1	1.913	0.00042	7.079						
ILMN_1361302	Klf5	1.314	0.00050	6.790				1.660	0.00220	5.620
ILMN_1369190	Pdlim7	1.460	0.00050	6.715						
ILMN_1371753	F5_mapped	1.749	0.00050	6.731	-1.118	0.04691	2.173			
ILMN_1351274	RGD1565374_predicted	3.232	0.00057	6.525						
ILMN_1371493	Edg6_predicted	1.630	0.00067	6.318	-1.224	0.03012	2.912			
ILMN_1364468	Coro1a	1.890	0.00070	6.218	-1.274	0.04691	2.097			
ILMN_1349113	Sell	3.062	0.00071	6.162						
ILMN_1376772	Stom	1.446	0.00075	5.969						
ILMN_1374896	Napsa	2.981	0.00075	5.955						
ILMN_1371081	Mmp8	3.197	0.00075	5.994						
ILMN_1359464	Emb	1.079	0.00077	5.818	-0.747	0.04691	1.933			
ILMN_1350897	Pfc_mapped	1.366	0.00077	5.715						
ILMN_1370817	Stk17b	1.477	0.00077	5.798	-1.024	0.04691	1.932			
ILMN_1362534	Retnla	1.535	0.00077	5.681	-1.115	0.04691	2.150			
ILMN_1376557	Nfe2	2.065	0.00077	5.668						
ILMN_1374845	MGC105649	2.161	0.00077	5.821						
ILMN_1349895	RGD1565140_predicted	2.490	0.00077	5.714						
ILMN_1366212	Errf1	2.443	0.00082	5.571						
ILMN_1368490	LOC24906	1.528	0.00084	5.512						
ILMN_1376621	Adck4	1.446	0.00089	5.431						
ILMN_1357059	Alox5ap	2.163	0.00092	5.365						
ILMN_1370198	LOC363060	1.153	0.00092	5.335	-0.873	0.04691	2.139			
ILMN_1368846	Pacsin2	-1.159	0.00097	5.110						
ILMN_1364945	LOC315883	1.008	0.00097	5.244				0.996	0.03663	3.447
ILMN_1350738	Gpr109a	1.181	0.00097	5.165						
ILMN_1353693	Cd53	1.495	0.00097	5.229						
ILMN_1373383	Tiparp_predicted	1.516	0.00097	5.145						
ILMN_1368402	Uap1_predicted	2.082	0.00097	5.104						
ILMN_1350798	Slc16a3	3.702	0.00097	5.109						
ILMN_1372724	RGD1562136_predicted	1.132	0.00098	5.028						
ILMN_1362834	Dusp6	1.623	0.00098	5.024						
ILMN_1370981	Akap12	2.237	0.00098	5.005						
ILMN_1375048	LOC684525	3.839	0.00098	5.052						
ILMN_1361277	Il1rn	1.802	0.00100	4.931						
ILMN_1367672	RGD1564330_predicted	1.830	0.00100	4.948						
ILMN_1354586	Ptafr	1.973	0.00100	4.913						
ILMN_1357030	Laptm5	0.939	0.00101	4.753						
ILMN_1355211	Pim1	0.964	0.00101	4.782						
ILMN_1355039	Actb	1.228	0.00101	4.847						
ILMN_2040884	RGD1309802_predicted	1.233	0.00101	4.840						
ILMN_1354445	Rassf1	1.442	0.00101	4.753						
ILMN_1358241	Adamts9_predicted	1.615	0.00101	4.777						
ILMN_1362702	Gmfg	2.158	0.00101	4.761						
ILMN_1356721	Cor1	2.271	0.00101	4.863						
ILMN_1369063	LOC497722	1.146	0.00103	4.714						
ILMN_1376726	Dgat2	2.026	0.00108	4.655						
ILMN_1348962	Lrrc10_predicted	-1.596	0.00113	4.580						
ILMN_1366128	RGD1562311_predicted	1.027	0.00113	4.565	-0.835	0.04691	1.979			
ILMN_1360909	Ednrb	1.204	0.00113	4.595						
ILMN_1349030	Il1r2	4.183	0.00113	4.546						
ILMN_1351430	Serpib10	2.044	0.00114	4.508						
ILMN_1351830	Retnlg	3.781	0.00114	4.523						

APPENDIX 7: continued

ID	SYMBOL	Sham vs. MI			MI vs. BMMNC			Sham vs. BMMNC		
		logFC	adj.P.Val	B	logFC	adj.P.Val	B	logFC	adj.P.Val	B
ILMN_1356202	Tlr6	1.107	0.00116	4.471						
ILMN_1372185	RGD1566118_predicted	0.949	0.00119	4.406						
ILMN_1362741	Ccr5	1.091	0.00119	4.406						
ILMN_1376363	Cnksr3	1.665	0.00119	4.431						
ILMN_1376301	Enpp3	1.783	0.00121	4.370						
ILMN_1370914	Dok3_predicted	1.179	0.00130	4.286	-1.065	0.04206	2.472			
ILMN_1348979	MGC93707	-1.083	0.00140	4.175						
ILMN_1376851	Rnd3	1.392	0.00140	4.199						
ILMN_1357799	LOC497748	2.069	0.00140	4.174						
ILMN_1376661	Lbp	1.194	0.00140	4.152						
ILMN_1360947	Tgm1	1.407	0.00140	4.130						
ILMN_1351237	Txnrd1	1.749	0.00140	4.138						
ILMN_1353208	G7c	-0.949	0.00143	4.040						
ILMN_1359365	Mttr7_predicted	0.873	0.00143	4.048						
ILMN_1376641	Chst1	1.015	0.00143	4.053	-1.095	0.01897	3.479			
ILMN_1364252	Btg3_predicted	1.101	0.00143	4.035						
ILMN_1357312	Mcl1	1.445	0.00143	4.041						
ILMN_1376579	Bst1	1.505	0.00143	4.026						
ILMN_1351679	LOC500040	1.829	0.00143	4.042						
ILMN_1357171	Adfp	1.649	0.00145	3.994						
ILMN_1353817	Prok2	3.131	0.00148	3.968						
ILMN_1375025	Fgr	1.189	0.00150	3.943						
ILMN_1358168	LOC363897	0.865	0.00151	3.916						
ILMN_1356655	Ii17r_predicted	1.583	0.00151	3.909						
ILMN_1351690	LOC500687	1.075	0.00159	3.847						
ILMN_1375922	Nr4a3	2.273	0.00163	3.814						
ILMN_2038944	RGD1309802_predicted	1.041	0.00165	3.780						
ILMN_1651184	Hp	3.531	0.00165	3.790						
ILMN_1374611	RGD1306595	-0.956	0.00168	3.745						
ILMN_1363228	Eli2	1.240	0.00168	3.726						
ILMN_1358531	Tubb6	1.967	0.00168	3.732						
ILMN_1373523	Igfbp3	1.114	0.00170	3.707						
ILMN_1370551	RGD1563888_predicted	1.230	0.00173	3.681						
ILMN_1350690	S100a8	3.645	0.00175	3.654						
ILMN_1359028	RGD1559988_predicted	0.735	0.00176	3.640						
ILMN_1370088	LOC311984	1.250	0.00177	3.627						
ILMN_1367232	RGD1307396_predicted	1.115	0.00180	3.599						
ILMN_1373122	Arpc5	0.801	0.00184	3.564						
ILMN_1354808	LOC500904	1.219	0.00185	3.552						
ILMN_1353924	Anxa1	1.612	0.00187	3.529						
ILMN_1376249	Tf	1.814	0.00187	3.524						
ILMN_1650006	Angpt2	1.155	0.00187	3.513						
ILMN_1354357	Jmjd1c	0.996	0.00187	3.492						
ILMN_1352340	Ii8rb	2.213	0.00187	3.501						
ILMN_2040847	Adrb2	0.752	0.00188	3.477						
ILMN_1363594	Zfp655	0.872	0.00192	3.450						
ILMN_1369168	Ccl6	2.130	0.00197	3.413						
ILMN_1357948	Trem1_predicted	2.881	0.00199	3.395						
ILMN_1374520	RGD1563073_predicted	1.138	0.00201	3.377						
ILMN_1362898	Clecsf9	2.174	0.00204	3.354						
ILMN_1363939	Ccni1	1.521	0.00204	3.337						
ILMN_1367877	Fcgr3	1.716	0.00204	3.332						
ILMN_1366054	Abcc8	-0.887	0.00207	3.229						
ILMN_1367596	Mocs2	-0.803	0.00207	3.232						
ILMN_1364579	Gnai3	0.750	0.00207	3.236						
ILMN_1364576	Verge	0.880	0.00207	3.255						
ILMN_1366777	Slc2a6_predicted	0.955	0.00207	3.235						
ILMN_1650307	Galnt3	0.979	0.00207	3.311						
ILMN_1353336	Rbm3	1.158	0.00207	3.292						
ILMN_1364910	RGD1561967_predicted	1.835	0.00207	3.289						
ILMN_1368419	Sat	1.874	0.00207	3.239						
ILMN_1359143	Samsn1	2.019	0.00207	3.272						
ILMN_2040190	Ifit1_predicted	3.072	0.00207	3.238						
ILMN_1363716	Sorl1_predicted	1.051	0.00209	3.206	-1.017	0.04691	2.025			
ILMN_1649963	Tpm3	1.356	0.00209	3.205						
ILMN_1650056	RGD1306658	1.145	0.00214	3.170						
ILMN_1370898	RGD1308872_predicted	0.893	0.00216	3.156						
ILMN_1370369	Egr2	1.539	0.00220	3.128						
ILMN_1376442	Nedd9	0.933	0.00222	3.110						
ILMN_1359590	Fgl2	1.979	0.00224	3.096						
ILMN_1355177	Dusp5	1.223	0.00225	3.077						
ILMN_1359732	Tfpi2	2.580	0.00225	3.080						

APPENDIX 7: continued

ID	SYMBOL	Sham vs. MI			MI vs. BMMNC			Sham vs. BMMNC		
		logFC	adj.P.Val	B	logFC	adj.P.Val	B	logFC	adj.P.Val	B
ILMN_1363727	Thbd	1.540	0.00227	3.058						
ILMN_1354499	Ltb	2.069	0.00234	3.022						
ILMN_1374656	RGD1565451_predicted	0.678	0.00238	2.998						
ILMN_1366607	Trh	0.987	0.00243	2.969				1.211	0.03663	3.082
ILMN_1373357	Sphk1	2.672	0.00243	2.963						
ILMN_1359089	Coq3	-0.813	0.00250	2.925						
ILMN_1369798	Hnrpf	0.704	0.00252	2.907						
ILMN_1351496	Pglyrp1	3.535	0.00252	2.905						
ILMN_1375583	Crem	1.966	0.00255	2.884						
ILMN_1357658	Wsb1	1.349	0.00260	2.860						
ILMN_1372404	Tyrobp	1.357	0.00261	2.848						
ILMN_1359659	Mrpl50_predicted	-0.754	0.00262	2.838						
ILMN_1359578	RGD1305574_predicted	-0.640	0.00275	2.778						
ILMN_1372165	Nckap1l_predicted	0.733	0.00275	2.761						
ILMN_1356132	RGD1561016_predicted	0.929	0.00275	2.760						
ILMN_1365682	Pdk3_mapped	0.988	0.00275	2.771						
ILMN_1351139	LOC498279	1.382	0.00275	2.757						
ILMN_1650285	Hmox1	1.200	0.00276	2.739						
ILMN_1365751	Kpnb3_predicted	1.314	0.00276	2.738						
ILMN_1354240	Ripk3	0.882	0.00277	2.721						
ILMN_1358144	Hspca	1.928	0.00277	2.724						
ILMN_1356369	Glrx1	1.930	0.00277	2.708						
ILMN_1363160	Plac8_predicted	2.169	0.00277	2.708						
ILMN_1358127	Plat	1.319	0.00278	2.697						
ILMN_1354457	LOC316207	1.187	0.00285	2.669						
ILMN_1358847	Fcar	1.177	0.00285	2.660						
ILMN_1651181	Cap1	0.874	0.00285	2.637						
ILMN_1369735	Odc1	0.931	0.00285	2.635						
ILMN_1374672	Nol5	1.298	0.00285	2.642						
ILMN_1368002	Snag1_predicted	1.534	0.00285	2.640						
ILMN_1370665	Zfand2a	2.502	0.00301	2.576						
ILMN_1349466	Plp2	0.692	0.00303	2.546						
ILMN_1358946	Cotl1_predicted	0.959	0.00303	2.542						
ILMN_1376877	Arhgap9	1.337	0.00303	2.558						
ILMN_1368364	Pstip1_predicted	1.366	0.00303	2.548						
ILMN_1355213	Ppp1r3b	1.412	0.00303	2.538						
ILMN_1360286	Slpi	3.302	0.00304	2.530						
ILMN_1364243	MGC94207	-0.717	0.00308	2.510						
ILMN_1372349	Arhgdib	0.864	0.00313	2.487						
ILMN_1372294	LOC499078	1.077	0.00315	2.458						
ILMN_1366909	LOC683463	1.509	0.00315	2.462						
ILMN_1371053	RGD1562655_predicted	1.687	0.00315	2.466						
ILMN_1352135	Ceacam10	3.236	0.00315	2.464						
ILMN_1361027	Mafb	0.829	0.00329	2.410						
ILMN_1373913	Ywhaz	0.985	0.00329	2.402						
ILMN_1362451	Rgs2	1.951	0.00330	2.395						
ILMN_1359219	Aif1	0.688	0.00341	2.350						
ILMN_1373687	RGD1307618_predicted	0.796	0.00341	2.349						
ILMN_1349555	RGD1359509	1.428	0.00344	2.337						
ILMN_1357127	Nalp12_predicted	0.710	0.00346	2.319						
ILMN_1368423	Fbxl5_predicted	1.074	0.00346	2.320						
ILMN_1352911	Plek	2.248	0.00353	2.294						
ILMN_1359982	Ccdc51	-1.003	0.00365	2.255						
ILMN_1356828	Arg1	1.045	0.00372	2.228						
ILMN_1366543	RGD1560119_predicted	1.305	0.00372	2.224						
ILMN_1355936	Adss_predicted	0.929	0.00374	2.214						
ILMN_1374695	Oldlr1	1.266	0.00384	2.182						
ILMN_1650241	Tmem60_predicted	-0.727	0.00386	2.154						
ILMN_1353169	Sema4d_predicted	0.604	0.00386	2.156						
ILMN_1356425	Ptbp1	0.857	0.00386	2.163						
ILMN_2038799	Actb	0.951	0.00386	2.164						
ILMN_1367061	RGD1561141_predicted	-0.865	0.00391	2.112						
ILMN_1349844	Maea	-0.719	0.00391	2.116						
ILMN_1368068	RGD1562105_predicted	0.709	0.00391	2.114						
ILMN_1353551	Itgb7	0.955	0.00391	2.130						
ILMN_1370840	Lgals3	0.963	0.00391	2.107						
ILMN_1356957	LOC687856	1.104	0.00391	2.105						
ILMN_1362050	RGD1563994_predicted	1.333	0.00391	2.108						
ILMN_1365809	Ptbrc	1.147	0.00391	2.100						
ILMN_1373013	Hck	1.160	0.00392	2.094						

APPENDIX 7: continued

ID	SYMBOL	Sham vs. MI			MI vs. BMMNC			Sham vs. BMMNC		
		logFC	adj.P.Val	B	logFC	adj.P.Val	B	logFC	adj.P.Val	B
ILMN_1371475	Gmpr	-0.774	0.00393	2.077						
ILMN_1357924	Gnl3	1.026	0.00393	2.081						
ILMN_1371943	Runx1	1.135	0.00393	2.084						
ILMN_1364500	Hspcal3_predicted	1.905	0.00399	2.057						
ILMN_1371205	Map4k1_predicted	1.258	0.00399	2.051						
ILMN_1363936	Fem1a	-0.861	0.00407	2.014						
ILMN_1350981	Ripk1_predicted	0.897	0.00407	2.013						
ILMN_1355065	Ptpn1	0.975	0.00407	2.021						
ILMN_1365729	Slc7a5	1.349	0.00407	2.014						
ILMN_1349008	H3f3b	0.948	0.00407	2.008						
ILMN_1352529	Ier2	1.202	0.00413	1.988						
ILMN_1352096	Cspg4	-1.059	0.00414	1.962						
ILMN_1361386	Abhd14a	-0.623	0.00414	1.959						
ILMN_1350279	Syk	0.670	0.00414	1.962						
ILMN_1350976	Arpc3_predicted	0.730	0.00414	1.957						
ILMN_1359095	Mat2a	0.969	0.00414	1.976						
ILMN_1369914	Rasd1	1.064	0.00414	1.964						
ILMN_1361387	Trim45_predicted	-0.868	0.00422	1.915						
ILMN_1350620	Gp1bb	0.988	0.00422	1.919						
ILMN_1361672	Tm4sf1_predicted	1.143	0.00422	1.933						
ILMN_1349889	Cyp4f5	1.154	0.00422	1.928						
ILMN_1368412	Jmjd3_predicted	1.473	0.00422	1.920						
ILMN_1353022	Jph2	-0.751	0.00425	1.899						
ILMN_1359516	Gclc	1.118	0.00425	1.902						
ILMN_1363777	Scap2	1.056	0.00429	1.886						
ILMN_2040557	Serpine1	2.271	0.00431	1.876						
ILMN_1362293	RGD1562305_predicted	-0.885	0.00435	1.860						
ILMN_1364569	Cd24	0.752	0.00435	1.853						
ILMN_2039240	Mmp9	1.775	0.00435	1.855						
ILMN_1353276	RGD1559981_predicted	-0.706	0.00440	1.833						
ILMN_1353943	Lrg1	0.983	0.00440	1.832						
ILMN_1352095	Myl7_predicted	-1.108	0.00441	1.827						
ILMN_1348782	Etfhd	-0.584	0.00443	1.818						
ILMN_1367516	LOC363331	-1.092	0.00450	1.798						
ILMN_1360607	Numb1_predicted	0.797	0.00450	1.793						
ILMN_1376913	Zc3h8	-0.698	0.00459	1.769						
ILMN_1359661	Nasp	0.783	0.00460	1.754						
ILMN_1368793	Cdr2	1.102	0.00460	1.758						
ILMN_1353896	Tlr2	2.223	0.00460	1.762						
ILMN_1366783	Vps13d_predicted	-0.737	0.00461	1.732						
ILMN_1365622	Pcyt2	-0.664	0.00461	1.730						
ILMN_1364613	Rhoj	0.764	0.00461	1.718						
ILMN_1356330	Lst1	0.998	0.00461	1.718						
ILMN_2038798	Actb	1.123	0.00461	1.741						
ILMN_1357368	LOC497841	1.702	0.00461	1.738						
ILMN_1370638	LOC498277	2.038	0.00461	1.725						
ILMN_1352285	Serpinb1a	3.028	0.00461	1.746						
ILMN_1364192	RGD1560523_predicted	1.012	0.00487	1.659						
ILMN_1365557	Cyb5r3	-0.698	0.00487	1.655						
ILMN_1359146	Zswim6	0.664	0.00488	1.638						
ILMN_1370131	RGD1564130_predicted	1.042	0.00488	1.644						
ILMN_1351826	Ippk	1.073	0.00488	1.647						
ILMN_1353078	Pde4b	1.877	0.00488	1.636						
ILMN_1361128	Acat2	0.687	0.00491	1.626						
ILMN_1364095	LOC362703	1.095	0.00495	1.613						
ILMN_2040035	Trem1_predicted	1.783	0.00496	1.608						
ILMN_1358347	Pls3	1.088	0.00498	1.599						
ILMN_1349016	Rabgef1_predicted	0.767	0.00505	1.583						
ILMN_1363372	Ets2_mapped	0.773	0.00505	1.578						
ILMN_1362278	Slc5a3	2.139	0.00505	1.573						
ILMN_1349287	Hiat1_predicted	0.794	0.00512	1.556						
ILMN_1363628	Nt5m_predicted	-0.868	0.00516	1.541						
ILMN_1361561	Pten	0.654	0.00516	1.532						
ILMN_1356110	Klf4	1.136	0.00516	1.536						
ILMN_1360736	Ugdh	1.887	0.00516	1.537						
ILMN_1353729	Pgd	0.771	0.00523	1.505						
ILMN_1353820	Actr3	0.816	0.00523	1.504						
ILMN_1359024	Myd88	1.247	0.00523	1.511						
ILMN_1357730	Npy	3.309	0.00523	1.509						
ILMN_1364203	Pcna	0.713	0.00535	1.478						

APPENDIX 7: continued

ID	SYMBOL	Sham vs. MI			MI vs. BMMNC			Sham vs. BMMNC		
		logFC	adj.P.Val	B	logFC	adj.P.Val	B	logFC	adj.P.Val	B
ILMN_1368356	Fos	3.750	0.00542	1.461						
ILMN_1360418	RGD1302996	-0.819	0.00545	1.448						
ILMN_1359200	Timp1	2.038	0.00545	1.449						
ILMN_1349137	Ptpro	0.964	0.00551	1.433						
ILMN_1367417	Polmt_predicted	-0.669	0.00552	1.416						
ILMN_1358564	Pabpc1	0.736	0.00552	1.426						
ILMN_1367519	Idi1	0.821	0.00552	1.417						
ILMN_1360373	Ptpn6	0.998	0.00552	1.417						
ILMN_1530409	Ier5	1.038	0.00552	1.413						
ILMN_1374891	Cyp11a1	-0.651	0.00555	1.395						
ILMN_1351646	Gpr4	0.930	0.00555	1.402						
ILMN_2039673	Arc	1.405	0.00555	1.398						
ILMN_1365610	RGD1565319_predicted	2.368	0.00555	1.393						
ILMN_1650001	Ociad1	-0.560	0.00560	1.377						
ILMN_1350180	Emp1	1.938	0.00560	1.376						
ILMN_1376722	MGC94736	-0.599	0.00562	1.364						
ILMN_1359287	LOC310086	0.568	0.00562	1.363						
ILMN_1374870	Pafah1b1	1.103	0.00562	1.364						
ILMN_1359784	LOC362115	0.929	0.00564	1.356						
ILMN_1350250	Soat1	0.577	0.00576	1.330						
ILMN_1376946	Clec4d	1.113	0.00584	1.313						
ILMN_1375131	MGC125015	0.953	0.00584	1.309						
ILMN_1373952	Cspg2	1.714	0.00586	1.302						
ILMN_1370049	Zfp180	-0.622	0.00605	1.263						
ILMN_1351911	RGD1310168_predicted	0.743	0.00605	1.264						
ILMN_1373876	Pmp22	0.728	0.00607	1.257						
ILMN_1359759	Scnn1a	0.885	0.00609	1.243						
ILMN_1362786	Cias1_predicted	1.156	0.00609	1.242						
ILMN_1376417	Serpine1	2.025	0.00609	1.247						
ILMN_1650650	Gypc	-0.618	0.00629	1.206						
ILMN_1371223	Fbl	0.756	0.00636	1.192						
ILMN_1374737	Ifitm6_predicted	3.015	0.00639	1.183						
ILMN_1370087	LOC498062	-0.597	0.00648	1.164						
ILMN_1366126	RGD1564040_predicted	0.709	0.00648	1.159						
ILMN_1375100	Atf4	1.266	0.00648	1.159						
ILMN_1375084	RGD1559897_predicted	0.678	0.00651	1.151						
ILMN_1371126	Procr	2.277	0.00659	1.135						
ILMN_1362330	Slc25a29	-0.733	0.00665	1.123						
ILMN_1355677	RGD1305246	0.952	0.00669	1.110						
ILMN_1367946	Baz1a_predicted	0.967	0.00669	1.108						
ILMN_1369706	Dnajb1_predicted	2.419	0.00669	1.108						
ILMN_1357240	RGD1564549_predicted	-0.600	0.00671	1.101						
ILMN_1364370	Klrb1b	0.838	0.00671	1.097						
ILMN_1365821	RGD1566093_predicted	0.539	0.00683	1.076						
ILMN_1361776	MGC72584	-0.754	0.00687	1.064						
ILMN_1375833	Crem	2.041	0.00687	1.065						
ILMN_1373900	MGC72974	-1.236	0.00696	1.039						
ILMN_1363911	MGC94339	-0.698	0.00696	1.045						
ILMN_1350548	Neurl2_predicted	-0.598	0.00696	1.032						
ILMN_1373883	S100a11	0.848	0.00696	1.041						
ILMN_1360748	Pgsq	0.887	0.00696	1.034						
ILMN_1365695	Dnaja1	1.471	0.00696	1.032						
ILMN_1357140	Irx4_predicted	-0.782	0.00698	1.012						
ILMN_1358668	Ddt	-0.768	0.00698	1.009						
ILMN_1362991	Vps45	-0.580	0.00698	1.006						
ILMN_1364441	Gja3	-0.553	0.00698	0.999						
ILMN_1650489	Isoc2b	-0.550	0.00698	1.020						
ILMN_1375233	Vps24	-0.517	0.00698	1.009						
ILMN_1373962	Gp9	0.712	0.00698	0.995						
ILMN_1372586	Ell_predicted	0.715	0.00698	1.012						
ILMN_1374460	Yars	0.969	0.00698	1.018						
ILMN_1365800	Rac2	1.031	0.00698	0.995						
ILMN_1362080	Klf6	1.121	0.00698	0.996						
ILMN_1373510	Pskh1_predicted	-0.554	0.00705	0.982						
ILMN_1350364	RGD1563798_predicted	-0.762	0.00705	0.979						
ILMN_1371051	Hk3	0.924	0.00705	0.975						
ILMN_1367615	Spsb1_predicted	0.845	0.00708	0.965						
ILMN_1349218	Casp3	1.023	0.00708	0.968						
ILMN_1365196	Sertad1	1.147	0.00711	0.958						
ILMN_1376319	Fus	0.585	0.00711	0.955						

APPENDIX 7: continued

ID	SYMBOL	Sham vs. MI			MI vs. BMMNC			Sham vs. BMMNC		
		logFC	adj.P.Val	B	logFC	adj.P.Val	B	logFC	adj.P.Val	B
ILMN_1360968	Arl5a	0.676	0.00721	0.937						
ILMN_1357555	LOC307907	-0.811	0.00727	0.926						
ILMN_1373668	RGD1310553	-0.728	0.00727	0.917						
ILMN_1356615	Gpr65_predicted	0.537	0.00727	0.921						
ILMN_1360656	Gfpt2	2.044	0.00727	0.918						
ILMN_1366301	RGD1561143_predicted	0.648	0.00729	0.911						
ILMN_1370116	LOC501594	0.591	0.00731	0.903						
ILMN_1367573	Slc25a25	1.071	0.00731	0.902						
ILMN_1366898	Irf2bp1_predicted	-0.701	0.00735	0.894						
ILMN_1348939	C1qr1	1.014	0.00740	0.884						
ILMN_1362859	Mrlp22_predicted	-0.527	0.00741	0.881						
ILMN_1371034	Acsl4	0.642	0.00748	0.867						
ILMN_1376914	Akap2	1.526	0.00748	0.864						
ILMN_1372499	Lad1_predicted	-0.746	0.00750	0.857						
ILMN_1376380	P2ry13	0.766	0.00750	0.859						
ILMN_1366394	Timm13	-0.570	0.00756	0.842						
ILMN_1367954	Ddx39	0.687	0.00756	0.842						
ILMN_1355362	Mca32	0.744	0.00758	0.837						
ILMN_1357130	Cflar	0.897	0.00759	0.833						
ILMN_1357039	RGD1310357_predicted	0.815	0.00762	0.826						
ILMN_1363774	Tpm3	0.713	0.00773	0.807						
ILMN_1360221	Tacstd1	1.765	0.00773	0.806						
ILMN_1369005	Egr1	2.664	0.00776	0.799						
ILMN_1367927	Ly49i8	0.695	0.00783	0.785						
ILMN_1349873	Cd302	0.881	0.00783	0.784						
ILMN_1363263	Lrrc8c	0.743	0.00797	0.763						
ILMN_1372107	Nos2	1.905	0.00800	0.756						
ILMN_1353390	Mxd1	1.368	0.00802	0.751						
ILMN_1352342	Eif5	0.823	0.00802	0.745						
ILMN_1376646	Bag3	0.859	0.00802	0.741						
ILMN_1349269	Sgk	1.012	0.00802	0.743						
ILMN_1362622	Rhoh	1.293	0.00802	0.740						
ILMN_1376312	Mar-07	0.960	0.00814	0.722						
ILMN_1357241	Pmm1	-0.618	0.00816	0.717						
ILMN_1351668	Pcf11_predicted	0.676	0.00818	0.712						
ILMN_1371731	LOC501284	-0.750	0.00822	0.705						
ILMN_1357763	Rhoq	0.781	0.00832	0.689						
ILMN_1350091	G0s2	1.818	0.00838	0.679						
ILMN_1356563	Ptges2_predicted	-0.584	0.00853	0.658						
ILMN_1369599	Cxcl4	2.063	0.00853	0.655						
ILMN_1366226	RGD1359713	0.672	0.00860	0.644						
ILMN_1349422	Ptgs2	2.647	0.00865	0.636						
ILMN_1368524	Glg1	-0.762	0.00865	0.633						
ILMN_1357506	Gpsm1	-0.657	0.00867	0.624						
ILMN_1357886	Mrlp16	-0.582	0.00867	0.627						
ILMN_1650950	Josd3	0.825	0.00867	0.623						
ILMN_1367384	Mox2r	0.949	0.00871	0.616						
ILMN_1367435	Pdzd7_predicted	-0.581	0.00871	0.612						
ILMN_1355544	LOC498276	1.684	0.00871	0.610						
ILMN_1364338	Zcchc12	0.783	0.00873	0.606						
ILMN_1351557	Tmem9_predicted	-0.548	0.00885	0.589						
ILMN_1357664	Sema6a_predicted	0.557	0.00898	0.571						
ILMN_1361429	Arlh1	1.117	0.00905	0.561						
ILMN_1359238	Rock2	0.563	0.00907	0.555						
ILMN_1363954	Nip7	0.863	0.00914	0.545						
ILMN_1372842	Cars_predicted	0.845	0.00928	0.524						
ILMN_1369410	Sec23b_predicted	0.882	0.00928	0.524						
ILMN_1354751	Leng4_predicted	0.632	0.00933	0.517						
ILMN_1352021	Tmx2	-0.652	0.00933	0.511						
ILMN_1351674	Gdf15	1.061	0.00933	0.511						
ILMN_1349147	Mar-03	1.448	0.00933	0.508						
ILMN_1370633	Itpkc	1.651	0.00937	0.502						
ILMN_1376777	Mpst	-0.663	0.00937	0.496						
ILMN_1376818	Tubb3	0.626	0.00937	0.495						
ILMN_1371385	Gpsm3	0.770	0.00937	0.494						
ILMN_1367486	Dusp1	1.266	0.00940	0.489						
ILMN_1373864	RGD1308113	-0.535	0.00949	0.474						
ILMN_1352642	Spp1	1.816	0.00949	0.475						
ILMN_1362482	Nkx2-5	-0.749	0.00950	0.470						
ILMN_1349318	Tmem49	0.651	0.00950	0.468						

APPENDIX 7: continued

ID	SYMBOL	Sham vs. MI			MI vs. BMMNC			Sham vs. BMMNC		
		logFC	adj.P.Val	B	logFC	adj.P.Val	B	logFC	adj.P.Val	B
ILMN_1361287	Surb7_predicted	0.595	0.00951	0.464						
ILMN_1364113	Ctgf	1.265	0.00956	0.456						
ILMN_1363587	Slc25a19	-0.549	0.00959	0.446						
ILMN_1369550	RGD1305622	-0.501	0.00959	0.451						
ILMN_1349697	Midn_predicted	0.704	0.00959	0.446				1.115	0.03795	2.678
ILMN_1351900	Fcnb	1.580	0.00959	0.444						
ILMN_1353563	Aacs	0.572	0.00962	0.438						
ILMN_1352848	Cdc42ep3_predicted	0.584	0.00962	0.435						
ILMN_1354419	Bcl2a1	1.952	0.00967	0.428						
ILMN_1349102	RGD1562922_predicted	-1.096	0.00968	0.422						
ILMN_1363106	Ndel1	0.538	0.00968	0.422						
ILMN_1366871	Bmyc	-0.652	0.00969	0.416						
ILMN_1356848	Btg1	1.075	0.00969	0.416						
ILMN_1366459	LOC499612	-0.519	0.00971	0.411						
ILMN_1367494	Vdac3	-0.611	0.00996	0.382						
ILMN_1365578	RGD1561055_predicted	0.747	0.00996	0.380						
ILMN_1357616	Casq2	-0.690	0.01157	0.061	1.253	0.01897	3.553			
ILMN_1372230	Rnf149				-1.778	0.03978	2.595			

APPENDIX 8: Probe level data for the top 433 probes found to be altered in the LIMMA analysis Including all probes with significant difference in MI vs. BMMNC ($p < 0.05$) and all probes with significant alteration in Sham vs. MI ($p < 0.01$). Illumina probe ID, gene symbol, gene accession code and gene definition are shown alongside the average signal and standard deviation for each experimental group for every probe found to be significantly altered in the LIMMA analysis.

ID	SYMBOL	ACCESSION	DEFINITION	Ave Sham	StDev Sham	Ave MI	StDev MI	Ave MNC	StDev MNC
ILMN_1349147	Mar-03	NM_001007759.1	membrane-associated ring finger (C3HC4) 3 (March3), mRNA.	310.27	127.65	805.87	96.58	656.82	146.01
ILMN_1376312	Mar-07	NM_001012087.1	membrane-associated ring finger (C3HC4) 7 (March7), mRNA.	65.03	3.23	128.15	26.46	84.69	19.24
ILMN_1353563	Aacs	NM_023104.1	acetoacetyl-CoA synthetase (Aacs), mRNA.	69.56	4.28	103.34	4.51	73.87	8.34
ILMN_1366054	Abcc8	NM_013039.1	ATP-binding cassette, sub-family C (CFTR/MRP), member 8 (Abcc8), mRNA.	349.47	25.65	188.78	7.87	279.42	41.74
ILMN_1361386	Abhd14a	NM_001009670.1	abhydrolase domain containing 14A (Abhd14a), mRNA.	122.07	5.55	79.26	2.79	96.01	5.11
ILMN_1361128	Acat2	NM_001006995.1	acetyl-Coenzyme A acetyltransferase 2 (Acat2), mRNA.	142.35	16.10	228.24	8.25	185.16	3.38
ILMN_1371034	Acsl4	NM_053623.1	acyl-CoA synthetase long-chain family member 4 (Acsl4), mRNA.	57.67	3.59	90.15	8.78	63.07	4.85
ILMN_1355039	Actb	NM_031144.2	actin, beta (Actb), mRNA.	2171.06	190.60	5099.52	661.78	3093.01	347.33
ILMN_2038799	Actb	NM_031144.2	actin, beta (Actb), mRNA.	6518.84	445.31	12717.95	2202.32	9038.88	622.88
ILMN_2038798	Actb	NM_031144.2	actin, beta (Actb), mRNA.	1824.31	95.97	4011.43	688.48	2575.02	701.59
ILMN_1362269	Actg_predicted	XM_213540.3	actin, gamma, cytoplasmic (predicted) (Actg_predicted), mRNA.	2320.65	284.09	7905.07	912.57	4916.95	306.69
ILMN_1353820	Actr3	NM_031068.1	ARP3 actin-related protein 3 homolog (yeast) (Actr3), mRNA.	877.15	61.60	1554.57	239.11	1223.41	27.10
ILMN_1358241	Adamts9_predicted	XM_232202.3	a disintegrin-like and metalloprotease (repolysin type) with thrombospondin type 1 motif, 9 (predicted) (Adamts9_predicted), mRNA.	224.34	47.34	682.70	106.97	486.05	54.44
ILMN_1376621	Adck4	XM_001077748.1	aarF domain containing kinase 4 (Adck4), mRNA.	105.76	10.89	289.94	47.95	183.14	5.75
ILMN_1357171	Adfp	NM_001007144.1	adipose differentiation related protein (Adfp), mRNA.	998.42	277.46	3057.84	314.88	1799.12	132.96
ILMN_2040847	Adrb2	NM_012492.2	adrenergic receptor, beta 2 (Adrb2), mRNA.	135.12	2.97	227.67	10.20	166.96	11.30
ILMN_1355936	Adss_predicted	XM_001059694.1	adenylosuccinate synthetase, non muscle (predicted) (Adss_predicted), mRNA.	335.87	53.56	634.73	27.10	470.35	64.74
ILMN_1359219	Aif1	NM_017196.2	allograft inflammatory factor 1 (Aif1), mRNA.	445.08	22.78	717.68	50.58	485.35	1.68
ILMN_1370981	Akap12	NM_001033653.1	A kinase (PRKA) anchor protein (gravin) 12 (Akap12), transcript variant 2, mRNA.	92.18	24.28	430.43	93.11	248.46	37.10
ILMN_1376914	Akap2	NM_001011974.1	A kinase (PRKA) anchor protein 2 (Akap2), mRNA.	217.57	94.66	596.60	104.70	515.17	34.89
ILMN_1357059	Alox5ap	NM_017260.2	arachidonate 5-lipoxygenase activating protein (Alox5ap), mRNA.	124.13	15.81	572.79	190.00	204.58	5.30
ILMN_1650006	Angpt2	XM_001065522.1	angiopoietin 2 (Angpt2), mRNA.	80.77	6.57	180.85	27.02	134.11	20.16
ILMN_1353924	Anxa1	NM_012904.1	annexin A1 (Anxa1), mRNA.	776.54	203.90	2337.85	367.13	1199.98	183.60
ILMN_1650752	Aplra1	NM_001005896.1	antigen presenting cell lectin-like receptor A1 (Aplra1), mRNA.	31.56	1.61	112.74	23.00	36.05	1.03
ILMN_2039673	Arc	NM_019361.1	activity regulated cytoskeletal-associated protein (Arc), mRNA.	55.01	2.68	149.95	45.66	123.59	39.37
ILMN_1356828	Arg1	NM_017134.1	arginase 1 (Arg1), mRNA.	67.68	11.87	139.29	21.43	93.98	0.91
ILMN_1376877	Arhgap9	XM_001056068.1	Rho GTPase activating protein 9 (Arhgap9), mRNA.	122.64	7.06	318.54	94.72	154.14	0.17
ILMN_1372349	Arhgdib	NM_001009600.1	Rho, GDP dissociation inhibitor (GDI) beta (Arhgdib), mRNA.	704.63	90.43	1278.90	113.09	755.44	10.56
ILMN_1361429	Arih1	NM_001013108.1	ariadne ubiquitin-conjugating enzyme E2 binding protein homolog 1 (Drosophila) (Arih1), mRNA.	240.10	27.32	524.82	97.23	351.20	116.69
ILMN_1360968	Arl5a	NM_053979.1	ADP-ribosylation factor-like 5A (Arl5a), mRNA.	159.18	16.90	253.42	1.82	220.25	29.14
ILMN_1350976	Arpc3_predicted	XM_213782.4	actin related protein 2/3 complex, subunit 3 (predicted) (Arpc3_predicted), mRNA.	521.98	8.95	869.53	96.85	593.22	45.73

APPENDIX 8: continued

ID	SYMBOL	ACCESSION	DEFINITION	Ave Sham	StDev Sham	Ave MI	StDev MI	Ave MNC	StDev MNC
ILMN_1373122	Arpc5	NM_001025717.1	actin related protein 2/3 complex, subunit 5 (Arpc5), mRNA.	1395.58	64.48	2433.05	147.58	1672.33	108.13
ILMN_1375100	Atf4	NM_024403.1	activating transcription factor 4 (Atf4), mRNA.	715.20	225.85	1680.93	276.36	1048.78	78.58
ILMN_1376646	Bag3	NM_001011936.1	Bcl2-associated athanogene 3 (Bag3), mRNA.	5864.32	561.22	10637.38	1066.30	10072.59	2513.78
ILMN_1367946	Baz1a_predicted	XM_001079067.1	bromodomain adjacent to zinc finger domain, 1A (predicted) (Baz1a_predicted), mRNA.	106.82	8.80	211.15	40.89	141.76	24.05
ILMN_1354419	Bcl2a1	NM_133416.1	B-cell leukemia/lymphoma 2 related protein A1 (Bcl2a1), mRNA.	218.10	62.25	884.98	404.62	435.03	183.89
ILMN_1366871	Bmyc	NM_001013163.2	brain expressed myelocytomatosis oncogene (Bmyc), mRNA.	106.32	2.40	68.13	10.07	78.78	4.95
ILMN_1376579	Bst1	NM_030848.1	bone marrow stromal cell antigen 1 (Bst1), mRNA.	82.83	9.12	237.59	47.59	122.61	22.63
ILMN_1356848	Btg1	NM_017258.1	B-cell translocation gene 1, anti-proliferative (Btg1), mRNA.	2563.41	778.38	5278.74	660.71	4233.48	381.62
ILMN_1364252	Btg3_predicted	XM_346415.2	B-cell translocation gene 3 (predicted) (Btg3_predicted), mRNA.	154.27	21.63	329.58	29.31	251.54	11.98
ILMN_1348939	C1qr1	NM_053383.1	complement component 1, q subcomponent, receptor 1 (C1qr1), mRNA.	715.02	144.89	1433.00	179.24	1044.88	212.32
ILMN_1651181	Cap1	NM_022383.2	CAP, adenylate cyclase-associated protein 1 (yeast) (Cap1), mRNA.	331.75	17.46	609.94	68.15	390.66	51.21
ILMN_1372842	Cars_predicted	XM_001065753.1	cysteinyl-tRNA synthetase (predicted) (Cars_predicted), mRNA.	86.23	4.67	156.43	28.47	128.03	23.55
ILMN_1349218	Casp3	NM_012922.2	caspase 3, apoptosis related cysteine protease (Casp3), mRNA.	100.94	18.45	205.83	42.52	154.22	9.37
ILMN_1357616	Casq2	NM_017131.1	calsequestrin 2 (Casq2), mRNA.	373.51	51.14	231.13	27.15	548.56	14.68
ILMN_1359982	Ccdc51	NM_001014098.1	coiled-coil domain containing 51 (Ccdc51), mRNA.	275.64	52.15	135.85	4.39	180.62	13.43
ILMN_1369168	Ccl6	NM_001004202.1	chemokine (C-C motif) ligand 6 (Ccl6), mRNA.	79.52	23.23	354.56	136.29	139.11	4.22
ILMN_1363939	Ccnl1	NM_053662.3	cyclin L1 (Ccnl1), mRNA.	545.56	54.46	1601.94	420.60	1145.80	58.62
ILMN_1356721	Ccr1	NM_020542.2	chemokine (C-C motif) receptor 1 (Ccr1), mRNA.	157.20	9.02	800.35	339.03	337.93	11.42
ILMN_1362741	Ccr5	NM_053960.3	chemokine (C-C motif) receptor 5 (Ccr5), mRNA.	149.85	20.62	317.37	14.72	189.77	9.37
ILMN_1364569	Cd24	NM_012752.2	CD24 antigen (Cd24), mRNA.	72.41	7.90	121.66	9.31	75.91	2.40
ILMN_1349873	Cd302	NM_001013916.1	CD302 antigen (Cd302), mRNA.	404.90	72.67	743.44	108.43	532.18	15.96
ILMN_1353693	Cd53	NM_012523.1	CD53 antigen (Cd53), mRNA.	49.61	4.63	141.19	27.52	69.84	2.47
ILMN_1352848	Cdc42ep3_predicted	XM_233815.3	CDC42 effector protein (Rho GTPase binding) 3 (predicted) (Cdc42ep3_predicted), mRNA.	86.19	1.60	129.28	4.26	113.97	17.67
ILMN_1368793	Cdr2	NM_001025682.1	cerebellar degeneration-related 2 (Cdr2), mRNA.	77.06	16.02	163.32	7.68	127.90	29.74
ILMN_1352135	Ceacam10	NM_173339.1	CEA-related cell adhesion molecule 10 (Ceacam10), mRNA.	106.51	88.67	825.24	188.88	323.97	37.71
ILMN_1357130	Cflar	NM_057138.2	CASP8 and FADD-like apoptosis regulator (Cflar), transcript variant 2, mRNA.	163.20	23.45	303.36	36.92	298.58	60.51
ILMN_1376641	Chst1	NM_001011955.1	carbohydrate (keratan sulfate Gal-6) sulfotransferase 1 (Chst1), mRNA.	125.50	10.53	254.17	30.19	118.42	3.41
ILMN_1362786	Cias1_predicted	XM_220513.4	cold autoinflammatory syndrome 1 homolog (human) (predicted) (Cias1_predicted), mRNA.	42.57	3.09	95.89	18.11	59.38	18.58
ILMN_1376946	Clec4d	NM_001003707.1	C-type lectin domain family 4, member d (Clec4d), mRNA.	43.52	3.97	95.59	23.01	46.77	9.49
ILMN_1362898	Clecsf9	NM_001005897.1	macrophage-inducible C-type lectin (Clecsf9), mRNA.	61.15	17.33	278.70	89.36	133.05	36.45
ILMN_1376363	Cnksr3	NM_001012061.1	Cnksr family member 3 (Cnksr3), mRNA.	226.39	30.31	715.76	65.37	605.90	205.24
ILMN_1359089	Coq3	NM_019187.1	coenzyme Q3 homolog, methyltransferase (yeast) (Coq3), mRNA.	1902.05	142.71	1083.30	90.34	1600.73	75.83
ILMN_1364468	Coro1a	NM_130411.2	coronin, actin binding protein 1A (Coro1a), mRNA.	266.39	63.32	974.45	115.04	401.07	14.26
ILMN_1358946	Cotl1_predicted	XM_341700.3	coactosin-like 1 (Dictyostelium) (predicted) (Cotl1_predicted), mRNA.	136.57	3.01	268.14	45.36	191.22	15.73
ILMN_1375583	Crem	NM_013086.1	cAMP responsive element modulator (Crem), transcript variant 1, mRNA.	240.86	102.82	891.12	50.86	518.30	141.69
ILMN_1375833	Crem	NM_017334.1	cAMP responsive element modulator (Crem), transcript variant 2, mRNA.	120.33	66.63	454.24	57.72	249.39	98.22
ILMN_1373952	Cspg2	XM_215451.4	chondroitin sulfate proteoglycan 2 (Cspg2), mRNA.	220.02	84.84	685.31	94.23	467.99	92.62

APPENDIX 8: continued

ID	SYMBOL	ACCESSION	DEFINITION	Ave Sham	StDev Sham	Ave MI	StDev MI	Ave MNC	StDev MNC
ILMN_1352096	Cspg4	NM_031022.1	chondroitin sulfate proteoglycan 4 (Cspg4), mRNA.	383.02	71.90	181.61	9.62	284.08	49.70
ILMN_1364113	Ctgf	NM_022266.2	connective tissue growth factor (Ctgf), mRNA.	2627.23	292.69	6377.17	1333.44	4432.42	1881.46
ILMN_1369599	Cxcl4	NM_001007729.1	chemokine (C-X-C motif) ligand 4 (Cxcl4), mRNA.	401.42	125.03	1812.68	1028.71	747.93	63.31
ILMN_1365557	Cyb5r3	NM_138877.1	cytochrome b5 reductase 3 (Cyb5r3), mRNA.	172.20	15.31	105.96	5.84	134.74	12.27
ILMN_1374891	Cyp11a1	NM_017286.1	cytochrome P450, family 11, subfamily a, polypeptide 1 (Cyp11a1), mRNA.	928.96	92.56	589.78	8.86	775.62	54.54
ILMN_1349889	Cyp4f5	NM_173124.1	cytochrome P450 4F5 (Cyp4f5), mRNA.	112.13	28.52	245.60	27.47	231.84	20.71
ILMN_1358668	Ddt	NM_024131.1	D-dopachrome tautomerase (Ddt), mRNA.	794.24	58.87	469.30	73.96	736.45	57.57
ILMN_1367954	Ddx39	NM_053563.2	DEAD (Asp-Glu-Ala-Asp) box polypeptide 39 (Ddx39), mRNA.	367.17	52.35	587.75	31.95	421.64	7.41
ILMN_1376726	Dgat2	NM_001012345.1	diacylglycerol O-acyltransferase homolog 2 (mouse) (Dgat2), mRNA.	324.31	45.07	1353.14	424.38	693.82	150.36
ILMN_1365695	Dnaja1	NM_022934.1	DnaJ (Hsp40) homolog, subfamily A, member 1 (Dnaja1), mRNA.	3209.10	518.65	9060.12	2422.20	7138.14	2588.04
ILMN_1369706	Dnajb1_predicted	XM_001069407.1	DnaJ (Hsp40) homolog, subfamily B, member 1 (predicted) (Dnajb1_predicted), mRNA.	1344.65	300.56	7498.73	2955.22	5987.70	4038.05
ILMN_1370914	Dok3_predicted	XM_001069255.1	docking protein 3 (predicted) (Dok3_predicted), mRNA.	45.54	2.57	103.67	14.44	49.42	6.51
ILMN_1367486	Dusp1	NM_053769.2	dual specificity phosphatase 1 (Dusp1), mRNA.	2072.98	249.79	5006.80	805.89	2747.02	1212.61
ILMN_1355177	Dusp5	NM_133578.1	dual specificity phosphatase 5 (Dusp5), mRNA.	59.71	2.10	140.01	17.29	111.27	31.88
ILMN_1362834	Dusp6	NM_053883.2	dual specificity phosphatase 6 (Dusp6), mRNA.	357.57	24.08	1103.01	107.52	560.51	178.21
ILMN_1371493	Edg6_predicted	XM_234930.2	endothelial differentiation, G-protein-coupled receptor 6 (predicted) (Edg6_predicted), mRNA.	56.54	6.17	176.20	31.04	74.68	1.26
ILMN_1360909	Ednrb	NM_017333.1	endothelin receptor type B (Ednrb), mRNA.	368.70	23.34	854.64	126.16	561.09	47.29
ILMN_1369005	Egr1	NM_012551.1	early growth response 1 (Egr1), mRNA.	827.65	642.83	4409.36	983.34	3400.53	1181.62
ILMN_1370369	Egr2	NM_053633.1	early growth response 2 (Egr2), mRNA.	309.83	21.28	909.30	165.34	731.31	258.58
ILMN_1352342	Eif5	NM_020075.1	eukaryotic translation initiation factor 5 (Eif5), mRNA.	241.20	39.49	425.35	56.25	310.67	4.11
ILMN_1372586	Ell_predicted	XM_001070626.1	elongation factor RNA polymerase II (predicted) (Ell_predicted), mRNA.	160.00	21.30	261.41	14.73	235.28	20.98
ILMN_1363228	Eil2	XM_001054852.1	elongation factor RNA polymerase II 2 (Eil2), mRNA.	230.65	31.36	545.77	81.39	324.11	36.40
ILMN_1359464	Emb	NM_053719.1	embigin (Emb), mRNA.	59.57	1.27	126.22	11.37	75.02	1.62
ILMN_1350180	Emp1	NM_012843.2	epithelial membrane protein 1 (Emp1), mRNA.	649.71	180.90	2475.14	562.87	1242.37	682.92
ILMN_1376301	Enpp3	NM_019370.1	ectonucleotide pyrophosphatase/phosphodiesterase 3 (Enpp3), mRNA.	205.62	33.34	710.41	133.16	356.94	94.76
ILMN_1366212	Erff1	NM_001014071.1	ERBB receptor feedback inhibitor 1 (Erff1), mRNA.	315.12	36.61	1742.82	423.28	845.72	316.24
ILMN_1348782	Etfdh	NM_198742.2	electron-transferring-flavoprotein dehydrogenase (Etfdh), mRNA.	2596.67	61.04	1733.27	71.60	1881.43	1.67
ILMN_1363372	Ets2_mapped	XM_239510.4	v-ets erythroblastosis virus E26 oncogene homolog 2 (avian) (mapped) (Ets2_mapped), mRNA.	99.53	7.54	169.83	7.87	138.36	25.16
ILMN_1371753	F5_mapped	XM_222831.4	coagulation factor 5 (mapped) (F5_mapped), mRNA.	43.26	4.42	146.05	21.85	67.12	9.81
ILMN_1371223	Fbl	NM_001025643.1	fibrillarin (Fbl), mRNA.	907.53	134.23	1522.98	73.94	1264.83	89.42
ILMN_1368423	Fbxl5_predicted	XM_001060082.1	F-box and leucine-rich repeat protein 5 (predicted) (Fbxl5_predicted), mRNA.	1162.82	157.99	2456.44	416.12	1545.52	90.81
ILMN_1358847	Fcar	NM_201992.1	IgA Fc receptor (Fcar), mRNA.	41.23	4.12	94.55	22.02	49.32	0.98
ILMN_1367877	Fcgr3	XM_001077008.1	Fc receptor, IgG, low affinity III (Fcgr3), mRNA.	90.73	16.12	302.49	85.59	151.52	34.22
ILMN_1351900	Fcnb	NM_053634.1	ficolin B (Fcnb), mRNA.	84.93	29.52	253.33	85.20	108.97	29.92
ILMN_1363936	Fem1a	NM_001025706.1	feminization 1 homolog a (C. elegans) (Fem1a), mRNA.	1909.15	239.71	1048.28	96.73	1588.27	149.15
ILMN_1359590	Fgl2	NM_053455.1	fibrinogen-like 2 (Fgl2), mRNA.	139.23	15.32	555.69	126.98	312.10	153.32

APPENDIX 8: continued

ID	SYMBOL	ACCESSION	DEFINITION	Ave Sham	StDev Sham	Ave MI	StDev MI	Ave MNC	StDev MNC
ILMN_1375025	Fgr	NM_024145.2	Gardner-Rasheed feline sarcoma viral (Fgr) oncogene homolog (Fgr), mRNA.	61.50	2.31	141.81	27.51	80.08	6.47
ILMN_1368356	Fos	NM_022197.1	FBJ murine osteosarcoma viral oncogene homolog (Fos), mRNA.	320.70	294.32	3277.88	574.70	2391.67	1583.58
ILMN_1376319	Fus	NM_001012137.1	fusion, derived from t(12;16) malignant liposarcoma (human) (Fus), mRNA.	654.15	14.52	982.40	62.21	762.66	71.98
ILMN_1350091	G0s2	NM_001009632.1	G0/G1 switch gene 2 (G0s2), mRNA.	615.29	151.77	2275.52	1077.79	712.73	187.97
ILMN_1353208	G7c	NM_212499.1	G7c protein (G7c), mRNA.	686.94	30.26	356.72	35.45	532.58	49.06
ILMN_1650307	Galnt3	NM_001015032.2	UDP-N-acetyl-alpha-D-galactosamine:polypeptide N-acetylgalactosaminyltransferase 3 (Galnt3), mRNA.	40.45	4.04	79.83	9.22	45.20	3.61
ILMN_1359516	Gclc	NM_012815.2	glutamate-cysteine ligase, catalytic subunit (Gclc), mRNA.	341.60	41.42	747.93	150.56	456.10	72.12
ILMN_1351674	Gdf15	NM_019216.1	growth differentiation factor 15 (Gdf15), mRNA.	47.89	3.97	102.32	26.84	71.54	8.05
ILMN_1360656	Gfpt2	NM_001002819.2	glutamine-fructose-6-phosphate transaminase 2 (Gfpt2), mRNA.	187.72	81.63	744.63	184.08	550.46	290.15
ILMN_1364441	Gja3	NM_024376.1	gap junction membrane channel protein alpha 3 (Gja3), mRNA.	93.91	5.36	63.98	2.62	84.87	0.75
ILMN_1368524	Glg1	NM_017211.1	golgi apparatus protein 1 (Glg1), mRNA.	634.21	68.54	373.10	23.29	595.10	118.57
ILMN_1376740	Glipr1	NM_001011987.1	GLI pathogenesis-related 1 (glioma) (Glipr1), mRNA.	101.54	8.77	520.91	105.49	167.67	19.60
ILMN_1356369	Glrx1	NM_022278.1	glutaredoxin 1 (thioltransferase) (Glrx1), mRNA.	212.56	91.60	771.83	132.65	326.59	10.13
ILMN_1362702	Gmfg	NM_181091.2	glia maturation factor, gamma (Gmfg), mRNA.	292.50	58.00	1339.99	472.57	519.47	16.75
ILMN_1371475	Gmpr	NM_057188.1	guanosine monophosphate reductase (Gmpr), mRNA.	1417.92	143.76	828.62	73.13	1089.18	50.54
ILMN_1364579	Gnai3	NM_013106.1	guanine nucleotide binding protein, alpha inhibiting 3 (Gnai3), mRNA.	1289.60	56.72	2167.86	29.73	1769.68	163.11
ILMN_1357924	Gnl3	NM_175580.2	guanine nucleotide binding protein-like 3 (nucleolar) (Gnl3), mRNA.	106.09	18.75	215.48	31.63	132.62	3.69
ILMN_1350620	Gp1bb	NM_053930.3	glycoprotein Ib, beta polypeptide (Gp1bb), mRNA.	207.90	33.79	411.73	58.17	325.76	26.56
ILMN_1373962	Gp9	NM_001031825.1	glycoprotein 9 (Gp9), mRNA.	36.27	1.93	59.63	7.32	44.67	4.94
ILMN_1350738	Gpr109a	NM_181476.1	G protein-coupled receptor 109A (Gpr109a), mRNA.	33.34	1.43	75.95	9.76	43.16	3.47
ILMN_1351646	Gpr4	NM_001025680.1	G protein-coupled receptor 4 (Gpr4), mRNA.	172.94	14.90	333.22	67.27	241.20	5.88
ILMN_1356615	Gpr65_predicted	XM_234367.3	G-protein coupled receptor 65 (predicted) (Gpr65_predicted), mRNA.	40.67	1.70	59.00	2.74	41.74	0.31
ILMN_1357506	Gpsm1	NM_144745.1	G-protein signalling modulator 1 (AGS3-like, C. elegans) (Gpsm1), mRNA.	178.72	14.61	113.27	8.22	162.19	21.73
ILMN_1371385	Gpsm3	NM_001003974.2	G-protein signalling modulator 3 (AGS3-like, C. elegans) (Gpsm3), mRNA.	59.73	6.51	102.39	17.64	61.55	2.81
ILMN_1650650	Gypc	NM_001013233.1	glycophorin C (Gerbich blood group) (Gypc), mRNA.	503.54	34.24	328.19	23.58	418.98	15.72
ILMN_1349008	H3f3b	NM_053985.2	H3 histone, family 3B (H3f3b), mRNA.	1318.13	211.92	2530.97	262.41	2047.19	217.86
ILMN_1373013	Hck	NM_013185.2	hemopoietic cell kinase (Hck), mRNA.	70.02	13.10	156.37	28.86	113.44	12.67
ILMN_1349287	Hiat1_predicted	XM_001067587.1	hippocampus abundant gene transcript 1 (predicted) (Hiat1_predicted), mRNA.	202.69	15.08	353.18	49.25	258.83	9.68
ILMN_1371051	Hk3	NM_022179.2	hexokinase 3 (Hk3), mRNA.	56.24	12.12	105.58	11.47	75.29	5.17
ILMN_1650285	Hmox1	NM_012580.2	heme oxygenase (decycling) 1 (Hmox1), mRNA.	1619.45	246.27	3735.65	709.27	2799.72	320.78
ILMN_1369798	Hnrpf	NM_001037285.1	heterogeneous nuclear ribonucleoprotein F (Hnrpf), transcript variant 2, mRNA.	1471.44	38.38	2399.29	144.07	1831.40	72.42
ILMN_1651184	Hp	NM_012582.2	haptoglobin (Hp), mRNA.	157.98	123.35	1526.51	227.31	585.06	53.07
ILMN_1358144	Hspca	NM_175761.2	heat shock protein 1, alpha (Hspca), mRNA.	381.31	44.09	1451.86	180.53	920.48	506.44
ILMN_1364500	Hspcal3_predicted	XM_216334.3	heat shock 90kDa protein 1, alpha-like 3 (predicted) (Hspcal3_predicted), mRNA.	356.34	61.51	1334.04	224.31	966.14	548.05

APPENDIX 8: continued

ID	SYMBOL	ACCESSION	DEFINITION	Ave Sham	StDev Sham	Ave MI	StDev MI	Ave MNC	StDev MNC
ILMN_1367519	Idi1	NM_053539.1	isopenentenyl-diphosphate delta isomerase (Idi1), mRNA.	89.76	2.64	159.31	19.31	111.20	21.14
ILMN_1352529	ler2	NM_001009541.1	immediate early response 2 (ler2), mRNA.	459.09	99.66	1050.29	178.42	752.11	113.85
ILMN_1530409	ler5	NM_001025137.1	immediate early response 5 (ler5), mRNA.	43.33	8.34	88.17	8.45	66.44	14.37
ILMN_2040190	lfit1_predicted	XM_220058.2	interferon-induced protein with tetratricopeptide repeats 1 (predicted) (lfit1_predicted), mRNA.	92.50	49.38	760.25	310.13	275.58	70.23
ILMN_1374737	lfitm6_predicted	XM_219476.3	interferon induced transmembrane protein 6 (predicted) (lfitm6_predicted), mRNA.	117.43	86.70	889.26	510.79	405.87	103.70
ILMN_1373523	Igfbp3	NM_012588.1	insulin-like growth factor binding protein 3 (Igfbp3), mRNA.	289.42	20.22	631.42	107.59	422.74	26.05
ILMN_1356655	Il17r_predicted	XM_232247.4	interleukin 17 receptor (predicted) (Il17r_predicted), mRNA.	77.23	17.75	228.73	34.40	133.41	19.36
ILMN_1349030	Il1r2	NM_053953.1	interleukin 1 receptor, type II (Il1r2), mRNA.	222.44	133.60	3658.11	1179.89	1091.62	555.73
ILMN_1361277	Il1rn	XM_001071294.1	interleukin 1 receptor antagonist, transcript variant 1 (Il1rn), mRNA.	61.63	13.44	213.78	35.47	115.86	20.60
ILMN_1352340	Il8rb	NM_017183.1	interleukin 8 receptor, beta (Il8rb), mRNA.	38.09	4.42	188.36	89.92	84.66	10.98
ILMN_1351826	Ippk	NM_001008556.1	inositol 1,3,4,5,6-pentakisphosphate 2-kinase (Ippk), mRNA.	63.32	4.44	133.19	9.04	109.85	36.63
ILMN_1366898	Irf2bp1_predicted	XM_001075292.1	interferon regulatory factor 2 binding protein 1 (predicted) (Irf2bp1_predicted), mRNA.	278.63	18.30	172.27	24.85	207.48	2.58
ILMN_1357140	Irx4_predicted	XM_001057125.1	Iroquois related homeobox 4 (Drosophila) (predicted), transcript variant 1 (Irx4_predicted), mRNA.	204.69	24.63	119.21	16.01	148.31	6.68
ILMN_1650489	Isoc2b	NM_001008367.1	isochorismatase domain containing 2b (Isoc2b), mRNA.	241.92	8.59	165.34	9.50	232.00	4.31
ILMN_1353551	Itgb7	XM_001067562.1	integrin, beta 7 (Itgb7), mRNA.	54.54	4.35	106.68	20.27	73.18	2.10
ILMN_1370633	Itpkc	NM_178094.2	inositol 1,4,5-trisphosphate 3-kinase C (Itpkc), mRNA.	107.58	37.68	341.10	121.61	238.06	27.95
ILMN_1354357	Jmjd1c	XM_001080424.1	jumonji domain containing 1C (Jmjd1c), mRNA.	234.74	13.50	470.55	65.14	401.53	36.70
ILMN_1368412	Jmjd3_predicted	XM_001079385.1	jumonji domain containing 3 (predicted) (Jmjd3_predicted), mRNA.	139.10	19.69	397.01	118.94	348.85	22.84
ILMN_1650950	Josd3	NM_001014207.1	Josephin domain containing 3 (Josd3), mRNA.	114.46	17.62	201.56	16.67	123.67	20.58
ILMN_1353022	Jph2	NM_001037974.1	junctophilin 2 (Jph2), mRNA.	106.87	11.58	63.38	4.26	99.68	6.71
ILMN_1356110	Klf4	NM_053713.1	Kruppel-like factor 4 (gut) (Klf4), mRNA.	369.84	73.72	807.42	105.04	475.08	110.07
ILMN_1361302	Klf5	NM_053394.2	Kruppel-like factor 5 (Klf5), mRNA.	146.91	9.81	365.79	36.37	463.67	16.35
ILMN_1362080	Klf6	NM_031642.2	Kruppel-like factor 6 (Klf6), mRNA.	1029.62	275.41	2208.02	339.40	2168.59	191.84
ILMN_1364370	Klrb1b	NM_173292.1	killer cell lectin-like receptor subfamily B member 1B (Klrb1b), mRNA.	36.66	2.71	66.04	11.11	40.80	4.53
ILMN_1365751	Kpnb3_predicted	XM_224534.3	karyopherin (importin) beta 3 (predicted) (Kpnb3_predicted), mRNA.	428.79	45.77	1079.59	239.95	644.26	133.79
ILMN_1372499	Lad1_predicted	XM_001063663.1	ladinin (predicted) (Lad1_predicted), mRNA.	208.54	29.72	124.00	13.30	151.84	4.05
ILMN_1357030	Laptm5	NM_053538.2	lysosomal-associated protein transmembrane 5 (Laptm5), mRNA.	162.16	9.08	310.66	12.64	201.94	17.84
ILMN_1376661	Lbp	NM_017208.1	lipopolysaccharide binding protein (Lbp), mRNA.	90.41	14.35	206.15	23.06	113.00	1.09
ILMN_1376765	Lcp1	NM_001012044.1	lymphocyte cytosolic protein 1 (Lcp1), mRNA.	804.18	138.86	3023.13	478.44	1662.49	40.19
ILMN_1354751	Leng4_predicted	XM_001056203.1	leukocyte receptor cluster (LRC) member 4 (predicted) (Leng4_predicted), mRNA.	55.30	4.72	85.78	8.62	64.38	3.53
ILMN_1370840	Lgals3	NM_031832.1	lectin, galactose binding, soluble 3 (Lgals3), mRNA.	1292.35	150.44	2525.01	354.08	1305.17	142.72
ILMN_1368490	LOC24906	NM_031537.1	RoBo-1 (LOC24906), mRNA.	55.55	7.67	160.68	27.00	78.63	3.54
ILMN_1357555	LOC307907	XM_226529.3	similar to RIKEN cDNA 6430548M08 (predicted) (LOC307907), mRNA.	908.46	126.97	514.58	7.67	768.92	151.18
ILMN_1350326	LOC308990	NM_001025001.1	hypothetical protein LOC308990 (LOC308990), mRNA.	43.14	1.71	123.58	17.81	59.66	1.42
ILMN_1359287	LOC310086	XM_226757.3	similar to RIKEN cDNA D130064H19 (predicted) (LOC310086), mRNA.	125.07	4.38	185.50	8.42	139.24	5.21
ILMN_1370088	LOC311984	XM_001062783.1	similar to RIKEN cDNA A530088I07 gene (LOC311984), mRNA.	166.78	35.97	390.94	24.39	301.87	2.46
ILMN_1364945	LOC315883	NM_001014094.1	similar to phospholipid scramblase 2 (LOC315883), mRNA.	140.49	8.27	282.82	21.15	279.95	5.36

APPENDIX 8: continued

ID	SYMBOL	ACCESSION	DEFINITION	Ave Sham	StDev Sham	Ave MI	StDev MI	Ave MNC	StDev MNC
ILMN_1354457	LOC316207	XM_236901.3	similar to RIKEN cDNA B430306N03 gene (predicted) (LOC316207), mRNA.	34.11	2.66	78.93	18.95	41.92	3.44
ILMN_1359784	LOC362115	XM_342417.2	similar to RIKEN cDNA 9130404D14 (predicted) (LOC362115), mRNA.	174.18	8.06	336.60	69.53	205.17	3.12
ILMN_1364095	LOC362703	XM_001061088.1	similar to WD-repeat protein 43 (LOC362703), mRNA.	221.29	52.64	464.93	43.40	340.27	29.15
ILMN_1370198	LOC363060	NM_001014209.1	similar to RIKEN cDNA 1600029D21 (LOC363060), mRNA.	57.54	1.92	128.17	10.41	70.23	10.31
ILMN_1367516	LOC363331	XM_343669.2	similar to S3-12 (LOC363331), mRNA.	250.70	41.26	117.72	21.33	184.88	16.46
ILMN_1358168	LOC363897	XR_009066.1	similar to Ras-related protein Rap-1b precursor (GTP-binding protein smg p21B) (LOC363897), mRNA.	1701.37	53.12	3101.58	166.30	2162.57	241.79
ILMN_1651187	LOC497712	XM_579055.1	hypothetical gene supported by NM_001001511 (LOC497712), mRNA.	187.46	11.55	619.18	92.86	392.81	25.09
ILMN_1369063	LOC497722	XM_579583.1	hypothetical gene supported by NM_053905 (LOC497722), mRNA.	75.17	6.32	167.01	23.11	93.33	0.80
ILMN_1357799	LOC497748	XM_579551.1	hypothetical gene supported by NM_053313 (LOC497748), mRNA.	47.19	12.72	198.74	57.90	73.63	7.37
ILMN_1357368	LOC497841	XM_579384.1	hypothetical gene supported by NM_016994 (LOC497841), mRNA.	85.45	27.92	269.65	47.92	151.28	43.21
ILMN_1370087	LOC498062	XM_573260.1	similar to RIKEN cDNA 1190017O12 (LOC498062), mRNA.	598.42	33.23	395.75	27.77	522.03	17.68
ILMN_1355544	LOC498276	XM_573502.1	similar to Fc gamma (IgG) receptor II (low affinity) alpha precursor - rat (LOC498276), mRNA.	1119.06	412.70	3610.21	1428.77	2359.73	170.17
ILMN_1370638	LOC498277	XR_007542.1	similar to Low affinity immunoglobulin gamma Fc region receptor III precursor (IgG Fc receptor III) (Fc-gamma RIII) (FcRIII) (LOC498277), mRNA.	265.68	118.18	1068.85	389.98	537.18	56.89
ILMN_1351139	LOC498279	XM_001053627.1	similar to High affinity immunoglobulin epsilon receptor gamma-subunit precursor (FcεRI gamma) (IgE Fc receptor gamma-subunit) (Fc-epsilon RI gamma) (LOC498279), mRNA.	997.36	200.37	2604.83	574.13	1355.74	165.69
ILMN_1372294	LOC499078	XM_001070660.1	similar to glycoprotein 49b (LOC499078), mRNA.	40.48	1.65	86.72	18.92	48.42	2.63
ILMN_1366459	LOC499612	XM_574939.1	similar to NADH dehydrogenase (ubiquinone) 1, subcomplex unknown, 1 (LOC499612), mRNA.	88.77	2.72	62.00	3.66	73.56	3.91
ILMN_1351679	LOC500040	XM_575396.1	similar to Testis derived transcript (LOC500040), mRNA.	275.12	57.81	985.04	245.20	449.82	60.33
ILMN_1351690	LOC500687	XM_580105.1	LOC500687 (LOC500687), mRNA.	68.81	4.84	145.61	19.37	96.26	9.54
ILMN_1354808	LOC500904	XM_576306.2	similar to neutrophil cytosolic factor 4 (LOC500904), mRNA.	66.19	10.79	153.63	21.98	83.60	0.10
ILMN_1371731	LOC501284	XM_576699.1	similar to mKIAA1881 protein (LOC501284), mRNA.	233.07	11.76	139.83	23.93	191.24	11.06
ILMN_1370116	LOC501594	XM_580217.1	LOC501594 (LOC501594), mRNA.	720.42	34.82	1087.15	88.71	891.42	32.15
ILMN_1366909	LOC683463	XM_001066042.1	similar to paired-Ig-like receptor B (LOC683463), mRNA.	51.20	9.74	148.41	45.35	59.52	2.71
ILMN_1375048	LOC684525	XM_001070830.1	similar to stefin A2 like 1 (LOC684525), mRNA.	72.22	20.06	1106.89	547.23	261.25	110.29
ILMN_1356957	LOC687856	XM_001080365.1	similar to Myeloid cell surface antigen CD33 precursor (Siglec-3) (LOC687856), mRNA.	45.80	4.06	99.22	18.08	67.93	14.67
ILMN_1353943	Lrg1	NM_001009717.1	leucine-rich alpha-2-glycoprotein 1 (Lrg1), mRNA.	78.21	9.45	155.08	24.90	98.68	14.15
ILMN_1348962	Lrrc10_predicted	XM_001080952.1	leucine-rich repeat-containing 10 (predicted) (Lrrc10_predicted), mRNA.	927.68	171.55	305.51	46.52	483.32	65.76
ILMN_1363263	Lrrc8c	NM_001037179.1	leucine rich repeat containing 8 family, member C (Lrrc8c), mRNA.	187.50	21.26	312.84	21.04	241.51	38.96
ILMN_1356330	Lst1	NM_022634.1	leucocyte specific transcript 1 (Lst1), mRNA.	54.58	9.92	108.43	12.98	67.80	8.23
ILMN_1354499	Ltb	NM_212507.2	lymphotoxin B (Ltb), mRNA.	64.67	13.30	280.95	107.97	136.67	33.79
ILMN_1367927	Ly49i8	NM_001009486.1	Ly49 inhibitory receptor 8 (Ly49i8), mRNA.	46.13	6.42	74.34	5.32	51.68	2.37
ILMN_1349844	Maea	NM_001008319.1	macrophage erythroblast attacher (Maea), mRNA.	1042.82	108.39	631.44	19.11	816.16	43.48
ILMN_1361027	Mafb	NM_019316.1	v-maf musculoaponeurotic fibrosarcoma oncogene family, protein B (avian) (Mafb), mRNA.	94.92	12.87	167.59	4.40	122.56	3.74

APPENDIX 8: continued

ID	SYMBOL	ACCESSION	DEFINITION	Ave Sham	StDev Sham	Ave MI	StDev MI	Ave MNC	StDev MNC
ILMN_1371205	Map4k1_predicted	XM_001074916.1	mitogen activated protein kinase kinase kinase 1 (predicted) (Map4k1_predicted), mRNA.	77.68	14.51	187.05	41.10	119.02	3.76
ILMN_1359095	Mat2a	NM_134351.1	methionine adenosyltransferase II, alpha (Mat2a), mRNA.	124.22	2.21	245.77	46.07	159.38	24.68
ILMN_1355362	Mca32	NM_021585.1	mast cell antigen 32 (Mca32), mRNA.	43.37	3.61	72.91	9.92	46.93	3.95
ILMN_1357312	Mcl1	NM_021846.2	myeloid cell leukemia sequence 1 (Mcl1), mRNA.	775.05	80.62	2102.88	38.08	1250.33	412.47
ILMN_1374845	MGC105649	NM_001008518.1	hypothetical LOC302884 (MGC105649), mRNA.	60.83	15.83	269.28	50.66	128.55	20.01
ILMN_1375131	MGC125015	NM_001037356.1	similar to PAK/PLC-interacting protein 1 (MGC125015), mRNA.	123.09	20.62	237.93	36.86	201.99	10.61
ILMN_1361776	MGC72584	NM_001009535.1	similar to postmeiotic segregation increased 1 (MGC72584), mRNA.	283.51	34.42	167.92	17.53	201.73	9.64
ILMN_1373900	MGC72974	NM_198772.1	hypothetical LOC316976 (MGC72974), mRNA.	572.32	148.92	239.71	44.21	330.37	18.56
ILMN_1348979	MGC93707	NM_001005556.1	similar to RIKEN cDNA D430028G21 (MGC93707), mRNA.	757.48	33.82	357.45	11.87	532.07	112.63
ILMN_1364243	MGC94207	NM_001007751.1	similar to RIKEN cDNA C030006K11 (MGC94207), mRNA.	277.60	17.90	168.89	11.81	230.81	3.08
ILMN_1363911	MGC94339	NM_001007703.1	similar to BC002216 protein (MGC94339), mRNA.	157.69	19.78	96.80	6.46	129.80	0.55
ILMN_1376722	MGC94736	NM_001007685.1	similar to hypothetical protein MGC35097 (MGC94736), mRNA.	239.50	13.32	158.09	8.49	235.24	9.80
ILMN_1349697	Midn_predicted	XM_001076784.1	midnolin (predicted) (Midn_predicted), mRNA.	61.48	3.61	100.93	17.15	132.99	0.75
ILMN_1371081	Mmp8	NM_022221.1	matrix metalloproteinase 8 (Mmp8), mRNA.	68.25	16.86	634.17	210.11	192.97	79.93
ILMN_2039240	Mmp9	NM_031055.1	matrix metalloproteinase 9 (Mmp9), mRNA.	68.78	14.46	239.77	77.34	127.06	48.33
ILMN_1367596	Mocs2	XM_001067999.1	molybdenum cofactor synthesis 2, transcript variant 1 (Mocs2), mRNA.	2299.10	37.03	1319.29	71.40	1878.18	228.46
ILMN_1367384	Mox2r	NM_023953.1	antigen identified by monoclonal antibody MRC OX-2 receptor (Mox2r), mRNA.	55.50	6.31	108.67	25.79	72.75	6.18
ILMN_1376777	Mpst	NM_138843.1	mercaptopyruvate sulfurtransferase (Mpst), mRNA.	860.99	114.67	540.78	24.65	742.18	46.13
ILMN_1357886	Mrpl16	NM_001009647.1	mitochondrial ribosomal protein L16 (Mrpl16), mRNA.	409.72	36.47	273.26	16.68	396.72	2.15
ILMN_1362859	Mrpl22_predicted	XM_213307.4	mitochondrial ribosomal protein L22 (predicted) (Mrpl22_predicted), mRNA.	1180.24	23.60	819.95	43.23	971.27	15.75
ILMN_1359659	Mrpl50_predicted	XM_342835.2	mitochondrial ribosomal protein L50 (predicted) (Mrpl50_predicted), mRNA.	601.49	38.59	356.60	22.66	499.33	26.93
ILMN_1359365	Mttr7_predicted	XM_240417.4	myotubularin related protein 7 (predicted) (Mttr7_predicted), mRNA.	38.96	0.59	71.49	5.49	46.61	3.89
ILMN_1353390	Mxd1	XM_001074696.1	max dimerization protein 1 (Mxd1), mRNA.	57.54	13.70	148.83	38.83	94.83	27.91
ILMN_1359024	Myd88	NM_198130.1	myeloid differentiation primary response gene 88 (Myd88), mRNA.	210.97	63.76	489.85	67.26	381.41	34.71
ILMN_1352095	Myl7_predicted	XM_214074.4	mRNA.	156.75	28.88	72.73	13.88	91.28	1.94
ILMN_1357127	Nalp12_predicted	XM_001066862.1	NACHT, leucine rich repeat and PYD containing 12 (predicted) (Nalp12_predicted), mRNA.	43.95	1.34	72.00	5.20	45.06	3.97
ILMN_1374896	Napsa	NM_031670.1	napsin A aspartic peptidase (Napsa), mRNA.	135.04	49.64	1045.92	279.59	437.30	109.46
ILMN_1359661	Nasp	NM_001005543.1	nuclear autoantigenic sperm protein (histone-binding) (Nasp), mRNA.	191.73	19.78	330.21	36.88	252.29	1.95
ILMN_1372165	Nckap1l_predicted	XM_001070373.1	NCK associated protein 1 like (predicted) (Nckap1l_predicted), mRNA.	87.78	4.54	146.05	10.96	102.93	0.60
ILMN_1363106	Ndel1	NM_133320.1	nudE nuclear distribution gene E homolog like 1 (A. nidulans) (Ndel1), mRNA.	1367.59	55.34	1985.93	80.85	1630.05	159.65
ILMN_1376442	Nedd9	NM_001011922.1	neural precursor cell expressed, developmentally down-regulated gene 9 (Nedd9), mRNA.	363.14	15.30	695.11	68.06	501.56	81.14
ILMN_1350548	Neur12_predicted	XM_230848.4	neuronalized-like 2 (Drosophila) (predicted) (Neur12_predicted), mRNA.	492.37	32.52	325.37	23.82	464.72	6.51
ILMN_1376557	Nfe2	NM_001012224.1	nuclear factor, erythroid derived 2 (Nfe2), mRNA.	46.31	12.39	191.83	38.04	76.78	0.09
ILMN_1363954	Nip7	NM_138847.1	nuclear import 7 homolog (S. cerevisiae) (Nip7), mRNA.	214.10	49.21	382.77	11.36	258.86	19.92

APPENDIX 8: continued

ID	SYMBOL	ACCESSION	DEFINITION	Ave Sham	StDev Sham	Ave MI	StDev MI	Ave MNC	StDev MNC
ILMN_1362482	Nkx2-5	NM_053651.1	NK2 transcription factor related, locus 5 (Drosophila) (Nkx2-5), mRNA.	236.89	26.98	140.87	15.21	180.21	26.75
ILMN_1374672	Nol5	NM_021754.1	nucleolar protein 5 (Nol5), mRNA.	705.98	160.46	1721.32	287.68	1177.47	66.15
ILMN_1372107	Nos2	NM_012611.2	nitric oxide synthase 2, inducible (Nos2), mRNA.	44.56	16.40	167.91	61.36	104.26	33.95
ILMN_1357730	Npy	NM_012614.1	neuropeptide Y (Npy), mRNA.	155.37	125.07	1334.89	620.78	404.56	141.81
ILMN_1375922	Nr4a3	NM_031628.1	nuclear receptor subfamily 4, group A, member 3 (Nr4a3), transcript variant 1, mRNA.	82.53	28.13	395.77	112.96	298.34	65.78
ILMN_1363628	Nt5m_predicted	XM_213318.4	5',3'-nucleotidase, mitochondrial (predicted) (Nt5m_predicted), mRNA.	140.50	20.78	76.85	9.49	109.20	1.90
ILMN_1360607	Numbl_predicted	XM_218360.3	numb-like (predicted) (Numbl_predicted), mRNA.	84.64	10.52	146.72	13.29	102.42	6.78
ILMN_1358567	Oas1k	NM_001009489.1	2'-5' oligoadenylate synthetase 1K (Oas1k), mRNA.	76.05	6.23	452.29	58.14	150.21	13.88
ILMN_1650001	Ociad1	NM_001013874.1	OClA domain containing 1 (Ociad1), mRNA.	4272.09	187.72	2896.93	82.75	3988.63	101.31
ILMN_1369735	Odc1	NM_012615.1	ornithine decarboxylase 1 (Odc1), mRNA.	226.70	15.92	433.98	59.05	310.55	37.38
ILMN_1374695	Oldlr1	NM_133306.1	oxidized low density lipoprotein (lectin-like) receptor 1 (Oldlr1), mRNA.	48.48	7.96	116.15	14.02	84.84	25.55
ILMN_1376380	P2ry13	NM_001002853.1	purinergic receptor P2Y, G-protein coupled, 13 (P2ry13), mRNA.	54.55	4.92	93.24	14.57	64.82	3.61
ILMN_1358564	Pabpc1	NM_134353.2	poly(A) binding protein, cytoplasmic 1 (Pabpc1), mRNA.	1173.91	109.23	1950.43	101.30	1483.39	207.30
ILMN_1368846	Pacsin2	NM_130740.2	protein kinase C and casein kinase substrate in neurons 2 (Pacsin2), mRNA.	279.08	26.19	125.08	13.38	223.29	0.70
ILMN_1374870	Pafah1b1	NM_031763.3	platelet-activating factor acetylhydrolase, isoform 1b, alpha subunit 45kDa (Pafah1b1), mRNA.	65.57	17.87	137.79	10.68	109.03	9.92
ILMN_1351668	Pcf11_predicted	XM_001062815.1	cleavage and polyadenylation factor subunit homolog (S. cerevisiae) (predicted) (Pcf11_predicted), mRNA.	304.06	23.75	485.90	39.64	318.60	43.67
ILMN_1364203	Pcna	NM_022381.2	proliferating cell nuclear antigen (Pcna), mRNA.	978.97	106.37	1600.08	75.53	1061.50	104.31
ILMN_1365622	Pcyt2	NM_053568.1	phosphate cytidylyltransferase 2, ethanolamine (Pcyt2), mRNA.	489.48	17.65	309.62	28.75	455.53	9.47
ILMN_1353078	Pde4b	NM_017031.2	phosphodiesterase 4B, cAMP specific (Pde4b), mRNA.	127.64	65.36	435.45	66.14	324.68	6.86
ILMN_1365682	Pdk3_mapped	XM_001056460.1	pyruvate dehydrogenase kinase, isoenzyme 3 (mapped) (Pdk3_mapped), mRNA.	52.51	3.91	104.79	16.33	62.44	7.11
ILMN_1369190	Pdim7	NM_173125.1	PDZ and LIM domain 7 (Pdim7), mRNA.	257.62	25.10	709.05	74.89	397.81	27.06
ILMN_1367435	Pdzd7_predicted	XM_001057829.1	PDZ domain containing 7 (predicted) (Pdzd7_predicted), mRNA.	171.34	9.97	114.68	9.88	123.73	3.48
ILMN_1350897	Pfc_mapped	XM_001056015.1	properdin factor, complement (mapped) (Pfc_mapped), mRNA.	106.40	6.17	276.18	42.57	145.29	11.63
ILMN_1353729	Pgd	XM_342979.2	phosphogluconate dehydrogenase (Pgd), mRNA.	482.53	65.54	820.60	72.28	566.39	7.06
ILMN_1351496	Pglyrp1	NM_053373.1	peptidoglycan recognition protein 1 (Pglyrp1), mRNA.	104.08	78.40	1064.75	445.19	326.43	53.91
ILMN_1360748	Pgsg	NM_020074.2	proteoglycan peptide core protein (Pgsg), mRNA.	81.93	2.93	153.37	30.95	90.72	13.28
ILMN_1355211	Pim1	NM_017034.1	proviral integration site 1 (Pim1), mRNA.	68.04	2.52	132.99	12.22	102.12	1.99
ILMN_1363160	Plac8_predicted	XM_001067597.1	placenta-specific 8 (predicted) (Plac8_predicted), mRNA.	332.93	171.50	1375.66	94.19	746.39	15.21
ILMN_1358127	Plat	NM_013151.2	plasminogen activator, tissue (Plat), mRNA.	545.29	60.06	1357.55	105.18	820.87	285.04
ILMN_1352911	Plek	NM_001025750.1	pleckstrin (Plek), mRNA.	314.79	132.73	1467.68	485.05	805.87	268.58
ILMN_1349466	Plp2	NM_207601.1	proteolipid protein 2 (Plp2), mRNA.	686.52	22.31	1108.94	40.08	874.21	80.64
ILMN_1358347	Pls3	XM_001057425.1	plastin 3 (T-isoform) (Pls3), mRNA.	164.24	6.51	353.26	65.61	205.21	51.73
ILMN_1357241	Pmm1	NM_001008323.1	phosphomannomutase 1 (Pmm1), mRNA.	502.91	40.26	327.77	26.88	414.60	26.64
ILMN_1373876	Pmp22	NM_017037.1	peripheral myelin protein 22 (Pmp22), mRNA.	553.39	50.47	918.55	113.50	608.41	9.99
ILMN_1367417	Polrmt_predicted	XM_001074109.1	polymerase (RNA) mitochondrial (DNA directed) (predicted) (Polrmt_predicted), mRNA.	213.57	13.80	134.29	7.69	162.87	18.33
ILMN_1355213	Ppp1r3b	NM_138912.2	protein phosphatase 1, regulatory (inhibitor) subunit 3B (Ppp1r3b),	133.96	15.60	365.25	108.45	259.00	22.72

APPENDIX 8: continued

ID	SYMBOL	ACCESSION	DEFINITION	Ave Sham	StDev Sham	Ave MI	StDev MI	Ave MNC	StDev MNC
ILMN_1371126	Procr	NM_001025733.2	protein C receptor, endothelial (Procr), mRNA.	243.22	40.05	1212.86	379.12	802.35	561.64
ILMN_1353817	Prok2	NM_138852.1	prokineticin 2 (Prok2), transcript variant 2, mRNA.	56.56	25.76	497.54	203.18	138.22	19.10
ILMN_1373510	Pskh1_predicted	XM_344760.2	protein serine kinase H1 (predicted) (Pskh1_predicted), mRNA.	153.84	7.36	104.75	4.06	144.94	8.00
ILMN_1368364	Pstpip1_predicted	XM_217152.3	proline-serine-threonine phosphatase-interacting protein 1 (predicted) (Pstpip1_predicted), mRNA.	76.13	10.25	199.72	54.58	98.43	9.00
ILMN_1354586	Ptafr	NM_053321.2	platelet-activating factor receptor (Ptafr), mRNA.	107.31	17.37	424.03	90.33	182.54	47.91
ILMN_1356425	Ptbp1	NM_022516.4	polypyrimidine tract binding protein 1 (Ptbp1), transcript variant 2, mRNA.	293.32	27.71	531.93	58.42	398.81	43.25
ILMN_1361561	Pten	NM_031606.1	phosphatase and tensin homolog (Pten), mRNA.	130.21	7.82	204.85	12.82	151.60	13.17
ILMN_1356563	Ptges2_predicted	XM_231144.4	prostaglandin E synthase 2 (predicted) (Ptges2_predicted), mRNA.	340.60	13.80	227.18	8.21	344.92	44.58
ILMN_1349422	Ptgs2	NM_017232.2	prostaglandin-endoperoxide synthase 2 (Ptgs2), mRNA.	224.50	156.54	1202.39	224.74	626.41	315.74
ILMN_1355065	Ptpn1	NM_012637.1	protein tyrosine phosphatase, non-receptor type 1 (Ptpn1), mRNA.	199.35	40.74	386.19	7.61	331.03	5.03
ILMN_1360373	Ptpn6	NM_053908.1	protein tyrosine phosphatase, non-receptor type 6 (Ptpn6), mRNA.	183.89	19.78	371.32	78.38	233.35	21.16
ILMN_1365809	Ptprc	XM_001063971.1	protein tyrosine phosphatase, receptor type, C (Ptprc), mRNA.	57.39	8.62	127.89	27.54	67.15	3.77
ILMN_1349137	Ptpro	NM_017336.1	protein tyrosine phosphatase, receptor type, O (Ptpro), mRNA.	99.28	19.03	192.56	26.05	107.90	5.40
ILMN_1349760	Pygl	NM_022268.1	liver glycogen phosphorylase (Pygl), mRNA.	79.13	16.61	399.31	65.97	170.98	25.87
ILMN_1349016	Rabgef1_predicted	XM_001072217.1	RAB guanine nucleotide exchange factor (GEF) 1 (predicted) (Rabgef1_predicted), mRNA.	123.75	8.42	211.55	27.85	167.00	8.06
ILMN_1365800	Rac2	NM_001008384.1	RAS-related C3 botulinum substrate 2 (Rac2), mRNA.	549.40	132.23	1107.26	144.55	770.88	0.74
ILMN_1369914	Rasd1	XM_340809.3	RAS, dexamethasone-induced 1 (Rasd1), mRNA.	145.41	15.69	307.52	62.98	254.11	10.42
ILMN_1354445	Rassf1	NM_001007754.1	Ras association (RalGDS/AF-6) domain family 1 (Rassf1), transcript variant 2, mRNA.	267.11	43.39	721.87	66.95	456.31	85.23
ILMN_1353336	Rbm3	XM_001063211.1	RNA binding motif protein 3 (Rbm3), mRNA.	115.28	17.05	256.52	28.62	177.26	29.26
ILMN_1362534	Retnla	NM_053333.1	resistin like alpha (Retnla), mRNA.	54.61	1.29	160.33	31.13	73.17	6.18
ILMN_1351830	Retnlg	NM_181625.1	resistin-like gamma (Retnlg), mRNA.	139.04	99.32	1683.53	474.49	423.33	48.37
ILMN_1360418	RGD1302996	NM_213610.1	hypothetical protein MGC:15854 (RGD1302996), mRNA.	1116.47	65.83	635.16	74.67	915.61	157.12
ILMN_1355677	RGD1305246	NM_001014028.1	similar to Cgi67 serine protease precursor (RGD1305246), mRNA.	236.23	12.61	464.14	107.32	374.05	46.03
ILMN_1359578	RGD1305574_predicted	XM_341388.2	similar to polymerase (RNA) III (DNA directed) (155kD) (predicted) (RGD1305574_predicted), mRNA.	167.35	0.92	107.40	1.74	116.00	3.83
ILMN_1369550	RGD1305622	NM_001013854.1	hypothetical LOC287173 (RGD1305622), mRNA.	470.85	26.94	332.45	3.98	426.20	4.70
ILMN_1374611	RGD1306595	NM_001025626.1	similar to hypothetical protein (RGD1306595), mRNA.	390.42	30.05	201.57	20.12	299.96	22.61
ILMN_1650056	RGD1306658	NM_001014216.1	similar to 5830411E10Rik protein (RGD1306658), mRNA.	328.28	51.00	725.00	100.22	535.91	22.80
ILMN_1367232	RGD1307396_predicted	XM_341029.3	similar to RIKEN cDNA 6330406115 (predicted) (RGD1307396_predicted), mRNA.	168.75	28.59	362.29	24.39	278.81	0.76
ILMN_1373687	RGD1307618_predicted	XM_001070654.1	similar to chondroitin beta1,4 N-acetylgalactosaminyltransferase (predicted), transcript variant 3 (RGD1307618_predicted), mRNA.	77.38	6.43	134.55	13.39	112.13	5.24
ILMN_1373864	RGD1308113	NM_001008296.1	similar to CGI-112 protein (RGD1308113), mRNA.	474.44	14.46	327.77	20.57	419.55	28.19
ILMN_1370898	RGD1308872_predicted	XM_214620.4	similar to Retinoblastoma-binding protein 8 (RBBP-8) (CtBP interacting protein) (CtIP) (Retinoblastoma-interacting protein and myosin-like) (RIM) (predicted) (RGD1308872_predicted), mRNA.	105.91	5.60	197.17	19.92	148.90	17.19
ILMN_2040884	RGD1309802_predicted	XM_233480.3	similar to RIKEN cDNA 3110037116 (predicted) (RGD1309802_predicted), mRNA.	89.29	6.70	210.77	29.56	113.78	12.13

APPENDIX 8: continued

ID	SYMBOL	ACCESSION	DEFINITION	Ave Sham	StDev Sham	Ave MI	StDev MI	Ave MNC	StDev MNC
ILMN_2038944	RGD1309802_predict	XM_233480.3	similar to RIKEN cDNA 3110037116 (predicted) (RGD1309802_predicted), mRNA.	91.43	5.37	189.39	29.86	107.77	1.45
ILMN_1351911	RGD1310168_predict	XM_219540.4	similar to cDNA sequence BC032204 (predicted) (RGD1310168_predicted), mRNA.	68.49	5.59	115.07	15.56	78.81	3.51
ILMN_1357039	RGD1310357_predict	XM_001065047.1	similar to RIKEN cDNA 2810457106 (predicted) (RGD1310357_predicted), mRNA.	82.31	6.11	145.83	23.56	131.92	16.42
ILMN_1373668	RGD1310553	NM_001008517.1	similar to expressed sequence AI597479 (RGD1310553), mRNA.	274.91	18.44	166.63	22.34	208.90	21.29
ILMN_1349555	RGD1359509	NM_001009671.1	similar to hypothetical protein FLJ13448 (RGD1359509), mRNA.	898.78	210.14	2405.41	476.33	1697.21	179.72
ILMN_1366226	RGD1359713	NM_001005882.1	hypothetical RNA binding protein RGD1359713 (RGD1359713), mRNA.	49.47	4.64	78.94	9.29	63.54	0.77
ILMN_1375084	RGD1559897_predict	XM_001066538.1	similar to osteoclast-associated receptor mOSCAR-M1 (predicted) (RGD1559897_predicted), mRNA.	39.50	1.08	63.54	8.57	36.86	0.18
ILMN_1353276	RGD1559981_predict	XM_001056018.1	similar to leucine rich repeat containing 27 (predicted), transcript variant 1 (RGD1559981_predicted), mRNA.	1099.02	47.57	674.26	47.79	987.32	115.99
ILMN_1359028	RGD1559988_predict	XM_222107.4	similar to RIKEN cDNA 2410018M08 (predicted) (RGD1559988_predicted), mRNA.	49.87	1.75	82.99	2.54	69.51	1.50
ILMN_1366543	RGD1560119_predict	XR_008328.1	similar to actin alpha 1 skeletal muscle protein (predicted) (RGD1560119_predicted), mRNA.	73.72	14.73	183.26	45.11	125.64	0.15
ILMN_1364192	RGD1560523_predict	XM_573428.2	similar to S-adenosylmethionine synthetase gamma form (Methionine adenosyltransferase) (predicted) (RGD1560523_predicted), mRNA.	346.17	57.33	695.54	94.40	565.18	66.52
ILMN_1364315	RGD1560676_predict	XM_573293.1	similar to stefin A2 (predicted) (RGD1560676_predicted), mRNA.	124.35	41.77	3162.73	733.71	527.78	27.13
ILMN_1356132	RGD1561016_predict	XM_575925.2	similar to BC013712 protein (predicted) (RGD1561016_predicted), mRNA.	49.49	8.47	93.39	2.56	68.46	1.49
ILMN_1365578	RGD1561055_predict	XM_577041.2	similar to Ferritin light chain 2 (Ferritin L subunit 2) (Ferritin subunit LG) (predicted) (RGD1561055_predicted), mRNA.	1790.45	312.18	2983.14	265.73	2081.58	111.28
ILMN_1367061	RGD1561141_predict	XR_007837.1	similar to solute carrier family 25 (mitochondrial carrier, Aralar), member 12 (predicted) (RGD1561141_predicted), mRNA.	1690.24	215.21	926.47	98.85	1443.93	1.53
ILMN_1366301	RGD1561143_predict	XM_222031.4	similar to cell surface receptor FDFACT (predicted) (RGD1561143_predicted), mRNA.	49.71	4.49	77.81	5.99	50.48	3.70
ILMN_1364910	RGD1561967_predict	XM_573497.2	similar to UDP-N-acetylglucosamine pyrophosphorylase 1 homolog (predicted) (RGD1561967_predicted), mRNA.	1161.06	247.13	4166.40	1038.30	2879.18	674.82
ILMN_1368068	RGD1562105_predict	XM_001070699.1	similar to Rho-GTPase-activating protein 25 (predicted) (RGD1562105_predicted), mRNA.	42.02	0.94	68.75	4.24	44.19	5.40
ILMN_1372724	RGD1562136_predict	XM_001070947.1	similar to D1Ert0622e protein (predicted) (RGD1562136_predicted), mRNA.	139.30	17.80	304.06	19.33	176.43	6.88
ILMN_1362293	RGD1562305_predict	XM_214902.4	similar to suprabasal-specific protein suprabasin (predicted) (RGD1562305_predicted), mRNA.	154.52	10.66	83.69	6.14	119.67	26.55
ILMN_1366128	RGD1562311_predict	XR_008266.1	similar to PIRA5 (predicted) (RGD1562311_predicted), mRNA.	43.86	4.51	89.26	7.07	49.94	0.30
ILMN_1371053	RGD1562655_predict	XR_007646.1	similar to toll-like receptor 13 (predicted) (RGD1562655_predicted), mRNA.	98.54	18.28	325.91	111.82	151.88	5.58
ILMN_1349102	RGD1562922_predict	XM_001057256.1	similar to ankyrin repeat-containing SOCS box protein 10 (predicted) (RGD1562922_predicted), mRNA.	159.99	35.80	74.98	17.72	89.10	13.25
ILMN_1374520	RGD1563073_predict	XR_009371.1	similar to SIGLEC-like 1 (predicted) (RGD1563073_predicted), mRNA.	38.55	2.04	85.64	14.68	42.02	5.47
ILMN_1350364	RGD1563798_predict	XR_007778.1	similar to BC040823 protein (predicted) (RGD1563798_predicted), mRNA.	193.88	27.13	114.09	12.60	193.44	5.81
ILMN_1370551	RGD1563888_predict	XM_001068357.1	similar to DNA segment, Chr 16, ERATO Doi 472, expressed (predicted) (RGD1563888_predicted), mRNA.	75.61	10.16	177.46	24.27	125.57	18.62

APPENDIX 8: continued

ID	SYMBOL	ACCESSION	DEFINITION	Ave Sham	StDev Sham	Ave MI	StDev MI	Ave MNC	StDev MNC
ILMN_1362050	RGD1563994_predicted	XM_001064713.1	similar to hypothetical protein A330042H22 (predicted) (RGD1563994_predicted), mRNA.	37.64	4.37	96.88	28.14	49.41	7.50
ILMN_1366126	RGD1564040_predicted	XM_001062502.1	similar to methylenetetrahydrofolate dehydrogenase (NAD) (EC 1.5.1.15)/methenyltetrahydrofolate cyclohydrolase (EC 3.5.4.9) precursor (predicted) (RGD1564040_predicted), mRNA.	102.13	12.56	166.40	11.69	129.87	1.44
ILMN_1370131	RGD1564130_predicted	XM_347206.3	similar to TBP-associated factor 172 (TAF-172) (TAF(II)170) (predicted) (RGD1564130_predicted), mRNA.	148.49	16.52	308.98	64.66	203.66	18.10
ILMN_1367672	RGD1564330_predicted	XM_343179.3	similar to PML-RAR alpha-regulated adaptor molecule-1 (predicted) (RGD1564330_predicted), mRNA.	44.31	6.40	160.20	39.97	67.57	1.50
ILMN_1357240	RGD1564549_predicted	XM_214831.4	similar to hypothetical protein FLJ20512 (predicted) (RGD1564549_predicted), mRNA.	944.73	76.18	622.44	33.09	888.45	7.81
ILMN_1349895	RGD1565140_predicted	XM_001067977.1	similar to Clec3f12 protein (predicted) (RGD1565140_predicted), mRNA.	55.13	3.25	321.56	110.97	116.31	31.47
ILMN_1365610	RGD1565319_predicted	XM_001070153.1	similar to Delta-interacting protein A (Hepatitis delta antigen interacting protein A) (predicted) (RGD1565319_predicted), mRNA.	109.44	47.94	564.76	231.02	257.77	102.31
ILMN_1351274	RGD1565374_predicted	XM_573339.2	similar to hypothetical protein LOC199675 (predicted) (RGD1565374_predicted), mRNA.	62.83	21.05	579.22	132.62	149.33	54.37
ILMN_1374656	RGD1565451_predicted	XR_007981.1	similar to ring finger protein 127 (predicted) (RGD1565451_predicted), mRNA.	39.39	1.76	62.98	0.99	50.14	0.60
ILMN_1365821	RGD1566093_predicted	XM_001060226.1	similar to Fusion (involved in t(12;16) in malignant liposarcoma) (predicted) (predicted) (RGD1566093_predicted), mRNA.	1538.69	45.20	2236.50	97.12	1844.17	46.52
ILMN_1372185	RGD1566118_predicted	XM_001076548.1	RGD1566118 (predicted) (RGD1566118_predicted), mRNA.	323.39	28.20	623.03	31.58	464.06	26.69
ILMN_1362451	Rgs2	NM_053453.1	regulator of G-protein signaling 2 (Rgs2), mRNA.	583.76	173.37	2257.89	721.32	1280.72	341.84
ILMN_1362622	Rhoh	NM_001013430.1	ras homolog gene family, member H (Rhoh), mRNA.	103.19	22.28	257.22	74.85	126.16	4.28
ILMN_1364613	Rhoj	NM_001008320.1	ras homolog gene family, member J (Rhoj), mRNA.	364.52	23.96	619.29	47.19	631.05	95.00
ILMN_1357763	Rhoq	NM_053522.1	ras homolog gene family, member Q (Rhoq), mRNA.	811.99	98.33	1391.56	116.30	1086.59	196.17
ILMN_1350981	Ripk1_predicted	XM_225262.4	receptor (TNFRSF)-interacting serine-threonine kinase 1 (predicted) (Ripk1_predicted), mRNA.	74.12	7.75	138.32	18.19	134.05	16.08
ILMN_1354240	Ripk3	NM_139342.1	receptor-interacting serine-threonine kinase 3 (Ripk3), mRNA.	51.51	6.71	94.64	8.00	62.26	1.95
ILMN_1376851	Rnd3	NM_001007641.1	Rho family GTPase 3 (Rnd3), mRNA.	128.58	12.42	336.72	16.40	277.47	82.71
ILMN_1372230	Rnf149	XM_343561.3	ring finger protein 149 (Rnf149), mRNA.	247.84	57.38	324.53	95.53	92.18	5.85
ILMN_1359238	Rock2	NM_013022.1	Rho-associated coiled-coil forming kinase 2 (Rock2), mRNA.	182.54	4.36	270.48	25.41	229.64	9.04
ILMN_1371943	Runx1	NM_017325.1	runt related transcription factor 1 (Runx1), mRNA.	135.27	34.31	291.56	19.63	231.01	23.68
ILMN_1373883	S100a11	NM_001004095.1	S100 calcium binding protein A11 (calizzarin) (S100a11), mRNA.	2054.54	371.03	3675.86	401.00	2787.39	9.15
ILMN_1350690	S100a8	NM_053822.1	S100 calcium binding protein A8 (calgranulin A) (S100a8), mRNA.	718.96	527.49	7860.78	2652.69	3148.98	532.70
ILMN_1359143	Samsn1	NM_130821.1	SAM domain, SH3 domain and nuclear localization signals, 1 (Samsn1), mRNA.	65.72	16.51	268.31	79.28	151.82	50.14
ILMN_1368419	Sat	NM_001007667.1	spermidine/spermine N1-acetyl transferase (Sat), mRNA.	678.58	182.52	2504.56	720.99	1506.77	79.16
ILMN_1363777	Scap2	NM_130413.1	src family associated phosphoprotein 2 (Scap2), mRNA.	151.43	26.88	314.80	55.32	216.52	7.89
ILMN_1359759	Scnn1a	NM_031548.2	sodium channel, nonvoltage-gated 1 alpha (Scnn1a), mRNA.	43.71	7.29	80.30	9.35	59.86	3.99
ILMN_1369410	Sec23b_predicted	XM_001054580.1	SEC23B (S. cerevisiae) (predicted) (Sec23b_predicted), mRNA.	170.46	2.18	319.06	68.35	252.47	39.02
ILMN_1349113	Sell	NM_019177.1	selectin, lymphocyte (Sell), mRNA.	69.50	28.71	557.81	104.89	151.57	39.20

APPENDIX 8: continued

ID	SYMBOL	ACCESSION	DEFINITION	Ave Sham	StDev Sham	Ave MI	StDev MI	Ave MNC	StDev MNC
ILMN_1376428	Sema4a	NM_001012078.1	sema domain, immunoglobulin domain (Ig), transmembrane domain (TM) and short cytoplasmic domain, (semaphorin) 4A (Sema4a), mRNA.	138.78	2.66	662.06	47.25	265.59	26.33
ILMN_1353169	Sema4d_predicted	XM_001053912.1	sema domain, immunoglobulin domain (Ig), transmembrane domain (TM) and short cytoplasmic domain, (semaphorin) 4D (predicted) (Sema4d_predicted), mRNA.	44.75	1.66	67.97	0.26	50.54	1.44
ILMN_1357664	Sema6a_predicted	XM_341612.3	sema domain, transmembrane domain (TM), and cytoplasmic domain, (semaphorin) 6A (predicted) (Sema6a_predicted), mRNA.	93.46	4.16	137.76	11.47	106.47	1.55
ILMN_1351430	Serpib10	NM_153733.2	serine (or cysteine) peptidase inhibitor, clade B (ovalbumin), member 10 (Serpib10), mRNA.	36.48	4.15	155.97	56.66	53.00	7.85
ILMN_1352285	Serpib1a	NM_001031642.1	serine (or cysteine) proteinase inhibitor, clade B, member 1a (Serpib1a), mRNA.	226.46	187.90	1543.90	475.42	948.79	65.11
ILMN_2040557	Serpine1	NM_012620.1	serine (or cysteine) peptidase inhibitor, clade E, member 1 (Serpine1), mRNA.	374.87	134.64	1808.98	685.09	942.06	388.97
ILMN_1376417	Serpine1	NM_012620.1	mRNA.	401.65	119.17	1639.90	500.09	1222.81	584.15
ILMN_1365196	Sertad1	NM_001007735.1	SERTA domain containing 1 (Sertad1), mRNA.	154.62	45.51	333.88	22.09	268.26	51.74
ILMN_1349269	Sgk	NM_019232.1	serum/glucocorticoid regulated kinase (Sgk), mRNA.	1246.45	152.58	2506.70	224.04	1908.03	619.89
ILMN_1350798	Slc16a3	NM_030834.1	solute carrier family 16 (monocarboxylic acid transporters), member 3 (Slc16a3), mRNA.	163.41	95.65	2006.89	779.92	540.08	79.08
ILMN_1363587	Slc25a19	NM_001007674.1	solute carrier family 25 (mitochondrial thiamine pyrophosphate carrier), member 19 (Slc25a19), mRNA.	361.32	16.07	247.33	20.69	312.83	8.88
ILMN_1367573	Slc25a25	NM_145677.1	solute carrier family 25 (mitochondrial carrier, phosphate carrier), member 25 (Slc25a25), mRNA.	231.67	10.76	493.30	99.54	414.07	116.11
ILMN_1362330	Slc25a29	NM_001010958.1	solute carrier family 25 (mitochondrial carrier, palmitoylcarnitine transporter), member 29 (Slc25a29), mRNA.	261.58	9.33	157.78	14.69	189.38	32.22
ILMN_1366777	Slc2a6_predicted	XM_238321.4	solute carrier family 2 (facilitated glucose transporter), member 6 (predicted) (Slc2a6_predicted), mRNA.	47.24	3.90	91.92	12.23	62.09	0.22
ILMN_1362278	Slc5a3	NM_053715.2	solute carrier family 5 (inositol transporters), member 3 (Slc5a3), mRNA.	148.78	21.03	697.49	282.97	462.26	194.77
ILMN_1365729	Slc7a5	NM_017353.1	solute carrier family 7 (cationic amino acid transporter, y+ system), member 5 (Slc7a5), mRNA.	115.18	27.55	290.88	56.60	215.60	21.06
ILMN_1360286	Slpi	NM_053372.1	secretory leukocyte peptidase inhibitor (Slpi), mRNA.	814.07	610.81	6911.15	2215.57	2699.06	60.41
ILMN_1368002	Snag1_predicted	XM_226769.4	sorting nexin associated golgi protein 1 (predicted) (Snag1_predicted), mRNA.	103.52	9.72	300.16	34.40	183.10	79.09
ILMN_1350250	Soat1	NM_031118.1	sterol O-acyltransferase 1 (Soat1), mRNA.	36.72	2.13	54.72	1.05	44.00	2.21
ILMN_1363716	Sorl1_predicted	XM_001065506.1	sortilin-related receptor, L(DLR class) A repeats-containing (predicted) (Sorl1_predicted), mRNA.	117.63	4.67	246.28	45.18	120.59	8.87
ILMN_1373357	Sphk1	NM_133386.2	sphingosine kinase 1 (Sphk1), mRNA.	174.40	97.11	1017.34	222.37	744.30	114.44
ILMN_1352642	Spp1	NM_012881.1	secreted phosphoprotein 1 (Spp1), mRNA.	69.25	14.16	261.23	113.96	98.64	2.57
ILMN_1367615	Spsb1_predicted	XM_001075317.1	spiA/ryanodine receptor domain and SOCS box containing 1 (predicted) (Spsb1_predicted), mRNA.	274.79	45.21	489.31	18.68	431.18	71.66
ILMN_1352951	Stfa2_predicted	XM_001070786.1	stefin A2 (predicted) (Stfa2_predicted), mRNA.	126.73	43.19	3042.27	493.95	545.40	88.64
ILMN_1370817	Stk17b	NM_133392.1	serine/threonine kinase 17b (apoptosis-inducing) (Stk17b), mRNA.	107.00	5.26	300.92	55.99	146.57	12.05
ILMN_1376772	Stom	NM_001011965.1	stomatin (Stom), mRNA.	104.52	9.08	284.28	14.35	193.70	41.15

APPENDIX 8: continued

ID	SYMBOL	ACCESSION	DEFINITION	Ave Sham	StDev Sham	Ave MI	StDev MI	Ave MNC	StDev MNC
ILMN_1361287	Surb7_predicted	XM_001074060.1	SRB7 (suppressor of RNA polymerase B) homolog (S. cerevisiae) (predicted) (Surb7_predicted), mRNA.	310.59	28.26	468.28	26.11	371.14	29.01
ILMN_1350279	Syk	NM_012758.1	spleen tyrosine kinase (Syk), mRNA.	52.06	0.71	83.00	6.96	51.10	3.23
ILMN_1360221	Tacstd1	NM_138541.1	tumor-associated calcium signal transducer 1 (Tacstd1), mRNA.	36.87	3.67	133.22	59.79	87.62	34.94
ILMN_1376249	Tf	NM_001013110.1	transferrin (Tf), mRNA.	1058.85	21.41	3870.74	1343.10	1975.94	431.07
ILMN_1359732	Tfpi2	NM_173141.1	tissue factor pathway inhibitor 2 (Tfpi2), mRNA.	150.35	61.07	860.96	129.71	454.37	250.93
ILMN_1360947	Tgm1	NM_031659.1	transglutaminase 1 (Tgm1), mRNA.	70.92	8.64	189.66	36.52	139.59	14.78
ILMN_1363727	Thbd	NM_031771.2	thrombomodulin (Thbd), mRNA.	261.50	68.98	743.89	57.04	385.82	92.83
ILMN_1366394	Timm13	NM_145781.1	translocase of inner mitochondrial membrane 13 homolog (yeast) (Timm13), mRNA.	175.81	9.77	118.51	7.99	156.13	5.86
ILMN_1359200	Timp1	NM_053819.1	tissue inhibitor of metalloproteinase 1 (Timp1), mRNA.	1987.37	1022.76	7652.86	1713.85	5378.48	1201.80
ILMN_1373383	Tiparp_predicted	XM_001060648.1	TCDD-inducible poly(ADP-ribose) polymerase (predicted) (Tiparp_predicted), mRNA.	321.23	29.93	927.12	170.06	680.68	79.09
ILMN_1353896	Tlr2	NM_198769.2	toll-like receptor 2 (Tlr2), mRNA.	225.41	123.74	987.04	297.04	431.23	60.43
ILMN_1356202	Tlr6	NM_207604.1	toll-like receptor 6 (Tlr6), mRNA.	131.21	17.10	281.48	20.57	157.43	9.98
ILMN_1361672	Tm4sf1_predicted	XM_001060042.1	transmembrane 4 superfamily member 1 (predicted) (Tm4sf1_predicted), mRNA.	883.72	172.10	1930.61	116.98	1381.63	346.34
ILMN_1349318	Tmem49	NM_138839.2	transmembrane protein 49 (Tmem49), mRNA.	730.41	46.35	1148.61	111.71	799.03	106.46
ILMN_1650241	Tmem60_predicted	XM_001063081.1	transmembrane protein 60 (predicted) (Tmem60_predicted), mRNA.	441.07	33.77	266.57	22.68	341.11	4.47
ILMN_1351557	Tmem9_predicted	XM_001063617.1	transmembrane protein 9 (predicted) (Tmem9_predicted), mRNA.	123.42	5.72	84.44	4.75	105.98	7.19
ILMN_1352021	Tmx2	NM_001007643.1	thioredoxin-related transmembrane protein 2 (Tmx2), mRNA.	454.56	13.32	289.75	23.26	388.13	65.57
ILMN_1649963	Tpm3	NM_173111.1	tropomyosin 3, gamma (Tpm3), transcript variant 2, mRNA.	290.51	75.31	731.52	86.76	426.76	20.77
ILMN_1363774	Tpm3	NM_057208.2	tropomyosin 3, gamma (Tpm3), transcript variant 1, mRNA.	46.04	4.40	75.38	4.98	51.43	8.34
ILMN_1357948	Trem1_predicted	XM_217336.4	triggering receptor expressed on myeloid cells 1 (predicted) (Trem1_predicted), mRNA.	73.74	29.13	563.45	296.86	180.36	15.81
ILMN_2040035	Trem1_predicted	XM_217336.4	triggering receptor expressed on myeloid cells 1 (predicted) (Trem1_predicted), mRNA.	58.11	13.68	209.13	95.15	90.69	5.17
ILMN_1366607	Trh	NM_013046.2	thyrotropin releasing hormone (Trh), mRNA.	133.94	20.47	263.55	11.61	308.35	29.69
ILMN_1361387	Trim45_predicted	XM_215666.4	tripartite motif protein 45 (predicted) (Trim45_predicted), mRNA.	319.90	52.11	174.12	13.12	300.45	5.12
ILMN_1376818	Tubb3	NM_139254.1	tubulin, beta 3 (Tubb3), mRNA.	46.55	2.91	71.93	5.87	66.72	8.18
ILMN_1358531	Tubb6	NM_001025675.1	tubulin, beta 6 (Tubb6), mRNA.	323.13	128.48	1200.03	54.74	870.44	14.77
ILMN_1351237	Txnrd1	NM_031614.1	thioredoxin reductase 1 (Txnrd1), mRNA.	187.87	60.30	611.44	40.72	363.16	13.89
ILMN_1372404	Tyrobp	NM_212525.1	Tyro protein tyrosine kinase binding protein (Tyrobp), mRNA.	92.37	22.05	234.61	39.68	120.07	10.15
ILMN_1368402	Uap1_predicted	XM_222863.4	UDP-N-acetylglucosamine pyrophosphorylase 1 (predicted) (Uap1_predicted), mRNA.	179.04	17.63	768.40	167.01	475.60	158.24
ILMN_1360736	Ugdh	NM_031325.1	UDP-glucose dehydrogenase (Ugdh), mRNA.	651.00	314.27	2271.01	406.04	1445.61	356.63
ILMN_1367494	Vdac3	NM_031355.1	voltage-dependent anion channel 3 (Vdac3), mRNA.	6275.70	772.14	4092.54	197.67	5355.04	226.18
ILMN_1364576	Verge	NM_001003403.1	vascular early response gene protein (Verge), mRNA.	115.96	8.67	213.56	17.96	170.45	16.94
ILMN_1366783	Vps13d_predicted	XM_001073610.1	vacuolar protein sorting 13D (yeast) (predicted) (Vps13d_predicted), mRNA.	581.05	75.28	346.87	9.12	522.07	21.93
ILMN_1375233	Vps24	NM_172331.1	vacuolar protein sorting 24 (yeast) (Vps24), mRNA.	1015.45	6.69	709.81	24.66	895.42	16.15
ILMN_1362991	Vps45	NM_172072.2	vacuolar protein sorting 45 (yeast) (Vps45), mRNA.	135.69	5.96	90.88	7.12	131.71	0.04

APPENDIX 8: continued

ID	SYMBOL	ACCESSION	DEFINITION	Ave Sham	StDev Sham	Ave MI	StDev MI	Ave MNC	StDev MNC
ILMN_1357658	Wsb1	NM_001025664.1	WD repeat and SOCS box-containing 1 (Wsb1), transcript variant 2,	281.42	20.58	732.82	186.89	475.90	34.11
ILMN_1374460	Yars	NM_001025696.1	tyrosyl-tRNA synthetase (Yars), mRNA.	294.88	49.12	576.29	85.34	495.76	72.70
ILMN_1373913	Ywhaz	NM_013011.2	tyrosine 3-monooxygenase/tryptophan 5-monooxygenase activation protein, zeta polypeptide (Ywhaz), mRNA.	1647.25	172.62	3276.01	542.88	2166.15	156.36
ILMN_1376913	Zc3h8	NM_001012090.1	zinc finger CCCH type containing 8 (Zc3h8), mRNA.	228.20	12.20	141.00	13.36	164.61	9.93
ILMN_1364338	Zcchc12	NM_001014065.1	zinc finger, CCHC domain containing 12 (Zcchc12), mRNA.	51.28	1.44	89.35	16.70	71.38	0.22
ILMN_1370665	Zfand2a	NM_001008363.1	zinc finger, AN1-type domain 2A (Zfand2a), mRNA.	263.29	40.16	1554.32	551.71	960.21	552.65
ILMN_1370049	Zfp180	NM_144757.1	zinc finger protein 180 (Zfp180), mRNA.	261.91	0.72	170.61	14.08	261.85	22.32
ILMN_1363594	Zfp655	NM_001008362.1	zinc finger protein 655 (Zfp655), mRNA.	338.78	24.44	620.30	47.24	484.53	40.74
ILMN_1359146	Zswim6	XM_226779.4	zinc finger, SWIM domain containing 6 (Zswim6), mRNA.	60.34	2.22	95.84	9.06	80.02	3.59

APPENDIX 9: continued

Band		Protein Name	MASCOT Score	Queries matched	Species	Theoretical		coverage	Matched peptides	MASCOT ion Score
						Mr	PI			
BWB02			156	5	Rattus	68686	6.09	7%	R.FPNAEFAEITK.L	65
BWB02		NO RESULT	111	2	Rattus	68686	6.09	4%		
BWB03	ODO1_RAT	oxoglutarate dehydrogenase E1 component, mt	89	10	Rattus	116221	6.3	8%		
BWB03		NO RESULT								
BWB04										
BWB04		NO RESULT								
BWB05										
BWB05		NO RESULT								
BWB06										
BWB06		NO RESULT								
BWB07										
BWB07		NO RESULT								
BWB08										
BWB08		NO RESULT								
BWB09										
BWB09		NO RESULT								
BWB10										
BWB10		NO RESULT								
BWB11										
BWB11		NO RESULT								
BWB12										
BWB12		NO RESULT								
BWB13										
BWB13		NO RESULT								
BWB14	ATPB_RAT	ATP synthase subunit beta, mitochondrial	419	18	Rattus	56318	5.19	36%	R.LVLEVAQHLGESTVR.T	56
									K.VVDLLAPYAK.G	43
									R.VALTGLTVAEYFR.D	72
									R.FTQAGSEVSALLGR.I	49
									R.AIAELGIYPAVDPLDSTR.I	42
BWB14	ATPB_RAT	ATP synthase subunit beta, mt	262	5	Rattus	56318	5.19	14%		
BWB15	ECHB_RAT	Trifunctional enzyme subunit beta, mitochondrial	68	4	Rattus	51382	9.5	8%	K.VGAPPLEK.F	36
BWB15	ECHB_RAT	Trifunctional enzyme subunit beta, mt	36	1	Rattus	51382	9.5	2%		
BWB16										
BWB16		NO RESULT								
BWB17	KCRS_MOUSE	Creatine kinase, sarcomeric mitochondrial	105	8	Mouse	47443	8.64	18%		
BWB17		NO RESULT								
BWB18			55	2	Bovine	19870	4.93	15%	R.VYVEELKPTPEGDLEILLQK.W	51
BWB18		NO RESULT	51	1	Bovine	19870	4.93	11%		
BWB19			64	2	Bovine	19870	4.93	15%	R.VYVEELKPTPEGDLEILLQK.W	46
BWB19		NO RESULT	46	1	Bovine	19870	4.93	11%		
BWB20	1433E_RAT	14-3-3 protein epsilon	70	3	Rattus	29155	4.63	10%	R.YLAEFATGNDR.K	36
BWB20	1433E_RAT	14-3-3 protein epsilon	36	1	Rattus	29155	4.63	4%		

APPENDIX 9: continued

Band		Protein Name	MASCOT Score	Queries matched	Species	Theoretical		coverage	Matched peptides	MASCOT ion Score
						Mr	PI			
BWB21	1433E_RAT	14-3-3 protein epsilon	103	8	Rattus	29155	4.63	29%	K.LAEQAER.Y	35
BWB21	1433E_RAT	14-3-3 protein epsilon	35	1	Rattus	29155	4.63	3%		
BWB22	1433E_RAT	14-3-3 protein epsilon	1090	61	Rattus	29155	4.63	55%	K.LAEQAER.Y	49
									K.VAGMDVELTVEER.N	83
									K.VAGMDVELTVEER.N (M)	95
									R.NLLSVAYK.N	48
									R.IISSIEQK.E	50
									R.IISSIEQKEENK.G	78
									R.QMVETELK.L (M)	45
									K.LICCDILDVLDK.H 2 (C)	94
									K.HLIPAANTGESK.V	72
									R.YLAEFATGNDR.K	85
									K.EAAENSLVAYK.A	73
									K.AASDIAMTELPPTHPIR.L	103
									K.AASDIAMTELPPTHPIR.L (M)	89
									K.AAFDDAIAELDTLSEESYK.D	71
									K.AAFDDAIAELDTLSEESYKDSLIMQLLR.D	133
									K.DSTLIMQLLR.D	51
									K.DSTLIMQLLR.D (M)	44
BWB22	1433E_RAT	14-3-3 protein epsilon	1263	17	Rattus	29155	4.63	55%		
BWB23										
BWB23		NO RESULT								
BWB24	CY1_MOUSE	Cytochrome c1, heme protein, mitochondrial	98	8	Mouse	35305	9.24	17%	R.AANNGALPPDLSYIVR.A	58
BWB24	CY1_MOUSE	Cytochrome c1, heme protein, mt	58	1	Mouse	35305	9.24	5%		
BWB25	HBB1_RAT	Hemoglobin subunit beta-1	70	6	Rattus	15969	7.88	25%		
BWB25		NO RESULT								
BWB26	HBB1_RAT	Hemoglobin subunit beta-1 (or HBB2_RAT)	78	4	Rattus	15969	7.88	19%		
	HBA_RAT	Hemoglobin subunit alpha-1/2	55	3	Rattus	15319	7.82	25%	R.MFAAFPTTK.T	36
BWB26	HBA_RAT	Hemoglobin subunit alpha-1/2	36	1	Rattus	15319	7.82	6%		
BWB27	HBA_RAT	Hemoglobin subunit alpha-1/2	210	12	Rattus	15319	7.82	57%	R.MFAAFPTTK.T	37
									R.MFAAFPTTK.T (M)	46
									K.TYFSHIDVSPGSAQVK.A	63
	HBB1_RAT	Hemoglobin subunit beta-1	128	8	Rattus	15969	7.88	25%	M.VHLTDAEK.A	39
									R.LLVVYPWTQR.Y	52
BWB27	HBA_RAT	Hemoglobin subunit alpha-1/2	146	3	Rattus	15319	7.82	18%		
BWB27	HBB1_RAT	Hemoglobin subunit beta-1	91	2	Rattus	15969	7.88	12%		
BWB28	HBA_RAT	Hemoglobin subunit alpha-1/2	289	13	Rattus	15319	7.82	57%	R.MFAAFPTTK.T	38
									R.MFAAFPTTK.T (M)	42
									K.TYFSHIDVSPGSAQVK.A	93
									K.KVADALAK.A	38
									K.AADHVEDLPGALSTLSLHAHK.L	74
	HBB1_RAT	Hemoglobin subunit beta-1	159	10	Rattus	15969	7.88	38%	M.VHLTDAEK.A	46
									R.LLVVYPWTQR.Y	48
BWB28	HBA_RAT	Hemoglobin subunit alpha-1/2	285	5	Rattus	15319	7.82	39%		
BWB28	HBB1_RAT	Hemoglobin subunit beta-1	94	2	Rattus	15969	7.88	12%		

APPENDIX 9: continued

Band		Protein Name	MASCOT Score	Queries matched	Species	Theoretical		coverage	Matched peptides	MASCOT ion Score
						Mr	PI			
BWB29	QCR6_RAT	Cytochrome b-c1 complex subunit 6, mitochondrial	147	6	Rattus	10417	4.9	29%	R.SQTEEDCTEELDFLHAR.D (C)	114
	USMG5_RAT	Up-regulated during skeletal muscle growth protein 5	92	3	Rattus	6403	9.84	43%	M.AGPESDGGQFQFTGIK.K	72
	ATP5I_RAT	ATP synthase subunit e, mitochondrial	92	2	Rattus	8249	9.34	32%	M.VPPVQVSPLIK.F	62
BWB29	QCR6_RAT	Cytochrome b-c1 complex subunit 6, mt	114	1	Rattus	10417	4.9	20%		
BWB29	USMG5_RAT	Up-regulated during skeletal muscle growth protein 5	72	1	Rattus	6403	9.84	26%		
BWB29	ATP5I_RAT	ATP synthase subunit e, mt	62	1	Rattus	8249	9.34	15%		
BNB01										
BNB01		NO RESULT								
BNB02			54	3	Bovine	19870	4.93	23%		
BNB02		NO RESULT								
BNB03	NDUS1_RAT	NADH-ubiquinone oxidoreductase 75 kDa subunit, mitochondrial	78	5	Rattus	79362	5.65	7%		
	K1C15_RAT	Keratin, type I cytoskeletal 15	70	3	Rattus	48840	4.8	5%		
BNB03		NO RESULT								
BNB04										
BNB04		NO RESULT								
BNB05										
BNB05		NO RESULT								
BNB06										
BNB06		NO RESULT								
BNB07	EF1A2_RAT	Elongation factor 1-alpha	259	10	Rattus	50422	9.11	12%	K.YYITIIDAPGHR.D	38
									R.EHALLAYTLGVK.Q	56
									R.LPLQDVYK.I	51
									K.IGGIGTVPVGR.V	65
BNB07	EF1A2_RAT	Elongation factor 1-alpha	210	4	Rattus	50422	9.11	9%		
BNB08	SUCA_RAT	Succinyl-CoA ligase [GDP-forming] subunit alpha, mitochondrial	704	27	Rattus	36125	9.54	35%	R.KNIYIDK.N	50
									K.VICQGFQTK.Q (C)	48
									K.QGTFHSQQALEYGTK.L	95
									K.LVGGTTPGK.G	65
									K.HLGLPVFNTVK.E	73
									R.LIGPNCPGIINPGECK.I 2 (C)	107
									K.DPATEGIVLIGEIGHAEENAAEFLK.E	123
									K.AKPVVFSIAGITAPPGR.R	44
									R.MGHAGAIAGGK.G (M)	84
BNB08	SUCA_RAT	Succinyl-CoA ligase [GDP-forming] subunit alpha, mt	689	9	Rattus	36125	9.54	35%		
BNB09	CY1_BOVIN	Cytochrome c1, heme protein, mitochondrial	91	5	Bovine	35274	9.14	16%		
BNB09		NO RESULT								
BNB10	HBB2_RAT	Hemoglobin subunit beta-2	105	7	Rattus	15972	8.91	25%		
	NDUV2_RAT	NADH dehydrogenase [ubiquinone] flavoprotein 2, mitochondrial	89	3	Rattus	27361	6.23	12%	R.DSDSILETLQR.K	40
BNB10	NDUV2_RAT	NADH dehydrogenase [ubiquinone] flavoprotein 2, mt	40	1	Rattus	27361	6.23	4%		

APPENDIX 9: continued

Band		Protein Name	MASCOT Score	Queries matched	Species	Theoretical		coverage	Matched peptides	MASCOT ion Score
						Mr	PI			
BNB11	HBB2_RAT	Hemoglobin subunit beta-2	141	5	Rattus	15972	8.91	25%	R.LLVVYPWTQR.Y	40
	K2C4_RAT	Keratin, type II cytoskeletal 4	53	1	Rattus	57631	7.52	1%	K.NEISELNR.M	54
BNB11	HBB2_RAT	Hemoglobin subunit beta-2	141	5	Rattus	15972	8.91	7%		
BNB11	K2C4_RAT	Keratin, type II cytoskeletal 4	53	1	Rattus	57631	7.52	1%		
BNB12	HBB2_RAT	Hemoglobin subunit beta-2	289	11	Rattus	15972	8.91	53%	M.VHLTDAEK.A	49
									K.ATVSGLWGK.V	38
									R.LLVVYPWTQR.Y	52
									K.FGDLSSASAIMGNPQVK.A (M)	35
									K.VINAFNDGLK.H	46
									K.VVAGVASALAHK.Y	69
	HBA_RAT	Hemoglobin subunit alpha-1/2	52	5	Rattus	15319	7.82	33%		
BNB12	HBB2_RAT	Hemoglobin subunit beta-2	289	6	Rattus	15319	7.82	53%		
BNB13	HBA_RAT	Hemoglobin subunit alpha-1/2	680	21	Rattus	15319	7.82	71%	M.VLSADDKTNK.N	52
									K.IGGHGGGEYGEEALQR.M	125
									R.MFAAFPTTK.T	38
									R.MFAAFPTTK.T (M)	70
									K.TYFSHIDVSPGSAQVK.A	119
									K.KVADALAK.A	55
									K.AADHVEDLPGALSTLSLHHAHK.L	127
									K.LRVDPVNFK.F	47
									K.FLASVSTVLTSK.Y	91
	HBB1_RAT	Hemoglobin subunit beta-1	545	21	Rattus	15969	7.88	78%	M.VHLTDAEK.A	51
									K.VNPDDVGGALGR.L	90
									R.LLVVYPWTQR.Y	52
									R.YFDSFGDLSSASAIMGNPK.V (M)	40
									K.VINAFNDGLK.H	55
									K.GTFAHLSLHCDK.L (C)	53
									K.LHVDPENFR.L	46
									K.EFTPCAQAQAFQK.V (C)	61
									K.VVAGVASALAHK.Y	86
	HBB2_RAT	Hemoglobin subunit beta-2	441	19	Rattus	15972	8.91	56%	M.VHLTDAEK.A	51
									K.ATVSGLWGK.V	37
									R.LLVVYPWTQR.Y	52
									K.VINAFNDGLK.H	55
									K.GTFAHLSLHCDK.L (C)	53
									K.LHVDPENFR.L	46
									K.EFTPCAQAQAFQK.V (C)	61
									K.VVAGVASALAHK.Y	86
BNB13	HBA_RAT	Hemoglobin subunit alpha-1/2	724	9	Rattus	15319	7.82	71%		
BNB13	HBB1_RAT	Hemoglobin subunit beta-1	534	9	Rattus	15969	7.88	78%		
BNB13	HBB2_RAT	Hemoglobin subunit beta-2	441	8	Rattus	15972	8.91	56%		

APPENDIX 9: continued

Band		Protein Name	MASCOT Score	Queries matched	Species	Theoretical		coverage	Matched peptides	MASCOT ion Score
						Mr	PI			
BNB14	QCR6_RAT	Cytochrome b-c1 complex subunit 6, mitochondrial	168	5	Rattus	10417	4.9	38%	R.SQTEEDCTEELDFDLHAR.D (C)	112
	HBA_RAT	Hemoglobin subunit alpha-1/2	85	3	Rattus	15319	7.82	35%	K.FLASVSTVLTSK.Y	58
	CX6B1_MOUSE	Cytochrome c oxidase subunit 6B1	60	3	Rattus	10065	8.96	34%	K.GGDVSVCEWYR.R (C)	44
	NDUS6_RAT	NADH dehydrogenase [ubiquinone] iron-sulfur protein 6, mitochondrial	57	1	Rattus	12775	9.37	12%	R.IIACDGGGGALGHPK.V (C)	57
BNB14	QCR6_RAT	Cytochrome b-c1 complex subunit 6, mt	112	1	Rattus	10417	4.9	20%		
BNB14	HBA_RAT	Hemoglobin subunit alpha-1/2	58	1	Rattus	15319	7.82	3%		
BNB14	CX6B1_MOUSE	Cytochrome c oxidase subunit 6B1	44	1	Rattus	10065	8.96	13%		
BNB14	NDUS6_RAT	NADH dehydrogenase [ubiquinone] iron-sulfur protein 6, mt	57	1	Rattus	12775	9.37	12%		

APPENDIX 10: Manuscript submitted to Atherosclerosis

Bone Marrow Mononuclear Cells Reduce Myocardial Reperfusion Injury by Activating the PI3K/Akt Survival Pathway.

Authors

Matthew J. Lovell*¹, Mohammed Yasin*², Kate L. Lee¹, Kenneth Cheung^{4,5}, Yasunori Shintani², Massimo Collino², , Ahila Sivarajah², Kit-yi Leung¹, Kunihiko Takahashi², Amar Kapoor², Mohammed M. Yaqoob², Ken Suzuki², Mark F. Lythgoe⁴, John Martin³, Patricia B. Munroe¹, †Chris Thiemermann², and †Anthony Mathur¹.

1 Centre for Clinical Pharmacology, The William Harvey Research Institute, Barts and the London School of Medicine and Dentistry, Queen Mary University of London, London, EC1M 6BQ, UK

2 Centre for Translational Medicine & Therapeutics, The William Harvey Research Institute, Barts and the London School of Medicine and Dentistry, Queen Mary University of London, London, EC1M 6BQ, UK

3 British Heart Foundation Laboratories, Department of Medicine, University College London, London WC1E 6JJ, UK

4 Centre for Advanced Biomedical Imaging, Department of Medicine and Institute of Child Health, University College London, London WC1E 6DD, UK

5 Department of Medical Physics and Bioengineering, University College London, London WC1E 6DD, UK

* These authors have contributed equally and are joint first authors of this article.

† These authors have contributed equally and are joint last authors of this article.

Prof A. Mathur Corresponding Author

Fax no. 0044 208 983 2381

Tel No. 0044 208 983 2216

Email: a.mathur@qmul.ac.uk

Key words

Bone marrow, mononuclear cells, ischaemia-reperfusion, stem cell, myocardial infarction, proteomics

Disclosures

The authors acknowledge the support of the Medical Research Council (K.L. Lee and M. Yasin), William Harvey Research Foundation (M. Yasin), the British Heart Foundation (M. Lythgoe and M. Lovell), and the Engineering and Physical Sciences Research Council (K.C.). No conflicts of interest are declared.

APPENDIX 10: continued

Author Contributions

Study concept and design: MJL, MY, MMY, KS, MFL, CT, AM; Phenotype studies (infarct size, effects on apoptosis and necrosis, cardiac function and myocardial fibrosis: MJL, MY, KC, YS, AS, KT, AK, KS, MFL, JM, AM; 2-DE and mass spectrometry: KLL; PI3/Akt survival analyses: MY, MC, AK; Data analyses and interpretation: MJL, MY, KLL, MC, KYL, PBM, CT, AM; Writing of the paper: MJL, MY, KLL, CT, AM; Critical review of the manuscript: MJL, KLL, MFL, JM, PBM, CT, AM

Abstract

Objective - Adult bone marrow mononuclear cells (BMMNCs) can restore cardiac function following myocardial necrosis. Protocols used to date have administered cells relatively late after ischemia/reperfusion injury, but there is the opportunity with elective procedures to infuse cells shortly after restoration of blood flow, for example after angioplasty. Our aim was therefore to try and quantify protection from myocardial injury by early infusion of BMMNCs in a rat ischaemia reperfusion (I/R) model.

Methods and Results - Male Wistar rats underwent 25 minutes of ischaemia followed by 2 hours reperfusion of the left anterior descending coronary artery. Ten million BMMNCs were injected i.v. at reperfusion. We found BMMNCs caused a significant reduction in infarct size at two hours when assessed by staining the area at risk with p-nitro blue tetrazolium (42% reduction, $P < 0.01$). Apoptosis and necrosis of isolated cardiomyocytes was significantly reduced in the area at risk. Functional assessment at 7 days using echocardiography and left ventricular catheterisation showed improved systolic and diastolic function in the BMMNC treatment group (LVEF: BMMNC $71 \pm 3\%$ vs PBS $48 \pm 4\%$, $P < 0.0001$). In functional studies BMMNC injected animals showed increased activation of Akt, inhibition of GSK-3 β , amelioration of p38 MAP kinase phosphorylation and NF- κ B activity compared to control myocardium. Inhibition of PI3K with LY294002 abolished all beneficial effects of BMMNC treatment. Proteomic analysis also demonstrated that BMMNC treatment induced alterations in proteins within known cardioprotective pathways, e.g., heat shock proteins, stress-70 protein as well as the chaperone protein 14-3-3epsilon.

Conclusions - Early BMMNC injection during reperfusion preserves the myocardium, with evidence of reduced apoptosis, necrosis, and activation of survival pathways.

Introduction

Bone marrow mononuclear cells (BMMNCs) are emerging as a therapeutic modality for the treatment of ischaemic heart disease and its sequelae. The majority of animal experiments, forming the foundation for clinical translation of cell therapy, have been conducted after myocardial infarction has been established, i.e., cells were injected more than one hour after reperfusion or whilst the coronary artery remained

APPENDIX 10: continued

occluded[1]. The possibility that cell therapy may have a beneficial outcome if administered near the time of reperfusion, in a model many ways analogous to patients undergoing primary angioplasty (i.e. ischaemia-reperfusion injury - IRI) for acute myocardial infarction, has not been investigated.

BMMNCs have been demonstrated to improve cardiac function and a variety of explanations have been promoted as the cause of induced benefit. A key suggested mechanism of action is transdifferentiation or plasticity, these terms describe the observation that BMMNCs can engraft within ischaemic and non-ischaemic myocardium and modify their cell phenotype to that of cardiac muscle or vascular cells thus improving cardiac function by direct contribution to contractile function and increasing perfusion of cardiac tissue[2].

Others have failed to observe transdifferentiation[3] and subsequent investigators have suggested local release of paracrine factors as the key mechanism of action of transplanted cells. BMMNCs are capable of secreting a wide range of cytokines[4]. The paracrine factors themselves have been shown to induce a number of beneficial effects including induction of angiogenesis in host tissues[1], reducing apoptosis[4], immunomodulation of injury, e.g., benefits of transplantation following myocardial ischaemia have been shown to be dependent on cytokines such as IL-10[5], a further documented paracrine benefit is the stimulation of, the recently described, resident cardiac stem cells[6].

The optimum timing of BMMNC cell injection in acute myocardial infarction has been identified as an unanswered question[7], and currently there is little published data to answer this question.

We speculated that an early time point of injection could optimise benefits: the earlier the offending coronary artery is treated during myocardial infarction the more cardiac tissue is preserved, and the better the outcome[8]. If the stem cells evoke their beneficial effect through paracrine actions, rather than 'de-novo' myogenesis, in acute myocardial infarction, then the biggest opportunity to save muscle would be before completion of infarction. Thus we suggest that the stem cell delivery would ideally be in less than three hours after ischaemia onset, an important threshold observed in thrombolysis trials[8]. This viewpoint is underlined by observations in a rat stroke model that earlier intervention led to greater brain tissue survival and improved functional outcome[9]. Early intervention, ideally in minutes, is also needed to ameliorate ischaemia-reperfusion injury, an important modifiable determinant of infarct size, and an obvious potential target for paracrine factors released by BMMNCs[10].

Our hypothesis was that early injection of BMMNCs would induce a significant benefit after ischaemia-reperfusion injury and that this benefit would be induced by paracrine factors affecting the ischaemia-reperfusion injury pathway. Thus, we

APPENDIX 10: continued

designed a series of experiments to test whether there is an early window of opportunity during which injection of bone marrow derived cells leads to a significant decrease in infarct size, in an animal model of IRI.

Materials and methods

All experiments were performed in accordance with the Guide for the Care and Use of Laboratory Animals published by the US National Institutes of Health (NIH Publication No. 85-23, revised 1996). All studies were performed using male Wistar rats (Charles River, UK) weighing 250-350 g receiving a standard diet and water ad libitum.

1 Experiment Outline

We performed five experimental protocols in parallel, due to the mutually exclusive nature of the outcome measures used in our study (See supplementary Figure 1). The aim of each study was to assess the effect of intravenous delivery of 107 BMMNCs in a rat IRI model. The first two studies were designed to assess changes in infarct size, and effects on apoptosis and necrosis. The third study evaluated cardiac function and myocardial fibrosis after seven days reperfusion. The fourth study evaluated activation of the PI3K/Akt survival pathway including downstream mediators, finally we attempted to quantify proteomic changes (See online supplementary Figure 1 for the experimental designs). We chose 107 BMMNCs as our therapeutic dose since several studies have shown functional benefit at this dose[11,12], in addition a dose response effect has been documented so we tried to take advantage of this[13].

2 Donor bone marrow mononuclear cell preparation

Whole bone marrow was harvested from femurs and tibias of male Wistar rats, BMMNCs were isolated by Percoll (Amersham Biosciences, UK) density gradient centrifugation, as previously described[14]. BMMNCs were characterised by flow cytometry using monoclonal antibodies for c-kit (Santa Cruz, sc-5535, USA), CD34 (Santa Cruz, sc-9095, USA), CD45 (BD, 554875, USA) and CD133 (Santa Cruz, sc-30219, USA). BMMNCs were c-Kit⁺ ($7 \pm 1\%$, $n = 10$), CD34⁺ ($7 \pm 1\%$, $n = 10$), CD45⁺ ($54 \pm 6\%$, $n = 10$), and CD133⁺ ($15 \pm 1\%$, $n = 10$).

3 Measurement of infarct size

Rats were anaesthetised with thiopentone, tracheotomised and ventilated with air oxygen mix (30 %), and subjected to LAD occlusion (25 minutes)[15] and reperfusion (for 30 min, 2 hours or 7 days). Area at risk (AAR) of the left ventricle was demarcated by perfusion with Evans Blue and infarct size was measured by staining the AAR with nitro blue tetrazolium, as previously described[16].

4 Detection of apoptosis and necrosis in cardiac myocytes

Cardiomyocytes (CMCs) from the AAR of the previously ischaemic and reperfused (2 hours) myocardium were isolated and analysed for CMC apoptosis and necrosis by flow cytometry as previously described[17]. Gating of the CMC population was

APPENDIX 10: continued

determined by the degree of binding of troponin-T monoclonal antibody (SC-20025, Santa Cruz, USA). Troponin-T binding in the gated population was $70 \pm 6\%$ ($n = 5$). Annexin 5-FITC/propidium iodide apoptosis detection kit (BD Biosciences Pharmingen, UK) was used to dual stain live AAR CMC isolates. All stained AAR CMC isolate samples were analysed within 1 hour using a flow cytometer (FACScan, Becton Dickinson, UK) with Cell-Quest software (BD, UK). Cardiomyocyte apoptosis was also confirmed using a caspase-9 FLICA assay kit (Sigma-Aldrich, UK).

5 Determination of cardiac function after 7 days reperfusion

Cardiac function was analysed using echocardiography (Vevo-770 imaging system and 23.5MHz probe, Visual Sonics, USA) under anesthetic (1.5% isoflurane) on the day before and 7 days post I/R injury. The percentage fractional area of contraction (%FAC) was assessed with 2-D images at the papillary muscle level. Left ventricle ejection fraction (LVEF) was measured by M-mode. Haemodynamic catheter analysis of LV function was performed (on the same days as above) by inserting a 2 Fr micro tipped pressure transducer (Millar Instruments; SPR-320) through the right carotid artery and advanced into the LV for measurement of ventricular pressure. Left ventricular peak systolic pressure (LVPS), end diastolic pressure (LVEDP), maximal slope of systolic pressure increment (+dP/dt), diastolic decrement (-dP/dt), the relaxation time constant (τ), and heart rate were all analysed using ChartPro software.

6 Determination of LV fibrosis after 7 days reperfusion

Excised hearts were immediately fixed by perfusion (via aortic cannulation) with 4% paraformaldehyde, followed by immersion in 4% paraformaldehyde, on ice for 30 minutes. The hearts were then washed with PBS and incubated in PBS containing 30% sucrose (w/v) at 4°C overnight. The fixed hearts were then cut transversely into three pieces, each of which was embedded in OCT compound (BDH, UK), frozen in liquid nitrogen-cooled isopentane and stored at -80°C. Subsequently, cryosections were stained with 0.1% picosirius red F3B (BDH, UK) for 10 minutes at room temperature. The sections were rinsed 5 times in deionised water and then rinsed for 1 minute in picric alcohol (20 ml absolute alcohol; 70 ml H₂O; 10 ml saturated aqueous picric acid). The sections were then dehydrated through a methanol series and mounted in DPX (VWR, UK). The degree of picosirius red staining was visualized by an all-in-one microscope (Keyence BZ8000, UK).

7 Determination of activation of the PI3K/Akt-signaling pathways by Western blot analysis

Animals were subjected to 25 minutes ischaemia followed by 30 minutes reperfusion and ex vivo hearts were frozen in liquid nitrogen. Cytosolic and nuclear protein homogenates were prepared from the frozen myocardium (AAR only) as described[18]. Protein extracts from the cytosol were analysed for phosphorylation of Akt, GSK-3 β , and p38 MAPK by western blots as previously described[19]. Protein

APPENDIX 10: continued

extracts from both the cytosol and nucleus were analysed for nuclear translocation of p65 NF- κ B, as described[19]. Immunodetection was performed using primary antibodies against mouse anti-phosphorylated AktSer473 mouse, antiphosphorylated p38 MAPK (both from Cell Signaling Biotechnology), rabbit antitotal Akt, rabbit anti-total GSK-3 β , goat anti-phosphorylated GSK-3 β Ser9, and mouse anti-NF- κ B p65 (all from Santa Cruz). Blots were then incubated with specific secondary antibodies conjugated with horseradish peroxidase and developed with an ECL detection system (Amersham). Immunoreactive bands were visualised by autoradiography and band density was evaluated using the Gel Pro®Analyzer 4.5, 2000 software (Media Cybernetics). The proportion of phosphorylated to total protein was normalised to the vehicle treated group. Membranes were then stripped and incubated with β -actin monoclonal antibody and subsequently with anti-mouse antibody to assess gel-loading homogeneity.

8 Analysis of the cardiac proteome after LAD-occlusion and reperfusion (6 hours)

We assessed changes in the cardiac proteome by two-dimensional gel electrophoresis (2-DE) coupled with electro-spray ionization (ESI) mass spectrometry (MS) to identify differentially expressed protein spots in myocardial samples from sham operated animals plus PBS, ischaemia/reperfusion (25min/6h) plus PBS, and from ischaemia/reperfusion (25min/6h) plus BMMNC (n=3, for all groups). Protein homogenates were individually prepared for each rat from 80–140 mg of ground frozen myocardium (AAR only) using 1 ml lysis buffer per 100 ug tissue (9.5M Urea, 4% CHAPS, 1% DTT, complete protease inhibitor [Roche, UK], Phosphatase inhibitor cocktail [Sigma]). Protein concentration of homogenates was quantified by Bio-Rad protein assay (Bio-Rad). Duplicate 2D gels were produced for each sample using 200 ug total protein separated on 18 cm non-linear (NL) pH4-7 immobilised pH gradient (IPG) strips (GE-Healthcare Lifesciences, UK). Large format, homogenous, 12% SDS PAGE gels were used for second dimension separation and then stained using the plus one silver staining kit (GE-Healthcare Lifesciences, UK). Images were scanned and analyzed using PDQuest software (BioRad, UK). Spot intensity values were 'normalised' using 'total density in gel' method. Fold changes and unpaired Mann-Whitney p-values were calculated for 'SHAM vs. PBS' and 'PBS vs. BMMNC' comparisons. Over a hundred spots had significant > 2.5 fold differences ($p \leq 0.05$) in either or both of the comparisons, and were selected for trypsin digestion, peptide extraction, and protein identification using LC-MS/MS, Q-ToF Micro (Micromass, UK). The resultant peak list data (PKL file) was then used to search the SwissProt database using the MASCOT (Matrix Science) online server for a match. Only peptides with scores over 45 were considered to be significant, the MASCOT scores were calculated from these.

9 Validation of proteomic data

Twenty ug of protein homogenate was electrophoresed in duplicate on 10% Bis-tris gels (Invitrogen, UK) and transferred to PVDF membranes (GE Healthcare

APPENDIX 10: continued

Lifesciences, UK), and subsequently blocked in Tris buffered saline containing 0.05% Tween-20 (TBS-Tween) with 3% non-fat dry milk at 4°C overnight. Blots were probed with either anti-14-3-3ε or anti-SDHA antibodies (Abcam, UK). Loading was verified by probing the duplicate gel with anti-GAPDH antibodies (Abcam, UK) for each experiment. Blots were incubated with the appropriate secondary antibody (Santa Cruz Biotechnology, USA). Chemiluminescence was detected using ECL reagents (GE Healthcare, UK). Bands were detected and quantified using TotalLab v1.1 (Phoretix, UK), and volumes were normalised to the GAPDH volumes for the duplicate gels.

10 Statistical Analyses

GraphPad Prism 5 statistics package was used to analyse the results. Data for physiological variables are expressed as means ± standard error, and analysed by one way ANOVA followed by Dunnet's post hoc test for multiple comparisons. For western blots, a one-way ANOVA followed by Bonferroni's post hoc test for multiple comparisons was used. For 2-DE data a two-tailed unpaired Mann-Whitney P-value <0.05 was considered to be statistically significant.

Results

1 Intravenous administration of BMMNCs upon reperfusion reduces infarct size
Intravenous jugular administration of 10 million BMMNCs, in 0.5 ml PBS, immediately upon reperfusion to animals subjected to ischaemia then reperfusion for 2 hours resulted in a 42% reduction in infarct size (Figure 1). There was no significant difference in the percentage of left ventricle at risk for the BMMNC group compared to the PBS control group (50.85 vs 49.65% respectively, $P=0.68$). From experiments not shown here, we quantified donor cells within the rat hearts using a cell tracker dye, CFDA SE, we estimate that <1% of the injected cells remained in the heart two hours following injection. We next demonstrated that administration of BMMNCs, at the beginning of a 7 days reperfusion period, reduced IRI-induced infarct size and fibrosis, i.e., cardiac scar formation. These findings were associated with prevention of impairment in systolic and diastolic LV function measured by echocardiography and haemodynamic catheterization. Improvements in systolic function by BMMNC therapy were demonstrated by significantly higher values for LVEF (BMMNC $71 \pm 3\%$ vs. PBS $48 \pm 4\%$, $n=11$, $P < 0.0001$); FAC (BMMNC $47 \pm 2\%$ vs. PBS $36 \pm 3\%$, $n=11$, $P < 0.01$); dP/dtmax (BMMNC $10 \times 10^3 \text{ mmHg-s}^{-1} \pm 0.4\%$ vs. PBS $8 \times 10^3 \text{ mmHg-s}^{-1} \pm 1\%$ $n=7$, $P < 0.05$); and Contractility Index (BMMNC 162 ± 10 vs. PBS 113 ± 3 , $n=7$, $P < 0.001$). Similarly, improvements in diastolic function by BMMNC-therapy were demonstrated by lower values for LVEDP (BMMNC $4 \pm 1 \text{ mmHg}$ vs. PBS $16 \pm 3 \text{ mmHg}$, $n=7$, $P < 0.01$); dP/dtmin (BMMNC $-9 \times 10^3 \pm 0.5 \text{ mmHg-s}^{-1}$ vs. PBS $-7 \times 10^3 \pm 1 \text{ mmHg-s}^{-1}$, $n=7$, $P < 0.01$); and Tau (BMMNC $12 \times 10^{-3} \pm 0.5$ vs. PBS $10 \times 10^{-3} \pm 1$, $n=7$, $P = 0.075$)(Figures 1b-i).

APPENDIX 10: continued

2 Apoptosis and Necrosis

A significant decrease in the number of necrotic myocytes was seen when BMMNCs were injected immediately upon reperfusion (n=5 all groups, $6.1 \pm 1.1\%$ in shams vs $16.3 \pm 1.3\%$ myocyte necrosis in control vs $4.9 \pm 1\%$ myocyte necrosis in BMMNC treated animals, $P < 0.01$). Similarly, injection of BMMNCs immediately after ischaemia significantly reduced the proportion of cells undergoing apoptosis (n=5 all groups, $7.8 \pm 0.5\%$ in shams, $27.7 \pm 3.2\%$ in vehicle controls, and $13.9 \pm 3.4\%$ in BMMNC group, $P < 0.05$, Figure 2). This observation was confirmed by measurement of caspase 9 expression, the percentage of cells isolated from the area at risk expressing caspase 9 was measured and found to be significantly reduced in cell treated compared to vehicle treated animals (BMMNCs $12.7 \pm 2.6\%$ vs PBS $30.6 \pm 4.2\%$, n=5, $P < 0.01$).

3 The reduction in infarct size caused by BMMNC is associated with activation of PI3K/Akt survival pathway

The cardioprotective effect of BMMNCs was associated with the increased expression of the pro-survival PI3K/Akt signalling pathway. BMMNCs resulted in a significant increase, in phosphorylation of serine-473Akt and serine-9GSK-3 β (Figure 3) which was abolished by the pre-treatment of animals with the PI3-K inhibitor LY294002 (0.3mg/ kg i.v.), indicating that the activation of Akt (and the subsequent inhibition of GSK-3 β) were secondary to the activation of PI3K. Furthermore, BMMNCs resulted in a significant reduction in the phosphorylation of p38-MAPK and nuclear translocation of NF- κ B, and both effects were attenuated by the PI3K inhibitor (0.3mg/kg i.v.).

4 The cardioprotection afforded by BMMNCs is associated with a reversal in metabolism and mitochondrial protein disturbances

We next investigated changes in the cardiac proteome of hearts that had been subjected to IRI by comparing the Sham operated group to PBS, and then we investigated the proteomic alterations attributable to BMMNC application by comparing the PBS group to the BMMNC group in the hope this would elucidate pro survival mechanisms afforded by the treatment. The proteins identified from spots found to be significantly altered are detailed in Table 1. Fold changes and p-values of these proteins are shown in Table 2 along with the observed and theoretical Mr and pI. The proteins identified as being altered by IRI were involved in mitochondrial respiration, stress, cellular energy metabolism, and sarcomeric/cytoskeletal structure and function. Disturbances in mitochondrial oxidative phosphorylation components (complex I and complex III and ATP synthase) were observed in IRI suggesting mitochondrial dysfunction. Several stress responsive proteins were also altered in IRI: stress-70 protein (Hspa9), and the cytoplasmic antioxidant Peroxiredoxin-6 were both affected by IRI. The expression levels of several energy metabolism enzymes were also disturbed, possibly reflecting a switch in substrate preference[20]. Galectin-5, a beta-galactoside-binding lectin, was up-regulated from undetectable levels in the PBS myocardial samples compared to Sham. Many of these alterations were largely reversed when the BMMNC group was compared to PBS, such that levels were

APPENDIX 10: continued

similar to that seen in the Sham group. For example, the spots identified as NADH-ubiquinone oxidoreductase 75kDa subunit, and cytochrome b-c1 subunit 6 which had -10 and 6 fold changes respectively in the Sham vs. PBS comparison were seen to have 7 and -10 fold changes respectively in PBS vs. BMMNC. Fragments of ATP synthase subunit beta, identified in 16 different spots, all showed down-regulation in Sham vs. PBS, possibly reflecting enhanced protein degradation in IRI, and up-regulation in PBS vs. BMMNC, four of these had significant alteration in both comparisons showing similar degree of expression change (-13, -6, -3 and -2 fold decrease in Sham vs. PBS; 13, 9, 3 and 3 fold increase in PBS vs. BMMNC). IRI related expression changes were also 'corrected' for Enoyl CoA hydratase and lactate dehydrogenase, hinting at a reversal of the IRI related substrate switch. We also observed a 12-fold up-regulation in the chaperone protein 14-3-3epsilon in the BMMNC group compared to PBS. The expression of two proteins (Shda and 14-3-3 epsilon) were validated by Western blot (see Figure 4).

Discussion

We have discovered that the intravenous systemic administration of BMMNCs (10 million: c-Kit+, CD34+, CD45+, CD133+) at the beginning of reperfusion, in a myocardial ischaemia-reperfusion injury model (25 minutes ischaemia, 2 hours reperfusion), results in a significant reduction in myocardial infarct size, and reduces the number of cardiomyocytes undergoing apoptosis within the area subjected to IRI. The cardioprotection induced by BMMNCs was not transient, but remained evident when hearts were subjected to regional myocardial ischaemia and treated with BMMNCs upon reperfusion, followed by 7 days of reperfusion. Under these experimental conditions, BMMNCs reduced the development of a scar tissue (reduction of necrosis and intra-mural fibrosis assessed by histology) and prevented the development of a significant systolic and diastolic cardiac dysfunction, which was seen in control animals. Notably, the cardioprotection afforded by BMMNCs was similar to that afforded by ischaemic preconditioning, a known gold standard for the experimental reduction of myocardial infarct size[21]. The cardioprotective effect of preconditioning is induced by pro-survival kinases such as PI3K-Akt and MEK1/Erk1/2, these protective kinases are collectively termed the reperfusion injury salvage kinase pathway (RISK).

Activation of the RISK pathway at the time of myocardial reperfusion can confer powerful infarct size reduction. A diverse range of activating mechanisms have been demonstrated, these include growth factors[22], many of which have been shown to be released by stem cells, for example VEGF and FGF[23]. The cardioprotective actions of RISK pathway activation remain to be completely resolved, but leading suggestions with experimental evidence include inhibition of the mitochondrial permeability transition pore (mPTP), activation of anti-apoptotic mechanisms including inhibition of pro-apoptotic factors, e.g., BAD and BAX, and facilitation of calcium uptake into the sarcoplasmic reticulum ameliorating calcium triggered mPTP opening[24].

APPENDIX 10: continued

We next investigated possible mechanisms for our observations. The small quantity of cell engraftment two hours after injection, <1%, (measured in experiments not shown here), combined with the speed of the cardioprotective effect of BMMNC administration, coupled to the finding that BMMNCs can secrete mediators of the RISK pathway suggested to us that the observed cardioprotective effects could be due to activation of the RISK pathway. Various mediators of reperfusion injury — oxidative stress, changes in pH, inflammation, intracellular calcium levels, and the mitochondrial permeability transition pore are all possible targets for interaction with BMMNCs injected at the time of reperfusion. As BMMNCs have already been shown to exhibit release of paracrine factors and expression of cardioprotective genes that may act beneficially on the RISK pathway we chose to investigate this possibility preferentially over other hypotheses[4]. Specific growth factors released by BMMNCs that have been shown to be cardioprotective include vascular endothelial growth factor (VEGF), hepatocyte growth factor (HGF), fibroblast growth factor (FGF), insulin-like growth factor 1 (IGF-1), and transforming growth factor (TGF) [23].

A number of our observations support the hypothesis that paracrine growth factors secreted by BMMNCs contribute to the cardioprotective effects of BMMNCs observed here. This hypothesis is supported by the following findings, administration of BMMNCs upon reperfusion was associated with activation of the PI3K/Akt phosphorylation survival kinase pathway, and when PI3K activity was inhibited, with LY294002, the cardioprotective effect seen with injection of BMMNCs was negated, highlighting the key importance of the activation of the PI3K/ Akt pro-survival pathway in the observed beneficial effects. The increase in Ser-473Akt phosphorylation also resulted in the inhibition of GSK3 β , suppression of which has been documented to reduce infarct size and to cause pronounced anti inflammatory effects[25], which are, at least in part, due to prevention of the activation of NF- κ B24. The findings that the inhibition of activation of PI3K with LY294002 abolished all of the above effects of BMMNCs on cell signaling as well as their cardioprotective effects supports the view that the cardioprotective effects of BMMNC may be secondary to activation of the PI3K/Akt survival pathway. In order to further investigate the down stream molecular mechanisms associated with PI3K/Akt signaling we analysed changes in the global proteome of hearts subjected to IRI and treated upon reperfusion with BMMNCs. Within the proteomic dataset, many of the protein alterations measured in the BMMNC group compared to PBS control seem likely to be secondary to the reduced cell death associated with treatment, however, several proteins with a possible mechanistic role in cardioprotection were identified in the BMMNC treated group. Two significant proteins were the heat shock protein stress-70 protein (aka HSPA9 or HSP70), which has also been shown to be up-regulated in cardioprotection as afforded by hydrogen sulphide[26], and the chaperone protein 14-3-3epsilon which is known to have pro-survival functions including its ability to bind and inhibit the Bcl-2 related protein

APPENDIX 10: continued

Bad in its phosphorylated conformation[27]. Bad phosphorylation is thought to be one of the many downstream actions of the PI3K/Akt pathway [28].

In conclusion, a single dose of systemic intravenous BMMNCs upon reperfusion reduces infarct size and cardiac dysfunction caused by regional myocardial ischaemia and reperfusion. This reduction in infarct size was associated with activation of the PI3K/Akt survival pathway. Furthermore, BMMNC treatment induced alterations in protein expression consistent with known cardioprotective pathways. Results from clinical BMMNC trials suggest positive effects on cardiac function when cells are administered 5 days after successful reperfusion of myocardial infarction[29]. However, in another study when cells were injected at a time closer to the point of successful reperfusion (24 hours) no beneficial effect was seen[30]. The data presented in this paper suggests that there may be a very early window of opportunity (i.e., less than 24 hours following reperfusion) that exists for bone marrow derived cell therapy to prevent myocardial necrosis, and that this time point should be considered when designing future clinical trials. In addition, it appears that the cardioprotective benefit shown here is too rapid to be related to stem cell plasticity and may be attributable to activation of the RISK pathway. This raises the possibility of unearthing one or more molecules that could be administered 'in lieu' of BMMNCs to achieve similar protection, thus avoiding the need for cell collection and any potential harmful effects that may manifest as a consequence of cell injection.

Figure Legends

Figure 1: (A) Infarct size was measured in animals subjected to 25 minutes regional myocardial ischaemia followed by 2 hours reperfusion (I/R2h) treated with phosphate buffered saline (PBS), bone marrow mononuclear cells (BMMNCs) or ischaemic preconditioning (IPC), sham animals received a thoracotomy only and were not rendered ischaemic. The area at risk (AAR) was expressed as a % of the left ventricle (LV) and the infarct size was expressed as a % of the AAR. (B-H) Cardiac function was analysed by echocardiography and LV hemodynamic catheterisation in animals subjected to 25 minutes LAD occlusion followed by 7 days reperfusion (I/R7D). When compared to vehicle, administration of BMMNCs upon reperfusion prevented systolic and diastolic dysfunction. (I) Myocardial fibrosis in hearts subjected to (I/R7D) was assessed by picrosirius red staining of myocardial cryosections. When compared with PBS, administration of BMMNC dramatically attenuated the degree of post I/R fibrosis. Statistical significance was determined by ANOVA followed by Dunnett's post hoc test * P < 0.05, ** P < 0.01.

Figure 2: BMMNC treatment significantly reduced apoptosis, necrosis and caspase 9 activation compared to controls. The area at risk (AAR) of rat myocardium, following LAD ischaemia for 25 minutes then reperfusion for 2 hours, was isolated from animals in sham, vehicle, and BMMNC treated groups. The cardiomyocyte (CMC) fraction, for all groups, was then assessed for: (A) Necrosis (B) Apoptosis (C)

APPENDIX 10: continued

Caspase 9 activation. Statistical significance was determined by ANOVA followed by Dunnett's post hoc test * $P < 0.05$, ** $P < 0.01$.

Figure 3: (A) Infarct size was measured in animals subjected to 25 minutes regional myocardial ischemia followed by 2 hours reperfusion (I/R2h) or sham animals. The area at risk (AAR) was expressed as a % of the left ventricle (LV) and the infarct size was expressed as a % of the AAR. When compared with PBS, pre-treatment with the LY294002 (0.3mg/kg IV) abolished the attenuation of infarct size caused by the systemic intravenous injection of 10 million BMMNC upon reperfusion in I/R2h (B-E). Western blots demonstrating that systemic intravenous injection of 10 million BMMNC upon reperfusion significantly augmented the phosphorylation of Aktserine-473 and GSK-3 β serine-9, reduced the phosphorylation of p38-mitogen activated protein kinase (MAPK) and the nuclear translocation of NF- κ B. The PI3-K inhibitor LY294002 abolished all of these effects of BMMNCs. Statistical significance was determined by ANOVA followed by Dunnett's post hoc test * $P < 0.05$, ** $P < 0.01$.

Figure 4: A Western blot of expression levels of 14-3-3 epsilon with the normalized volumes shown in panel B. C shows western blot of expression levels of succinate dehydrogenase with the normalised volumes shown in D. Figure B and D show average normalised volumes and standard deviations, lines with stars indicate significance as calculated by one-way ANOVA followed by Bonferroni's post hoc test for multiple comparisons.

Table Legends

Table 1: Spots with significant fold changes for which a single protein ID was found. SSP are spot identification numbers assigned by PDQuest software. Mascot details are as follows; mascot score (the sum of the peptide scores), the number of peptides found and the sequence coverage of these peptides (only including peptides with individual scores over 35). Theoretical Mr and PI values for the protein identified are shown as well as the observed Mr and PI of the spot as estimated from its position in the gel.

Table 2: Proteins identified from spots that had significant fold changes in either the Sham vs. PBS or the PBS vs. BMMNC comparisons. Average spot volumes and standard deviations for each group are shown alongside fold changes and p-values (unpaired, 2 tailed, Mann-Whitney). 'On' and 'Off' in the FC column indicate changes to presence or absence in spots, e.g, in spot 1206 'On' indicates the spot was absent in Sham but present in PBS.

References

[1] Kocher, AA, Schuster, MD, Szabolcs, MJ et al., Neovascularization of ischemic myocardium by human bone-marrow-derived angioblasts prevents cardiomyocyte apoptosis, reduces remodeling and improves cardiac function. *Nat Med* 2001;7(4):430-6.

APPENDIX 10: continued

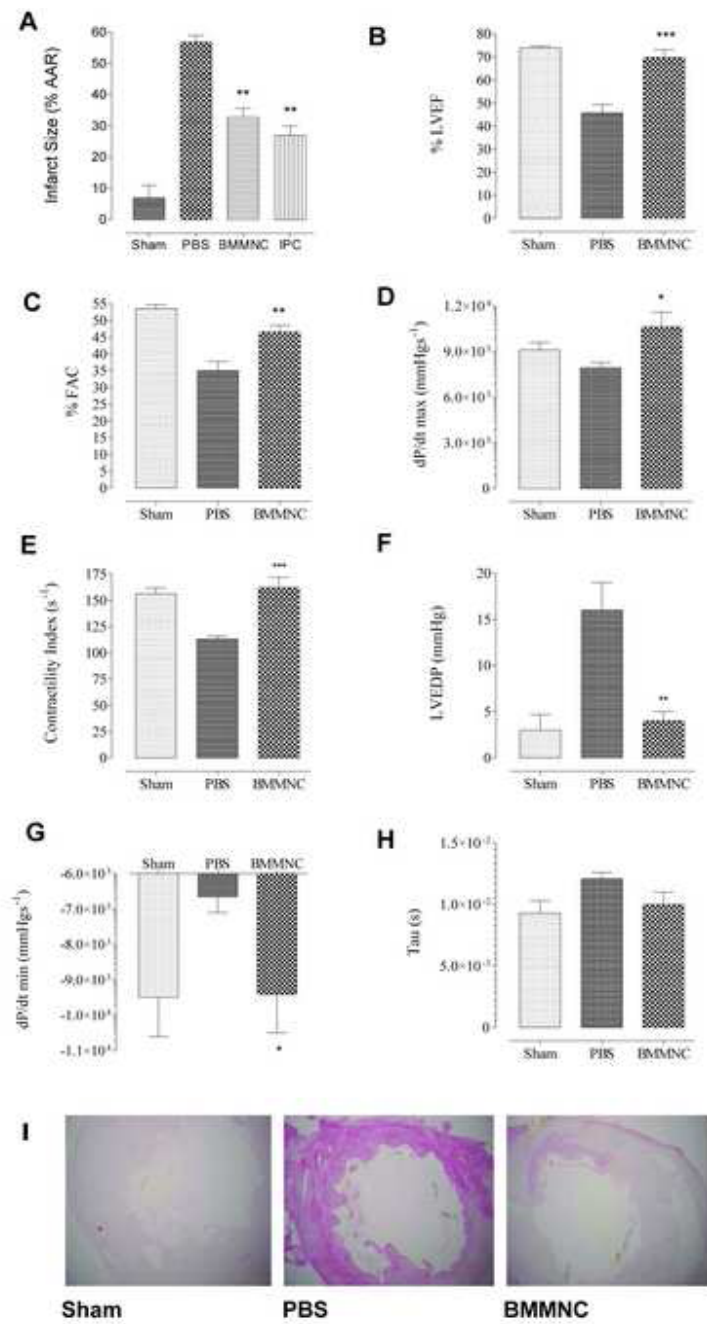
- [2] Rota, M, Kajstura, J, Hosoda, T et al., Bone marrow cells adopt the cardiomyogenic fate in vivo. *Proc Natl Acad Sci U S A* 2007;104(45):17783–8.
- [3] Balsam, LB, Wagers, AJ, Christensen, JL et al., Haematopoietic stem cells adopt mature haematopoietic fates in ischaemic myocardium. *Nature* 2004;428(6983):668–73.
- [4] Xu, M, Uemura, R, Dai, Y et al., In vitro and in vivo effects of bone marrow stem cells on cardiac structure and function. *J Mol Cell Cardiol* 2007;42(2):441–8.
- [5] Burchfield, JS, Iwasaki, M, Koyanagi, M et al., Interleukin-10 from transplanted bone marrow mononuclear cells contributes to cardiac protection after myocardial infarction. *Circ Res* 2008;103(2):203–11.
- [6] Rota, M, Padin-Iruegas, ME, Misao, Y et al., Local activation or implantation of cardiac progenitor cells rescues scarred infarcted myocardium improving cardiac function. *Circ Res* 2008;103(1):107–16.
- [7] Dimmeler, S, Zeiher, AM, Cell therapy of acute myocardial infarction: open questions. *Cardiology* 2009;113(3):155–60.
- [8] Boersma, E, Maas, AC, Deckers, JW et al., Early thrombolytic treatment in acute myocardial infarction: reappraisal of the golden hour. *Lancet* 1996;348(9030):771–5.
- [9] Iihoshi, S, Honmou, O, Houkin, K et al., A therapeutic window for intravenous administration of autologous bone marrow after cerebral ischemia in adult rats. *Brain Res* 2004;1007(1-2):1–9.
- [10] Rodríguez-Sinovas, A, Abdallah, Y, Piper, H et al., Reperfusion injury as a therapeutic challenge in patients with acute myocardial infarction. *Heart Fail Rev* 2007;12(3-4):207–16.
- [11] Tse, HF, Kwong, YL, Chan, JK et al., Angiogenesis in ischaemic myocardium by intramyocardial autologous bone marrow mononuclear cell implantation. *Lancet* 2003;361(9351):47–9.
- [12] Hamano, K, Li, TS, Kobayashi, T et al., Therapeutic angiogenesis induced by local autologous bone marrow cell implantation. *Ann Thorac Surg* 2002;73(4):1210–5.
- [13] Schuster, MD, Kocher, AA, Seki, T et al., Myocardial neovascularization by bone marrow angioblasts results in cardiomyocyte regeneration. *Am J Physiol Heart Circ Physiol* 2004;287(2):H525–32.
- [14] Kamihata, H, Matsubara, H, Nishiue, T et al., Implantation of bone marrow mononuclear cells into ischemic myocardium enhances collateral perfusion and regional function via side supply of angioblasts, angiogenic ligands, and cytokines. *Circulation* 2001;104(9):1046–52.
- [15] Wayman, NS, Hattori, Y, McDonald, MC et al., Ligands of the peroxisome proliferator-activated receptors (PPAR-gamma and PPAR-alpha) reduce myocardial infarct size. *Faseb J* 2002;16(9):1027–40.
- [16] Thiernemann, C, Bowes, J, Myint, FP et al., Inhibition of the activity of poly(ADP ribose) synthetase reduces ischemia-reperfusion injury in the heart and skeletal muscle. *Proc Natl Acad Sci U S A* 1997;94(2):679–83.

APPENDIX 10: continued

- [17] Sivarajah, A, Collino, M, Yasin, M et al., Anti-apoptotic and anti-inflammatory effects of hydrogen sulfide in a rat model of regional myocardial I/R. *Shock* 2009;31(3):267–74.
- [18] Meldrum, DR, Shenkar, R, Sheridan, BC et al., Hemorrhage activates myocardial NFkappaB and increases TNF-alpha in the heart. *J Mol Cell Cardiol* 1997;29(10):2849–54.
- [19] Collino, M, Aragno, M, Mastrocola, R et al., Oxidative stress and inflammatory response evoked by transient cerebral ischemia/reperfusion: effects of the PPARalpha agonist WY14643. *Free Radic Biol Med* 2006;41(4):579–89.
- [20] Stanley, WC, Sabbah, HN, Metabolic therapy for ischemic heart disease: the rationale for inhibition of fatty acid oxidation. *Heart Fail Rev* 2005;10(4):275–9.
- [21] Murry, CE, Jennings, RB, Reimer, KA, Preconditioning with ischemia: a delay of lethal cell injury in ischemic myocardium. *Circulation* 1986;74(5):1124–36.
- [22] Hausenloy, DJ, Yellon, DM, Reperfusion injury salvage kinase signalling: taking a RISK for cardioprotection. *Heart Fail Rev* 2007;12(3-4):217–34.
- [23] Kinnaird, T, Stabile, E, Burnett, MS et al., Bone-marrow-derived cells for enhancing collateral development: mechanisms, animal data, and initial clinical experiences. *Circ Res* 2004;95(4):354–63.
- [24] Hausenloy, DJ, Yellon, DM, Cardioprotective growth factors. *Cardiovasc Res* 2009;83(2):179–94.
- [25] Tong, H, Imahashi, K, Steenbergen, C et al., Phosphorylation of glycogen synthase kinase-3beta during preconditioning through a phosphatidylinositol-3-kinase-- dependent pathway is cardioprotective. *Circ Res* 2002;90(4):377–9.
- [26] Calvert, JW, Jha, S, Gundewar, S et al., Hydrogen sulfide mediates cardioprotection through Nrf2 signaling. *Circ Res* 2009;105(4):365–74.
- [27] Masters, SC, Yang, H, Datta, SR et al., 14-3-3 inhibits Bad-induced cell death through interaction with serine-136. *Mol Pharmacol* 2001;60(6):1325–31.
- [28] Datta, SR, Dudek, H, Tao, X et al., Akt phosphorylation of BAD couples survival signals to the cell-intrinsic death machinery. *Cell* 1997;91(2):231–41.
- [29] Schachinger, V, Erbs, S, Elsasser, A et al., Intracoronary bone marrow-derived progenitor cells in acute myocardial infarction. *N Engl J Med* 2006;355(12):1210–21.
- [30] Janssens, S, Dubois, C, Bogaert, J et al., Autologous bone marrow-derived stemcell transfer in patients with ST-segment elevation myocardial infarction: doubleblind, randomised controlled trial. *Lancet* 2006;367(9505):113–21.

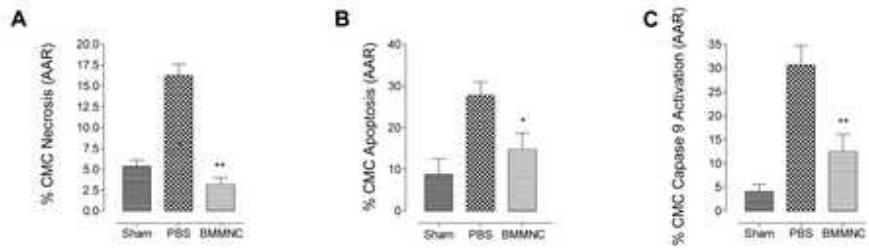
APPENDIX 10: continued

Figure 1



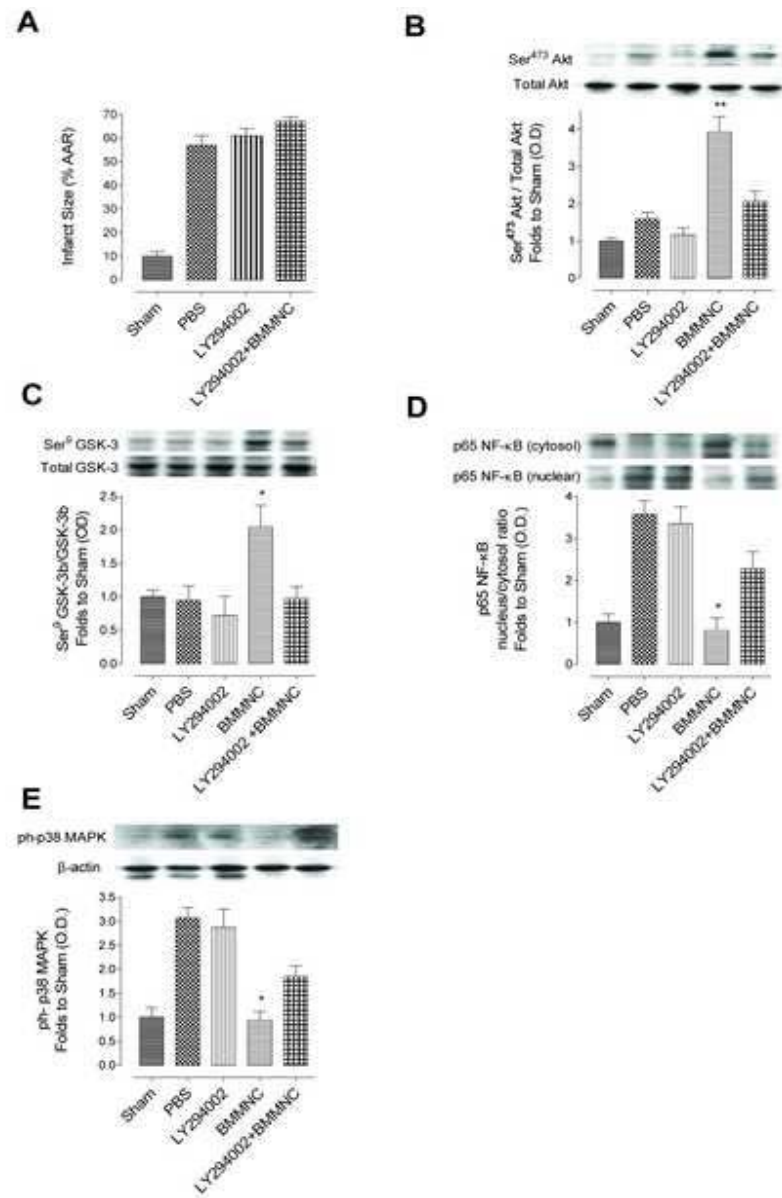
APPENDIX 10: continued

Figure 2



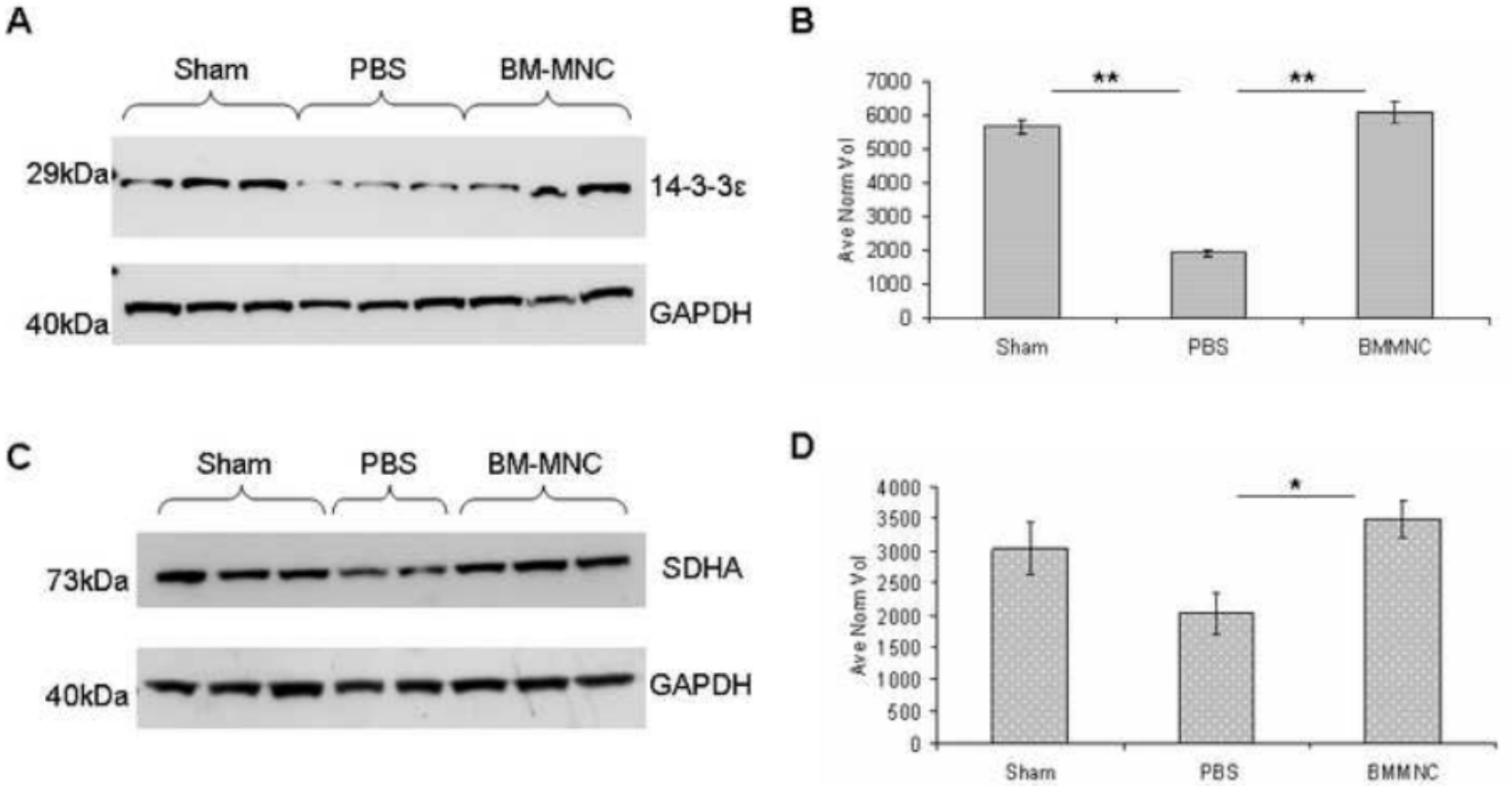
APPENDIX 10: continued

Figure 3



APPENDIX 10: continued

Figure 4



APPENDIX 10: continued

Table 1

SSP	Observed		Theoretical		Protein name	UniProtKB/ Swiss-Prot Accession	Mascot		
	Mr	PI	Mr	PI			Score	pep's	% sc
1430	34500	4.40	29155	4.63	14-3-3 protein epsilon	P62260	164	3	20
2616	47500	4.80	32803	4.80	40S ribosomal protein SA	P38983	50	1	4
2546	45000	4.80	51556	7.16	Adenylyl cyclase-associated protein 1	Q08163	55	1	4
3209	20000	5.00	56318	5.19	ATP synthase subunit beta	P10719	144	2	5
1225	21000	4.50	56318	5.19	ATP synthase subunit beta	P10719	192	2	7
3208	22000	5.00	56318	5.19	ATP synthase subunit beta	P10719	51	1	4
4235	24000	5.40	56318	5.19	ATP synthase subunit beta	P10719	110	2	4
4329	29000	5.40	56318	5.19	ATP synthase subunit beta	P10719	69	1	2
1424	34000	4.60	56318	5.19	ATP synthase subunit beta	P10719	131	2	8
3433	34000	5.00	56318	5.19	ATP synthase subunit beta	P10719	436	6	18
2443	35000	4.80	56318	3.00	ATP synthase subunit beta	P10719	91	1	3
3523	40000	5.20	56318	5.19	ATP synthase subunit beta	P10719	280	4	14
3632	47000	5.20	56318	5.19	ATP synthase subunit beta	P10719	314	5	16
2609	47500	4.80	56318	5.19	ATP synthase subunit beta	P10719	457	6	12
2626	52500	4.90	56318	5.19	ATP synthase subunit beta	P10719	167	3	8
3626	54500	5.20	56318	5.19	ATP synthase subunit beta	P10719	711	9	29
3636	57000	5.10	56318	5.19	ATP synthase subunit beta	P10719	226	5	15
3706	57000	5.10	56318	5.19	ATP synthase subunit beta	P10719	215	3	9
2712	57500	4.90	56318	5.19	ATP synthase subunit beta	P10719	707	8	26
2119	14500	4.80	10417	4.90	Cytochrome b-c1 complex subunit 6	Q5M9I5	131	1	20
3627	57000	5.20	53424	5.21	Desmin	P48675	463	7	20
7722	62000	6.60	67123	8.76	Dihydrolipoyllysine-residue acetyltransferase component of pyruvate dehydrogenase complex	P08461	228	4	9
7323	31500	6.60	31496	8.39	Enoyl-CoA hydratase	P14604	71	1	3
7110	16000	6.30	16186	6.17	Galectin-5	P47967	157	3	21
7702	70000	6.40	58307	5.85	Hydroxysteroid dehydrogenase-like protein 2	Q4V8F9	75	2	4
6425	37000	6.20	36589	5.70	L-lactate dehydrogenase B chain	P42123	77	1	6
4521	37000	5.40	36589	5.70	L-lactate dehydrogenase B chain (or LDHA)	P42123	72	1	3
8853	67500	6.70	79293	7.70	Methylcrotonoyl-CoA carboxylase subunit alpha, mitochondrial (mouse)	Q5I0C3	166	3	6
3305	25000	5.00	22142	5.03	Myosin light chain 3	P16409	334	5	33
1206	17500	4.40	18868	4.86	Myosin regulatory light chain 2	P08733	57	1	8
1213	17500	4.40	18868	4.86	Myosin regulatory light chain 2	P08733	108	2	16
3228	15000	5.20	18868	4.86	Myosin regulatory light chain 2	P08733	135	3	20
4207	19000	5.40	223370	5.59	Myosin-6	P02563	279	4	3
1207	19000	4.40	113780	8.4	NAD(P) transhydrogenase	Q61941	58	1	2
7112	17000	6.50	79362	5.65	NADH-ubiquinone oxidoreductase 75 kDa	Q66HF1	102	2	2
5408	32000	5.80	24803	5.64	Peroxisome protein 6	O35244	388	7	44
3518	42500	5.10	73812	5.97	Stress-70 protein (aka HSPA9)	P48721	85	1	2
4702	60000	5.20	73812	5.97	Stress-70 protein (aka HSPA9)	P48721	739	10	21
7723	67500	6.60	71570	6.75	Succinate dehydrogenase [ubiquinone] flavoprotein subunit, mitochondrial	Q920L2	73	1	2
1320	29000	4.50	32661	4.69	Tropomyosin alpha-1 chain (or Tropomyosin beta chain)	P04692	58	1	4
1248	25000	4.50	35709	4.95	Troponin T, cardiac muscle	P50753	59	1	3
4523	43000	5.60	49892	4.95	Tubulin alpha-4A chain	Q5XIF6	191	3	11
8710	67000	6.60	66140	6.15	WD repeat-containing protein 1	Q5RKI0	157	4	11

APPENDIX 10: continued

Table 2

SSP	Protein name	Sham		PBS		BMMNC		SHAM vs. PBS		PBS vs. BMMNC	
		Average	StDev	Average	StDev	Average	StDev	FC	p-value	FC	p-value
Mitochondrial/Oxidative Phosphorylation											
4329	ATP synthase subunit beta	110.16	35.61	19.83	23.57	106.70	92.44	-5.6	0.0095	5.4	ns
1225	ATP synthase subunit beta	291.53	151.54	22.25	23.86	283.33	231.65	-13.10	0.0238	12.7	0.0476
3636	ATP synthase subunit beta	271.00	120.04	47.25	52.81	411.01	114.47	-5.7	0.0190	8.7	0.0095
3433	ATP synthase subunit beta	924.75	333.91	357.85	251.86	1052.96	350.05	-2.6	0.0022	2.9	0.0087
2609	ATP synthase subunit beta	621.15	297.10	311.42	168.21	781.41	136.07	-2.0	ns	2.5	0.0022
3523	ATP synthase subunit beta	468.32	318.28	244.35	136.88	670.89	119.11	-1.9	ns	2.7	0.0022
1424	ATP synthase subunit beta	394.95	298.27	272.46	165.49	776.50	227.39	-1.5	ns	2.8	0.0022
3632	ATP synthase subunit beta	130.97	81.35	76.08	59.83	218.44	101.06	-1.7	ns	2.9	0.0152
3626	ATP synthase subunit beta	846.73	155.91	386.66	214.61	1178.68	396.37	-2.2	0.0043	3.0	0.0022
2712	ATP synthase subunit beta	708.74	441.93	292.35	251.10	955.57	597.67	-2.4	ns	3.3	0.0260
2443	ATP synthase subunit beta	652.00	498.23	177.28	268.43	639.85	170.64	-3.7	ns	3.6	0.0152
2626	ATP synthase subunit beta	91.75	60.28	90.81	52.64	334.31	223.37	-1.0	ns	3.7	0.0303
3208	ATP synthase subunit beta	248.58	168.64	133.85	129.33	511.89	119.33	-1.9	ns	3.8	0.0043
3706	ATP synthase subunit beta	368.77	159.79	172.42	95.57	776.99	334.44	-2.1	ns	4.5	0.0095
3209	ATP synthase subunit beta	261.67	224.65	101.93	124.18	470.32	252.87	-2.6	ns	4.6	0.0260
4235	ATP synthase subunit beta	70.55	65.79	21.61	12.18	176.25	102.63	-3.3	ns	8.2	0.0238
2119	Cytochrome b-c1 complex subunit 6	330.30	406.92	1901.07	1217.20	185.77	128.67	5.8	0.0303	-10.2	0.0087
7112	NADH-ubiquinone oxidoreductase 75 kDa subunit	156.83	102.34	16.00	10.00	113.15	111.86	-9.8	0.0022	7.1	0.0260
1207	NAD(P) transhydrogenase	384.6	636.9	1474.3	808.7	1325.4	851.1	3.83	0.026	-1.1	ns
7723	Succinate dehydrogenase [ubiquinone] flavoprotein subunit	314.78	202.61	115.62	63.81	282.54	143.14	-2.7	ns	2.4	0.0260
Energy Metabolism											
7722	Dihydrolipoylysine-residue acetyltransferase component of pyruvate dehydrogenase complex	39.01	24.22	225.82	164.74	45.42	22.77	5.8	0.0411	-5.0	ns
7323	Enoyl-CoA hydratase	696.98	400.62	1634.53	371.06	639.89	608.94	2.4	0.0022	-2.6	0.0152
6425	L-lactate dehydrogenase B chain	426.25	148.40	69.00	82.66	385.72	480.03	-6.2	0.0087	5.6	0.0303
4521	L-lactate dehydrogenase B chain (or LDHA)	700.40	749.67	252.34	315.77	676.73	160.45	-2.8	ns	2.7	0.0317
8853	Methylcrotonoyl-CoA carboxylase subunit alpha (mouse)	320.41	221.74	120.29	80.60	403.40	239.65	-2.7	ns	3.4	0.0173

APPENDIX 10: continued

Table 2 continued.

Antioxidants											
5408	Peroxiredoxin-6	410.63	200.37	162.61	156.60	393.45	123.55	-2.5	ns	2.4	0.0260
Heat Shock Proteins											
3518	Stress-70 protein (aka HSPA9)	369.67	142.60	112.02	144.99	323.75	223.68	-3.3	0.0260	2.9	0.0411
4702	Stress-70 protein (aka HSPA9)	508.89	402.11	1035.09	584.46	360.54	271.60	-1.9	ns	2.7	0.0152
Cytoskeletal/Sarcomeric											
3627	Desmin	491.87	264.82	206.72	46.34	545.80	182.40	-2.4	0.0159	2.6	0.0043
3305	Myosin light chain 3	1691.27	957.03	545.68	498.17	1472.06	904.54	-3.1	0.0411	2.7	ns
1206	Myosin regulatory light chain 2			490.18	236.51	305.05	331.21	On		-1.6	ns
1213	Myosin regulatory light chain 2	147.58	126.06	1049.19	385.02	626.65	440.62	7.1	0.0095	-1.7	ns
3228	Myosin regulatory light chain 2	204.57	219.47	1850.40	1241.85	1218.78	1357.75	9.1	0.0022	-1.5	ns
4207	Myosin-6	508.89	402.11	1035.09	584.46	360.54	271.60	2.0	ns	-2.9	0.0152
1320	Tropomyosin alpha-1 chain (or Tropomyosin beta chain)	172.31	68.46	17.32	9.72	195.82	115.85	-9.95	0.0238	11.30	0.0238
1248	Troponin T, cardiac muscle	133.87	228.64			173.79	243.95	Off		On	
4523	Tubulin alpha-4A chain	705.21	218.21	157.23	193.67	404.76	319.42	-4.5	0.0087	2.6	ns
Others											
1430	14-3-3 protein epsilon	225.70	167.56	24.77	15.25	309.80	180.01	-9.1	ns	12.5	0.0043
2616	40S ribosomal protein SA	98.56	104.48	83.32	54.58	278.01	167.07	-1.2	ns	3.3	0.0173
2546	Adenylyl cyclase-associated protein 1	89.10	44.41	21.66	13.56	134.59	57.71	-4.1	0.0303	6.2	0.0043
7110	Galectin-5			654.97	1246.68	66.30	101.51	On		-9.9	ns
7702	Hydroxysteroid dehydrogenase-like protein 2	150.13	98.79	54.77	48.38	200.66	103.56	-2.7	ns	3.7	0.0087
8710	WD repeat-containing protein 1	358.36	214.12	169.16	88.09	454.56	216.81	-2.1	ns	2.7	0.0043